ISSN 0021-9673

VOL. 704 NO. 2 9 JUNE 1995

THIS ISSUE COMPLETES VOL. 704

# JOURNAL OF CHROMATOGRAPHY A

## INCLUDING ELECTROPHORESIS AND OTHER SEPARATION METHODS



ELSEVIER

# JOURNAL OF CHROMATOGRAPHY A

INCLUDING ELECTROPHORESIS AND OTHER SEPARATION METHODS

**Scope.** The *Journal of Chromatography A* publishes papers on all aspects of **chromatography, electrophoresis** and related methods. Contributions consist mainly of research papers dealing with chromatographic theory, instrumental developments and their applications. In the *Symposium volumes*, which are under separate editorship, proceedings of symposia on chromatography, electrophoresis and related methods are published. *Journal of Chromatography B: Biomedical Applications* —This journal, which is under separate editorship, deals with the following aspects: developments in and applications of chromatographic and electrophoretic techniques related to clinical diagnosis or alterations during medical treatment; screening and profiling of body fluids or tissues related to the analysis of active substances and to metabolic disorders; drug level monitoring and pharmacokinetic studies; clinical toxicology; forensic medicine; veterinary medicine; occupational medicine; results from basic medical research with direct consequences in clinical practice.

**Submission of Papers.** The preferred medium of submission is on disk with accompanying manuscript (see *Electronic manuscripts* in the Instructions to Authors, which can be obtained from the publisher, Elsevier Science B.V., P.O. Box 330, 1000 AH Amsterdam, Netherlands). Manuscripts (in English; *four* copies are required) should be submitted to: Editorial Office of *Journal of Chromatography A*, P.O. Box 681, 1000 AR Amsterdam, Netherlands, Telefax (+31-20) 485 2304, or to: The Editor of *Journal of Chromatography B: Biomedical Applications*, P.O. Box 681, 1000 AR Amsterdam, Netherlands. Review articles are invited or proposed in writing to the Editors who welcome suggestions for subjects. An outline of the proposed review should first be forwarded to the Editors for preliminary discussion prior to preparation. Submission of an article is understood to imply that the article is original and unpublished and is not being considered for publication elsewhere. For copyright regulations, see below.

**Publication information.** *Journal of Chromatography A* (ISSN 0021-9673): for 1995 Vols. 683–714 are scheduled for publication. *Journal of Chromatography B: Biomedical Applications* (ISSN 0378-4347): for 1995 Vols. 663–674 are scheduled for publication. Subscription prices for *Journal of Chromatography A*, *Journal of Chromatography B: Biomedical Applications* or a combined subscription are available upon request from the publisher. Subscriptions are accepted on a prepaid basis only and are entered on a calendar year basis. Issues are sent by surface mail except to the following countries where air delivery via SAL is ensured: Argentina, Australia, Brazil, Canada, China, Hong Kong, India, Israel, Japan, Malaysia, Mexico, New Zealand, Pakistan, Singapore, South Africa, South Korea, Taiwan, Thailand, USA. For all other countries airmail rates are available upon request. Claims for missing issues must be made within six months of our publication (mailing) date. Please address all your requests regarding orders and subscription queries to: Elsevier Science B.V., Journal Department, P.O. Box 211, 1000 AE Amsterdam, Netherlands. Tel.: (+31-20) 485 3642; Fax: (+31-20) 485 3598. Customers in the USA and Canada wishing information on this and other Elsevier journals, please contact Journal Information Center, Elsevier Science Inc., 655 Avenue of the Americas, New York, NY 10010, USA, Tel. (+1-212) 633 3750, Telefax (+1-212) 633 3764.

**Abstracts/Contents Lists** published in Analytical Abstracts, Biochemical Abstracts, Biological Abstracts, Chemical Abstracts, Chemical Titles, Chromatography Abstracts, Current Awareness in Biological Sciences (CABS), Current Contents/Life Sciences, Current Contents/Physical, Chemical & Earth Sciences, Deep-Sea Research/Part B: Oceanographic Literature Review, Excerpta Medica, Index Medicus, Mass Spectrometry Bulletin, PASCAL-CNRS, Referativnyi Zhurnal, Research Alert and Science Citation Index.

**US Mailing Notice.** *Journal of Chromatography A* (ISSN 0021-9673) is published weekly (total 52 issues) by Elsevier Science B.V., (Sara Burgerhartstraat 25, P.O. Box 211, 1000 AE Amsterdam, Netherlands). Annual subscription price in the USA US$ 5389.00 (US$ price valid in North, Central and South America only) including air speed delivery. Second class postage paid at Jamaica, NY 11431. **USA POSTMASTERS**: Send address changes to *Journal of Chromatography A*, Publications Expediting, Inc., 200 Meacham Avenue, Elmont, NY 11003. Airfreight and mailing in the USA by Publications Expediting.

**See inside back cover** for Publication Schedule, Information for Authors and information on Advertisements.

---



0021-9673/95/$09.50



Printed in the Netherlands

# CONTENTS

*(Abstracts/Contents Lists published in Analytical Abstracts, Biochemical Abstracts, Biological Abstracts, Chemical Abstracts, Chemical Titles, Chromatography Abstracts, Current Awareness in Biological Sciences (CABS), Current Contents/Life Sciences, Current Contents/Physical, Chemical & Earth Sciences, Deep-Sea Research/Part B: Oceanographic Literature Review, Excerpta Medica, Index Medicus, Mass Spectrometry Bulletin, PASCAL-CNRS, Referativnyi Zhurnal, Research Alert and Science Citation Index)*

## REGULAR PAPERS

*Column Liquid Chromatography*

Consolidation of the packing material in chromatographic columns under dynamic axial compression. I. Fundamental study
by G. Guiochon and M. Sarker (Knoxville and Oak Ridge, TN, USA) (Received 13 February 1995) . . . . . 247

Naproxen-derived segmented and sidechain-modified polysiloxanes as chiral stationary phases
by W.H. Pirkle and G.J. Terfloth (Urbana, IL, USA) (Received 13 February 1995) . . . . . 269

Retentive and enantioselective properties of ovomucoid-bonded silica columns. Influence of protein purity and isolation method
by J. Haginaka, C. Seyama and T. Murashima (Nishinomiya, Japan) (Received 7 February 1995) . . . . . 279

Retention and selectivity of flavanones on homopolypeptide-bonded stationary phases in both normal- and reversed-phase liquid chromatography
by B.A. Siles, H.B. Halsall and J.G. Dorsey (Cincinnati, OH, USA) (Received 17 February 1995) . . . . . 289

High-performance affinity chromatography of proteins on non-porous polystyrene beads
by W.-C. Lee (Chiayi, Taiwan) and C.-H. Lin, R.-C. Ruaan and K.-Y. Hsu (Chungli, Taiwan) (Received 16 February 1995) . . . . . 307

Immobilized-liposome chromatographic analysis of drug partitioning into lipid bilayers
by F. Beigi, Q. Yang and P. Lundahl (Uppsala, Sweden) (Received 10 February 1995) . . . . . 315

Nitrobenzenes in reversed-phase liquid chromatography. New candidates for internal standards
by S. Yamauchi (Tokushima, Japan) (Received 21 February 1995) . . . . . 323

Determination of aldehydes in used engine oils by liquid chromatography with chemiluminescence detection
by A.N. Gachanja, S.W. Lewis and P.J. Worsfold (Plymouth, UK) (Received 9 February 1995) . . . . . 329

Preferred high-performance liquid chromatographic anion-exchange chromatographic contact region for recombinant rat cytochrome $b_5$
by D.J. Roush, D.S. Gill and R.C. Willson (Houston, TX, USA) (Received 5 December 1994) . . . . . 339

Chromatographic determination of constituents of the genus *Colchicum* (Liliaceae)
by P. Ondra, I. Válka and J. Vičar (Olomouc, Czech Republic), N. Sütlüpinar (Istanbul, Turkey) and V. Šimánek (Olomouc, Czech Republic) (Received 6 February 1995) . . . . . 351

Determination of indole alkaloids from *R. serpentina* and *R. vomitoria* by high-performance liquid chromatography and high-performance thin-layer chromatography
by V.E. Klyushnichenko, S.A. Yakimov, T.P. Tuzova, Ya.V. Syagailo, I.N. Kuzovkina, A.N. Wulfson and A.I. Miroshnikov (Moscow, Russia) (Received 13 January 1995) . . . . . 357

High-performance liquid chromatographic analysis of mevinolin as mevinolinic acid in fermentation broths
by J. Friedrich, M. Žužek, M. Benčina, A. Cimerman and A. Štrancar (Ljubljana, Slovenia) and I. Radež (Novo Mesto, Slovenia) (Received 16 January 1995) . . . . . 363

Analysis and purification of modified methoxy(polyethylene glycol) compounds of similar molecular mass by high-performance liquid chromatography
by W.H. Leister, L.E. Weaner and D.G. Walker (Spring House, PA, USA) (Received 14 December 1994) . . . . . 369

Characterization of poly(naphthalenesulfonate) salts by ion-pair chromatography and ultrafiltration
by M. Piotte, F. Bossányi, F. Perreault and C. Jolicoeur (Sherbrooke, Canada) (Received 13 February 1995) . . . . 377

*Gas Chromatography*

Pair-wise interactions by gas chromatography. VI. Interaction free enthalpies of solutes with primary methoxyalkane, cyanoalkane and alkanethiol groups
by K.S. Reddy, R. Cloux and E.s. Kováts (Lausanne, Switzerland) (Received 9 February 1995) . . . . . 387



*(Continued overleaf)*

*Contents (continued)*

Prediction of gas chromatographic retention times, column efficiency and resolution as a function of temperature and flow-rate. Application for gas chromatographic separation of eight *p*-hydroxybenzoic esters
by Y. Guillaume, M. Thomassin and C. Guinchard (Besançon, France) (Received 21 February 1995) . . . . . 437

Comparison of gas chromatographic and spectrophotometric techniques for the determination of formaldehyde in water
by Š. Velikonja, I. Jarc, L. Zupančič-Kralj and J. Marsel (Aškerčeva, Slovenia) (Received 5 January 1995) . . . . . 449

Accurate quantitation of short-, medium-, and long-chain fatty acid methyl esters by split-injection capillary gas–liquid chromatography
by F. Ulberth and F. Schrammel (Vienna, Austria) (Received 10 February 1995) . . . . . 455

Breakthrough volume of monoterpenes on Tenax TA: influence of temperature and concentration for $\alpha$-pinene
by V. Simon, M.-L. Riba, A. Waldhart and L. Torres (Toulouse, France) (Received 13 February 1995) . . . . . 465

Chromatographic determination of trace amounts of amines using a surface ionization detector
by U.K. Rasulev, E.G. Nazarov and G.B. Khudaeva (Tashkent, Uzbekistan) (Received 21 October 1994) . . . . . 473

Hygrine, bona fide alkaloid or artifact: its chemical reduction, novel di-heptafluorobutyrylation and sensitive detection in South American coca leaves using capillary gas chromatography–electron capture detection
by J.M. Moore, J.F. Casale, P.A. Hays, R.F.X. Klein and D.A. Cooper (McLean, VA, USA) (Received 16 February 1995) . . . . . 483

Improved chromatographic analysis of volatile sulfur compounds by the static headspace technique on water–alcohol solutions and brandies with chemiluminescence detection
by M. Nedjma and A. Maujean (Reims, France) (Received 20 December 1994) . . . . . 495

*Electrophoresis*

Capillary zone electrophoresis of aldose enantiomers: separation after derivatization with *S*-(−)-1-phenylethylamine
by C.R. Noe and J. Freissmuth (Frankfurt, Germany) (Received 28 December 1994) . . . . . 503

SHORT COMMUNICATIONS

*Column Liquid Chromatography*

Determination of benzoylurea insecticides in apples by high-performance liquid chromatography
by T. Tomšej (Karlovy Vary, Czech Republic) and J. Hajšlová (Prague, Czech Republic) (Received 7 February 1995) 513

Determination of eight constituents of Hsiao-cheng-chi-tang by high-performance liquid chromatography
by S.-J. Sheu and C.-F. Lu (Taipei, Taiwan) (Received 13 February 1995) . . . . . 518

Separation and quantification of tetraethylene glycol monoheptanoate and diheptanoate by high-performance liquid chromatography
by V. Baudrand, Z. Mouloungui and A. Gaset (Toulouse, France) (Received 14 February 1995) . . . . . 524

Determination of chlorine, sulphur and phosphorus in organic materials by ion chromatography using electrodialysis sample pretreatment
by M. Novič, A. Dovžan, B. Pihlar and V. Hudnik (Ljubljana, Slovenia) (Received 19 January 1995) . . . . . 530

*Gas Chromatography*

Monitoring the esterification of sorbitol and fatty acids by gas chromatography
by J. Giacometti and Č. Milin (Rijeka, Croatia) and N. Wolf (Zagreb, Croatia) (Received 8 February 1995) . . . . . 535

*Planar Chromatography*

Thin-layer chromatographic detection of dichlorvos and dimethoate using orcinol
by B.D. Mali, M.V. Garad, V.B. Patil and S.V. Padalikar (Aurangabad, India) (Received 18 January 1995) . . . . . 540

BOOK REVIEW

Carbohydrate Analysis–High-Performance Chromatography and Capillary Electrophoresis (edited by Z. El Rassi), reviewed by E.F. Hounsell (London, UK) 544

AUTHOR INDEX . . . . . 546

ELSEVIER

Journal of Chromatography A, 704 (1995) 247–268

JOURNAL OF CHROMATOGRAPHY A

# Consolidation of the packing material in chromatographic columns under dynamic axial compression. I. Fundamental study

Georges Guiochon[a,b,*], Matilal Sarker[a,b]

[a]*Department of Chemistry, University of Tennessee, Knoxville, TN, 37996-1600, USA*

[b]*Division of Chemical and Analytical Sciences, Oak Ridge National Laboratory, Oak Ridge, TN, 37831-6120, USA*

First received 30 November 1994; revised manuscript received 13 February 1995; accepted 20 February 1995

**Abstract**

Packing materials do consolidate progressively inside chromatographic columns. The process is slow. The literature on the phenomenon of soil consolidation is critically reviewed and the concepts relevant to the behavior of sands are applied to conventional packing materials. Preliminary experimental results obtained with irregular-shaped particles are presented to illustrate the concepts introduced by and the conclusions of the literature survey. These results show that the consolidation of packing material in chromatographic columns is a slow process which may sometimes appear to take place as a series of "catastrophic" events. It involves changes in the apparent packing density of the bed which are large enough to account for the formation of large voids at the column inlet, as has been frequently reported by operators of analytical as well as large-size preparative columns.

## 1. Introduction

There is serious experimental evidence that the packing of chromatographic columns is not homogeneous. Knox and Parcher [1], Knox et al. [2], and Horne et al. [3] showed conclusively that there is a wall region in packed columns which is severely perturbed. This region extends to ca. 30 particle diameters from the wall. The column core, on the other hand, appears to be much more homogeneous. So, these authors suggested that if the sample is injected at the center of a wide enough column, the analyte bands would never have time to reach the wall region and the column performance would be as good as if the column were entirely homogeneous. If the column is narrow, however, a significant fraction of its molecules enters the wall region and propagates inside it. As a consequence of the heterogeneity of the packing in the wall region, the apparent efficiency of the column drops markedly when the band has access to it. Knox's data [1–3] were confirmed by Eon [4] who demonstrated that the local value of the axial plate height (characterizing band spreading in the direction of the flow velocity) increases as the location gets closer to the wall, that the apparent height equivalent of a theoretical plate (HETP) is not constant along the wall, around the column, and that radial compression [5] may im-

* Corresponding author. Address for correpondence: Department of Chemistry, University of Tennessee, 575 Buehler Hall, Knoxville, TN 37996-1600, USA.

0021-9673/95/$09.50 
*SSDI* 0021-9673(95)00242-1

prove markedly column performance, presumably because it reduces the density difference between the wall and the core regions.

Unfortunately, the concept of the infinite-diameter column would not be practical in preparative chromatography. A large fraction of the packing material contained in the column and of the solvent used would not be involved in the retention and the separation process. Their loss would represent a high cost to pay for a gain in column efficiency which is rarely perceived to be worth so much. For analytical applications, the equipment would be markedly more complex as local injection and detection would be required [1–7]. The HPLC equipment has evolved in a direction opposite to the requirements of operation under the infinite-diameter column concept. Although the decision of the community, instrument designers and analysts alike, to reject the concept of infinite-diameter column operation does not seem unreasonable, it does not justify our complete amnesia regarding the lack of radial homogeneity of packed columns which has been demonstrated twenty years ago.

The early experimental results of Knox [1–3] and Eon [4] were confirmed later by Baur et al. [6] and, more recently, by Farkas et al. [7]. These authors have shown that the distribution of the residence times of the molecules of a nonretained tracer in the exit cross-sectional area of a chromatographic column depends on the distance to the column center. Thus, the retention time of a nonretained band and the axial plate height vary across the column section. Baur et al. [6] found that the retention time of a nonretained tracer and the HETP along the axial direction vary with the radial position, are minimum at the column center, and maximum at the wall. Farkas et al. [7] found also that the retention time is maximum at the wall but observed a minimum at approximately two thirds of the radius from the center. The retention time remains nearly constant in the core region. The retention time is typically 6 to 10% higher at the wall and 3 to 4% lower at the ridge than in the core region [7]. The column HETP remains constant in the same core region, exhibits a weak minimum at about two thirds of a radius from the center and raises very rapidly close to the wall where it may be between three [7] and five [6] times larger than in the core region. It was also shown that these experimental results cannot be explained by a nonplanar injection [7]. The difference between the results of Baur et al. [6] and those of Farkas et al. [7] are explained by a difference in the packing technology used. It is important to note at this stage that the velocity distribution observed is opposite in the earlier work [1–4] (velocity minimum at the column center) and in the more recent one [6,7] (velocity minimum at the wall).

Early studies in gas chromatography reported an effect similar to the one observed by Knox [1–3] and Eon [4]. Giddings and Fuller [8] showed that particles segregate spontaneously during packing, the large particles accumulating along the column wall and the small ones at the center, an effect due to dry packing. A cone is formed at the column center and the large particles roll more easily to the wall. As a result of this discrimination, the packing permeability is 25 to 45% larger at the column wall than in the center [8]. This simple phenomenon could explain completely the velocity variation measured by Huyten et al. [9] across a wide column. In a study done on packed beds used as heat exchangers, Schwartz and Smith [10] had shown a velocity 30 to 100% larger at the wall than in the center, with a velocity peak at about one pellet diameter from the column wall. These results suggest that the layer of packing close to the wall has a lower density than the core. However, these experimental results were achieved with values of the column-to-particle diameter ratio of the order of 30, much smaller than in any conventional LC columns. The recent results reported [6,7], showing that the packing density is higher along the column wall, have been obtained with column-to-particle diameter ratios in the range from 100 to 1500.

Comparing the data reported in Refs. [1–4] and [8–10] on the one hand, with those of Refs. [6,7] on the other hand suggests that the difference originates in the use of dry-packing techniques in the former series of experiments, slurry packing in the latter. With slurry packing, the

velocity of the packing solvent, hence the viscous drag on the particles, are larger in the regions where the bed density is lower, thus providing for a drive toward column homogeneity. Furthermore, the mechanism leading to radial discrimination of the particles on the basis of their size, which is so effective in dry packing, is not operative in slurry packing. Thus, the systematic variations across the column of the mobile-phase velocity and the axial dispersion coefficient reported by Baur et al. [6] and Farkas et al. [7] cannot be accounted for by a systematic variation of the average particle size along the diameter. They suggest rather a nonhomogeneous density of the column packing.

Other phenomena reported in the literature could be explained by column-to-column variations of the packing density. For example, it is well known that excellent columns can be packed by mere sedimentation of a slurry but these columns are unstable, i.e., their packing collapses after a certain time, resulting into a nonhomogeneous bed, an important void at the column inlet, and possible cracks. It is often observed in analytical laboratories that well-packed columns lose their efficiency after a while. In most cases, opening the column inlet shows the beginning of the column to be empty. This phenomenon is clearly illustrated by recent results obtained in NMR imaging using a column packed by sedimentation [11]. Filling this void usually restores the column performance to its original level. This effect can be explained simply by a progressive consolidation of the column bed, resulting in a slow increase of its packing density.

The column-to-column reproducibility of retention data has always been a serious concern among chromatographers. The same is true for the reproducibility of equilibrium isotherms. It has been reported in the literature that isotherms measured under identical conditions on two columns prepared successively with the same material, using the same packing method are significantly different [12]. Recently, a systematic study has shown important differences in the packing density of series of columns, explaining the differences between the isotherms measured on these columns [13]. Other studies have shown that the packing density of columns prepared with a given packing material is different depending on the type of column used: analytical column, dynamic axial compression column, dynamic radial compression column [14,15]. The important conclusion is that various independent observations suggest that the density of a packing material is not a physical property characterizing it in the same way as its density can characterize a solvent.

A chromatographic bed is submitted to compression stress of various origins. In addition to axial [15] or radial [14] compression which are now widely used in preparative chromatography or to annular compression which has also been suggested, a bed is always subject to several types of stress. First, the inlet pressure also causes a compression of the entire bed due to the pressure gradient which acts on each particle of the packing, while the inlet pressure acts on the entire bed: withdrawing the exit frit and applying a high inlet pressure results usually in the expulsion of the entire packing material from the column. The friction of the bed against the column wall opposes the sliding movement of the bed. Second, the viscous flow of the mobile phase results in an intense friction which tends to move particles along the column in the direction of the flow. Finally, the presence of the mobile phase may change the interaction energy between particles, e.g., if of electrostatic origin. These stresses are continuously applied during column operation and may cause more or less extensive reorganization of the packing whenever one particle moves or breaks.

The application of stress to any material causes strains. Solid mechanics is the science studying the relationships between applied stress, resulting strains and the ensuing deformation of the material [16]. In the particular case of column packing, we deal with an unusual solid, which has no proper shape, like a liquid, and can deform almost as freely. The structure of the packing is a skeleton of solid grains enclosing voids filled with the mobile phase. There are weak interactions between the particles of packing material. The intensity of these interactions

depend on the nature of the surface of the particles and on their size. Spheres with a glassy surface will interact the least. Spheres with rugous surface will interact somewhat more. Irregular-shaped particles will interact the most. Small particles will interact more strongly than large particles of the same nature. These interactions will have an important role when the bed consolidates or reacts physically under compression [16].

A bed of packing material has little elasticity (although it is not entirely negligible, as we will see later). If a certain amount of packing material is compressed, as it is during the procedure of packing the column or afterward during its operation, the particles and the packing skeleton are placed under stress and at least one will deform. Depending on the rigidity of the particles, widely different results may be observed. If the packing is made of plastic materials, such as gels of crosslinked polyacrylamide particles, the particles deform easily, filling the void between them. The external porosity of the bed decreases rapidly and consequently the permeability decreases dramatically. As polymers tend to flow unless they are strongly crosslinked, their deformation is permanent. The particles do not recover their initial shape when the stress is released and the column permeability does not return to its initial value. This sets a rather low limit to the maximum pressure at which the column can be operated. For this reason, gels and many polymer-based packing materials are not mechanically suitable for high-performance chromatography in spite of otherwise attractive performance. An abundant literature originating from a single well [17] has tried to make virtue from this drawback. This should not delude the separation chemist [18]. Although there are cases in which a most favorable equilibrium thermodynamics can offset the consequences of the inability of the particles of a packing material to withstand a relatively high pressure drop, this drawback constitutes a more and more definitive roadblock.

If the packing material is made of hard, strong (under compression), brittle material, such as silica, alumina, zeolites, or other inorganic substances, the particles deform very little until the break point is reached. The nearly entire stress is conveyed to the skeleton which has to deal with it [16]. Some grains will slide or roll over their neighbors while other ones may break apart. The volume occupied by the packing material decreases accordingly. When the stress is released, however, there is no mechanism and little driving force for the particles which have moved to return to their initial position in the bed. The volume rebound is not so great as the compression. It is limited to the elastic compression of the particles and of the skeleton, both rather small [16]. In the same way as soil on an oft travelled footpath, at the bottom of a rut, or on a dirt road hardens progressively and remains permanently hardened (rain or shine), the packing in a chromatographic column becomes more compact as a response to the stress applied to the packing. This phenomenon is accompanied by a decrease of the external porosity and the column permeability. Although this is not intuitive, the apparent density of the packing is not a constant. It depends on the size of the column (diameter and length), on the packing method used, and on the previous consolidation history of the column.

At this stage we must introduce a distinction between the two different consolidation processes which are used in the packing of chromatographic columns. Analytical columns are consolidated under the influence of the viscous stress applied to the particles by the solvent stream percolating through them. Fluid mechanics shows that this stress is equivalent to the stress afforded by an intense gravity field acting parallel to the column axis. This equivalence will be discussed in a later report [19]. Dynamic compression columns are consolidated under the influence of mechanical compression of the bed by a compression stress applied through a piston (axial compression [15]), or the column wall (radial compression [14]). In this latter case, the stress is not distributed through the entire packing, as in the former case, but conveys from a surface toward the inside of the packing. Because of friction between particles and between the packing bed and the wall, the distribution of stress inside the column bed is not

homogeneous [20]. Because the stress applied to a liquid conveys instantaneously and homogeneously, two different situations are possible depending on whether the container of packing material is open or closed. If it is closed, the liquid is under compression and, because liquid compressibility is small, the packing material is under weak stress. This situation will not be considered further in this work. If the container is open, as a chromatographic column, the liquid is under no stress, unless there is a flow. The packing material is under the mechanical compression stress, distributed heterogeneously through the bed. In the case of a dynamically compressed chromatographic column, the viscous stress due to the local flow velocity (or rather to the pressure gradient) which is described above adds to the mechanical stress.

The main difference between soils such as sand and chromatographic beds is that the latter are entirely confined in a closed vessel, so the packing cannot shear. There is still a stability problem in our case, and the particles can break. Another significant difference is in the particle size distribution, somewhat wider in soils [16] than in packing materials. Other major differences are in the orders of magnitude. In most current problems of soil mechanics the volume involved are millions or billions times larger than in chromatography, the time scale is similarly much longer (typically years), while the pressure gradients and the flow velocities are much lower. Nevertheless, the phenomena observed are similar in nature. If a given mass of packing is compressed, its volume decreases. This results from a combination of (i) the compression of the individual, solid particles, (ii) the compression of the particle skeleton, (iii) the compression of the mobile phase surrounding the particles (which is negligible), and (iv) the escape of the mobile phase from the interstitial voids, between the particles. As far as the classical, silica-based phases are concerned, the contribution of the first phenomenon is negligible and it is accurate enough to consider only the fourth one. For polymeric phases, the first and last phenomena are significant. The process by which the bed responds to the external compression and settles, is called consolidation [16]. The extent of consolidation depends on the compression pressure applied. The phenomenon is not instantaneous. Results of soil mechanics suggest that the kinetics is different for a dry bed and for a wet one [16].

Finally, we must recognize that the interactions between the packing material and the mobile phase are important in any study of packed bed stability. If a glass column packed with silica, and fed by gravity, is left to dry, its bed cracks in a random fashion and voids extending across the entire column can be seen. Admittedly, HPLC columns made of stainless steel or titanium tubings are more consolidated than conventional columns made of glass tubes which cannot stand any significant pressure[1]. Nevertheless, this suggests that the packing density (expressed in weight of silica per unit volume of column) depends on the presence of a liquid phase and probably on its nature. This is confirmed by another phenomenon, which is ignored in soil mechanics, but may have to be taken into account in chromatography, although it has not been documented yet.

The apparent density of a sedimented bed depends on the surface tension of the solid particles and the liquid in contact [22]. When the mobile-phase composition changes, so does its surface tension. This may cause a change of the apparent density of the packing material, provided it can accommodate it. This phenomenon has been applied by Barford [22] to the measurement of the surface tension of packing materials. It may not play an important role with chemically bonded $C_{18}$ silica because these materials are not wetted by water-rich solvents, anyway. However, it is probably significant in hydrophobic interaction chromatography. If the packing is strongly consolidated, there will be no change in its density, unless the stress becomes strong enough to break some particles. If the packing is only weakly consolidated, a concentration gra-

[1] Unfortunately, we cannot see the packing material inside our metal columns. This may provide another illustration to the profound comment of Eyring, "What the eye does not see, does not bother the mind" [21].

dient, caused either by a change in the mobile phase composition or by the injection of a large sample, may lead to an increase in the packing density. Like other causes of increased consolidation, this effect should be transient and after a certain time, the bed should remain stable under the experimental conditions used. There is no mechanism for the extent of consolidation to decrease when the stress which caused it is removed. The particles cannot bounce back to their original position.

The goal of this work is to present new data on the extent of the consolidation of the packing material in chromatographic columns, on the difference between consolidation and elasticity of the bed, and on the time scale of this phenomenon. Further publications will apply these new concepts to the study of various packing materials used in preparative chromatography [23].

## 2. Theoretical

Sands are the types of soil closest in properties to packing materials for chromatography. The main difference between sands and packing materials is in the particle size distribution. Sands are very heterogeneous, with a range of particle sizes extending over several orders of magnitude, from a few mm to less than 1000 Å. As a consequence, their porosity in compacted beds can be as low as 27%. They are also nonporous and stronger than the porous silica particles used in HPLC.

### 2.1. Kinetics of consolidation

The time lag during compression of sands [16], hence most probably of all packing materials, is mostly of a frictional nature. After a compression increment is applied, there is no uniform and smooth reordering of the particles, but an irregular, chaotic succession of local build-up of stress between groups of particles, leading to a rupture of the equilibrium, grains rolling over each other or being separated abruptly by the local avalanche of grains resulting from the break-up of a bridge at some distance. As a consequence, consolidation tends toward a limit following a quasi-exponential decay with a pseudo time constant which may be of the order of hours for a small preparative column and increases with increasing bed volume.

The simplest case of consolidation considered in soil mechanics is the one which results from linear compression (i.e., compression in one direction). This case applies exactly to the situation encountered in dynamic axial compression and in chromatographic columns which are not dynamically compressed but where the bed is stressed by the pressure applied to the top of the bed (the inlet pressure) and the shear force generated by the friction of the mobile phase percolating through the bed. Typically, plots of the void volume versus the compression pressure can be represented by the following equation:

$$e = \frac{\epsilon_e}{1-\epsilon_e} = e_0 - C_c \log \frac{P}{p_0} \quad (1)$$

where $e$ is the void ratio or ratio of the volume fraction of the column available to the mobile phase percolating around the particles to the volume occupied by the particles assumed to be nonporous, $\epsilon_e$ is the external, interparticle, or interstitial porosity, $e_0$ is the void volume at the reference pressure $p_0$, usually the atmospheric pressure, $P$ is the compression pressure, and $C_c$ is a numerical coefficient. The compression diagram is a plot of the void ratio, $e$, versus the logarithm of the compression pressure, $P$. As an example, Fig. 1 shows a typical compression diagram recorded for a sample of a well-known packing material having irregular-shape particles (see Section 3 for relevant details). This diagram will be discussed later together with the reasons for the broken plot (dotted lines). Suffice it to say at this stage that Eq. 1 is approximately valid for the consolidation of the dry-packing material (solid line) and is valid in a certain pressure range for the consolidation of the wet material (dotted lines). Note that, because the particles are porous, the total porosity which is derived directly from the value of the hold-up volume should be corrected for the contribution of the internal porosity. The latter cannot be measured simply but is estimated by assuming that the

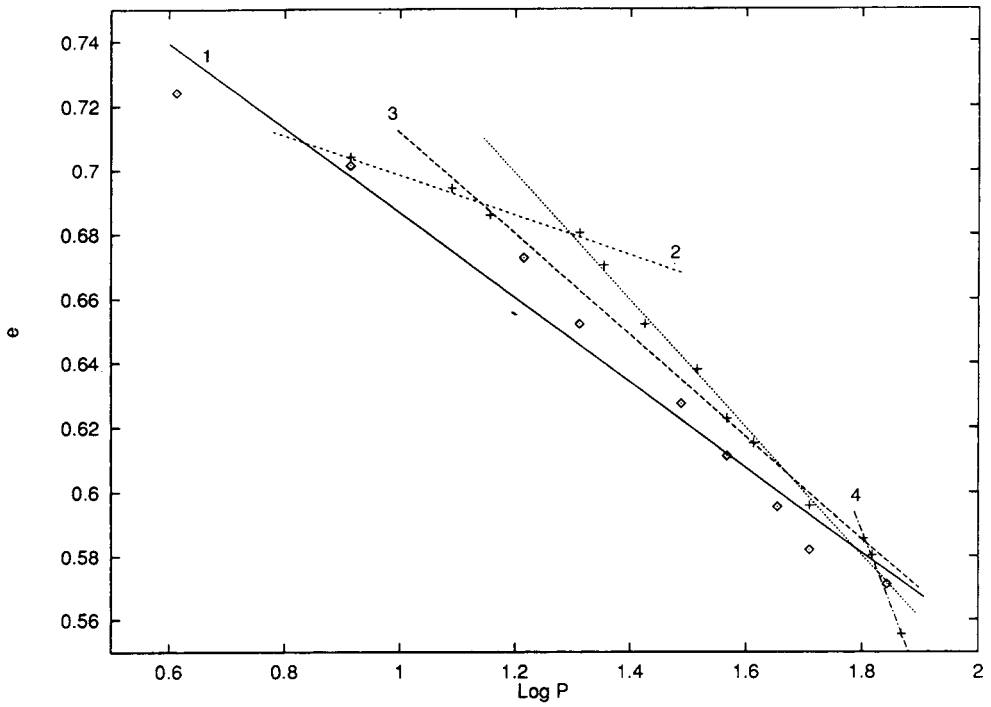


Fig. 1. Compression diagram. Plot of the void ratio versus the compression pressure for the dry (◇) and wet (+) packing material: 1 = compression of the dry packing; 2 = compression of the wet packing, least-squares fit of the first five data points on a straight line; 3 = compression of the wet packing, least-squares fit of data points 4 to 12 on a straight line; 4 = compression of the wet packing, least-squares fit of the last three data points on a straight line.

internal porosity is constant and independent of the stress applied to the particles and that the external porosity of the material sedimenting freely is 41%. Fig. 2 illustrates the kinetics of the bed consolidation. These results are discussed later for their significance in chromatography.

Two phenomena explain the finite rate at which a bed of sand or the packing of a chromatographic column consolidates. The first is the frictional nature of the compression process, just explained. Thus, consolidation is expected to be slower with irregular and rugous particles than with spherical or smooth particles, *not that this may necessarily affect the chromatographic performances themselves*. The second is the finite time it takes to eliminate the mobile phase inside the skeleton of particles when compression takes place. This hydrodynamic lag is due to the finite permeability of the bed which controls the escape of the mobile phase. Its importance increases with decreasing particle size and increasing column length. The particle size distribution of the silica materials for chromatography is narrower than that of sand and their average diameter is much larger than the finest sand grains found in nature, so their consolidation appears to be faster.

The theory of the kinetics of consolidation of Terzaghi [24] neglects the frictional lag and takes into account only the hydrodynamic lag. This theory assumes that the void ratio, $e$, decreases linearly with increasing pressure, which is only approximate since we have said above that the experimental data are better fitted by a logarithmic dependence (Eq. 1). When the pressure applied to the sample is increased from $P_1$ to $P_2$, there cannot be a change in strain of the packing unless part of the mobile phase flows out. If the column is closed and the compression pressure applied to the bed is raised while the liquid is

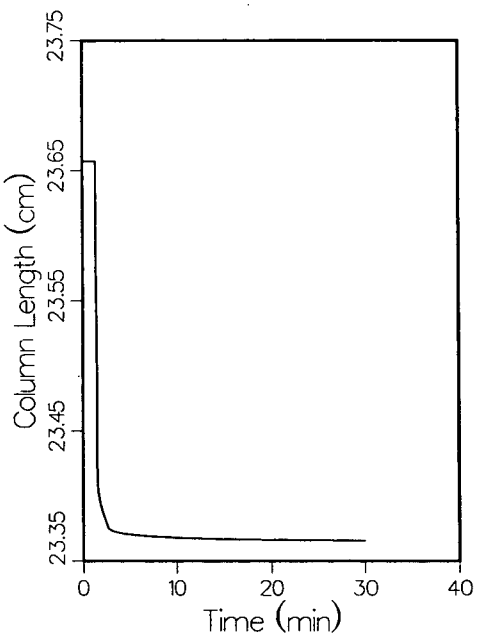


Fig. 2. Kinetics of the consolidation of the dry-packing material. Plot of the column length versus time at constant compression pressure after a pressure jump from 4.2 to 8.4 bar.

unable to leak out, the only change which occurs is due to the compression of the liquid and the silica itself, a very small change. Fig. 3 illustrates the phenomenon.

Consider a differential element of the packing material, in the middle of a column filled with mobile phase, but with no flow-rate; hence the static pressure of the mobile phase is atmospheric. A constant compression pressure, $P_1$ is applied to the packing. Initially, the state of this packing is represented by the point A, with void ratio $e_1$ and pressure $P_1$. At time $t = 0$, the compression pressure is raised to $P_2$, but the void ratio remains the same and the pressure $\Delta P = P_2 - P_1$ is applied to the liquid, forcing it out of the bed through both ends of the column. The liquid cannot exit instantaneously. At time $t = \infty$, the compression pressure applied to the bed has become $P_2$ and the void ratio $e_2$; the state of the packing is represented by point C. At an intermediate time, $t$, the bed is compressed with the pressure $P$ and the void ratio is $e$, the state being represented by point B. The liquid inside the element of the bed is under the pressure $\delta P = P_2 - p$. Thus, $\delta P$ decreases from $\Delta P$ to 0, while the pressure supported by the bed increases from $P_1$ to $P_2$ and the bed consolidates, its void ratio decreasing from $e_1$ to $e_2$. The consolidation ratio, $U$ is given by:

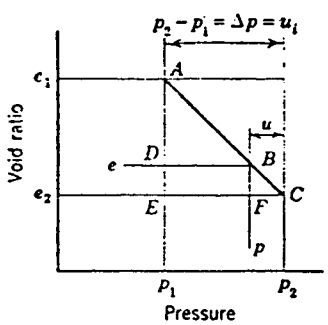


Fig. 3. Relationship between the pressure and the void volume for a small pressure increment.

$$U = \frac{e_1 - e}{e_2 - e_1} \tag{2a}$$

$$= \frac{p - P_1}{P_2 - P_1} = 1 - \frac{\delta P}{\Delta P} \tag{2b}$$

The first equation above is the definition of the consolidation ratio; the second results from the assumption that the void ratio decreases linearly with increasing compression pressure. This assumption is expressed by considering the coefficient:

$$a_v = \frac{e_1 - e_2}{P_2 - P_1} = -\frac{de}{dP} \tag{3}$$

as a constant. This coefficient is called the coefficient of compressibility of the packing. The consolidation ratio, $U$, increases from 0 to 1 during the process, while the hydrostatic pressure inside the bed dissipates from $\Delta P$ to 0 (we assume here that there is no flow; this restrictive assumption will be waived later).

The Terzaghi theory [16,24] makes the following assumptions: (1) the bed is homogeneous; (2) the bed is completely saturated with the mobile phase (no residual gas); (3) the compressibility of the mobile phase and of the particles are negli-

gible; (4) the compression and the flow are unidimensional and parallel; (5) Darcy's law [25] is valid; (6) the parameters considered are independent of the pressure.

In fact, all these assumptions are valid in the case of the packing of chromatographic columns. They are indeed better fulfilled than in the case of most sand deposits. Darcy's law gives the rate of change of volume of liquid under a pressure gradient as:

$$\frac{\partial V}{\partial t} = -\frac{kS}{\eta}\frac{\partial p}{\partial z} \tag{4}$$

where $V$ is the volume of fluid, $z$ the position, $k$ the column permeability, $p$ the local pressure, $S$ the cross-sectional area of the column, and $\eta$ the mobile-phase viscosity. It has been shown that Darcy's law is valid in a porous medium as long as the Reynolds number is lower than 1 [26]. Typical values of Reynolds numbers in liquid chromatography are lower than 0.01 [27].

As long as the bed is in the process of consolidation, the permeability is not constant along the column. We assume, however, that the bed remains radially homogeneous. We consider a slice of column of thickness dz. The flow-rates of the mobile phase entering and leaving the slice are, respectively:

$$F_{v,i} = \frac{k}{\eta}\left(-\frac{\partial p}{\partial z} + \frac{\partial^2 p}{\partial z^2}\frac{dz}{2}\right)S \tag{5a}$$

$$F_{v,o} = \frac{k}{\eta}\left(-\frac{\partial p}{\partial z} - \frac{\partial^2 p}{\partial z^2}\frac{dz}{2}\right)S \tag{5b}$$

where $k$ is the column permeability, as derived from Darcy's law at low flow-rates, $S$ is the cross-sectional area of the column, and $\eta$ is the mobile-phase viscosity. The difference is the volume which has left the slice during the consolidation process. It is also equal to the rate of change of this volume, thus:

$$-\frac{kS}{\eta}\frac{\partial^2 p}{\partial z^2} = \frac{\partial}{\partial t}\left(\frac{e}{1+e}S\,dz\right) \tag{6}$$

Because of the definition of $e$, the volume occupied by the particles in the slice is $Sdz/(1+e)$, and this volume remains constant. Hence, combination with Eq. 3 gives:

$$\frac{k}{\eta}\frac{\partial^2 p}{\partial z^2} = \frac{a_v}{1+e}\frac{\partial p}{\partial t} \tag{7a}$$

$$C_v\frac{\partial^2 p}{\partial z^2} = \frac{\partial p}{\partial t} \tag{7b}$$

with $C_v = k(1+e)/(a_v\eta)$. Eq. 7b describes the kinetics of bed consolidation in the presence of a liquid. This equation can be solved in closed form [16]. The solution depends on the value of the dimensionless time:

$$T = \frac{4C_v}{L^2}t \tag{8}$$

where $t$ is the time and $L$ is the length of the column, which is assumed to be drained at both ends, as is the case in liquid chromatography with an axial compression column if the entrance is left open (see Section 4). The variation of the column permeability during the consolidation is not taken into account, although it may not be negligible.

When the experiment is carried out under static conditions, with a constant initial pressure, $P_0$, and with no flow, an analytical solution of Eq. 7 is given by [16]:

$$p = \sum_{m=0}^{m=\infty}\frac{2P_0}{M}\left(\sin\frac{2Mz}{L}\right)e^{-M^2T} \tag{9}$$

where $P_0$ is the initial pressure of the liquid in the column, before the compression experiment begins, $m$ is an integer, and $M = (2m+1)\pi/2$. Then, under these same static conditions, the local consolidation ratio, $U_z$, is given by the equation:

$$U_z = 1 - \sum_{m=0}^{m=\infty}\frac{2}{M}\left(\sin\frac{2Mz}{L}\right)e^{-M^2T} \tag{10}$$

The average consolidation ratio for the entire column is given by:

$$\overline{U} = 1 - \sum_{m=0}^{m=\infty}\frac{2}{M^2}e^{-M^2T} \tag{11}$$

However, it is possible to show [16,24] that this equation applies also in the case of a linear

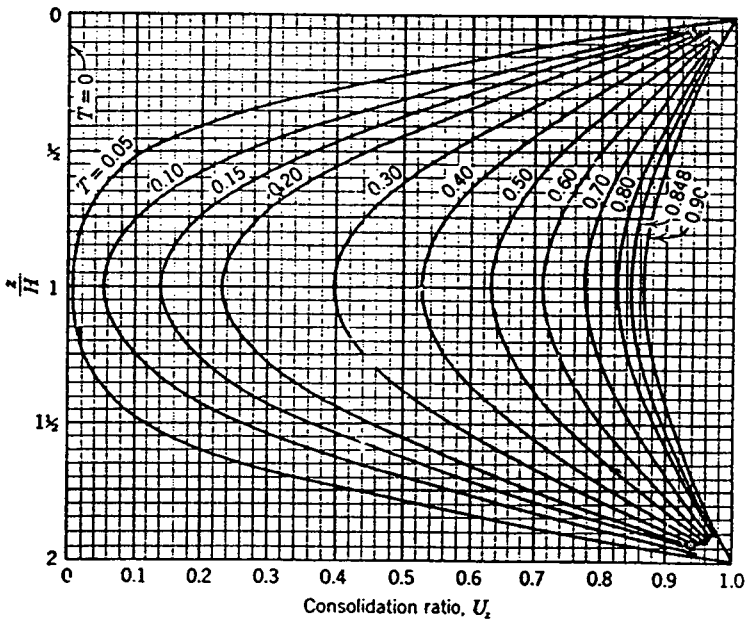


Fig. 4. Dependence of the local consolidation factor on time and on the position in the column. Reduced coordinates, see Eq. 7.

pressure gradient along the column, that is under the conventional conditions under which chromatographic columns are operated.

Fig. 4 illustrates the dependence of the local consolidation ratio as a function of time and position in the column, in the case of a constant pressure of the liquid in the column (i.e., under static compression of the bed). The column has a height equal to $2H$, is open for drainage at both ends and is supposed to have a diameter large compared to its length, so that friction of the packing against the wall has a negligible effect. Fig. 5 shows the variation of the average consolidation ratio as a function of time. This ratio increases rapidly with the dimensionless time, $T$. In the case of consolidation without flow (curve

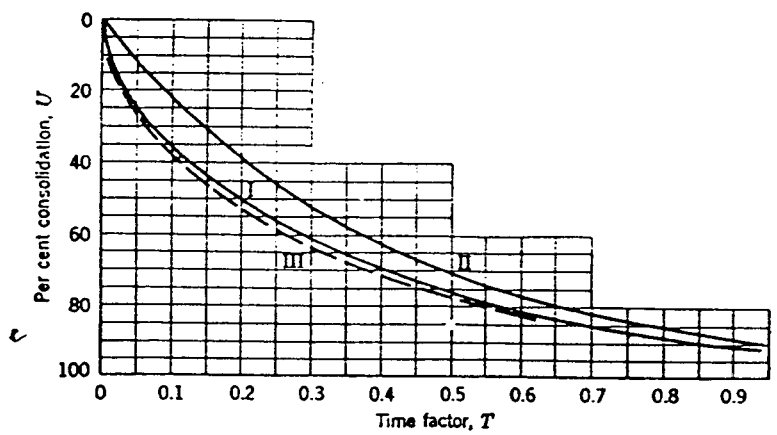


Fig. 5. Consolidation curve. Increase in the average consolidation factor of the column as a function of time. $T$ is given by Eq. 8.

I) is 50% after 0.2 $T$, 80% after 0.57 $T$, and 90% after 0.87 $T$. So, the value of $T$ is an important characteristic of packing materials for preparative chromatography. The other two curves in Fig. 5 correspond to consolidation in the presence of two different types of lateral stream of water percolating through the soil, a case of importance in soil mechanics but irrelevant in chromatography.

### 2.2. The time constant of consolidation

The value of the time constant of consolidation is given by Eq. 8. We need to translate the parameters involved in this equation into parameters which are more conventional in chromatography. The column permeability is given by the Blake–Kozeny eqation [26]

$$k = \frac{d_p^2 \epsilon_e^3}{h_0(\epsilon_i + \epsilon_e)(1 - \epsilon_e)^2} \tag{12}$$

where $d_p$ is the average particle diameter, $\epsilon_i$ is the internal porosity of the packing (or volume fraction of the column occupied by the stagnant mobile phase, inside the particles), and $h_0$ is a geometrical constant, usually of the order of 180, but which can vary from one packing material to the next and is probably somewhat smaller for spherical particles than for irregular ones. The void ratio, $e$, is the ratio of the volume available to the flowing mobile phase and the volume occupied by the particles, so:

$$e = \frac{\epsilon_e}{1 - \epsilon_e} \tag{13}$$

The compressibility coefficient, $a_v$, is also related to the external porosity:

$$a_v = -\frac{de}{dP} = \frac{-1}{(1 - \epsilon_e)^2} \frac{d\epsilon_e}{dP} \tag{14}$$

Accordingly, $T$ becomes:

$$T = \frac{4}{h_0} \frac{\epsilon_e^3}{(\epsilon_i + \epsilon_e)(1 - \epsilon_e)} \frac{-1}{d\epsilon_e/dP} \frac{d_p^2}{L^2} t \tag{15}$$

The parameter $h_0$ cannot be changed. There is little which can be done about the mobile-phase viscosity, as the solvent is selected for chromatographic reasons, to maximize the separation factor and to obtain a reasonable value of the retention. The values of the porosities in most packing materials are close and there is little we can do about them. The second factor of the RHS of Eq. 15 does not vary by a factor 2 in the entire range of packing materials available and of experimental conditions used, if we do not take into account the influence of the consolidation itself. There are few data available at present, if any, regarding the packing compressibility, $d\epsilon_e/dP$. So, the time scale in column compressibility is essentially controlled by the ratio $(L/d_p)^2 = N^2 h^2$, that is by the column efficiency required ($N$) and by the column quality ($h$). The last term in Eq. 15 may vary by orders of magnitude from one column to another. The most efficient columns will tend to consolidate much more slowly than the least efficient ones.

### 2.3. Limitation of the consolidation theory

The theoretical discussion presented in the previous two sections assumes that the time required for the consolidation to take place is essentially controlled by the flow of the liquid expelled from the packed bed. Any other contribution is neglected. In this work, we assume that the particles are elastic but rather rigid. Thus, each particle adjusts rapidly to the stress received from its neighbors. It may deform locally (elastically or not) or it can break, but it does it quickly; there is no plastic flow of the particles. This could be different for rigid resin-based particles which may flow somewhat before they eventually break. Soft gels would flow quickly and obstruct the interparticulate channels, which makes them unsuitable for preparative HPLC. Any delay in the consolidation must result from the time required for the particles to move around each other and, in so doing, to decrease the phase ratio. This time is called the plastic time lag.

In soil mechanics, two steps are recognized during the compression of a material. The primary compression is fast and controlled by the

permeability of the bed. The hydrostatic pressure falls to 0 at the end of the primary compression stage. During the secondary compression, the rate of compression is so slow that the escape of water takes place freely and the kinetics is controlled by plastic resistance. The plastic time lag is more important for clays than for sands but it could still be significant for packed beds, although actual binding can take place between packing particles. There is no information available at this time on this property. The plastic lag time depends on the energy of the particle–particle interactions. Thus, differences between the consolidation kinetics of irregular and spherical particles, if any were to be found, could be explained by a higher plastic time lag for the former, due to stronger interactions between its particles. Such differences could be explained also by the narrow size distribution of the particles used in chromatography. This distribution results in a much larger value of the interparticle porosity and a much larger average volume of the cavities between neighbor particles in columns than in sand beds.

Since there is no clay nor any colloidal material in packing materials for chromatography, it is easy to handle the same materials either dry or wet and to do so without affecting their integrity, something which is difficult for soils and present little interest in the applications of soil mechanics. Although the structure of a wet and a dry column are different, the study of the consolidation of dry-packing materials may provide some clues regarding the importance of this effect.

## 3. Experimental

### 3.1. Principle

Tests carried out in soil mechanics are done with samples between 2.5 and 5 cm thick and 10 cm wide, using successive pressure increments increasing by a factor 2 and starting from a rather low value of 1/8 kg/cm$^2$. We have modified these experimental conditions although the literature shows that they are required for reproducibility. As a matter of fact, what is required is the standardization of the determinations to permit valuable comparisons. We have carried out the experiments reported here with 15–25 cm long beds in a 5-cm diameter column. Thus, the results are not directly comparable to those obtained on sands. The main difference is in the much different aspect ratio ($L/d_c$), 3 to 3.5 in our experiments versus 0.5 in soil mechanics, a large difference because the distribution of stress inside the bed is different and depends on $L/d_c$. Also, we have used a larger initial pressure of 4 kg/cm$^2$ and larger pressure increments.

These changes present the advantage of giving a test which is more closely relevant to our purpose, the study of chromatographic beds under experimental conditions close to those used in the practical applications. Differences between experimental results obtained on large-size columns and those extrapolated from our data could be significant for columns having an aspect ratio lower than 2, but no information on this question is available yet. Further studies will involve measurements made with beds of different lengths [23].

### 3.2. Equipment

We used a dynamic axial compression column, 5.0 cm I.D. and 59 cm long (maximum), LC.50.VE.500.100 (Prochrom, Champigneulles, France). The piston is actuated by a hydraulic jack driven by an air compression pump from Haskel (Burbank, CA, USA). A pressure up to 100 bar may be applied to the packing material.

### 3.3. Packing material

Because the results presented here are preliminary, have been obtained with a single packing material, and are not clearly related to the chromatographic performance of the material under the conventional conditions used in preparative chromatography, it seems unfair at this stage to give the origin of the material used for the experiments. This information will be given later, with data regarding a number of other similar products of various origins [23]. The material used is a $C_{18}$ bonded silicagel, made of

irregular-shaped particles, with an average size between 15 and 20 $\mu$m and an average pore size of 100 Å. It was dried in a beaker for 12 h at 120° prior to use.

### 3.4. Procedures

During the following operations, the column length was monitored using a position sensor previously described [14]. The range of the sensor is approximately 0.8 cm, while the changes measured in the column length totaled approximately 6 cm. This required adjustments of the sensor position during the experiments.

*Dry compression*

An amount of 238 g of packing material was weighed and dried, then poured into the empty column with a funnel. Before closing the column top, the piston was brought slowly upward until the silica level reached the column rim. The burst of a few air bubbles on the top of the packing was observed during this process, illustrating clearly that pouring a powder in a vessel results in a low-density packing. After the piston had been stopped, the upper side of the column was tapped 20 to 30 times with the handle of a small hammer, which brought the level of the packing material slightly down. The piston was raised again and the operation repeated three times. Afterward, the top flange was closed, with its frit resting directly in contact with the top of the bed. The column was compressed at 4.1 bar, and then by increasing progressively the compression pressure to 69.7 bar. The initial column length was 24.38 cm, the final length 22.22 cm. At each new set pressure, the column length was monitored continuously until apparent stabilization, which usually took about 30 min, although may be quite insufficient some times (see later). Then, the new pressure was set.

*Decompression*

The design of the equipment does not permit to perform gradual decreases of the compression pressure. The leak of the hydraulic system is too small. The compression mechanism is switched to neutral, the new desired compression pressure is set, and the equipment is switched back on compression, at the new set value.

*Wetting a dry packing*

After completion of the compression and decompression experiments on the dry-packed bed, the mobile phase (methanol–water, 40:60, w/w) was introduced into the column at an axial compression of 73 bar. After about an hour and a half, the column length had decreased and stabilized again and the solution was replaced by pure methanol. Then, it was observed that, after a few minutes, air bubbles began to leave the column. Methanol–water mixtures below 50:50 do not wet chemically bonded silica, which explains the tardy gas expulsion. After a few hours, the column length had stabilized at 18.9 cm. Then, a series of determinations of the column efficiency were made, using nonretained acetone as the probe.

*Slurry compression*

An amount of 238 g of packing material was weighed and dried, then slurried in 900 ml of isopropanol. The slurry was poured into the column and left to sediment. The supernatant was collected periodically with a large syringe and the piston brought up slowly until the slurry level reached the top of the column. After 4 h, when a total of 300 ml of isopropanol had been collected, the top flange was closed, a graduated cylinder was connected to the column exit to collect the expelled solvent, and the axial compression was applied at 1 bar. The length of the column was measured manually and the displacement sensor set to follow the changes in the column length. The first compression step was to 4.1 bar. The pressure was then raised by a series of steps to a maximum of 73.8 bar, at which pressure crushing noises began to be heard. A total volume of liquid of 153.2 ml was collected. The initial column length was 27.3 cm, the final one 19.1 cm, corresponding to a volume reduction of 161.0 ml. The difference can be explained by evaporation loss during 4 h, error in the determination of the initial column length, and losses during the closing of the top flange.

The maximum pressure during recompression

was 77.9 bar. After the end of the experiments, the column was washed with fresh methanol and equilibrated for a few hours in closed circuit. Its efficiency was then measured using acetone, with a compression pressure of 57.4 bar, at a length of 18.9 cm.

## 4. Results and discussion

### 4.1. Consolidation of a dry bed of packing material

Fig. 2 shows a typical example of the consolidation kinetics obtained with the dry-packing material. The column had been previously stabilized at 8.2 bar for 30 min. After 2 min in the experiment, the pressure was raised to 16.4 bar. The column length decreased initially very rapidly, then much more slowly. In this case, it was completely stabilized after 30 min. Similar results were obtained at all compression pressures.

Fig. 6 shows the plot of the column length after stabilization versus the compression pressure (circles). Consolidation progresses with increasing compression pressure and appears to tend toward a limit which is nearly reached at 70 bar, when the column length has decreased by approximately 10% from its initial value. These experiments are long when high compression pressures are applied and it is difficult to make sure that equilibrium is reached. An experiment to measure the extent of rebound at decompression was started after the reading at a compression pressure of 69.7 bar (highest stress in Fig. 6). This was done by releasing the gas pressure in the Haskel pump (see Section 3). However, the leakage of the hydraulic system was so low that the pressure had not decreased significantly after 6 h. The column length had decreased from 22.22 to 22.19 cm. However, the following morning, after 16 h, the pressure had decreased to 57.4 bar and the column length to 21.9 cm. Then, the decompression procedure described in Section 3 was used. This explains the jump between the last compression point (Fig. 6, circle) and the first decompression data point (Fig. 6, dot). The variation of the column length with the compression pressure upon column decompression is also shown in Fig. 6. It is practically insignificant. The rebound is from 21.9 to 22.03 cm, i.e., less than ca. 0.6%.

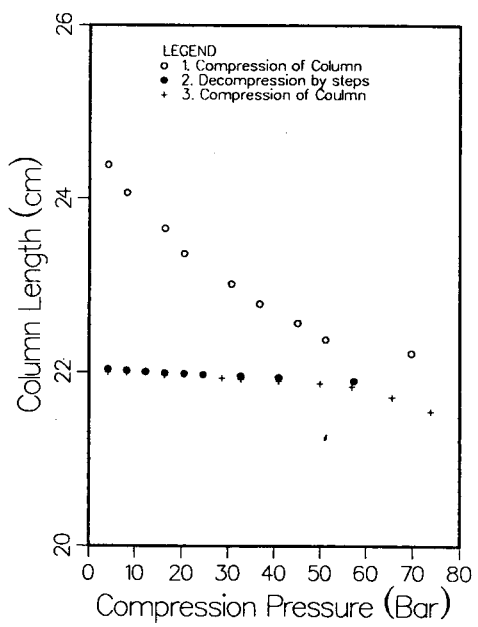


Fig. 6. Compression (O), decompression (●), and recompression ( + ) curves of the dry-packing material.

The recompression of the packing after decompression does not result in a significant decrease in the column volume up to 60 bar. At higher pressures, however, the column length decreases again and is reduced to 21.55 cm after recompression up to 73.8 bar. The fact that recompression from 0 to 60 bar shows no change in the column length demonstrates that the bed was completely consolidated at a pressure of 60 bar when it was decompressed. However, consolidation would certainly progress further at higher pressures, as the following results will show. Experiments cannot be carried out at pressures above 75 bar without crushing the particles.

Fig. 1 includes the compression diagram of the dry-packing material (solid line). This diagram has been derived from the data in Fig. 6, assuming an external porosity equal to 0.42 for the bed at the beginning of the compression.

This value is somewhat arbitrary, although consistent with results obtained with other dry-particle beds [9,10,26]; however, we have checked that changes in this initial value of the porosity between 0.40 and 0.43 have negligible effects on our conclusions (with only minor changes in the values of the empirical parameters derived from the data). We also assume that the volume of the particles remains unchanged, hence the volume of solid and the pore volumes remain constant. In other words, we assume that the consolidation reduces only the external porosity. The compression diagram of the dry packing shown in Fig. 1 (solid line) shows that, except for the first one, slightly low, the data points exhibit a linear relationship, in agreement with Eq. 1. The coefficient $a_v$ calculated from the slope of the least-squares straight line is equal to 0.13.

Fig. 7 shows a plot of the external porosity, calculated using the same data, versus the pressure. A satisfactory linear relationship is found, except for the first data point, which deviates slightly, and the last one, which is markedly off. The slope of the least-squares straight line for the central 7 data points gives a value of $d\epsilon_e/dP$ equal to $-1.0 \cdot 10^{-3}$ bar$^{-1}$. Introduction of this value in Eq. 15, with an average external porosity of 0.39, an internal porosity of 0.355, $h_0 = 180$, gives for a 25-cm long column packed with 15-$\mu$m particles, a reduced time, $T$, equal to 0.0104 $t$ (s). In this case, the consolidation of the packing should be rapid, taking less than 100 s. With a 50-cm long column, packed with 5-$\mu$m particles, the time constant becomes almost 1 h (3500 s), still not unreasonably long. Note, however, that the consolidation of the packing of a chromatographic column is not instantaneous, even under dynamic compression.

### 4.2. Wetting a bed of dry packing

Introduction of a stream of a methanol–water solution (40:60, w/w) results in an immediate contraction of the packing, by about 1.4% (from

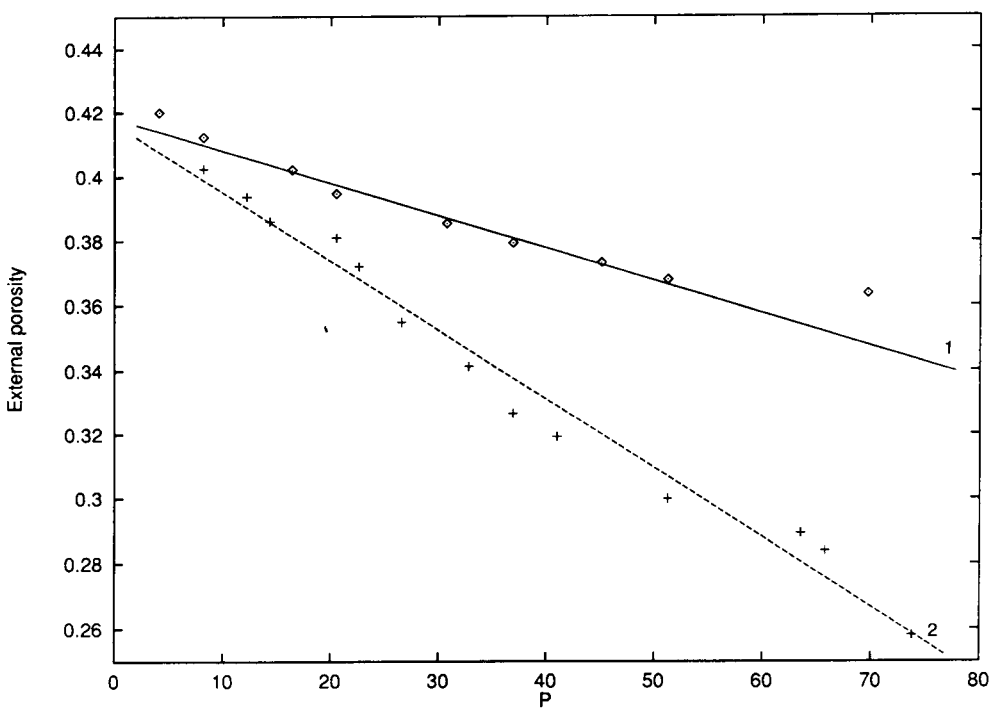


Fig. 7. Plot of the external porosity of the column bed versus the compression pressure: 1 = compression of the dry packing (◇); 2 = compression of the wet packing (+).

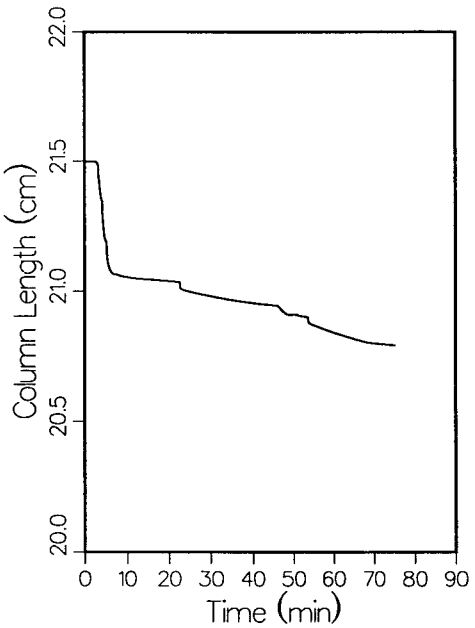


Fig. 8. Shrinking of a bed of dry packing material when wetted by a 40:60 (w/w) methanol–water solution.

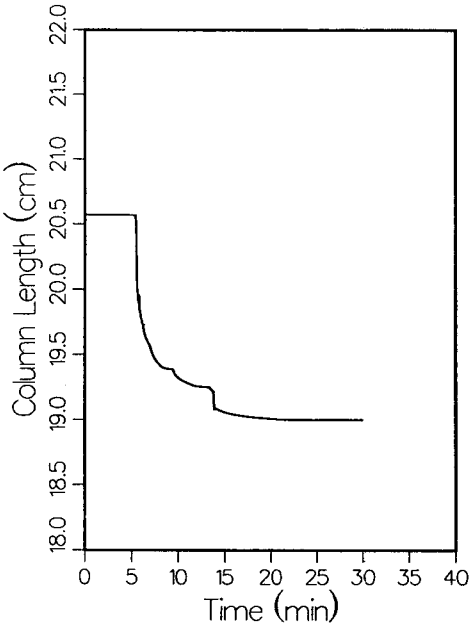


Fig. 9. Shrinking of a bed of packing material wetted by a 40:60 methanol–water solution when this solution is replaced by pure methanol.

21.50 to 21.19 cm), followed by a further, slow decrease in the column length. The data obtained are shown in Fig. 8. The recording was stopped after 82 min, the sensor being at the end of its range and having to be adjusted. After this adjustment, the column length shrank by an additional 1% after another hour (not shown).

Finally, pure methanol was introduced (Fig. 9). The column shrank again rapidly, by more than 5% in the first 7 min. Gas bubbles were observed in the exit stream. After 30 min the column length has decreased by a total of 1.57 cm since liquid began to be introduced into it. The initial column length (24.6 cm) has been reduced to 19.0 cm at the end of the series of experiments. This loss of nearly a quarter has been achieved at constant mass of packing and, practically, at constant total volume of the particles. The loss is due to a decrease of the sole external porosity. The granulometric analysis done on samples of packing material taken from the region close to the wall and the piston, where the stress is highest in an axial compression column, shows that breakage has taken place but to a limited extent [23].

### 4.3. Column efficiency, dry-packed column

The column efficiency was measured, as a function of the mobile-phase velocity, after the series of experiments described above was completed. The results are shown in Fig. 10. The efficiency is very poor, reminiscent of what was obtained in preparative gas chromatography columns which had to be dry-packed [28]. The simple pouring technique used here resulted in reduced efficiencies of the order of 50 or larger [8,9,28]. It is important to report that the values found initially were still worse and that, after a few hours, the efficiency improved, particularly at high flow-rates, the slope of the slanted asymptote decreased, as if some local reorganization, with minimum change in volume, had taken place under the influence of the continu-

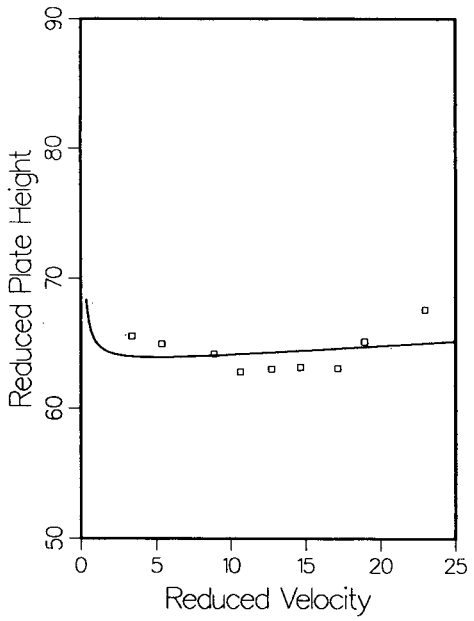


Fig. 10. Efficiency of the consolidated dry column after wetting by pure methanol. Solute: acetone (nonretained).

ous stream of eluent. No change in the column length was observed, however.

We explain the poor column efficiency under these experimental conditions (the reduced plate height is around 65) by particle size discrimination across the column, a well-known effect which accompanies dry packing in nearly all cases [8,9,28]. This effect has often been reported and is strongly documented [8,9]. The abundant literature [28] on the packing technology of gas chromatographic columns provides further justifications. For this reason and because of the profound difference in the behavior of wet and dry packing under compression, work was not pursued on this issue and efforts were shifted to the study of the consolidation of beds obtained by the more conventional slurry method. However, because some, who ignore the troubles encountered by a past generation, may be attracted by the idea of resuscitating the old dry-packing technique, we felt it appropriate to report the results obtained and to point out the poor efficiency achieved.

### *4.4. Consolidation of a bed of wet-packing material*

While the data recorded for the consolidation kinetics of a wet packing at low or moderate compression pressure tend to be like that shown in Fig. 2 for a dry bed, a different behavior is observed at high pressures, when the bed has already lost a significant fraction of its interparticle void volume. Fig. 11 shows a typical consolidation curve obtained at high pressures. While the plots of the extent of consolidation versus time are different for the dry (Fig. 2) and the wet (Fig. 11) packing, the latter are quite similar to the plots illustrating the consolidation kinetics during the wetting of the column packing (Figs. 8 and 9). The presence of a liquid seems necessary for the abrupt collapses observed (Figs. 8, 9 and 11) to take place. Like for some other features of the consolidation curves, it is difficult at this stage to determine which ones are general and to be found in the consolidation of all packing materials and which ones are specific of the

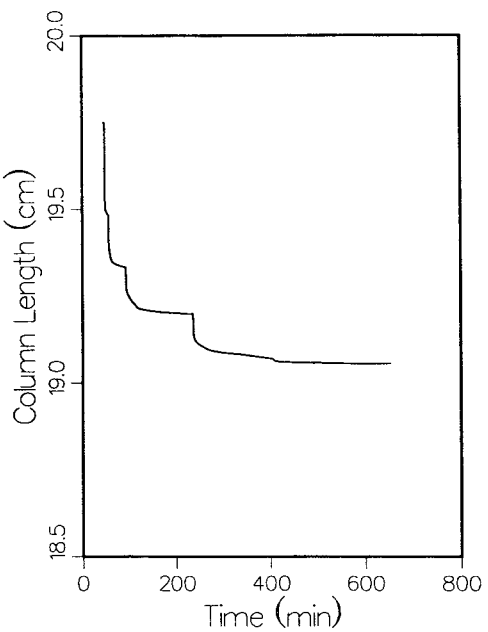


Fig. 11. Consolidation kinetics under isobar conditions of the wet-packing material after compression from 65 to 74 bar.

material used here. At any compression pressure, the degree of consolidation achieved in wet compression is higher than in dry compression. This may be due to a reduction in the interparticle interaction energy caused by the presence of the solvent. We have seen in the study of dry packing that the dielectric constant or the dipole moment of the solvent is less critical to explain consolidation than the wettability, since methanol induces a stronger increase in packing density than water–methanol mixtures. This conclusion, however, does not necessarily extend to the consolidation of beds of silica particles.

The unexpected result is certainly the random character of the process. Catastrophic events, in the probable form of avalanches inside the packed bed, take place for no apparent reasons. They occur after long periods, up to several hours. This phenomenon may explain the formation of holes at the beginning of columns after a certain time during which satisfactory performance is recorded. At the end of the experiment illustrated in Fig. 11, the column was whipped 20 times with a rubber vacuum hose to no effect[1]. It seems that total consolidation had been achieved at the operating pressure. Nevertheless, this phenomenon slows down considerably the kinetics of consolidation of the packing compared to what is predicted by the Terzaghi theory [16,24]. For irregular-shaped particles at least, the frictional lag to consolidation causes a much more serious problem than the hydrodynamic lag.

Fig. 12 shows the plot of the column length as a function of the compression pressure. The curve obtained is qualitatively similar to the one recorded during dry packing. However, the quantitative differences are important. The same amount of packing was used in both experiments (238 g). Within 0.1 cm, the same final length was obtained at nearly the same compression pressure. However, dry packing itself could not

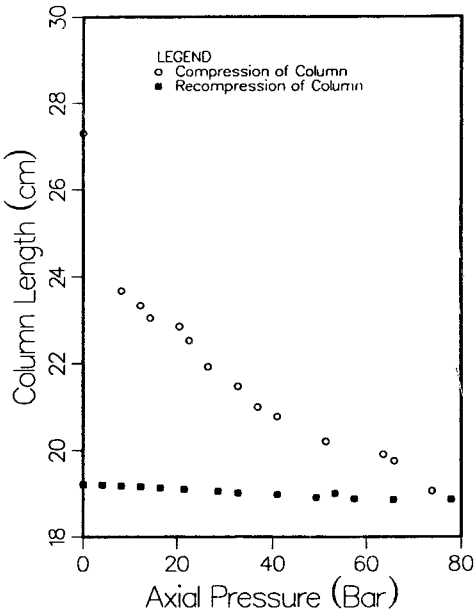


Fig. 12. Compression (O) and decompression (■) curves of the wet-packing material.

reduce the column length by more than ca. 10% and the final consolidation is achieved by percolating methanol through the bed. By contrast, wet packing reduces the column length directly to 19.06 cm, corresponding to a final density of 0.636 g/ml. The same density cannot be achieved with dry packing unless the bed is wet with methanol afterward, in which case the same packing density is achieved. The decompression curves are nearly identical for dry and wet packing. With the wet-packed bed, recompression up to 80 bar gives a curve which overlays the decompression curve, showing that the phenomenon involved is limited to elastic deformation of the particles and of the bed structure. The bed has been completely consolidated at 80 bar.

The compression diagram of the wet column is shown also in Fig. 1 (dotted lines). Surprisingly, the data points are not correctly fitted by one single straight line but rather by three different ones. At low pressures, up to approximately 20 bar, the data points are on a line which is much

[1] Whipping the column was an attempt at rapidly triggering a collapse of local instabilities of the packing. It is not suggested as a reliable procedure to improve the quality of the column packing.

less steep than the one observed for dry packing, with a slope $a_v = 0.062$ (versus 0.132 for dry packing). The intermediate points are on a line with a slope $a_v = 0.20$, slightly steeper than the dry-packing points, and the last three points, above 63 bar, on a steep line of slope $a_v = 0.47$. The first stage involves mere slippage of the particles over each other, leading to a closer packing [20]. Rapidly, the particles become too close to each other to move easily, which limits the process. It gives place to the second stage of consolidation, the formation of temporary vaults protecting small voids. These vaults are compressed, deformed and give way by abrupt slippage or breakage of the keystone. The second break of the plot (at ca. 63 bar) corresponds to the onset of the third mechanism of consolidation, particle breakage. This explanation is in agreement with the independent observation that crushing noises are heard around 65 bar with this material. A similar broken-line plot has been reported in the compression of particles into pellets (e.g., drug tablets) [20]. It has been given the same explanation. The two break points observed in the compaction of magnesium carbonate (particle size, 200–240 mesh, B.S.) took place at 13 and 70 bar, respectively [20]. These values are very close to those found in this work. All the data points have been determined after waiting for hours, which largely exceed the time constant of the compression (see below). We have yet no satisfactory explanation for the different behavior of beds obtained by dry- and wet-packing techniques under compression. The phenomenon is under investigation.

It remains possible, however, that we are attempting to overinterpret the results. The plot of the external porosity versus the pressure in Fig. 7 shows a straight line with a slope of $-2.1 \cdot 10^{-3}$ bar$^{-1}$. The scatter of the data points is expected, given the small variations of the porosity measured. However, the trend is clear. The value of $d\epsilon_e/dP$ being twice as large as for the dry compression, the time constant of compression would be double. This time remains negligible in practice, except for columns having an unusually high efficiency. The need to wait an indeterminate period of time for the relaxation of the bed instabilities (see Fig. 10) remains the controlling factor in the consolidation of column beds.

The packing density can easily be derived from our results. A plot of the packing density versus the compression pressure (not shown) is very well approximated by a straight line of equation $Pd = 0.500 + 0.00184P$, where $Pd$ is the packing density. This relationship permits a rapid calculation of the apparent pressure of consolidation of a column bed when knowing its packing density. This parameter is an indication of the bed stability.

### 4.5. Column efficiency, wet-packed column

The results obtained are shown in Fig. 13. They are much better than with the dry-packed column since the minimum reduced HETP is 6. Much better results ($h_{min}$ around 3) are obtained routinely with a more conventional slurry-packing technique than the one used here [14]. This is probably in connection with the observation that fast compression of the slurry tends to give

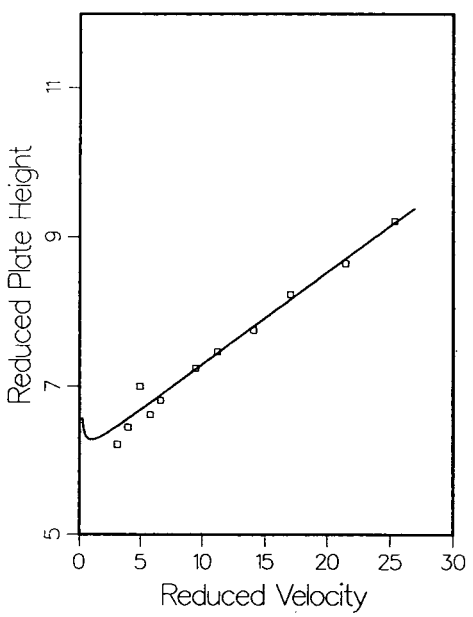


Fig. 13. Efficiency of the consolidated column after wet compression of the packing. Solute: acetone (nonretained).

better efficiencies than slow compression. There are, however, many reports in the literature that sedimentation gives highly efficient but unstable columns (e.g., Ref. [11]). The sedimentation step in our slurry-packing procedure does not let the slurry undisturbed for the whole operation, which may explain the fair efficiency of the column.

## 5. Conclusion

The results obtained are in excellent agreement with the predictions derived from soil mechanics and demonstrate the considerable uncertainty surrounding the concept of packing density. The dry-packed column contains 238 g of silica material. If we assume an approximate density of silica of 2.21, this weight corresponds to a total volume of solid of 107.7 ml. Initially, the dry bed has a length of 24.9 cm, hence a volume of 488.9 ml, a packing density of 0.487, and a total porosity of 0.778, taken at 0.78 in the following, approximate calculations. Estimating the external porosity at 42% gives an internal porosity of 0.36 and a total pore volume of 176 ml. The final column length is 19.1 cm, hence the packing volume is 375.0 ml, the packing density is now 0.635. Assuming that the volume occupied by the pores and by the solid have remained constant (i.e., assuming that the particles are not compressible to any significant extent), the volume left for the external porosity is 87.4 ml, giving an external porosity of 0.24, an extremely low value, which is comparable to that of compressed sands. This value is slightly lower than the one obtained by wet packing at the same compression pressure.

A packing density of 0.547 g/cm$^3$ was found for an analytical column packed with the same material as the one used here. Using the relationship given previously between the packing density and the compression pressure, we find that this analytical column was consolidated at 25.5 bar only. Both the value of the consolidation pressure and that of the packing density are rather low. It would not be surprising in such a case that some additional consolidation takes place slowly, during operation of the column. An increase of the packing density by up to 10% could easily occur, with a correlative decrease of 10% in the column length. The formation of a void of such a magnitude at the column inlet would cause a dramatic loss of efficiency. The phenomenon could come at any time, or could possibly be triggered by a minor shock to the column.

Further work is in progress to unravel the intricacies of the relationships between the structure of the column bed and the performance of the column. The behavior of different packing materials used in preparative chromatography will be investigated and the results obtained with materials with different shapes (spherical vs. irregular), average size, and average pore size diameter (which may affect breakage resistance) [23]. So will be the homogeneity of the column packing in the radial and the axial directions. The distribution of stress in a compressed bed of particles is certainly not homogeneous as is the distribution of the hydrostatic pressure. This is demonstrated by the obvious differences in packing densities between the two ends of a column. Accordingly, it is highly probable that the column packing density is not homogeneous either, whether in the axial or the radial direction. The uneven consolidation of the packing in a column provides a source of explanation for the chromatographic phenomena observed by others [1–4,6,7].

It may seem surprising that a research field as extensively investigated in the past as the behavior of packing materials for liquid chromatography still contains nearly unexplored areas. This might be interpreted as meaning that the knowledge accumulated so far on this issue is sufficient for our needs. A proof that this conclusion is not correct has been recently given by the investigation of the behavior of chromatographic bands by NMR Imaging [11]. While the minimum reduced HETP of the column measured with a conventional UV detector was between 2.1 (first measurements) and 5 (after several experiments had degraded its performance), the same HETP measured from the local thickness of the band seen inside the column by the NMR

imager was 1.0, although injection had to be done with a 150-cm long, 0.8 mm I.D. connecting tube to place the column far enough from the instrument magnet. We should never forget that there is no theoretical lower limit to the column reduced HETP, although the opposite is widely believed. Long ago, Giddings [29] has reported a reduced HETP well below 1 in gas chromatography, for a column packed with glass beads covered with a thin layer of liquid as the stationary phase. It should be possible to achieve routinely an efficiency in that range. However, we are of the opinion that we can never approach that goal without a much more profound knowledge of the properties of consolidated beds of packing materials.

**Acknowledgements**

We acknowledge fruitful discussions with Jean Salençon and Luc Dormieux (Laboratoire de Mécanique des Solides, Ecole Polytechnique, Paris) and with A.M. Katti (Malinckrodt Chemical Co., St-Louis, MO, USA). This work was supported in part by the cooperative agreement between the University of Tennessee and the Oak Ridge National Laboratory. GG thanks the Alexander von Humboldt Stifftung (Bonn, Germany) for a research award allowing his stay in the Institut für Organische Chemie of the University of Tübingen, Germany, where this work was conceived.

**List of symbols**

| | |
|---|---|
| $\Delta P = P_2 - P_1$ | Compressibility coefficient. |
| $C_c$ | Numerical coefficient. |
| $C_v$ | Coefficient of consolidation. |
| $d_c$ | Column diameter. |
| $d_p$ | Average particle diameter. |
| $e$ | Void volume fraction (volume available to the mobile phase around the particles). |
| $e_0$ | Void volume at the reference pressure ($p_0$). |
| $e_1$ | Initial void ratio |
| $e_2$ | Final void ratio. |
| $h_0$ | Constant in the Blake–Kozeny equation. |
| $k$ | Permeability of the packing. |
| $L$ | Column length. |
| $P$ | Compression pressure. |
| $P_1$ | Initial value of the compression pressure. |
| $P_2$ | Final value of the compression pressure. |
| $p$ | Pressure. |
| $p_0$ | Reference pressure (usually the atmospheric pressure). |
| $S$ | Cross-sectional area of the column. |
| $T$ | Dimensionless time, $T = 4C_v t/L^2$, Eq. 8. |
| $t$ | Time. |
| $U$ | Consolidation ratio. |
| $V$ | Volume of fluid. |
| $z$ | Position along the column. |
| $\Delta P = P_2 - P_1$ | Excess pressure applied to the liquid. |
| $\epsilon_e$ | External, interparticular, or interstitial porosity. |
| $\epsilon_i$ | Internal porosity or porosity of the particles. |
| $\eta$ | Mobile phase viscosity. |

**References**

[1] J.H. Knox and J.F. Parcher, Anal. Chem., 41 (1969) 1599.
[2] J.H. Knox, G.R. Laird and P.A. Raven, J. Chromatogr., 122 (1976) 129.
[3] D.S. Horne, J.H. Knox and L. McLaren, Sep. Sci., 1 (1966) 531.
[4] C. Eon, J. Chromatogr., 149 (1978) 29.
[5] J.N. Little, R.L. Cohen, J.A. Pendergast and P.D. McDonald, J. Chromatogr., 126 (1976) 439.
[6] J.E. Baur, E.W. Kristensen and R.M. Wightman, Anal. Chem., 60 (1988) 2338.
[7] T. Farkas, J.Q. Chambers and G. Guiochon, J. Chromatogr. A, 679 (1994) 231.
[8] J.C. Giddings and E.N. Fuller, J. Chromatogr., 7 (1962) 255.
[9] F.H. Huyten, W. van Beersum and G.W.A. Rijnders, in R.P.W. Scott (Editor), Gas Chromatography, Butterworths, London, 1960, p. 224.

[10] C.E. Schwartz and J.M. Smith, Ind. Eng. Chem., 45 (1953) 1209.
[11] U. Tallarek, E. Baumeister, K. Albert, E. Bayer and G. Guiochon, J. Chromatogr. A, 696 (1995) 1.
[12] A.M. Katti, M. Czok and G. Guiochon, J. Chromatogr., 556 (1991) 205.
[13] H. Guan and G. Guiochon, J. Chromatogr. A, 687 (1994) 179.
[14] M. Sarker and G. Guiochon, J. Chromatogr. A, 683 (1994) 293.
[15] M. Sarker and G. Guiochon, J. Chromatogr. A, (1995) in press.
[16] D.W. Taylor, Fundamentals of Soil Mechanics, Wiley, New York, NY, 1948.
[17] G.K. Sofer and L.E. Nystrom, Process Chromatography–A Practical Guide, Harcourt Brace Jovanovich, Sidkup, UK, 1989.
[18] S. Golshan-Shirazi and G. Guiochon, J. Chromatogr., 511 (1990) 402.
[19] G. Guiochon, in preparation.
[20] D. Train, J. Pharm. Pharmacol., 8 (1956) 745.
[21] H. Eyring, Anal. Chem., 20 (1948) 98.
[22] D.R. Absolom and R.A. Barford, Anal. Chem., 60 (1988) 2120.
[23] M. Sarker, A.M. Katti and G. Guiochon, in preparation.
[24] K. Terzaghi, Erdbaumechanik auf Bodenphysikalischer Grundlage, Deuticke, Leipzig, 1925, Section 20.
[25] H. Darcy, Les Fontaines Publiques de la Ville de Dijon, Dijon, 1856.
[26] R.B. Bird, W.E. Stewart and E.N. Lightfoot, Transport Phenomena, Wiley, New York, NY, 1960.
[27] E. Baumeister, U. Klose, K. Albert, E. Bayer and G. Guiochon, J. Chromatogr. A, 694 (1995) 321.
[28] A. Zlatkis and V. Pretorius, Preparative Gas Chromatography, Interscience, New York, NY, 1971.
[29] J.C. Giddings and R.A. Robinson, Anal. Chem., 34 (1962) 885.

ELSEVIER

Journal of Chromatography A, 704 (1995) 269–277

JOURNAL OF CHROMATOGRAPHY A

# Naproxen-derived segmented and sidechain-modified polysiloxanes as chiral stationary phases

William H. Pirkle*, Gerald J. Terfloth

*School of Chemical Sciences, University of Illinois, Urbana, IL 61801, USA*

First received 7 September 1994; revised manuscript received 13 February 1995; accepted 17 February 1995

**Abstract**

The preparation of a series of polysiloxane-based chiral stationary phases (CSPs) derived from (*S*)-naproxen diallyl amide is described. Two types of chiral polysiloxanes have been synthesized. Segmented polymers were obtained by double hydrosilylation of the diallyl amide with difunctional oligomethylhydrosiloxanes. The latter are obtained by a linear homologation strategy, thus allowing systematic variation of the spacing of the chiral selectors along the polymer chain. This spacing clearly affects chromatographic behavior, for increased spacing decreases retention even when the total amount of chiral selector present is unaltered. Alternatively, chiral polysiloxanes were prepared by adding, through hydrosilylation, the diallyl amide as pendent sidechains to a polymethylhydrosiloxane. The resulting polymers were coated on silica gel, packed into HPLC columns and evaluated using normal and reversed-phase conditions. Comparison of the performance of both types of chiral polysiloxane-based CSPs shows them to afford less retention and comparable or higher enantioselectivity than does the corresponding brush-type CSP.

## 1. Introduction

Chiral biopolymers have found extensive usage as chiral stationary-phase (CSP) components. In many instances, how the biopolymer is deposited (or immobilized) greatly influences the performance of the CSP [1]. This behavior, also noted for some chiral synthetic polymers, occurs when the secondary and tertiary structure of the polymer is largely responsible for its ability to discriminate between the enantiomers of analytes. In contrast, the chiral selectors developed for brush-type CSPs largely function independently of their neighbors, a feature which greatly facilitates the understanding of their modes of action. Since the introduction of Chirasil-Val [2], it has been clear that polysiloxane-based CSPs have much to offer in terms of desirable chromatographic properties. Accordingly, the incorporation of effective "brush-type" chiral selectors into polysiloxane-based CSPs was deemed to be a fruitful field of study.

Initial studies in which brush-type chiral selectors of proven ability were incorporated into polysiloxane-based CSPs suggested that it is selector structure and not the secondary or tertiary structure of the polymer which is largely responsible for the enantiodiscrimination abilities of the CSP [3–5]. This is clearly an advantage in terms of understanding the details of the operative chiral recognition processes, something which augers well for the develop-

* Corresponding author.

0021-9673/95/$09.50 
*SSDI* 0021-9673(95)00223-5

ment of still better chiral selectors. Polysiloxane CSPs have several additional advantages. For example, the polymers may be prepared reproducibly on large scale, thus leading to greater batch-to-batch column uniformity [6–11]. As with brush-type CSPs, the structure of the chiral selectors is completely controllable. Additionally, while the mass transfer characteristics of polymeric CSPs often cause them to have lower chromatographic efficiencies than brush-type CSPs, this is not the case for the polysiloxane CSPs, presumably because of their nonpolar backbones. Finally, the thickness of the polymeric layer coated onto the support can be controlled. Residual silanol groups are detrimental to the performance of CSPs, hence the need to end-cap to lessen the effect of these groups. In the case of silica, the polysiloxanes appear to blanket residual silanol groups since end-capping produces little effect. In some circumstances, the spacing between strands of bonded phase influences the ability of brush-type CSPs to differentiate between enantiomers. These interstrand spacings are not yet controllable for brush-type CSPs. However, the spacings between selectors along a polymeric backbone are potentially controllable [8–11]. Hence, the effect of this variable in the primary structure of a polymeric CSP is one to be studied. The chiral polysiloxanes which might evolve from such studies are potentially useful as physically and chemically stable coatings for porous and nonporous supports which can be used as CSPs in GC, SFC, CE, and HPLC.

In this paper, we report the design, synthesis, and evaluation of CSPs based on segmented and sidechain-modified polysiloxanes. A series of ABAB-type copolymers of (*S*)-naproxen diallyl amide [12] and difunctional oligomethylhydrosiloxanes were prepared by hydrosilylation of the former by the latter using hexachloroplatinic acid as a catalyst. Sidechain-modified chiral polysiloxanes were obtained by similarly attaching the chiral selector to a polymethylhydrosiloxane containing 10 mol% Si–H groups. The resulting polymers were chemically bonded to silica gels of different pore size by thermal treatment. The chromatographic performance of these CSPs, studied by HPLC using normal-phase and reversed-phase conditions, is compared to that of the brush-type phase derived from the same chiral selector.

## 2. Experimental

Chromatography was carried out on a system consisting of an Alcott 760 HPLC pump equipped with a Rheodyne 7125 injector (20-$\mu$l sample loop) and a Milton Roy UV monitor D fixed-wavelength (254 nm) detector. Data was collected using a HP3394A recording integrator. The columns were immersed in a constant temperature bath. Tri-*tert.*-butylbenzene and sodium iodide were used as void volume markers. The analytes were available from prior studies [12,13].

China clay and hexachloroplatinic acid were purchased from Aldrich (Milwaukee, WI, USA). All other silicon reagents were obtained from Petrarch Systems (Bristol, MA, USA). Silica (Rexchrom 300 Å, 5 $\mu$m, and 100 Å, 5 $\mu$m) was provided by Regis Technologies (Morton Grove, IL, USA). LiChrospher Si 1000, 10 $\mu$m, and Si 4000, 10 $\mu$m, was from EM Science (Gibbstown, NJ, USA) as were the solvents used for HPLC analyses. (*S*)-Naproxen diallyl amide [12], the difunctional oligomethylhydrosiloxanes [14], and polymethylhydrosiloxane [5], were available from prior studies or were prepared using literature procedures.

### 2.1. Preparation of 1,1,3,3,5,5,7,7,9,9,11,11-dodecamethylhexasiloxane ($^{H}MD_4M^{H}$)

The described procedure is typical for the linear homologation of cyclosiloxanes. Following the reported procedure [14], 48.0 g (0.5 mol) of dimethylchlorosilane were added at room temperature to a slurry of 50.0 g (0.17 mol) octamethyltetrasiloxane, 30.4 g (0.169 mol) of water, and 5.0 g of silica gel over 2 h. After 4 h, the silica gel was removed by filtration and volatile byproducts were removed from the filtrate by rotary evaporation. The residue was diluted with 50 ml of benzene and, after separation of the

phases, the upper layer was washed sequentially with 50 ml of water, 50 ml of 1% sodium hydrogencarbonate solution (twice), and 50 ml of water (twice). The organic phase was dried over sodium sulfate and evaporated to afford a colorless liquid which was purified by vacuum distillation (bp 81°C, 0.1 torr) to give 10.9 g (29.2% based on consumed octamethyltetrasiloxane) of $^{H}MD_4M^{H}$.

### 2.2. Dimethyl-hydromethyl siloxane copolymer (10 mol% Si–H groups) [5]

To a slurry of 0.7 g of china clay in a mixture of 4.54 g (2.0 mmol, 68.0 mmol SiH) polymethylhydrosiloxane (PS 120) and 45.38 g (153 mmol) octamethylcyclotetrasiloxane was added 0.2 μl of 36 *M* sulfuric acid. The suspension was heated to 70°C under a nitrogen atmosphere for 24 h. The mixture was cooled and 150 ml of diethyl ether was added. The china clay was removed by suction filtration and the filtrate was washed with water until neutral. The ethereal solution was dried over, then decanted from, sodium sulfate and concentrated to leave a colorless viscous liquid which was vacuum distilled to remove residual octamethylcyclotetrasiloxane. The copolymer (33.75 g; 67.7%) remained as a highly viscous residue.

### 2.3. General procedure for the preparation of sidechain-modified polymethylsiloxanes

A typical synthetic method is given for a (*S*)-naproxen diallyl amide (2, see Fig. 1) modified polymer. (*S*)-Naproxen diallyl amide (2, 336 mg, 1.09 mmol), polymethylhydrosiloxane (1.0 g, 1.36 mmol SiH), and 100 ml of dry toluene were heated to 70°C under a nitrogen atmosphere. Then 50 μl of 1% hexachloroplatinic acid in tetrahydrofuran were added. After one hour, the temperature was lowered to 55°C and the mixture was stirred for 72 h. Evaporation of the solvent was followed by addition of 20 ml of dichloromethane, 20 ml of methanol, and 10 ml of water. The mixture was stirred thoroughly and the water–methanol layer was removed. This process was repeated three times. The remaining dichloromethane solution was concentrated and the residue was dried under vacuum at 50°C to give 1.30 g (97%) of the chiral polymer. The proton NMR spectrum is consistent with the anti-Markovnikov addition of the silane to the double bond.

### 2.4. General procedure for the preparation of diene–oligosiloxane copolymers

The same synthetic method as described for the preparation of sidechain-modified polymethylsiloxanes was used. A typical reaction is described for the copolymer of (*S*)-naproxen diallyl amide with 1,1,3,3,5,5,7,7,8,8,11,11-dodecamethylhexasiloxane. (*S*)-Naproxen diallyl amide (2, 309 mg, 1.0 mmol), 1,1,3,3,5,5,7,7,8,8,11,11-dodecamethylhexasiloxane (370 mg, 1.0 mmol), and 50 ml of toluene were treated with 50 μl of 1% hexachloroplatinic acid in tetrahydrofuran, as described above, to give 314.5 mg (85%) of the copolymer. The proton NMR of the copolymer does not show a resonance for Si–H protons.

### 2.5. Preparation of the CSPs

Brush-type phases (CSPs 7 and 8) were prepared as described in [12] by bonding of the organosilane to silica gel (CSP 7: 100 Å pore size, 5 μm diameter; CSP 8: 300 Å, 5 μm). Segmented and sidechain-modified polysiloxane

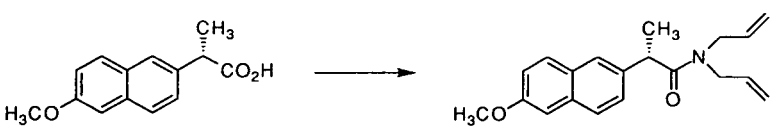


1 2

Fig. 1. Preparation of (*S*)-naproxen diallyl amide 2.

derived CSPs were obtained using the same procedure, simply substituting the chiral polymer for the organosilane. The loadings of the stationary phases are summarized in Table 2. The CSPs were packed into stainless steel columns of 250 × 4.6 mm I.D. as methanol slurries. Residual silanol groups were end-capped by passing a solution of 2 ml of hexamethyldisilazane in 50 ml of dichloromethane through a dichloromethane equilibrated column at a flow-rate of 1.0 ml/min.

## 3. Results and discussion

### 3.1. Syntheses of the CSPs

It has previously been observed that the manner in which a chiral selector is immobilized sometimes exerts a secondary influence on the separation process [15,16]. Steric repulsion, attractive interactions with the underlying support, and simultaneous interaction of the analyte with more than one selector may result in nonreciprocal behavior [17,18]. Incorporation of the chiral selector into suitably designed polymers allows for a control of these effects. The approach chosen to control the mode of attachment and spacing between the chiral sites uses principles developed in polymer chemistry. Polymers of the ABAB-type (monomer A: selector, monomer B: spacer) allow for the precise control of spacing between the chiral selectors. Reaction of difunctional oligomethylhydrosiloxanes with dienes in the presence of hexachloroplatinic acid provides a versatile route to segmented polymers with variable spacer length. Sidechain-modified polymers can be generated by hydrosilylation of a polymethylhydrosiloxane with a chiral olefin. (*S*)-Naproxen diallyl amide (2) was used as a model compound for the preparation of different polymeric and brush-type CSPs. The chiral selector was prepared from commercially available

Table 1
(S)-Naproxen diallyl amide-derived CSPs

| CSP | Polysiloxane[a] | Silica | Column length[c] (cm) |
|---|---|---|---|
| 1 | $^{H}MD_1M^{H}$ | A | 25 |
| 2 | $^{H}MD_2M^{H}$ | A | 25 |
| 3 | $^{H}MD_3M^{H}$ | A | 25 |
| 4 | $^{H}MD_4M^{H}$ | A | 25 |
| 5 | $^{H}MD_5M^{H}$ | A | 25 |
| 6 | $MD^{H}_1D_{9.3}M$ | A | 25 |
| 7[d] | none, brush-type | B | 25 |
| 8 | none, brush-type | A | 25 |
| 9 | $MD^{H}_1D_{9.3}M$ | C | 15 |
| 10 | $MD^{H}_1D_{9.3}M$ | D | 15 |

[a] $^{H}MD_nM^{H}$: $Me_2HSiO\text{-}(Me_2SiO)_nSiHMe_2$. Descriptors M and D are conventionally used in silicon chemistry to denote $Me_3Si\text{-O-}$ and $\text{-O-}SiMe_2\text{-O-}$. Superscripts on these descriptors denote a ligand or ligands substituting a Me or $Me_2$ ligands attached to silicon [14].
[b] Silica A: 300 Å, 5 μm; silica B: 100 Å, 5 μm; silica C: 1000 Å, 10 μm; silica D: 4000 Å, 10 μm.
[c] All columns: 4.6 mm I.D.
[d] This CSP was prepared by Patrick L. Spence of this group [12].

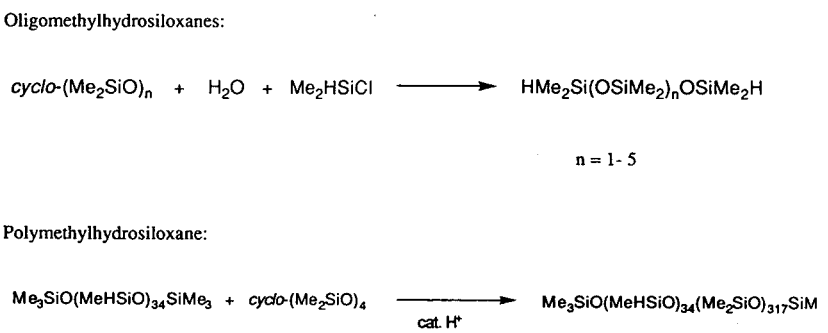


Fig. 2. Preparation of the polysiloxanes.

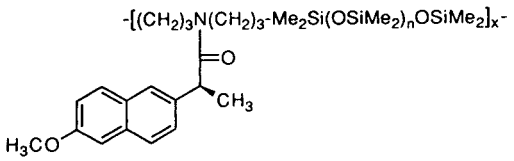


Segmented Polysiloxane (n = 1-5)

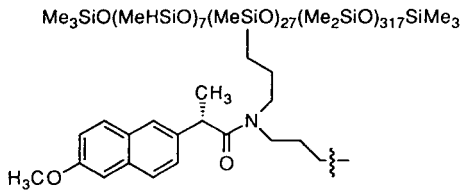


Sidechain Modified Polysiloxane

Fig. 3. Strucutral features of the segmented and sidechain-modified polysiloxanes.

(*S*)-naproxen (1) via the acid chloride by standard procedures (Fig. 2) [12]. A linear homologation strategy for the synthesis of oligosiloxanes developed by Uchida et al. [14] was used to prepare the difunctional oligosiloxanes $^{H}MD_nM^{H}$ ($n$ = 3–5, see legend of Table 1 for use of the descriptors) [14]. The first two homologues ($n$ = 1, 2) are commercially available products (Fig. 3).

In order to study the effect of the length of the dimethylsilyloxy spacer segments on chromatographic performance, the amounts of the various segmented polymers loaded onto the silica were adjusted so as to afford the same amount of selector in each column. The microanalytical data for each of these CSPs indicate a comparable selector content in each of the columns (Table 2).

The polymethylhydrosiloxane used for the preparation of a sidechain-modified polymeric phase was obtained by equilibrating an SiH-containing polysiloxane of suitable molecular weight with cyclooctamethyltetrasiloxane (Fig. 2) [3–5]. Hydrosilylation of this polymer with less than the stoichiometric amount of chiral olefin affords a sidechain-modified polysiloxane (Fig. 3).

Residual SiH groups were used for the chemical bonding to silica gel of 300, 1000, and 4000 Å pore size. (*S*)-Naproxen diallylamide (2) was transformed to the bis(dimethylethoxysilyl)-derivative and bonded to silica gel of 100 and 300 Å pore size to give the brush-type CSPs. All CSPs were slurry packed into 250 × 4.6 mm I.D. stainless steel columns as methanolic slurries and residual silanol groups were endcapped by pass-

Table 2
Microanalytical data of the CSPs

| CSP | Found (%) | | | Loading calculated by %N (mmol selector/g silica) |
|---|---|---|---|---|
| | C | H | N | |
| 1 | 7.64 | 1.26 | 0.25 | 0.18 |
| 2 | 6.84 | 1.15 | 0.23 | 0.16 |
| 3 | 7.76 | 1.50 | 0.20 | 0.14 |
| 4 | 6.47 | 0.92 | 0.30 | 0.21 |
| 5 | 10.86 | 2.16 | 0.30 | 0.21 |
| 6 | 10.04 | 2.07 | 0.25 | 0.18 |
| 7 | 6.32 | 0.95 | 0.30 | 0.21 |
| 8 | 6.46 | 0.97 | 0.35 | 0.28 |
| 9 | 13.22 | 2.59 | 0.35 | 0.28 |
| 10 | 13.04 | 2.48 | 0.33 | 0.24 |

ing a solution of hexamethyldisilazane through the packed columns [5].

### 3.2. Chromatographic properties of the CSPs

Racemic and partially resolved 3,5-dinitrobenzamides available from prior studies were used to evaluate the performance of the CSPs (Table 3). The results, using 20% 2-propanol in *n*-hexane as the mobile phase at a flow-rate of 2.0 ml/min, are summarized in Table 4.

For CSPs 1–5, prepared from segmented polysiloxanes, a decrease of retention is observed for a given analyte with an increase in the length of the oligosiloxane spacer. Since CSPs 1–5 were prepared from the same batch of silica, differences in the properties of the initial support cannot account for this observation. The microanalytical data obtained for these CSPs indicate that while there is some variation in the amount of chiral selector present in each of the columns containing CSPs 1–5 (Table 2), there is no correlation between these variations and retention. CSP 5 has the greatest nitrogen content but the lowest retention. Reduced retention with increasing spacer length might suggest (i) a more effective shielding of the support resulting in a suppression of superfluous interaction, (ii)

Table 3
Analytes used for the evaluation of the CSPs

| Analyte | |
|---|---|
| 3 | N-(3,5-Dinitrobenzoyl)alanine methyl ester |
| 4 | N-(3,5-Dinitrobenzoyl)phenylalanine methyl ester |
| 5 | N-(3,5-Dinitrobenzoyl)valine methyl ester |
| 6 | 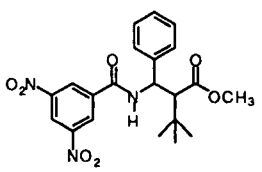 |
| 7 | 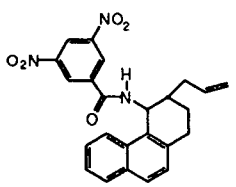 |
| 8 | 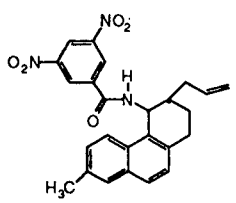 |
| 9 | 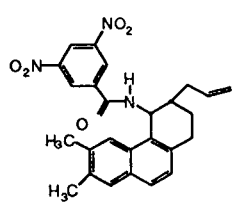 |

Table 4
Conditions: *n*-hexane–2-propanol (8:2), flow-rate: 2.0 ml/min

| Analyte | | CSP | | | | | | | | | |
|---|---|---|---|---|---|---|---|---|---|---|---|
| | | 1 | 2 | 3 | 4 | 5 | 6 | 7 | 8 | 9 | 10 |
| 3 | $k_1'$ | 0.76 | 0.70 | 0.62 | 0.48 | 0.28 | 0.70 | 6.44 | 2.63 | 0.34 | 0.19 |
| | $k_2'$ | 1.61 | 1.56 | 1.06 | 0.87 | 0.67 | 1.50 | 13.27 | 4.96 | 0.71 | 0.36 |
| | $\alpha$ | 2.12 | 2.22 | 1.7 | 1.81 | 2.39 | 2.14 | 2.06 | 1.88 | 2.04 | 1.92 |
| 4 | $k_1'$ | 0.93 | 0.91 | 0.44 | 0.41 | 0.18 | 0.63 | 8.02 | 3.25 | 0.29 | 0.15 |
| | $k_2'$ | 1.95 | 1.82 | 0.81 | 0.75 | 0.47 | 1.35 | 15.89 | 6.77 | 0.61 | 0.29 |
| | $\alpha$ | 2.10 | 1.99 | 1.84 | 1.79 | 2.61 | 2.12 | 1.98 | 2.08 | 2.09 | 2.00 |
| 5 | $k_1'$ | 0.70 | 0.59 | 0.37 | 0.33 | 0.18 | 0.55 | 4.77 | 2.00 | 0.25 | 0.13 |
| | $k_2'$ | 1.67 | 1.55 | 1.00 | 0.73 | 0.52 | 1.46 | 12.30 | 4.49 | 0.69 | 0.33 |
| | $\alpha$ | 2.38 | 2.63 | 2.70 | 2.20 | 2.88 | 2.62 | 2.58 | 2.25 | 2.73 | 2.50 |
| 6 | $k_1'$ | 0.59 | 0.59 | 0.25 | 0.37 | 0.08 | 0.66 | 4.12 | 2.11 | 0.31 | 0.13 |
| | $k_2'$ | 3.77 | 3.36 | 1.62 | 1.80 | 0.97 | 3.27 | 27.49 | 10.29 | 1.63 | 0.77 |
| | $\alpha$ | 6.39 | 5.69 | 6.50 | 4.86 | 12.12 | 4.91 | 6.67 | 4.88 | 5.30 | 5.80 |
| 7 | $k_1'$ | 1.15 | 0.93 | 0.56 | 0.46 | 0.30 | 0.68 | 6.93 | 3.67 | 0.48 | 0.24 |
| | $k_2'$ | 5.95 | 4.82 | 2.91 | 1.89 | 1.84 | 3.82 | 38.31 | 15.12 | 2.57 | 1.26 |
| | $\alpha$ | 5.19 | 5.16 | 5.19 | 4.12 | 6.14 | 5.56 | 5.53 | 4.12 | 5.36 | 5.27 |
| 8 | $k_1'$ | 1.04 | 0.91 | 0.50 | 0.66 | 0.28 | 0.59 | 13.50 | 2.03 | 0.40 | 0.23 |
| | $k_2'$ | 5.25 | 4.96 | 2.25 | 2.55 | 1.66 | 3.42 | 46.00 | 11.23 | 2.20 | 1.12 |
| | $\alpha$ | 5.05 | 5.45 | 4.50 | 3.83 | 5.93 | 5.80 | 3.41 | 4.27 | 5.50 | 4.91 |
| 9 | $k_1'$ | 0.93 | 0.91 | 0.50 | 0.54 | 0.18 | 0.74 | 7.00 | 3.56 | 0.30 | 0.13 |
| | $k_2'$ | 6.38 | 6.02 | 2.75 | 2.54 | 1.95 | 5.09 | 40.75 | 17.92 | 1.84 | 0.93 |
| | $\alpha$ | 6.87 | 6.61 | 5.50 | 4.71 | 10.83 | 6.87 | 5.82 | 5.03 | 6.41 | 6.87 |

more effective solvation of the chiral selectors owing to their greater spacing, (iii) a reduced extent of bridging of analytes between adjacent selectors owing to their greater spacing. However, reduction of retention does not reduce enantioselectivity nor should it necessarily do so. More effective masking of silanols can reduce retention while increasing enantioselectivity. Some separation factors are suspiciously large (e.g. Table 4: analytes 6, 9), presumably owing to elution of the least retained enantiomer so near the system void volume. The values are reported as determined but we hasten to point out that small errors in determining void volumes greatly affect separation factors when the retention of the least retained enantiomer is so slight. We also point out that injection of the sample in a solvent stronger than the mobile

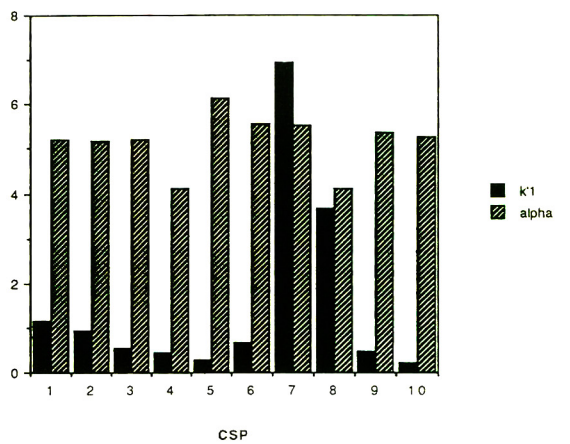


Fig. 4. Representation of the $k_1'$ and $\alpha$ values observed for analyte 7 on CSPs 1–10. Conditions: *n*-hexane–2-propanol (8:2) at a flow-rate of 2.0 ml/min.

phase can reduce the retention of an analyte, particularly when that retention is small to begin with. In the present case, enantioselectivity could be artificially increased.

Bonding of the chiral selector to a preformed polymethylhydrosiloxane affords CSP 6. The capacity and separation factors of the analytes on this phase are comparable to those on the lower homologues of the segmented polysiloxanes. To study the effect of varying the pore size of the underlying support, the sidechain-modified polymer was immobilized on Si 1000 (CSP 9) and Si 4000 (CSP 10). The chromatographic data show a clear reduction of retention with increasing pore size (Table 4: CSPs 6, 9, 10), doubtless because of the lesser surface area of the large pore silica. As a reference, two brush-type columns (CSPs 7 [12] and 8) were used. Increasing the pore size of the silica support from 100 Å (CSP 7) to 300 Å (CSP 8) decreases retention by a factor of 2–3 (Table 4). Comparison of brush-type CSP 8 with CSPs 1–5, prepared from segmented polysiloxanes, and CSP 6, prepared from a sidechain-modified polysiloxane, shows that resolutions of comparable or higher selectivity can be obtained on the polymeric CSPs in one third to one fifth the time using the same conditions. A graphic representation of these findings for analyte 7 is shown in Fig. 4.

The chromatographic data obtained on CSP 10 in the reversed-phase mode using the same set of analytes is shown in Table 5. Interestingly, the

Table 5
Chromatographic data obtained on CSP 10 at a flow-rate of 2.0 ml/min

| Analyte | | Solvent: × water/(100 − ×) methanol | | | | | | | | | | | | |
|---|---|---|---|---|---|---|---|---|---|---|---|---|---|---|
| | | 10 | 20 | 30 | 40 | 50 | 60 | 70 | 80 | 90 | 95 | 97 | 98 | 99 |
| 3 | $k_1'$ | n.r.[a] | n.r. | 0.04 | 0.21 | 0.56 | 2.21 | 6.56 | 15.14 | 31.25 | 51.10 | 61.93 | 65.34 | 66.69 |
| | $k_2'$ | | | | 0.38 | 1.04 | 3.85 | 11.13 | 25.19 | 49.89 | 77.77 | 93.56 | 98.46 | 99.68 |
| | $\alpha$ | 1.0 | 1.0 | 1.0 | 1.79 | 1.84 | 1.74 | 1.69 | 1.66 | 1.59 | 1.52 | 1.51 | 1.49 | 1.51 |
| 4 | $k_1'$ | n.r. | n.r. | n.r. | 0.04 | 0.05 | 0.14 | 0.74 | 1.31 | 1.68 | 2.55 | 2.96 | 3.00 | 3.19 |
| | $k_2'$ | | | | | | 0.29 | 1.64 | 3.18 | 3.30 | 3.48 | 4.01 | 4.10 | 4.31 |
| | $\alpha$ | 1.0 | 1.0 | 1.0 | 1.0 | 1.0 | 2.07 | 2.22 | 2.43 | 1.96 | 1.36 | 1.35 | 1.37 | 1.34 |
| 5 | $k_1'$ | n.r. | 0.03 | 0.04 | 0.1 | 0.16 | 0.68 | 1.73 | 3.26 | 6.13 | 9.36 | 11.01 | 11.43 | 11.67 |
| | $k_2'$ | | | | | 0.45 | 1.70 | 3.41 | 6.15 | 10.98 | 16.02 | 18.44 | 19.20 | 19.61 |
| | $\alpha$ | 1.0 | 1.0 | 1.0 | 1.0 | 2.80 | 2.50 | 1.97 | 1.88 | 1.79 | 1.71 | 1.67 | 1.68 | 1.68 |
| 6 | $k_1'$ | n.r. | 0.01 | 0.13 | 0.50 | 1.48 | 4.66 | 24.78 | n.d.[b] | n.d. | n.d. | n.d. | n.d. | n.d. |
| | $k_2'$ | | 0.19 | 0.45 | 1.71 | 5.22 | 17.38 | 85.91 | | | | | | |
| | $\alpha$ | 1.0 | 15.8 | 3.55 | 3.38 | 3.52 | 3.72 | 3.47 | | | | | | |
| 7 | $k_1'$ | 0.08 | 0.59 | 1.78 | 6.77 | 28.35 | n.d. | n.d. | n.d. | n.d. | n.d. | n.d. | n.d. | n.d. |
| | $k_2'$ | 0.43 | 2.61 | 8.28 | 31.88 | 141.75 | | | | | | | | |
| | $\alpha$ | 5.40 | 4.42 | 4.65 | 4.71 | 5.00 | | | | | | | | |
| 8 | $k_1'$ | 0.13 | 0.83 | 2.65 | 10.0 | 53.0 | n.d. | n.d. | n.d. | n.d. | n.d. | n.d. | n.d. | n.d. |
| | $k_2'$ | 0.55 | 3.49 | 11.72 | 43.67 | n.d. | | | | | | | | |
| | $\alpha$ | 4.11 | 4.18 | 4.42 | 4.36 | n.d. | | | | | | | | |
| 9 | $k_1'$ | 0.05 | 0.27 | 1.89 | 10.14 | n.d. | n.d. | n.d. | n.d. | n.d. | n.d. | n.d. | n.d. | n.d. |
| | $k_2'$ | 0.92 | 1.58 | 9.97 | n.d. | | | | | | | | | |
| | $\alpha$ | 10.08 | 5.81 | 5.27 | n.d. | | | | | | | | | |

[a] n.r.: not retained.
[b] n.d.: not determined, no peak detected after 2.5 h.

composition of the mobile phase can be altered over a wide range without a significant alteration of enantioselectivity. As expected, decreasing the concentration of the organic component in the mobile phase results in increased retention of the analytes. This feature is valuable as it allows one to adjust the mobile-phase composition for better separation of multicomponent mixtures without adversely affecting the separation of the enantiomers of interest. These columns have been used with a variety of mobile phases (hexane, 2-propanol, methanol, ethanol, acetonitrile, water, tetrahydrofuran, ethyl acetate, dichloromethane, buffers) for over a year with no adverse effects. Some of these columns have been used at temperatures exceeding 100°C with no lasting effect. Since these polysiloxanes are anchored to silica, one might suppose that the usual admonitions about pH extremes should be heeded but we have not yet sought the tolerable limits of these CSPs.

## 4. Conclusions

In summary, ten (*S*)-naproxen-derived CSPs were utilized to study the properties of brush-type and polymeric coatings of a chromatographic support. Reduction of retention times without significant loss of enantioselectivity was observed upon increasing the pore size of the silica gel used to prepare the CSPs. Synthesis of a series of difunctional oligosiloxanes provided starting materials for the preparation of copolymers with variable spacer length. CSPs based on these segmented polysiloxanes show strongly reduced retention times and enantioselectivities comparable or higher than those obtained on the corresponding brush-type CSPs. Immobilization of a sidechain-modified polysiloxane affords CSPs capable of rapid resolutions of enantiomers. It has been shown that the incorporation of a chiral selector into polysiloxanes affords CSPs of high enantioselectivity in combination with short analysis time under either normal- or reversed-phase conditions.

## Acknowledgements

This work has been supported by EM Science, Regis Chemical Company, the National Science Foundation, and the Deutsche Forschungsgemeinschaft (Postdoctoral Fellowship to GJT).

## References

[1] S. Anderson, R.A. Thompson, S. Allenmark, J. Chromatogr., 591 (1992) 65.
[2] H. Frank, G.J. Nicholson, E. Beyer, J. Chromatogr. Sci., 15 (1977) 174.
[3] W. Röder, F.-J. Ruffing, G. Schomburg, W.H. Pirkle, HRC and CC, 10 (1987) 665.
[4] F.-J. Ruffing, J.A. Lux, W. Röder, G. Schomburg, Chromatographia, 26 (1988) 19.
[5] M. Schleimer, V. Schurig, W.H. Pirkle, J. Chromatogr. A, 679 (1994) 23.
[6] V. Schurig, H.-P. Nowotny, Angew. Chem., Int. Ed. Engl., 29 (1990) 939.
[7] D.F. Johnson, J.S. Bradshaw, M. Eguchi, B.E. Rossiter, M.L. Lee, P. Petersson, K.E. Markides, J. Chromatogr., 594 (1992) 283.
[8] J.S. Bradshaw, G.-L. Yi, B.E. Rossiter, S.L. Reese, P. Petersson, K.E. Markides, M.L. Lee, Tetrahedon Lett., 34 (1993) 79.
[9] G. Yi, J.S. Bradshaw, B.E. Rossiter, A. Malik, W. Li, M.L. Lee, J. Org. Chem., 58 (1993) 4844.
[10] H. Frank, HRC and CC, 11 (1988) 787.
[11] H. Frank, I. Abe, G. Fabian, HRC and CC, 15 (1992) 444.
[12] W.H. Pirkle, P.L. Spence, J. Chromatogr. A, 659 (1994) 69.
[13] W.H. Pirkle, C.J. Welch, B. Lamm, J. Org. Chem., 57 (1992) 3854.
[14] H. Uchida, Y. Kabe, K. Yoshino, A. Kawamata, T. Tsumuraya, S. Masamune, J. Am. Chem. Soc., 112 (1990) 7077.
[15] W.H. Pirkle, M.H. Hyun, B. Bank, J. Chromatogr., 316 (1984) 585.
[16] W.H. Pirkle, P.G. Murray, J.A. Burke, J. Chromatogr., 641 (1993) 21.
[17] W.H. Pirkle, R.S. Readnour, Anal. Chem., 63 (1991) 16.
[18] W.H. Pirkle, C.J. Welch, J. Chromatogr., 589 (1992) 45.

ELSEVIER

Journal of Chromatography A, 704 (1995) 279–287

JOURNAL OF CHROMATOGRAPHY A

# Retentive and enantioselective properties of ovomucoid-bonded silica columns. Influence of protein purity and isolation method

Jun Haginaka*, Chikako Seyama, Tokiko Murashima

*Faculty of Pharmaceutical Sciences, Mukogawa Women's University, 11-68, Koshien Kyuban-cho, Nishinomiya 663, Japan*

First received 12 December 1994; revised manuscript received 7 February 1995; accepted 17 February 1995

**Abstract**

The influence of protein purity and isolation method on the chiral resolution of racemates on ovomucoid-bonded materials has been investigated. Chicken ovomucoid (OMCHI) and turkey ovomucoid (OMTKY) were obtained from commercial sources, and were isolated by precipitation with acetone from their corresponding egg whites. Further, crude OMCHI protein was fractionated by cation-exchange chromatography into two fractions, pure OMCHI and an unknown protein fraction. The OMCHI, fractionated OMCHI and OMTKY proteins were characterized by N-terminal sequencing and trypsin-inhibitory activity. Their purity was checked by reversed-phase chromatography. The results reveal that the commercial OMCHI, and the isolated OMCHI and OMTKY are crude preparations and that an unknown protein fraction is present in each crude ovomucoid protein. The OMCHI, fractionated OMCHI and OMTKY proteins were bound to aminopropyl-silica gels activated by N,N'-disuccinimidyl carbonate to test the retentive and enantioselective properties of those materials. The result suggests that the unknown protein fraction could be responsible for chiral recognition ability of the OMCHI and OMTKY columns.

## 1. Introduction

Protein-bonded stationary phases including albumins such as bovine serum albumin (BSA) [1] and human serum albumin [2], and glycoproteins such as $\alpha_1$-acid glycoprotein [3] and chicken ovomucoid (OMCHI) [4] and avidin [5], and enzymes such as cellulase [6], trypsin [7], $\alpha$-chymotrypsin [8] and lysozyme [9] have been developed for the separation of enantiomeric forms. Among these, an OMCHI-bonded silica column is of special interest because of its long-term stability [10] and because it is suited for separating a wide range of enantiomeric mixtures [10–12]. The column is now commercially available as an Ultron ES-OVM column.

It is well known that the protein purity and/or the isolation method affect the physiological activity of a protein. In this study, we investigated the influence of ovomucoid protein purity and isolation method on the retention and enantioselectivity of various solutes on OMCHI- and turkey ovomucoid (OMTKY)-bonded silica columns. Also, preliminary result on the origin of

* Corresponding author.

0021-9673/95/$09.50 
*SSDI* 0021-9673(95)00230-8

the chiral recognition ability of ovomucoid-bonded column will be discussed.

## 2. Experimental

### 2.1. Reagents and materials

Ketoprofen and chlorpheniramine maleate were kindly donated by Kaken Pharmaceutical Co. (Tokyo, Japan) and Essex Nippon (Osaka, Japan), respectively. Benzoin was purchased from Sigma (St. Louis, MO, USA). The Structures of the racemic compounds used in this study are shown in Fig. 1. Chicken ovomucoid (OMCHI) from Eisai Co. (Tokyo, Japan), Sigma, Taiyo Chemicals (Yokkaichi, Mie, Japan) were abbreviated OMCHI-C1, OMCHI-C2 and OMCHI-C3, respectively. OMTKY from Sigma was abbreviated OMTKY-C. Sephadex G-75, Sephadex G-25 (fine) and SP Sepharose FF were from Pharmacia Biotec (Tokyo, Japan). N,N'-Disuccinimidyl carbonate (DSC) was purchased from Sigma. Ethanol of HPLC grade was obtained from Wako Pure Chemical Industries (Osaka, Japan). 3-Aminopropyltriethoxysilane was obtained from Chisso Co. (Tokyo, Japan). Silica gels (Ultron-120, 5-$\mu$m diameter, 120-Å pore size, 300 $m^2/g$) used were from Shinwa Chemical Industries (Kyoto, Japan). An Ultron ES-OVM column was kindly donated by Shinwa Chemical Industries. Other solvents and reagents of analytical-reagent grade were used without further purification.

Water purified with a Nanopure II unit (Barnstead, Boston, MA, USA) was used for the preparation of the eluent and the sample solution.

### 2.2. Isolation of OMCHI and OMTKY from egg whites

OMCHI and OMTKY were isolated from their corresponding egg whites according to a modified form of the method reported previously [13]. A 900-ml volume of cold 0.5 M trichloroacetic acid–acetone (1:2, v/v) at pH 3.5 was added to 450 ml of the egg white, and the mixture was stirred for 4 h at 4°C. The solution was centrifuged at 5500 g rpm for 30 min at 4°C using polypropylene bottles. Two volumes of cold acetone were added to the supernatant and after stirring the solution for 2 h at 4°C, it was centrifuged at 5500 g rpm for 40 min at 4°C. The precipitate was dissolved and dialized against water and then lyophilized. The remaining product is further purified by the two methods described below.

The first purification method is a modification of the method reported by Kato et al. [4]. The remaining product was purified through a 90 × 5 cm Sephadex G-75 column equilibrated with 10 m*M* Tris buffer (pH 8.0) including 0.3 *M* NaCl at a flow-rate of 180 ml/h. The eluate was monitored at 280 nm. The separation was performed at 4°C. The eluted major component was fractionated and lyophilized. The lyophilized sample was desalted on a Sephadex G-25 (fine) column (20 × 5 cm) using 15 m*M* $NH_4HCO_3$ buffer with an average flow-rate of 120 ml/h. The eluate was collected and lyophilized. The obtained product was termed OMCHI-I1 or OMTKY-I.

The second purification method is based on a modification of the method reported by Waheed and Salahuddin [15]. The lyophilized product was brought to 90% $(NH_4)_2SO_4$ saturation, pH

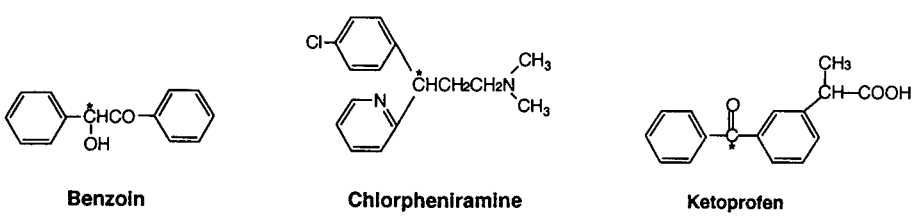


Fig. 1. Structures of the racemic compounds used in this study.

4.6. The solution was centrifuged at 5500 g for 40 min at 4°C. The precipitate was dissolved and dialized against water and then lyophilized. The remaining product was dissolved in water. The obtained solution was centrifuged again at 5500 g for 40 min at 4°C. The supernatant was lyophilized. The obtained product was termed OMCHI-I2.

### 2.3. Fractionation of crude OMCHI protein

The OMCHI, OMCHI-C1, from Eisai was further separated on a SP Sepharose FF column (12 × 5 cm) that was equilibrated with 10 m*M* $CH_3COONH_4$ (pH 4.6) applying a liner gradient to 500 m*M* $CH_3COONH_4$ (pH 4.6) for 4.5 h at an average flow-rate of 100 ml/h, and then the eluent was changed to 800 m*M* $CH_3COONH_4$ (pH 4.6). The separation was performed at 4°C. Detection was carried out at 280 nm. Two fractions were collected and lyophilized. The lyophilized samples were desalted with a Sephadex G-25 (fine) column as described above, and the eluate was collected and lyophilized. The isolated fractions were termed fractions A and B.

### 2.4. Characterization of OMCHI, fractionated OMCHI and OMTKY protein

#### N-Terminal sequencing

A 70-μg amount of each protein was reconstituted with 50 μl of water. A 5-μl portion of the dilution was spotted on a solid support for N-terminal sequencing using an ABI 473A Protein Sequencer (Applied Biosystems Division, Perkin Elmer Japan, Tokyo, Japan).

#### Trypsin-inhibitory activity

Trypsin-inhibitory activity measurement is based on a modification of the method reported by Waheed and Salahuddin [15].

### 2.5. Preparation of aminopropyl-silica gels

Ultron-120 silica gel (5 g) was dried in vacuo over $P_2O_5$ at 150°C for 6 h and the dry silica gel was added to 120 ml of dry toluene. The mixture was heated to reflux until all the water had been removed as an azeotrope into a Dean-Stark-type trap. Next, 3.32 g of 3-aminopropyltriethoxylsilane, corresponding to 10 μmol/m$^2$ of the

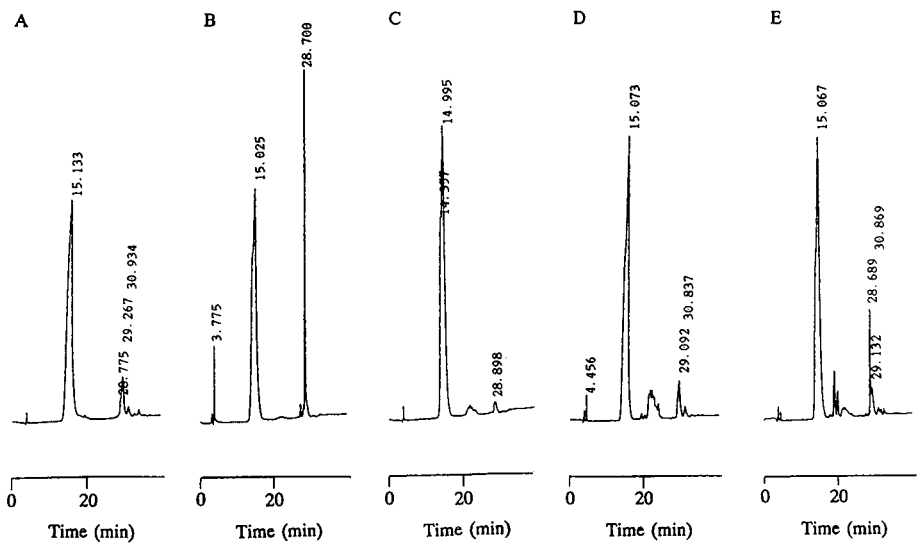


Fig. 2. Chromatograms of commercial and isolated OMCHI proteins on a $C_{18}$ column. (A) OMCHI-C1; (B) OMCHI-C2; (C) OMCHI-C3; (D) OMCHI-I1; (E) OMCHI-I2. Column: Cosmosil 5C18-AR (250 × 4.6 mm I.D.). Eluents: eluent A, $H_2O$–$CH_3CN$ (80:20, v/v) including 0.1% TFA; eluent B, $H_2O$–$CH_3CN$ (20:80, v/v) including 0.1% TFA; linear gradient from 0% eluent B at 0 min to 100% eluent B at 90 min. Flow-rate, 1.0 ml/min; Detection, 280 nm; Loaded amount, 200 μg.

specific surface area, was added and reacted for 8 h. The reaction mixture was cooled to room temperature, filtered and washed with toluene and methanol. The isolated silica gels were dried in vacuo over $P_2O_5$ at 60°C for 2 h.

### 2.6. Activation of aminopropyl-silica gels

Aminopropyl-silica gels were activated by DSC. Five grams of the gels were slurried in 70 ml of acetonitrile and reacted with 5 g of DSC for 24 h at 30°C. The reaction mixture was filtered and washed with acetonitrile, water and methanol. The obtained silica gels were dried in vacuo over $P_2O_5$ at 60°C for 2 h.

### 2.7. Preparation of ovomucoid-bonded materials

Each protein was bound to DSC-activated aminopropyl-silica gels as follows: 1.2 g of the DSC-activated silica gels were slurried in 20 ml of 20 m*M* phosphate buffer (pH 6.8). To the mixture, 400 mg of each ovomucoid protein, except for the fractionated protein portion (fraction B), dissolved in 5 ml of the same buffer was added slowly at room temperature for 1 h by adjusting pH to 6.6, and further stirred for 15 h at 30°C. For fraction B protein, 100 mg of protein were used and treated as described above. The reaction mixture was washed with water and further reacted with 2-aminoethanol–water (1:50) adjusted to pH 6.6 with hydrochloric acid at room temperature for 1 h. Then the reaction mixtures were filtered, and washed with water and methanol. The isolated materials were dried in vacuo over $P_2O_5$ at 40°C for 6 h.

The ovomucoid-bonded materials were packed into a 100 × 4.6 mm I.D. stainless-steel column by the slurry packing method using 5% ethanol as the slurry and packing solvent.

### 2.8. Elemental analysis

Elemental analysis of the ovomucoid-bonded silica materials was performed using ion-chromatography combined with oxygen-flask method for sulfur.

### 2.9. Chromatography

For the chiral resolution of solutes, the HPLC system consisted of an LC-9A pump, an SPD-6A spectrophotometer, an SIL-6B autoinjector, a

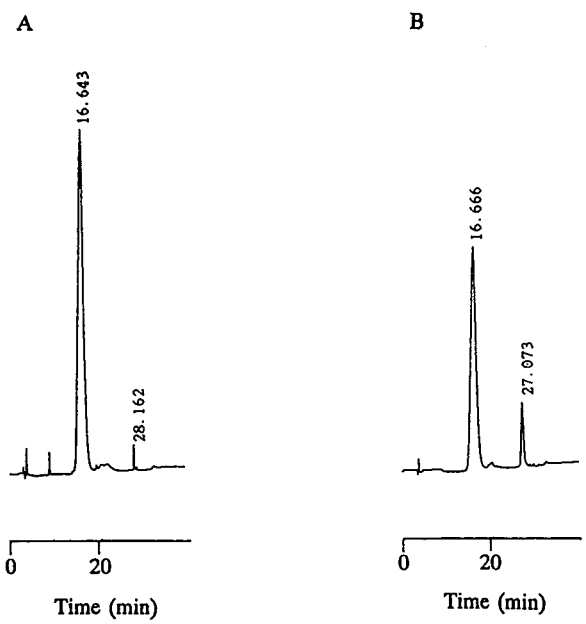


Fig. 3. Chromatograms of commercial and isolated OMTKY proteins on a $C_{18}$ column. (A) OMTKY-C; (B) OMTKY-I. Other conditions as in Fig. 2.

Table 1
Amounts of bonded proteins on OMCHI and OMTKY Materials

| Material | Sulfur content[a] (%) | Amount of bonded ovomucoid (μmol/g) |
|---|---|---|
| OMCHI-C1 | 0.15 | 2.3 |
| OMCHI-C2 | 0.20 | 3.1 |
| OMCHI-C3 | 0.23 | 3.6 |
| OMCHI-I1 | 0.18 | 2.8 |
| OMCHI-I2 | 0.16 | 2.5 |
| OMTKY-C | 0.23 | 3.6 |
| OMTKY-I | 0.21 | 3.3 |
| OVM[b] | 0.26 | 4.1 |

[a] Estimated from the elemental analysis data of sulfur.
[b] Commercial available Ultron-ES OVM column.

C-R4A integrator and an SCL-6B system controller (all from Shimadzu, Kyoto, Japan). The flow-rate was maintained at 0.8 ml/min. Detection was performed at 220 or 254 nm. Capacity factors were calculated from the equation $k' = (t_R\text{-}t_0)/t_0$, where $t_R$ and $t_0$ are the elution times of retained and unretained solutes, respectively; $k'_1$ and $k'_2$ are the capacity factors of the first- and second-eluted peaks, respectively. The retention time of unretained solute, $t_0$, was measured by injection of a solution, the organic modifier content of which was slightly different from that of the eluent used. The enantioseparation factor is calculated from the equation $\alpha = k'_2/k'_1$. Resolution is calculated from the equation $R_s = 2(t_2 - t_1)/(t_{w1} + t_{w2})$, where $t_1$ and $t_2$ are the retention times of the first- and second-eluted peaks, respectively, and $t_{w1}$ and $t_{w2}$ are the peak widths. All separation were carried out at 25°C using a CO-1093C column oven (Uniflows, Tokyo, Japan). The composition of eluents, which are prepared by using phosphoric acid–sodium dihydrogenphosphate or sodium dihydrogenphosphate–disodium hydrogenphosphate and organic modifier, are specified in the table and figure legends.

For reversed-phase chromatography of the ovomucoid protein, the same HPLC system as described above was used except that two pumps were used for gradient elution. The eluents used are as follows: eluent A, $H_2O$–$CH_3CN$ (80:20, v/v) including 0.1% trifluoroacetic acid (TFA); eluent B, $H_2O$–$CH_3CN$ (20:80, v/v) including 0.1% TFA; linear gradient from 0% eluent B at 0 min to 100% eluent B at 90 min. The column used was a Cosmosil 5C18-AR column (250 × 4.6 mm I.D.) (Nacalai Tesque, Kyoto, Japan). Detection was carried out at 280 nm. The flow-rate was 1.0 ml/min. All separations were performed at 30°C.

## 3. Results and discussions

### 3.1. Characterization of ovomucoid proteins

Fig. 2A–E shows chromatograms of the separation of OMCHI-C1, OMCHI-C2, OMCHI-C3,

Table 2
Capacity factor, enantioselectivity and resolution of benzoin, chlorpheniramine and ketoprofen on several OMCHI and OMTKY columns[a]

| Column | Benzoin | | | Chlorpheniramine | | | Ketoprofen | | |
|---|---|---|---|---|---|---|---|---|---|
| | $k'_1$ | $\alpha$ | $R_s$ | $k'_1$ | $\alpha$ | $R_s$ | $k'_1$ | $\alpha$ | $R_s$ |
| OMCHI-C1 | 2.86 | 2.37 | 5.64 | 1.30 | 1.77 | 1.52 | 10.8 | 1.06 | 0.54 |
| OMCHI-C2 | 1.85 | 2.29 | 3.87 | 1.33 | 1.49 | 1.16 | 6.01 | 1.07 | 0.56 |
| OMCHI-C3 | 1.52 | 1.90 | 3.30 | 0.75 | 1.42 | 1.28 | 6.39 | 1.00 | – |
| OMCHI-I1 | 3.68 | 2.70 | 9.57 | 1.83 | 1.91 | n.c.[b] | 11.1 | 1.11 | 1.38 |
| OMCHI-I2 | 2.45 | 2.33 | 4.49 | 1.53 | 1.76 | 3.11 | 8.10 | 1.14 | 1.06 |
| OMTKY-C | 0.61 | 1.00 | – | 0.33 | 1.00 | – | 3.83 | 1.00 | – |
| OMTKY-I | 2.80 | 2.03 | 6.21 | 1.97 | 1.20 | n.c. | 8.87 | 1.16 | 1.60 |
| OVM | 4.08 | 2.62 | 8.72 | 1.63 | 1.80 | 3.07 | 14.3 | 1.10 | 1.18 |
| Fraction A | 0.46 | 1.00 | – | 3.57 | 1.00 | – | 4.15 | 1.00 | – |
| Fraction B | 9.19 | 3.08 | 11.0 | 4.63 | 2.28 | 6.24 | 20.7 | 1.24 | 2.08 |

[a] HPLC conditions: column, each material packed into 100 × 4.6 mm I.D. stainless steel column except for the OVM column, which is the commercially available Ultron ES-OVM column (150 × 4.6 mm I.D.); eluent, 20 m*M* phosphate buffer (pH 5.0)–ethanol (90:10, v/v); flow-rate: 1.0 ml/min for the Ultron-ES OVM column and 0.8 ml/min for other columns; detection, 220 nm; $t_0$ was 2.1 min for the Ultron ES-OVM column and 1.9 min for the other columns.

[b] n.c. means that resolution is not calculated because of overlapping of the peaks of one enantiomer and maleic acid.

OMCHI-I1 and OMCHI-I2 proteins, respectively, on a $C_{18}$ column. The first three OMCHI proteins were from commercial sources, while the last two proteins were isolated from chicken egg whites. It was found that the commercial and isolated OMCHI proteins are crude preparations, and that the OMCHIs contain one major protein fraction at a retention time of 15 min and one or two minor protein fractions at retention times of 30 min or 20 and 30 min.

Next, we separated the OMCHI-C1 into two fractions, fractions A and B, by cation-exchange chromatography. The obtained fractions A and B showed broad peaks at retention times of about 15 min and 30 min, respectively, on the same $C_{18}$ column as used in Fig. 2. Note that the protein fraction giving the sharp peak at a retention time of 29 min observed with OMCHI-C2 and OMCHI-I2 proteins is different from the fraction B protein. The N-terminal sequencing results of the first 15 amino acid in proteins of fraction A are A-E-V-D-X-S-R-F-P-X-A-T-D-K-E, where X deviates cystine or glycosylated amino acid residue. These amino acid sequences are in good agreement with those of the OMCHI reported by Kato et al. [14]. However, the N-terminal sequencing results of the first 5 amino acid in proteins of fraction B are T-E-S-P-X. The second sequences were not observed with the N-terminal sequencing results of fractions A and B. Also, fraction A protein as well as commercial and isolated OMCHI proteins showed trypsin-inhibitory activity as reported previously [15], while fraction B protein had no trypsin-inhibitory activity. These results suggest that the major protein fraction at a retention time of 15 min should be the OMCHI, and that the minor protein fraction with a retention time of 30 min should be other protein. At present we have not yet identified the minor protein fraction, and thus this protein fraction is termed "unknown protein".

Fig. 3A, B shows chromatograms of OMTKY-C and OMTKY-I proteins, respectively, on a $C_{18}$ column. The former OMTKY protein was from commercial sources, while the latter protein was isolated from turkey egg whites. Taking into account the results of the amino acid sequencing and the trypsin-inhibitory activity of the OMTKY, the protein fraction at a retention time of 16 min should be the OMTKY, and the minor protein fraction at a retention time of 27 min could be the unknown protein as in the case of the commercial and isolated OMCHI proteins. It is interesting that the OMTKY-C has no protein fraction at a retention time of 27 min.

We do not know how the commercial OMCHI and OMTKY are isolated. However, the above results reveal that the commercial and isolated OMCHI and OMTKY are crude, except for the commercial OMTKY, and that they include minor unknown protein fractions. Also, the isolation method affects the OMCHI and OMTKY purity.

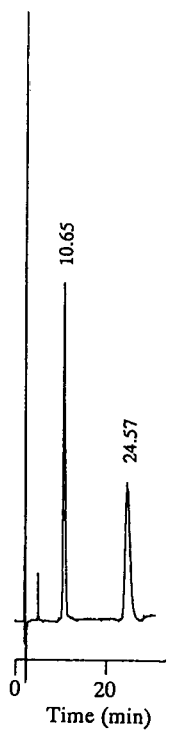


Fig. 4. Chiral resolution of benzoin on a commercial OMCHI-bonded column (Ultron ES-OVM column). HPLC conditions: column, 150 × 4.6 mm I.D.; eluent, 20 m*M* phosphate buffer (pH 5.0)–ethanol (90:10, v/v); flow-rate, 1.0 ml/min; detection, 220 nm.

### 3.2. Amounts of the bonded ovomucoid proteins

Next, we bound these proteins to DSC-activated aminopropyl-silica gels. Table 1 shows the amounts of bonded ovomucoid proteins on the various OMCHI and OMTKY materials. Assuming that the protein is pure, the amount of the bonded protein was estimated by elemental analysis of sulfur. The results show that the amounts of bonded OMCHI and OMTKY proteins range from 2.3 to 3.6 $\mu$mol/g. The amounts of bonded proteins on commercial OMCHI materials (Ultron ESOVM) was estimated to be 4.1 $\mu$mol/g.

### 3.3. Chiral recognition properties of the OMCHI, fractionated OMCHI and OMTKY columns

Next, we examined the chiral recognition properties of the OMCHI, fractionated OMCHI (fractions A and B) and OMTKY columns. Table 2 shows the capacity factor ($k'_1$), enantioselectivity ($\alpha$) and resolution ($R_s$) of benzoin, chlorpheniramine and ketoprofen on the columns made with the various proteins. For comparison, those values on the commercial OMCHI-bonded column (Ultron ES-OVM) are also cited in Table 2. Figs. 4–6 show chromatograms of benzoin on Ultron ES-OVM, OMCHI and fractionated OMCHI (fractions A and B) columns, respectively. Fig. 7 shows chromatograms of benzoin on the OMTKY columns. It was found that commercial and isolated OMCHI columns give a chiral recognition ability comparable to that of a commercial Ultron ES-OVM column. Also, the pure OMCHI (fraction A) has no chiral recognition ability, but the unknown protein (fraction B) has. These results show that the chiral recognition ability of the crude OMCHI-bonded column originates from the unknown protein fraction in the crude OMCHI proteins. The differences in retention and enantioselective properties of the various OMCHI columns were easily elucidated. It depends on how much of the unknown protein is isolated from egg whites with the pure OMCHI. It is plausible that the isolation method and/or the protein purity much affect the chiral recognition

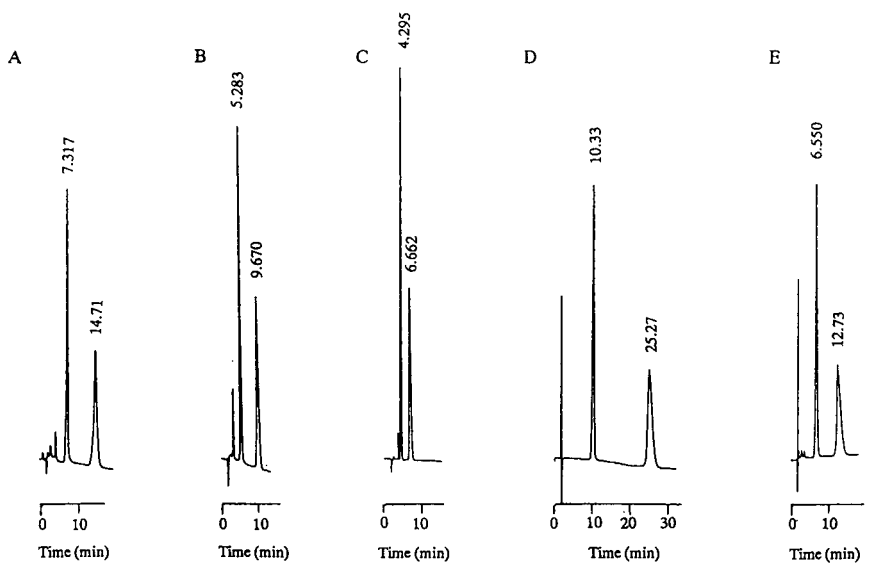


Fig. 5. Chiral resolution of benzoin on columns made with commercial and isolated OMCHI. (A) OMCHI-C1; (B) OMCHI-C2; (C) OMCHI-C3; (D) OMCHI-I1, (E) OMCHI-I2. HPLC conditions: column, 100 × 4.6 mm I.D.; flow-rate, 1.0 ml/min. Other conditions as in Fig. 4.

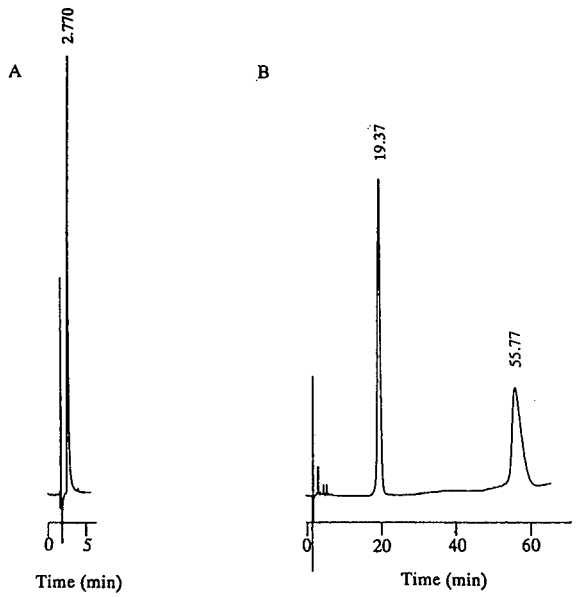


Fig. 6. Chiral resolution of benzoin on columns made with the fractionated OMCHI. (A) fraction A; (B) fraction B. Other conditions as in Fig. 5.

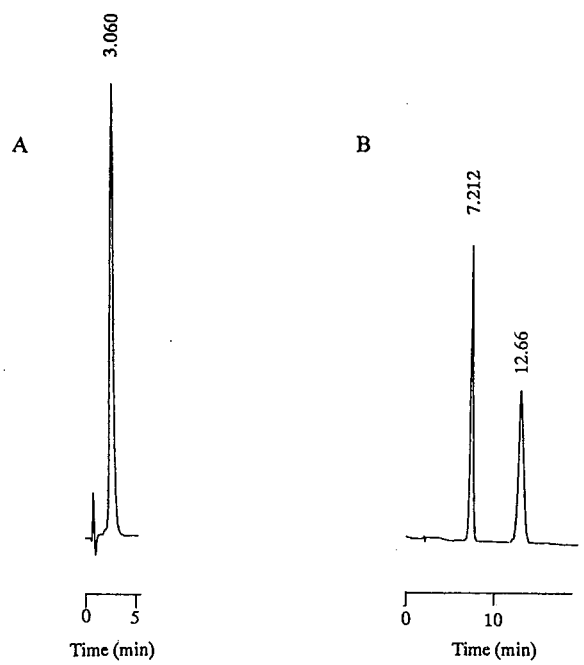


Fig. 7. Chiral resolution of benzoin on columns made with commercial and isolated OMTKY. (A) OMTKY-C; (B) OMTKY-I. Other conditions as in Fig. 5.

properties of the OMCHI columns made with crude proteins.

As shown in Table 2 and Fig. 7, the OMTKY-C column made with the commercial OMTKY had no chiral recognition ability, whereas the OMTKY-I column made with the isolated OMTKY showed good chiral recognition ability. The OMTKY-C column still gave no chiral recognition ability when the ethanol content in the eluent was decreased from 10% to 1%. If the chiral recognition ability of the OMTKY-I column should originate from the protein fraction with a retention time of 27 min, the presence and absence of the chiral recognition ability of the two OMTKY columns could be well explained in the case of the crude OMCHI columns. The lack of chiral recognition ability of the OMTKY-C column is due to the absence of the protein fraction with a retention time of 27 min.

In conclusion, an unknown protein fraction is present in crude ovomucoid protein from commercial sources and isolated from egg whites. This unknown protein fraction could be responsible for the chiral recognition of the solutes tested. Further work is on-going to characterize the unknown protein fraction in crude ovomucoid proteins.

## Acknowledgements

We wish to thank Dr. H. Wada of Shinwa Chemical Industries (Kyoto, Japan) for kind donation of silica materials and an Ultron ES-OVM column. Thanks are also due to Mr. T. Tsukamoto of Taiho Pharmaceutical Co. (Tokushima, Japan) for elemental analysis of the protein-bonded materials. This work was partly supported by a Grant-in-Aid for Scientific Research (No. 05671799 and No. 06672159) from the Ministry of Education, Science and Culture, Japan.

## References

[1] S. Allenmark, J. Liq. Chromatogr., 9 (1986) 425.
[2] E. Domenici, C. Bertucci, P. Salvadori, G. Felix, I. Cahagne, S. Montellier and I.W. Wainer, Chromatographia, 29 (1990) 170.

[3] J. Hermansson, J. Chromatogr., 269 (1983) 71.
[4] T. Miwa, M. Ichikawa, M. Tsuno, T. Hattori, T. Miyakawa, M. Kayano and Y. Miyake, Chem. Pharm. Bull., 35 (1987) 682.
[5] T. Miwa, T. Miyakawa and T. Miyake, J. Chromatogr., 457 (1988) 227.
[6] P. Erlandsson, I. Marle, L. Hansson, R. Isaksson, C. Pettersson and G. Pettersson, J. Am. Chem. Soc., 112 (1990) 4573.
[7] S. Thelohan, P. Jadaud and I.W. Wainer, Chromatographia, 28 (1989) 551.
[8] I.W. Wainer, P. Jadaud, G.R. Schombaum, S.V. Kadodkar and M.P. Henry, Chromatographia, 25 (1988) 903.
[9] J. Haginaka, T. Murashima and Ch. Seyama, J. Chromatogr. A, 666 (1994) 203.
[10] K.M. Kirkland, K.L. Nelson and D.A. McCombs, J. Chromatogr., 545 (1991) 43.
[11] J. Haginaka, J. Wakai, H. Yasuda, K. Takahashi and T. Katagi, Chromatographia, 29 (1990) 587.
[12] J. Iredale, A.-F. Aubry and I.W. Wainer, Chromatographia, 31 (1991) 329.
[13] H. Lineweaver and C.W. Murray, J. Biol. Chem., 171 (1947) 565.
[14] I. Kato, J. Shrode, W.J. Kohr and M. Laskowski Jr., Biochemistry, 26 (1987) 193.
[15] A. Waheed and A. Salahuddin, Biochem. J., 147 (1975) 139.

ELSEVIER

Journal of Chromatography A, 704 (1995) 289–305

JOURNAL OF CHROMATOGRAPHY A

# Retention and selectivity of flavanones on homopolypeptide-bonded stationary phases in both normal- and reversed-phase liquid chromatography

Barbara A. Siles[1], H. Brian Halsall, John G. Dorsey*,[2]

*Department of Chemistry, University of Cincinnati, Cincinnati, OH 45221-0172, USA*

First received 15 August 1994; revised manuscript received 17 February 1995; accepted 23 February 1995

**Abstract**

Three linear polymers of repeating amino acid units, or homopolypeptides, have been individually covalently bonded to microparticulate silica and evaluated for liquid chromatographic separations. The retention and selectivity of seven flavanones were investigated on these stationary phases and a structurally similar, commercially available reference stationary phase, Chiraspher. All three of the homopolypeptide stationary phases retain solutes in the normal-phase mode. The aromatic-containing homopolypeptide stationary phases also retain solutes in the reversed-phase mode. Selectivity values for the flavanones were higher in the normal-phase mode; chiral selectivity was observed for the amphiphilic homopolypeptide stationary phase in the reversed-phase mode. The retention mechanism of each stationary phase is suggested based on the chemical nature and conformation of the corresponding homopolypeptide ligand.

## 1. Introduction

Conformational transitions of stationary-phase ligands as a function of mobile-phase composition and column temperature have been investigated in relation to fundamental retention and selectivity in liquid chromatography (LC) [1]. In both theoretical treatments and practical applications of reversed-phase LC, the conformational ordering of alkyl chains has been thoroughly investigated [2–4]. Conformational properties of chiral stationary-phase ligands in liquid chromatography have been directly related to, and in some instances simply inferred, in the mechanism of enantiomeric recognition. For instance, ( + )-poly(triphenylmethacrylate) forms a helical coil structure that has been directly related to its enantioselectivity as a stationary-phase ligand [5–7]. The process of chiral recognition of biomolecules, such as proteins, is more complex, however. The folding of the amino acid chain of a protein into a native three-dimensional tertiary structure may create one or more binding sites that have stereochemical preference for analytes. The most commonly used proteins for chiral stationary-phase ligands have been bovine serum albumin (BSA) and $\alpha_1$-acid glycoprotein (AGP). BSA-silica was developed by Allenmark et al. [8]

* Corresponding author.

[1] Present address: National Institute of Standards and Technology, Building 222, Room A217, Gaithersburg, MD 20899, USA.

[2] Present address: Department of Chemistry, Florida State University, Tallahassee, FL 32306-3006, USA.

0021-9673/95/$09.50 
*SSDI* 0021-9673(95)00269-3

and is now commercially available as Resolvosil-BSA. According to retention studies of aromatic pharmaceuticals and amino acid derivatives, varying mobile-phase composition, hydrophobic and electrostatic interactions contribute significantly to retention, and hydrogen-bonding and charge transfer interactions are of secondary importance [9–12]. Subtle changes in mobile-phase composition and column temperature cause dramatic differences in the performance of BSA as a chromatographic ligand. Gilpin et al. [13] related the change in selectivity of L-tryptophan versus D-tryptophan in binding to BSA-silica as a function of temperature to a complex phenomenological local conformational change of the protein. AGP-silica, introduced by Hermansson [14] and now commercially available as Enantiopac, has been most commonly used for enantiomeric separations of racemic mixtures of cationic pharmaceuticals. Chromatographic investigations using aqueous buffer mobile phases in the pH range 4–7 have revealed that this acidic protein retains species based on ion-pairing, hydrophobic (related to its hydrophobic core) and hydrogen-bonding interactions [15–17], as have other studies [18,19]. Changes in retention and enantioselectivity with pH suggest that AGP is conformationally dynamic in nature [17].

More recently, Armstrong et al. [20] have introduced a new class of chiral selectors for liquid chromatography, macrocyclic antibodies. These LC stationary phases are multimodal in nature, demonstrating high enantioselectivity in both the normal- and reversed-phase modes. The macrocyclic antibodies possess the chemical diversity of the glycoproteins without irreversible denaturation of structure in nonpolar mobile-phase media. The enantioselectivity of these stationary phases was related to hydrophobic interactions (possibly inclusion into hydrophobic clefts of the antibodies) in the reversed-phase mode and related to hydrogen-bonding interactions in the normal-phase mode.

In this paper, we report the investigation of homopolypeptides as stationary-phase ligands for liquid chromatography. Homopolypeptides are analogous to proteins in their primary structure, existing as linear polymers of covalently bonded amino acids. Under the appropriate experimental conditions, proteins and peptides exist in ordered secondary structures, such as $\alpha$-helices and extended $\beta$-strands or $\beta$-sheets. In contrast to proteins, homopolypeptides consist of a repeating sequence of the same amino acid, and tend to exist in predominantly one conformation. For this reason, synthetic homopolypeptides have been used extensively as physicochemical models of protein folding [21–23]. In separation science, polylysine-coated glass beads have been used in biochemistry to isolate cell membranes [24]. Spherical particles of poly-$\gamma$-methyl-L-glutamate have been used as packing material for gel permeation separations of polysaccharide and polystyrene standards [25]. Alpert has extensively investigated amino acid homopolymers, polymerized in situ on the activated silica surface, as cation exchange stationary phases for the separation of peptides, proteins, nucleic acids and polar compounds [26–29]. In liquid chromatography, the homopolypeptide stationary phases may demonstrate the effect of protein secondary structure on mechanisms of solute retention. To our knowledge, this is the first report relating the conformation of the homopolypeptide ligands to retention and selectivity in liquid chromatographic separations. In fundamental studies of retention and selectivity, a knowledge of the chemical nature and corresponding conformational properties of the homopolypeptide should aid in understanding the mechanism of retention of solutes by the stationary phases. Since synthetic homopolypeptides are also chiral, they may show enantioselectivity for racemates in LC separations.

## 2. Experimental

### 2.1. Chemicals

HPLC-grade methanol (MeOH), chloroform ($CHCl_3$), tetrahydrofuran (THF), 1,4-dioxane, electronic-grade isopropanol (IPA), hexane, methylene chloride, ethyl ether, toluene, nitric acid, potassium hydroxide (KOH), molecular

sieves (Davison, 4 Å), triethylamine, phosphorus pentoxide ($P_2O_5$), 85% phosphoric acid and dibasic anhydrous potassium phosphate were obtained from Fisher Scientific (Fair Lawn, NJ, USA). Poly-L-lysine ($M_r$ 4600, $n = 22$), poly-β-benzyl-L-aspartate ($M_r$ 13 900, $n = 68$), poly-L-tyrosine ($M_r$ 13 900, $n = 85$ and $M_r$ 22 500, $n = 138$) and 4-dimethylaminopyridine (4-DMAP) were obtained from Sigma (St. Louis, MO, USA). Deuterium oxide, β-mercaptoethanol and solid sodium were obtained from Aldrich (Milwaukee, WI, USA). Flavanones were obtained from Indofine (Belle Meade, NJ, USA). γ-Glycidoxypropyltrimethoxysilane, γ-glycidoxypropyldimethylethoxysilane and trimethylchlorosilane were obtained from Huls (Bristol, PA, USA). THF was dried over and distilled from solid sodium immediately before use. Methylene chloride was dried over and distilled from $P_2O_5$ immediately before use. Toluene was dried and stored over oven-dried 4-Å molecular sieves. All of the above chemicals were reagent-grade and used without further purification, unless otherwise noted. Distilled water obtained in-house was further purified using a Barnstead Nanopure II system (Barnstead, Boston, MA, USA) fitted with a 0.45-μm filter. Buffers were prepared with Barnstead water, dibasic potassium phosphate and 85% phosphoric acid. The pH was adjusted using a Corning pH meter (Model 125; Corning Glass Co., Corning, NY, USA). Solvents used in mobile-phase compositions that were not HPLC-grade were filtered before use with 0.45-μm filters (Micro Separations). Mobile-phase solvents were degassed by sparging with helium (Wright Brothers, Cincinnati, OH, USA) and mixed in the appropriate proportions by a ternary pump. Bare silica was obtained from Phase Separations (Norwalk, CT, USA) and epoxide-activated silica (Hydropore EP) was obtained from Rainin Instrument Co. (Woburn, MA, USA).

### 2.2. Synthesis equipment

Glassware for silanization reactions was pretreated with 5% (by volume) trimethylchlorosilane in chloroform for at least 4 h. Reactions requiring an anhydrous atmosphere were carried out in an air-tight glove box, constructed in-house from 1/4-inch-thick Plexiglas (Cincinnati Plastics, Cincinnati, OH, USA). The glove box was purged with dry nitrogen (Wright Brothers, Cincinnati, OH, USA) for at least 1 h prior to mixing the reagents. Nitrogen was dried by passing the gas through a tube filled with Drierite desiccant (W.A. Hammond Drierite, Xenia, OH, USA) just prior to entering the glove box. Distillation of methylene chloride, gentle agitation of trimethylsilanization reactions and acid washing of silica were accomplished using a rotary evaporator (Model RE121, Buchi Laboratoriums Technik, Flawil, Switzerland). Epoxide-blocking reactions were agitated using a laboratory stirrer (Model 106, T-Line Co., Emerson, NJ, USA) with an attached variable voltage regulator (Talboys Engineering Corp., Emerson, NJ, USA) and an adapter constructed in-house to hold the reaction vessel. Glassware, drying agents, silicas and some reactants were dried in Isotemp vacuum ovens (Model 281A, Fisher Scientific, Fair Lawn, NJ, USA). Epoxidations and peptide coupling reactions were heated in a mineral oil bath. Silicas were efficiently rinsed in polyallomer and PTFE bottles (Nalge, Rochester, NY, USA) of 250 ml capacity using a Sorvall centrifuge (Model Dupont RC5C, Sorvall Instruments). Volumes less than 1 ml were measured using an automatic electronic digital Pipetman (Rainin Instrument Co., Woburn, MA, USA).

### 2.3. Stationary-phase synthesis

Homopolypeptides were covalently bonded to epoxide-activated microparticulate silica, both pre-activated and activated in-house, under the appropriate solvent and temperature conditions as shown in Fig. 1. Stationary-phase identification and reaction conditions are given in Table 1. Further details of the synthesis of these stationary phases are described below. Percent elemental analyses were performed by Robertson Microlit Laboratories (Madison, NJ, USA).

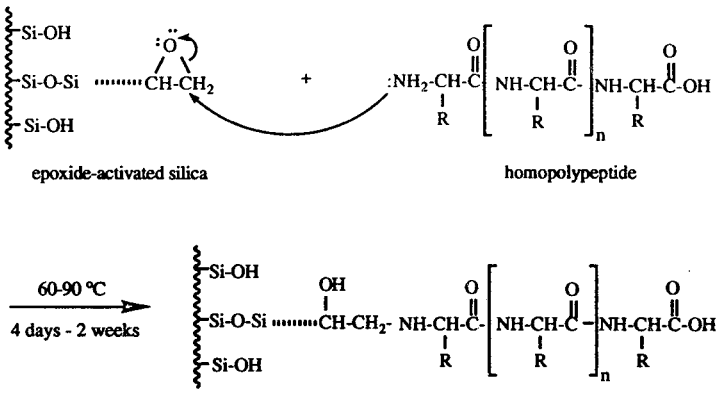


Fig. 1. The coupling of a homopolypeptide to epoxide-activated silica, where R is the amino acid sidechain group and $n + 2$ is the mean degree of polymerization of the homopolypeptide.

*Silica pretreatment*

Microparticulate silica (10 g) was added to 0.1 *M* nitric acid (100 ml) and heated at 90°C for 24 h under atmospheric conditions on a rotary evaporator. The silica was rinsed to neutrality (tested using pH paper) with Barnstead-purified water and then with two volumes of methanol to facilitate air-drying. The silica was dried under vacuum (30 inches of Hg) at 240°C for at least 4 h immediately prior to monomeric silanization reactions. Molar excesses of reagents for silanization reactions were calculated according to Eq. 1, assuming 5 $\mu$mol/m$^2$ sterically accessible silanol groups:

$$(5 \cdot 10^{-6})(\text{S.A.})(\text{g})(M_r) = \text{one molar excess} \quad (1)$$

where S.A. is the specific surface area of the silica (m$^2$/g), g is grams of silica reacted and $M_r$ is the molecular mass of the silane (g/mol).

*Monomeric epoxide silanization*

The following reagents were added to a 250-ml round-bottom flask under a dry nitrogen atmos-

Table 1
Reaction conditions for the covalent attachment of homopolypeptides to epoxide-activated silicas

| Stationary phase identification | Ligand | Epoxide-activated Silica | Reaction conditions | | |
|---|---|---|---|---|---|
| | | | Time (days) | Solvent | Temperature (°C) |
| PL22-R | PL, $n = 22$ | Hydropore EP[a] | 5 | pH 7.5, phosphate buffer | 60 |
| PBA68-R | PBA, $n = 68$ | Hydropore EP[a] | 5 | $CHCl_3$ | 65 |
| PT85-R | PT, $n = 85$ | Hydropore EP[a] | 5 | THF | 65 |
| PT138-M | PT, $n = 138$ | Phase Separations[b] with monomeric activation[c] | 15 | THF | 65 |
| PT138-P | PT, $n = 138$ | Phase Separations[b] with polymeric activation[d] | 15 | THF | 65 |

[a] Particle diameter = 12 $\mu$m, nominal pore diameter = 300 Å, surface area = 74 m$^2$/g.
[b] Particle diameter = 5 $\mu$m, nominal pore diameter = 300 Å, surface area = 109 m$^2$/g.
[c] 1.97 $\mu$mol epoxide/m$^2$.
[d] 1.94 $\mu$mol epoxide/m$^2$.

phere in order: vacuum-dried, acid-washed silica (5 g); a four-fold molar excess of γ-glycidoxypropyldimethylethoxysilane, 8 μl triethylamine (dried over oven-dried KOH for 24 h); and 50 ml toluene (dried over 4-Å oven-dried molecular sieves for 24 h). The mixture was swirled, quickly connected to a continuously nitrogen purging condenser apparatus and heated at 90°C in an oil bath with magnetic stirring for 16 h. The mixture was removed and rinsed with three 50-ml volumes each of toluene, tetrahydrofuran and methanol, then air-dried overnight. Percent elemental carbon was determined and the surface density (μmol/m$^2$) of epoxide functionalities was calculated using Eq. 2:

$$\frac{\mu\text{mol}}{\text{m}^2} = \frac{(\%\text{C})(10^6)}{(\text{S.A.})(n_c)(12.001)\left[100 - \frac{\%\text{C}}{(n_c)(12.001)}(M_r)\right]} \quad (2)$$

where S.A. is the specific surface area of the silica, $n_c$ is the number of carbon atoms in the ligand and $M_r$ is the molecular mass of the ligand minus the molecular mass of the leaving group. Epoxide-activated silica was vacuum-dried (30 inches of Hg) at 125°C for at least 4 h immediately prior to endcapping.

*Polymeric epoxide silanization*

A 5% (by volume) aqueous solution of γ-glycidoxypropyltrimethoxysilane was prepared by simultaneous dropwise addition of the silane and 0.01 *M* KOH into Barnstead-purified water, maintaining solution pH between 5.0 and 6.5 (tested using pH paper). This solution (10 ml) was then added to air-dried, acid-washed silica (5 g) in a 250-ml round-bottom flask and heated at 90°C under atmospheric conditions in an oil bath with magnetic stirring for 16 h. The mixture was removed and thoroughly rinsed with Barnstead-purified water and then with methanol to facilitate air-drying overnight. The epoxide-activated silica was dried under vacuum (30 inches of Hg) at 125°C for at least 4 h immediately prior to endcapping. Percent elemental carbon was determined and the surface density of epoxide functionalities was calculated using Eq. 2.

*Deactivation of residual silanol groups*

The following reagents were added to a 250-ml round-bottom flask under a dry nitrogen atmosphere in order: vacuum-dried silica; a two-fold molar excess of trimethylchlorosilane; a four-fold molar excess of 4-dimethylaminopyridine; and 100 ml methylene chloride (dried over and distilled from $P_2O_5$, under dry nitrogen). The mixture was swirled and quickly connected to a continuously nitrogen-purging condenser and heated in a mineral oil bath at 28°C for 24 h. The mixture was then removed and rinsed with three 100-ml volumes each of methylene chloride, methanol, 50:50 (v/v) methanol–water, methanol and ethyl ether and allowed to air-dry.

*Polypeptide coupling*

A solution of polypeptide and organic solvent or buffer was added to Rainin Hydropore EP silica or epoxide-activated Phase Separations silica (5 μm in diameter) to create a concentrated slurry (approximately 2 ml solvent or buffer per gram of silica) in a dry-nitrogen purged glove box. Each silica was previously vacuum-dried (30 inches of Hg) at 125°C for at least 4 h. The mixture was heated to the appropriate temperature in an oil bath for 4 days to 2 weeks to achieve the desired ligand coverage with continuous nitrogen purging and occasional manual agitation. Percent elemental nitrogen was determined and the surface density (μmol/m$^2$) of homopolypeptide was calculated using Eq. 3:

$$\frac{\mu\text{mol}}{\text{m}^2} = \frac{(\%\text{N})(10^6)}{(\text{S.A.})(n_N)(14.0067)\left[100 - \frac{\%\text{N}}{(n_N)(14.0067)}(M_r)\right]} \quad (3)$$

where S.A. is the specific surface area of the silica, $n_N$ is the number of nitrogen atoms in the ligand and $M_r$ is the molecular mass of the ligand minus the molecular mass of the leaving group.

*Deactivation of residual epoxide functionalities*

Polypeptide-bonded silicas were agitated on a rotary evaporator with 1 *M* β-mercaptoethanol (adjusted to pH 8.0 with phosphoric acid, tested using a pH meter) under atmospheric conditions for 2 h at 25°C. The reaction mixture was then rinsed thoroughly to neutrality (using pH paper) with three 50-ml volumes of Barnstead-purified water and then rinsed with two 50-ml volumes of methanol to facilitate air-drying.

*Column packing procedure*

Unreacted Rainin Hydropore EP silica and homopolypeptide-bonded silicas were suspended in $CHCl_3$ (approximately 2 g of silica per 50 ml $CHCl_3$) and the slurry was degassed by immersing in an ultrasonic bath for 15 min. The slurry was then transferred to the precolumn assembly of an air-driven fluid pump. Compressed air (Wright Brothers, Cincinnati, OH, USA) was applied at 60 p.s.i. to deliver 300 ml 50:50 (v/v) $CHCl_3$–MeOH, 300 ml each of MeOH and 200 ml 50:50 (v/v) MeOH–$H_2O$ sequentially through the stainless-steel column and then to waste. Chiraspher (EM Science, Darmstadt, Germany), a commercial chiral stationary phase, and Rainin Hydropore EP epoxide-activated silica were used as reference stationary phases. Ligand coverages of the stationary phases and dimensions of the columns used are shown in Table 2.

*2.4. Chromatographic equipment and analysis*

The chromatographic system consisted of a Spectra-Physics ternary pump (Model SP8800, ThermoSeparations, San Jose, CA, USA), a VICI 6-port injector (Valco Instruments Co., Houston, TX, USA) fitted with a 20-μl injection loop and a TosoHaas variable-wavelength detector (Model TSK-6041, Philadelphia, PA, USA). Two stainless-steel columns were positioned in series before the injector; a static mobile-phase mixer column (80 × 4.6 mm, packed with stainless-steel ball bearings) and a 12 cm × 4.6 mm I.D. column hand-packed with 10 μm, 300 Å PhaseSep silica (Phase Separations, Norwalk, CT, USA). The latter column maintained system back pressure above 300 p.s.i. for optimal pump performance. Both columns before the injector and the analytical column placed after the injector were water-jacketed and were temperature-controlled using a Fisher Scientific Isotemp refrigerated circulator (Model 9100, Fisher Scientific, Fair Lawn, NJ, USA) circulating a mixture of 50:50 (v/v) methanol–water. The column was allowed to equilibrate to temperature for 1 h prior to data collection. Flavanones were dissolved in hexane for normal-phase separations and dissolved in HPLC-grade methanol and mixed with Barnstead-purified water to match the mobile-phase composition for reversed-phase separations. Sample solutions ($10^{-4}$ *M*) were

Table 2
Stationary-phase identification, surface coverage for homopolypeptide stationary phases and column dimensions for LC experiments

| Stationary phase identification | Surface coverage (μmol/m²) | | Stationary phase deactivated?[a] | Column dimensions (mm) |
|---|---|---|---|---|
| | Homopolypeptide | Amino acid | | |
| Rainin | – | – | no | 60 × 4.6 |
| PL22-R | 0.064 | 1.4 | no | 100 × 4.6 |
| PBA68-R | 0.10 | 6.8 | no | 250 × 4.6 |
| PT85-R | 0.061 | 5.2 | no | 250 × 4.6 |
| PT138-M | 0.040 | 5.5 | yes | 150 × 4.6 |
| PT138-P | 0.025 | 3.4 | yes | 150 × 4.6 |
| Chiraspher | – | – | – | 250 × 4.6 |

[a] Refers to deactivation of residual silanol groups and residual epoxide functionalities.

filtered through 0.45-$\mu$m porosity nylon Aerodisc filters (Gelman Sciences, Ann Arbor, MI, USA). Each solute was injected in duplicate and the average capacity factor was reported. Data were collected using Turbochrom 3.1 software (PE Nelson, Cupertino, CA, USA) installed on a 486 PC with a CTX color monitor (Integrity Computers and Electronics, Cincinnati, OH, USA) with a Series 900 PE Nelson interface (PE Nelson, Cupertino, CA, USA). For the majority of experiments, a flow-rate of 2 ml/min was used, columns were maintained at 20°C and solutes were detected at 254 nm. Deuterium oxide was injected to determine the column void time, $t_0$. Capacity factors, $k'$, were calculated based on the retention time of the solute $t_r$ relative to $t_0$:

$$k' = \frac{t_r - t_0}{t_0} \quad (4)$$

Selectivity values were calculated as ratios of capacity factors.

## 3. Results and discussion

The monomers of the three homopolypeptides chosen for this study, poly-L-lysine (PL), poly-$\beta$-benzyl-L-aspartate (PBA) and poly-L-tyrosine (PT) possessing hydrophilic, hydrophobic and amphiphilic properties, respectively, are shown in Fig. 2. The secondary structures of homopolypeptide ligands are not irreversibly denatured under polar or nonpolar solvent conditions. The application of such stationary phases under both normal- and reversed-phase mobile-phase conditions extends their usefulness in LC. Existing protein chiral stationary phases only operate in the reversed-phase mode.

Poly-L-lysine exists in three distinct conformations: $\beta$-sheet, right-handed $\alpha$-helix and unordered coil. Conformational transition from unordered coil to $\alpha$-helix occurs as a function of deprotonation of the ionizable amino sidechain groups ($pK_a = 10.5$) reducing electrostatic repulsion along the polypeptide [30–32]. The presence of salts shields the electrostatic repulsion and conformational transitions occur at pH values

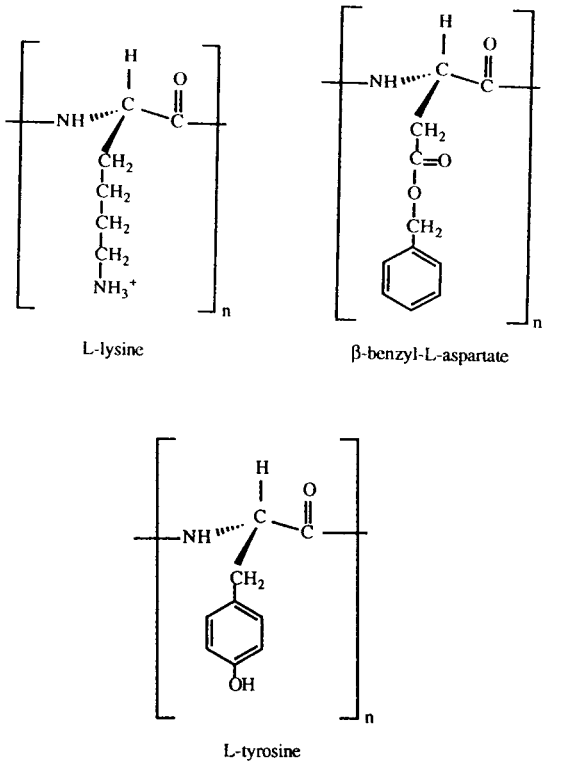


Fig. 2. The chemical structures of the homopolypeptides, where $n$ represents the mean degree of polymerization.

below the $pK_a$ [30]. In aqueous solutions above 40°C, the $\alpha$-helical conformation is converted to $\beta$-sheet structure [33]. High alcohol content in aqueous solutions favors the $\alpha$-helical formation even when the polypeptide is in the fully charged state [34,35]. Thus, it is suggested that PL would exist as an $\alpha$-helix in the normal-phase mobile-phase compositions used here. The PL ($n = 22$) lot used here may not be of sufficient length to form a stable secondary structure, however. In addition, it is likely that the PL was attached to the silica surface at multiple sites as both the amino terminus and the amino sidechain groups could react with the epoxide functionalities. The PL, therefore, would be able to undergo minor conformational transitions.

Due to steric interactions between sidechain groups and the amide backbone, poly-$\beta$-benzyl-L-aspartate may exist in a left-handed as well as a right-handed $\alpha$-helical conformation. PBA also

exists in β-sheet and unordered conformations. The homopolypeptide exists in the left-handed α-helical conformation in solvents such as chloroform and carbon tetrachloride [36–38]. The unordered conformation is obtained by the addition of strong organic acids [39,40] or dimethylsulfoxide [41]. PBA exists in the right-handed α-helical conformation in the solid state at room temperature [42]. By Fourier-transform infrared (FT-IR) spectroscopic studies, we have concluded that PBA, $n = 68$, exists in a right-handed α-helical conformation under reversed-phase mobile-phase conditions used in this investigation [43]. Based on literature reports, it is suggested that PBA also would exist in a right-handed α-helix in the normal-phase mobile-phase conditions used here.

Poly-L-tyrosine (PT) contains ionizable phenolic groups in its sidechains, rendering this polypeptide amphiphilic in nature. Therefore, the polypeptide may undergo conformational transitions based on the degree of ionization of the phenolic groups (electrostatic interactions) and according to aggregation of sidechain groups in aqueous/organic solvent mixtures (hydrophobic interactions). Three prominent conformations have been observed for this polypeptide: unordered, right-handed α-helical and β-sheet. PT undergoes an unordered to intramolecular antiparallel β-sheet conformational transition as pH is decreased over a narrow range (11.2 to 11.5), related to the $pK_a$ of the phenolic group [44,45]. In aqueous alcohol mixtures, conformational transitions between the β-sheet and the α-helical conformations are observed [46,47]. We have determined by FT-IR spectroscopic studies that PT, $n = 85$, undergoes a conformational transition between β-structure and an α-helix near 50% methanol in water [43]. It is assumed that PT, $n = 138$, would undergo the same conformational transition. Based on investigations in the literature it is suggested that each lot of PT exists in an α-helical conformation under the normal-phase mobile-phase conditions used here.

A set of flavanone derivatives was chosen as solutes to compare the fundamental retention and selectivity of the stationary phases under both normal- and reversed-phase mobile-phase conditions. The chemical structure of flavanone and identification of hydroxy- and methoxy-substituted derivatives used in this study are given in Table 3. Some flavanones are central intermediates in the synthesis of flavanoids, responsible for the coloration of plants, and others are secondary plant metabolites [48]. All the flavanones investigated here are chiral; they exist as pairs of nonsuperimposable optical isomers. Chiraspher was chosen as a reference stationary phase since a variety of optical isomers, including flavanones [49] have been resolved previously on this stationary phase in both the normal-phase mode [50,51] and the reversed-phase mode [52]. The chemical structure of the Chiraspher polymer differs from polypeptides in that it has a hydrocarbon backbone and its aromatic and amide groups exist as "sidechains" (Fig. 3).

### 3.1. Separation of flavanones in the reversed-phase mode

The capacity factors for the flavanones under reversed-phase mobile-phase compositions are given in Table 4. In order to obtain capacity factors of appropriate values, three different

Table 3
The structure of flavanone with positions labeled for derivative identification

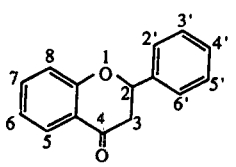


| Derivative | Identification |
|---|---|
| Flavanone | F |
| 2′-Hydroxy | 2′H |
| 4′-Hydroxy | 4′H |
| 7′-Methoxy | 7′M |
| 4′-Methoxy | 4′M |
| 5-Hydroxy-7-methoxy | 5H–7M |
| 4′,5-Dihydroxy-7-methoxy | 4′,5H–7M |

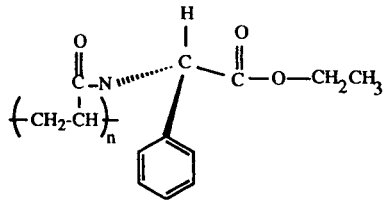

Fig. 3. The monomer of the Chiraspher stationary-phase polymer, N-acryloyl-(*S*)-phenylalanine ethyl ester.

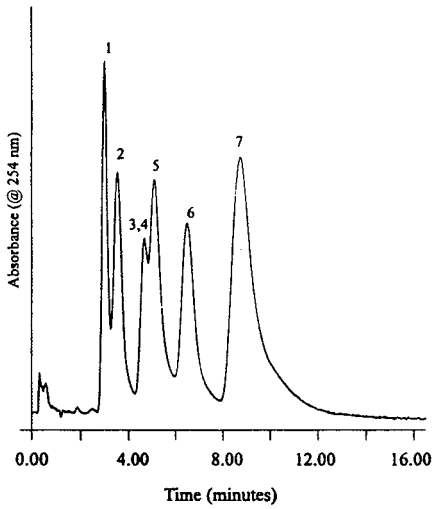


Fig. 4. The separation of the seven flavanones on the PT138-M stationary phase in 50:50 MeOH–$H_2O$ at 20°C and 2 ml/min. Peak identification: 1 = 4′-hydroxy-flavanone; 2 = 2′-hydroxy-flavanone; 3 = 4′,5-dihydroxy-7-methoxy-flavanone; 4 = flavanone; 5 = 4′-methoxy-flavanone; 6 = 7-methoxy-flavanone; 7 = 5-hydroxy-7-methoxy-flavanone.

MeOH–$H_2O$ mobile-phase compositions were used: 40:60 MeOH–$H_2O$ to compare the PBA and PT85-R stationary phases, 50:50 MeOH–$H_2O$ to compare the three PT stationary phases, and finally 60:40 MeOH–$H_2O$ to compare the PT85-R stationary phase with the Chiraspher stationary phase. A chromatogram of the seven flavanones on the PT138-M stationary phase at 50:50 MeOH–$H_2O$ is given in Fig. 4. Relative retention plots were constructed from calculated capacity factors in order to compare the stationary phases for the retention of flavanones in the same mobile-phase composition and at the same temperature. The linearity of relative retention plots suggests that each solute in the set is being retained by a similar mechanism on each stationary phase. Deviation from a slope equal to one indicates that differences exist in the relative loadings, structure or chemical nature of the two stationary-phase ligands.

The PBA and PT stationary-phase ligands differ from many stationary-phase ligands used in RPLC in that they contain polar functionalities in addition to hydrophobic aryl groups. A relative retention plot for the two phases for the separation of the flavanones is shown in Fig. 5. The solutes were retained significantly longer on the PT85-R stationary phase than the PBA68-R stationary phase. Differences in retention based on the chemical nature of the activation groups may be discounted here since the same pre-activated silica was used in synthesizing each phase. Instead, differences in retention may

Table 4
Capacity factors for flavanone derivative pairs for specified stationary phases and MeOH–$H_2O$ mobile-phase compositions at 20°C

| Flavanone | Capacity factor | | | | | | |
|---|---|---|---|---|---|---|---|
| | PBA68-$R_{40:60}$ | PT85-$R_{40:60}$ | PT138-$P_{50:50}$ | PT85-$R_{50:50}$ | PT138-$M_{50:50}$ | PT85-$R_{60:40}$ | Chiraspher$_{60:40}$ |
| F | 0.639 | 7.85 | 2.64 | 3.16 | 3.95 | 1.25 | 5.30, 5.52 |
| 2′H | 0.618 | 4.71, 5.33 | 1.43 | 2.04 | 2.58 | 0.827 | 7.97 |
| 4′H | 0.444 | 3.83 | 1.21 | 1.63 | 1.91 | 0.687 | 5.02 |
| 7M | 0.743 | 12.1, 12.8 | 3.56 | 4.59 | 5.73 | 1.69 | 5.84, 6.20 |
| 4′M | 0.701 | 11.1 | 3.40 | 4.13 | 5.11 | 1.56 | 5.89, 6.05 |
| 5H–7M | 1.16 | 19.9 | 4.93 | 6.87 | 8.23 | 2.31 | 13.2, 13.7 |
| 4′,5H–7M | 0.757 | 9.31 | 2.22 | 3.39 | 3.81 | 1.27 | 13.2 |

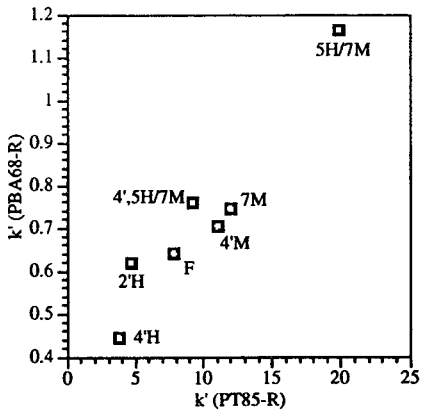


Fig. 5. Relative retention plot for flavanones on PT85-R and PBA68-R stationary phases in 40:60 MeOH–$H_2O$ mobile-phase composition at 20°C. Linear coefficient of determination ($r^2$) = 0.9111, slope ($m$) = 0.0388 and $1/m$ = 25.8.

reflect differences in inherent hydrophobicities of the constituent amino acids of the polypeptides. The elution orders of the flavanones on the two phases are similar and a high linear correlation exists in their relative retention plot. This may be related to their common structural feature, the amide backbone. Slight differences in elution order may, however, be attributed to differences in the chemical nature of the polypeptide sidechains. Each polypeptide contains polar functionalities in its sidechains; PT contains an ionizable *p*-phenolic group in each sidechain, and PBA an ester linkage. The phenolic group, however, is more polar, and hence may undergo more interactions with the flavanones. Alternatively, the polypeptide ligands may differ in their hydrogen-bonding capabilities, dictated by their secondary structures. Peptide conformations differ fundamentally in the extent of intramolecular hydrogen-bonding that they possess. Therefore as a chromatographic ligand, the polypeptide will be more or less able to hydrogen-bond to solutes based on its conformation at a particular mobile-phase composition. The PT ligand exists in a more extended conformation than the PBA ligand in this mobile-phase composition [43]. Therefore, more amide bonds along the polypeptide backbone are able to participate in hydrogen-bonding with the polar solutes. Also, the PT85-R phase demonstrated enantioselectivity for both the 2'-hydroxy- and 7-methoxy-flavanone derivatives under these chromatographic conditions, yielding selectivities of 1.13 and 1.06, respectively. Higher resolution of the chiral enantiomers was observed at lower column temperatures and slower mobile-phase flow-rates. The partial chiral resolution of 2'-hydroxy-flavanone at 40:60 MeOH–$H_2O$, 10°C and 1 ml/min is shown in Fig. 6. The aromatic group of L-tyrosine is in closer proximity to the chiral carbon center of the amino acid compared to β-benzyl-L-aspartate, facilitating chiral interactions of the solutes with PT [53]. The lower apparent efficiency of the homopolypeptide stationary phases in general may be related to the mass transfer of the solute through a noncovalent (hydrogen-bonded) polymeric network. In addition, the chromatographic ligands used here are much longer than those typically used in liquid chromatographic coatings. Longer homopolypeptides, able to form stable secondary structures, were most desirable for this investigation, however. Slow solute desorption rates have been observed also for protein stationary-phase ligands [54].

In comparing the three PT stationary phases for the retention of flavanones in the slightly stronger mobile-phase composition, an elution order reversal is observed on the PT85-R phase relative to the other PT stationary phases (Table

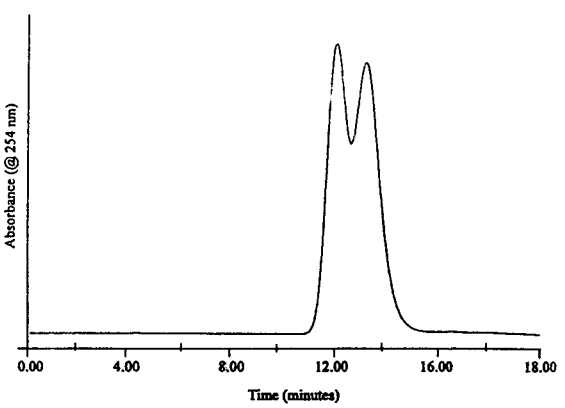


Fig. 6. The partial resolution of the 2'-hydroxy-flavanone optical isomers on the PT85-R stationary phase in 40:60 MeOH–$H_2O$ at 10°C and 1 ml/min.

4). Flavanone elutes before its tri-substituted derivative on the PT85-R phase but the opposite elution order is observed on the other PT phases. This may be due to the different activation chemistry of this phase (pre-activated Rainin Hydropore EP silica) compared to the two PT phases of more similar activation chemistries, synthesized in-house. Despite slight differences in retention due to the activation chemistries of the PT85-R phase and the PT138 phases, the flavanones appear to be retained by a similar retention mechanism overall (Figs. 7 and 8). Despite differences in total amino acid loadings, the PT138 phases retain the polar species by a similar mechanism as well (Fig. 9). The greatest correlation does exist, however, between the PT phases of more comparable amino acid loadings, PT85-R and PT138-M (Fig. 7). These observations suggest that retention on the polypeptide stationary phases is dominated by the total amino acid content of the phase and not the nature of activation groups (polymeric versus monomeric) or ligand length. The relative capacity factors of the PT phases do not correlate directly with relative tyrosine loadings of the stationary phases. A variety of interactions, both polar and nonpolar, complicate the retention mechanism of the flavanones on these stationary phases. At this slightly stronger mobile-phase composition, the PT phases were not able to discriminate optical isomers of the flavanones.

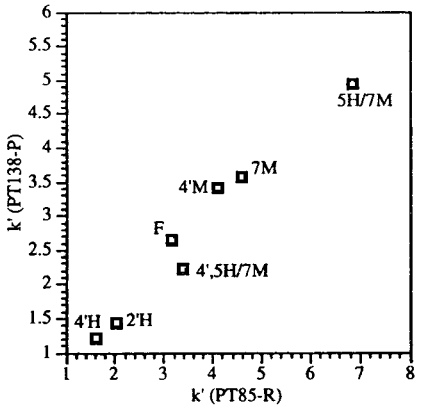


Fig. 8. Relative retention plot for flavanones on PT85-R and PT138-P stationary phases in 50:50 MeOH–$H_2O$ mobile-phase composition at 20°C. Linear coefficient of determination ($r^2$) = 0.9672, slope ($m$) = 0.732 and $1/m$ = 1.37.

The PT85-R stationary phase was then compared with the commercial chiral stationary phase, Chiraspher, for the retention of flavanones at an even stronger mobile-phase composition. Chiraspher preferentially retained the solutes, by a factor of approximately three. This is likely due to differences in the surface area of the base silicas or alternatively differences in the inherent hydrophobicities of the

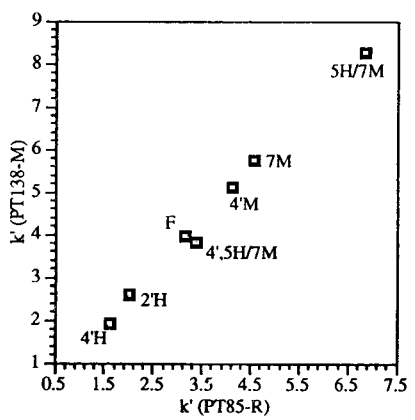


Fig. 7. Relative retention plot for flavanones on PT85-R and PT138-M stationary phases in 50:50 MeOH–$H_2O$ mobile-phase composition at 20°C. Linear coefficient of determination ($r^2$) = 0.9938 and slope ($m$) = 1.21.

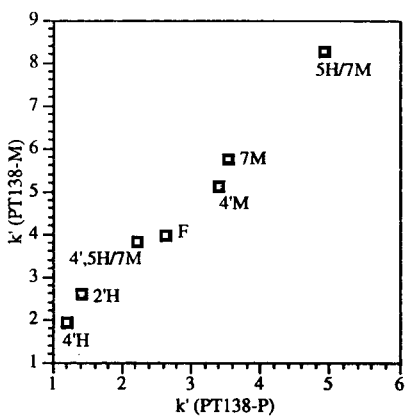


Fig. 9. Relative retention plot for flavanones on PT138-P and PT138-M stationary phases in 50:50 MeOH–$H_2O$ mobile-phase composition at 20°C. Linear coefficient of determination ($r^2$) = 0.9836 and slope ($m$) = 1.61.

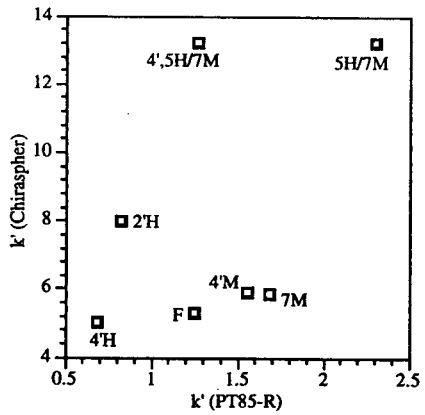


Fig. 10. Relative retention plot for flavanones on PT85-R and Chiraspher stationary phases in 60:40 MeOH–$H_2O$ mobile-phase composition at 20°C. Linear coefficient of determination ($r^2$) = 0.2227 and slope ($m$) 3.13.

ligands. PT has a polar amide backbone, whereas the Chiraspher ligand has a more hydrophobic hydrocarbon backbone. On both the PT85-R and Chiraspher stationary phases, 2'-hydroxyflavanone is retained least and 5-hydroxy-7-methoxy-flavanone is retained most. Otherwise, the elution orders of the flavanones on the two phases are significantly different, indicating the influence of the amide backbone structure. The differences in elution order are shown in Fig. 10, in the relative retention plot for the two stationary phases. These results suggest that the amide backbone of the PT phase may dramatically influence the separation of polar species. Therefore, significant differences would be anticipated in the retention mechanisms between PT stationary phases and traditional RPLC stationary phases containing phenyl or alkyl stationary phases.

The selectivity values calculated for pairs of flavanones give insight into the retention processes for polar aromatic solutes on these phases (Table 5). The PT85-R phase had greater methoxy- and hydroxy-selectivity than the PBA68-R phase, while comparable selectivities are found for the two phases in the separation of molecular mass isomers. All three PT phases had similar selectivities for the flavanone pairs, despite differences in length, activation chemistry, surface coverage of ligands and stationary-phase deactivation. The PT85-R stationary phase also demonstrated greater methoxy- and hydroxy-selectivities than the Chiraspher phase, but the Chiraspher was able to separate more optical isomer pairs under these experimental conditions.

### *3.2. Separation of flavanones in the normal-phase mode*

In comparing stationary phases, separations were performed in the same mobile-phase composition (92.5:6.0:1.5 hexane–1,4-dioxane–IPA) and at the same temperature (20°C). Thus, all differences in retention and selectivity are attributable to differences in stationary-phase properties. The mobile phase chosen for this

Table 5
Selectivity values for flavanone derivative pairs for specified stationary phases and MeOH–$H_2O$ mobile-phase compositions at 20°C

| Flavanone Pair | $\alpha$ | | | | | | |
|---|---|---|---|---|---|---|---|
| | PBA68-$P_{40:60}$ | PT85-$P_{40:60}$ | PT138-$P_{50:50}$ | PT85-$R_{50:50}$ | PT138-$M_{50:50}$ | PT85$R_{60:40}$ | Chiraspher$_{60:40}$ |
| 7M–F | 1.16 | 1.54 | 1.35 | 1.45 | 1.45 | 1.35 | 1.10 |
| 4'M–F | 1.10 | 1.41 | 1.29 | 1.29 | 1.29 | 1.25 | 1.11 |
| 2'H–4'H | 1.39 | 1.23 | 1.18 | 1.25 | 1.35 | 1.20 | 1.59 |
| 7M–4'M | 1.06 | 1.09 | 1.05 | 1.11 | 1.12 | 1.08 | 0.992 |
| F–4'H | 1.44 | 2.05 | 2.18 | 1.94 | 2.07 | 1.82 | 1.06 |
| F–2'H | 1.03 | 1.67 | 1.85 | 1.55 | 1.53 | 1.51 | 0.665 |
| 4',5H–7M/5H–7M | 1.53 | 2.13 | 2.22 | 2.03 | 2.16 | 1.82 | 1.00 |

investigation was similar to that used previously for the separation of flavanones on Chiraspher [49].

The capacity factors for the seven flavanones on the various homopolypeptide, Rainin and Chiraspher stationary phases are given in Table 6. The elution order for this set of compounds was the same on the four homopolypeptide stationary phases and two reference stationary phases. Also, there is approximately an order of magnitude difference in retention for flavanone and the 5-hydroxy-7-methoxy-, 4′-methoxy- and 7-methoxy-flavanone derivatives versus 2′-hydroxy-, 4′-hydroxy- and 4′,5-dihydroxy-7-methoxy-flavanone derivatives. A chromatogram of the separation of the seven flavanones on the PT138-M stationary phase in 92:6:2 hexane–1,4-dioxane–IPA is given in Fig. 11. This stationary phase was synthesized using silica activated in-house. The homopolypeptide stationary phases, PL22-R, PBA68-R and PT85-R were synthesized using Rainin Hydropore EP preactivated silica. Therefore, retention of the flavanones on the Rainin silica was included to determine the contribution of its hydrophilic polymeric activation groups, of proprietary chemical structure, to the retention of polar solutes under normal-phase conditions. Low retention of the flavanones is observed on the Rainin silica in comparison with the polypeptide phases; retention is more significant on the Rainin silica for the 2′-hydroxy-, 4′-hydroxy- and 4′,5-dihydroxy-7-methoxy-flavanone derivatives.

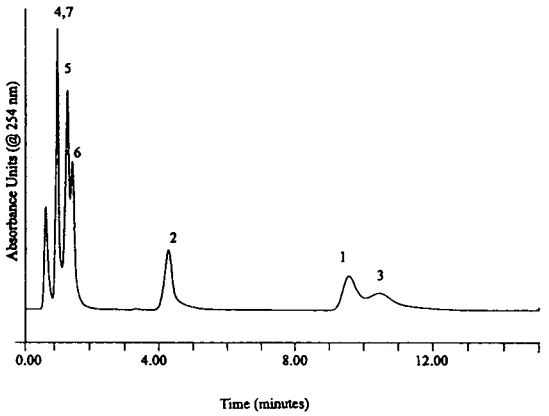


Fig. 11. The separation of the seven flavanones on the PT138-M stationary phase in 92:4:2 hexane–1,4-dioxane–IPA at 20°C and 2 ml/min. Peak identification is the same as that given in Fig. 4. The first peak is the system peak.

All of the polypeptide phases were able to retain polar species due to interactions with their polar amide backbones. Retention of the flavanones on the homopolypeptide-bonded stationary phases in the normal-phase mode is expected to increase with increasing polarity of the homopolypeptide according to the following trend, PBA < PT < PL. This trend in retention is most pronounced for the hydroxy-containing flavanones. Differences in the relative retention of polar species on the PL22-R, PBA-68-R and PT85-R stationary phases may be related to differences in the chemical structure of their sidechains. In addition, differences in their secondary structures, due to the amount of hydro-

Table 6
Capacity factors for flavanones on Rainin Hydropore EP silica, various homopolypeptide and Chiraspher stationary phases in 92.5:6.0:1.5 hexane–1,4-dioxane–IPA mobile-phase composition at 20°C

| Flavanone | Capacity factor | | | | | |
|---|---|---|---|---|---|---|
| | Rainin | PL22-R | PBA68-R | PT85-R | PT138-M | Chiraspher |
| F | 0.0645 | 0.270 | 0.272 | 0.713 | 0.677 | 1.00, 1.09 |
| 2′H | 0.548 | 10.1 | 2.28 | 3.67 | 4.05 | 13.3, 14.3 |
| 4′H | 0.935 | 13.6 | 4.00 | 7.75 | 7.84 | 26.5, 27.6 |
| 7M | 0.129 | 0.492 | 0.503 | 1.50 | 1.33 | 1.88, 2.04 |
| 4′M | 0.0968 | 0.413 | 0.435 | 1.19 | 1.04 | 1.69, 1.80 |
| 5H–7M | 0.0968 | 0.381 | 0.388 | 0.880 | 0.785 | 1.55, 1.63 |
| 4′,5H–7M | 1.06 | 18.8 | 5.35 | 9.41 | 8.77 | 40.3 |

gen-bonding along the polypeptide backbone, may affect the retention of polar species.

PL22-R demonstrated greater retention for most of the hydroxy-containing flavanones than would be predicted based on its relative loading of total amino acid. This may be related to the additional primary amino groups of strongly basic nature in the sidechains of PL. As with amino-bonded phases, there is strong affinity for the acidic hydroxy groups [55,56]. Alternatively, these primary amino functionalities may contribute to enhanced hydrogen-bonding with the solutes. As stated previously, based on reports in the literature, the PL lot used here would exist in an unordered coil in such nonpolar conditions. This more extended conformation would also contribute to the hydrogen-bonding ability of the stationary-phase ligand.

The PBA68-R stationary phase had significantly lower retention for the flavanones than would be predicted based on its high coverage of total amino acid. The ether linkage in the sidechain of PBA must only be slightly basic in nature compared to a primary amino group, lowering the overall retention for this stationary phase under normal-phase conditions [57]. In addition, charged ligands such as PL and PT tend to be more polar than uncharged ligands such as PBA. Since the chemical structure of PBA is remarkably similar to that of Chiraspher, the lower retention on PBA68-R phase may be related to a higher surface coverage of ligands or higher specific surface area for the Chiraspher phase. Alternatively, the lower retentivity of the PBA68-R stationary phase may be related to its secondary structure. As stated previously, based on reports in the literature, the PBA lot used here would exist predominantly in a right-handed $\alpha$-helical conformation in the nonpolar mobile phase. This secondary structure has a significant amount of hydrogen-bonding along the polypeptide backbone, possibly contributing to the low retentive properties of this stationary phase. Such polar interactions are accentuated under nonpolar normal-phase mobile-phase conditions.

The PT85-R stationary phase contains ionizable hydroxyl groups in its sidechains. These groups are expected to be slightly acidic in nature, similar to diol-bonded phases. Therefore, one would expect lower retentivity due to charge repulsion for the potentially negatively charged PT stationary phases with potentially negatively charged flavanones. The higher retentivity of this stationary phase then may reflect the importance of hydrogen-bonding interactions. Alternatively, the relatively high retention for this stationary phase may be related to its conformation. Based on reports in the literature, PT ($n = 85$) would predominantly exist in intramolecularly hydrogen-bonded antiparallel single $\beta$-sheet structure in more nonpolar solvents. This polypeptide conformation is more extended than $\alpha$-helical conformation with less intramolecular hydrogen-bonding. Therefore, its amide backbone groups would contribute more significantly to retention of polar species than that observed for the PBA stationary phase.

The PT138-M stationary phase was synthesized from silica activated with a monofunctional glycidoxypropylsilane under anhydrous conditions forming a monomeric structure. No significant differences were observed in retention for this stationary phase and the PT85-R stationary phase with polymeric activation. Both homopolypeptides should exist in the same secondary structure under these mobile-phase conditions. In addition, PT138-M was endcapped by deactivating the residual hydroxyl groups on the silica surface with hydrophobic trimethyl functionalities.

As noted in the literature, under similar mobile-phase conditions the Chiraspher stationary phase was able to separate six of the seven flavanones into their optical isomers [49]. The homopolypeptide phases did not demonstrate chiral selectivity, however, since their aromatic groups are more removed from the chiral center of the polymer than in the chemical structure for the Chiraspher polymer. Close proximity of an aromatic functionality to the chiral center of a selector allows more favorable chiral interactions [53].

Since an order of magnitude difference in retention existed for this set of data, probably due to large differences in solute polarity, the

data will be referred to as two sets in order to emphasize individual retention effects. Set A includes flavanone and the 5-hydroxy-7-methoxy-, 4′-methoxy- and 7-methoxy-flavanone derivatives. Set B includes the more polar 2′-hydroxy-, 4′-hydroxy- and 4′,5-dihydroxy-7-methoxy-flavanone derivatives.

Overall, the PT85-R phase is the most retentive of the four homopolypeptide stationary phases for set A flavanones. The enhanced retention of this set of solutes displayed by the PT85-R phase may be related to hydrogen-bonding interactions with the phenolic sidechain group of this amphiphilic stationary phase. The PBA68-R and PL22-R phases show parallel behavior for retention of set A flavanones. This suggests that the retention of these four flavanones is dominated by the amide bonds of the polypeptide backbone, their common structural feature. The presence of aromatic functionalities in the PBA stationary phases may not significantly affect retention of these compounds. The PL22-R stationary phase is the most retentive of the set B flavanones of the four homopolypeptide phases. The basic nature and hydrogen-bonding ability of the primary amino group sidechains of PL may be a dominant factor in retaining the more acidic polar solutes. There is a high linear correlation between the PBA68-R stationary phase and Chiraspher stationary phase for the retention of all seven flavanones (Fig. 12). This is not surprising, however, due to the great similarity in chemical structure of their corresponding ligands.

The selectivity values for flavanone pairs are given in Table 7. The PL, PBA and PT ligands had similar methoxy-selectivity that appeared to be position-dependent. In addition, all the homopolypeptide phases were able to discriminate molecular mass isomers. The selectivity is greater between the more polar pair of hydroxy-flavanone derivatives versus the methoxy-flavanone derivatives. In terms of hydroxy-selectivity, differences in stationary-phase properties became apparent. As expected, due to the basic nature and hydrogen-bonding ability of the amino sidechain groups of PL, the PL22-R phase demonstrated the greatest hydroxy-selectivity.

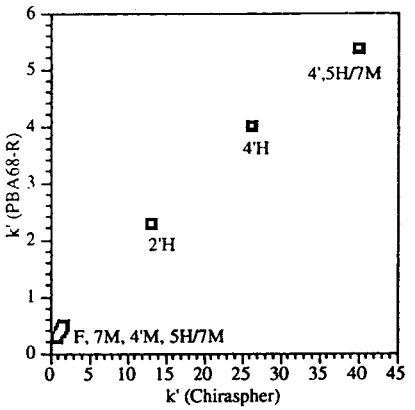


Fig. 12. Relative retention plot for flavanones on the PBA68-R stationary phases versus the Chiraspher stationary phase in 92.5:6.0:1.5 hexane–1,4-dioxane–IPA mobile-phase composition at 20°C. Linear coefficient of determination ($r^2$) = 0.9921, slope ($m$) = 0.132 and $1/m$ = 7.58.

The PT phases demonstrated the least hydroxy-selectivity and this was anticipated due to the acidic nature of its phenolic sidechain groups. Even though the PBA68-R phase had the lowest retention of the three types of polypeptide phases, the PBA68-R stationary phase showed intermediate hydroxy-selectivity.

## 4. Conclusions

The retention mechanism for the homopolypeptide stationary phases under reversed-phase conditions primarily involves hydrophobic interactions between the solutes and the aromatic rings of the ligands. The sidechain chemistry of the homopolypeptide determines its overall hydrophobicity. Elution orders varied for the stationary phases especially between the Chiraspher and PT stationary phases and all the flavanones eluted within the same order of magnitude.

In contrast to reversed-phase conditions, the retention of the solutes was "normalized" for the overall polarity of the phases under normal-phase conditions due to the amide backbone common to each ligand. The same elution order for the flavanones was observed for all the

Table 7
Selectivity values for flavanone derivative pairs on specified stationary phases in 92.5:6.0:1.5 hexane–1,4-dioxane–IPA mobile-phase composition at 20°C

| Flavanone pair | $\alpha$ | | | | |
|---|---|---|---|---|---|
| | PL22-R | PBA68-R | PT85-R | PT138-M | Chiraspher |
| 7M–F | 1.82 | 1.85 | 2.10 | 1.96 | 1.88 |
| 4'M–F | 1.53 | 1.60 | 1.67 | 1.54 | 1.69 |
| 4'H–2'H | 1.35 | 1.75 | 2.11 | 1.94 | 1.99 |
| 7M–4'M | 1.19 | 1.16 | 1.26 | 1.28 | 1.11 |
| 4'H–F | 37.4 | 8.38 | 5.15 | 5.98 | 13.3 |
| 2'H–F | 50.4 | 14.7 | 10.9 | 11.6 | 26.5 |
| 4',5H–7M/5H–7M | 49.3 | 13.8 | 13.8 | 11.2 | 26.0 |

homopolypeptide stationary phases and the Chiraspher stationary phase. In addition, the separation of the flavanones under normal-phase conditions was highly sensitive to the polarity of the solutes as they eluted in two distinct groups whose capacity factors differed by an order of magnitude. Under nonpolar mobile-phase conditions, polar interactions between the ligand and the solute are enhanced. Both modes of liquid chromatography allowed the separation of flavanone molecular mass isomers. Hydroxy-, methoxy- and molecular mass isomer selectivities were higher under normal-phase conditions, however. Sidechain chemistries of the homopolypeptides played a dominant role in retention processes.

The stationary phases derivatized with PT offer great potential in future applications, especially in the separation of polar solutes. Shorter homopolypeptide ligands are recommended for separations of higher efficiency, however. In comparison with PBA and PL phases, the PT phases were able to retain solutes strongly under both normal- and reversed-phase conditions. The PT phases demonstrated chiral selectivity under reversed-phase conditions as well. These chiral recognition properties of the PT phases should be more fully investigated and applied to the separation of other racemic mixtures. In an additional practical application of these stationary phases, their low retentivity may lead to their use in hydrophobic interaction chromatography. The advantage of amphiphilic PT stationary-phase ligand is that it may be used in hydrophilic interaction chromatography as well for less polar biomolecules such as histones, membrane proteins and phosphorylated amino acids and peptides.

## Acknowledgements

The authors would like to thank Dr. A.H. Pinhas for helpful discussions during the synthesis of the homopolypeptide stationary phases, Dan DeVido for assistance in obtaining some chromatograms, EM Science for kindly donating the Chiraspher LC column, and the National Institutes of Health (GM-48561) for financial support for this project.

## References

[1] J.F. Wheeler, T.L. Beck, S.J. Klatte, L.A. Cole and J.G. Dorsey, J. Chromatogr. A, 656 (1993) 317–333.
[2] L.C. Sander and S.A. Wise, CRC Crit. Rev. Anal. Chem., 18 (1987) 299–415.
[3] D.E. Martire and R.E. Boehm, J. Phys. Chem., 87 (1983) 1045–1062.
[4] M.E. Montgomery Jr. and M.J. Wirth, Anal. Chem., 66 (1994) 680–684.
[5] H. Yuki, Y. Okamoto and I. Okamoto, J. Am. Chem. Soc., 102 (1980) 6358–6359.
[6] Y. Okamoto, I. Okamoto and H. Yuki, Chem. Lett., (1981) 835–838.
[7] Y. Okamoto and K. Hatada, J. Liq. Chromatogr., 9 (1986) 369–384.

[8] S. Allenmark, B. Bomgren and H. Boren, J. Chromatogr., 264 (1983) 63–68.
[9] S. Allenmark, B. Bomgren and H. Boren, J. Chromatogr., 316 (1984) 617–624.
[10] S. Allenmark, J. Liq. Chromatogr., 9 (1986) 425–442.
[11] S. Allenmark, S. Andersson and J. Bojarski, J. Chromatogr., 436 (1988) 479–483.
[12] S. Andersson and S. Allenmark, J. Liq. Chromatogr., 12 (1989) 345–357.
[13] R.K. Gilpin, S.E. Ehtesham and R.B. Gregory, Anal. Chem., 63 (1991) 2825–2828.
[14] J. Hermansson, J. Chromatogr., 269 (1983) 71–80.
[15] J. Hermansson, J. Chromatogr., 298 (1984) 67–78.
[16] G. Schill, I.W. Wainer and S. Barkan, J. Liq. Chromatogr., 9 (1986) 641–666.
[17] J. Hermansson and M. Eriksson, J. Liq. Chromatogr., 9 (1986) 621–639.
[18] T.L. Kirley, E.D. Sprague and H.B. Halsall, Biophys. Chem., 15 (1982) 209–216.
[19] M.L. Friedman, K.T. Schlueter, T.L. Kirley and H.B. Halsall, Biochem. J., 232 (1985) 863–867.
[20] D.W. Armstrong, Y. Tang, S. Chen, Y. Zhou, C. Bagwill and J. Chen, Anal. Chem., 66 (1994) 1473–1484.
[21] G.D. Fasman, in G.D. Fasman (Editor), Poly-$\alpha$-amino Acids, Marcel Dekker, New York, NY, 1967, pp. 499–604.
[22] J. Yang, C.S. Wu and H.M. Martinez, Methods Enzymol., 130 (1986) 208–269.
[23] S. Song and S.A. Asher, J. Am. Chem. Soc., 111 (1989) 4295–4305.
[24] D.I. Kalish, C.M. Cohen, B.S. Jacobson and D. Branton, Biochim. Biophys. Acta, 506 (1978) 97–110.
[25] C. Hirayama and H. Ihara, J. Chromatogr., 347 (1985) 357–361.
[26] A.J. Alpert, J. Chromatogr., 266 (1983) 23–37.
[27] A.J. Alpert, J. Chromatogr., 359 (1986) 85–97.
[28] A.J. Alpert and P.C. Andrews, J. Chromatogr., 443 (1988) 85–96.
[29] A.J. Alpert, J. Chromatogr., 499 (1990) 177–196.
[30] J. Applequist and P. Doty, in M.A. Stahmann (Editor), Polyamino Acids, Polypeptides and Proteins, The University of Wisconsin Press, Madison, WI, 1962, pp. 161–177.
[31] S. Yu. Venyaminov and N.N. Kalnin, Biopolymers, 30 (1990) 1259–1271.
[32] H. Noguchi, Biopolymers, 4 (1966) 1105–1113.
[33] B. Davidson and G.D. Fasman, Biochemistry, 6 (1967) 1616–1629.
[34] R.F. Epand and H.A. Scheraga, Biopolymers, 6 (1968) 1383–1386.
[35] M. Barteri and B. Pispisa, Biopolymers, 12 (1973) 2309–2327.
[36] E.M. Bradbury, L. Brown, A.R. Downie, A. Elliot, W.E. Hamburg and T.R.R. McDonald, Nature, 183 (1959) 1736–1737.
[37] H. Obata and H. Kanetsuna, J. Polym. Sci., Part A-2, 9 (1971) 1977–1989.
[38] H. Kyotoni and H. Kanetsuna, J. Polym. Sci., Part A-2, 10 (1972) 1931–1939.
[39] D.N. Silverman, G.T. Taylor and H.A. Scheraga, Arch. Biochem. Biophys., 146 (1971) 587–590.
[40] T. Norisuye, K. Misumi, A. Teramoto and H. Fujita, Biopolymers, 12 (1973) 1533–1541.
[41] E.M. Bradbury, C. Crane-Robinson, L. Paolillo and P. Temussi, J. Am. Chem. Soc., 95 (1973) 1683–1684.
[42] T. Akieda, H. Mimura, S. Kuroki, H. Kurosa and I. Ando, Macromolecules, 25 (1992) 5794–5797.
[43] B.A. Siles, Doctoral Thesis, University of Cincinnati, Cincinnati, OH, 1993.
[44] E. Patrone, C. Giuseppina and S. Brighetti, Biopolymers, 9 (1970) 897–910.
[45] R.P. McKnight and H.E. Auer, Macromolecules, 9 (1976) 939–944.
[46] C. Conio, E. Patrone and F. Salaris, Macromolecules, 4 (1971) 283–288.
[47] E. Peggion, A. Cosani and M. Terbojevich, Macromolecules, 7 (1974) 453–459.
[48] W. Heller and G. Forkman, in J.B. Harborne (Editor), The Flavanoids, Advances in Research, Chapman and Hall, New York, NY, 1988, pp. 399–422.
[49] M. Krause and R. Galensa, J. Chromatogr., 514 (1990) 147–159.
[50] M. Huffer and P. Schreier, J. Chromatogr., 469 (1989) 137–141.
[51] S. Hunig, N. Klaunzer and K. Gunther, J. Chromatogr., 481 (1989) 387–390.
[52] H. Stampfli, G. Patil, R. Sato and C.Y. Quon, J. Liq. Chromatogr., 13 (1990) 1285–1290.
[53] W.H. Pirkle and T.C. Pochapsky, Chem. Rev., 89 (1989) 347–362.
[54] A.F. Bergold, A.J. Muller, D.A. Hanggi and P.W. Carr, in C. Horvath (Editor), High-Performance Liquid Chromatography: Advances and Perspectives, Academic Press, San Diego, CA, 1989, pp. 95–209.
[55] L.R. Snyder and T.C. Schunk, Anal. Chem., 54 (1982) 1764–1772.
[56] M.C. Pietrogrande, F. Dondi, G. Blo, P.A. Borea and P.A. Bighi, J. Liq. Chromatogr., 11 (1988) 1313–1333.
[57] P.L. Smith and W.T. Cooper, Chromatographia, 25 (1988) 55–60.

ELSEVIER

Journal of Chromatography A, 704 (1995) 307–314

JOURNAL OF CHROMATOGRAPHY A

# High-performance affinity chromatography of proteins on non-porous polystyrene beads

Wen-Chien Lee[a,*], Chang-Hung Lin[b], Ruoh-Chyu Ruaan[b], Keh-Ying Hsu[b]

[a]*Department of Chemical Engineering, National Chung Cheng University, Chiayi, 621, Taiwan*

[b]*Department of Chemical Engineering, Chung Yuan Christian University, Chungli, 320, Taiwan*

First received 24 November 1994; revised manuscript received 16 February 1995; accepted 23 February 1995

**Abstract**

Non-porous monodisperse polystyrene (PS) beads with an average diameter of 3.7 $\mu$m and a surface area of 1.56 $m^2/g$ were prepared for the rapid analytical and micropreparative high-performance affinity chromatography of proteins. The PS was nitrated with acetic acid–sulfuric acid–nitric acid and reduced to yield hydrophilic amino groups by hydrogenation. Two affinity ligands, *p*-aminophenyl-$\beta$-D-glucopyranoside and *p*-aminobenzamidine, were immobilized on the amino-containing support via a cross-linker, hexamethylene diisocyanate. When the column (5 cm × 0.46 cm I.D.) packed with the resultant *p*-aminophenyl-$\beta$-D-glucopyranoside–PS was employed, the retained component of the concanavalin A (Con A) samples could be completely eluted in 3 min following a stepwise change of pH from 7.4 to 4.8. Thus, a calibration graph could be established from the peak area versus amount of Con A injected. A column (1 cm × 0.46 cm I.D.) packed with immobilized *p*-aminobenzamidine was also examined for protein chromatography. For a sample containing up to 200 $\mu$g of trypsin, the retained portion of proteins could be completely eluted in ca. 4.5 min. In summary, the prepared non-porous PS-based affinity adsorbent was found to be very efficient for analytical and micropreparative applications.

## 1. Introduction

Non-porous adsorbents of small particle diameter have been gaining in interest in recent years for protein chromatography using high-performance liquid chromatography (HPLC). Non-porous polystyrene-based adsorbents have been employed for the reversed-phased chromatography of proteins [1] and anion-exchange chromatography of proteins [2] and other small molecules [3–5]. Polystyrene (PS) or cross-linked poly(styrene–divinybenzene) can be used directly as an adsorbent for reversed-phase chromatography. In addition, it can be either surface sulfonated to give negative sulfonic groups or surface coated with polyethyleneimine for applications in ion chromatography. Only a few studies on the application of non-porous PS in affinity chromatography of proteins have been reported. Cross-linked poly(styrene–divinybenzene) microbeads have been coupled with dinitrophenylamino acids for the affinity chromatography of immunoglobulin E [6]. In a recent paper [7], PS microbeads were coated with poly(vinyl alcohol) and coupled with the reactive dye Cibacron Blue F3G-A for albumin adsorption. PS is inexpensive, readily available in different particle sizes and possesses mechanical

* Corresponding author.

0021-9673/95/$09.50 
*SSDI* 0021-9673(95)00267-7

rigidity. The great advantage of a PS-based over a silica-based support is its stability, covering a wide range of pH values. In this paper, we report a procedure for surface modification and ligand immobilization on microsized non-porous PS. PS was converted into aromatic amino-containing PS by nitration and successive reduction (hydrogenation). This amino-containing PS was ready for immobilization of affinity ligands via covalent binding.

Two affinity ligands, *p*-aminophenyl-β-D-glucopyranoside and *p*-aminobenzamidine, were covalently coupled to the chemically modified PS beads to make HPLC packings for the chromatographic analysis of concanavalin A (Con A) and trypsin, respectively. Affinity chromatography operated in the HPLC mode is called high-performance affinity chromatography (HPAC) and has been widely used as an analytical tool in biochemical research.

## 2. Experimental

### 2.1. Preparation and modification of non-porous PS beads

Non-porous PS beads with an average diameter of 3.7 μm were made by dispersion polymerization in ethanol with 2,2-azobisisobutyronitrile (AIBN) and polyvinylpyrrolidone (PVP) as the initiator and stabilizer, respectively. The apparatus for the polymerization consisted of a water-bath and a 250-ml three-necked round-bottomed flask, equipped with a mechanical (overhead) stirrer, a condenser and a connection with a nitrogen reservoir. The monomer solution was prepared by mixing 22 ml of styrene with 49 ml of ethanol in the flask at 60°C. AIBN (0.4 g) and PVP (1.6 g) were dissolved in 8 ml of ethanol and mixed with the monomer solution. Polymerization was carried out under nitrogen pressure and stirring (150 rpm) at 60°C for 1 day. The resultant PS beads were washed with methanol and dried in a vacuum oven at room temperature for 24 h.

Nitration of PS was carried out in a mixture of acids. Dried PS (10 g) was suspended in a flask containing 20 ml of 99.8% anhydrous acetic acid and stirred for 20 min at 60°C. A mixture of 65% nitric acid (20 ml) and 70% sulfuric acid (23 ml) was cooled to about 5°C and then added to the flask. After reaction for 3 h, the product was diluted with ice–water and washed successively with 0.1 *M* NaOH and distilled water. For the preparation of resins containing amino groups, 8 g of the nitrated PS, denoted PS-$NO_2$, were suspended in 15 ml of 99.8% anhydrous acetic acid and mixed with 59 ml of 6 *M* HCl containing 20 g of $SnCl_2 \cdot 2H_2O$. The hydrogenation reaction mixture was stirred for 2.5 days and the product was washed with 0.1 *M* NaOH and distilled water. The zeta potential of the non-porous beads was measured with a Zetasizer 3 (Malvern Instruments), in which beads were dispersed in 0.02 *M* phosphate buffer (pH 7).

### 2.2. Preparation of affinity adsorbents

Beads of the aromatic amino-containing PS, denoted PS-$NH_2$, were covalently coupled with *p*-aminophenyl-β-D-glucopyranoside and *p*-aminobenzamidine. PS-$NH_2$ (5 g) and 1,4-diazo[2,2,2]bicyclooctane (DABCO) (0.5 g) were mixed with 99.8% anhydrous acetic acid and stirred at 50°C for 15 min under nitrogen pressure. The cross-linker hexamethylene diisocyanate was then added to the above solution. After stirring for 8 h at 50°C, the unreacted hexamethylene diisocyanate was washed out with anhydrous acetic acid. The diisocyanate-activated PS was resuspended in fresh anhydrous acetic acid with the ligand, *p*-aminophenyl-β-D-glucopyranoside (0.01 g) or *p*-aminobenzamidine (0.5 g), and stirred for 16 h. The final product was washed with methanol and dried in a vacuum oven. The amount of *p*-aminobenzamidine bound to PS was determined spectrophotometrically, measuring the *p*-aminobenzamidine content of the acid hydrolysate.

### 2.3. Affinity chromatography of concanavalin A

The non-porous PS beads coupled with *p*-aminophenyl-β-D-glucopyranoside were slurry

packed into a 5.0 cm × 4.6 mm I.D. stainless-steel column using a Model CPP-085 column packer (Chemco). Pure Con A (Fluka) dissolved in 0.05 *M* Tris–HCl buffer containing 1 m*M* $MnCl_2$, 1 m*M* $CaCl_2$ and 0.1 *M* NaCl (pH 7.4) was applied to the HPAC column at a flow-rate of 1.5 ml/min. The retained component was eluted with 0.01 *M* acetic acid buffer containing 1 m*M* $MnCl_2$, 1 m*M* $CaCl_2$ and 0.01 *M* NaCl (pH 4.8). A mixture of Con A and bovine serum albumin (BSA) (Sigma) was also used as the sample injected on to the column. Peaks eluted from the HPAC column were detected at 280 nm using a Gilson Model 115 UV spectrophotometric detector. The peak area was integrated with an SIC Chromatocorder 12 integrator (System Instruments).

### 2.4. Affinity chromatography of trypsin

The affinity adsorbents coupled with *p*-aminobenzamidine were slurry packed into a 1.0 cm × 4.6 mm I.D. stainless-steel column using the same column packer. Trypsin (Type III, obtained from Sigma) dissolved in 0.05 *M* Tris–HCl buffer containing 0.25 *M* NaCl and 1 m*M* EDTA (pH 7.5) was applied into the HPAC column at a flow-rate of 1 ml/min. The elution buffer was 0.1 *M* glycine–HCl buffer containing 0.1 *M* NaCl (pH 2.6). Eluted peaks were detected at 280 nm and integrated with the SIC Chromatocorder 12 integrator. The peak data were also collected via a PCL-812 A/D converter (Advantech) connected to a personal computer.

For batch adsorption of trypsin, *p*-aminobenzamidine-immobilized PS (0.1 g) was placed in each tube with 10 ml of buffered trypsin (Type II, obtained from Sigma) solution with different initial concentrations. The buffer used was Tris–HCl (50 m*M* Tris–HCl, 0.5 *M* NaCl, 0.2 *M* $CaCl_2$, pH 7.8). The tube was gently rotated end-over-end at 4°C until an equilibrium between the proteins in the solution and on the adsorbents was reached. The concentration of protein was determined by measuring the UV absorbance at 280 nm.

## 3. Results and discussion

### 3.1. Properties of non-porous PS beads

PS beads with a monodisperse distribution of size ranging from 0.5 to 13.2 μm were prepared. The size distribution as shown in Fig. 1 was narrow. The average diameter of the non-porous beads was 3.7 μm and the surface area was 1.56 $m^2/g$, determined with an ASAP 2000 instrument (Micromeritics Instruments), and calculated with the BET equation using nitrogen as adsorbate. It was observed that the particle size of PS was controlled by the amounts of monomer, initiator and stabilizer and the type of dispersion medium, i.e., solvent, used for polymerization. When the solvent was methanol instead of ethanol, smaller beads (average diameter 2.0 μm) could be obtained. Both 3.7- and 2.0-μm PS beads are suitable for packings of HPLC columns.

### 3.2. Modification of PS beads

For utility as affinity adsorbents, PS should be chemically modified to become hydrophilic and contain functional groups for ligand immobilization. In the nitration procedure, sulfuric acid was present as a catalyst for the production of tran-

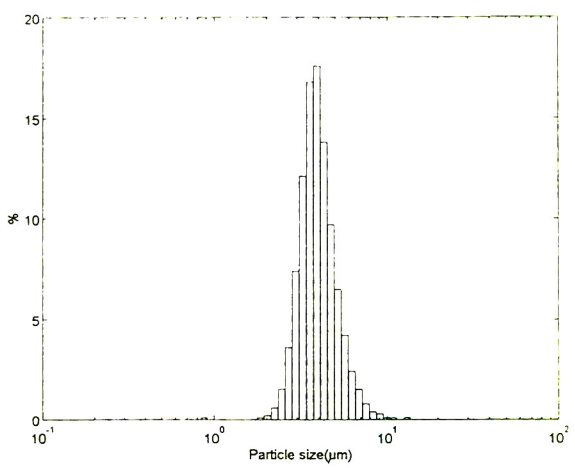


Fig. 1. Particle-size distribution of the polystyrene beads prepared by the method of dispersion polymerization.

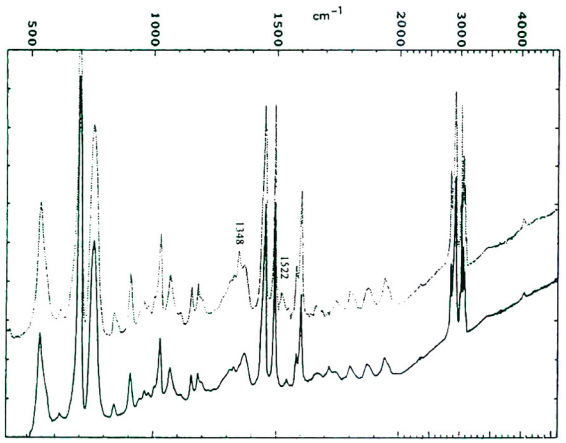


Fig. 2. FT-IR spectra of the prepared non-porous PS (solid curve) and nitrated PS (dashed curve).

sient nitronium ion ($NO_2^+$) during reaction. However, the long-term exposure of PS in sulfuric acid could cause undesirable sulfonation. No sulfonation was observed on the surface of PS that was exposed to 70% sulfuric acid for 3 h. However, sulfonation became evident when the time exceeded 3 h, which could be detected from the decline in the zeta potential of the PS beads. Therefore, the nitration of PS in the presence of sulfuric acid must be concluded within 3 h to avoid any possible sulfonation that could occur. In comparison with the unmodified PS, the FT-IR spectra of the resultant nitrated PS contain two additional peaks at 1522 and 1348 $cm^{-1}$, as shown in Fig. 2. These peaks were contributed by $NO_2$ groups on the benzene rings. Results from elemental analysis of the PS-$NO_2$ are given in Table 1. The experimental N:O ratio, which is close to the theoretical value (0.5), suggests that the nitration of PS was successful. No significant

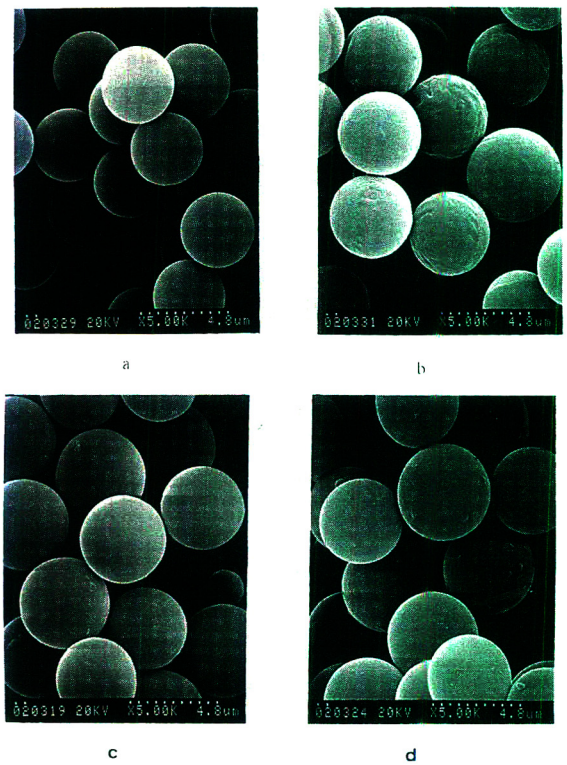


Fig. 3. Scanning electron micrographs of (a) non-porous PS beads, (b) PS-$NO_2$, (c) PS-$NH_2$ and (d) PS coupled with *p*-aminobenzamidine.

deformation of the PS beads after nitration and successive hydrogenation was observed on the scanning electron micrographs (Fig. 3).

The PS-$NO_2$ was converted into aromatic amino-containing PS by hydrogenation in acetic acid with HCl and $SnCl_2$ at 60°C for 2 days. The zeta potential of the beads changed significantly from −35 to −19 mV. An increase in zeta potential suggests that $NO_2$ groups were reduced

Table 1
Characterization of nitrated PS by elemental analysis

| Run No. | C (%) | H (%) | N (%) | O (%) | N:O |
|---|---|---|---|---|---|
| 1 | 91.14 | 8.01 | 0.28 | 0.57 | 0.56 |
| 2 | 91.02 | 8.04 | 0.29 | 0.65 | 0.51 |

to $NH_2$ groups. The zeta potential of the unmodified PS was −32 mV, which approached that of nitrated PS.

### 3.3. Immobilization of affinity ligands

The immobilization of low-molecular mass ligands on the surface of PS via the method of covalent binding is described here. The reactant hexamethylene diisocyanate played the role of a cross-linker and also a spacer between PS and the ligand. Diisocyanate reacted with the amino group on the benzene ring at one end and on the amino group of the ligand at the other end. The reaction of diisocyanate with amino-containing PS under a dry nitrogen pressure could be concluded in 8 h using DABCO as the catalyst. DABCO is an effective base catalyst for the reaction of amines and isocyanate. The unreacted diisocyanate should be removed by washing with acetic acid. For further reaction of immobilizing ligands, fresh acetic acid and DABCO were added to the isocyanate-activated PS and stirred for 16 h. The amount of *p*-aminobenzamidine bound to PS was determined as 1.1 μmol/g. This value corresponds to 0.7 μmol/$m^2$, which is higher than that reported [8] for coupling to porous silica (Fractosil 500) beads, 0.32 μmol/$m^2$. The specific surface area of the porous silica is 43.46 $m^2$/g and the density of *p*-aminobenzamidine ligands immobilized on the silica is 13.8 μmol/g.

### 3.4. High-performance affinity chromatography of Con A

When a 5-cm long column was operated at a flow-rate of 1.5 ml/min, the retained component of the Con A sample (20 μl) could be eluted by a stepwise change of pH from 7.4 to 4.8, as shown in Fig. 4. The non-retained peak in the Con A chromatogram constitutes ca. 20% of the total proteins. The retention time of the non-retained component did not change with sample size, as shown in Fig. 5, indicating that this retention time (0.32 min) is the time for the mobile phase to pass through all void spaces.

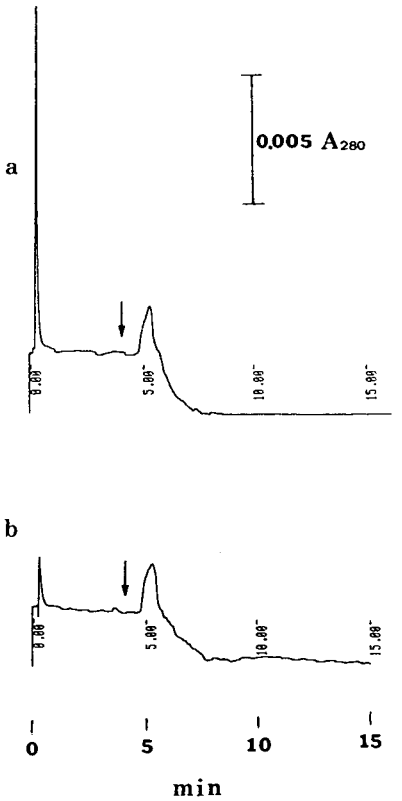


Fig. 4. Analysis of 20-μl samples containing (a) 40 μg each of Con A and BSA and (b) 40 μg of Con A only, using the column packed with *p*-aminophenyl-β-D-glucopyranoside–PS. The arrows indicate stepwise changes in the mobile phase pH from 7.4 to 4.8. Flow-rate, 1.5 ml/min; pressure, 170 bars.

The void volume, which is 0.48 ml, includes the extra-column volume, which was determined as 0.16 ml. The retained portion of the samples containing up to 55 μg of Con A could be completely eluted in 3 min after a stepwise change of pH. A significant shift of the baseline was observed owing to the change of buffers during pH elution. The composition of the starting buffer (Tris–HCl) was different from that of the elution buffer (acetic acid). However, the quantitative properties of the elution peaks were not affected by the shift of the baseline. The problem of the shift in baseline became even worse when elution was effected with a buffer containing competing free ligand, glucose. This

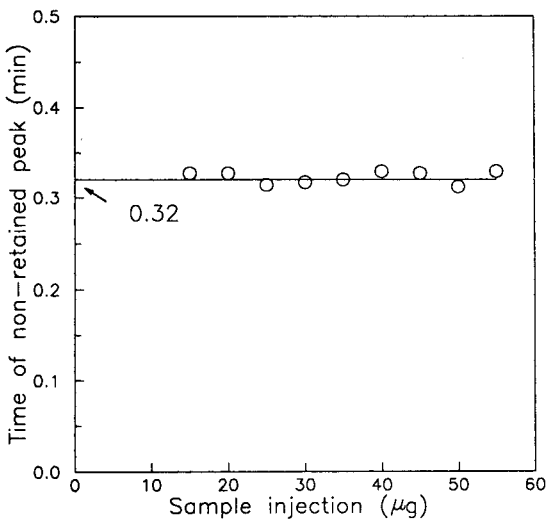


Fig. 5. Variation of retention time of the non-retained peak with sample loading. Flow-rate of effluent, 1.5 ml/min.

suggests that the use of the elution buffer should be subjected to further investigation.

Fig. 6 shows that when 20-μl samples with Con A content ranging from 15 to 55 μg were prepared as standards, a straight line was obtained in the plot of peak area versus Con A content. A straight line could also be obtained in the plot of peak height versus Con A content up to 40 μg. Each data point in Fig. 6 represents an average value resulting from two or three experimental runs. When a sample containing equal amounts (40 μg) of Con A and BSA was applied to the column, the chromatogram as shown in Fig. 4a was obtained. Results from sodium dodecyl sulfate polyacrylamide gel electrophoresis of the peak fractions indicated that no BSA appeared in the retained fraction. Comparison of Fig. 4b and a suggests that the retained peaks in each instance are almost identical in their shape and area. The data indicate that this affinity column is suitable for the chromatographic determination of Con A. The error in the HPLC analysis using the affinity column was within 4%.

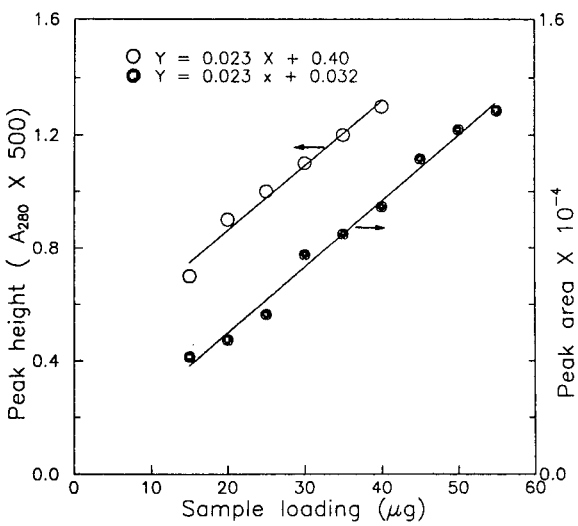


Fig. 6. Calibration graphs of peak height (peak area) versus Con A concentration. The HPAC column (5 cm × 0.46 cm I.D.) was operated at a flow-rate of 1.5 ml/min and 20-μl samples were injected.

### 3.5. Affinity chromatography of trypsin

The utility of the 1-cm column packed with the *p*-aminobenzamidine-immobilized PS for trypsin (Type III) chromatography is demonstrated in Fig. 7. Elution was achieved by a stepwise change of buffers from Tris–HCl (pH 7.5) to glycine–HCl (pH 2.6). A linear relationship was observed between the elution peak area and the trypsin content in the sample (Fig. 8). The retention time of the retained peak was approximately 1.7 min. In contrast to the elution of Con A, no significant shift of the baseline was observed in the elution of bound trypsin. The small fluctuations that appeared on the peaks in Fig. 7a and b were caused by the truncation of the digits of the data collected by the A/D converter. For a sample containing up to 200 μg of trypsin, bound proteins could be eluted completely in ca. 4.5 min following the stepwise change of pH. This suggests that the affinity column was suitable for rapid micropreparative chromatography even though it is only 1 cm long. The total void volume of this column was determined as 0.22 ml, which includes the extra-column volume, 0.14 ml.

The density of bound trypsin (Type II crude)

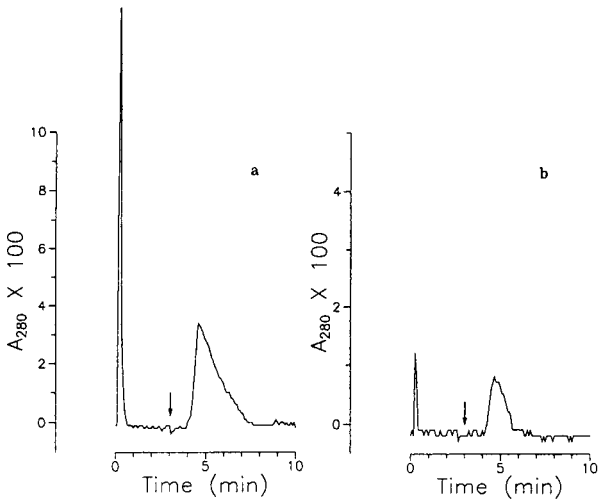


Fig. 7. Chromatograms of trypsin samples (20 $\mu$l) with concentrations of (a) 10 and (b) 0.5 mg/ml. The HPAC column (1 cm × 0.46 cm I.D.) packed with *p*-aminobenzamidine-immobilized PS was operated at a flow-rate of 1 ml/min. The arrows indicate stepwise changes in mobile phase pH from 7.5 to 2.6.

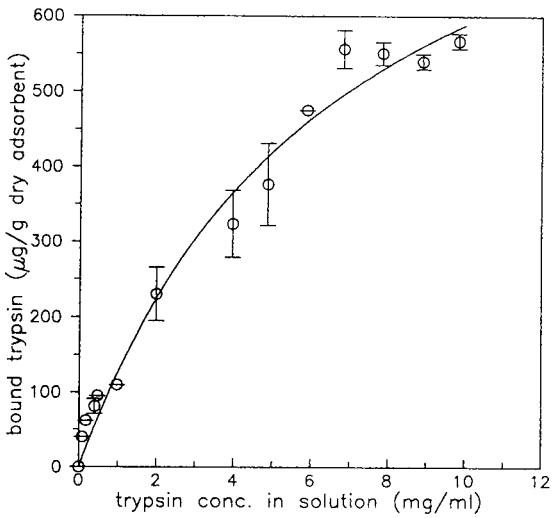


Fig. 9. Adsorption isotherm for trypsin (Type II, Sigma) and *p*-aminobenzamidine-immobilized PS. A 0.1-g amount of adsorbent was placed in each tube with 10 ml of buffered trypsin solution with different initial concentrations. The buffer used was Tris–HCl (50 m*M* Tris–HCl, 0.5 *M* NaCl, 0.2 *M* $CaCl_2$, pH 7.8). The tubes were gently rotated end-over-end at 4°C for 6 h. Protein adsorption was determined by measuring the loss of solution protein.

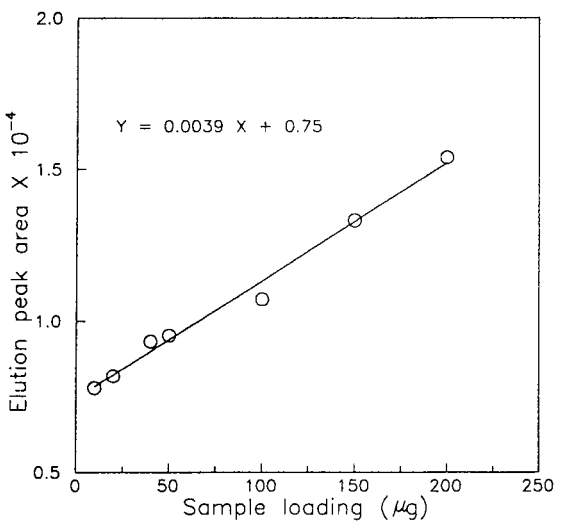


Fig. 8. Calibration graph of peak area vs. trypsin concentration. The HPAC column (1 cm × 0.46 cm I.D.) was operated at a flow-rate of 1 ml/min and 20-$\mu$l samples were injected.

was plotted against the equilibrium trypsin concentration in the solution (Fig. 9). The maximum binding capacity was observed to be ca. 550 $\mu$g/g. The adsorption capacity at this level due to the use of non-porous adsorbents with a low specific surface area suggests that the prepared affinity adsorbent is suitable for the analysis of protein samples of microgram size. The solid line in Fig. 9 was generated from the best fit of the data with the Langmuir model. It is evident that the equilibrium relationship is not exactly of Langmuir type.

## Acknowledgement

This study was supported by the National Science Council of the Republic of China under the contracts NSC 83-0402-E194-002 and NSC 84-2214-E194-006.

## References

[1] Y.-F. Maa and C. Horvath, J. Chromatogr., 445 (1988) 71–86.
[2] M.A. Rounds and F.E. Regnier, J. Chromatogr., 443 (1988) 73–83.
[3] Y. Miura and J.S. Fritz, J. Chromatogr., 482 (1989) 155–163.
[4] L.M. Warth, J.S. Fritz and J.O. Naples, J. Chromatogr., 462 (1991) 165–176.
[5] R.F. Strasburg, J.S. Fritz and J.O. Naples, J. Chromatogr., 547 (1991) 11–19.
[6] S. Wongyai, J.M. Varga and G.K. Bonn, J. Chromatogr., 536 (1991) 155–164.
[7] A. Tuncel, A. Denizli, D. Purvis, C.R. Lowe and E. Piskin, J. Chromatogr., 634 (1993) 161–168.
[8] R.-M. Chang and W.-C. Lee, J. Chem. Technol. Biotechnol., 59 (1994) 133–139.

ELSEVIER

Journal of Chromatography A, 704 (1995) 315–321

JOURNAL OF CHROMATOGRAPHY A

# Immobilized-liposome chromatographic analysis of drug partitioning into lipid bilayers ☆

Farideh Beigi, Qing Yang, Per Lundahl*

*Department of Biochemistry, Biomedical Center, Uppsala University, Box 576, S-751 23 Uppsala, Sweden*

First received 2 January 1995; revised manuscript received 10 February 1995; accepted 16 February 1995

**Abstract**

The chromatographic retardation of drugs on a gel bed with immobilized liposomes was shown to correlate with the absorption of the drugs through epithelial cell layers, which is related to drug partitioning into the lipid bilayers of cell membranes. The capacity factors were divided by the lipid concentration (m$M$) in the gel bed to obtain specific capacity factors, $K_s$. The logarithm of the octanol–water distribution ratios showed a linear correlation with log $K_s$, whereas the logarithm of the apparent permeability coefficients in epithelial cell monolayers and the absorption of drugs orally administered in humans (data from other laboratories) increased over the interval $0 < \log K_s < 1$ and attained a saturation level in the interval $1 < \log K_s < 3$. Immobilized-liposome chromatography may be applicable for prediction of drug uptake through epithelial cell membranes.

## 1. Introduction

The epithelium of the human small intestine absorbs drugs through the cell membranes or the tight junctions between the cells. The rate of absorption can be studied in a human intestinal epithelial cell line monolayer model [1,2]. Drug absorption across the cell membrane is related to the hydrophobicity of the drugs in terms of their experimental octanol–water distribution ratio, $D$, which is defined as the ratio between the sums of the concentrations of all drug species (non-charged and charged, monomeric and oligomeric) in the organic phase and in the aqueous phase, whereas the octanol–water partition coefficient, $P_{oct}$, applies strictly only to non-charged drug monomers, as is discussed extensively in the literature [3]. Among numerous investigations in this field, thermodynamic studies of partitioning of chemical compounds and pharmaceutical drugs between an aqueous phase and phosphatidylcholine (PC) liposomes, cyclohexane or $n$-octanol can be mentioned [4–6]. An optical method is available for determining drug partitioning into lipid bilayers and utilizes measurements of refractive index changes in a lipid bilayer deposited onto a planar optical waveguide [7]. Partitioning of drugs into a hydrophobic phase can also be analyzed by HPLC with suitable stationary phases [8]. How-

* Corresponding author.

☆ Paper presented at the *5th Symposium of the European Society for Biochromatography, Nancy, 17–19 May, 1994.*

0021-9673/95/$09.50 
*SSDI* 0021-9673(95)00214-6

ever, analysis of partitioning into lipid monolayers or bilayers seems advantageous, since organic phases cannot account for the existence of specific polar interactions between the compounds and phospholipid bilayers [9]. Recently, HPLC beds with PC coatings have been used with aqueous eluents containing an organic modifier [8,10,11], particularly for drugs of high $P_{oct}$ values. Columns containing monolayers of phospholipids covalently bonded to silica gel beads for "immobilized artificial membrane (IAM)" chromatography seemed useful in model studies related to the transport of drugs through human skin [12]. For the prediction of rates of drug transport across membranes, chromatographic analysis of the interaction of drugs with liposomes should be preferable, since liposomal lipid bilayers are structurally similar to biological membrane bilayers and suitable for experiments under physiological conditions, avoiding organic solvents as eluent modifiers for eluting the most hydrophobic drugs. Furthermore, the restraint posed by the covalent immobilization of each individual lipid molecule in the IAM monolayer does not exist in the liposomal system.

Chromatography on immobilized liposomes and proteoliposomes, for example, of proteins on liposomes ("liposome chromatography") and of glucose on glucose transporter (Glut1) proteoliposomes ("transport retention chromatography") have been described earlier [13–15]. In the present work, drugs were applied to immobilized-liposome chromatographic (ILC) columns to study the partitioning of drugs into liposomes. For this new approach, liposomes were immobilized by freeze–thawing [16] in small agarose–dextran gel beads, which were packed into columns. Pharmaceutical drugs of various structures and with a wide range of log $P_{oct}$ values were applied to the columns and showed widely different retention volumes. The ILC results were compared with partition coefficients determined with free liposomes [19], and with data on drug absorption through monolayers of cultured epithelial cells of the cell line Caco-2 [1,2] and on absorption of orally administered doses [2].

## 2. Experimental

### 2.1. Materials

Egg PC (95% or 99%) was purchased from Avanti Polar Lipids (Alabaster, AL, USA). Sephadex G-50 M and Superdex 200 HR (13-$\mu$m crosslinked agarose beads with grafted dextran) were obtained from Pharmacia Biotech AB (Uppsala, Sweden). Acetylsalicylic acid (aspirin) (A-5376), alprenolol (A-8676), atenolol (A-7655), chlorpromazine (C-8138), corticosterone (C-2505), hydrocortisone (H-4001), metoprolol (M-5391), polyethylene glycol (PEG) (P-3015), salicylic acid (S-3007), terbutaline (T-2528) and warfarin (A-2250) were purchased from Sigma (St. Louis, MO, USA). DL-propranolol (P-0884) was a gift from P. Artursson, Dept. Pharmaceutics, Uppsala University. Other chemicals were of analytical grade.

Eluent A was 10 m*M* Tris-HCl, pH 7.4, and 150 m*M* NaCl. Eluent B was 10 m*M* sodium phosphate, pH 7.4, and 150 m*M* NaCl. The eluents were passed through a 0.2-$\mu$m filter (11107-47-N, Sartorius, Göttingen, Germany) and were simultaneously degassed.

### 2.2. Preparation and immobilization of liposomes

Liposomes were prepared by removal of cholate from cholate–lipid solutions on Sephadex G-50 M gel beds in eluent A at 22°C, concentrated in a membrane concentrator (Minicon B15, Amicon, Beverly, MA, USA) at 4°C, mixed with partially dried gel beads and immobilized by freeze–thawing, all essentially as described in Ref. [16], except that Superdex 200 HR beads were utilized. Briefly, beads were partially dried with a water aspirator, or were ethanol-dried for the immobilization of 99% PC liposomes, and were thoroughly mixed with a liposome suspension of 180–280 m*M* phospholipid concentration. The mixture (0.5–2 ml) was vortexed and kept at room temperature ($\approx$22°C) for at least one hour to allow the liposomes to enter the swelling gel beads and

was frozen in ethanol–$CO_2$ (s) at −75°C and thawed at 25°C. This procedure effected steric immobilization by increasing the liposome size to dimensions similar to the spaces available in the network of the gel matrix. The beads with immobilized liposomes were left at room temperature for one hour. Nonimmobilized liposomes were removed by suspending the gel-liposome mixture in buffer A and washing five times at 20°C by centrifugation at 350 *g* for 15 min (see also Discussion). The amount of phospholipids per packed gel volume was determined by phosphorus analysis [16,17].

### 2.3. Immobilized-liposome chromatography (ILC) of drugs

ILC of drugs was performed on PC liposomes in Superdex 200 HR gel beads packed in 5-mm I.D. glass columns (HR 5/5 and HR 5/10, Pharmacia Biotech). Three immobilized-liposome gel beds were used: 1.0-ml bed volume, 95% PC, 53 or 63 m*M* phospholipid; and 2.0-ml bed volume, 99% PC, 43 m*M* phospholipid. The drugs were dissolved in eluent B at 0.02–10 mg/ml or were dissolved in ethanol or 0.1 *M* NaOH and diluted with eluent B to a concentration in that range. Aliquots (30–50 μl) were applied to the column and were eluted at 22°C with eluent B at a flow-rate of 0.1–0.5 ml/min with an HPLC pump (No. 2248, Pharmacia Biotech AB) with absorbance detection at 210 or 220 nm (Waters 486 detector, Millipore, Milford, MA, USA). After the ILC experiments, the liposomes were eluted with 100 m*M* cholate solution, the amount of phospholipids was determined [17], and the drugs were run on the liposome-free gel beds in order to estimate the contribution of the gel matrix to the retardation on the liposome-Superdex gel bed.

### 2.4. The specific capacity factor ($K_s$)

The retention volume, $V_R$, on a liposome column and the corresponding retention volume, $V_0$, after removal of the liposomes, were used to calculate the specific capacity factor, $K_s$, defined as

$$K_s = [V_R - (V_0 - V_L)]/[(V_0 - V_L)B].$$

The liposome volume, $V_L$, estimated by chromatography of [$^{14}$C]glucose before and after removal of the liposomes [18], was introduced to correct for the difference in total column volume between the columns with and without liposomes. The concentration of immobilized phospholipids, B, expressed as μmol phosphorus/ml gel bed, was introduced for combining data from the different columns. $K_s$ was thus expressed in the unit m$M^{-1}$.

Strongly hydrophobic drugs showed high retardation on the liposome columns and minor retardation even on the liposome-free columns. The latter retardation was taken into account by the term $V_0$ in the above definition of the specific capacity factor $K_s$.

## 3. Results

### 3.1. Immobilized-liposome chromatography with PC liposomes

All drugs were run two to six times on each of the three immobilized-liposome columns and showed an essentially constant retention volume and a constant peak area for a given drug on a given column, which indicates that no appreciable loss of liposomes or adsorption of the drug occurred during a run. The nearly symmetric peaks showed that equilibration was essentially attained even at high flow-rate [20]. The average loss of lipids after ≈100 runs over a period of three weeks was 7%.

A typical pair of drug elution profiles in runs with and without liposomes is shown in Fig. 1. The peaks were relatively broad, especially for the drugs that were strongly retarded on immobilized liposomes. These drugs were slightly retarded even on the liposome-free columns. Other drugs showed no significant retardation on the liposome-free columns.

The log $K_s$ values were essentially indepen-

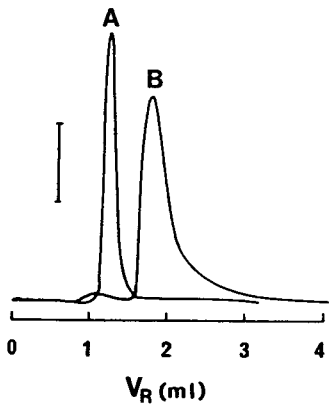


Fig. 1. Elution profiles for terbutaline on an immobilized-liposome Superdex 200 HR column (peak B) and on the same column after removal of the liposomes (peak A). Gel bed: 5 × 0.5 cm I.D. (0.98 ml). Liposome composition: PC, 99%. Phospholipid amount: 63 μmol. Eluent: B. Flow-rate: 0.1 ml/min. Terbutaline amount: 0.5 μg. The bar indicates an absorbance at 220 nm of 0.02 (peak A) and 0.01 (peak B).

dent of the column length and the phospholipid concentrations in the gel beds in the range used, 40–65 m*M* (Fig. 2). The slightly negative slopes are barely significant, but may be due to multilamellarity of the liposomes (see Discussion).

The logarithm of the octanol–water partition coefficients (log $P_{oct}$) [6] showed poor correlation with the logarithm of the specific capacity factor, log $K_s$, (linear correlation coefficient $r \approx 0.7$; not illustrated). The retardations did not only depend only on the hydrophobicity of the drugs as reflected by their partition coefficients (log $P_{oct}$), since most of the tested drugs have ionizable groups with different p$K_a$ values [6] and are charged at pH 7.4. The logarithm of the octanol–water distribution ratio *D* (the concentration ratio for all species of the drug [3]; see Introduction) correlated fairly well with the logarithm of the specific capacity factor, log $K_s$ (Fig. 3). The linear correlation coefficient was $r = 0.94$ for the combined results from three series of determinations. The drugs tested were nonhomologous. Within homologous series of drugs a better correlation can be expected.

The series of experiments on the three columns showed almost the same pattern. An additional experiment (not illustrated) was done

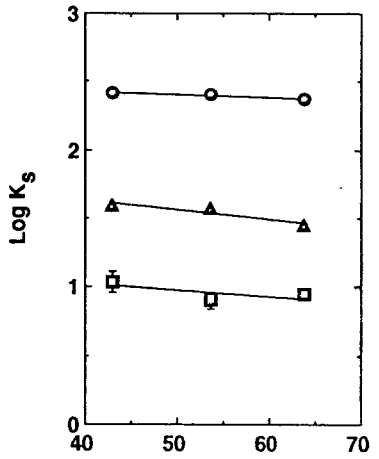


Fig. 2. The logarithm of the specific capacity factor, $K_s$, versus the phospholipid concentration in three ILC columns with PC liposomes (see Experimental) for two drugs of different hydrophobicities: terbutaline (□) (error bars shown) and alprenolol (○) (error bars contained within the solid circles). The average of the log $K_s$ values on each column for terbutaline, aspirin, corticosterone, warfarin and alprenolol (▲) was also calculated (no error bars, since the drugs have widely different $K_s$ values).

on immobilized PC-liposomes with a mixture of eight drugs, which separated on a 0.3-ml gel bed (0.5 × 1.5 cm) into one moderately retarded zone and three broad and strongly retarded zones, the latter ones corresponding to the three most hydrophobic drugs. On a 1.8-ml gel bed (0.5 × 9.3 cm) the first zone split into two zones. For drugs of low log *D* values a long column may be suitable for precise determination of $K_s$ values, whereas for more hydrophobic drugs a short column saves time and reduces diffusional effects.

### *3.2. Correlation with permeability of epithelial cells and absorption in humans*

For several drugs, the apparent drug permeability $P_{app}$ into monolayers of cultured epithelial cells of the cell line Caco-2 has been determined by Artursson [1] and Artursson and Karlsson [2]. Their determinations showed that the absorption of orally distributed doses in-

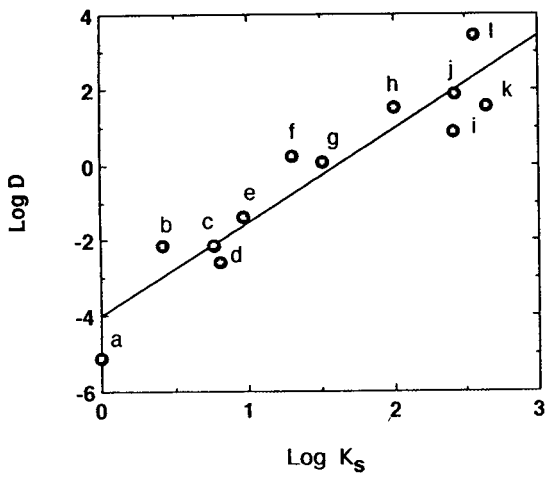


Fig. 3. The logarithm of the octanol–water distribution ratio $D$, versus the average log $K_s$ value from runs of each drug on three ILC columns with different lipid amounts. The drugs were: a = PEG; b = atenolol; c = salicylic acid; d = aspirin; e = terbutaline; f = warfarin; g = metoprolol; h = hydrocortisone; i = alprenolol; j = corticosterone; k = chlorpromazine; l = DL-propranolol. The amount applied was in the range 0.5–20 $\mu$g. The log $D$ values are from Ref. [2].

creased monotonically with increasing $P_{app}$ values and reached 100% above $P_{app} = 10^{-6}$ cm $s^{-1}$ [2] (Fig. 4). The absorption data also increased

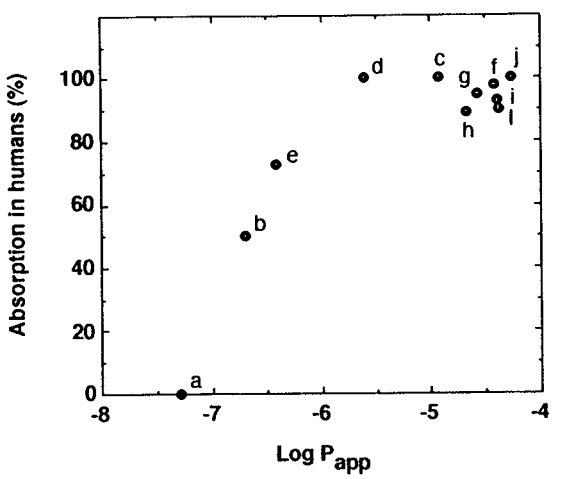


Fig. 4. Absorption of orally administered doses of drugs in humans versus log $P_{app}$ values. Chlorpromazine (k) is excluded, other drugs are denoted as in Fig. 3. Both log $P_{app}$ values and absorption data are from Ref. [2].

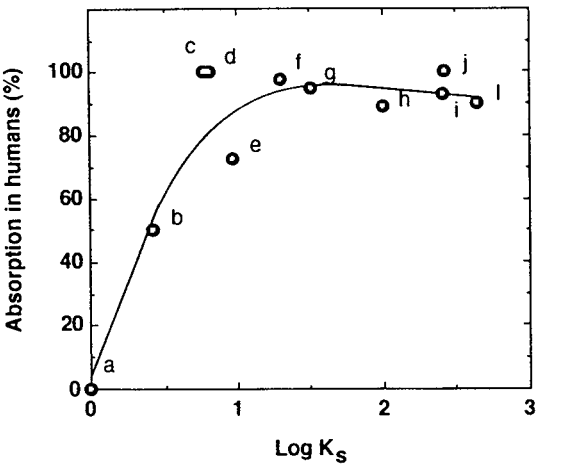


Fig. 5. Absorption of orally administered doses of drugs in humans versus the same log $K_s$ values as in Fig. 3. The drugs are denoted as in Figs. 3 and 4. Absorption values are from Ref. [2].

with increasing log $K_s$ values for ILC (Fig. 5), although less regularly. The absorption values tended to decrease slightly when log $K_s$ increased from 1 to 2.7. Drugs with log $K_s > 1$ ($K_s$ in $mM^{-1}$) seem to have favorable absorption properties. ILC may thus be used for the estimation of drug partitioning and drug absorption through cell membranes.

### *3.3. Correlation with apparent partition coefficients in fluid liposomal membranes*

Apparent ion-corrected partition coefficients for $\beta$-blockers have been determined with free liposomes [19]. The corresponding non-corrected partition coefficients were calculated and compared with our $K_s$ values from the ILC columns for the four $\beta$-blockers atenolol, metoprolol, alprenolol and propranolol (Fig. 6). The linear correlation coefficient was relatively high ($r$ = 0.90).

## 4. Discussion

Superdex 200 HR gel beads were chosen for ILC, since the small and rigid beads were found to be suitable for liposome immobilization [16]

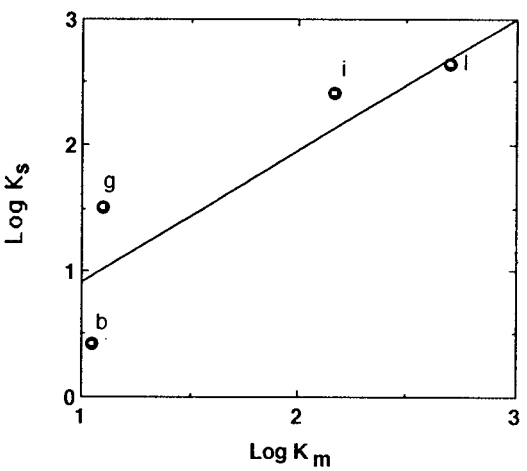


Fig. 6. Log $K_s$ values, obtained by runs on ILC columns, versus the apparent partition coefficients determined with free liposomes [19] (without ion-correction, see text) for: b = atenolol; g = metoprolol; i = alprenolol; and l = propranolol.

and allowed a flow-rate of 0.1–1 ml/min. The PC liposomes showed good stability during the runs, although the most hydrophobic drugs tended to cause release of a minimal fraction of the immobilized liposomes, as was detected by low-angle laser light-scattering flow-cell photometry. For long-term use of a liposome column, the immobilized-liposome stability and the reproducibility of retention volumes should be checked by use of suitable standard compounds, similarly as in Fig. 5B of Ref. [20]. The columns showed good stability during runs over three weeks. By modifying the washing procedure after immobilization, a still higher stability of liposome [20] or proteoliposome (Yang and Lundahl, manuscript in preparation) immobilization was achieved. For example, a column with immobilized PC proteoliposomes was run under 45 days with a moderate loss of lipids (10%). Improved ILC columns can therefore presumably be run for at least 2–3 months with a large number of drug applications, provided that calibration with a standard drug is performed regularly. Over a long period of time, lipid degradation may affect the column performance.

The log $K_s$ values for the drugs seemed to decrease slightly with increasing lipid concentration in the gel beds. Increasing amounts of liposomes in the bed during the freeze–thawing immobilization presumably results in increasing multilamellarity of the liposomes formed and immobilized [16], which would decrease the liposome outer surface area leading to a decrease in drug retention volume and trailing of the elution peaks caused by non-equilibrium partitioning of the drug into the internal bilayers. The small effect observed in the present experiments (Fig. 2) indicates that any differences in multilamellarity that occurred over the lipid concentration range used were of little consequence at the flow-rates employed.

Most of the drugs tested in the present study were charged at pH 7.4. The chromatographic retention of drugs expressed as the logarithm of the specific capacity factor (log $K_s$) correlated better with log $D$ than with log $P_{oct}$. This indicates that the retardation of drugs on liposome columns reflects both hydrophobic and other properties of the drugs. The hydrophobic effect certainly plays an important role in the interaction between drugs and liposomes. Electron-spin resonance spectroscopy has revealed that drugs can be located either in the hydrophobic interior of the lipid bilayers or on the surface of the bilayers [4]. Hydrogen-bonding and other electrostatic interactions may affect drug distribution between the aqueous phase and the lipid bilayer.

The correlation between absorption of orally distributed drugs in humans and the log $K_s$ values from the ILC experiments shows that log $K_s$ can be related to the uptake of a drug into a lipid bilayer. The difference in the correlation between the absorption of orally administered drugs and $P_{app}$ or log $K_s$ presumably reflects the role of tight junctions in drug uptake through the epithelial cell layers. ILC may therefore become useful for the characterization of drugs, for example, in the screening of drug prototypes available only in small amounts, for rapid preliminary prediction of drug uptake in humans. The preparation of the columns is very simple. For high-volume screening, commercial columns will hopefully soon be available. Furthermore,

ILC seems applicable for detailed model studies of non-specific or specific interactions between drugs and biomembranes.

Future ILC studies should, for instance, reveal effects of the lipid composition and the net electric drug charge on drug partitioning into lipid bilayers. Different homologous series of drugs should be compared. Computer modelling of drug conformations upon interaction with lipid bilayers may be useful for interpretation of experimental $K_s$ values, for example, for peptides.

## Acknowledgements

We thank Per Artursson (Department of Pharmaceutics, Uppsala University, Uppsala) for encouragement and valuable discussions, Eva Greijer for a series of experiments and good advice, Lili Lu and Eggert Brekkan for useful assistance, and David Eaker for linguistic revision of the manuscript. This work was supported by the Swedish Natural Science Research Council, the O.E. and Edla Johansson Science Foundation, the Magnus Bergvall Foundation and Grant-in-Aid for Scientific Research for International Academic Exchange from the Ministry of Education, Science and Culture of Japan.

## References

[1] P. Artursson, J. Pharm. Sci., 79 (1990) 476.
[2] P. Artursson and J. Karlsson, Biochem. Biophys. Res. Commun., 175 (1991) 880.
[3] P.J. Taylor, in C. Hansch, P.G. Sammes and J.B. Taylor (Editors), Comprehensive Medicinal Chemistry, Vol. 4, Pergamon Press, Oxford, 1990, p. 241.
[4] A.M.S. Ahmed, H.F. Farah and I.W. Kellaway, Pharm. Res., 2 (1985) 119.
[5] G.V. Betageri and S.R. Dipali, J. Pharm. Pharmacol., 45 (1993) 931.
[6] P.N. Craig, in C. Hansch, P.G. Sammes and J.B. Taylor (Editors), Comprehensive Medicinal Chemistry, Vol. 6, Pergamon Press, Oxford, 1990, p. 237.
[7] J.J. Ramsden, Experientia, 49 (1993) 688.
[8] R. Kaliszan, Quant. Struct.-Act. Relat., 9 (1990) 83.
[9] J.A. Rogers and A. Wong, Int. J. Pharm., 6 (1980) 339.
[10] K. Miyake, F. Kitaura, N. Mizuno and H. Terada, J. Chromatogr., 398 (1987) 47.
[11] R. Kaliszan, A. Kaliszan and I.W. Wainer, J. Pharm. Biomed. Anal., 11 (1993) 505.
[12] F.M. Alvarez, C.B. Bottom, P. Chikhale and C. Pidgeon, in T.T. Ngo (Editor), Molecular Interactions in Bioseparations, Plenum Press, New York, 1993, p. 151.
[13] P. Lundahl and Q. Yang, Protein Nucleic Acid Enzyme (Tokyo) 35 (1990) 1983 (in Japanese).
[14] P. Lundahl and Q. Yang, J. Chromatogr., 544 (1991) 283.
[15] L. Lu, E. Brekkan, L. Haneskog, Q. Yang and P. Lundahl, Biochim. Biophys. Acta, 1150 (1993) 135.
[16] Q. Yang and P. Lundahl, Anal. Biochem., 218 (1994) 210.
[17] G.R. Bartlett, J. Biol. Chem., 234 (1959) 466.
[18] Q. Yang, M. Wallstén and P. Lundahl, Biochim. Biophys. Acta, 938 (1988) 243.
[19] G.V. Betageri and J.A. Rogers, Int. J. Pharm., 36 (1987) 165.
[20] E. Brekkan, L. Lu, and P. Lundahl, J. Chromatogr. A, in press.

ELSEVIER

Journal of Chromatography A, 704 (1995) 323–328

JOURNAL OF CHROMATOGRAPHY A

# Nitrobenzenes in reversed-phase liquid chromatography. New candidates for internal standards

Shiro Yamauchi

*Analytical Development, Formulation Research Institute, Otsuka Pharmaceutical Co., 224-18 Hiraishi Ebisuno, Kawauchi-cho, Tokushima-shi, Tokushima 771-01, Japan*

First received 14 March 1994; revised manuscript received 21 February 1995; accepted 23 February 1995

**Abstract**

The utility of nitrobenzenes as candidates for internal standards in reversed-phase HPLC was investigated. Among many kinds of commercial reagents, 21 nitrobenzenes were selected as candidates, based on the chromatographic results obtained under various conditions. These have higher UV absorption within a wider range of wavelengths than the phenols previously reported. The wavelength range extends up to at least 310 nm and the molar absorptivity is more than 500 l $mol^{-1}$ $cm^{-1}$. The twenty-one nitrobenzenes showed a constant order of elution regardless of the separation conditions. The mobile phases consisted of 20–70% aqueous–organic solutions (organic solvent = acetonitrile, methanol, tetrahydrofuran and mixtures thereof). The packing materials used were hydrocarbon-bonded silica gels ($C_1$, phenyl, $C_8$ and $C_{18}$ columns). Moreover, the capacity factors of the 21 nitrobenzenes were independent of the acidity and basicity of mobile phases within the pH range 2.5–12.0 with an octadecyl-bonded polymer gel.

## 1. Introduction

Our previously reported 31 phenols are very useful in systematically searching for a suitable internal standard in RP-HPLC using a hydrocarbon-bonded silica gel column [1,2] because they show a constant elution order over a wide range of HPLC conditions. We have been using them as first-choice candidates for internal standards, and the most suitable internal standard can usually be selected from among them. However, some phenols do not show very high UV absorption over a wide range of wavelengths owing to their spectrophotometric characteristics. Therefore, the detectable wavelength range is restricted to within a narrow range when using several phenols, e.g., halogenated phenols and alkyl parabens.

Detection at long wavelengths is useful for eliminating interferences from other components of a complex mixture or the background of the mobile phase.

On the other hand, the capacity factor of each phenol is independent of the pH of mobile phase (within the pH range 2.0–7.0). In general, it is recommended that the mobile phase should be controlled in the acidic to neutral range in RP-HPLC using the chemically bonded silica gel columns. In recent years, chemically bonded silica gels that are stable even with alkaline (up to pH 10) mobile phases have been developed and are now commercially available [3]. Another

0021-9673/95/$09.50 
*SSDI* 0021-9673(95)00268-5

type of packing material, the support of which is not silica gel, can be obtained and is stable in alkaline (pH 13) mobile phases [4]. Using these packing materials, alkaline mobile phases can be utilized in RP-HPLC. However, at pH >7.0, the capacity factor of each phenol changes in accordance with its $pK_a$ (7.5–10.2). Alkyl 4-hydroxybenzoates are not stable in alkaline solutions.

As new candidates for internal standards in RP-HPLC, we have searched for other benzene derivatives that should satisfy the following conditions: (1) have high UV absorption within a wide wavelength range, at least up to 320 nm; (2) have no dissociating group; and (3) be commercially available and usable without further purification.

Nitrobenzene derivatives satisfy these criteria. Nitrobenzene has a high UV absorption within a wide wavelength range, owing to the resonance between the phenyl ring and nitro group, which is a chromophore. It contains no dissociating group. There are several reports relevant to aromatic nitro compounds [5–7] and 1-nitroalkanes as retention index standards [8] in RP-HPLC. In this paper, we report the results for a series of 21 nitrobenzenes that are potential internal standards in RP-HPLC and their comparison with phenols.

## 2. Experimental

### 2.1. Chemicals

Nitrobenzenes were purchased from Wako (Osaka, Japan), Tokyo Kasei (Tokyo, Japan) and Lancaster (Morecambe, UK) and were used as received.

### 2.2. Apparatus

The HPLC system consisted of a Model 510 pump, a Model 440 detector fixed at 254 and 280 nm and a WISP 710B automatic sample injector (Waters, Milford, MA, USA). Chromatograms were recorded on a LabChart 180 (System Instrument, Tokyo Japan). For measurement of the UV spectra of nitrobenzenes, a U-3200 spectrophotometer (Hitachi, Tokyo Japan) was used.

Table 1
HPLC conditions employed for evaluating the chromatographic behaviour of nitrobenzenes and influence of packing material and mobile phase

| Stationary phase | | | | Mobile phase[b] |
|---|---|---|---|---|
| Material | Bonded group | Carbon content (%)[a] | End-capping | |
| Nucleosil $5C_{18}$ | $C_{18}$ | 14 | Treated | ACN–water (20:80, 30:70, 40:60, 50:50, 60:40)<br>MeOH–water (30:70, 40:60, 50:50, 60:40, 70:30)<br>ACN–MeOH–water (20:20:60)<br>ACN–THF–water (30:10:60)<br>ACN–20 m*M* $Na_2SO_4$ (40:60)<br>ACN–5 m*M* sodium octanesulfonate (pH 2.5) (40:60) |
| μBondapak $C_{18}$ | $C_{18}$ | 10 | Treated | ACN–water (40:60) |
| Zorbax ODS | $C_{18}$ | 10 | Untreated | ACN–water (40:60) |
| Nucleosil $5C_8$ | $C_8$ | 9 | Untreated | ACN–water (40:60) |
| Cosmosil 5Ph | $C_6H_5$ | 9 | Treated | ACN–water (40:60) |
| Shodex TMS | $C_1$ | 5 | Treated | ACN–water (40:60) |
| Asahikak ODP-50 | $C_{18}$ | 17 | – | ACN–water (40:60)<br>ACN–10 m*M* $KH_2PO_4$ (pH 2.5, 7, 12) (40:60) |

[a] Values taken from manufacturers' catalogues.
[b] ACN = acetonitrile; MeOH = methanol; THF = tetrahydrofuran.
[c] pH adjusted with 85% phosphoric acid.

### 2.3. Analytical columns and mobile phases

In the chromatography of nitrobenzenes, the analytical columns and mobile phases used in this study were equivalent to those reported previously [1]. The analytical conditions are summarized in Table 1. In the chromatography using alkaline mobile phase, the following conditions were used: column, Asahipak ODP-50 (15 cm × 4.6 mm I.D.) (Asahikasei, Tokyo, Japan) [4]; mobile phase, acetonitrile–10 m*M* $KH_2PO_4$ (pH 2.5, 7.0 and 12.0, adjusted with 85% phosphoric acid or 1 *M* sodium hydroxide) (40:60); and flow-rate, 0.5 ml $min^{-1}$.

### 2.4. Sample preparation and chromatographic procedure

A 20-mg amount of each nitrobenzene was weighed accurately and dissolved in methanol to make exactly 100 ml [0.02% (w/v) solution]. A 5-$\mu$l volume of sample solution was injected for HPLC determination. The flow-rate was adjusted to between 0.5 and 1.0 ml $min^{-1}$ to keep the column pressure below 2000 p.s.i. at 25°C. The retention time of uracil was taken as the column void volume and used for the calculation of the capacity factor of each nitrobenzene.

### 2.5. UV spectrophotometric procedure

Sample solutions for HPLC were diluted exactly fivefold with methanol and were scanned from 210 to 500 nm with reference to methanol.

## 3. Results and discussion

UV spectra of phenol and nitrobenzene in methanol are shown in Fig. 1. Apparently, nitrobenzene has advantageous spectrophotometric properties with respect to sensitivity and detectable wavelength range.

The capacity factors of all the nitrobenzenes decreased with increase in the content of organic solvent (acetonitrile or methanol) and increased in order of the hydrophobicity of the bonded alkyl groups ($C_{18} > C_8 \approx$ phenyl > methyl).

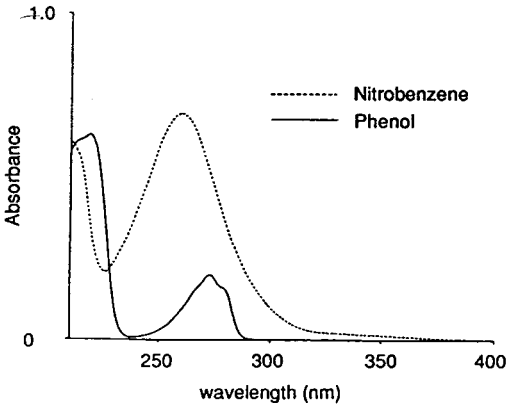


Fig. 1. UV spectra of (dotted line) nitrobenzene and (solid line) phenol in methanol solution. Concentration of each solution is 0.001 mg/ml.

These results agreed with the general retention tendencies in RP-HPLC.

Many nitrobenzenes were rejected as candidates for internal standards on the basis of the

Table 2
Series of nitrobenzene derivatives selected as potential internal standards in RP-HPLC

| No. | Derivative | Substituent | λ (nm)[a] |
|---|---|---|---|
| 1 | 1,3-Diamino-4-nitrobenzene | 2,4-$(NH_2)_2$ | 450 |
| 2 | 4-Nitroaniline | 4-$NH_2$ | 440 |
| 3 | 3-Nitroaniline | 3-$NH_2$ | 430 |
| 4 | 4-Nitroacetanilide | 4-NHCOMe | 370 |
| 5 | 2-Amino-4-nitrobenzene | 3-$NH_2$-4-Me | 430 |
| 6 | 4-Nitroacetophenone | 4-COMe | 330 |
| 7 | 2,4-Dinitroaniline | 3-$NO_2$-4-$NH_2$ | 430 |
| 8 | Nitrobenzene | H | 310 |
| 9 | 2-Amino-3-nitrotoluene | 2-$NH_2$-3-Me | 480 |
| 10 | 2-Nitrotoluene | 2-Me | 320 |
| 11 | 4-Nitrotoluene | 4-Me | 320 |
| 12 | 3-Nitrotoluene | 3-Me | 320 |
| 13 | 4-Bromonitrobenzene | 4-Br | 320 |
| 14 | 3-Bromonitrobenzene | 3-Br | 320 |
| 15 | 2,4-Dimethylnitrobenzene | 2,4-$Me_2$ | 350 |
| 16 | 4-Chloro-2-nitrotoluene | 2-Me-5-Cl | 320 |
| 17 | 2-Chloro-4-nitrotoluene | 4-Me-3-Cl | 320 |
| 18 | 3,5-Dichloronitrobenzene | 3,5-$Cl_2$ | 320 |
| 19 | 2-Nitromesitylene | 2,4,5-$Me_3$ | 350 |
| 20 | 2,4,5-Trichloronitrobenzene | 2,4,5-$Cl_3$ | 320 |
| 21 | 4-*tert*-Butylnitrobenzene | 4-*tert*-Bu | 320 |

[a] Maximum available detectable wavelength at which the molar absorptivity is more than 500 l $mol^{-1}$ $cm^{-1}$.

same criteria as reported previously [1] and also toxicological data [9–11].

We selected 21 nitrobenzenes as the candidates for potential internal standards in RP-HPLC, and they are listed in Table 2 in order of elution with the practically available maximum detection wavelengths at which the molar absorptivities are more than 500 l $mol^{-1}$ $cm^{-1}$. The capacity factors ($k'$) of the 21 nitrobenzenes are given in Table 3 and 4. The nitrobenzenes were eluted every 2–5 min within a 20-min operating period under the conditions given in Table 1.

1,3-Diamino-4-nitrobenzene, 4-nitroanaline, 3-nitroaniline, 2-amino-4-nitrotoluene, 2,4-dinitroaniline and 2-amino-3-nitrotoluene each have one or two amino groups (dissociating group), being aniline derivatives and basic compounds. Their peak shapes were sharp and symmetrical, and showed no tailing under all the HPLC conditions summarized in Table 1, even though uncapped columns where residual silanol groups were not treated, Zorbax ODS and Nucleosil $5C_8$, were used. As expected, their capacity factors were independent of the pH (2.5, 7.0 and 12.0) of the mobile phase in which the concentration of acetonitrile was fixed at 40% on the Asahipak ODP-50 column.

These phenomena can be explained as follows. Anilines with a nitro group bonded at the position of the benzene ring have low $pK_a$ values, owing to the electron-inductive effect of the nitro group and a direct resonance effect between the amino and nitro groups. For example, the $pK_a$ values of 4- and 3-nitroaniline are 1.02 and 2.50, respectively. Hence the basicity of the amino group in nitrobenzenes is very weak, and the $pK_a$ may not be more than 3.0. Accordingly, the interaction between amino and residual silanol groups seems to be very slight or negligible.

The retention times and peak shapes of the 21

Table 3
Capacity factors ($k'$) of 21 nitrobenzenes on Nucleosil $5C_{18}$ column

| Nitrobenzene[a] | Mobile phase | | | | | | | | | |
|---|---|---|---|---|---|---|---|---|---|---|
| | Acetonitrile–water[b] | | | | | Methanol–water[b] | | | | |
| | 20 | 30 | 40 | 50 | 60 | 30 | 40 | 50 | 60 | 70 |
| 2,4-$(NH_2)_2$ | 2.335 | 1.327 | 0.853 | 0.576 | 0.331 | 1.675 | 0.897 | 0.463 | 0.260 | 0.141 |
| 4-$NH_2$ | 5.665 | 3.047 | 1.767 | 1.101 | 0.574 | 3.565 | 1.974 | 1.037 | 0.578 | 0.304 |
| 3-$NH_2$ | 7.015 | 3.895 | 2.221 | 1.342 | 0.695 | 4.170 | 2.454 | 1.368 | 0.765 | 0.413 |
| 4-NHCOMe | 7.951 | 3.439 | 1.767 | 1.044 | 0.546 | 8.595 | 4.062 | 2.047 | 1.064 | 0.554 |
| 3-$NH_2$-4-Me | 13.98 | 6.561 | 3.423 | 1.918 | 0.924 | 9.814 | 5.088 | 2.500 | 1.274 | 0.658 |
| 4-COMe | 13.50 | 6.444 | 3.337 | 1.886 | 0.939 | 10.47 | 5.366 | 2.716 | 1.402 | 0.728 |
| 3-$NO_2$-4-$NH_2$ | 14.32 | 6.357 | 3.135 | 1.677 | 0.796 | 10.73 | 5.206 | 2.884 | 1.534 | 0.799 |
| H | 15.33 | 8.058 | 4.307 | 2.449 | 1.185 | 11.59 | 6.686 | 3.547 | 1.912 | 1.011 |
| 2-$NH_2$-3-Me | 21.76 | 9.526 | 4.589 | 2.456 | 1.170 | 20.37 | 9.062 | 4.405 | 2.137 | 1.065 |
| 2-Me | 34.92 | 15.12 | 7.018 | 3.551 | 1.578 | 27.58 | 13.95 | 6.426 | 3.039 | 1.467 |
| 4-Me | 37.36 | 16.58 | 7.577 | 3.779 | 1.673 | 30.35 | 14.35 | 6.958 | 3.304 | 1.555 |
| 3-Me | 41.17 | 17.45 | 7.878 | 3.968 | 1.740 | 32.57 | 16.36 | 7.600 | 3.627 | 1.707 |
| 4-Br | 50.96 | 21.89 | 9.601 | 4.589 | 1.950 | 35.46 | 18.15 | 8.600 | 3.966 | 1.848 |
| 3-Br | 56.19 | 23.40 | 10.13 | 4.823 | 2.058 | 45.54 | 20.54 | 10.62 | 4.980 | 2.326 |
| 2,4-$Me_2$ | – | 31.50 | 12.29 | 5.551 | 2.276 | – | 32.75 | 13.59 | 5.623 | 2.440 |
| 2Me-5-Cl | – | 36.25 | 14.17 | 6.291 | 2.501 | – | 39.10 | 16.33 | 6.931 | 3.000 |
| 4-Me-3-Cl | – | 39.72 | 15.48 | 6.791 | 2.743 | – | 39.47 | 18.85 | 8.078 | 3.494 |
| 3,5-$Cl_2$ | – | 42.67 | 16.79 | 7.405 | 2.934 | – | 42.89 | 19.73 | 8.706 | 3.897 |
| 2,4,5-$Me_3$ | – | 63.69 | 21.44 | 8.519 | 3.159 | – | 67.14 | 25.93 | 9.456 | 3.744 |
| 2,4,5-$Cl_3$ | – | 69.26 | 23.83 | 9.532 | 3.455 | – | 72.94 | 28.44 | 11.29 | 4.663 |
| 4-*tert*-Bu | – | 110.6 | 33.60 | 12.20 | 4.171 | – | 109.7 | 41.17 | 14.17 | 5.244 |

[a] Each nitrobenzene is expressed using abbreviations of substituents (see Table 2).
[b] The contents (%) of organic solvents in the mobile phases are given.

Table 4
Retention data for nitrobenzenes in acetonitrile water (40:60) with various columns

| Nitrobenzene[a] | Column | | | | | | |
|---|---|---|---|---|---|---|---|
| | Nucleosil $5C_{18}$ | μ Bondapak $C_{18}$ | Zorbax ODS | Nucleosil $5C_8$ | Cosmosil 5Ph | Shodex TMS | Asahipak ODP-50 |
| 2,4-$(NH_2)_2$ | 0.853 | 0.799 | 0.660 | 0.781 | 0.868 | 0.764 | 2.096 |
| 4-$NH_2$ | 1.767 | 1.557 | 1.359 | 1.415 | 1.500 | 1.254 | 3.664 |
| 3-$NH_2$ | 2.221 | 1.872 | 1.861 | 1.620 | 1.743 | 1.501 | 4.477 |
| 4-NHCOMe | 1.767 | 1.480 | 1.357 | 1.446 | 1.297 | 1.210 | 1.795 |
| 3-$NH_2$-4-Me | 3.423 | 2.710 | 2.838 | 2.220 | 2.330 | 1.941 | 5.900 |
| 4-COMe | 3.337 | 2.652 | 2.848 | 2.124 | 2.282 | 1.974 | 3.867 |
| 3-$NO_2$-4-$NH_2$ | 3.135 | 2.587 | 2.409 | 2.030 | 2.214 | 1.891 | 6.144 |
| H | 4.307 | 3.323 | 3.915 | 2.573 | 2.643 | 2.152 | 5.624 |
| $2NH_2$-3-Me | 4.589 | 3.456 | 3.865 | 2.689 | 2.743 | 2.217 | 7.459 |
| 2-Me | 7.018 | 5.077 | 6.450 | 3.686 | 3.784 | 3.076 | 8.211 |
| 4-Me | 7.577 | 5.443 | 6.949 | 3.814 | 3.820 | 3.186 | 8.755 |
| 3-Me | 7.878 | 5.747 | 7.330 | 3.995 | 3.962 | 3.228 | 9.296 |
| 4-Br | 9.601 | 6.787 | 9.053 | 4.405 | 4.617 | 3.699 | 15.123 |
| 3-Br | 10.135 | 7.049 | 9.620 | 4.615 | 4.562 | 3.620 | 14.847 |
| 2,4-$Me_2$ | 12.288 | 8.508 | 11.578 | 5.472 | 5.363 | 4.517 | 13.095 |
| 2-Me-5-Cl | 14.165 | 9.617 | 13.554 | 5.990 | 5.878 | 4.743 | 17.370 |
| 4-Me-3-Cl | 15.478 | 10.304 | 15.195 | 6.144 | 5.840 | 4.809 | 18.760 |
| 3,5-$Cl_2$ | 16.791 | 11.179 | 17.588 | 6.299 | 6.172 | 5.006 | 23.039 |
| 2,4,5-$Me_3$ | 21.435 | 14.051 | 20.376 | 8.200 | 7.987 | 6.597 | 19.950 |
| 2,4,5-$Cl_3$ | 23.828 | 15.781 | 23.617 | 8.537 | 8.918 | 6.738 | 34.033 |
| 4-*tert*-Bu | 33.601 | 21.881 | 32.435 | 11.181 | 10.980 | 9.247 | 31.373 |

[a] Each nitrobenzenes is expressed using abbreviations of substituents (see Table 2).

nitrobenzenes were independent of the counter ion and ionic strength of the mobile phase. They maintained a constant elution order on all the columns studied with the exception of the Asahipak ODP column. The retention behaviour of the 21 nitrobenzenes on the latter column was different from that on the hydrocarbon bonded silica gel columns. The capacity factors of the 21 nitrobenzenes are plotted logarithmically in Fig. 2. ODP gel can be obtained by introduction of octadecyl groups in place in hydroxyl groups in vinyl alcohol copolymers [4]. The difference in selectivity between the two types of packing materials may be mainly due to the difference in the supports (silica gel vs. vinyl alcohol copolymer). No satisfactory explanation could be found for this behaviour.

The difference in retention behaviours of several nitrobenzenes between a ODS column and a polystyrene gel column, using Smejkal et

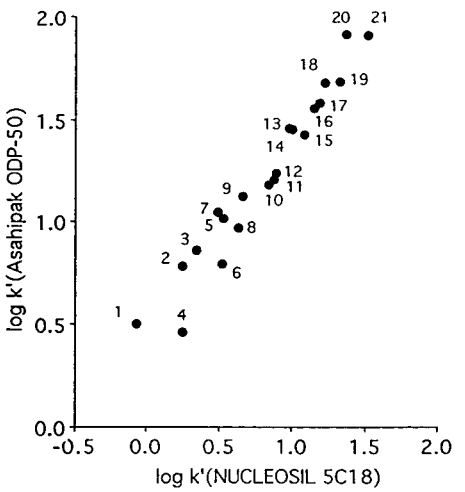


Fig. 2. Log $k'$(Nucleosil $5C_{18}$) vs. log $k'$(Asahipak ODP) of nitrobenzenes in acetonitrile–water(40:60). Nitrobenzenes are expressed using the numbers listed in Table 2.

al's retention data [7], could be discussed, but this is omitted in this paper.

## 4. Conclusion

A large number of commercial nitrobenzenes were chromatographed under different conditions including alkaline mobile phases, and 21 nitrobenzenes were selected as candidates for internal standards in RP-HPLC. These maintained a constant elution order over a wide range of RP-HPLC conditions, including alkaline mobile phases (up to pH 12).

Compared with the previously reported phenols, the nitrobenzenes have the following advantages: (1) nitrobenzenes maintain a constant elution order even at mobile phase pH values in the range 2.5–12.0; (2) the practically available detection wavelength range is at least 200–310 nm. We expect that it will become easier and quicker to choose a suitable internal standard from these 21 nitrobenzenes in combination with the previously reported phenols.

## References

[1] S. Yamauchi and H. Mori, J. Chromatogr., 515 (1990) 305.
[2] S. Yamauchi, J. Chromatogr., 635 (1993) 61.
[3] Y. Ohtsu, H. Fukui, T. Kanda, K. Nakamura, M. Nakano, O. Nakata and Y. Fujiyama, Chromatographia, 24 (1987) 351 and 380.
[4] K. Yasukawa, Y. Tamura, T. Uchida, Y. Yanagihara and K. Noguchi, J. Chromatogr., 410 (1987) 129.
[5] J. Zukowski, D. Sybilska and J. Jurczak, Anal. Chem., 57 (1985) 2215.
[6] P.J. Schoenmaker, H.A.H. Billiet and L. de Galan, J. Chromatogr., 218 (1981) 261.
[7] F. Smejkal, M. Popl, A. Cihova and M. Zazvorkova, J. Chromatogr., 197 (1980) 147.
[8] M. Bogusz and R. Aderjan, J. Chromatogr., 435 (1988) 43.
[9] Tokyo Kasei Organic Chemicals Catalog, No. 32, Tokyo Kasei, Tokyo 1994.
[10] Aldrich Catalog Handbook of Fine Chemicals 1994–95, Aldrich, Milwaukee, WI, 1994.
[11] Wako Pure Chemicals Catalogue, Wako, Osaka, 28th ed., 1994.

ELSEVIER

Journal of Chromatography A, 704 (1995) 329–337

JOURNAL OF CHROMATOGRAPHY A

# Determination of aldehydes in used engine oils by liquid chromatography with chemiluminescence detection

Anthony N. Gachanja, Simon W. Lewis[1], Paul J. Worsfold*

*Department of Environmental Sciences, University of Plymouth, Plymouth PL4 8AA, UK*

First received 2 August 1994; revised manuscript received 9 February 1995; accepted 21 February 1995

**Abstract**

Straight-chain aliphatic aldehydes ($C_6$–$C_{14}$) were selectively derivatised in oxidised engine-oil dialysates with the fluorophore 3-aminofluoranthene. The derivatives were separated by reversed-phase liquid chromatography on a mid-bore (3.2 mm I.D.) column and detected by monitoring the chemiluminescence emission from a post-column reaction with bis-(2,4,6-trichlorophenyl)oxalate and hydrogen peroxide. Calibrations for the aldehydes in an oil matrix ($0–5.0 \cdot 10^{-4}$ mol $l^{-1}$) were linear ($0.9980 < r^2 < 0.9997$) with limits of detection ($S/N = 3$) in the range $3.0 \cdot 10^{-7}$–$3.4 \cdot 10^{-6}$ mol $l^{-1}$ (0.7–75 fmol on-column). Analysis of oil samples taken from an engine test at different times (0, 16, 24 and 32 h) showed that the concentration of aldehydes increased throughout the duration of the test.

## 1. Introduction

The oxidation of oils in engines results in the formation of polar oxidation products including alcohols, aldehydes, ketones, carboxylic acids and water [1]. These species undergo further reactions to form sludges which degrade the performance of the oil. Characterisation and measurement of the polar oxidation products is therefore useful in monitoring the degradation of engine oils and elucidating the oxidation pathways.

Procedures for the determination of carboxylic acids in used engine oils by liquid chromatography (LC) with chemiluminescence (CL) [2] and fluorescence detection [3] have been described. As aldehydes are intermediate in the oxidation process it would be advantageous to monitor them in conjunction with the carboxylic acids in order to obtain a greater understanding of the oxidation process.

Ultraviolet (UV) absorbing [4,5] and fluorescence [6–9] labels based on nucleophilic addition to the aldehyde with nitrogen containing nucleophiles, e.g. oximes, hydrazines and semicarbazides, have been used for the pre-column derivatisation of aldehydes and photo-initiated peroxyoxalate CL has been applied to the detection of dansylhydrazone derivatives of airborne aldehydes [10]. However, all of these reactions were carried out in aqueous conditions which are incompatible with a used oil matrix.

A procedure for the labelling of aldehydes and ketones, based on reaction with 3-aminofluoran-

* Corresponding author.

[1] Present address: School of Biological and Chemical Sciences, Deakin University, Geelong, Vic. 3217, Australia.

0021-9673/95/$09.50 
*SSDI* 0021-9673(95)00244-8

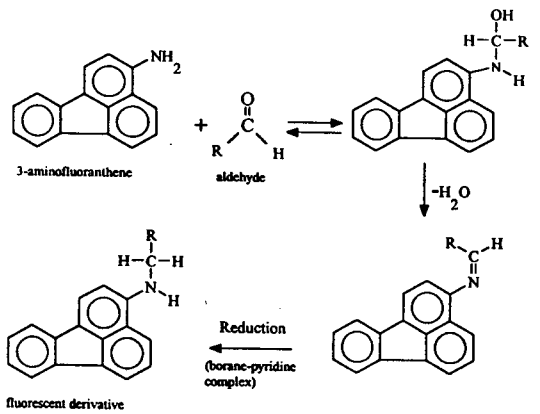


Fig. 1. Reductive amination of aldehydes with 3-aminofluoranthene in the presence of borane–pyridine complex as a reducing agent. R = aliphatic or aromatic substituent.

thene in non-aqueous media, followed by fluorescence and peroxyoxalate CL detection, has been reported [11]. The reaction scheme involved reductive amination of an aldehyde with 3-aminofluoranthene in the presence of a reducing agent (borane–pyridine complex) and is shown in Fig. 1. The high CL efficiency of amino polycyclic aromatic hydrocarbons (amino-PAHs), including 3-aminofluoranthene, has been studied and used to quantify amino-PAHs in shale and coal oils [12]).

This paper describes a procedure for the determination of aliphatic aldehydes ($C_6$–$C_{14}$) in oxidised engine oils by off-line derivatisation with 3-aminofluoranthene followed by removal of excess label by solid-phase extraction and isocratic reversed-phase LC with post-column peroxyoxalate CL detection. Results are presented for a series of oxidised oils sampled from a test engine after different periods of operation (0, 16, 24 and 32 h) using the optimised procedure.

## 2. Experimental

### 2.1. Reagents

High quality de-ionised water from a Milli-Q system (Millipore, USA) and analytical grade reagents were used unless otherwise stated. Acetonitrile (ACN), tetrahydrofuran (THF), hexane, ethyl acetate and toluene were of HPLC grade (Rathburn, UK).

Solutions of 3-aminofluoranthene (Janssen, Belgium) were prepared daily in acetic acid (glacial, BDH, UK)–toluene (2:7, v/v). The borane–pyridine complex (BAP, Aldrich, UK) was used as the liquid. Solutions of hexanal ($C_6$), octanal ($C_8$) (both Aldrich), decanal ($C_{10}$), dodecanal ($C_{12}$) and tetradecanal ($C_{14}$) (all Fluka, UK) were prepared in toluene. All aldehydes were of reagent grade.

Imidazole buffer ($3.0 \cdot 10^{-2}$ mol $l^{-1}$, pH 7.5) was prepared by dissolving imidazole (Fluka) in water; the pH was adjusted with nitric acid (0.1 mol $l^{-1}$, Merck, UK). Mobile-phase solvents were degassed in an ultrasonic bath for 10 min immediately before use. A mixed CL reagent of bis-(2,4,6-trichlorophenyl)oxalate ($1.3 \cdot 10^{-3}$ mol $l^{-1}$; TCPO, Fluka) and hydrogen peroxide ($8.8 \cdot 10^{-2}$ mol $l^{-1}$; Fluka) was prepared by dissolving 0.120 g TCPO in 198 ml acetonitrile, adding 2.0 ml of 100 volume (30%, m/v) stock hydrogen peroxide solution and mixing the combined solution in an ultrasonic bath for 15 min. This mixed reagent solution was left to stand for 45 min before use. Fresh CL reagents were prepared daily.

The oil samples were initially fractionated using a continuous dialysis system as described previously [3]. A solution of oil was dissolved in light petroleum spirit (b.p. 60–80°C) and contained in a semipermeable membrane (the molecular mass cutoff was $M_r$ 1000) around which warm petroleum spirit (b.p. 60–80°C) was continuously circulated, allowing low molecular mass material to diffuse through the membrane for 24 h. This was done to remove polymeric additives, organometallic oxidation products and solid debris which could interfere with the pre-column derivatisation.

### 2.2. Off-line derivatisation

The reaction was carried out at room temperature using the following reaction conditions unless otherwise stated.

Aldehyde standards in toluene, oil dialysate samples and oil dialysates spiked with aldehyde standards (50 μl) were added to a mixture of 3-aminofluoranthene ($1.0 \cdot 10^{-3}$ mol $l^{-1}$ in glacial acetic acid–toluene (2:7, v/v), 2 ml) and BAP (5 μl). Toluene (195 μl) was added to bring the final volume of the reaction mixture to 2.25 ml. The reaction mixture was shaken and an aliquot (100 μl) removed after 3 min for solid-phase clean-up.

Neutral alumina Sep-Pak Plus cartridges (Waters, USA) were used to remove the excess 3-aminofluoranthene before LC analysis of the aldehyde derivatives. Each cartridge was pre-cleaned with 10 ml hexane. A 100-μl sample, dissolved in the reaction solvent mixture, was loaded on the alumina cartridge and the aldehyde derivatives eluted with 15 ml of 20% (v/v) ethyl acetate in hexane. The solvent was removed by rotary evaporation and the residue redissolved in 10 ml acetonitrile–tetrahydrofuran (4:1) prior to LC analysis.

### 2.3. Instrumentation

A schematic diagram of the instrumental configuration is given in Fig. 2. Samples (5 μl) were injected (Rheodyne Model 7010) into a mobile phase of ACN–THF–imidazole buffer (75:15:10, v/v) pumped at 0.5 ml $min^{-1}$ (Model 9012 inert quaternary pump, Varian, USA). Separation was achieved using a stainless-steel column (250 × 3.2 mm I.D.) packed with Spherisorb S5 ODS2-5 (5 μm, Phenomenex, UK). A Spherisorb S5 ODS2-5 cartridge guard column (Hichrom, UK) was also used. The post-column CL reagent was pumped at 1.0 ml $min^{-1}$ by a peristaltic pump (Gilson Minipuls 2, France) fitted with silicone pump tubing (Labsystems, UK) and merged with the column eluate at a low dead volume stainless-steel T-piece (Anachem, UK) before passing into a photodiode-based CL detector (Camspec CL-1, Camspec, Cambridge CB2 4BG, UK) fitted with a specially designed 120-μl flow cell.

Polyetheretherketone (PEEK) tubing (0.5 mm I.D., 1.6 mm O.D.) was used for all of the connections between the LC pump and the analytical column; polytetrafluoroethylene (PTFE) tubing (0.8 mm I.D.) was used for all other connections. The length of tubing between the T-piece and the flow cell was kept as short as possible (4 cm). The output from the detector was recorded on a strip chart recorder (Chessell BD 4004, UK) and a PC-based integration system (Nelson PC integrator, Perkin Elmer, USA).

Signals were measured manually as peak heights and noise measured as the amplitude of the baseline on the chart recorder. Response factors were determined as the signal-to-noise ratio from the chart recorder and peak areas from the integrator were used for quantitative analysis.

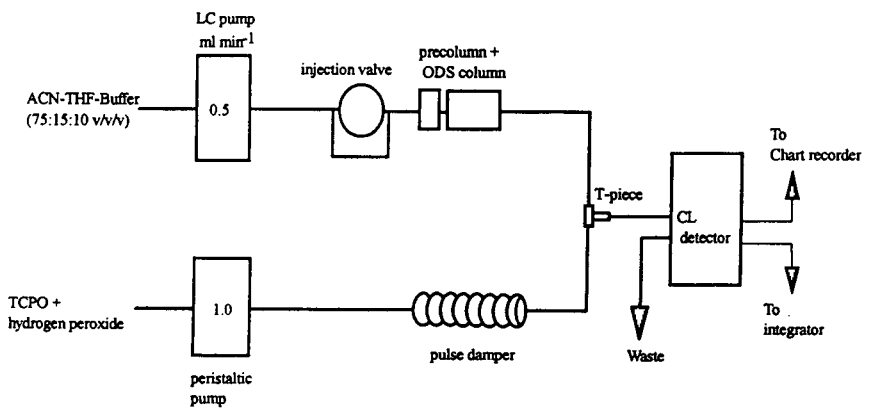


Fig. 2. LC–CL manifold for the determination of aldehydes in a non-aqueous medium.

## 3. Results and discussion

All concentrations quoted relate to the original sample.

### 3.1. Off-line derivatisation

Aliphatic aldehydes do not possess a strong chromophore or fluorophore and therefore derivatisation is needed to achieve the required selectivity and sensitivity. The most common derivatising reagent for aldehydes is dinitrophenylhydrazine, which produces strongly UV absorbing hydrazones [4,5]. This method has found wide application in environmental analysis, e.g. automobile exhaust gas [5], indoor and outdoor air [13], and sea and river waters [4]. Fluorescence derivatisation reagents that have been applied to the determination of aldehydes include benzofurazans [6], cyclohexanediones [7], quinolizinocoumarins [8], quinoxalinones [9] and dansylhydrazine [10]. These reagents were unsuitable for application to the analysis of used oils in a process environment because the reaction conditions were either incompatible with the used oil matrix (non-aqueous) or the procedures were lengthy and complex and, in most cases [6–9], the derivatising agent needed to be synthesized and purified prior to use.

Amino-substituted polycyclic aromatic hydrocarbons are amongst the most efficient sensitisers for peroxyoxalate CL [12] due to their low oxidation potentials and high fluorescence quantum yields. Aldehydes and ketones can be labelled with the amino-PAH 3-aminofluoranthene in a non-aqueous medium, which is compatible with the oil matrix, by acid catalysed reduction of the aldehydes in the presence of BAP [11]. Aldehydes react immediately with 3-aminofluoranthene in the presence of BAP, whilst ketones require heating for up to 14 h. Therefore, if no heating is applied, this procedure is selective for aldehydes.

Hexanal ($5.0 \cdot 10^{-4}$ mol $l^{-1}$) was derivatised with varying concentrations of 3-aminofluoranthene (0–$4.0 \cdot 10^{-3}$ mol $l^{-1}$) to determine the optimum concentration of the label. The yield of the reaction, measured by the signal-to-noise ratio, was directly related to the concentration of label. However, a large (160 ×) molar excess of the label (ca. $2 \cdot 10^{-3}$ mol $l^{-1}$) resulted in early breakthrough during solid-phase clean-up due to overloading of the Sep-Pak Plus cartridge. A concentration of $1.0 \cdot 10^{-3}$ mol $l^{-1}$ gave the best compromise between sensitivity and the solid-phase clean-up efficiency.

In a similar manner, the volume of BAP (0–100 $\mu$l) added to the reaction mixture was varied using hexanal as the model compound. When no catalyst was present, the derivatisation product was not detected. The optimum level of BAP was 5 $\mu$l (the smallest volume that could be added accurately) because volumes of BAP greater than 5 $\mu$l decreased the yield of the derivative. This decrease was probably due to the increased formation of non-fluorescent by-products, as no additional peaks were observed in the chromatogram.

The recovery of the aldehyde derivatives ($C_6$–$C_{14}$) spiked on a 0-h oil matrix from an alumina Sep-Pak Plus cartridge was in the range 97–100% (duplicate analysis). In addition, the solid-phase extraction procedure removed excess 3-aminofluoranthene label (thus minimising the possibility of further reactions during storage), a compound in the 0-h oil matrix that interfered with the octanal derivative peak and many other compounds in the oil matrix, e.g. phthalate esters which would otherwise accumulate in the LC column. Separation was achieved by greater retention of the more basic components on the alumina cartridge.

### 3.2. Liquid chromatography

Aryl oxalate esters and solvents are relatively expensive and therefore an LC procedure that reduces CL reagent and LC solvent consumption would be advantageous. This is realised using mid-bore (3.2 mm I.D.) columns, the diameter necessary to reduce the flow-rate of a conventional column (4.6 mm I.D.) by half and still retain an equivalent linear velocity. Furthermore, improved sensitivity for the same injection volume is possible as the peak volumes are lower, leading to less dilution of the injected

sample by the mobile phase, and specialised pumps, fittings or flow cells are not required [14,15]. Use of a larger sample volume with a conventional column would degrade resolution and column lifetime due to the nature of the oil matrix.

For the CL detection procedure reported here, a mixed TCPO-hydrogen peroxide post-column reagent was used, allowing for simpler instrument geometry than is possible with other peroxyoxalates (with the exception of bis[-4-nitro-2-(3,6,9-trioxadecyloxycarbonyl)phenyl]oxalate (TDPO) [16]). The other commonly used aryl oxalate bis(2,4-dintrophenyl)oxalate (DNPO) is unstable in the presence of hydrogen peroxide [17] and therefore cannot be used in this manner. The stability of the mixed reagent (TCPO and hydrogen peroxide concentrations of $1.0 \cdot 10^{-3}$ mol $l^{-1}$ and 0.1 mol $l^{-1}$, respectively) was assessed by replicate injections of a solution of 3-aminofluoranthene ($1 \cdot 10^{-6}$ mol $l^{-1}$) in acetonitrile over a period of 8 h. The decrease in signal-to-noise ratio over this time period was less than 5%.

Mann and Grayeski [11] did not remove the excess label prior to LC separation. However it was partially separated from 3-aminofluoranthene derivatives of $C_6$–$C_{10}$ straight-chain aldehydes on a $C_{18}$ column using a mobile phase of ACN–aqueous tris(hydroxymethyl)-aminomethane buffer ($4.0 \cdot 10^{-3}$ mol $l^{-1}$, pH 7.5, 85:15, v/v) [11]. In the work reported here, the excess 3-aminofluoranthene was completely removed using solid-phase extraction and 3-aminofluoranthene derivatives were then separated on an ODS2-5 column with a mobile phase of ACN–THF–imidazole buffer ($3.0 \cdot 10^{-2}$ mol $l^{-1}$, pH 7.5). The inclusion of THF ensured that the mobile phase was compatible with the derivatised oil dialysate samples [2]. Imidazole not only acts as a buffer but also has a marked catalytic effect on the kinetics of peroxyoxalate CL reaction leading to enhanced CL response [18].

THF is relatively non-polar compared with the other mobile phase components and increasing its relative concentration increases the eluting power of the mobile phase for the aldehyde-3-aminofluoranthene derivatives. However, increasing the THF concentration also results in quenching of the CL emission, which in turn decreases the signal-to-noise ratio [2]. Using a mixture of hexanal- and octanal-3-aminofluoranthene derivatives, the ACN–THF ratio was therefore varied from 80:10 to 70:20 whilst keeping the imidazole buffer constant at 10% v/v. The optimum mobile phase composition for separation was ACN–THF–imidazole buffer (75:15:10, v/v). A mixture of straight-chain aliphatic aldehydes ($C_6$, $C_8$, $C_{10}$, $C_{12}$ and $C_{14}$) dissolved in toluene and spiked on the 0-h oil matrix was derivatised and separated using this mobile phase. Retention data and capacity factors for the aldehydes in toluene and in 0-h and 32-h oil dialysate matrices are given in Table 1 and a chromatogram of the separation is shown in Fig. 3.

Table 1
Capacity factors for synthetic mixture of aldehyde derivatives in toluene and spiked on 0-h and 32-h oil dialysates and concentrations of aldehydes in the 32-h used oil dialysate

| Aldehyde | Capacity factor ($k'$)[a] in toluene matrix | Capacity factor ($k'$)[a] in 0-h oil dialysate matrix | Capacity factor ($k'$)[a] in 32-h oil dialysate matrix | Concentration in 32-h used oil dialysate (nmol $ml^{-1}$) |
|---|---|---|---|---|
| Hexanal | 1.9 | 2.1 | 2.2 | 46 |
| Octanal | 3.0 | 3.2 | 3.4 | 15 |
| Decanal | 4.8 | 5.0 | 5.3 | 66 |
| Dodecanal | 8.0 | 8.0 | 8.6 | 77 |
| Tetradecanal | 13.3 | 12.8 | 13.8 | 186 |

[a] $t_0 = 2.0$ min.

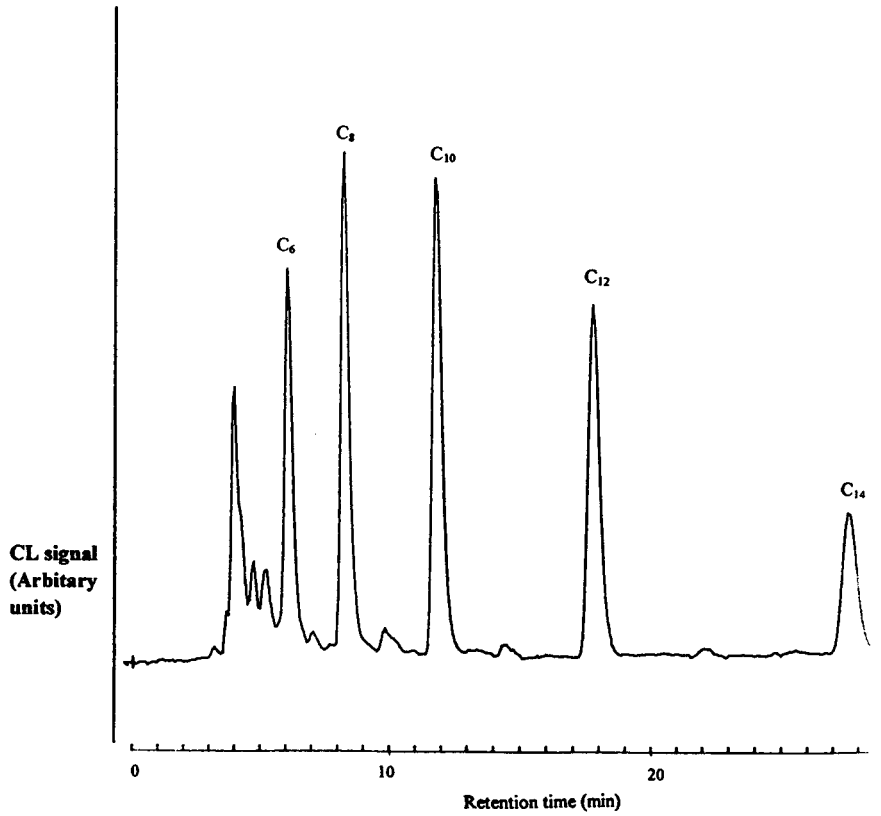


Fig. 3. Chromatogram of aliphatic straight-chain aldehyde-3-aminofluoranthene derivatives of $C_6$–$C_{14}$ aldehydes spiked on a 0-h oil matrix.

### 3.3. Chemiluminescence detection

CL reagent flow-rate and concentration were investigated using the hexanal derivative as a model compound. The CL emission intensity was directly related to reagent flow-rate up to 1.0 ml $min^{-1}$. Higher flow-rates led to lower observed CL emission intensities as the maximum intensity occurred after the analyte had passed through the flow cell. The CL emission intensity was also directly related to the concentrations of TCPO and hydrogen peroxide which are limited by the solubility of TCPO in water.

The optimum conditions, which were used in all subsequent experiments were: TCPO $1.3 \cdot 10^{-3}$ mol $l^{-1}$, hydrogen peroxide $8.8 \cdot 10^{-2}$ mol $l^{-1}$, CL reagent flow-rate 1.0 ml $min^{-1}$. Using these conditions the mixed CL reagent was stable for a period of 24 h, but degraded thereafter and could not be used after 48 h.

### 3.4. Calibration data

Calibration data for straight-chain aliphatic aldehydes ($C_6$, $C_8$, $C_{10}$, $C_{12}$ and $C_{14}$) spiked on the 0-h oil matrix were all linear over the range from the detection limit to $5.0 \cdot 10^{-4}$ mol $l^{-1}$ ($0.9980 < r^2 < 0.9997$). The limits of detection ($S/N = 3$) were in the range $3.0 \cdot 10^{-7}$ ($C_6$)–$3.4 \cdot 10^{-6}$ ($C_{14}$) mol $l^{-1}$ (which includes the derivatisation step) and is equivalent to 0.7–75 fmol on-column (5-$\mu$l injection). These results are an order of magnitude lower than those reported previously [11].

Recoveries were in the range 83–104% for a mixture of straight-chain aliphatic aldehydes ($C_6$,

$C_8$, $C_{10}$, $C_{12}$ and $C_{14}$) derivatised at the $2.5 \cdot 10^{-4}$ mol $l^{-1}$ level in toluene. The precision (relative standard deviation) of the complete analytical procedure for a mixture of decanal and dodecanal ($2.5 \cdot 10^{-5}$ mol $l^{-1}$) was 5.6% and 7.1% ($n = 6$), respectively.

### 3.5. Oil analysis

An oil was sampled from the sump of a car engine after 0, 16, 24 and 32 h of continuous running. Analysis of the 32 h used oil dialysate by LC with fluorescence detection [3] showed the presence of an homologous series of straight-chain aliphatic acids, with hydrocarbon chain lengths from $C_7$ to $C_{22}$.

The oil dialysates sampled from the car engine were derivatised with 3-aminofluoranthene and analysed using the optimum conditions described above. Two distinct series of peaks first appeared in the 16-h used oil dialysate and their peak heights increased in magnitude in the 24-h and 32-h used oil dialysates (Fig. 4). These two series are labelled * and Ø on the chromatogram of the 24-h used oil dialysate (Fig. 4). Several peaks of the series labelled * were identified as straight-chain aldehydes by capacity factors in the 32-h used oil dialysate (Table 1). This was confirmed by spiking the used oil dialysate with a mixture of the aldehydes prior to derivatisation.

A plot of log (capacity factor of the aldehyde-3-aminofluoranthene derivatives) against carbon

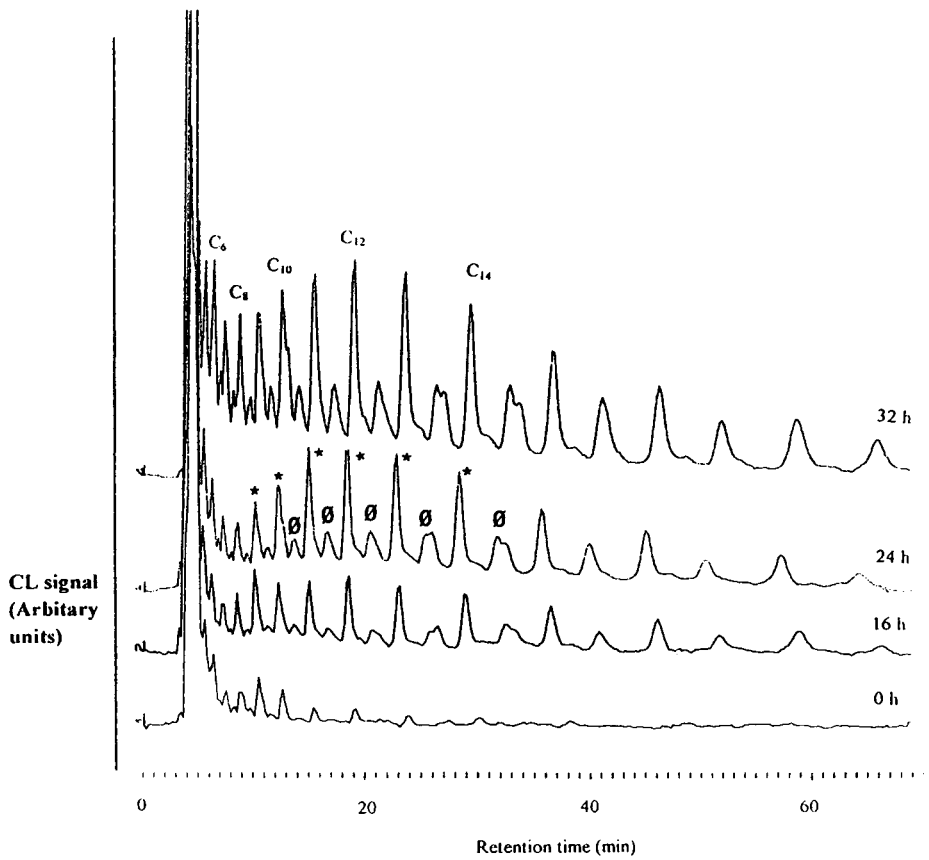


Fig. 4. Chromatograms showing the formation of aldehydes in an engine oil over the 32-h time course of an engine test The chromatogram of the 24-h used oil dialysate shows homologous series of aliphatic straight chain aldehydes (*) and unidentified derivatives, possibly branched-chain aldehydes (Ø).

Table 2
Identification of aldehydes in the 32-h used oil dialysate derived from the equation: $\log(k') = 0.09985$ (number of carbon atoms) − 0.2640

| Capacity factor ($k'$)[a] | Calculated number of carbon atoms | Aldehyde |
|---|---|---|
| 2.73 | 7.0 | heptanal ($C_7$) |
| 4.25 | 8.9 | nonanal ($C_9$) |
| 6.76 | 10.9 | undecanal ($C_{11}$) |
| 10.88 | 13.0 | tridecanal ($C_{13}$) |
| 17.57 | 15.1 | pentadecanal ($C_{15}$) |
| 22.41 | 16.2 | hexadecanal ($C_{16}$) |
| 28.72 | 17.2 | heptadecanal ($C_{17}$) |

[a] $t_0 = 2.0$ min.

number of the aldehydes ($C_6$–$C_{14}$) was linear (equation of line of best fit: $\log(k') = 0.09985$ (number of carbon atoms) − 0.2640) with a correlation coefficient ($r^2$) of 0.9994. This is characteristic of a homologous series and can be used to predict the capacity factor of any member of that series when using isocratic elution [19]. The aliphatic straight-chain aldehydes observed in the chromatogram shown in Fig. 4 were identified using the equation above and are listed in Table 2. A second series of peaks (Ø) has been tentatively identified as branched-chain aliphatic aldehydes. The formation of aldehydes in the oil is directly related to the length of the engine test, as shown graphically in Fig. 5.

## 4. Conclusions

Straight-chain aliphatic aldehydes ($C_6$–$C_{14}$) in non-aqueous media can be rapidly determined by selective derivatisation with 3-aminofluoranthene and reversed-phase LC with CL detection. A single stream CL reagent line containing mixed TCPO–hydrogen peroxide reagent can be used. Calibration data over the range from the detection limit to $5 \cdot 10^{-4}$ mol $l^{-1}$ were linear ($0.9980 < r^2 < 0.9997$) and limits of detection ($S/N = 3$), including the derivatisation step, were in the range $3.0 \cdot 10^{-7}$–$3.4 \cdot 10^{-6}$ mol $l^{-1}$ (0.7–75 fmol on-column). Analysis of oil from an engine test showed that straight-chain aliphatic aldehydes ($C_6$–$C_{14}$) are formed during the oxidation of engine oils and that their concentration increases with running time. Bis-(2-nitrophenyl)oxalate would be an attractive alternative to TCPO because the solubility is relatively high and it can also be mixed with hydrogen peroxide but this reagent is much more difficult to obtain from commercial sources.

## Acknowledgements

Part of this study was funded by SERC grant GR/H49528 as part of a DTI/SERC TAPM LINK award. The authors would also like to

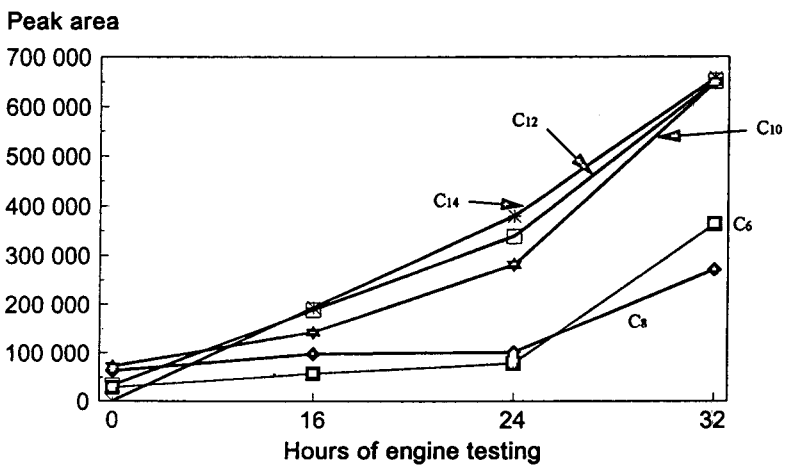


Fig. 5. Graph showing the rate of increase of the individual aldehydes in an engine oil during the course of an engine test.

thank Dr. Tony Moss (Camspec, Cambridge) for providing the photodiode-based CL detector.

## References

[1] D. Klamen, Lubricants and Related Products, Verlag Chemie, Basel, 1984, p. 14.
[2] S.W. Lewis, P.J. Worsfold, A. Lynes and E.H. McKerrell, Anal. Chim. Acta, 266 (1992) 257.
[3] S.W. Lewis, P.J. Worsfold and E.H. McKerrell, J. Chromatogr. A, 667 (1994) 91.
[4] K. Takami, K. Kuwata, A. Sugimae and M. Nakamoto, Anal. Chem., 57 (1985) 243.
[5] A.C. Geng, Z.L. Chen and G.G. Siu, Anal. Chim. Acta, 257 (1992) 99.
[6] H. Koizumi and Y. Suzuki, J. Chromatogr., 457 (1988) 299.
[7] W.L. Stahovec and K. Mopper, J. Chromatogr., 298 (1984) 399.
[8] F. Traore, M. Tod, J. Chalom, R. Farinotti and G. Mahuzier, Anal. Chim. Acta, 269 (1992) 211.
[9] T. Iwata, T. Hirose, M. Nakamura and M. Yamaguchi, Analyst, 118 (1993) 517.
[10] L. Nondek, R.E. Milofsky and J.W. Birks, Chromatographia, 32 (1991) 33.
[11] B. Mann and M.L. Grayeski, J. Chromatogr., 386 (1987) 149.
[12] K.W. Sigvardson, J.M. Kennish and J.W. Birks, Anal. Chem., 56 (1984) 1096.
[13] D. Grosjean and E.L. Williams, Atmos. Environ., 26A (1992) 2923.
[14] N.A. Parris, Instrumental Liquid Chromatography, 2nd ed., Elsevier, Amsterdam, 1984, p. 52.
[15] M. Miyaguchi, K. Honda, T. Toyo'oka and K. Imai, J. Chromatogr., 352 (1986) 255.
[16] K. Imai, Y. Matsunaga, Y. Tsukamoto and A. Nishitani, J. Chromatogr., 400 (1987) 169.
[17] G.J. de Jong, N. Lammers, F.J. Spruit, U.A.Th. Brinkman and R.W. Frei, Chromatographia, 18 (1984) 129.
[18] N. Hanaoka, R.S. Givens, R.L. Schowen and T. Kuwana, Anal. Chem., 60 (1988) 2193.
[19] P. Dufek and E. Smolkova, J. Chromatogr., 257 (1983) 247.

ELSEVIER

Journal of Chromatography A, 704 (1995) 339–349

JOURNAL OF CHROMATOGRAPHY A

# Preferred high-performance liquid chromatographic anion-exchange chromatographic contact region for recombinant rat cytochrome $b_5$

David J. Roush[1], Davinder S. Gill[2], Richard C. Willson*

*Department of Chemical Engineering, University of Houston, 4800 Calhoun Avenue, Houston, TX 77204-4792, USA*

Received 5 December 1994; accepted 8 February 1995

**Abstract**

The HPLC anion-exchange isocratic retention behaviors of site-directed charge mutants of the recombinant soluble core of rat cytochrome $b_5$ on Mono Q HR 5/5 were investigated as a function of sodium chloride concentration, at a fixed temperature and eluent flow-rate. The retention behavior of the charge mutants was observed to depend on both the net charge of the protein and on the distribution of charged residues on the protein surface. Site-directed mutants of the same net charge differed significantly in retention behavior; differences in retention were observed to increase with decreasing ionic strength. The retention results were interpreted in terms of the stoichiometric displacement model (SDM) to obtain the apparent number of binding sites in the contact region, $Z$. Elimination of a single negatively charged residue, in an apparent preferred chromatographic contact region, resulted in disproportionately large changes in the retention behavior as compared with elimination of a single negatively charged residue on other areas of the protein surface. The experimentally determined preferred chromatographic contact region compares favorably with the results of batch equilibrium adsorption studies on the same system and with previously reported results of computational molecular electrostatic modeling. The results of this study indicate that the observed protein ion-exchange retention represents the summation of many fractional electrostatic interactions of varying interaction energies. Therefore, protein ion-exchange retention is a function of both the number of contacts and the individual electrostatic interaction energies of the contacts between the protein and the ion-exchange surface.

## 1. Introduction

Electrostatic interactions between oppositely charged groups on the protein and adsorbent surfaces are the primary interactions in the ion-exchange chromatography of proteins. However, the precise contributions of the charged groups located on the surfaces of the protein and the ion-exchanger to retention have not been well characterized. Several studies have indicated that the distribution of charges on the protein surface can influence the observed retention behavior to the extent that a protein may be retained on an ion-exchange surface of the same sign as the net charge of the protein [1,2]. The ion-exchange

* Corresponding author.

[1] Present address: Merck and Co., Bioprocess R&D, P.O. Box 2000, Rahway, NJ 07065, USA.

[2] Present address: Department of Surgery, Massachusetts General Hospital and Harvard Medical School, Boston, MA 02114, USA.

0021-9673/95/$09.50 
*SSDI* 0021-9673(95)00180-8

adsorption of a protein has also been observed to be dominated by patches or clusters of charge on the protein's surface [1–6]. These observations are in contrast to the traditional assumption that ion-exchange retention is governed by the net charge of the protein so that a protein will be retained on an anion-exchange surface at any pH above the protein's isoelectric point. The surface topography of the protein has also been noted to sterically restrict electrostatic interactions between a protein and an ion-exchange surface [6].

The non-mechanistic stoichiometric displacement model (SDM) originally proposed by Boardman and Partridge [7] and first applied to HPLC by Kopaciewicz et al. [1] has been widely employed to determine the regression parameter $Z$, the apparent number of contacts between the protein and the ion-exchange surface participating in the adsorption/desorption process [1,3,5,6,8–10]. $Z$-values have been found to be fractional and have been observed to change as a function of loading [4,11,12]. The change in the observed value of $Z$ with different loading levels has been attributed to changes in the orientations of absorbed protein molecules as the concentration of the absorbed protein increases. The existence of a heterogeneous distribution of orientations for adsorbed protein molecules is supported by observations from other systems mediated by electrostatic interactions, especially protein–protein interactions. For example, the cytochrome $b_5$/cytochrome c complex has been suggested to adopt multiple binding orientations which appear to vary as a function of ionic strength [13–15]. These studies experimentally confirmed molecular modeling studies by Wendoloski et al. [16], who determined that the flexibility of the two proteins allows for the sampling of multiple binding conformations. This investigation of the existence of multiple binding orientations for an electrostatically mediated protein–protein complex can also aid in understanding of protein ion-exchange interactions, as fractional chromatographic $Z$-values can also be interpreted to represent the summation of many fractional interactions between the protein and ion-exchange surface.

It is important to note that the observed protein ion-exchange retention behavior reflects the contributions of both the protein and the adsorbent. Wu and Walters [17] investigated the effects of varying the charge density of a cation-exchanger on the isocratic retention of lysozyme and cytochrome c. The value of $Z$ and even the elution order was observed to vary as a function of the adsorbent charge density, illustrating the importance of the adsorbent's contributions to retention behavior [17]. These researchers [17] also noted that the heterogeneity of the ion-exchange surface can affect the observed protein ion-exchange retention behavior, in agreement with the results of Gill et al. [10].

This study examines retention of wild type and site-directed charge mutants of recombinant soluble tryptic core of rat cytochrome $b_5$ on the strong anion-exchanger, Mono Q. This protein was chosen as an experimental model because of the wealth of related structural [18–21] and biochemical data available and the existence of an efficient system for its expression in *E. coli* [22]. The protein is well-suited for use in anion-exchange adsorption studies because of its great stability in solution, strong chromophore, moderate molecular mass ($M_r$ = 13 603) and negative net charge at pH values near neutrality; p*I* 4.6 by isoelectric focusing (IEF); 23 negative groups (including the protoporphyrin) and 15 positive groups (allowing for partial titration of histidines) resulting in net charge −9.4 at pH 8.0.

The goals of this investigation were to: (a) determine the contributions of the individual charged amino acid residues located on the protein's surface to the observed anion-exchange retention behavior, (b) to verify the existence of a "preferred chromatographic contact region" on the protein surface for interaction with the anion-exchange surface and (c) to determine the contributions of the other charged residue clusters by providing a more complete map of the protein surface. The HPLC anion-exchange retention results are compared to equilibrium batch adsorption data for the same protein/ion-exchanger system by Gill et al. [12].

## 2. Experimental

### 2.1. Reagents and proteins

The reagents, proteins, and protein purification and characterization methods used in these investigations were the same as those previously described [9,10,12].

### 2.2. Equipment

The experimental system and the control experiments verifying the precision and estimating the accuracy of the experimental apparatus have been previously described in detail [9] and are therefore described only briefly. The entire HPLC system, with the exception of the computer (NEC 386/25 CPU; NEC Technologies, Foxborough, MA, USA), and the computer interface (System Interface Module; Waters, Milford, MA, USA) was located in a temperature-controlled environment room (Norlake, Hudson, WI, USA) regulated to within ±0.5°C. Data were analyzed using Maxima 3.0 (Dynamic Solutions) software. All chromatographic experiments were performed with a Waters HPLC system consisting of two Model 510 positive displacement pumps, a WISP 710B automated sample injection system and either a Model 441 UV–Vis single wavelength detector operating at 405 nm or a Model 481 variable-wavelength detector. The 405 nm wavelength was used for rat cytochrome $b_5$ retention measurements because it is close to the oxidized protoporphyrin Soret band maximum at 412 nm.

Mono Q (Pharmacia) prepacked strong anion-exchange columns (HR 5/5, 50 × 5 mm I.D.) were used in all studies. Each determination of the SDM parameter $Z$ was carried out entirely on a single column to avoid any effects of inter-column variations. Columns were replaced when the plate count fell below the Pharmacia specification of 25 000 theoretical plates/m.

### 2.3. Chromatography

Protein samples were prepared in 10 m$M$ Tris, pH 8.0 plus the appropriate NaCl concentration corresponding to the intended elution conditions. Protein samples of 50 $\mu$l were injected and eluted isocratically with eluents containing 10 m$M$ Tris, pH 8.0 and NaCl in the range of 150 to 700 m$M$, matching the injection buffer. Protein sample concentrations were 0.26 ± 0.01 mg/ml for the experiments designated 0.25 mg/ml. Retention was studied at a fixed nominal temperature of 25°C (25.0 ± 0.25°C) with a nominal eluent flow-rate of 0.5 ml/min (0.48 ± 0.01 ml/min). For each eluent flow-rate, the protein was assigned a non-retained volume corresponding to the elution volume at 700 m$M$ NaCl, corrected for non-column system volume, based on control experiments which showed that retention does not vary significantly in the range of 600 to 700 m$M$ NaCl.

Protein recovery calculations were performed as described previously [9]. The recoveries of cytochrome $b_5$ were 100 ± 6%. A gradient cleaning run, employing 10 m$M$ Tris, pH 8.0 and 2 $M$ NaCl, was performed after isocratic runs of less than 300 m$M$ NaCl. The ratio of peak area to baseline noise integrated over a period equal to the peak width at baseline was typically ca. 75 under conditions of strong retention.

As discussed previously [9,23], the $k'$ value can be a strong function of temperature. Therefore, the protein samples and eluents were pre-equilibrated at the experimental temperature. Previous studies on the effect of variations in the mean system temperature in the range of 25.0 ± 0.4°C indicated that at 150 m$M$ a variation in temperature of 0.4°C would produce a change in $k'$ or $Z$ of ca. 5% and 0.4%, respectively.

## 3. Data analysis

The capacity factor, $k'$ was calculated based on the protein retention volume, $V_R$ and the protein non-retained volume, $V_o$, corrected for non-column system volume. Retained and non-retained volumes were obtained from the retention time and the eluent volumetric flow-rate determined gravimetrically using the measured

eluent density for each run. Retention data were also analyzed through application of the stoichiometric displacement model [1] to yield the apparent number of protein-adsorbent contacts, $Z$. For the one-to-one electrolyte employed in this study, NaCl, the value of $Z$ equals half the slope of the plot of log $k'$ versus the log of the reciprocal ionic strength. Values of the capacity factor, $k'$ calculated for representative runs from the peak maximum and from the mean retention time for the wild type protein were in agreement within experimental error [9]. The $k'$ data presented in this work were determined from the peak maxima.

The mutations examined in this work consisted of conservative carboxylic acid to amide substitutions located on surface residues. The mutations examined are designated using the single letter code for each amino acid where the site-directed mutation(s) occurred; e.g. E47,48Q represents the mutation from residue E (glutamic acid) to Q (glutamine) at both residues 47 and 48. Representative conservative site-directed charge mutants used in this study have been previously examined by NMR spectroscopy [18] to determine if any substantial tertiary conformational change resulted from the charge mutation. The NMR results indicated that only the double charge substitution E47,48Q resulted in a significant difference in tertiary structure when compared with the wild type; more conservative mutations did not result in an experimentally observable tertiary structural change. The other site-directed mutants studied by Rodgers et al. [18] also involved the loss of one negative charge and are denoted as D60N and E48Q, where D represents aspartic acid and N represents asparagine. Based on the tertiary structural results for D60N and E48Q (which represent the same type of conservative mutation as the other mutant proteins examined) and in the absence of any direct structural data, the other site directed mutants employed in this study will be assumed to have essentially the same tertiary structure as the wild type protein. The sole exception is the mutant D70K which represents a substitution of a positively charged lysine residue for a negatively charged aspartic acid. This amino acid mutation involves residues of significantly different side-chain geometry, and the charge reversal and associated local structural changes associated with this mutation might substantially alter the tertiary structure of the protein in the local environment of the substitution. Hence, the conclusions based on the investigation of the D70K mutant will take the possibility of mutation-induced local conformational changes into account.

## 4. Results

The contributions of various charged amino acid residues to the overall protein retention were inferred by comparing the retention values of the site-directed mutant proteins to that of the wild type protein, as a function of NaCl concentration. Retention data for the mutant and wild type proteins over a range of NaCl concentrations are presented in Fig. 1.

As illustrated in Fig. 1, the resolution among the mutant proteins decreases as the ionic strength increases. The loss of resolution ($R_s$) is so pronounced that for NaCl concentrations of 300 and 400 m$M$, the mutant proteins are not well resolved from the wild type protein; average $R_s$ ($\pm$ S.D. over mutant proteins) decreases from $0.48 \pm 0.30$ (300 m$M$) to $0.20 \pm 0.21$ (400 m$M$). Resolution is clearly enhanced as the NaCl concentration is reduced from 400 to 150 m$M$. A potential explanation for this change is that as the ionic strength increases, the electrostatic screening of the protein surface potentials increases, masking the differences among the mutants on all but the local length scale (less than 10 Å). Therefore, patches or clusters of charge on the protein surface could dominate retention behavior on a local scale.

The differences in the relative contributions of the various charged amino acid groups to retention can be analyzed from the site-directed mutant protein retention data presented in Fig. 1. All of the site-directed unit charge change mutant proteins studied have the same net charge at pH 8.0 of $-8.4$, yet their retention behaviors vary significantly. Examples are the

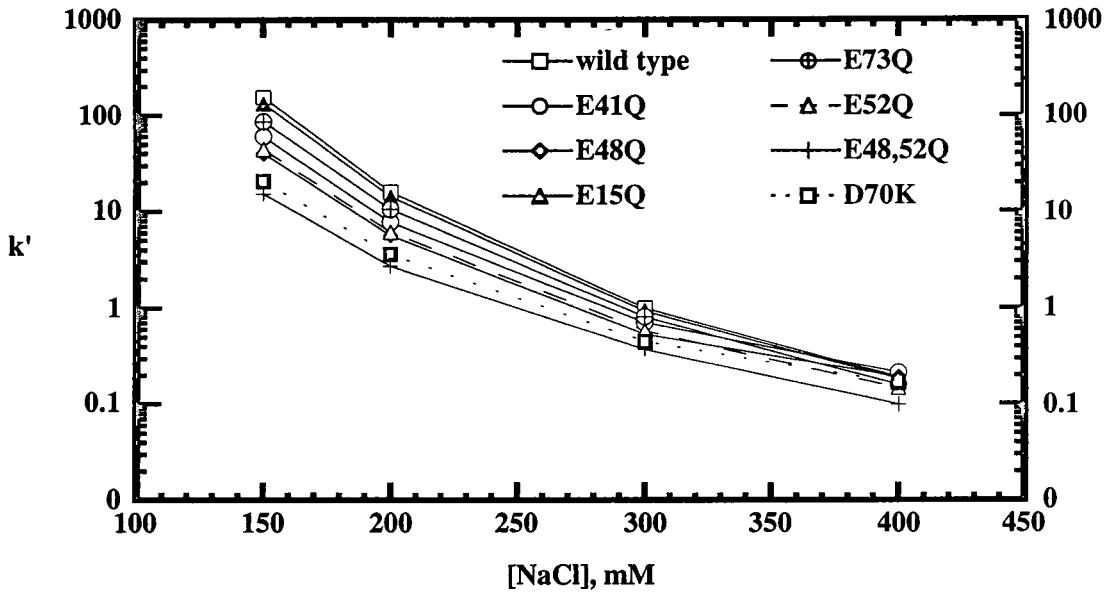


Fig. 1. A semilog plot of the capacity factor, $k'$, versus the NaCl concentration, comparing the retention of wild type and site-directed mutant forms of rat cytochrome $b_5$ on Mono Q. All retention data were acquired at a nominal eluent flow-rate of 0.5 ml/min and at a mean system temperature of 25°C. The data presented are the results of duplicate retention measurements. Error bars have been omitted for clarity. The average percentage errors from duplicate retention measurements are 5.5 (150 m*M*), 3.6 (200 m*M*), 4.8 (300 m*M*) and 14.0 (400 m*M*).

mutant proteins E15Q, E41Q, and E48Q which have the respective isocratic capacity factors (in 10 m*M* Tris, pH 8.0 and 150 m*M* NaCl) of 132.8 ± 5.5, 59.6 ± 0.6, and 40.0 ± 1.7, compared to 155.6 ± 21.2 for the wild type protein. Deletion of a single charge, therefore, can have only a minor effect on retention (15% loss of retention for E15Q) or may significantly reduce retention (62 and 74% for E41Q and E48Q) as compared to the wild type protein. The reduction in the net charge of the protein by two units to −7.4, either through the double mutant E48,52Q or the double charge change mutant D70K, resulted in even more dramatic losses in relative retention of 87 and 94%, respectively. However, results obtained with the double charge mutants must be viewed carefully since these mutant proteins could have a slightly different tertiary structure than the wild type protein. These retention results, combined with the results from stoichiometric displacement model analysis of the wild type protein retention data ($Z$ of 3.4 at 25°C), clearly indicate that only a small fraction of the 23 negative residues of rat cytochrome $b_5$ available for interaction with the anion-exchange surface of Mono Q are actually fully involved in the anion-exchange adsorption process. The anion-exchange retention results for the site-directed charged mutants indicate that the relative contribution of a particular charged residue is a strong function of its location on the protein surface.

The SDM analyses allow one to determine the change in the value of $Z$ ($\Delta Z$) resulting from charge mutagenesis. For comparison, the values for $Z$ and of $\Delta Z$ of the site-directed mutants and the wild type cytochrome $b_5$ obtained from both HPLC (with the corresponding mean system temperatures) and equilibrium batch adsorption experiments [10,12] are tabulated in Table 1. The $Z$ values obtained by the two experimental methods are in good agreement with respect to the relative contributions of the various residues. For instance, both methods indicate that the residue E15 does not appear to substantially contribute to the anion-exchange retention of

Table 1
The values for $Z$ obtained from isocratic, isothermal HPLC retention measurements at 0.5 ml/min (in 10 m$M$ Tris, pH 8.0 and the associated NaCl concentration) for the wild type and site-directed mutant forms of rat cytochrome $b_5$ at a mean system temperature of 25.0 ± 0.25°C for each set of Z determinations (HPLC)

| Protein | $Z$ (HPLC) | $\Delta Z$ (HPLC) | $Z$ (Batch) | $\Delta Z$ (Batch) |
|---|---|---|---|---|
| Wild type | 3.42 ± 0.01 | N/A | 2.92 ± 0.32 | N/A |
| E15Q | 3.37 ± 0.04 | −0.05 | 2.95 ± 0.25 | 0.03 |
| E41Q | 2.89 ± 0.07 | −0.53 | 2.18 ± 0.27 | −0.74 |
| E48Q | 2.76 ± 0.07 | −0.66 | 2.33 ± 0.34 | −0.59 |
| E52Q | 2.91 ± 0.04 | −0.51 | N.D. | N.D. |
| E48,52Q | 2.56 ± 0.08 | −0.86 | N.D. | N.D. |
| E73Q | 3.20 ± 0.03 | −0.22 | N.D. | N.D. |
| D70K | 2.49 ± 0.08 | −0.93 | N.D. | N.D. |

$Z$-values determined from equilibrium batch adsorption experiments [10,12] at a nominal temperature of 25°C are included for reference. Errors are standard deviations for $Z$-values determined from replicate experiments.

cytochrome $b_5$, since $Z$ values obtained for E15Q are not statistically significantly different from those obtained for the wild type protein. Both methods indicate approximately the same contribution (within experimental error) for the residues E41 and E48, based on the $\Delta Z$ values obtained for the mutant proteins E41Q and E48Q.

The importance of the location of a charged amino acid residue to its contribution to the observed retention behavior of cytochrome $b_5$ can be better understood by examining the tertiary structure of the protein [21]. The locations of the site-directed mutations and the associated $\Delta Z$ values resulting from the charge mutations are illustrated on the Cα (carbon backbone) trace in Fig. 2, for both HPLC and batch equilibrium adsorption experiments [12]. Fig. 2 reveals the presence of a patch on the protein surface which appears to preferentially mediate protein anion-exchange adsorption. Deletion of a negative charge (glutamate to glutamine site-directed mutant) from the residues E41, E48 or E52 results in the largest observed change in the apparent number of contacts, $Z$ (Table 1) and this appears to be a dominant patch mediating retention. These residues, along with E47 and E42, form a patch (refer to Fig. 2) on the left side of the protoporphyrin heme prosthetic group. As a comparison, elimination of a negative charge on the opposite side of the prosthetic group, as in D64N ($\Delta Z = -0.17$, batch adsorption), E60Q ($\Delta Z = -0.06$, batch adsorption) and E73Q ($\Delta Z = -0.22$) results in only a small change in the value of $Z$. Deletion of two charges (resulting in a protein of net charge −7.4) to form mutant D70K, however, did result in a substantial change in the apparent number of contacts with respect to the wild type

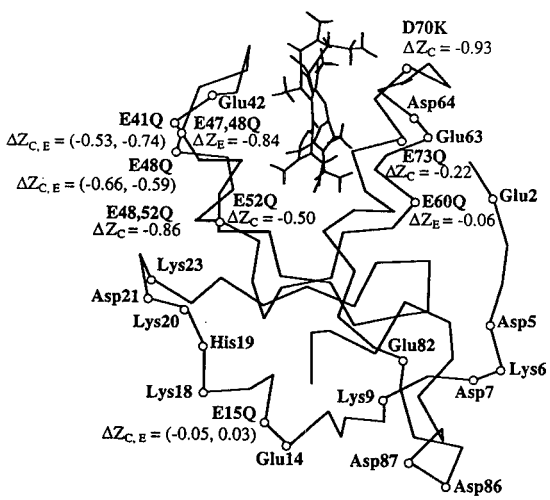


Fig. 2. A Cα trace of rat cytochrome $b_5$ [21] depicting the site-directed mutant proteins examined in this investigation (single letter amino acid designations) and the associated $\Delta Z$ values (with respect to the wild type protein). Results from the isocratic, isothermal HPLC retention measurements [9] and equilibrium batch adsorption experiments [10,12] are denoted by C and E, respectively.

protein, $\Delta Z = -0.93 \pm 0.08$. The retention results for this mutant, combined with those for E73Q, indicate that the patch of negative residues (D64, D70 and E73) located on the opposite side of the heme from the dominant patch is somewhat involved in anion-exchange retention of the protein. These results are also in agreement with earlier results for the mutants D70K and E73Q (see Fig. 1), which indicated that elimination of a single negative charge resulted in a substantial loss in retention (87 and 45%, respectively, relative to the wild type protein). These comparisons indicate that HPLC is a robust method for analyzing changes in retention behavior resulting from charge mutations and that HPLC can be used to approximate the results of equilibrium batch adsorption studies.

The varying contributions of different charged amino acid residues to the anion-exchange retention behavior of the protein are further illustrated by the distribution of retention times of the site-directed mutant proteins of the same net charge (Fig. 1). These results indicate that certain residues contribute more strongly to the ion-exchange retention behavior than do others. The combination of these two analyses is presented in Fig. 3; a plot of the relative retention of the mutant protein (with respect to the wild type protein), $k'_r$, versus the change in apparent number of contacts ($\Delta Z$) resulting from mutagenesis. The results from both the HPLC and equilibrium batch adsorption experiments [12] are presented to provide a better map of the protein surface, although some differences did exist between the protocols for HPLC and batch adsorption experiments. Both data were acquired at a nominal temperature of 25°C (see Table 1) in 10 m*M* Tris, pH 8.0 (batch experiments also included 0.1 m*M* EDTA in the buffer). The HPLC data were acquired over a range of NaCl concentrations of 150 to 400 m*M* whereas the batch adsorption data were acquired

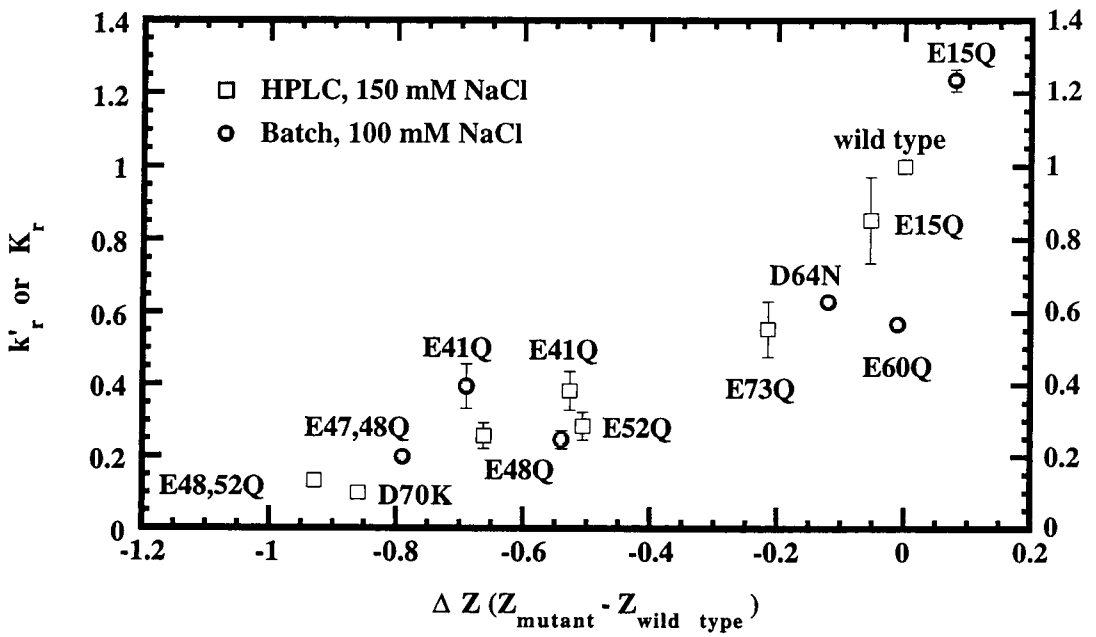


Fig. 3. Plot of the reduced or relative capacity factor, $k'_r$, ($k'_r = k'_{mutant}/k'_{wild\ type}$) versus the change in the apparent number of contacts, $\Delta Z$, (determined using the stoichiometric displacement model) resulting from the mutation. The value for the analogous relative Hill binding constant ($K_r$) from equilibrium batch adsorption experiments [10,12] have been included to provide a better map of the protein surface and for comparison purposes. HPLC and batch adsorption experiments were both performed at a nominal temperature of 25°C. Error bars represent standard deviations based on the results of replicate experiments.

over a range of NaCl concentrations of 75 to 175 m$M$, the range in which equilibrium adsorption is most accurately quantifiable.

Despite the differences in data acquisition protocols between the HPLC and batch adsorption methods, several important comparisons can be made among the data. Combining these two analyses (relative retention and change in apparent number of contacts) indicates that even when the apparent number of interactions ($Z$-value) is similar, relative retentions are different. For instance, the apparent number of contacts between the protein and the anion-exchange surface, $Z$, and the relative retention with respect to the wild type protein (in parentheses) for E73Q and E15Q are $3.20 \pm 0.03$ (0.55) and $3.37 \pm 0.04$ (0.85), respectively. Thus, large changes in retention can result from only a small change in $Z$. This comparison can be generalized across the data resulting in the following observations.

First, the elimination of a single charged residue (through site-directed mutagenesis) on the protein surface produces less than a unit decrease in $Z$, for all the proteins examined in both HPLC and batch adsorption experiments (Table 1, Fig. 3). The fractional change in $Z$ resulting from a unit change in charge suggests that the overall number of contacts between the protein and the ion-exchanger is the summation of many fractional interactions or is the statistical average over diverse orientations of individual charge–charge interactions. The nature of the electrostatic interactions between the protein and the ion-exchanger has been further investigated through computational electrostatic modeling calculations [24]. The electrostatic modeling results indicate that two patches of residues, including residues E47, E48, D70, R72, and E73 (surrounding the heme prosthetic group) (patch 1) and residues E60, D64, H67 (patch 2) are primarily involved in the anion-exchange adsorption behavior of cytochrome $b_5$, in agreement with the experimental results.

Deletion of two negative charges by site-directed mutagenesis (e.g., in E48,52Q) produces a value of $\Delta Z$ less than the sum of the $\Delta Z$'s of the independent E48Q and E52Q mutations (Table 1). This observation is clarified by comparing the relative changes in retention for the single charge mutants E48Q and E52Q to the relative change in retention of the double mutant E48,52Q. Values of reduced $k'$ ($k'_{\text{mut}}/k'_{\text{wild type}}$) are 0.25 and 0.28 for the single mutants E48Q and E52Q and 0.1 for the double mutant E48,52Q. Therefore, these two mutants display reductions in retention (with respect to the wild type protein) of 75% and 72%, respectively, while the double charge reduction mutant E48,52Q displays approximately a 90% reduction in retention. The results for E48,52Q must be viewed with some caution since NMR data on this mutant [18] indicated that a significant local conformational change results from this double mutation. Even taking into account the limitations of the comparison, it is clear that the electrostatic interactions between the protein and the ion-exchange surface are fractional in nature and that the summation of these interactions is not linearly additive.

The relative contributions of various residues are further explored by the data analyses presented in Fig. 4, which presents a plot of the relative retention, $k'_r$ versus relative $Z_r$ which is equal to $Z_{\text{mutant}}/Z_{\text{wild type}}$. These results indicate that the deletion of a single charged residue can have dramatic effects on retention behavior, while resulting in only a small percentage reduction in the apparent number of contacts. The retention results for the site-directed mutants E73Q and E48Q clearly illustrate this phenomenon. E73Q and E48Q have retentions reduced by 45% and 74% but $Z$ reduced by 6% and 19%, respectively. Changing a contact residue from a negative to a positive charge in the case of D70K results in virtually a complete loss of retention (87% reduction) with a decrease in $Z$ of only 27%. A related example is E41Q, which has a relative retention ($k'_r$) of 0.38 while retaining 85% of the apparent number of contacts ($Z_r$ of 0.85) of the wild type protein. For the extreme case of E48,52Q the relative retention ($k'_r$) is 0.098 with an associated $Z_r$ value of 0.75. These results imply, therefore, that under the conditions examined in this study, only a small fraction (less than 30%) of the apparent contacts between the protein and the ion-exchange sur-

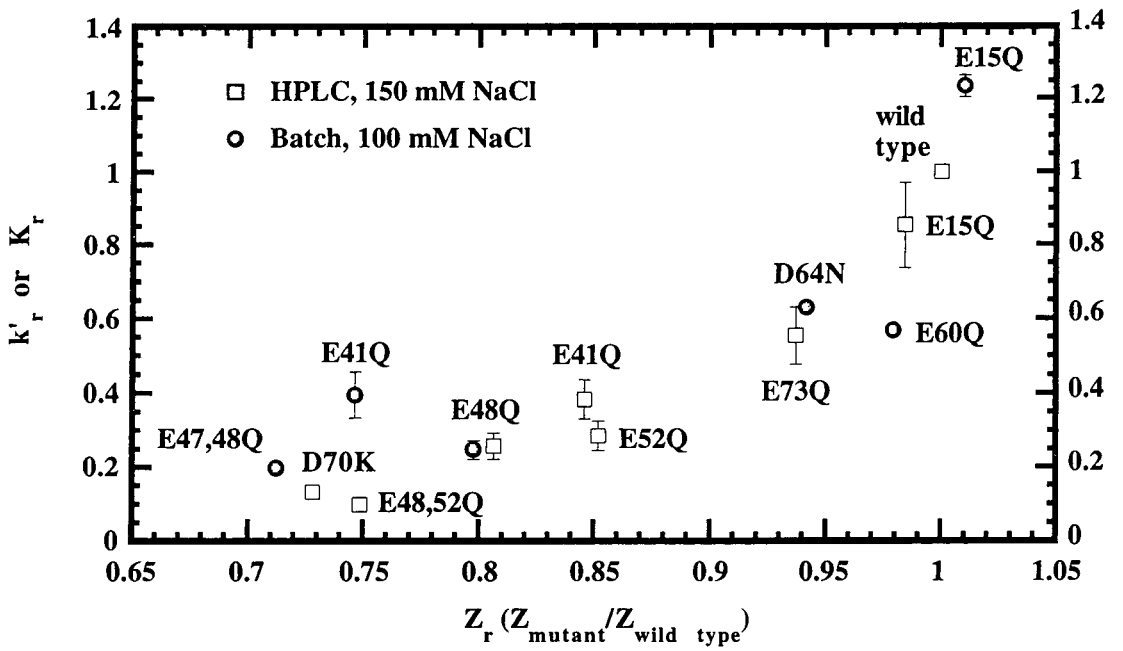


Fig. 4. A plot of the relative retention, $k'_r$, versus relative $Z$, $Z_r$, ($Z_r = Z_{mutant}/Z_{wild\ type}$). Error bars represent standard deviations estimated from replicate experiments.

face are responsible for the vast majority of the overall anion-exchange retention behavior of rat cytochrome $b_5$. The remainder of the electrostatic interactions make only a minor contribution to the observed retention behavior.

## 5. Discussion

In this work, the anion-exchange retention of wild type cytochrome $b_5$ and its site-directed charge mutants has been characterized by measuring the effects of ionic strength on retention in isocratic HPLC. The best-characterized influence on the chromatographic capacity factor $k'$ is that of ionic strength, as presented in Fig. 1. Based on results presented in Fig. 1, the resolution of the charge mutant proteins declines with increasing NaCl concentration and is virtually lost for NaCl concentrations greater than 300 m*M*. The protein purification implications of this loss of resolution with increasing NaCl concentration are important. If one were attempting to purify a desired wild type protein from closely related contaminants (e.g., deamidation products, charge mutant forms, translational variants), a high degree of resolution would best be achieved through operation at low ionic strengths. The use of a low ionic strength gradient would result in extended protein retention (process time) and reduced throughput for the purification system. In contrast, high throughput would require operation under high ionic strength conditions, with degraded resolution. Therefore, a compromise in the choice of ionic strength must be made in order to optimize the tradeoff between selectivity and productivity generally observed in separations processes.

The observation that only a small fraction of the charged amino acid residues on the protein surface participate in ion-exchange adsorption has been discussed in the literature [25] and has been demonstrated experimentally for the ion-exchange adsorption of other proteins. Chicz and Regnier [5] noted that the apparent number of contacts between subtilisin and an ion-exchange

surface fell into two distinct domains, with a sharp transition with increasing ionic strength of the eluent. Chicz and Regnier [6] also observed that when compared with the wild type subtilisin, the apparent number of contacts between the mutant proteins and ion-exchanger could increase while the retention times of the mutant proteins actually decreased, indicating possibly that electrostatic interactions between a protein and an ion-exchanger have varying interaction energies. The authors concluded that the protein tertiary structure sterically limits the number of contacts between the protein and the ion-exchange surface and that the local environment and position of each amino acid residue is important in determining its contribution to retention. The results obtained for the site-directed mutants of rat cytochrome $b_5$ concur with the conclusions of Chicz and Regnier [6] regarding the variable contributions of a single amino acid residue to retention. A good example of the effect of local environment is the retention result for the cytochrome $b_5$ mutant E15Q, which was observed to have a value of $Z$ indistinguishable from the wild type protein, even though its net charge was reduced by one unit. Although the residue is sterically accessible for interaction with the anion-exchange surface, the location of this negative charge in an area of predominantly positive charge limits its influence on retention behavior.

Previous batch adsorption experiments had shown participation of a single major contact region [12] mediating ion-exchange retention of cytochrome $b_5$. This result was corroborated and extended by this investigation to reveal the presence of an additional secondary region contributing to ion-exchange retention. The two negatively charged patches on the surface of rat cytochrome $b_5$ which dominate anion-exchange retention (as determined from retention studies of site-directed charged mutants) can be compared with the cation binding sites on the surface of bovine cytochrome $b_5$ identified by Whitford et al. [13] using NMR techniques. The following description of the sites located by Whitford et al. [13] identifies homologous residues in the rat form of the protein with the rat amino acid sequence number based on the method of Ozols [26]. Three cation-binding sites were located, including site I which was composed of the heme propionates and amino acid residues E41, E42, E47, E48, E52. Site II was found to be located near the histidine residue H30 and to contain the residues E60, D57 and D64 while site III was located near the histidine residue H84 and contained residues E82, D86, and D87. D87, located in the patch of negative residues identified by Whitford et al. [13] as site III, is involved in a salt bridge with K90. E14, located near site III, is involved in a salt bridge with K18. The salt-bridging of these two negatively charged residues probably reduces the contributions of the residues in site III to the anion-exchange retention of rat cytochrome $b_5$. The two patches which dominate anion-exchange adsorption behavior of rat cytochrome $b_5$ coincide with Whitford's sites I and II. This agreement suggests that NMR may be useful in identifying surface accessible clusters of negative charge which can participate in anion-exchange adsorption.

The contribution of the heme propionates was not investigated in this study, but the location of these negatively charged species would allow for their interaction with the anion-exchange adsorbent concurrent with either of the two charged patches. The potential interaction of the residues in the third cluster identified by Whitford were not examined in these ion-exchange retention behavior experiments, but the contribution of residue E15 was examined and it was determined not to contribute substantially to the anion-exchange retention behavior. The electrostatic interactions between the soluble tryptic fragment of rat cytochrome $b_5$ and a model anion-exchange adsorbent have been previously investigated using molecular electrostatic modeling [24]. Computational modeling revealed the presence of three major clusters of negative potential surrounding the heme prosthetic group including (a) the cluster containing Glu47, Glu48 and Glu52; (b) the cluster containing Glu41 and Glu42; and (c) the cluster containing Asp70 and Glu73. The negative potential associated with the heme functional groups is also evident from electrostatic equipotential plots. The relative

contributions of the residues in these three clusters to the overall electrostatic interaction energy between the protein and the anion-exchange surface is also in agreement with those obtained from chromatographic retention results.

Factors other than the net charge of the protein and the adsorbent can also play a large effect in mediating protein ion-exchange retention behavior. The importance of protein tertiary structure in determining the number of interactions between the protein and the ion-exchanger has been noted by Drager and Regnier [27] for the anion-exchange adsorption of lactate dehydrogenase. Drager and Regnier concluded that multiple parts of the protein surface could potentially interact cooperatively to determine the observed protein retention behavior. The observed heterogeneous contributions of amino acid residues and the distribution of retention times for charged mutants of the same net charge for cytochrome $b_5$ is in accord with the ideas proposed by Drager and Regnier.

The results of these HPLC retention studies combined with the results from equilibrium batch adsorption experiments [10,12] indicate that the observed cytochrome $b_5$ ion-exchange retention behavior results from the summation of many fractional electrostatic interactions of varying energies. Protein ion-exchange retention is therefore governed by both the number and the character of the contacts between the protein and the adsorbent surface.

## Acknowledgements

*E. coli* strain TB1 expressing recombinant soluble core of rat cytochrome $b_5$ was the generous gift of Dr. Stephen Sligar of the University of Illinois. We would like to thank Dr. Sligar and Dr. Karla Rodgers for helpful discussions. Support was provided by NSF under CTS-8910087, by the Welch Foundation, and by an NSF Presidential Young Investigator Award to RCW. Additional support was provided by the 3M Corporation, by Pharmacia and by Waters.

## References

[1] W. Kopaciewicz, M.A. Rounds, J. Fausnaugh and F.E. Regnier, *J. Chromatogr.*, 266 (1983) 3.
[2] V. Lesins and E. Ruckenstein, *Colloid Polym. Sci.*, 266 (1988) 1187.
[3] J. Fausnaugh-Pollitt, G. Thevenson, L. Janis and F.E. Regnier, *J. Chromatogr.*, 443 (1988) 221.
[4] I. Mazsaroff, S. Cook and F.E. Regnier, *J. Chromatogr.*, 443 (1988) 119.
[5] R. Chicz and F.E. Regnier, *J. Chromatogr.*, 443 (1988) 193.
[6] R. Chicz and F.E. Regnier, *Anal. Chem.*, 61 (1989) 2059.
[7] N.K. Boardman and S.M. Partridge, *Biochem. J.*, 59 (1955) 543.
[8] W. Kopaciewicz, M.A. Rounds and F.E. Regnier, *J. Chromatogr.*, 318 (1985) 157.
[9] D.J. Roush, D.S. Gill and R.C. Willson, *J. Chromatogr. A*, 653 (1993) 207.
[10] D.S. Gill, D.J. Roush and R.C. Willson, *J. Colloid Interface Sci.*, 167 (1994) 1.
[11] R.D. Whitley, R. Wachter, F. Liu and N.-H.L. Wang, *J. Chromatogr.*, 465 (1989) 137.
[12] D.S. Gill, D.J. Roush and R.C. Willson, *J. Chromatogr. A*, 684 (1994) 55.
[13] D. Whitford, D.W. Concar, N.C. Veitch and R.J.P. Williams, *Eur. J. Biochem.*, 192 (1990) 715.
[14] A. Willie, P.S. Stayton, S.G. Sligar, B. Durham and F. Millett, *Biochemistry*, 31 (1992) 7237.
[15] M. Rivera, F.A. Walker, M.R. Mauk, A.G. Mauk, M.A. Cusanovich and G. Tollin, *Biochemistry*, 32 (1993) 622.
[16] J.J. Wendoloski, J.B. Matthew, P.C. Weber and F.R. Salemme, *Science*, 238 (1987) 794.
[17] D. Wu and R.R. Walters, *J. Chromatogr.*, 598 (1992) 7.
[18] K. Rodgers, T. Pochapsky and S.G. Sligar, *Science*, 240 (1988) 1657.
[19] R.D. Guiles, V.J. Basus, I.D. Kuntz and L. Waskell, *Biochemistry*, 31 (1992) 1365.
[20] R.D. Guiles, V.J. Basus, S. Sarma, S. Malpure, K.M. Fox, I.D. Kuntz and L. Waskell, *Biochemistry*, 32 (1993) 8329.
[21] D.S. Gill, D.J. Roush and R.C. Willson, *J. Biomol. Struct. Dyn.*, 11 (1994) 1003.
[22] S. Beck von Bodman, M. Schuler, D. Jollie and S. Sligar, *Proc. Natl. Acad. Sci. USA*, 83 (1986) 9443.
[23] T. Takeuchi, M. Masayoshi and D. Ishii, *J. Chromatogr.*, 235 (1982) 309.
[24] D.J. Roush, D.S. Gill and R.C. Willson, *Biophys. J.*, 66 (1994) 1290.
[25] F.E. Regnier, *Science*, 238 (1987) 319.
[26] J. Ozols, *Biochem. Biophys. Acta*, 997 (1989) 121.
[27] R.P. Drager and F.E. Regnier, *J. Chromatogr.*, 406 (1987) 237.

ELSEVIER

Journal of Chromatography A, 704 (1995) 351–356

JOURNAL OF CHROMATOGRAPHY A

# Chromatographic determination of constituents of the genus *Colchicum* (Liliaceae)☆

Peter Ondra[a], Ivo Válka[a], Jaroslav Vičar[a], Nurhayat Sütlüpinar[b], Vilím Šimánek[a,*]

[a]*Institute of Medical Chemistry, Palacký University, 775 15 Olomouc, Czech Republic*

[b]*Department of Pharmacognosy, University of Istanbul, 34452 Istanbul, Turkey*

First received 13 October 1994; revised manuscript received 6 February 1995; accepted 9 February 1995

**Abstract**

A high-performance liquid chromatographic method for the determination of colchicinoid alkaloids in plant material is described. The determination is performed separately in neutral and basic alkaloid fractions using a $C_{18}$-bonded silica column. Nine alkaloids, i.e., 3-demethylcolchicine, 2-demethylcolchicine, colchifoline, N-deacetyl-N-formylcolchicine, colchicine, cornigerine, 2-demethyldemecolcine, 3-demethyldemecolcine and demecolcine, in seven *Colchicum* plants were assayed. For identification of phenolic compounds, a method using gas chromatography–mass spectrometry was elaborated and twenty phenolic compounds were identified in extracts from five *Colchicum* species. As the presence of luteolin appeared to be of value for chemotaxonomic purposes, its simple densitometric determination was developed.

## 1. Introduction

The plants of the genus *Colchicum* have been known for more than 2000 years for their marked biological effects. Colchicine, the main alkaloid, was isolated from all species of genera *Colchicum*, *Merendera* and *Gloriosa* (subfamily Wurmbaeoideae, Liliaceae). Colchicine and its congeners are chemotaxonomic markers for the subfamily Wurmbaeoideae. The genus *Colchicum* includes 42 species, most of which are endemic for the Middle East [1]. In most of the earlier studies, column and thin-layer chromatography were used for the isolation and identification of these alkaloids; other constituents, with the exception of flavones, were not studied [2].

For systematic phytochemical studies of *Colchicum* growing wild in Turkey, we developed methods of analysis for colchicinoid and phenolic compounds in plant extracts. So far, only three Turkish *Colchicum* species, *C. bivonae* [3], *C. micranthum* [4] and *C. sovitsii* [5] have been qualitatively investigated for their alkaloid content. This paper describes the results of the HPLC determination of colchicinoids in seven plants, GC–MS identification of phenolics in five

* Corresponding author.

☆ Presented at the International Symposium on Chromatographic and Electrophoretic Techniques, Bled, Slovenia, October 10–13, 1994.

0021-9673/95/$09.50 
*SSDI* 0021-9673(95)00185-9

plants and densitometric determination of luteolin in seven *Colchicum* plants.

## 2. Experimental

Alkaloids and luteolin used as reference compounds originated from the collection at our Institute and their structures were confirmed by their melting points and ultraviolet, infrared and nuclear magnetic resonance spectra. Phenolic reference compounds were obtained from Aldrich (Milwaukee, WI, USA) and ICN Biomedicals (Bucks, UK).

### 2.1. Extraction of plant material

Dried powdered plant material was extracted with methanol in a Soxhlet apparatus. The dried methanolic extracts were taken up in 0.01 *M* $H_2SO_4$ and extracted with diethyl ether. The solvent was evaporated after drying and the phenolic compounds were identified by GC–MS in the crude evaporation residue; luteolin was determined by densitometry. The aqueous solution was then extracted with chloroform and the extract was dried and evaporated, yielding a crude mixture of neutral alkaloids. The acidic aqueous residue was made alkaline (pH 9–10) with ammonia and extracted again with chloroform. After drying and evaporation of the extract, a crude mixture of basic alkaloids was obtained. The alkaloids in both fractions were identified and determined by HPLC. Details of extraction procedure are given in Ref. [6].

### 2.1. HPLC of alkaloids

Extracts were analysed using an SP 8700 apparatus and SP 4290 detector (Spectra Physics,

Table 1
Alkaloid composition in corms of the studied Turkish *Colchicum* species

| Plant | Alkaloid[a] (μg/g dried drug) (R.S.D., %)[b] | | | | | | | | |
|---|---|---|---|---|---|---|---|---|---|
| | 2MCO | 3MCO | CFNE | NFOCO | COL | COR | 2MDE | 3MDE | DEM |
| *C. macrophyllum* [7] | [c] | 2276 (0.05) | [c] | 168 (0.05) | 2223 (0.05) | [c] | [c] | 1 (0.03) | 67 (0.01) |
| *C. turcicum* [8] | [c] | 56 (0.03) | 19 (0.03) | [c] | 323 (0.04) | 7 (0.23) | 4 (0.14) | 2 (0.15) | 225 (0.02) |
| *C. cilicicum* [9] | n.a.[d] | n.a. | n.a. | n.a. | 300 (0.02) | n.a. | n.a. | n.a. | 1100 (0.01) |
| *C. kotschyi* [10] | 109 (0.01) | 289 (0.01) | 16 (0.01) | [c] | 1058 (0.04) | [c] | 0.9 (0.01) | 5 (0.03) | 6 (0.01) |
| *C. bornmuelleri* | [c] | 844 (0.03) | 91 (0.01) | [c] | 3063 (0.01) | 5 (0.03) | 23 (0.04) | 18 (0.02) | 720 (0.02) |
| *C. speciosum* | 13 (0.05) | 10 (0.06) | 220 (0.01) | 61 (0.03) | 4245 (0.01) | 187 (0.01) | 92 (0.03) | 106 (0.03) | 3159 (0.03) |
| *C. triphyllum* | 54 (0.02) | 88 (0.03) | 63 (0.03) | [c] | 958 (0.01) | 75 (0.02) | 65 (0.01) | 187 (0.03) | 105 (0.02) |

Quantification of alkaloids in other plant parts is given in refs. [7–10].

[a] 3MCO 3-demethylcolchicine, 2MCO 2-demethylcolchicine, CFNE colchifoline, NFOCO N-deacetyl-N-formylcolchicine, COL colchicine, COR cornigerine, 2MDE 2-demethyldemecolcine, 3MDE 3-demethyldemecolcine, DEM demecolcine. Retention times (min) in elution system for neutral alkaloids: 3MCO 5.9, 2MCO 6.7, CFNE 9.7, NFOCO 10.4, COL 11.0, COR 12.4; in elution system for basic alkaloids: 2MDE 3.9, 3MDE 4.7, DEM 6.3.

[b] In parentheses.

[c] Below detection limit.

[d] n.a. = Not analysed.

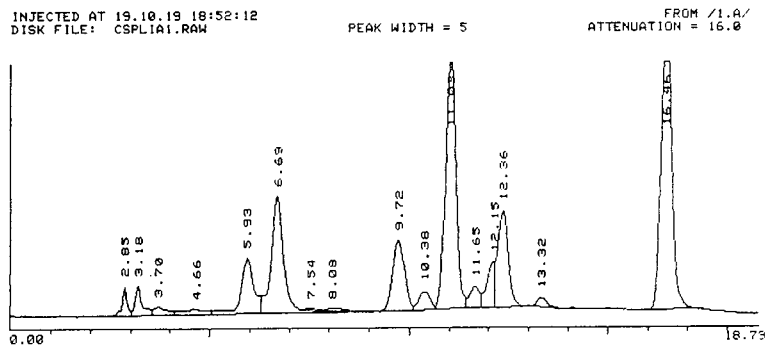


Fig. 1. HPLC separation of neutral alkaloid fraction from *Colchicum speciosum*. Separation was performed on a Separon SGX $C_{18}$ octadecylsilyl column (250 × 4.6 mm I.D.) with a gradient of MeCN–MeOH in 0.02 *M* phosphate buffer (pH 7.5) (0–6 min, 13:20; 16–21 min, 18:25; 23 min, 13:20, v/v) at ambient temperature and a flow-rate of 1.5 ml/min, with UV detection at 353 nm. Peaks: 5.93 min = 3-demethylcolchicine; 6.69 min = 2-demethylcolchicine; 9.72 min = colchifoline; 10.38 min = N-deacetyl-N-formylcolchicine; 11.03 min = colchicine; 12.36 min = cornigerine; 16.46 min = demecolcine.

Santa Clara, CA, USA), equipped with a 250 × 4.6 mm I.D. column filled with octadecyl-modified Separon SGX $C_{18}$ (Tessek, Prague, Czech Republic), particle size 7 $\mu$m. The solvent system for neutral alkaloids was a gradient of MeCN–MeOH in 0.02 *M* phosphate buffer (pH 7.5) as follows: 0–6 min, 13:20; 16–21 min, 18:25, 23 min, 13:20 (v/v); for basic alkaloids 13% tetrahydrofuran in 0.02 *M* acetate buffer (pH 5.5) was used; in both instances the flow-rate was 1.5 ml min. UV absorbance detection at 353 nm was applied.

The methanolic solutions of the chloroform extracts (2 mg) were percolated through modified silica gel cartridges (Separcol SI $C_{18}$) and the solvent was evaporated under nitrogen. The dry residues were dissolved in 1 ml of mobile phase and filtered through a 0.45-$\mu$m filter. Samples were injected in amounts of 10 $\mu$l and the alkaloids were identified by their retention

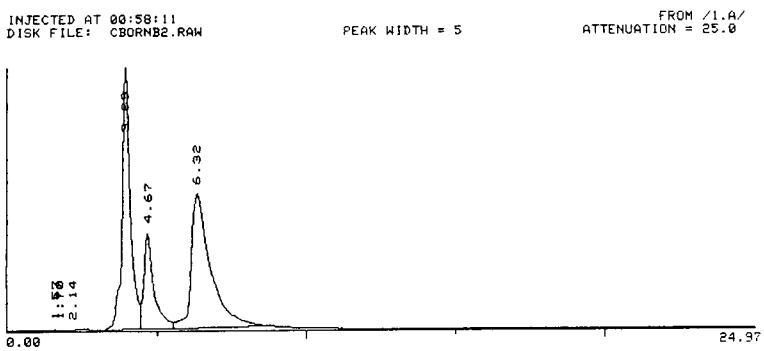


Fig. 2. HPLC separation of basic alkaloid fraction from *Colchicum bornmuelleri*. Separation was performed on a Separon SGX $C_{18}$ octadecylsilyl column (250 × 4.6 mm I.D.) with 13% tetrahydrofuran in 0.02 *M* acetate buffer (pH 5.5) at ambient temperature and a flow-rate of 1.5 ml/min, with UV detection at 353 nm. Peaks: 3.89 min = 2-demethyldemecolcine; 4.67 min = 3-demethyldemecolcine; 6.32 min = demecolcine.

Table 2
Phenolic compounds found in the studied Turkish *Colchicum* species

| Species | Compound | Retention time (min) | Plant part | | | |
|---|---|---|---|---|---|---|
| | | | Corms | Leaves | Seeds | Flowers |
| *C. bornmuelleri* | 4-Methoxybenzoic acid | 16.6 | – | + | – | – |
| | 4-Hydroxy-3-methoxybenzaldehyde (vanillin) | 16.7 | + | – | + | – |
| | 2,4-Dihydroxybenzoic acid | 17.4 | – | + | – | – |
| | 2,5-Dihydroxybenzoic acid | 19.2 | + | – | + | + |
| | 4-Hydroxybenzoic acid | 17.6 | + | + | + | + |
| | 3,4-Dihydroxybenzaldehyde | 18.8 | + | + | + | – |
| | 4-Hydroxy-3-methoxybenzoic acid (vanillic acid) | 19.3 | + | + | + | – |
| | 3,4-Dihydroxybenzoic acid | 19.9 | + | + | + | + |
| | 3-(4-Hydroxyphenyl)-2-propenoic acid (coumaric acid) | 21.7 | + | + | + | + |
| | 3-(3,4-Dimethoxyphenyl)-2-propenoic acid | 22.2 | – | + | – | – |
| | 3-(4-Hydroxy-3-methoxyphenyl)-2-propenoic acid (ferulic acid) | 24.0 | + | + | + | + |
| | 3-(3,4-Dihydroxyphenyl)-2-propenoic acid (caffeic acid) | 24.8 | + | + | + | + |
| | 3′,4′,5,7-Tetrahydroxyflavone (luteolin) | 38.6 | + | + | – | + |
| *C. speciosum* | 4-Hydroxyphenylmethanol | 15.3 | + | – | – | + |
| | 4-Hydroxy-3-methoxybenzaldehyde (vanillin) | 16.7 | + | – | – | – |
| | 3-Phenyl-2-propenoic acid (cinnamic acid) | 16.8 | + | – | – | – |
| | 2,5-Dihydroxybenzoic acid | 19.2 | – | + | – | + |
| | 2,6-Dihydroxybenzoic acid | 19.1 | – | – | – | + |
| | 4-Hydroxybenzoic acid | 17.6 | + | + | + | + |
| | 4-Hydroxy-3-methoxybenzoic acid (vanillic acid) | 19.3 | + | + | + | + |
| | 3,4-Dihydroxybenzoic acid | 19.9 | + | + | + | + |
| | 3-(4-Hydroxyphenyl)-2-propenoic acid (coumaric acid) | 21.7 | + | + | + | + |
| | 3-(3,4-Dihydroxyphenyl)-2-propenoic acid (caffeic acid) | 24.8 | + | + | – | + |
| | 3′,4′,5,7-Tetrahydroxyflavone (luteolin) | 38.6 | + | + | – | + |
| *C. kotschyi* | 4-Hydroxy-3-methoxybenzaldehyde (vanillin) | 16.7 | + | – | – | n.a.[a] |
| | 2,5-Dihydroxybenzoic acid | 19.2 | – | + | – | n.a. |
| | 4-Hydroxybenzoic acid | 17.6 | – | + | + | n.a. |
| | 3,4-Dihydroxybenzaldehyde | 18.8 | – | – | + | n.a. |
| | 3-(4-Hydroxyphenyl)propanoic acid | 19.2 | – | – | + | n.a. |
| | 4-Hydroxy-3-methoxybenzoic acid (vanillic acid) | 19.3 | + | + | + | n.a. |
| | 3-(4-Hydroxy-3-methoxyphenyl)propenol | 19.7 | + | – | – | n.a. |
| | 3,4-Dihydroxybenzoic acid | 19.9 | – | + | + | n.a. |
| | 3-(4-Hydroxy-3-methoxyphenyl)propanoic acid | 20.7 | + | – | + | n.a. |
| | 3-(4-Hydroxyphenyl)-2-propenoic acid (coumaric acid) | 21.7 | + | + | + | n.a. |
| | 3-(4-Hydroxy-3-methoxyphenyl)-2-propenoic acid (ferulic acid) | 24.0 | + | – | – | n.a. |
| | 3-(3,4-Dihydroxyphenyl)-2-propenoic acid (caffeic acid) | 24.8 | + | + | + | n.a. |
| | 3′,4′,5,7-Tetrahydroxyflavone (luteolin) | 38.6 | – | + | – | n.a. |
| *C. macrophyllum* | 2,5-Dihydroxybenzoic acid | 19.2 | + | + | – | + |
| | 2,6-Dihydroxybenzoic acid | 19.1 | + | + | – | + |
| | 4-Hydroxybenzoic acid | 17.6 | + | – | – | – |
| | 3-(4-Methoxyphenyl)propanoic acid | 18.7 | – | + | + | + |
| | 4-Hydroxy-3-methoxybenzoic acid (vanillic acid) | 19.3 | – | + | – | + |
| | 3,4-Dihydroxybenzoic acid | 19.9 | – | – | + | + |
| | 3-(4-Hydroxyphenyl)-2-propenoic acid (coumaric acid) | 21.7 | + | + | – | + |
| | 3-(4-Hydroxy-3-methoxyphenyl)-2-propenoic acid (ferulic acid) | 24.0 | – | + | + | + |
| | 3-(3,4-Dihydroxyphenyl)-2-propenoic acid (caffeic acid) | 24.8 | + | + | – | + |
| | 3′,4′,5,7-Tetrahydroxyflavone (luteolin) | 38.6 | + | + | + | + |
| *C. triphyllum* | 4-Hydroxy-3-methoxybenzaldehyde (vanillin) | 16.7 | + | + | + | – |
| | 2,5-Dihydroxybenzoic acid | 19.2 | + | – | – | – |
| | 2,6-Dihydroxybenzoic acid | 19.1 | + | – | – | – |
| | 4-Hydroxy-3-methoxybenzoic acid (vanillic acid) | 19.3 | + | + | – | + |
| | 3,4-Dihydrobenzoic acid | 19.9 | + | + | – | – |
| | 3-(4-Hydroxyphenyl)-2-propenoic acid (coumaric acid) | 21.7 | + | – | – | – |
| | 3-(4-Hydroxy-3-methoxyphenyl)-2-propenoic acid (ferulic acid) | 24.0 | – | – | + | + |
| | 3-(3,4-Dihydroxyphenyl)-2-propenoic acid (caffeic acid) | 24.8 | + | + | – | + |

[a] n.a. = Not analysed.

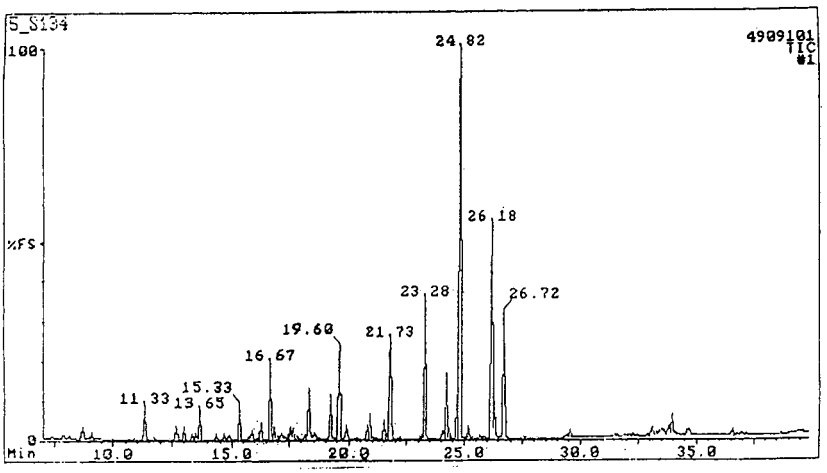


Fig. 3. GC profile of diethyl ether fraction from corms of *Colchicum speciosum*. Chromatographic conditions: column, Fisons 60 m × 0.32 mm I.D., coated with 0.5-μm DB-5 bonded phase; carrier gas, helium; flow-rate, 1.5 ml/min; column temperature gradient, 100°C for 7 min, then increased at 20°C/min to 220°C, at 4°C/min to 300°C and at 7°C/min to 320°C; injector temperature, 300°C. Peaks: 15.33 min = 4-hydroxyphenylmethanol; 16.67 min = vanillin; 16.81 min = cinnamic acid; 17.58 min = 4-hydroxybenzoic acid; 19.30 min = vanillic acid; 19.89 min = 3,4-dihydroxybenzoic acid; 21.73 min = coumaric acid; 24.82 min = caffeic acid.

times in comparison with reference compounds. Determination was carried out by the external calibration method. The results of three parallel determinations were processed using Student's *t*-test at the 95% confidence level for evaluation of the confidence interval. The limit of determination was ca. 1 μg of each substance per gram of dried drug.

Table 3
Content of luteolin in the studied Turkish *Colchicum* species

| Plant | Concentration (μg/mg dry material)[a] | | | |
|---|---|---|---|---|
| | Corms | Leaves | Seeds | Flowers |
| *C. macrophyllum* | 110.0 | 115.0 | [b] | 161.6 |
| *C. speciosum* | 56.1 | 153.8 | [b] | 278.9 |
| *C. kotschyi* | 145.7 | 42.1 | [b] | n.a. |
| *C. bornmuelleri* | 241.1 | 466.7 | [b] | 484.5 |
| *C. burtti* | 111.6 | n.a.[c] | n.a. | 85.0 |
| *C. triphyllum* | 219.1 | 202.2 | [b] | 150.9 |
| *C. umbrosum* | 89.4 | 118.7 | 1.8 | 334.8 |

[a] R.S.D. < 0.09%.
[b] Below detection limit.
[c] n.a. = Not analysed.

### 2.3. Capillary gas chromatography–mass spectrometry (GC–MS) of phenolic compounds

A diethyl ether extract (1 mg) after addition of 50 μl of pyridine and 100 μl of bis(trimethylsilyl) trifluoroacetamide containing 1% of trimethylchlorosilane was sealed and heated for 30 min at 100°C to produce trimethylsilyl derivatives for gas chromatography.

The derivatized samples were separated and analysed in an HRGC 5160 apparatus (Fisons, Middlewich, UK), equipped with a Fisons 60 m × 0.32 mm I.D. silica column, coated with 0.5-μm DB-5 bonded phase, and a splitless injector with a 7-min flush after sample injection to remove residual gases. The end of the column was introduced directly into the analyser chamber of a mass spectrometer. The system was operated under the following conditions: carrier gas, helium; flow-rate, 1.5 ml/min; injector temperature, 300°C; GC column temperature gradient, 100°C for 7 min, then increased at 20°C/min to 220°C, at 4°C/min to 300°C and at 7°C/min to 320°C. The mass spectrometer was set to scan 40–650 u per nominal second with an ionizing voltage of 70 eV. Samples of 0.3–0.5 μl

were injected. The identities of phenolic compounds in the ether extracts were established after GC separation by comparison of their retention times and mass spectra with those of reference compounds.

### 2.4. Determination of luteolin

Quantitative densitometric measurements were carried out on a Chromoscan MK II instrument (Joyce Loebl, Gateshead, UK) equipped with a device for evaluation of thin-layer chromatograms. The chromatograms (Silufol UV ready-to-use plates; Kavalier, Votice, Czech Republic) were used in duplicate, 0.1 mg of crude ether extract being applied to the plate. After elution with benzene–chloroform–ethanol (3:2:1), the quenching of fluorescence was measured at 260 nm. The spot area showed a linear dependence on the concentration of luteolin obtained in standard samples. The limit of determination was ca. 10 $\mu$g/mg dried drug.

## 3. Results and discussion

The alkaloid composition found in corms of the studied *Colchicum* species is presented in Table 1; representative chromatograms of neutral and basic alkaloid fractions are displayed in Figs. 1 and 2. Using the method described here, we determined nine of the 31 alkaloids found in *Colchicum* species [11]. Owing to the limit of determination (1 $\mu$g/g dried drug), we do not discuss the presence of other colchicine congeners in the plants studied. For colchiceines (colchicine derivatives with a hydroxyl instead of a methoxy group at C-10), the HPLC conditions used do not allow their determination. Compounds of this type can be determined in the form of Cu(II) complexes [12]. Lumi-colchicines, formed as artifacts during the extraction and which are without chemotaxonomic importance, cannot be determined by the method described.

Using GC–MS, we identified twenty phenolic compounds in five *Colchicum* species (see Table 2 and Fig. 3). Caffeic acid and leuteolin being the major phenolic compounds in studied plants, we consider luteolin to be the most suitable candidate for chemotaxonomic purposes. Therefore, a densitometric method for its determination was developed. The results for luteolin content in seven *Colchicum* species are given in Table 3.

## Acknowledgement

Financial support from the Grant Agency of the Czech Republic (Grant Reg. No. 303/93/2527) is gratefully acknowledged.

## References

[1] C.D. Brickell, in P.H. Davis (Editor), *Flora of Turkey and East Aegean Islands*, University Press, Edinburgh, 1984, p. 329.
[2] F. Šantavý, *Heterocycles*, 15 (1981) 1505.
[3] B. Orhon, *Thesis*, University of Istanbul, Istanbul, 1982.
[4] T. Baytop and G. Özcöbek, *J. Fac. Pharm. Istanbul*, 6 (1970) 21.
[5] E. Tojo, M.A. Önur, A.J. Freyer and M. Shamma, *J. Nat. Prod.*, 53 (1990) 634.
[6] F. Šantavý, S. Dvořáčková, V. Šimánek and H. Potěšilová, *Acta Univ. Palacki. Olomuc., Fac. Med.*, 105 (1983) 63.
[7] P. Ondra, J. Vičar, V. Šimánek, P. Indrák and N. Sütlüpinar, *Fitoterapia*, 65 (1994) 375.
[8] A. Husek, N. Sütlüpinar, P. Sedmera, F. Voegelein, I. Válka and V. Šimánek, *Phytochemistry*, 29 (1990) 3058.
[9] N. Sütlüpinar, A. Husek, H. Potěšilová, S. Dvořáčková, V. Hanuš, P. Sedmera and V. Šimánek, *Planta Med.*, 54 (1988) 243.
[10] P. Ondra, J. Vičar, V. Šimánek, W. Greenaway and N. Sütlüpinar, *Fitoterapia*, 65 (1994) 178.
[11] H.G. Capraro and A. Brossi, in A. Brossi (Editor), *The Alkaloids*, Vol. 23, Academic Press, New York, 1984, p. 1.
[12] E. Lacey and R.L. Brady, *J. Chromatogr.*, 315 (1984) 233.

ELSEVIER

Journal of Chromatography A, 704 (1995) 357–362

JOURNAL OF CHROMATOGRAPHY A

# Determination of indole alkaloids from *R. serpentina* and *R. vomitoria* by high-performance liquid chromatography and high-performance thin-layer chromatography ☆

V.E. Klyushnichenko[a,*], S.A. Yakimov[a], T.P. Tuzova[a], Ya.V. Syagailo[a], I.N. Kuzovkina[b], A.N. Wulfson[a], A.I. Miroshnikov[a]

[a]*Shemyakin and Ovchinnikov Institute of Bioorganic Chemistry, Russian Academy of Sciences, ul. Mikluho-Maklaya 16/10, 117871 GSP Moscow V-437, Russia*

[b]*Timiryazev Institute of Plant Physiology, Russian Academy of Sciences, ul. Botanicheskaja 35, 127276 Moscow, Russia*

First received 19 June 1994; revised manuscript received 13 January 1995; accepted 20 January 1995

**Abstract**

The separation of a model mixture of six indole alkaloids by high-performance liquid chromatography (HPLC) and high-performance thin-layer chromatography (HPTLC) on the normal- and reversed-phase Armsorb supports, respectively, was studied. A procedure for the analysis of extracts from plants cell callus culture of *Rauwolfia serpentina* and hairy roots of *R. serpentina* and *R. vomitoria* in the presence of these alkaloids and its derivatives with different chromatographic systems was elaborated. It was found that the alkaloid compositions of plant cell cultures and hairy roots of *R. serpentina* and *R. vomitoria* are identical. With HPLC analysis a higher precision of alkaloid determination in solution and measurements of concentration is achieved. HPTLC analysis gives a qualitative identification of the extracts. The combination of these high-performance methods provides quantitative and qualitative analyses of indole alkaloids such as ajmaline, ajmalicine, reserpine, raucaffricine, serpentine and yohimbine.

## 1. Introduction

Indole alkaloids such as ajmaline, reserpine, yochimbine and others, which are contained in plants of the *Rauwolfia* family, are biologically active substances, valuable drugs and semi-products which can be extracted [1].

In recent years, there has been widespread developments in biotechnological methods for obtaining indole alkaloids, apart from their isolation from natural plants. Metabolic biosynthesis in the natural plants may be different to that in the intact plants. An interesting technique for the synthesis of indole alkaloids by cell culture hairy root cultures of *Rauwolfia serpentina* was described recently [2,3]. Hence it is essential to develop methods for the identification of indole alkaloids.

Among the methods for the identification of alkaloids in solution, such as spectrometry, elec-

* Corresponding author.

☆ Presented at 20th International Symposium on Chromatography, Bournemouth, UK, June 19–24, 1994.

0021-9673/95/$09.50 
*SSDI* 0021-9673(95)00082-8

trophoresis and paper chromatography [4], surface adsorption [5,6], liquid column chromatography and affinity chromatography [7], high-performance liquid chromatography (HPLC) with electrochemical and UV detection [8,9], thin-layer liquid chromatography (TLC) [10] and their combinations have particular value.

For separation by TLC, some techniques exist for the identification of alkaloids such as spectrophotometry [11] and chromogenic reactions with different reagents. Court and Timmins [12] described specific chromogenic reactions for 22 indole alkaloids from *Rauwolfia* on a silica plate. In this case, TLC is suitable owing to the diversity of available elution systems [13,14]. A high selectivity was achieved in two-dimensional separation [15]. It is possible to use HPLC and TLC for the scaled-up isolation of pure alkaloids [16].

The aim of the work was to study the separation of a six-alkaloid mixture by high-performance thin-layer chromatography (HPTLC) and reversed-phase (RP) HPLC on Armsorb supports, and to develop qualitative and quantitative analyses for these alkaloids and their derivatives in biotechnological extracts of cell cultures and intact cell cultures of *R. serpentina* and *R. vomitoria* such as hairy roots.

## 2. Experimental

### 2.1. Cell cultures

A callus cell culture of *R. serpentina* was obtained as described [17]. The hairy roots of *R. serpentina* and *R. vomitoria* were grown in non-hormonal B-5 medium without light on a shaker (90 rpm) at 26°C for 21 days as described previously [18], then cells were dried under vacuum. Dried culture was kindly provided by Professor V.G. Winter (Kazan State University). The culture of hairy roots was obtained by genetic transformation of leaves of sterile plants of *R. serpentina* L. and *R. vomitoria* Afz. by Ri-plasmid of *Agrobacterium rhizogenes*, strain A-4. Genetic transformation of the plant occurs, which expresses the character of root formation and growth.

### 2.2. Alkaloid extraction

Amounts of 5 g of dried hairy roots of *R. serpentina* and *R. vomitoria* and cell culture of *R. serpentina* were extracted three times for 10 min in 20 ml of methanol using a Sonifer-250 ultrasound device (Branson Ultrasonics, Danbury, CT, USA). The extracts were evaporated to dryness under vacuum and the residues were dissolved in 100 ml of 0.01 *M* HCl. The filtered solutions were adjusted to pH 6 with 0.01 *M* NaOH and analysed by HPTLC and RP-HPLC.

### 2.3. Chromatography

For HPTLC, Armsorb HPTLC-KSKG-PZ-UV-254 (high-purity silica, regular particles, 300 $m^2/g$, pore size 100 Å) and Armsorb HPTLC-Sil-10-PZ-UV-254 (industrial silica, regular particles, 250 $m^2/g$, pore size 40–80 Å) plates (5 × 10 cm) with a 100-$\mu$m silica coating and a preadsorbent layer (Armchrom, Armeniya, Yerevan) were used. The column used for HPLC was Armsorb-300-$C_8$ (25 × 0.4 cm I.D., particle size 10 $\mu$m). Chromatography was performed with a Beckman Model 110B pump, Beckman Model 160 UV detector, Altex Model 210A injector and Waters Model 740 integrator, with an element flow-rate of 0.8 ml/min. Detection was carried out at 280 nm. The indole alkaloids used were ajmaline, ajmalicine, reserpine, raucaffricine, serpentine and yohimbine, kindly provided by Professor J. Stöckigt (Institut für Pharmazie, Johannes Gutenberg-Universität, Mainz, Germany). The samples of alkaloids were dissolved in acetonitrile at a concentration of 1 mg/ml. Internal and external standard methods were selected for quantification. Procedures for the preparation and concentration of the standards were as described above. For HPLC of 1–10 $\mu$l of each alkaloid sample and 5–100 $\mu$l of each extract were injected. For HPTLC of 1–5 $\mu$l of each alkaloid sample and 5–100 $\mu$l of each extract were applied.

Chloroform, acetonitrile, methanol, water purified with a Milli-Q system (Waters, Milford, MA, USA), ammonia and trifluoroacetic acid (TFA) were used. Before chromatography, the eluents were filtered through nitrocellulose and

GVWP filters (pore diameter 0.45 μm; Millipore) and degassed for 20 min by means of vacuum. The samples were applied to the preadsorbent layer with 3–4 samples per plate as spots with diameter 5–6 mm. The spots of the samples are transformed into lines at the border of the preadsorbent and separation layers after crossing the preadsorbent layer. Erlich reagent was prepared according to Ref. [19]. After spraying with Erlich reagent the plates were heated at 100°C for 5 min. Cerium ammonium sulphate (CAS) was dissolved in 1% $H_2SO_4$.

## 3. Results and discussion

The metabolism of intact plants may differ from each other and from that of natural plants owing to the biotechnological ways in which they were obtained. For reliable analyses for indole alkaloids and their derivatives it is advantageous to use chromatographic methods such as HPLC and HPTLC.

### 3.1. High-performance thin-layer chromatography

The samples of indole alkaloids (ajmaline, ajmalicine, yohimbine, raucaffricine, reserpine and serpentine) were applied under different conditions to the Armsorb HPTLC-KSKG-PZ-UV-254 and Armsorb HPTLC-Sil-10-PZ-UV-254 plates. TLC was performed using different polar and pH systems. The time of analysis was 30 min. Detection of the spots and thin lines was performed by exposure to UV radiation (254 and 365 nm) and chemical treatment with Erlich reagent followed by heat treatment, and with CAS.

On exposure of the plates to UV radiation some thin and one dominant lines are registered. At 254 nm, when spots of the alkaloid specimens are absorbed on the fluorescent covering of silica, the spots of ajmaline, ajmalicine and yohimbine have a grey colour, serpentine bright blue, raucaffricine dark grey and reserpine grey-blue on the bright green background of the surface. A more effective detection is obtained at 366 nm. In this instance the spots of the specimens showed many-coloured lines: ajmaline grey-blue, ajmalicine pink-yellow, yohimbine yellow, raucaffricine invisible, reserpine yellow-green and serpentine bright blue. With Erlich reagent and subsequent heating, ajmaline appears as a blue spot, yohimbine and ajmalicine brown-red, reserpine light-brown and raucaffricine invisible. With CAS treatment ajmaline appears as a red spot and other alkaloids with different tinges of yellow-brown.

Mobile phase systems for alkaloid separation with high resolution were developed. With separation under acidic conditions the reserpine spot was mostly washed out and the resolution was low. The main systems for elution were chloroform–methanol–ammonia (9.5:0.5:0.01 and 9.8:0.2:0.01) (Table 1, Fig. 1). We used these two chromatographic systems in the analysis, because of the small difference between the $R_F$ values of ajmalicine and reserpine in the first system and ajmaline and serpentine in the second system. The analyses of the extracts from cell cultures and hairy roots of *R. serpentina* and *R. vomitoria* were performed in the same systems. The results showed that *R. serpentina* cell culture extract contained mainly ajmaline and its derivatives (which with CAS treatment appeared as a red spot), reserpine and small impurities (Table 2, Fig. 1). Hairy root cultures of both *R. serpentina* and *R. vomitoria* contained mainly

Table 1
$R_F$ values of indole alkaloids in HPTLC separation on Armsorb HPTLC-KSKG-PZ-UV-254 and Armsorb HPTLC-Sil-10-PZ-UV-254 plates (5 × 10 cm). Mobile phase: $CHCl_3$–MeOH–$NH_3$ [(A) 9.8:0.2:0.01 and (B) 9.5:0.5:0.01]. Application of 2–5 μl of each alkaloid

| Indole alkaloid | $R_F$ | | | |
|---|---|---|---|---|
| | KSKG (A) | Sil-10 (A) | KSKG (B) | Sil-10 (B) |
| Ajmaline | 0.06 | 0.06 | 0.13 | 0.18 |
| Ajmalicine | 0.79 | 0.68 | 0.88 | 0.76 |
| Yohimbine | 0.19 | 0.10 | 0.46 | 0.38 |
| Reserpine | 0.53 | 0.31 | 0.85 | 0.75 |
| Serpentine | 0.01 | 0.01 | 0.03 | 0.03 |
| Raucaffricine | 0.01 | 0.01 | 0.01 | 0.01 |

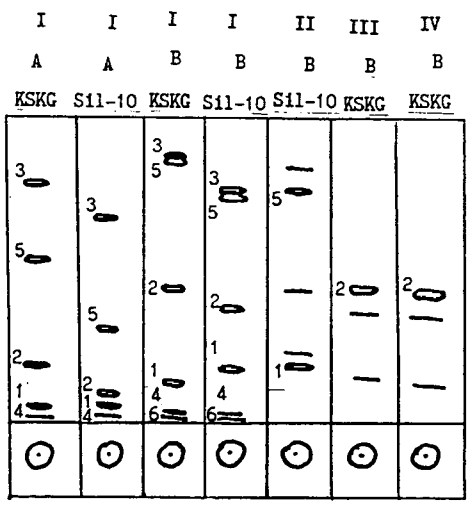


Fig. 1. Separation of (I) 5 μl each sample of indole alkaloids (1 = raucaffricine; 2 = ajmaline; 3 = yohimbine; 4 = ajmalicine; 5 = serpentine; 6 = reserpine), (II) methanol extract from cell culture of *R. serpentina*, (III) methanol extract from hairy roots of *R. serpentina* and (IV) methanol extract from hairy roots of *R. vomitoria*, by HPTLC on Armsorb HPTLC-KSKG-PZ-UV-254 (KSKG) and Armsorb HPTLC-Sil-10-PZ-UV-254 (Sil-10) plates (5 × 10 cm). Mobile phase: $CHCl_3$–MeOH–$NH_3$ [(A) 9.8:0.2:0.01 and (B) 9.5:0.5:0.01].

yohimbine on a background of small unidentified impurities (Table 3, Fig. 1).

### 3.2. Reversed-phase high-performance liquid chromatography

For a more effective alkaloid separation, ajmaline, ajmalicine, reserpine, raucaffricine, serpentine, yohimbine and their mixture were analysed by RP-HPLC on the Armsorb-300-$C_8$ column with different mobile phase systems. The best separation was achieved with acetonitrile–TFA (Fig. 2). The same analysis of extracts of cell cultures and hairy roots of *R. serpentina* and *R. vomitoria* was performed (Figs. 3 and 4). It can be seen from Table 2 and Fig. 3 that ajmaline is the main peak and reserpine and unidentified impurities are present in the *R. serpentina* cell culture. The peak of yohimbine is observed on a background of unidentified impurities in the hairy root cultures of both *R. serpentina* and *R. vomitoria*, as shown in Fig. 4. It is interesting that the amounts of yohimbine and other substances are the same in both hairy root cultures.

## 4. Conclusion

The separation of model mixtures of six indole alkaloids by RP-HPLC and HPTLC on the normal- and reversed-phase Armsorb supports, respectively, was studied. Procedure for the analysis of extracts from plant cell cultures and hairy roots of *R. serpentina* and *R. vomitoria* in the presence of these alkaloids and their derivatives using different chromatographic systems were elaborated.

It has been found that the alkaloid compositions of callus plant cell cultures and hairy roots of *R. serpentina* are different. The extract from callus cell culture of *R. serpentina* contains ajmaline as the main alkaloid and a small

Table 2
$R_F$ values of the compounds extracted with methanol from *R. serpentina* cell culture in HPTLC separation on the Armsorb HPTLC-KSKG-PZ-UV-254 and Armsorb HPTLC-Sil-10-PZ-UV-254 plates (5 × 10 cm). Mobile phase: $CHCl_3$–MeOH–$NH_3$ [(A) 9.8:0.2:0.01 and (B) 9.5:0.5:0.01]. Application of 100 μl of the extract

| Indole alkaloid | $R_F$ | | | |
|---|---|---|---|---|
| | KSKG (A) | Sil-10 (A) | KSKG (B) | Sil-10 (B) |
| Ajmaline | 0.06 | 0.06 | 0.14 | 0.17 |
| Reserpine | 0.54 | 0.32 | 0.84 | 0.76 |
| Other substances | 0.66 | 0.58 | 0.93 | 0.88 |
| | 0.24 | 0.22 | 0.42 | 0.40 |
| | 0.10 | 0.10 | 0.20 | 0.20 |

Table 3
$R_F$ values of compounds extracted with methanol from *R. serpentina* and *R. vomitoria* hairy roots culture in HPTLC separation on Armsorb HPTLC-KSKG-PZ-UV-254 and Armsorb HPTLC-Sil-10-PZ-UV-254 plates (5 × 10 cm). Mobile phase: $CHCl_3$–MeOH–$NH_3$ [(A) 9.8:0.2:0.01 and (B) 9.5:0.5:0.01]. Application of 100 μl of the extract

| Indole alkaloid | $R_F$ | | | |
|---|---|---|---|---|
| | KSKG (A) | Sil-10 (A) | KSKG (B) | Sil-10 (B) |
| Yohimbine | 0.18 | 0.11 | 0.45 | 0.39 |
| Other substances | 0.14 | 0.08 | 0.35 | 0.30 |
| | 0.05 | 0.05 | 0.10 | 0.09 |

amount of reserpine. The composition of *Rauwolfia* hairy root alkaloids is different to that of the roots of the native plant, but the alkaloid compositions of hairy roots of *R. serpentina* and *R. vomitoria* are identical.

More precise alkaloid separation and concentration determination in solution is achieved by

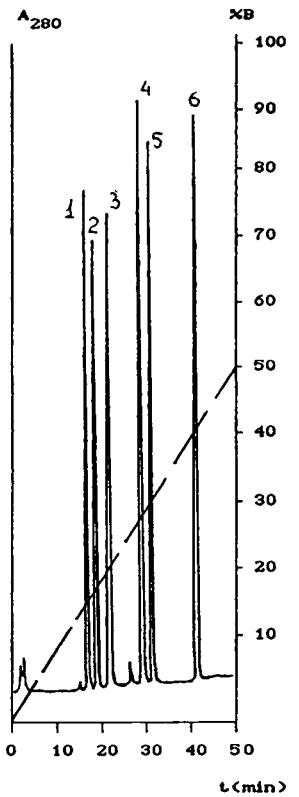


Fig. 2. Separation of indole alkaloids [1 = raucaffricine (5 μl); 2 = ajmaline (10 μl); 3 = yohimbine (3 μl); 4 = ajmalicine (2 μl); 5 = serpentine (8 μl); 6 = reserpine (5 μl)] by HPLC on the Armsorb-300-$C_8$ column (250 × 4 mm I.D.). Mobile phase: (A) 10% $CH_3CN$ and 0.1% TFA in $H_2O$; (B) 0.1% TFA in $CH_3CN$. The percentage of eluent B in the mobile phase is shown by the dashed line.

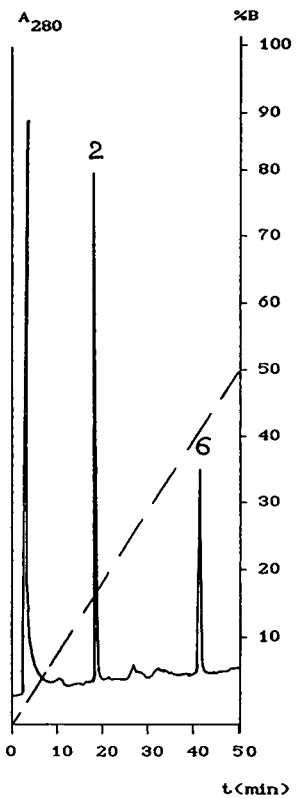


Fig. 3. Analysis of methanol extract from *R. serpentina* cell culture by HPLC on the Armsorb-300-$C_8$ column (250 × 4 mm I.D.). Mobile phase: (A) 10% $CH_3CN$ and 0.1% TFA in $H_2O$; (B) 0.1% TFA in $CH_3CN$. The percentage of eluent B in the mobile phase is shown by the dashed line. Injection volume, 20 μl of the extract.

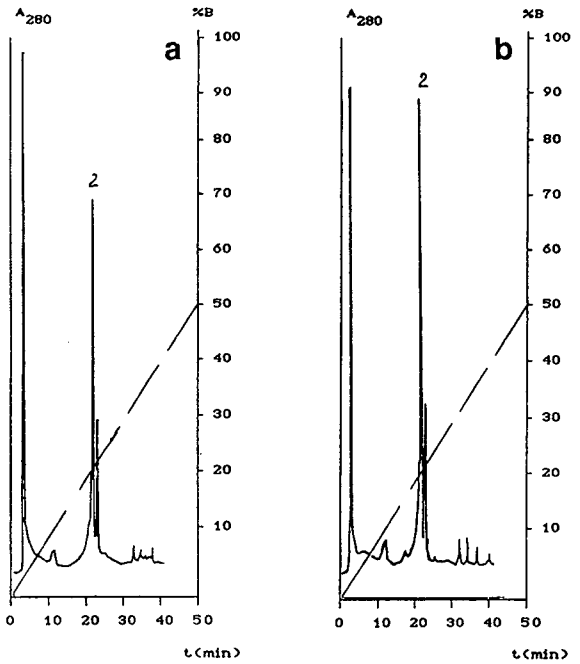


Fig. 4. Analysis of methanol extract from (a) *R. serpentina* and (b) *R. vomitoria* hairy roots by HPLC on the Armsorb-300-$C_8$ column (250 × 4 mm I.D.). Mobile phase: (A) 10% $CH_3CN$ and 0.1% TFA in $H_2O$; (B) 0.1% TFA in $CH_3CN$. The percentage of eluent B in the mobile phase is shown by the dashed line. Injection volume, 20 $\mu$l of the extract.

RP-HPLC than HPTLC. With the help of HPTLC, alkaloid identification is achieved by colour treatment under visible and UV light. In addition, this method is simpler than HPLC. The combination of these two high-performance methods provides effective qualitative and quantitative analyses for indole alkaloids.

## Acknowledgements

The authors express their gratitude to Dr. L.A. Nikolaeva (St. Petersburg Chemical-Pharmaceutical Institute) for providing sterile *Rauwolfia* plants and to Professor J. Stöckigt (Institut für Pharmazie, Johannes Gutenberg-Universität Mainz) for providing standards of indole alkaloids.

## References

[1] Yu.A. Ovchinnikov, Bioorganicheskaya Khimiya, Prosvescheniye, Moscow, 1987, pp. 665–666.
[2] H. Falkenhagen, J. Stöckigt, I. Kuzovkina, I. Alterman and H. Kolshorn, Can. J. Chem., 17 (1993) 2201.
[3] B.D. Benjamin, G. Roja and M.R. Heble, Phytochemistry, 35 (1994) 381.
[4] P. Duez, S. Chamart, M. Vanhaelen, R. Vanhaelen-Fastre, M. Hanocq and L. Molle, J. Chromatogr., 356 (1986) 334.
[5] F. Kargi, I. Friedel and K. Maricic, Abstr. Pap. Am. Chem. Soc. Meet., 196 (1988) MBTD 115.
[6] M. Asada and M.L. Shuler, Appl. Microbiol. Biotechnol., 30 (1988) 475.
[7] DE 6316-357: 16.05.85-GB-012438 (20.11.86) 15.05.86 as 616357. 86-312884/48.
[8] T. Naaranlahti, V.P. Ranta, P. Jarho, M. Nordstorm and S.P. Lapinjoki, Analyst., 114 (1989) 1229.
[9] S. Aurolia, T. Naaranlahti and S.P. Lapinjoki, J. Chromatogr., 554 (1991) 227.
[10] M. Monforte-Gonzalez, T. Aurora-Talavera, I.E. Maldonado-Menoza and U.M. Loyola-Vargas, Phytochem. Anal., 3 (1992) 117.
[11] B.A. Akinloye and W.E. Court, Phytochemistry, 19 (1980) 2741.
[12] W.E. Court and P. Timmins, Planta Med., 27 (1975) 319.
[13] U.R. Cieri, J. Assoc. Off. Anal. Chem., 66 (1983) 867.
[14] J.A. Martinez, C. Gomez, T. Santana and H. Velez, Planta Med., 55 (1989) 283.
[15] P. Le Huan, R.L. Munier and S. Meunier, Chromatographia, 13 (1980) 693.
[16] E. Manoilov, V.P. Komov, N.V. Kirillova, M.A. Strelkova, Yu.A. Samolin, L.S. Chernoborodova and L.A. Nicolaeva, J. Chromatogr., 440 (1988) 53.
[17] A.G. Volosovich, T.N. Puchinina and N.A. Listunova, Rastit. Resur., 18 (1982) 239.
[18] H. Falkenhagen, I. Kuzovkina, I. Alterman, L. Nikolaeva and J. Stöckigt, Nat. Prod. Lett., 3 (1993) 107.
[19] State Pharmacopoeia of USSR, 11th ed., (2), Meditsina, Moscow, 1990, p. 108.

ELSEVIER

Journal of Chromatography A, 704 (1995) 363–367

JOURNAL OF CHROMATOGRAPHY A

# High-performance liquid chromatographic analysis of mevinolin as mevinolinic acid in fermentation broths ☆

Jožica Friedrich[a,*], Mateja Žužek[a], Mojca Benčina[a], Aleksa Cimerman[a], Aleš Štrancar[b], Ivan Radež[c]

[a]*National Institute of Chemistry, Hajdrihova 19, 61115 Ljubljana, Slovenia*
[b]*BIA Ltd., Teslova 30, 61000 Ljubljana, Slovenia*
[c]*Krka Pharmaceutical and Chemical Works, Cesta Herojev 45, 68000 Novo Mesto, Slovenia*

First received 25 December 1994; revised manuscript received 16 January 1995; accepted 20 January 1995

**Abstract**

High-performance liquid chromatographic analysis of mevinolin in fermentation broth was initially performed after addition of acid and extraction with methanol using a mobile phase at pH 3.0. Under such conditions mevinolin was present in three different forms: as a lactone, as the corresponding β-hydroxy acid (mevinolinic acid) and as its methyl ester. To achieve accurate and reproducible results the method was modified such that only one form was present: mevinolinic acid. The fermentation broth samples were adjusted to pH 7.7 before the extraction with methanol, and the pH of the mobile phase was adjusted to 7.7 as well. For the separation a 250 × 4 mm I.D. column, termostated at 40°C, packed with Spherisorb ODS 2 of 5 μm particle size was used. Under these conditions mevinolin was detected at 237 nm as a single peak of a β-hydroxy acid, which has the lowest retention time of all three forms.

## 1. Introduction

Mevinolin (monacolin K, lovastatin) is an important fungal secondary metabolite inhibiting the enzyme which catalyses a rate-limiting step in the biosynthesis of cholesterol; it is an effective drug for the treatment of atherosclerosis and ischemic heart disease. Commercially this substance is produced biotechnologically by the fungi *Aspergillus terreus* or *Monascus rubber*.

The basic chemical structure of mevinolin contains a naphthalene ring system, a β-hydroxy-lactone and methyl butyric acid [1] as shown in Fig. 1a. The physiologically active form of the drug is the β-hydroxy acid which is formed by hydrolysis of the lactone ring (Fig. 1b).

Different analytical methods were developed for measuring mevinolin in blood [2,3], in bile [2], in tablets [4] and in fermentation broths [5,6]. Except for a method employing gas chromatography in combination with mass spectrometry [3], HPLC was used for mevinolin

* Corresponding author.

☆ Presented at the *International Symposium on Chromatographic and Electrophoretic Techniques, Bled, Slovenia, 10–13 October 1994.*

0021-9673/95/$09.50 
*SSDI* 0021-9673(95)00096-8

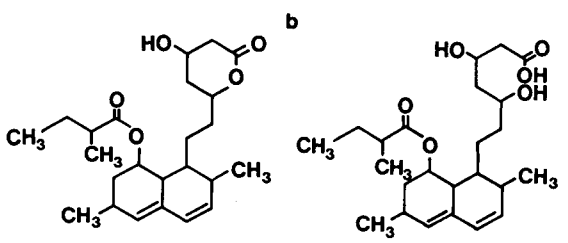


Fig. 1. Structural formulae of (a) mevinolin and (b) mevinolinic acid.

analyses. The separation was performed on reversed-phase columns with a mobile phase composed of a buffer solution and an organic modifier, and the drug was detected spectrophotometrically. To detect mevinolin in fermentation broths, Gullo et al. [5] derivatized the compounds to 4-nitrobenzoate derivatives. Mevinolin and the related compound hydroxymevinolin together with their $\beta$-hydroxy acids could be detected. The essential advantage of derivatization was the possibility to measure dihydromevinolin which has low UV absorption. Recently, a simple and fast method was described for analysing mevinolin directly without prior derivatization [6]. Kysilka and Křen [6] omitted the extraction of the broth, which is usually performed with methanol [5,7]. The substance was simultaneously present in two forms, as a lactone and as an acid and detected as two separate peaks.

In our laboratory biosynthesis of mevinolin by fungi was studied. For the detection during fermentation, the HPLC method by Monaghan et al. [8] had to be modified. This paper presents a new method for analysis of mevinolin in fermentation broths.

## 2. Experimental

### 2.1. Reagents and chemicals

As pure mevinolin was not available, a tablet of Mevacor (MSD, West Point, PA, USA) was used to prepare the standard solution. The tablet was dissolved in methanol, analytical-reagent grade (Serva, Heidelberg, Germany) and deionized water (1:1). The mobile phase consisted of HPLC-grade acetonitrile (Serva) and 0.02 *M* potassium phosphate buffer prepared from $KH_2PO_4$ and $K_2HPO_4$, both analytical-reagent grade (Kemika, Zagreb, Croatia). The initial pH value of the buffer was 3.0 and the proportion of acetonitrile–buffer was 35:65 (v/v). These values were changed during the experiments as indicated under Results and discussion. The mobile phase was filtered through a 0.22-$\mu$m filter (Millipore, Bedford, MA, USA).

### 2.2. Equipment

All analyses were performed on a Knauer (Berlin, Germany) isocratic system equipped with a data acquisition station of the same producer. The 250 × 4.0 mm I.D. column, thermostated at 40°C, packed with Spherisorb ODS 2 of 5 $\mu$m particle size, was from BIA (Ljubljana, Slovenia). During all experiments the flow-rate of the mobile phase was 0.7 ml/min. The detection was at 237 nm (UV detector, Knauer).

### 2.3. Sample preparation

After fermentation, the broth was harvested and the pH was adjusted to the appropriate value as indicated under Results and discussion. An equal volume of methanol was added and the suspension was shaken for 1 h on a rotary shaker at 200 rpm and 30°C. The suspension was then filtered, first through a filter paper ("black ribbon") and the filtrate obtained then through a micro filter (Millipore) of 0.22 $\mu$m pore diameter. The samples were injected into the HPLC column with a 20-$\mu$l sample loop injector.

To obtain the lactone form standard, a tablet of Mevacor was crushed in a mortar and suspended in a 1:1 mixture of deionized water (adjusted to pH 3.0 with 1 *M* HCl) and methanol. The suspension was sonicated for 20 min and filtered through a 0.22-$\mu$m filter. Subsequently, the filtrate was diluted to a concentration of 5 $\mu$g/ml and used in the analyses.

To obtain the acid form, the lactone was converted to acid through sodium salt according

to Brown et al. [9]. The crushed tablet was suspended in 0.1 *M* NaOH, sonicated and heated at 50°C for 1 h. Subsequently, the suspension was adjusted to pH 7.7 with 1 *M* HCl, filtered through a 0.22-$\mu$m filter (Millipore) and diluted to the concentration of 5 $\mu$g/ml.

## 3. Results and discussion

Initially we intended to determine mevinolin in the lactone form. According to the literature [8], mevinolinic acid can be converted to the lactone form at acidic pH. Therefore the broth samples were acidified to pH 3.0. Since the lactone was not soluble in water, methanol was added to the broth for extraction. After carrying out some analyses, it was found that mevinolin was not efficiently converted to the lactone and that a larger part was still present as mevinolinic acid. In addition to these two forms, a third unknown peak was observed in the samples as well as in the standard solution after some days of storing in the refrigerator (Fig. 2a). It could be the methyl ester of mevinolinic acid. To confirm this assumption, Mevacor tablets were dissolved in water–methanol (1:1, v/v), in water–ethanol (1:1, v/v) and in water–*n*-propanol (1:1, v/v). The solutions were stored at room temperature for three days and were subsequently analysed. It was shown that the retention time ($t_R$) of the unknown peak increased with the molecular mass of the alcohol used from 6 min 50 s to 8 min 7 s and 9 min 49 s, respectively. The results are shown in Fig 2. From these results it was concluded, that after extraction with methanol, mevinolin was present in the broth samples in three forms: as a lactone, as the corresponding $\beta$-hydroxy acid and as its methyl ester. The same forms were found in the aged solution of the standard, indicating that under acidic conditions the lactone slowly transformed to acid, which further reacted with methanol to form an ester (Fig. 2a).

A modified method for the analysis of mevinolin was developed. The following facts were taken into account:

(1) In the samples of our fermentation broth

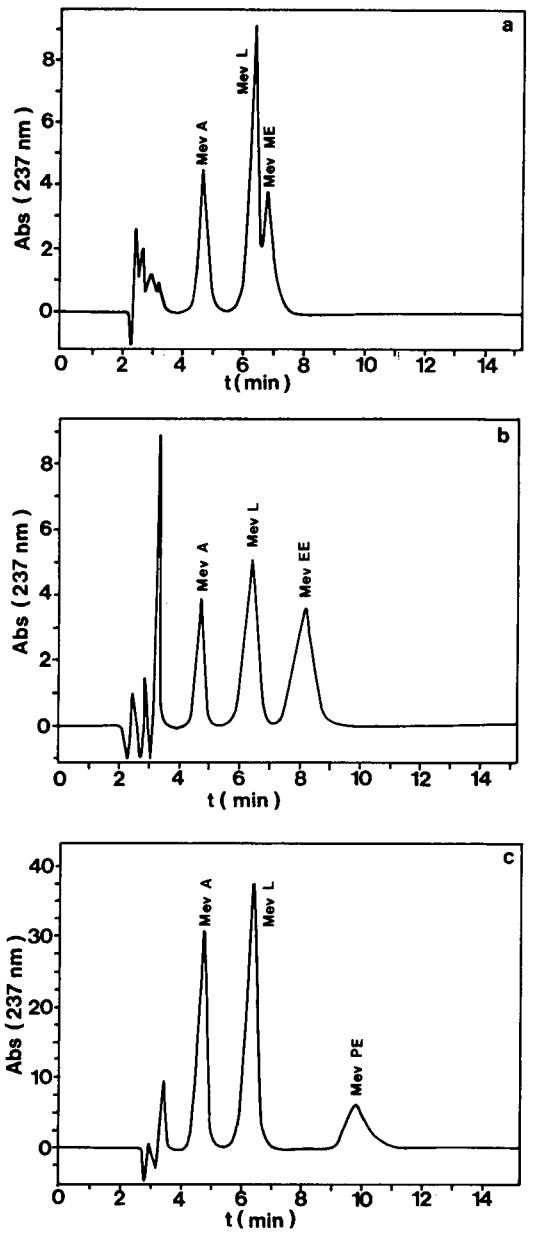


Fig. 2. HPLC analysis of a standard prepared in a lactone form, solubilized in (a) water–methanol (1:1), (b) water–ethanol (1:1), (c) water–*n*-propanol (1:1), after storing the solutions at room temperature for three days. Peaks: Mev A = mevinolinic acid; Mev L = mevinolin as lactone; Mev ME, Mev EE, Mev PE = methyl, ethyl and propyl ester of mevinolinic acid, respectively. Column: Spherisorb ODS 2, mobile phase: potassium phosphate buffer (pH 3.0)–acetonitrile (30:70, v/v), flow-rate: 0.7 ml/min, UV detection at 237 nm.

and according to the data found in the literature [8], the substance was "present in the fermentation broth largely as the hydroxycarboxylate (open lactone) form".

(2) From our experiments it followed that the acid was more stable in acidic water–methanol mixture than the lactone. The lactone form was stable only in pure methanol. Since water can not be avoided in the samples of fermentation broth, it is convenient to convert mevinolin to mevinolinic acid.

(3) The acid form had a lower $t_R$ than the lactone.

A method was developed in which the measured substance was present in the acid form as shown in Fig. 3. Since mevinolinic acid is stable at pH 7.7, the samples were prepared at this pH. The pH of the mobile phase had to be adjusted to the same value as well. For this purpose acetonitrile was mixed with 0.02 *M* potassium phosphate buffer at pH 7.7 in a 65:35 proportion. The broth samples were further treated as described above. The corresponding separation is shown in Fig. 4.

In order to check the necessity of extraction with methanol, some experiments were done by omitting the extraction step. However, the yield

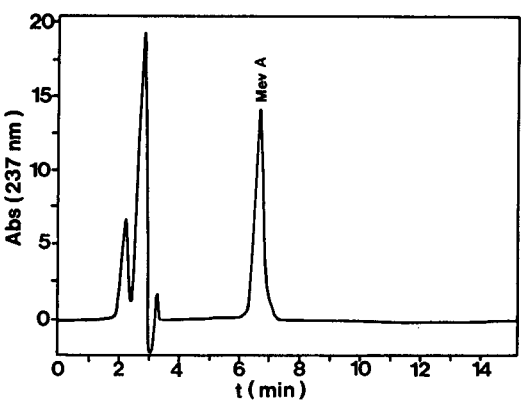


Fig. 3. Chromatogram of a standard in the acid form. Column: Spherisorb ODS 2, mobile phase: potassium phosphate buffer (pH 7.7)–acetonitrile (65:35, v/v), flow-rate: 0.7 ml/min, UV detection at 237 nm. Peak: Mev A = mevinolinic acid.

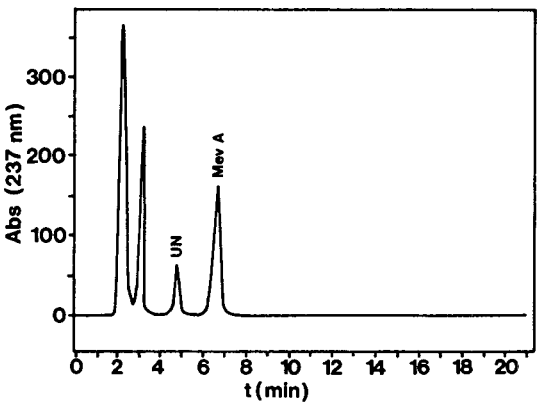


Fig. 4. HPLC chromatogram of a broth sample. Column: Spherisorb ODS 2, mobile phase: potassium phosphate buffer (pH 7.7)–acetonitrile (65:35, v/v), flow-rate: 0.7 ml/min, UV detection at 237 nm. Peaks: UN = unknown; Mev A = mevinolinic acid.

was much lower, attaining less than 60% of that obtained in the extracted samples.

From these results it can be assumed that a part of the substance was present as a lactone and solubilized only after addition of methanol, or that the substance was bound to the mycelium and released from it after methanol had changed the cell membrane composition and its permeability.

The effect of storage time on the standard solution was studied as well. The HPLC analysis was prolonged from 15 to 60 min in order to eliminate any doubt about the existence of the lactone form. The standard in the acid form was stable since no additional peak was detected after storing the solution for 10 days (data not shown).

Comparing this method with the one described by Kysilka and Křen [6], it can be seen that in our experiments the extraction of the broth was necessary. Without extraction of the fungal biomass with methanol, a great part of mevinolin was not detected. An additional advantage is the neutral pH, where all substance is in the form of one single compound. This proved to be the most stable, and had the lowest retention time during HPLC analysis under these conditions. In

the fermentation broth extracts mevinolin is found predominantly in its acid form and only in a small amount as the closed lactone [7]. Therefore the best way to determine the amount of mevinolin in fermentation studies is to measure it in the form of mevinolinic acid.

## 4. Conclusions

The HPLC analysis of mevinolin in fermentation broths extracted with methanol under acidic conditions results in three peaks corresponding to acid, lactone and methyl ester of mevinolin. By adjusting the pH of the samples and the mobile phase to 7.7, the substance can be detected as a single peak of mevinolinic acid, which is stable and has the lowest retention time of all three forms. It is not convenient to omit the extraction of the broth with methanol, since the yield is reduced by nearly half of the value detected after extraction.

## Acknowledgements

The financial supports of the Krka Pharmaceutical Factory and the Slovenian Ministry of Science and Technology are gratefully acknowledged.

## References

[1] B. Buckland, K. Gbewonyo, T. Hallada, L. Kaplan and P. Masurekar, in A.L. Demain, G.A. Somkuti, J.C. Hunter-Cevera and H.W. Rossmoore (Editors), *Novel Microbial Products for Medicine and Agriculture*, Elsevier, Amsterdam, 1989, pp. 161–169.
[2] R.J. Stubbs, M. Schwartz and W.F. Bayne, *J. Chromatogr.*, 383 (1986) 438–443.
[3] D. Wang-Iverson, E. Ivashkiv, M. Jemal and A.I. Cohen, *Rapid Commun. Mass Spectrom.*, 3 (1989) 132–134.
[4] *Pharmacopeial Forum*, 18 (1992) 2744–2747.
[5] V.P. Gullo, R.T. Goegelman, I. Putter and Y.-K. Lam, *J. Chromatogr.*, 212 (1981) 234–238.
[6] R. Kysilka and V. Křen, *J. Chromatogr.*, 630 (1993) 415–417.
[7] V.A. Vinci, T.D. Hoerner, A.D. Coffman, T.G. Schimmel, R.L. Dabora, A.C. Kirpekar, C.L. Ruby and R.W. Stieber, *J. Ind. Microbiol.*, 8 (1991) 113–120.
[8] R. Monaghan, A.W. Alberts, C.H. Hoffman and G. Albers-Schonberg, *US Pat.*, 4 231 938 (1980).
[9] M.S. Brown, J.R. Faust, J.L. Goldstein, I. Kaneko and A. Endo, *J. Biol. Chem.*, 253 (1978) 1121–1128.

ELSEVIER

Journal of Chromatography A, 704 (1995) 369–376

JOURNAL OF CHROMATOGRAPHY A

# Analysis and purification of modified methoxy(polyethylene glycol) compounds of similar molecular mass by high-performance liquid chromatography

William H. Leister*, Larry E. Weaner, Donald G. Walker

*Department of Chemical Development, The R.W. Johnson Pharmaceutical Research Institute, Spring House, PA 19477, USA*

Received 14 December 1994; accepted 16 February 1995

**Abstract**

The chromatographic analysis of monomethoxy(polyethylene glycol) (MPEG) derivatives, with an average molecular mass of 5000, and two related PEG compounds is described. The derivatives, containing neutral, basic, and acidic groups, were separated by HPLC using a cyanopropyl-bonded analytical column with UV detection. Collected chromatographic bands were identified using $^{1}H$ NMR. MPEG-amine 2 was also derivatized to form the corresponding MPEG-semicarbazide 5B labeled with $^{14}C$ to allow for sample quantification. A two-step purification method was devised to increase the radiochemical purity of crude 5B from 50% to over 95%.

## 1. Introduction

There has recently been a renewed interest in poly(ethylene glycol) (PEG) compounds and their derivatives for modifying the physical properties of drug candidates. When chemically linked to a protein, PEGs can have a mediating effect on the characteristics of the protein to which it is bound, while having little biological effect themselves [1]. PEGs have been shown to slow the rate of drug release and to reduce or control the antigenicity of immunogenic proteins [1–4]. To be useful in pharmaceutical applications, the starting PEG compound must be of high purity and well characterized. Numerous analytical methods have been reported for the analysis of these compounds including reversed-phase HPLC [1,5–9], high-temperature HPLC [10], size-exclusion chromatography (SEC) [2–4,7,11–13], HPLC with evaporative light scattering detection (ELSD) [14,15], thin-layer chromatography (TLC) [12], and supercritical fluid chromatography (SFC) [10]. Previously reported methods have been successful in resolving PEG compounds from non-PEG related compounds [5], in determining molecular mass distributions of a single PEG compound [3,10,14,15], and in resolving MPEG compounds that had different molecular mass distributions [3,7,10,11,13]. However, to our knowledge, there have been no reports on the separation of PEG compounds with the same molecular mass distribution and differing only by a single functional group.

We now report a method for the evaluation of PEG related compounds that is selective based on the terminating functional group of the glycol chain. Separation was accomplished using a cyanopropyl column with a sodium perchlorate–

* Corresponding author.

0021-9673/95/$09.50 
*SSDI* 0021-9673(95)00217-0

acetonitrile gradient. The compounds, consisting of distributions in the 3400 and 5000 molecular mass ranges, chromatographed as broad bands which were difficult to quantify by UV detection because of the lack of a suitable chromophore. In spite of low UV sensitivity and the poor peak shapes observed with these compounds, the method is useful for determining the presence of non-PEG impurities as well as for detecting the presence of other PEG related compounds. Factors affecting the separation, including sample pH, buffer pH, salt concentration, organic concentration, and temperature, have been investigated.

## 2. Experimental

### 2.1. Equipment

Analytical chromatography was performed with a Waters Millennium 2010 HPLC system consisting of a Model 600E system controller, a Model 996 diode-array detector and a Model 717 automatic injector. Wavelengths of 192 and 195 nm with a setting of 1.0 AUFS were used for UV detection. Sample injection volumes varied from 5 to 50 μl. The 150 × 4.6 mm I.D., 5 μm Zorbax cyanopropyl column was purchased from MAC-MOD (Chadds Ford, PA, USA).

Analytical chromatography of radioactive materials was performed with a Hewlett-Packard Model 1090 M liquid chromatograph with Chemstation software. A wavelength of 192 nm was used for detection, with an injection volume of 25 μl. Radiochemical detection was performed with a Radiomatic A250 detector. $^{1}H$ NMR spectra were recorded on a Bruker AC-300 instrument. The specific activity of the labeled sample was measured on a Beckman LS 6000LL liquid scintillation counter.

All samples were dissolved in a mixture of acetonitrile–0.5 *M* sodium perchlorate (pH 2.5) buffer (28:72, v/v) unless otherwise specified. Preparative chromatography was completed as previously reported [16].

### 2.2. Materials

Chemicals and reagents used in the study were certified ACS grade while solvents were of HPLC grade (Fisher Chemical, Fair Lawn, NJ, USA). Structures of the compounds studied are shown in Table 1. The MPEG compounds (1–6) were of average molecular mass 5000 and the PEG compounds (7 and 8) were of average molecular mass 3400 (Shearwater Polymers,

Table 1
Structure of MPEG and PEG compounds studied

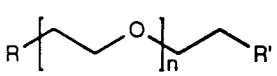


| Compound | R | R′ | Avg. molecular mass |
|---|---|---|---|
| 1 | $CH_3O$ | OH | 5000 |
| 2 | $CH_3O$ | $NH_2$ | 5000 |
| 3 | $CH_3O$ | $OCH_2CO_2H$ | 5000 |
| 4 | $CH_3O$ | $CH_2CO_2H$ | 5000 |
| 5A | $CH_3O$ | $NHCONHNH_2$ | 5000 |
| 5B | $CH_3O$ | $NH^*CONHNH_2$ | 5000 |
| 6 | $CH_3O$ | $OCO_2p\text{-}NO_2Ph$ | 5000 |
| 7 | $H_2N$ | OH | 3400 |
| 8 | $H_2N$ | $NH_2$ | 3400 |

* Indicates position of [$^{14}C$] label.

Table 2
Analytical HPLC gradient elution program

| Time (min) | 0 | 2 | 15 | 16 | 18 | 19 | 22 | 27 |
|---|---|---|---|---|---|---|---|---|
| % Acetonitrile | 25 | 25 | 27 | 27 | 75 | 75 | 25 | 25 |
| % Water | 75 | 75 | 0 | 0 | 25 | 25 | 75 | 75 |
| % 0.5 *M* Sodium perchlorate (pH 2.5) | 0 | 0 | 73 | 73 | 0 | 0 | 0 | 0 |
| Flow rate (ml/min) | 1 | 1 | 2 | 2 | 2 | 2 | 1 | 1 |

Table 3
Initial preparative HPLC gradient elution program

| Time (min) | 0 | 1 | 5 | 15 | 16 | 17 | 18 | 21 | 22 |
|---|---|---|---|---|---|---|---|---|---|
| % Acetonitrile | 34 | 34 | 34 | 35 | 35 | 35 | 75 | 75 | 34 |
| % Water | 66 | 66 | 66 | 32 | 0 | 0 | 0 | 0 | 66 |
| % 0.5 *M* Sodium perchlorate (pH 2.5) | 0 | 0 | 0 | 33 | 65 | 65 | 25 | 25 | 0 |
| Flow rate (ml/min) | 4 | 15 | 15 | 15 | 15 | 15 | 15 | 15 | 15 |

Huntsville, AL, USA). Details of the synthesis of the [$^{14}$C]-labeled MPEG-semicarbazide (5B) have been previously described [16]. The specific activity of this material was determined to be 7.7 $\mu$Ci/mg by liquid scintillation counting.

### 2.3. High-performance liquid chromatography

Analytical chromatography was performed using the gradient elution program described in Table 2. All gradients were linear and the column temperature was ambient.

The gradient programs employed for preparative chromatography have been previously reported [16] and are shown in Tables 3 and 4.

## 3. Results and discussion

### 3.1. The role of the buffer

The choice of the sodium perchlorate buffer was critical for the analysis of the MPEG and PEG compounds. It provided low UV absorbance in the wavelength region of interest and had good solubility in both aqueous and organic solutions. Additionally, separation of the various compounds could not be obtained on the cyanopropyl column without first complexing a minimum loading of sodium perchlorate onto the column. Equilibrating to the starting organic concentration prior to injection did not yield reproducible results until after conditioning the

Table 4
Final preparative HPLC gradient elution program

| Time (min) | 0 | 1 | 4 | 6 | 8 | 18 | 20 | 22 | 23 |
|---|---|---|---|---|---|---|---|---|---|
| % Acetonitrile | 0 | 0 | 0 | 32 | 33 | 45 | 100 | 100 | 0 |
| % Water | 0 | 100 | 100 | 68 | 67 | 55 | 0 | 0 | 0 |
| % 5% Acetic acid | 100 | 0 | 0 | 0 | 0 | 0 | 0 | 0 | 100 |
| Flow rate (ml/min) | 4 | 12 | 12 | 15 | 15 | 15 | 15 | 15 | 15 |

column with approximately 30 column volumes using the gradient program described in Table 2. Once conditioned, the gradient program satisfactorily maintained the sodium perchlorate concentration on the column and gave reproducible results. The selectivity of the complexed sodium perchlorate buffer was particularly effective in the case of MPEG 2, which was resolved into several components. Resolution of the first two eluting components was completely lost when water was substituted for the 0.5 *M* sodium perchlorate in the gradient program as illustrated in Fig. 1.

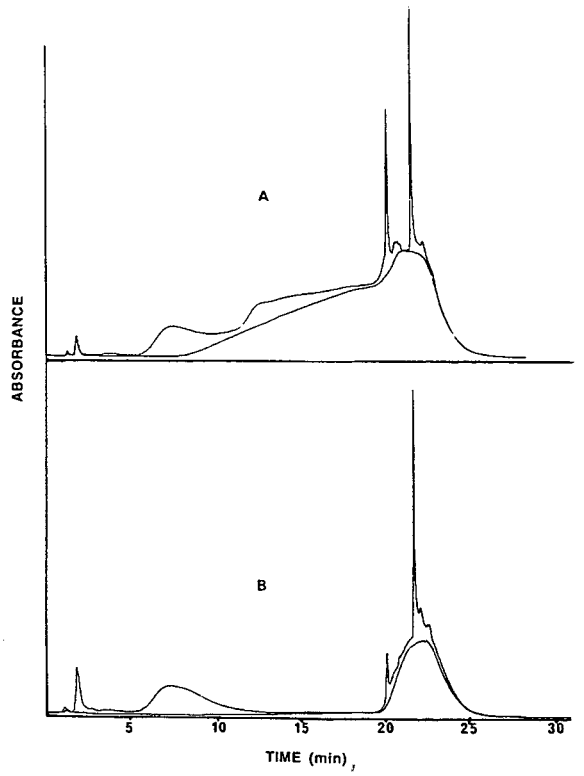


Fig. 1. Effect of buffer on the separation of compound 2, MPEG-$NH_2$. Chromatograms were obtained using the same column and injection vial, the only difference being that (A) used the sodium perchlorate gradient conditions outlined in Table 2 and (B) was obtained with water substituted for the 0.5 *M* sodium perchlorate. The baseline chromatogram is shown in each example.

### *3.2. Method of detection*

PEG compounds are frequently detected using an evaporative light scattering detector (ELSD) [14,15] or a refractive index detector (RI) [1,3,5,11,13] because of the low UV absorbance with these compounds. An ELSD was not available to us, and the use of an RI detector is severely limited for gradient applications. Since the compounds separated in this study differ only by one functional group, the use of a gradient elution program was essential for successful resolution. While the studies in this paper were completed using a UV detector, the use of an ELSD should enhance the performance of the method.

UV detection allows for gradient elution, however the problem of low sensitivity of the PEG compounds remains. UV detection has been used with some success with these compounds at low wavelengths [8,10] and by derivatization with a chromophore [6,7]. In this study, the lack of UV sensitivity was improved by using large concentrated samples (4.5 mg/injection). The high sample loading caused retention times to decrease with increased loading. To obtain reproducible results, all comparative chromatograms were prepared with the same sample loading and concentrations. The lack of pure reference materials prevented quantification of the chromatograms. However, interpretation of the results was aided by examining peak shape and absorbance spectra obtained using diode-array detection and, ultimately, by incorporation of a radiolabel and radioactive flow detection. All of the PEG and MPEG distributions chromatographed in broad bands with extensive peak tailing. Obtaining baseline resolution in most cases was not possible due to the large peak widths. Detection sensitivity improved as the monitoring wavelength was decreased, with the UV maxima observed at the lowest wavelength recorded (192 nm). At this wavelength, many of the non-MPEG/PEG impurities had very narrow peak widths and high UV absorbance. The UV absorbance of these impurities decreased at the lowest recorded wavelengths, with UV maxima between 210 and 220 nm. These differences allowed for qualitative

identification of PEG and non-PEG compounds, but quantification of results was not possible.

Detection at low wavelengths also made it difficult to achieve a reproducible, flat baseline with the gradient system employed. A blank injection showed a small peak at the void volume and a slow rise in the baseline was observed over the entire chromatogram as the concentration of the sodium perchlorate increased. Blank baselines are shown with all spectra for reference.

### 3.3. Band broadening

To effectively chromatograph the MPEG and PEG distributions it was necessary to increase the selectivity of the terminal functional groups, which comprise less than 1% of the total molecular weight, while minimizing the size of the broad bands observed with high molecular weight distributions. To limit band broadening, the effects of temperature and salt concentration were examined.

The MPEG and PEG compounds were analyzed at various temperatures up to 80°C using the sodium perchlorate gradient system. Increasing temperature has been previously reported to improve separation with MPEG compounds [10]. The acetonitrile concentration was adjusted as the temperature was increased to give acceptable retention times. The chromatograms obtained showed no corresponding increase in selectivity with increasing temperature and all of the compounds tested eluted with increased band widths and lower resolution values. Therefore, all subsequent analyses were performed at ambient temperature.

The best selectivity for the compounds was obtained with a water–acetonitrile gradient in the absence of buffer. However, under these conditions very wide peak widths were obtained. A gradient using sodium perchlorate with no change in organic concentration produced narrower peak widths but with reduced selectivity. Therefore, in order to obtain both tight bands and high selectivity, it was necessary to optimize the gradient for both buffer and organic composition. The best chromatographic results were achieved with a gradient using a large increase in salt concentration (72%) accompanied by a small increase in organic concentration (2%).

### 3.4. The effect of pH

The effect of pH on both the mobile phase and the sample solution was examined. Chromatography of the MPEG and PEG compounds tested showed no differences in retention using mobile phase compositions in the pH range of 2.5 to 5.9. A pH of 2.5 was chosen based on the high buffering capacity and good pH stability observed over several weeks of use.

The pH of the sample solution, however, was found to effect retention times even though the mobile phase was sufficiently buffered and maintained at pH 2.5 throughout the study. The relative retention and retention order of the MPEG compounds could be manipulated by adjusting the pH of the sample solution, while maintaining a constant concentration of the organic component. The retention time of basic compound 2 increased as sample pH was increased while retention of acidic compounds 3 and 4 decreased with increasing sample pH. Neutral compound 1 was unaffected by pH adjustment (Fig. 2). Therefore, the optimal pH of the sample solution was dependent upon the particular compound being chromatographed.

### 3.5. Analysis of starting materials and MPEG-semicarbazide

The method worked well in assaying the homogeneity of all of the compounds used in the study. Representative chromatograms of several compounds are shown in Fig. 3. The chromatography of compound 1 gave a single broad peak, which was subsequently identified by isolation and $^1$H NMR analysis. However, chromatography of the other compounds showed the presence of additional components. The MPEG acids, compounds 3 and 4, each showed a peak shoulder trailing the main peak. Chromatography of compounds 5A and 5B revealed the presence of multiple peaks, in addition to a late eluting compound. Chromatography of com-

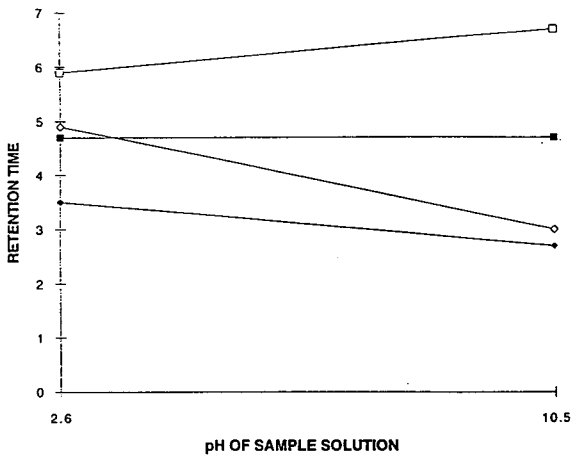


Fig. 2. The relative changes in retention times of MPEG compounds as a function of sample solution pH: (■) 1, MPEG-OH; (□) 2, MPEG-$NH_2$; (◆) 3, MPEG-$OCH_2CO_2H$; (◇) 4, MPEG-$CH_2CO_2H$ (see Experimental for HPLC conditions).

pound 6, the only MPEG compound analyzed containing an aromatic group, gave a single off-scale peak with a retention time of approximately 22 min. Compounds 7 and 8 were separated into several well resolved peaks.

Chromatography of MPEG 2 resulted in the separation of two broad, PEG-like bands as well as two more retained peaks. $^1H$ NMR spectra confirmed the identity of the first major peak to be compound 2. Impure compound 2 was further reacted to provide unlabeled 5A and [$^{14}C$]-labeled MPEG-semicarbazide, 5B. Due to the initial low purity of compound 2, several products were obtained from the reactions and HPLC purification was required. The major peak in the MPEG-semicarbazide chromatograms was isolated using the sodium perchlorate gradient program outlined in Table 3. A second chromatographic purification was required to remove unseparated reaction impurities as well as the sodium perchlorate salts carried through from the initial chromatography. Several different mixtures were evaluated to determine the optimal conditions for washing the perchlorate salts off the column. These solutions included aqueous mixtures of 5% $NaHCO_3$, 5% $CH_3COOH$, and 0.1% TFA, and were examined using the

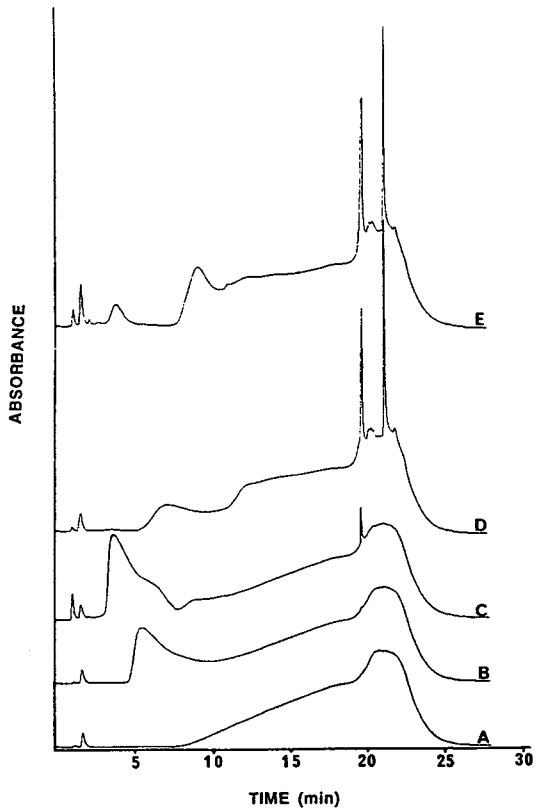


Fig. 3. The chromatograms of several representative compounds obtained under identical HPLC conditions (see text for conditions). MPEG-OH (1) is relatively pure while the other compounds show the presence of additional peaks: (A) blank, (B) 1, MPEG-OH, (C) 3, MPEG-$OCH_2CO_2H$, (D) 2, MPEG-$NH_2$, (E) 8, $H_2N$-PEG-$NH_2$.

gradient method described in Table 4. Each was found to have a great effect on both sample solubility and column stability.

A sodium bicarbonate (pH 8.3) wash resulted in increased retention and a loss of resolution. Following its use, an additional 5% acetonitrile was needed to elute the compounds off the column and reduced selectivity was observed. This was most likely a result of a partial stripping away of the bonded phase from the base silica. The presence of a cyanopropyl by-product in an isolated sample of compound 2 was confirmed by $^1H$ NMR. To avoid this problem, either acetic acid or trifluoroacetic acid could be substituted for the sodium bicarbonate solution in the gra-

dient program. No decrease in column stability was observed with either of these acids following their use. The final purification procedure was completed using 5% acetic acid in the gradient program (Table 4).

The preparation of MPEG-semicarbazide with a radioactive label (5B) allowed for the direct quantification of results which was not possible with UV detection. The initial radiochemical purity of 5B isolated from the reaction mixture was approximately 50% as measured using a radioactive flow detector (Fig. 4). The product was purified by preparative chromatography with the sodium perchlorate gradient system (Table 3). Further purification and removal of the sodium perchlorate salts was accomplished using the system described in Table 4. The radiochemical purity of the isolated product was determined to be 95% based on radioanalysis with a radioactive flow detector using a scintillation cocktail. The increase in chromatographic purity was even more significant as shown in Fig. 4. The identity of the purified [$^{14}$C]MPEG-semicarbazide was confirmed by $^{1}$H NMR.

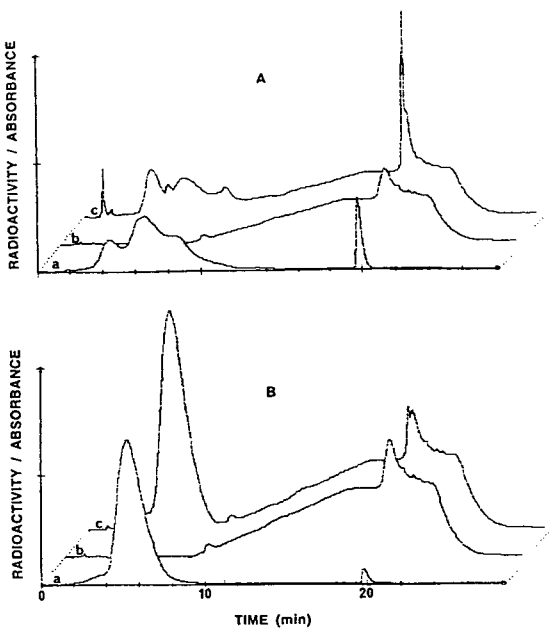


Fig. 4. Chromatograms of (A) crude 5B and (B) purified 5B obtained using UV (192 nm) detection and a radioactive flow detector. The HPLC purification increased the radiochemical purity from approximately 50% to over 95%: (a) [$^{14}$C] radiochromatogram, (b) baseline with UV detection, (c) UV detection (see text for HPLC conditions).

## 4. Conclusions

A combined organic and sodium perchlorate gradient on a cyanopropyl column has been shown to separate a number of PEG and MPEG compounds with similar molecular mass distributions. The use of a sodium perchlorate buffer allowed for detection at very low wavelengths while displaying unique chromatographic properties, obtained by interaction between the bonded phase and the perchlorate salt. The distributions chromatographed in broad bands but could be separated using a slight organic gradient coupled with a salt gradient to maintain good peak resolution. Additional selectivity was achieved by manipulating the pH of the sample solution. The method was used to determine the relative purity of PEG and MPEG compounds and to purify a sample of [$^{14}$C]-labeled MPEG semicarbazide (5B) from 50% to over 95% radiochemical purity.

## Acknowledgement

The authors acknowledge David C. Hoerr for his technical assistance and helpful discussions during the course of this work.

## References

[1] T. Suzuki and T. Tomono, J. Polym. Sci., Polym. Chem. Ed., 22 (1984) 2829.
[2] F.M. Veronese, P. Caliceti, A. Pastorino, O. Schiavon, L. Sartore, L. Banci and L.M. Scolaro, J. Controlled Release, 10 (1989) 145.
[3] B. Selisko, C. Delgado, D. Fisher and R. Ehwald, J. Chromatogr., 641 (1993) 71.
[4] R. Seraglia, P. Traldi, R. Mendichi, L. Sartore, O. Schiavon and F.M. Veronese, Anal. Chim. Acta, 262 (1992) 277.
[5] L.P. Turner, D. McCullough and A. Jackewitz, J. Am. Oil Chem. Soc., 53 (1976) 691.

[6] A. Warshawsky, N. Shoef and A. Tishbee, J. Liq. Chromatogr., 6 (1983) 2797.
[7] R. Murphy, A.C. Selden, M. Fisher, E.A. Fagan and V.S. Chadwick, J. Chromatogr., 211 (1981) 160.
[8] S. van der Wal and L.R. Snyder, J. Chromatogr., 255 (1983) 463.
[9] S.T. Lai, J. Chromatogr., 363 (1986) 444.
[10] R.E.A. Escott and N. Mortimer, J. Chromatogr., 553 (1991) 423.
[11] S. Mori, T. Mori and Y. Mukoyama, J. Liq. Chromatogr., 16 (1993) 2269.
[12] D.J. Larwood and F.C. Szoka, J. Labelled Compd. Radiopharm., 7 (1984) 603.
[13] M. Leonard and E. Dellacherie, Makromol. Chem., 189 (1988) 1809.
[14] K. Rissler, H.-P. Künzi and H.-J. Grether, J. Chromatogr., 635 (1993) 89.
[15] K. Rissler, U. Fuchslueger and H.-J. Grether, J. Liq. Chromatogr., 17 (1994) 3109.
[16] D.G. Walker, W.H. Leister and L.E. Weaner, J. Labelled Compd. Radiopharm., in press.

ELSEVIER

Journal of Chromatography A, 704 (1995) 377–385

JOURNAL OF CHROMATOGRAPHY A

# Characterization of poly(naphthalenesulfonate) salts by ion-pair chromatography and ultrafiltration

M. Piotte, F. Bossányi, F. Perreault, C. Jolicoeur*

*Department of Chemistry, Université de Sherbrooke, Sherbrooke, Que. J1K 2R1, Canada*

First received 15 November 1994; revised manuscript received 13 February 1995; accepted 17 February 1995

**Abstract**

The molecular mass distribution of naphthalenesulfonate condensation products (PNS) was investigated using ion-pair reversed-phase chromatography and ultrafiltration. The chromatograms obtained under an optimized solvent elution program yielded nearly 20 well resolved peaks corresponding to low and intermediate molecular mass species. A distinct broad peak was also resolved and attributed to polymeric species with relative molecular mass in excess of 5000. Under isocratic elution conditions, a linear relationship was obtained between the peak number and the log of the retention time for the first 17 peaks, thus indicating a homologous series of linear oligomers. The fractionation of the PNS mixtures by ultrafiltration enabled further resolution of the high molecular mass species; the latter also exhibited a broad distribution of molecular mass. Significant differences were also found amongst different commercial PNS products with similar average chemical composition.

## 1. Introduction

Poly(naphthalenesulfonic) acid is obtained by condensation of naphthalenesulfonic acid ($\alpha$ or $\beta$) with formaldehyde. A schematic representation of linear and singly-branched tetramers of poly($\beta$-naphthalenesulfonate) (PNS) sodium salts is shown in Fig. 1. These polymers are broadly used as dispersants of organic or mineral colloids in aqueous systems. The ability of this type of products to fluidize fresh concretes at very low water/cement ratios makes them an essential component in the production of high performance concrete [1,2]. Other applications, such as "water reducer" in gypsum board fabrication, as dye dispersant in the textile industry [3] and as leather tanning additive [4] are also widely known.

The dispersing/fluidizing properties of PNS salts have been suggested, or shown, to be dependent on their molecular mass [5–10]. The suggested mode of action of these polymers involves adsorption on the dispersed particles and particle–particle repulsion through electrostatic or steric effects [5,7,8,11–13]. A more detailed understanding of these mechanisms clearly requires an accurate characterization of the molecular species (e.g. molecular mass, branching, crosslinking, degree of sulfonation).

The nature and distribution of the species present in PNS condensation products have been investigated using several chromatographic methods: paper [4,14], size-exclusion [6,15,16], salting-out [17,18], anion-exchange [19] and ion-pair [19] chromatography.

* Corresponding author.

0021-9673/95/$09.50 
*SSDI* 0021-9673(95)00226-X

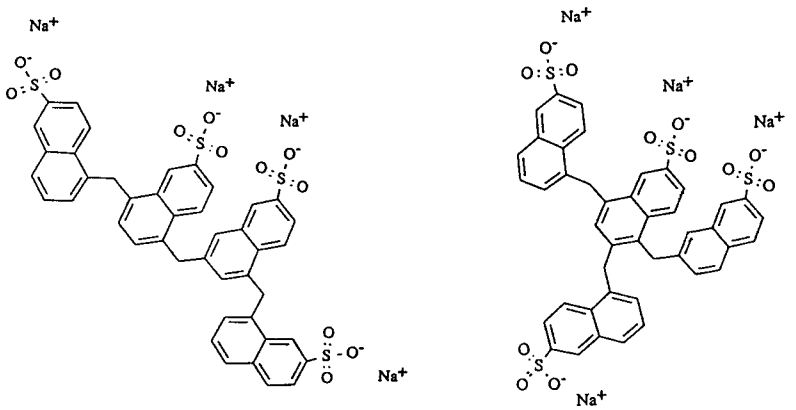

Fig. 1. Example of linear and branched tetramers of poly(β-naphthalenesulfonate) salts.

Fudano and Konishi [17] investigated various salting-out chromatographic columns and conditions and, under optimal conditions, resolved five distinct peaks; the first broad peak was further split up into five components by curve-shape analysis. The nine resulting peaks were compared with data from Hattori and Tanino [14], who had found nine spots in paper chromatographic analysis. Using size-exclusion chromatography (SEC), Garvey and Tadros [15] reported PNS oligomers with a degree of polymerization ($P$) between 1 and 9. Basile et al. [6] also used a SEC method to determine the number average $M_{r,n}$ of the fraction of PNS retained on an ultrafiltration membrane with a molecular mass cut-off (MWCO) of 1000. They obtained $M_r$ values ranging from 435 ($P = 1.8$) to 735 ($P = 3$), depending on the reaction time.

More recently, Miller [19] investigated PNS separation using ion-pair chromatography and could resolve two peaks, respectively attributed to linear and branched polymers. A comparison with poly(styrenesulfonate) data suggests that the degree of polymerization of the high molecular mass fraction of PNS may be as high as 90 ($M_r = 21\ 600$). With a similar method, Costa et al. [5] resolved the first peak into nearly ten peaks and identified ten additional peaks on the shoulder of the second broad peak.

As is apparent from the above overview, the polymeric species present in PNS mixtures are difficult to separate and identify. In view of the importance of the species distribution on the functional properties of the polymers, the present study was undertaken to reexamine some previously used analytical separation methods, and to further explore their potential for deriving information on the size and structure of PNS polymers.

## 2. Experimental

### 2.1. Material

Water was distilled and deionized with a Milli-Q (Millipore, Saint-Quentin-en-Yvelines, France) system (resistivity $> 17\ M\Omega\ cm^{-1}$) and then filtered over 0.22 μm filter. The acetonitrile used was of HPLC grade; glacial acetic acid and tetrabutylammonium bromide (TBAB) were ACS reagent grade. All other chemicals used were laboratory reagent grade. PNS compounds labelled A, B, C, D are all commercial preparations of sodium salts of PNS intended for fluidization of concrete or gypsum pastes, or for dispersion in other industrial applications.

### 2.2. Methods

Partisil 5 ODS-3 (Whatman, Clifton, NJ, USA) and Bondclone 10C18 (Phenomenex, Torrance, CA, USA) HPLC columns, 300 × 3.9 mm I.D., were used; the chromatographic ma-

terial consisted of $C_{18}$-grafted silica particles of 5 $\mu$m and 10 $\mu$m diameter, respectively. Detection was performed by measuring absorbance at 280 nm. Injections were made through a 50-$\mu$l or a 100-$\mu$l loop loaded with 10–50 $\mu$g of PNS (dry basis) in water. Integration was made using the area normalization method.

The eluent was a mixture of two solvents prepared as described by Miller [19]. Solvent A was 0.01 *M* TBAB in 99% water and 1% glacial acetic acid; solvent B was 0.01 *M* TBAB in 99% acetonitrile and 1% glacial acetic acid. The elution programs were executed by a gradient pump module (Dionex, Sunnyvale, CA, USA). The flow-rate of the eluent was maintained constant within ± 0.05 ml/min during each run; for any given run, it was adjusted at a value between 1.0 and 1.5 ml/min.

Ultrafiltration experiments were carried out in stirred cells (Amicon, Beverly, CA, USA) using the following series of membranes: YC05, YM2, YM5, PM10 (Amicon). The membrane specifications are given in Table 1. In the procedure followed here, a 10% solution of crude PNS was first filtered on the membrane with MWCO 500. The retained fraction was then diluted with water and filtered again on the same membrane; these operations were repeated for a total of at least five times. The membrane with the smaller pore size was used first in order to eliminate most of the electrolytes, thereby ensuring that the subsequent filtrations are performed at minimal ionic strength. The filtrates were combined and analyzed, while the final retained fraction was used as starting material for ultrafiltration on the membrane with the next larger pore size. The complete ultrafiltration procedure is illustrated schematically in Fig. 2.

Table 1
Ultrafiltration membrane specifications (Amicon)

| Membrane | Approximate pore diameter (Å) | Nominal $M_r$ cut-off |
|---|---|---|
| YC05 | 10.5 | 500 |
| YM2 | 12 | 1000 |
| YM5 | 13.5 | 5000 |
| PM10 | 15 | 10 000 |
| XM50 | 32 | 50 000 |
| YM100 | 51 | 100 000 |

Nominal cut-off and pore diameter are established with globular proteins 95% retained on the membrane.

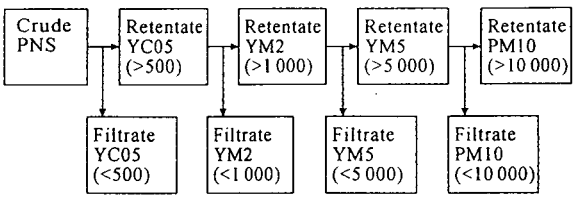


Fig. 2. Ultrafiltration procedure.

## 3. Results and discussion

### 3.1. Ion-pair chromatography

*Isocratic elution*

Although isocratic elution rarely represents the optimum condition to achieve separation of a complex mixture, it can nevertheless give valuable information on the partitioning between the static and the mobile phases. When pure water was used as the eluent, there was no retention and a single peak was detected. Conversely, when solvent A (water + TBAB) was used, no PNS was eluted. This stresses the critical role of ion-pairing on the retention mechanism. Using only solvent B, we detected a single peak at minimum retention time. Following various attempts with different A/B mixing ratios, a mixture containing 35% A and 65% B yielded the PNS chromatogram shown in Fig. 3. Because of considerable overlap, the precise integration of each of the twenty peaks observed can not be achieved, but their retention times yield valuable information. A plot of log ($t_R$) against the peak number is found to be linear (slope = 0.0615, R.S.D. = 0.6%, $r = 0.9996$); this relationship strongly indicates the presence of linear PNS oligomers and polymers [20–22] with a degree of polymerization as high as 17. Although the procedures used differ, the chromatogram shown in Fig. 3 is similar to that reported by Miller [19]; from NMR data, Miller attributed the first peak

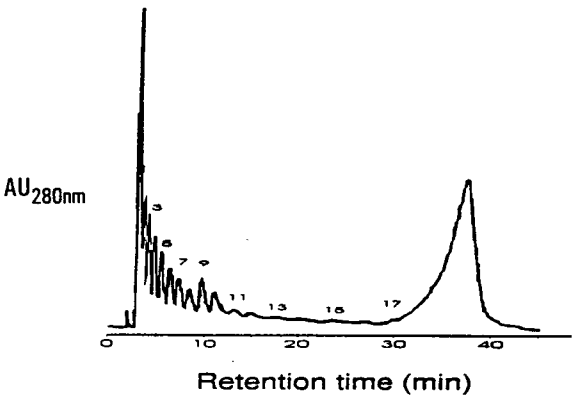


Fig. 3. Chromatogram of PNS-A with isocratic elution (35% A; 65% B).

(which corresponds to the group of 17 peaks found here) to linear PNS polymers.

*Programmed solvent elution*

Upon varying the A/B ratio, it was noticed that with 40% B, only the first four peaks of the PNS sample injected were eluted; with a higher content of solvent B (60%), the mid peaks were eluted, but the final broad peak was not. These experiments led to the conclusion that the resolution of either the first four peaks, or the mid peaks, was optimum when the eluent contained the minimum proportion of solvent B which achieved elution. All attempts to resolve the final peak into distinct components were unsuccessful. After numerous runs under varying conditions, the solvent elution program reported in Table 2 was adopted. It should be noted that the analytical separation is completed after the first 50 min of the elution program. The dual purpose of the rest of the elution program is first to prevent any micro-bubble formation and, second to ensure a regular purge of the column; in the absence of the latter procedure, the complex solubility behavior of PNS [10], can sharply reduce the column's life-time. Using this program, chromatograms were obtained for various naphthalenesulfonates; the $t_R$ values for these compounds are reported in Table 3. $\alpha$-Naphthalenesulfonate and $\beta$-naphthalenesulfonate exhibit the same retention time as the first peak of the chromatogram obtained for PNS (Figs. 4b, 5); naphthalene di- and tri-sulfonates were eluted in the mid peak region of the chromatogram.

Table 2
Elution program

| Time (min) | Solvent A (%) | Solvent B (%) |
|---|---|---|
| 0 | 60 | 40 |
| 10 | 35 | 65 |
| 25 | 35 | 65 |
| 35 | 20 | 80 |
| 45 | 20 | 80 |
| 47 | 0 | 100 |
| 50 | 0 | 100 |
| 52 | 20 | 80 |
| 54 | 20 | 80 |
| 55 | 60 | 40 |
| 60 | 60 | 40 |

Solvent A: TBAB 0.01 *M* in 99% water, 1% acetic acid.
Solvent B: TBAB 0.01 *M* in 99% acetonitrile, 1% acetic acid.

For PNS, the expected first and second peaks were only weakly resolved by this solvent elution program; however the mid peaks were well resolved. The chromatograms of Fig. 4b, 5 and 6 show that the first twenty peaks previously observed under isocratic elution are slightly asymmetric. Hence, while the maximum of each peak may correspond to a linear polymer, the area under the peaks cannot be exclusively attributed to linear polymer populations. The

Table 3
Retention time and peak area from chromatograms of various naphthalenesulfonate salts

| Compound | Retention time (min) | Relative peak area (%) |
|---|---|---|
| $\alpha$-Naphthalenesulfonate | 5.3 | 100.0 |
| $\beta$-Naphthalenesulfonate | 5.3 | 100.0 |
| 2,7-Naphthalenedisulfonate | 6.3 | 100.0 |
| 2,6-Naphthalenedisulfonate | 6.1 | 100.0 |
| Naphthalenetrisulfonate | 6.4 | 2.7 |
| | 7.0 | 1.6 |
| | 8.8 | 92.3 |
| | 12.7 | 3.3 |

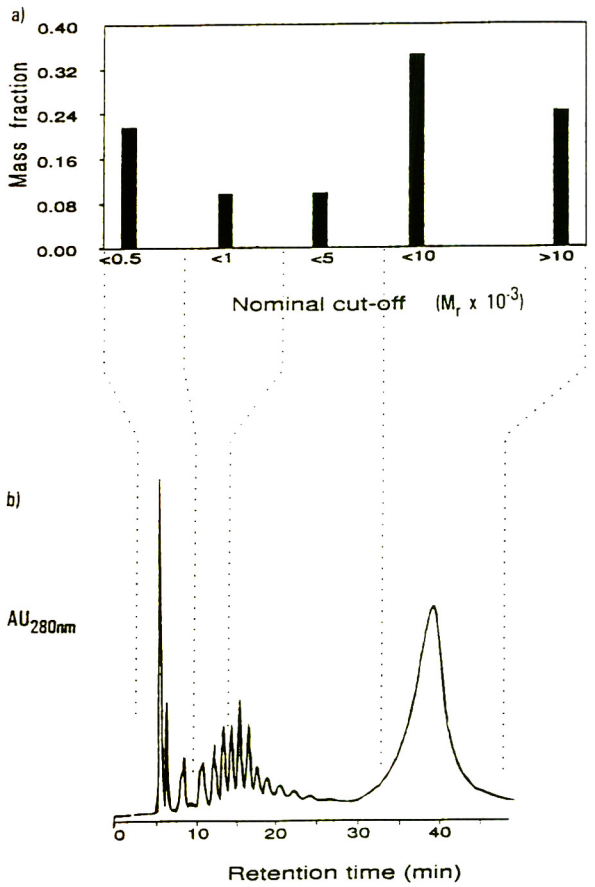


Fig. 4. (a) Size distribution of PNS-A obtained from successive ultrafiltrations; (b) Chromatogram of PNS-A using the elution program from Table 2.

relative areas computed from Fig. 4b gave about 7% for the first peak (which includes monomers and dimers), about 4% for the two following peaks (corresponding to oligomers with $P = 3,4$), about 25% for the rest of the mid peak region, and finally about 65% for the last broad peak (attributed to polymer with higher molecular mass). Since the extinction coefficient at 280 nm varies with the molecular mass of the polymer [10], the peak areas correspond only roughly to the relative populations; the smaller molecules have a lower specific absorbance, therefore their populations are underestimated. Nevertheless, the chromatograms provide a highly convenient relative basis for both qualitative and quantitative characterization of PNS mixtures as usually found in commercial preparations.

Fig. 5 shows chromatograms for three commercial PNS mixtures (B, C, D) and Table 4 lists the relative area under the peaks for all PNS samples investigated. Comparing the peak intensities for PNS-A (Fig. 4b) and PNS-B, it is readily seen that a higher proportion of PNS-A is eluted in the last peak; however, the overall patterns of polymer distribution, as reflected by the chromatographic peak intensities, are similar. The molecular mass distribution (intensities) of PNS-C and PNS-D are strikingly different from those of the A or B samples.

Number and mass average molecular mass values ($M_{r,n}$ and $M_{r,m}$) have been computed from the chromatograms and the results are collected in Table 5. For these calculations, it was assumed that the peaks numbered 1 to 20 are oligomers having the corresponding degree

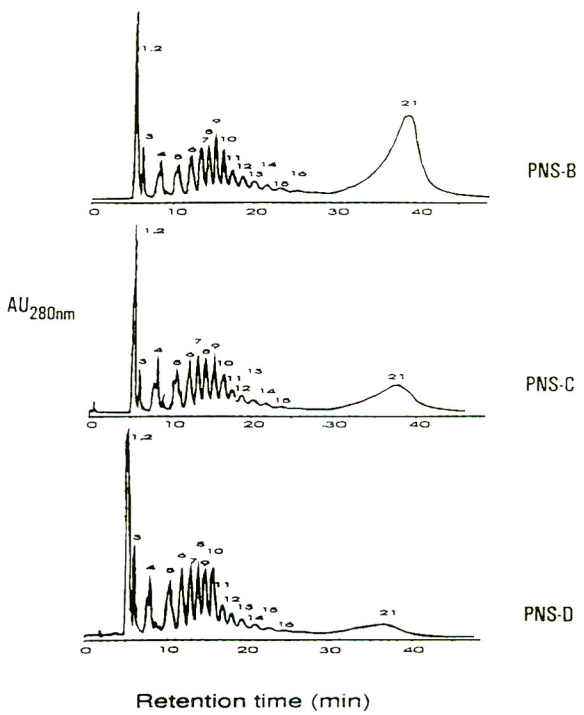


Fig. 5. Chromatograms of several commercial PNS preparations (B, C, D).

Table 4
Retention time and peak area of various PNS mixtures

| Peak | Retention time (min) | Relative area | | | |
|---|---|---|---|---|---|
| | | PNS-A (%) | PNS-B (%) | PNS-C (%) | PNS-D (%) |
| 1 | 5.4 | 7.4 | 8.4 | 17.8 | 21.0 |
| 2 | 5.7 | – | – | – | – |
| 3 | 6.2 | 1.9 | 1.9 | 2.7 | 5.7 |
| 4 | 8.3 | 2.2 | 3.2 | 7.7 | 8.6 |
| 5 | 10.7 | 2.6 | 3.7 | 7.9 | 8.3 |
| 6 | 12.2 | 2.8 | 3.6 | 7.3 | 8.1 |
| 7 | 13.3 | 3.0 | 3.7 | 7.0 | 7.4 |
| 8 | 14.2 | 2.9 | 3.6 | 6.4 | 6.4 |
| 9 | 15.3 | 3.7 | 4.2 | 6.6 | 7.4 |
| 10 | 16.3 | 3.2 | 3.7 | 5.7 | 8.0 |
| 11 | 17.4 | 2.0 | 2.6 | 3.9 | 3.8 |
| 12 | 18.7 | 1.6 | 2.1 | 3.0 | 2.8 |
| 13 | 20.1 | 1.2 | 1.7 | 2.2 | 1.9 |
| 14 | 21.9 | 0.7 | 1.2 | 1.2 | 1.1 |
| 15 | 23.0 | | 0.7 | | 0.6 |
| 16 | 25.0 | | 0.3 | | |
| 21 | 36–38 | 64.8 | 55.4 | 20.6 | 8.8 |

of polymerization. The $M_r$ value of the polymers under the last broad peak was taken as either 25 000 or 100 000. $M_{r,n}$ were found to be insensitive (within 5%) to the latter assumption; as expected, $M_{r,m}$ depended strongly on the assumed molecular mass of the larger polymers. The different PNS samples exhibit $M_{r,n}$ values between 700 and 2100, the lower value being in good agreement with earlier reports [6,14,15,17]. The polydispersity given by $M_{r,m}/M_{r,n}$ is very high, ranging between ~5 and ~30.

### 3.2. Fractionation through ultrafiltration

The ultrafiltration procedure described in Section 2.2 was used to separate a sample of the PNS-A into five fractions. Typical results are illustrated as a bar chart in Fig. 4a. This molecu-

Table 5
Molecular mass averages of PNS calculated from HPLC and ultrafiltration

| | HPLC | | | Ultrafiltration | | |
|---|---|---|---|---|---|---|
| | $M_{r,m}$ | | $M_{r,n}$ | $M_{r,m}$ | | $M_{r,n}$ |
| | A[a] | B[b] | | A[a] | B[b] | |
| PNS-A | 17 000 | 65 000 | 2100 | 11 000 | 35 000 | 2200 |
| PNS-B | 15 000 | 56 000 | 1800 | | | |
| PNS-C | 6000 | 22 000 | 910 | | | |
| PNS-D | 3500 | 10 000 | 770 | | | |

[a] Assumption A: $M_r$ of last peak is 25 000.
[b] Assumption B: $M_r$ of last peak is 100 000.

lar size distribution is very similar to the one found by ion-pair chromatography. As in the latter, a first peak is found corresponding to very low molecular mass species, followed by a minimum at the oligomer position. The "high molecular mass" region ($M_r > 5000$) is again found to represent about 60% of the total. It was also noticed that a large proportion of these high molecular mass species (retained on MWCO = 5000) was found in the lowest molecular mass side (passed MWCO = 10 000) of the band. Further ultrafiltration experiments using membranes having larger pore size indicated that substantial fractions of the polymers retained on the MWCO = 10 000 membrane were also retained on membranes with MWCO values of 50 000 and 100 000 (data not shown).

As with the HPLC data, the ultrafiltration results were used to derive average molecular mass values ($M_{r,n}$, $M_{r,m}$) under various assumption (Table 5). $M_r$ values of respectively 300, 750, 2500 and 7500 were assigned to the four passing fractions. For the retained fraction, $M_r$ values of either 25 000 or 100 000 were used, as in the treatment of the HPLC data. Comparison of the $M_r$ values obtained from the two techniques shows a rather good agreement.

### 3.3. Correlation between HPLC and ultrafiltration results

To evaluate the effectiveness of the membrane fractionation process, the different fractions were analyzed by the chromatographic method described above and the results are illustrated in Fig. 6. Monomers up to tetramers apparently passed through the YC05 membrane, indicating that the membrane has an actual MWCO for PNS of about 1000 (compared to the nominal MWCO of 500, Table 1). The chromatograms of the ultrafiltration fractions also show that pentamers, hexamers and heptamers were retained on the YC05 membrane and passed the YM2 membrane, along with some octamers to decamers; the effective MWCO of the YM2 membrane for PNS would thus be about 2000 (compared to the nominal MWCO of 1000). With the next membrane (YM5), PNS oligomers of $P$ up to 20 were

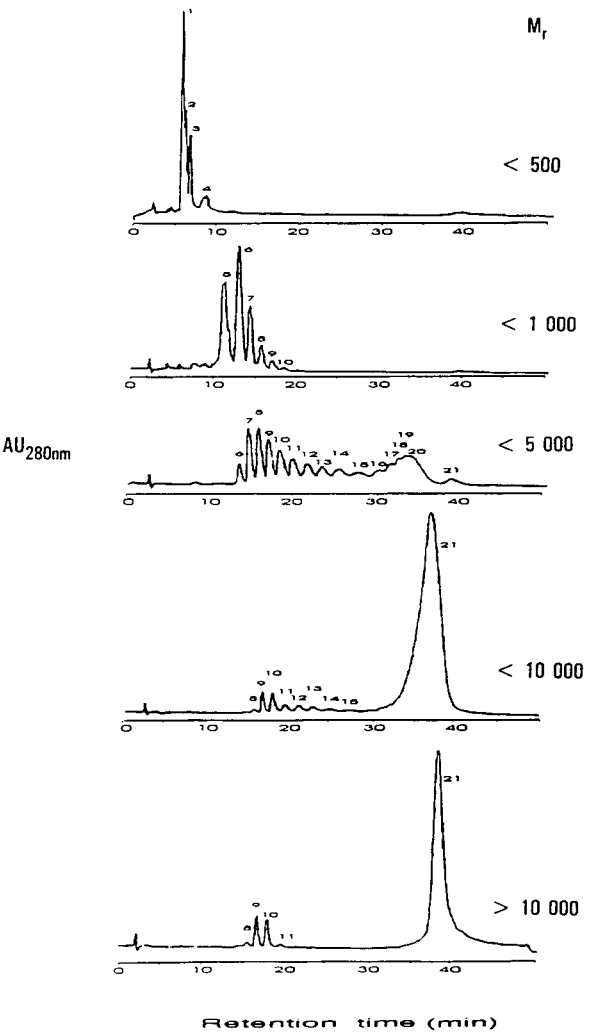


Fig. 6. Chromatograms of the fractions obtained by ultrafiltration.

allowed through; the effective PNS MWCO of this membrane would thus be of about 5000 (same as the nominal MWCO). Unfortunately, the resolution of the ion-pair chromatographic method does not provide further information on fractions that are retained on the YM5 membrane. All of those fractions showed small peaks in the region corresponding to $P \sim 10$ ($\approx 15$ min) and a large peak at around 38 min. As can be seen from Fig. 4, ion-pair chromatography yields

more detail in the low and intermediate molecular mass region, while ultrafiltration provides more information on the high molecular mass fractions of PNS.

## 4. Conclusions

The results presented above confirm the potential of ion-pair HPLC and ultrafiltration for the characterization of poly(naphthalenesulfonate) mixtures.

The HPLC technique, as used here, enables a separation of the monomers and oligomers with $P \approx 20$ (or $M_r$ up to $\sim 5000$) from mixed PNS condensation products. The method involves a relatively complex solvent elution program but, compared to other characterization methods (e.g. GPC), it is relatively rapid ($\sim 1$ h).

The ultrafiltration technique also enables an adequate separation of PNS polymers by $M_r$ classes; the technique is relatively long (many hours) and is particularly well-suited for high $M_r$ values, typically in the range $10^3$–$10^6$.

Overall, the results show that the PNS dispersant polymers exhibit a high degree of polydispersity. A similar trend, or shape, of the PNS species distribution was observed with both techniques. A typical mixture of PNS condensation products used as dispersant/fluidizer consists of a fairly high proportion of oligomers (about 10% of $P = 1$–$4$) in which the monomers are the more abundant species. Linear polymers can be found in the mixtures, with $M_r$ values as high as 5000 ($D \sim 20$), the maximum of this population being near 2500 ($P = 10$). The high molecular mass fraction contains $\sim 35\%$ of intermediate species ($M_r = 5000$ to 10 000; $P = 20$–$40$) and $\sim 25\%$ of species with $M_r$ values much higher. The presence of branched PNS polymers was not directly evidenced, but the high proportion of monomer, combined with the high polydispesity, strengthens the suggestion of chain branching proposed from considerations on the reaction path [10] and from NMR data [20].

Finally, calculations of average $M_r$ values show an excellent agreement between the ultrafiltration and HPLC data. The number average values ($M_{r,n}$) of PNS condensation products are usually low due to the presence of a high proportion of monomers. Hence, in order to adequately define the speciation of a PNS mixture, mass average molecular mass ($M_{r,m}$), or polydispersity values, must also be provided.

## Acknowledgements

The authors gratefully acknowledge financial support of this work by the Canadian Natural Sciences and Engineering Research Council, the Network of Centers of Excellence on High Performance Concrete and le ministère de l'Enseignement supérieur et de la Science du Québec. The assistance of Mr. Marc-André Simard is also gratefully acknowledged.

## References

[1] M.R. Rixom and N.P. Mailvaganam, Chemical Admixtures for Concrete, E. and F.N. Spon Ltd, 2nd edn., London, 1986.
[2] V.S. Ramachandran and V.M. Malhotra, in V.S. Ramachandran (Editor), Concrete Admixtures Handbook, Noyes Publications, Park Ridge, NJ, 1984, p. 211.
[3] T. Shibusawa, Sen-i Gakkaishi, 43 (1987) 614.
[4] K. Venkataboopathy, V.S. Sundara Rao, K.K. Reddy and C. Koteswara Rao, Leather Sci. (Madras), 28 (1981) 137.
[5] U. Costa, M. Goisis and G. Guerra, Proc. 9th International Congress on the Chemistry of Cement, Vol. 4, New Delhi, 1992, National Council for Cement and Building Material, New Delhi, 1992, p. 619.
[6] F. Basile, S. Biagini, G. Ferrari and M. Collepardi, Proc. 8th International Congress on the Chemistry of Cement, Vol. 6, Rio de Janeiro, 1986, Secretaria Geral do 8° CIQC, Rio de Janeiro, 1986, p. 260.
[7] P.J. Anderson, D.M. Roy and J.M. Gaidis, Cem. Concr. Res., 17 (1987) 805.
[8] A.A. Burk Jr, J.M. Gaidis and A.M. Rosenberg, in V.S. Ramachandran (Editor), Proc. of the 2nd CANMET/ACI International Conference on Superplasticizer and Other Admixtures in Concrete, Supplementary paper, Ottawa, 1981, American Concrete Institute, Detroit, 1981.
[9] S. Pieh, Angew. Makromol. Chem., 154 (1987) 145.
[10] M. Piotte, Ph.D. Thesis, Université de Sherbrooke, Sherbrooke, Qué., Canada, 1993.
[11] A. Pierre, C. Carquille, J.M. Lamarche, A. Foissy and R. Mercier, Cem. Concr. Res., 18 (1988) 18.

[12] C. Jolicoeur, P.C. Nkinamubanzi, M.A. Simard and M. Piotte, in V.S. Ramachandran (Editor), Proc. of the 4th CANMET/ACI International Conference on Superplasticizer and Other Admixtures in Concrete, Montreal, 1994, American Concrete Institute, Detroit, 1994, ACI SP148, p. 63.
[13] P.F.G. Banfill, Cem. Concr. Res., 9 (1979) 795.
[14] K. Hattori and Y. Tanino, Kogyo Kagaku Zasshi, 66 (1963) 55. (English translation); CA 59 (1963) 7743 d.
[15] M.J. Garvey and Th.F. Tadros, Kolloid-Z. Z. Polym., 250 (1972) 967.
[16] D.M. Roy, G. Váradi, F.D. Tamás, G. Pályi and B. Bartha, Cem. Concr. Res., 14 (1984) 439.
[17] S. Fudano and K. Konishi, J. Chromatogr., 56 (1971) 51.
[18] S. Fudano, J. Am. Oil Chem. Soc., 51 (1974) 514.
[19] T.G. Miller, J. Chromatogr., 347 (1985) 249.
[20] A.W. Ladon and S. Sandler, Anal. Chem., 45 (1973) 921.
[21] P. Jandera, J. Chromatogr., 449 (1988) 361.
[22] T.C. Schunk, J. Chromatogr. A, 656 (1993) 591.

ELSEVIER

Journal of Chromatography A, 704 (1995) 387–436

JOURNAL OF CHROMATOGRAPHY A

# Pair-wise interactions by gas chromatography VI. Interaction free enthalpies of solutes with primary methoxyalkane, cyanoalkane and alkanethiol groups

K.S. Reddy[1], R. Cloux, E. sz. Kováts*

*Laboratoire de Chimie Technique, Ecole Polytechnique Fédérale de Lausanne, CH-1015 Lausanne, Switzerland*

First received 28 December 1994; revised manuscript received 9 February 1995; accepted 21 February 1995

**Abstract**

Three polar-type liquids, P, having methoxy, cyano or thiol substituents in primary positions on a branched paraffin skeleton were used as stationary phases. The molecules of these stationary liquids have the same form and nearly the same size as that of the non-polar parent branched paraffin, $C_{78}H_{158}$ (C78). Gas chromatographic retention data of some 150 molecular probes were measured on pure P-type liquids and on P/C78 mixtures with a volume fraction $\varphi_P$ of 0.50. Based on these data interaction free enthalpies could be calculated between a probe and the polar substituent, both at infinite dilution in the alkane solvent.

## 1. Introduction

The objective of our project is the determination of interaction free enthalpies between molecular probe solutes, $j$, at infinite dilution and an interacting group, X, also at infinite dilution in an alkane solvent. Objective, experimental technique, synthesis of the stationary phases as well as first results have been communicated in Parts I–V of this series [1–5]. The measuring system consists of a family of isosteric, isomorphous solvents, L, shown in Fig. 1. The family includes a standard paraffin, A ≡ C78 ($C_{78}H_{158}$), and a series of polar compounds, P, in which a methyl or an ethyl group is substituted for an interacting group, X. The synthesis of members of this family has been reported in Parts III [3] and IV [4]. The method consists of measuring gas chromatographic data of molecular probes on a series of A–P mixtures at several temperatures, $T$, to convert these data to standard chemical potentials and to extrapolate data to infinite dilution of the interacting group, X [4]. The symbol $\Delta$ will be used throughout the paper to designate additional interaction data, $\Delta Y = \Delta Y^P - \Delta Y^A$, where $Y$ is interaction free enthalpy or retention index. The symbol $\Delta'$ will designate data in the hypothetical ideal solvent with reference to data in A ≡ C78, $\Delta' Y = \Delta Y^{idP} - \Delta Y^A \equiv Y^{idP} - Y^A$.

In the present paper we report data on inter-

* Corresponding author.

[1] Present address: Department of Chemistry, S.V. University, Tirupati - 517 502, India.

0021-9673/95/$09.50 
*SSDI* 0021-9673(95)000243-X

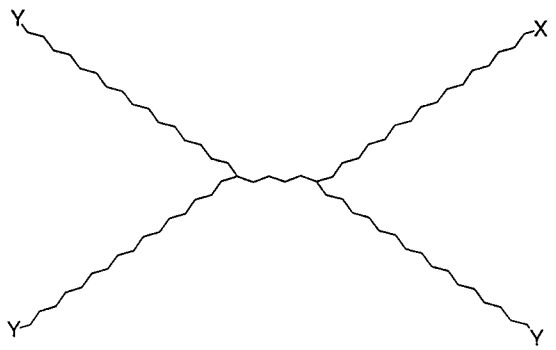


Fig. 1. The structure of the applied stationary phases: C78: $X = Y = CH_2CH_3$; TMO (for tetramethoxy): $X = Y = OCH_3$; PCN (for primary cyano): $X = CH_2CN$, $Y = CH_2CH_3$; PSH (for primary thiol): $X = CH_2SH$, $Y = CH_2CH_3$.

action free enthalpies between molecular probes and methoxy, cyano and thiol moieties as the interacting groups (X). For relationships, theory and symbols as well as for experimental details we refer to Refs. [1] and [4].

## 2. Experimental

### 2.1. Materials

For solutes see Ref. [1]. The synthesis of PCN is described in Ref. [3]. For the synthesis of TMO and PSH all the reagents were research-grade compounds from Fluka (Buchs, Switzerland). The stationary liquid TMO was prepared from dimethyl adipate and 16-bromo-1-methoxyhexadecane in an analogous procedure to that described previously [6] and the thiol phase PSH was synthesized from the bromide PBR (preparation see Ref. [3]) and thiourea as described in the following procedures.

*11-Bromo-1-methoxyundecane*

In a 250-ml 2-necked round-bottom flask equipped with a dropping funnel and a reflux condenser Mg (7.5 g, 0.31 mol) was covered with tetrahydrofuran (THF) (30 ml), activated with 1,2-dibromoethane (0.94 g, 5.0 mmol) and a solution of 1-bromobutane (27.4 g, 200 mmol) in THF (50 ml) was added dropwise.[1] At the end of the introduction THF (100 ml) was added and the reaction mixture was refluxed for 2.0 h. In a second 500-ml 2-necked round-bottom flask equipped with a reflux condenser and a dropping funnel 11-bromo-1-undecanol (50.2 g, 200 mmol) was dissolved in THF (100 ml) and dimethyl sulfate (50.4 g, 400 mmol) was added. The Grignard reagent from the first flask was now transferred into the dropping funnel and added within 20 min to the bromoalcohol. The mixture was refluxed for 28 h, cooled to room temperature and the excess dimethylsulfate was hydrolyzed with half-saturated aqueous $KHCO_3$ (200 ml). The organic layer was washed with brine (100 ml), the aqueous phase was extracted with diethyl ether ($2 \times 100$ ml) and the combined organic phase was dried ($Na_2SO_4$). The solvent was distilled in a rotary evaporator to give 57.1 g of crude 11-bromo-1-methoxyundecane which was dissolved in hexane (100 ml) and filtered on silica gel (100 g) with hexane–diethyl ether (9:1, 600 ml) as mobile phase to afford 51.1 g of colorless liquid. Distillation at 82.5–83.5°C/ $1.8 \times 10^{-2}$ mbar gave 46.3 g (87%) of pure 11-bromo-1-methoxyundecane. (GC: 98.9% pure, $I_{200} = 1695$). IR (film): $\nu/cm^{-1} = 2920$, 2850, 1465, 1385, 1120, 725, 645 and 570. $^1H$ NMR ($C^2HCl_3$, TMS): $\delta$/ppm = 1.28 (m, 14 protons ≡ H), 1.58 (m, 2H), 1.85 (quint., 2H, $J = 7.1$ Hz), 3.33 (s, 3H), 3.36 (t, 2H, $J = 6.5$) and 3.41 (t, 2H, $J = 6.9$). $^{13}C$ NMR ($C^2HCl_3$, TMS): $\delta$/ppm = 26.12, 28.16, 28.73, 29.38, 29.44, 29.50, 29.63, 32.85, 33.80, 58.44 and 72.94. MS (EI): $m/z = 266$ ($M^+ + 2$, 0.1% of 45), 264 ($M^+$, 0.1), 234 (4), 232 (4), 164 (9), 162 (9), 150 (11), 148 (11), 97 (20), 83 (35), 69 (38), 55 (38) and 45 (100).

*16-Bromo-1-methoxyhexadecane*

In a 500-ml 2-necked round-bottom flask Mg (4.86 g, 200 mmol) was covered with THF (150 ml) and activated with 1,2-dibromoethane (1.88 g, 10.0 mmol). A solution of 11-bromo-1-

[1] In this reaction the Grignard reagent of 1-bromobutane has been used as a base instead of KOH or the like. Hydroxyl bases would produce 1,11-undecanediol and oxacyclododecane as side products.

methoxyundecane (26.5 g, 100 mmol) in THF (100 ml) was added dropwise in 15 min and the mixture was refluxed for 1.5 h. In a second 1-l 2-necked round-bottom flask equipped with a dropping funnel and an Ar line 1,5-dibromopentane (69.0 g, 300 mmol) was dissolved in THF (250 ml). $Li_2CuCl_4$ (1 *M*) in THF (1.0 ml, 1.0 mmol; Kochi's reagent [7]) was added and the bright yellow solution was cooled to 0°C (ice bath). The Grignard reagent from the first flask was transferred into the dropping funnel and added slowly to the cold reaction mixture over a 1.0-h period. The mixture was stirred for 3.0 h at 0°C then it was allowed to warm to room temperature where it was stirred for another 2.0 h. Then it was hydrolyzed with saturated aqueous $NH_4Cl$ (200 ml). The organic phase was washed with a second portion of saturated aqueous $NH_4Cl$ (200 ml) then with brine (200 ml). The aqueous layer was extracted with diethyl ether (200 ml) and the combined organic phase was dried ($Na_2SO_4$). The solvent was removed in a rotary evaporator and the residue was chromatographed on silica gel (300 g). Hexane (2.0 l) eluted the excess 1,5-dibromopentane. The desired 16-bromo-1-methoxyhexadecane was eluted with a mixture of hexane–diethyl ether (90:10, 600 ml). Recrystallization from 94 wt% ethanol at 0°C gave 22.2 g (66%) of pure 16-bromo-1-methoxyhexadecane as colorless plates with a m.p. of 27.5–28.5°C. (GC: 99.4% pure, $I_{220} = 2204$). IR ($CCl_4$, $CS_2$): $\nu/cm^{-1}$ = 2930, 2850, 1465, 1385, 1120, 720, 645 and 570. $^1H$ NMR ($C^2HCl_3$, TMS): $\delta$/ppm = 1.27 (m, 24 protons ≡ H), 1.54 (m, 2H), 1.85 (quint., 2H, $J = 7.2$ Hz), 3.34 (s, 3H), 3.37 (t, 2H, $J = 6.6$) and 3.42 (t, 2H, $J = 6.9$). $^{13}C$ NMR ($C^2HCl_3$, TMS): $\delta$/ppm = 26.15, 28.19, 28.77, 29.42, 29.50, 29.52, 29.59, 29.63, 32.88, 33.83, 58.46 and 72.98. MS (EI): $m/z = 337$ ($M^+ + 3$, 0.1% of 45), 336 ($M^+ + 2$, 0.1), 335 ($M^+ + 1$, 0.1), 334 ($M^+$, 0.1), 304 (7), 302 (7), 150 (11), 148 (11), 97 (49), 83 (65), 69 (63), 55 (72), 45 (100).

*17,22-Bis-(16-methoxyhexadecyl)-1,38-dimethoxy-17,22-octatriacontanediol (TMO-diol)*

In a 250-ml 2-necked round-bottom flask equipped with a magnetic stirrer, a dropping funnel and a reflux condenser Mg (3.2 g, 132 mmol) was covered with THF (70 ml) and activated with 1,2-dibromoethane (0.94 g, 5.0 mmol). A solution of 16-bromo-1-methoxyhexadecane (22.13 g, 66.0 mmol) in THF (50 ml) was added dropwise within 30 min and the reaction mixture was refluxed for 2.0 h. At the same temperature a solution of dimethyladipate (2.61 g, 15.0 mmol) in THF (10 ml) was added dropwise and the reflux was maintained for 5.0 h. The reaction mixture was cooled to room temperature and hydrolyzed with half-saturated aqueous $NH_4Cl$ (100 ml). The organic phase was washed with brine (100 ml) and the aqueous phases were extracted with hexane (100 ml). The combined organic phase was dried ($Na_2SO_4$) and the solvent was distilled in a rotary evaporator to give 18.6 g of crude TMO-diol. The latter was dissolved in hexane (100 ml) and chromatographed on silica gel (100 g). Elution with benzene (1000 ml) afforded 4.54 g of a mixture of 1-methoxyhexadecane and 1,32-dimethoxydotriacontane. Elution with hexane–diethyl ether (1:1, 1000 ml) gave 13.56 g of TMO-diol. Recrystallization from abs. EtOH (400 ml) at 0°C gave 12.2 g (72%) of TMO-diol containing ca. 5% of a ketonic impurity that was removed in the next step; m.p. 63–63.5°C. IR ($CCl_4$, $CS_2$): $\nu/cm^{-1} = 2930$, 2850, 1465, 1385, 1195, 1120, 965 and 720. $^1H$ NMR ($C^2HCl_3$, TMS): $\delta$/ppm = 1.26 (m, 120 protons ≡ H), 1.57 (quint., 8H, $J = 6.4$ Hz), 3.34 (s, 12H) and 3.37 (t, 8H, $J = 6.5$). $^{13}C$ NMR ($C^2HCl_3$, TMS): $\delta$/ppm = 23.50, 24.12, 26.14, 29.49, 29.59, 29.65, 30.30, 39.33, 58.43, 72.97 and 74.33.

*17,22-Bis-(16-methoxyhexadecyl)-1,38-dimethoxyoctatriacontane (TMO)*

In a 250-ml round-bottom flask equipped with a Dean-Stark trap TMO-diol (11.52 g, 10.14 mmol), and *p*-toluenesulfonic acid monohydrate (0.39 g, 2.0 mmol) were dissolved in benzene (100 ml) and the water was removed by heating the solution to reflux for 9.0 h. The reaction mixture was then cooled to room temperature and successively washed with $H_2O$ (50 ml), half-saturated aqueous $KHCO_3$ (50 ml). The aqueous phases were extracted with hexane (100 ml), the combined organic phase was dried ($Na_2SO_4$) and

the solvent was removed in a rotary evaporator. The residue (11.37 g) was dissolved in a mixture of ethanol–cyclohexane (5:1, 120 ml), sodium borohydride (0.37 g, 10.0 mmol) was added and the reaction mixture was heated to 50°C for 30 min. The solvent was then removed in a rotary evaporator, the residue was extracted with cyclohexane (100 ml) and filtered on silica gel (30 g). Elution with benzene (300 ml) followed by cyclohexane–diethyl ether (95:5, 200 ml) afforded 6.84 g of TMO-diene. The latter was dissolved in cyclohexane (400 ml), 10% Pd-C (0.32 g) was added and the reaction mixture was hydrogenated at 40°C under 11 bar $H_2$ pressure for 18.0 h. The catalyst was removed by filtration on silica gel (30 g). Elution with a mixture of cyclohexane–diethyl ether (50:50, 200 ml) gave after evaporation of the solvent 6.50 g of TMO that was recrystallized from a mixture of ethanol–hexane (8:3, 110 ml) to give 6.21 g (55%) of pure TMO; mp 64.5–67.5°C. IR ($CCl_4$, $CS_2$): $\nu/cm^{-1} = 2930$, 2850, 1465, 1385, 1120 and 720. $^1H$ NMR ($C^2HCl_3$, TMS): $\delta/ppm = 1.26$ (m, 122 protons ≡ H), 1.58 (m, 8 H), 3.34 (s, 12 H) and 3.37 (t, 8H, $J = 6.5$ Hz). $^{13}C$ NMR ($C^2HCl_3$, TMS): $\delta/ppm = 26.16$, 26.77, 27.19, 29.51, 29.61, 29.71, 30.17, 33.80, 37.47, 58.46 and 72.99.

*18,23-Dioctadecyl-1-untetracontanylthiouronium bromide (PSTHIU)*

In a 250-ml round-bottom flask 1-bromo-18,23-dioctadecyluntetracontane (PBR, 6.60 g, 5.68 mmol) and thiourea (2.16 g, 28.4 mmol) were suspended in a mixture of cyclohexane–ethanol (1:2, 90 ml) and the reaction mixture was heated to reflux for 24 h (the mixture becomes homogeneous after ca. 4 h) and was allowed to cool to room temperature. The solvent was removed in a rotary evaporator and the solid residue was extracted with hot cyclohexane (50–60°C, 3 × 50 ml). The solvent was evaporated and the residue was recrystallized from ethanol–hexane (2:1, 90 ml) to give 6.86 g (98%) of a white solid, m.p. 143.5–144.5°C. $^1H$ NMR ($C^2HCl_3$, TMS): $\delta/ppm = 0.89$ (t, 9 protons ≡ H, $J = 6.4$ Hz), 1.25 (m, 142 H), 1.74 (quint., 2 H, $J = 7.2$), 3.32 (t, 2 H, $J = 7.2$). $^{13}C$ NMR ($C^2HCl_3$, TMS): $\delta/ppm = 14.05$, 22.67, 26.77, 26.83, 27.21, 28.24, 28.46, 29.05, 29.35, 29.41, 29.71, 30.17, 31.93, 32.31, 33.82, 37.50 and 172.57.

*18,23-Dioctadecyl-1-untetracontanethiol (PSH)*

In a 250-ml round-bottom flask equipped with a reflux condenser PSTHIU (6.78 g, 5.48 mmol) was dissolved in ethanol–cyclohexane (2:1, 75 ml) and a solution of KOH (0.72 g, 11 mmol) in $H_2O$ (4 ml) was added. The reaction mixture was heated to reflux for 1.0 h then stirred at room temperature overnight. The mixture was diluted with cyclohexane (100 ml), washed with $H_2O$ (3 × 50 ml) and the organic phase was dried ($Na_2SO_4$). The solvent was distilled in a rotary evaporator and the residue was chromato-

Table 1
Physical properties of the stationary phases

| L | | m.p. (°C) | $M$ (g mol$^{-1}$) | $\rho^\dagger$ (g cm$^{-3}$) | $v^\dagger$ (cm$^3$ mol$^{-1}$) | $\alpha^\dagger \cdot 10^4$ (K$^{-1}$) | B · 10$^7$ (K$^{-2}$) | $\sigma$ (g cm$^{-3}$) |
|---|---|---|---|---|---|---|---|---|
| Symbol | Formula | | | | | | | |
| C78 | $C_{78}H_{158}$ | 69–75 | 1096.1 | 0.7714 | 1420.9 | 7.62 | 1.26 | 0.0004 |
| TMO | $C_{70}H_{138}(OCH_3)_4$ | 65–68 | 1104.0 | 0.8039 | 1373.3 | 7.82 | 2.51 | 0.0004 |
| PCN | $C_{77}H_{155}CN$ | 66–68 | 1107.1 | 0.7826 | 1414.7 | 7.64 | 1.64 | 0.0003 |
| PSh | $C_{77}H_{155}SH$ | 70–74 | 1114.2 | 0.7870 | 1415.7 | 7.64 | 1.31 | 0.0002 |
| $\Delta_{95}$ | | | | ±0.00009 | ±0.17 | ±0.34 | ±0.93 | |

The symbol m.p. is for melting point and $M$ is for molar mass; the symbols $p^\dagger$, $\alpha^\dagger$ and B are regression coefficients of Eq. (1) for the calculation of the density in the temperature domain 80–210°C; $v^\dagger$ is for the molar volume at the standard temperature $T^\dagger = 403.15$K. Data for C78 are from Ref. [8], those for PCN are from Ref. [3].

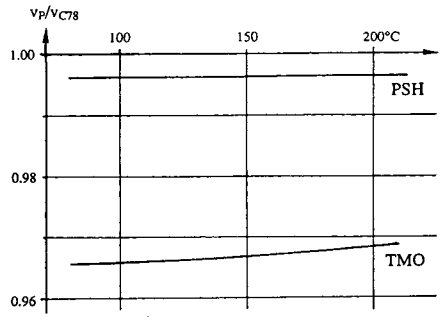


Fig. 2. Ratio of the molar volume of the P and C78 stationary phases as a function of temperature. P: TMO and PSH.

graphed on silica gel (100 g) with cyclohexane as mobile phase. Bis-(18,23-dioctadecyl-1-untetracontanyl)sulfide (1.2 g) was obtained as a first fraction followed by PSH (4.05 g). Recrystallization from ethanol–cyclohexane (2:1, 60 ml) at 0°C afforded 3.98 g (65%) of pure thiol as a white powder, m.p. 70.5–73.5°C. $^1$H NMR ($C^2HCl_3$, TMS): $\delta$/ppm = 0.89 (t, 9 protons ≡ H, $J$ = 6.4 Hz), 1.27 (m, 142 H), 1.82 (quint. 2 H, $J$ = 7.4) and 2.53 (q, 2H, $J$ = 7.3). $^{13}$C NMR ($C^2HCl_3$, TMS): $\delta$/ppm = 14.06, 22.68, 24.62, 26.79, 26.95, 27.22, 28.41, 29.10, 29.36, 29.55, 29.73, 30.19, 31.94, 33.84, 34.08 and 37.51.

Table 2
Characteristics of the chromatographic columns

| A/P | $100\varphi_P^\dagger$ (%) | $w_L$ (g) | $P_L$ (%) |
|---|---|---|---|
| C78/TMO | 50.0 (a) | 1.798 | 6.48 |
| | 50.0 (b) | 0.959 | 5.89 |
| | 100 (a) | 1.787 | 6.44 |
| | 100 (b) | 0.980 | 5.96 |
| C78/PCN | 50.0 | 1.750 | 6.26 |
| | 100 | 1.665 | 6.23 |
| C78/PSH | 50.0 | 1.761 | 5.28 |
| | 100 | 1.864 | 5.52 |

The symbol $\varphi_P^\dagger$ is for the volume fraction of the polar solvent in the A/P mixture at 130°C; $w_L$ is for the mass of the stationary liquid in the column and $P_L$ is for the weight percent of L of the packing ($100w_L$/total mass).

*Densities*

Densities were measured as described in part IV [4] in the temperature range of 80–200°C. Eq. (1) was fitted to the experimental points

$$\ln \rho_L = \ln M_L - \ln v_L = \ln \rho^\dagger - \alpha^\dagger \Delta T - B \Delta T^2 \quad (1)$$

where $\rho^\dagger$ is the density and $\alpha^\dagger$ is the isobaric coefficient of thermal expansion at $T^\dagger$ = 130.0 + 273.15 = 403.15 K. Coefficients of Eq. (1) for the stationary liquids are listed in Table 1. Fig. 2 shows that the ratio of the molar volumes of the stationary phases TMO and PSH is reasonably near unity. Characteristics of the columns used in this work are summarized in Table 2.

## 2.2. Apparatus

See part I [1] and IV [4].

## 2.3. Retention data

*Alkanes*

As in Refs. [1] and [4] absolute retention data of $n$-alkanes, $C_zH_{2z+2}$, with $5 \leq z \leq 10$ were determined in the temperature range 90–210°C. Specific retention volumes on the stationary phases C78/TMO and TMO were determined on two columns (a and b in Table 2). Data were converted to chemical potentials and those on

Table 3
Average ratio of specific retention volumes on columns of series (a) and (b): $f = V_g^{(b)}/V_g^{(a)}$, and the corresponding corrections to add to standard chemical potentials determined on columns of series (a)

| L | $f$ | $0.5RT \ln f$(cal mol$^{-1}$) | | | | | | |
|---|---|---|---|---|---|---|---|---|
| | | 90 | 110 | 130 | 150 | 170 | 190 | 210°C |
| C78/TMO | 0.989 | −4.0 | −4.2 | −4.4 | −4.7 | −4.9 | −5.1 | −5.3 |
| TMO | 1.004 | +1.4 | +1.5 | +1.6 | +1.7 | +1.8 | +1.8 | +1.9 |

TMO were corrected to the average of the two columns following the method given in Ref. [4]; corrections are given in Table 3. Variance analyses of the resulting data sets are shown in Tables 4, 5 and 6. Based on the variance analysis *n*-alkane data were fitted to the following equation:

$$\Delta\mu_z^{A/P} = \Delta\mu_0^{\dagger,A} + z\,\delta\mu_z^{\dagger,A} - \Delta T\,\Delta S_0^A - \Delta T z\,\delta S_z^A - \Delta T^2\frac{\Delta C_{P,0}^A}{2T^\dagger} - \Delta T^2 z\frac{\delta C_{P,z}^A}{2T^\dagger} + \varphi_P\,\Delta\mu_0^{\dagger,P} + \varphi_P z(\delta\mu_z^{\dagger,P} - \delta\mu_z^{\dagger,A}) - \Delta T\varphi_P\Delta S_0^P - \Delta T\varphi_P z(\delta S_z^P - \delta S_z^A)$$

Table 4
Analysis of variance of the set of 126 standard chemical potentials of the *n*-alkane solutes with $5 \leq z \leq 10$ in the temperature range 90–210°C at three compositions of the C78/TMO mixture

| Source | | *SQ* | $\Phi$ | *V'* | *F* | Sign. (%) | $b_X^{(i)}$ | Function |
|---|---|---|---|---|---|---|---|---|
| *X* | (*i*) | | | | | | | |
| $\Delta\bar{\mu}$ | (0) | | | | | | 42.5 | $\Delta\mu_0^{\dagger,A}$ |
| *T* | (1) | 2 195.8 | 1 | id | $6.55 \cdot 10^1$ | 0.1 | 2.09 | $\Delta S_0^A$ |
| | (2) | 260.2 | 1 | id | 7.77 | 5 | − 0.411 | $\Delta C_{P,0}^A$ |
| | (res. *T** | 261.0 | 4 | 65.3 | 1.95 | 20) | | |
| L | (1) | 116 935.5 | 1 | id | $3.49 \cdot 10^3$ | 0.01 | 37.310 | $\Delta\mu_0^{\dagger,P}$ |
| | (2) | 6 783.9 | 1 | id | $2.03 \cdot 10^2$ | 0.1 | −15.569 | $m_0^{\dagger,A/P}$ |
| *TL* | (1, 1) | 542.9 | 1 | id | $1.62 \cdot 10^1$ | 1 | 1.268 | $\Delta S_0^P$ |
| | (1, 2) | 671.5 | 1 | id | $2.00 \cdot 10^1$ | 0.1 | − 2.451 | $s_0^{A/P}$ |
| | (2, 1) | 121.3 | 1 | id | 3.62 | 10 | − 0.490 | $\Delta C_{P,0}^P$ |
| | (res. TL* | 174.5 | 9 | 19.4 | 0.58 | –) | | |
| 1st res. | (=Σ *X**) | 435.5 | 13 | 33.5 | | | | |
| *Z* | (1) | 2 892.1 | 1 | id | $2.75 \cdot 10^2$ | 0.01 | 2.8 | $\delta\mu_z^{\dagger,A}$ |
| | (2) | 537.8 | 1 | id | $5.12 \cdot 10^1$ | 0.1 | − 0.832 | |
| | (3) | 207.4 | 1 | id | $1.97 \cdot 10^1$ | 0.1 | 0.391 | |
| | (res. *Z*** | 35.6 | 2 | 17.8 | 1.69 | 20) | | |
| *TZ* | (1, 1) | 181.5 | 1 | id | $1.73 \cdot 10^1$ | 0.1 | 0.352 | $\delta S_z^A$ |
| | (2, 1) | 28.7 | 1 | id | 2.73 | 20 | − 0.083 | $\delta C_{P,z}^A$ |
| | (res. *TZ*** | 291.9 | 28 | 10.4 | 0.99 | –) | | |
| *LZ* | (1, 1) | 1 244.4 | 1 | id | $1.19 \cdot 10^2$ | 0.1 | 2.252 | $\delta\mu_z^{\dagger,P}$ |
| | (2, 1) | 223.7 | 1 | id | $2.13 \cdot 10^1$ | 0.1 | − 1.650 | $\delta m_z^{\dagger,A/P}$ |
| | (res. *LZ*** | 408.7 | 8 | 51.1 | 4.87 | 5) | | |
| *TLZ* | (1, 1, 1) | 49.9 | 1 | id | 4.75 | 5 | 0.232 | $\delta S_z^P$ |
| | (2, 1, 1) | 5.8 | 1 | id | 0.55 | – | − 0.041 | $\delta C_{P,z}^P$ |
| | (1, 2, 1) | 79.0 | 1 | id | 7.52 | 1 | − 0.489 | $\delta s_z^{A/P}$ |
| | (res. *TLZ*** | 258.8 | 57 | 4.5 | 0.43 | –) | | |
| 2nd res. | (=Σ *X***) | 995.0 | 95 | 10.5 | | | | |

* Sum of the residuals marked by one asterisk.
** Sum of the residuals marked by two asterisks.
$X^{(i)}$ is the systematic polynomial variation of $\Delta\mu^{A/P}$ on the effects *T* (temperature), *L* (composition of the liquid stationary phase, $100\,\varphi_P = 0.0$, 50.0 and 100.0%) and *Z* (carbon number of the solute). The subscripts in parentheses refer to the degree of the orthogonal polynomial: (1) linear; (2) quadratic; (3) cubic. *SQ* is the sum of squares, $\Phi$ is the number of degrees of freedom and $V' = V$ (res.) + $\nu_X V(X)$ is the combined variance to be analysed by Fisher's *F* ($\nu_X$ is the number of statistical units in one datum of the subset used for the evaluation of the effect) [9]. The values of the coefficients $b_X^{(i)}$ are also listed along with the corresponding thermodynamic coefficients. The meaning of the symbols of thermodynamic functions are described in the text. The abbreviations "res." is for residual variance, "sign." is for significance level and "id." means that $V' = SQ/\Phi$ is equal to the corresponding *SQ* ($\Phi = 1$).

Table 5
Analysis of variance of the set of 126 standard chemical potentials of the *n*-alkane solutes with $5 \leq z \leq 10$ in the temperature range 90–210°C at three compositions of the C78/PCN mixture

| Source | | *SQ* | $\Phi$ | *V'* | *F* | Sign. (%) | $b_X^{(i)}$ | Function |
|---|---|---|---|---|---|---|---|---|
| *X* | (*i*) | | | | | | | |
| $\Delta\bar{\mu}$ | (0) | | | | | | 66.8 | $\Delta\mu_0^{\dagger,A}$ |
| *T* | (1) | 3 051.3 | 1 | id | $1.01 \cdot 10^2$ | 0.1 | 2.46 | $\Delta S_0^A$ |
| | (2) | 131.9 | 1 | id | 4.35 | 10 | 0.295 | $\Delta C_{P,0}^A$ |
| | (res. *T** | 12.3 | 4 | 3.1 | 0.10 | –) | | |
| L | (1) | 306 167.7 | 1 | id | $1.01 \cdot 10^4$ | 0.01 | 60.373 | $\Delta\mu_0^{\dagger,P}$ |
| | (2) | 10 300.2 | 1 | id | $3.39 \cdot 10^2$ | 0.1 | −19.179 | $m_0^{\dagger,A/P}$ |
| *TL* | (1, 1) | 443.7 | 1 | id | $1.46 \cdot 10^1$ | 1 | 1.151 | $\Delta S_0^P$ |
| | (1, 2) | 1 733.6 | 1 | id | $5.72 \cdot 10^1$ | 0.1 | − 3.930 | $s_0^{A/P}$ |
| | (2, 1) | 63.1 | 1 | id | 2.08 | 20 | 0.252 | $\Delta C_{P,0}^P$ |
| | (res. TL* | 381.9 | 9 | 42.4 | 1.40 | –) | | |
| 1st res. | (=Σ *X**) | 394.2 | 13 | 30.3 | | | | |
| *Z* | (1) | 3 011.2 | 1 | id | $2.03 \cdot 10^2$ | 0.1 | 2.9 | $\delta\mu_z^{\dagger,A}$ |
| | (2) | 1 614.7 | 1 | id | $1.09 \cdot 10^2$ | 0.1 | − 1.435 | |
| | (3) | 581.7 | 1 | id | $3.93 \cdot 10^1$ | 0.1 | 0.654 | |
| | (res. *Z*** | 119.0 | 2 | 59.5 | 4.02 | 10) | | |
| *TZ* | (1, 1) | 227.6 | 1 | id | $1.54 \cdot 10^1$ | 0.1 | 0.391 | $\delta S_z^A$ |
| | (2, 1) | 163.6 | 1 | id | $1.11 \cdot 10^1$ | 1 | − 0.189 | $\delta C_{P,z}^A$ |
| | (res. *TZ*** | 44.4 | 28 | 1.6 | 0.11 | –) | | |
| *LZ* | (1, 1) | 1 570.8 | 1 | id | $1.06 \cdot 10^2$ | 0.1 | 2.531 | $\delta\mu_z^{\dagger,P}$ |
| | (2, 1) | 80.2 | 1 | id | 5.42 | 5 | − 0.990 | $\delta m_z^{\dagger,A/P}$ |
| | (res. *LZ*** | 1 158.7 | 8 | 144.8 | 9.78 | 1) | | |
| *TLZ* | (1, 1, 1) | 65.3 | 1 | id | 4.41 | 5 | 0.261 | $\delta S_z^P$ |
| | (2, 1, 1) | 30.4 | 1 | id | 2.05 | 20 | − 0.102 | $\delta C_{P,z}^P$ |
| | (1, 2, 1) | 53.8 | 1 | id | 3.64 | 10 | − 0.411 | $\delta s_z^{A/P}$ |
| | (res. *TLZ*** | 84.6 | 57 | 1.5 | 0.10 | –) | | |
| 2nd res. | (=Σ *X***) | 1 406.7 | 95 | 14.8 | | | | |

* Sum of the residuals marked by one asterisk.
** Sum of the residuals marked by two asterisks.
For explanation of symbols see Table 4.

$$- \Delta T^2 \varphi_P \frac{\Delta C_{P,0}^P}{2T^\dagger} - \Delta T^2 \varphi_P z \frac{\delta C_{P,z}^P - \delta C_{P,z}^A}{2T^\dagger} + \varphi_A \varphi_P m_0^{\dagger,A/P} + \varphi_A \varphi_P z\, \delta m_z^{\dagger,A/P} - \Delta T \varphi_A \varphi_P s_0^{A/P} - \Delta T \varphi_A \varphi_P z\, \delta s_z^{A/P} \quad (2)$$

Numerical values of the coefficients in Eq. (2) are listed in Table 7. The value of the derivative of Eq. (2) at zero concentration of the polar partner, P, gives the standard chemical potential of *n*-alkanes at ideal dilute solution of the functional group (see Ref. [1]) to give

$$\Delta' \mu_z^{idP} = \Delta' \mu_0^{\dagger,idP} + z\, \delta' \mu_z^{\dagger,idP} - \Delta T\, \Delta' S_0^{idP} - \Delta T z\, \delta' S_z^{idP} - \Delta T^2 \frac{\Delta' C_{P,0}^{idP}}{2T^\dagger} - \Delta T^2 z \frac{\delta' C_{P,z}^{idP}}{2T^\dagger} \quad (3)$$

Numerical values of the coefficients in Eq. (3) are listed in Table 7. The derivative of Eq. (2) with respect of the carbon number, *z*, gives the necessary equations for the "methylene increment" as follows

Table 6
Analysis of variance of the set of 126 standard chemical potentials of the *n*-alkane solutes with $5 \leq z \leq 10$ in the temperature range 90–210°C at three compositions of the C78/PSH mixture

| Source | | *SQ* | *Φ* | *V'* | *F* | Sign. (%) | $b_X^{(i)}$ | Function |
|---|---|---|---|---|---|---|---|---|
| *X* | (*i*) | | | | | | | |
| $\Delta\bar{\mu}$ | (0) | | | | | | 60.8 | $\Delta\mu_0^{\dagger,A}$ |
| *T* | (1) | 161.4 | 1 | id | 1.41 | – | 0.57 | $\Delta S_0^A$ |
| | (2) | 108.1 | 1 | id | 0.95 | – | 0.267 | $\Delta C_{P,0}^A$ |
| | (res. *T** | 636.5 | 4 | 159.1 | 1.39 | –) | | |
| L | (1) | 243 822.1 | 1 | id | $2.13 \cdot 10^3$ | 0.01 | 53.876 | $\Delta\mu_0^{\dagger,P}$ |
| | (2) | 12 088.9 | 1 | id | $1.06 \cdot 10^2$ | 0.1 | −20.779 | $m_0^{\dagger,A/P}$ |
| *TL* | (1, 1) | 183.6 | 1 | id | 1.61 | – | 0.739 | $\Delta S_0^P$ |
| | (1, 2) | 30.3 | 1 | id | 0.27 | – | 0.520 | $s_0^{A/P}$ |
| | (2, 1) | 114.6 | 1 | id | 1.00 | – | 0.337 | $\Delta C_{P,0}^P$ |
| | (res. TL* | 848.9 | 9 | 94.3 | 0.82 | –) | | |
| 1st res. | (=Σ *X**) | 1 485.4 | 13 | 114.3 | | | | |
| *Z* | (1) | 11 805.9 | 1 | id | $8.08 \cdot 10^2$ | 0.01 | 5.7 | $\delta\mu_z^{\dagger,A}$ |
| | (2) | 1 399.8 | 1 | id | $9.59 \cdot 10^1$ | 0.1 | − 1.336 | |
| | (3) | 485.3 | 1 | id | $3.32 \cdot 10^1$ | 0.1 | 0.597 | |
| | (res. *Z*** | 97.9 | 2 | 48.9 | 3.35 | 5) | | |
| *TZ* | (1, 1) | 224.5 | 1 | id | $1.54 \cdot 10^1$ | 0.1 | 0.391 | $\delta S_z^A$ |
| | (2, 1) | 0.0 | 1 | id | 0.00 | – | 0.000 | $\delta C_{P,z}^A$ |
| | (res. *TZ*** | 131.7 | 28 | 4.7 | 0.32 | –) | | |
| *LZ* | (1, 1) | 4 249.0 | 1 | id | $2.91 \cdot 10^2$ | 0.1 | 4.164 | $\delta\mu_z^{\dagger,P}$ |
| | (2, 1) | 1 661.3 | 1 | id | $1.14 \cdot 10^2$ | 0.1 | − 4.510 | $\delta m_z^{\dagger,A/P}$ |
| | (res. *LZ*** | 1 027.4 | 8 | 128.4 | 8.79 | 0.1) | | |
| *TLZ* | (1, 1, 1) | 75.9 | 1 | id | 5.19 | 1 | 0.278 | $\delta S_z^P$ |
| | (2, 1, 1) | 24.5 | 1 | id | 1.68 | 20 | 0.091 | $\delta C_{P,z}^P$ |
| | (1, 2, 1) | 37.1 | 1 | id | 2.54 | 10 | − 0.337 | $\delta s_z^{A/P}$ |
| | (res. *TLZ*** | 127.8 | 57 | 2.2 | 0.15 | –) | | |
| 2nd res. | (=Σ *X***) | 1 384.8 | 95 | 14.6 | | | | |

* Sum of the residuals marked by one asterisk.
** Sum of the residuals marked by two asterisks.
For explanation of symbols see Table 4.

$$\delta\mu_z^A = -510.5 + 1.2379\,\Delta T - 0.00244\,\Delta T^2 \quad (4a)$$

$$\delta\mu_z^{TMO} = -506.0 + 1.2745\,\Delta T - 0.00262\,\Delta T^2 \quad (4b)$$

$$\delta\mu_z^{PCN} = -507.4 + 1.2784\,\Delta T - 0.00263\,\Delta T^2 \quad (4c)$$

$$\delta\mu_z^{PSH} = -504.4 + 1.2288\,\Delta T - 0.00209\,\Delta T^2 \quad (4d)$$

"Methylene increments" for ideal polar solvents derived from Eq. (3) are as follows

$$\delta'\mu_z^{idMeO} = -506.8 + 1.2533\,\Delta T - 0.00249\,\Delta T^2 \quad (5a)$$

$$\delta'\mu_z^{idPCN} = -504.3 + 1.2998\,\Delta T - 0.00267\,\Delta T^2 \quad (5b)$$

$$\delta'\mu_z^{idPSH} = -481.0 + 1.2477\,\Delta T - 0.00195\,\Delta T^2 \quad (5c)$$

Let us note that the variance analyses refer to the approximate expression given in Eq. (2) which is the Taylor series of Eq. (6), where

Table 7
Coefficients for the description of the chemical potential of *n*-alkanes in real A/P mixtures, Eq. (2), and in ideal solution of the primary polar substituents, Eq. (3)

| Eq. (2) | | | | Eq. (3) | | | |
|---|---|---|---|---|---|---|---|
| P: | TMO | PCN | PSH | idP; | MeO | PCN | PSH |
| $\Delta\mu_0^{\dagger,A}$ | 3465.8 | 3465.8 | 3465.8 | $\Delta'\mu_0^{\dagger,idP}$ | 3481.1 | 3672.2 | 3511.5 |
| $\delta\mu_z^{\dagger,A}$ | −510.49 | −510.49 | −510.49 | $\delta'\mu_z^{\dagger,idP}$ | −506.78 | −504.30 | −481.03 |
| $\Delta S_0^A$ | −9.712 | −9.712 | −9.712 | $\Delta' S_0^{idP}$ | −9.865 | − 10.461 | −9.733 |
| $\delta S_z^A$ | −1.2379 | −1.2379 | −1.2379 | $\delta' S_z^{idP}$ | −1.2533 | −1.2998 | −1.2477 |
| $\Delta C_{P,0}^A$ | −3.47 | −3.47 | −3.47 | $\Delta' C_{P,0}^{idP}$ | −3.47 | −9.51 | −0.65 |
| $\delta C_{P,z}^A$ | 1.967 | 1.967 | 1.967 | $\delta' C_{P,z}^{idP}$ | 2.008 | 2.153 | 1.572 |
| $\Delta\mu_0^{\dagger,P}$ | 43.3 | 93.9 | 57.4 | | | | |
| $\delta\mu_z^{\dagger,P} - \delta\mu_z^{\dagger,A}$ | 4.09 | 3.08 | 6.12 | | | | |
| $\Delta S_0^P$ | 0.080 | 0.214 | −0.067 | | | | |
| $\delta S_z^P - \delta S_z^A$ | −0.0366 | −0.0405 | 0.0091 | | | | |
| $\Delta C_{P,0}^P$ | 0.40 | −3.95 | 2.02 | | | | |
| $\delta C_{P,z}^P - \delta C_{P,z}^A$ | 0.145 | 0.153 | −0.282 | | | | |
| $m_0^{\dagger,A/P}$ | 2.2 | 52.4 | − 25.9 | | | | |
| $\delta m_z^{\dagger,A/P}$ | 6.63 | 1.26 | 14.73 | | | | |
| $s_0^{A/P}$ | −0.489 | −0.627 | 0.073 | | | | |
| $\delta s_z^{A/P}$ | 0.0 | 0.0 | 0.0 | | | | |

Kirchhoff's approximation is used for the temperature dependence of $\Delta H$ and $\Delta S$.

$$\Delta\mu_j^{A/P} = \varphi_P\left[\Delta H_j^P - T\Delta S_j^P + \Delta C_{P,j}^P \times \left(T - T^\dagger - T\ln\frac{T}{T^\dagger}\right)\right] + \varphi_A\varphi_P(h_j - Ts_j) \quad (6)$$

In Tables 8, 9 and 10 results are listed. Data given under the heading "Thermodynamic data" refer to the coefficients in Eq. (6), which were obtained by non linear multiple regression.

*Other solutes*

For all *other solutes* retention indices were determined. Data in Tables 8, 9 and 10 describing the dependence of retention indices on composition and temperature are regression coefficients of Eq. (7)

$$\Delta I_j^P = I_j^P - I_j^A = \varphi_P(\Delta I_{130,j} + \Delta A_{T,j}\Delta T + \Delta A_{TT,j}\Delta T^2) + \varphi_A\varphi_P(A_{L,j} + A_{LT,j}\Delta T) \quad (7)$$

Retention indices were reconverted point by point to standard chemical potentials with the aid of *n*-alkane data (Eqs. 2 and 3) and Eq. (6) was fitted on the resulting data sets. Regression coefficients are listed under the heading "Thermodynamic data" in Tables 8, 9 and 10.

## 3. Results and discussion

The excess standard chemical potential of a solute in an A/P-mixture with respect to that in pure A ≡ C78 is described by Eq. (8)

$$\Delta\mu_j^{A/P} = \varphi_P\,\Delta\mu_j^P + \varphi_A\varphi_P m_j^{A/P} \quad (8)$$

i.e. this function is (slightly) curved, the extent of curvature being characterized by the constant $m_j^{A/P}$ For the experimental determination of this constant retention of solute *j* must be determined on at least three A/P-mixtures of different compositions (in our case $\varphi_P = 0$, 1/2 and 1). Knowledge of this constant is necessary to calculate the $\Delta'\mu$-value of a compound which is the difference of the std. chemical potential measured on a hypothetical stationary phase of a one molar ideal solution of the interacting group, X, in C78 and the same parameter on pure C78. Experimental evidence shows that the constant $m_j^{A/P}$ can be correlated with the standard chemi-

Table 8

Retention indices and thermodynamic data for 152 solutes in C78/TMO mixtures where data on an ideal solvent, a one molar solution of X = MeO, idMeO, are also given.

The symbol $n$ is for the number of data points used for regression where points for pure C78 were taken from Refs. [1,4,5]. Constants and functions, $Y$, preceded by $\Delta$ refer to those on C78, i.e. $\Delta Y(P) = Y(P) - Y(C78)$; $\Delta'$ values are for an "ideal solution" of group X. *Retention indices*: $I_{130}$ is for the retention index at the reference temperature $T^{\dagger} = 130 + 273.15$K; for the meaning of the coefficients, $A$, see Eq. (7). *Thermodynamic functions*: $H$ and $S$ are for partial molar enthalpy and entropy at $T^{\dagger}$, $C_p$ is for the mean partial molar heat capacity in the temperature range indicated; for the meaning of the coefficients $h$ and $s$ see Eq. (6). At the end of the table additive corrections are listed *to convert data A*: to those related to the partition coefficients $K_D$; $B$: to those where pressures are measured in units of bar (instead of atm). *Errors*. The symbol $\sigma$ is for the standard deviation around the regression and at the end of the table are listed standard deviations of constants and functions in units of the standard deviation around the regression, $f(\text{coeff}) = \sigma(\text{coeff})/\sigma$. Data marked by superscript, s, are significant at the 10% significance level if tested against $\sigma$. Data marked by one asterisk are at the 20% significance level, those marked by double asterisk are under this limit. Note that *linearity* of the following thermodynamic functions of *n-alkanes with carbon number* was imposed by the regression function: $\Delta H$, $\Delta S$, $\Delta C_p$, $h$, $s$, $\Delta' H$, $\Delta' S$ and $\Delta' C_p$.

| No. | Compound | Temp. range | n | Retention index : C78 / TMO | | | | | | | | | σ |
|---|---|---|---|---|---|---|---|---|---|---|---|---|---|
| | | | | TMO - C78 | | | Mixture | | id([OCH3]=1) - C78 | | | | |
| | | | | $\Delta I_{130}$ | $10 \times \Delta A_T$ ($K^{-1}$) | $100 \times \Delta A_{TT}$ ($K^{-2}$) | $A_L$ | $10 \times A_{LT}$ ($K^{-1}$) | $\Delta' I_{130}$ | $10 \times \Delta' A_T$ ($K^{-1}$ l mol$^{-1}$) | $100 \times \Delta' A_{TT}$ ($K^{-2}$ l mol$^{-1}$) | | |
| | | (°C) | | | | | | | | | | | |
| *HYDROCARBONS* | | | | | | | | | | | | | |
| *n-Alkanes* | | | | | | | | | | | | | |
| 00.05 | Pentane | 90-210 | 21 | | | | | | | | | | |
| 00.06 | Hexane | 90-210 | 21 | | | | | | | | | | |
| 00.07 | Heptane | 90-210 | 21 | | | | | | | | | | |
| 00.08 | Octane | 90-210 | 21 | | | | | | | | | | |
| 00.09 | Nonane | 90-210 | 21 | | | | | | | | | | |
| 00.10 | Decane | 90-210 | 21 | | | | | | | | | | |
| 00.11 | Undecane | 150-210 | 12 | | | | | | | | | | |
| 00.12 | Dodecane | 150-210 | 12 | | | | | | | | | | |
| 00.13 | Tridecane | 150-210 | 12 | | | | | | | | | | |
| 00.14 | Tetradecane | 150-210 | 12 | | | | | | | | | | |
| *Isoalkanes* | | | | | | | | | | | | | |
| 10.01 | 2,2-Dimethylbutane | 90-170 | 15 | + 1.0 | +0.16* | | + 1.0** | -0.08** | + 0.7 | +0.03 | | | 0.41 |
| 10.02 | 2,3-Dimethylbutane | 90-170 | 15 | + 1.2 | +0.20** | | + 0.1** | -0.04** | + 0.5 | +0.06 | | | 0.69 |
| 10.03 | 2,2-Dimethylpentane | 90-170 | 15 | + 0.7 | -0.02** | | + 0.9* | -0.22** | + 0.5 | -0.08 | | | 0.26 |
| 10.04 | 2,3-Dimethylpentane | 90-170 | 15 | + 0.9 | +0.09** | | - 0.2** | -0.26** | + 0.2 | -0.06 | | | 0.33 |
| 10.05 | 2,4-Dimethylpentane | 90-170 | 15 | + 0.2* | -0.16 | | + 0.4* | -0.18** | + 0.2 | -0.12 | | | 0.23 |
| 10.06 | 2,2-Dimethylhexane | 90-170 | 15 | + 0.4 | -0.02** | | + 0.4** | -0.28** | + 0.3 | -0.10 | | | 0.35 |
| 10.07 | 2,3-Dimethylhexane | 90-170 | 15 | + 0.9 | +0.10** | | - 0.4** | -0.09** | + 0.2 | +0.01 | | | 0.32 |
| 10.08 | 2,4-Dimethylhexane | 90-170 | 15 | - 0.1** | +0.03** | | - 0.3** | +0.16** | - 0.1 | +0.06 | | | 0.27 |
| 10.09 | 3,4-Dimethylhexane | 90-170 | 15 | + 1.0 | +0.05** | | - 0.4** | +0.23** | + 0.2 | +0.10 | | | 0.34 |
| 10.10 | 2,2,3-Trimethylbutane | 90-170 | 15 | + 1.3 | +0.48 | | + 0.1** | +0.84 | + 0.5 | +0.46 | | | 0.35 |

| No. | Thermodynamic data : C78 / TMO | | | | | | | | |
|---|---|---|---|---|---|---|---|---|---|
| | TMO- C78 | | | Mixture | | id([$OCH_3$]=1) - C78 | | | σ |
| | $\Delta H$ (cal $mol^{-1}$) | $\Delta S$ | $\Delta C_P$ ($cal\ mol^{-1}K^{-1}$) | $h$ (cal $mol^{-1}$) | $s$ ($cal\ mol^{-1}\ K^{-1}$) | $\Delta H$ ($cal\ l\ mol^{-2}$) | $\Delta S$ | $\Delta C_P$ ($cal\ l\ mol^{-2}K^{-1}$) | (cal $mol^{-1}$) |
| *HYDROCARBONS* | | | | | | | | | |
| *n-Alkanes* | | | | | | | | | |
| 00.05 | + 22 | -0.103 | + 1.1 | - 162 | -0.489 | - 59 | -0.230 | +0.2 | 6.6 |
| 00.06 | + 12 | -0.139 | + 1.2 | - 155 | -0.489 | - 61 | -0.245 | +0.3 | 5.6 |
| 00.07 | + 1 | -0.176 | + 1.4 | - 148 | -0.489 | - 64 | -0.261 | +0.3 | 4.2 |
| 00.08 | - 10 | -0.213 | + 1.5 | - 142 | -0.489 | - 66 | -0.276 | +0.3 | 2.6 |
| 00.09 | - 20 | -0.249 | + 1.7 | - 135 | -0.489 | - 69 | -0.291 | +0.4 | 3.4 |
| 00.10 | - 31 | -0.286 | + 1.8 | - 129 | -0.489 | - 71 | -0.307 | +0.4 | 4.5 |
| 00.11 | - 42 | -0.323 | + 1.9 | - 122 | -0.489 | - 74 | -0.322 | +0.5 | 5.9 |
| 00.12 | - 52 | -0.359 | + 2.1 | - 115 | -0.489 | - 76 | -0.338 | +0.5 | 5.5 |
| 00.13 | - 63 | -0.396 | + 2.2 | - 109 | -0.489 | - 79 | -0.353 | +0.5 | 6.6 |
| 00.14 | - 74 | -0.432 | + 2.4 | - 102 | -0.489 | - 81 | -0.368 | +0.6 | 6.9 |
| *Isoalkanes* | | | | | | | | | |
| 10.01 | + 44[s] | -0.043** | + 2.4* | - 190 | -0.552 | - 60 | -0.229 | +0.7 | 2.2 |
| 10.02 | + 49* | -0.035** | + 4.2* | - 170* | -0.521[s] | - 52 | -0.217 | +1.3 | 3.3 |
| 10.03 | - 4** | -0.172 | + 1.6* | - 214 | -0.627 | - 86 | -0.302 | +0.4 | 1.4 |
| 10.04 | + 12** | -0.137 | + 2.2* | - 204 | -0.625 | - 78 | -0.292 | +0.6 | 1.8 |
| 10.05 | - 29 | -0.238 | + 1.1** | - 200 | -0.599 | - 90 | -0.317 | +0.2 | 1.2 |
| 10.06 | - 11** | -0.202 | + 1.1** | - 212 | -0.645 | - 89 | -0.323 | +0.2 | 2.0 |
| 10.07 | + 4** | -0.166 | + 1.9** | - 159 | -0.532 | - 67 | -0.273 | +0.5 | 1.8 |
| 10.08 | + 4** | -0.174 | + 1.7* | - 111 | -0.407 | - 50 | -0.233 | +0.4 | 1.5 |
| 10.09 | - 9** | -0.199 | + 3.0 | - 91* | -0.366 | - 48 | -0.227 | +0.9 | 1.6 |
| 10.10 | + 93 | +0.071* | + 1.9* | + 22** | -0.059** | + 28 | -0.025 | +0.6 | 1.7 |

(Continued on pages 398 and 399)

Table 8 (*continued*)

| No. | Compound | Temp. range | n | Retention index : C78 / TMO | | | | | | | | | σ |
|---|---|---|---|---|---|---|---|---|---|---|---|---|---|
| | | | | TMO- C78 | | | Mixture | | id([OCH$_3$]=1) - C78 | | | | |
| | | (°C) | | $\Delta I_{130}$ | $10\times \Delta A_T$ ($K^{-1}$) | $100\times \Delta A_{TT}$ ($K^{-2}$) | $A_L$ | $10\times A_{LT}$ ($K^{-1}$) | $\Delta' I_{130}$ ($l\ mol^{-1}$) | $10\times \Delta' A_T$ ($K^{-1} l\ mol^{-1}$) | $100\times \Delta' A_{TT}$ ($K^{-2} l\ mol^{-1}$) | | |
| 10.11 | 2,2,4-Trimethylpentane | 90-170 | 15 | + 0.0** | +0.43 | | + 0.5** | +0.17** | + 0.2 | +0.21 | | | 0.41 |
| 10.12 | 2,3,4-Trimethylpentane | 90-170 | 15 | + 1.3 | +0.30 | | + 0.0** | +0.57 | + 0.5 | +0.30 | | | 0.25 |
| *1-Alkenes* | | | | | | | | | | | | | |
| 11.05 | 1-Pentene | 90-170 | 15 | + 6.3 | -0.10** | | - 2.2 | -0.75 | + 1.4 | -0.28 | | | 0.43 |
| 11.06 | 1-Hexene | 90-170 | 15 | + 7.4 | -0.14 | | + 0.4** | -0.91 | + 2.7 | -0.34 | | | 0.21 |
| 11.07 | 1-Heptene | 90-170 | 15 | + 8.2 | -0.01** | | + 1.5 | -0.53 | + 3.3 | -0.16 | | | 0.24 |
| 11.08 | 1-Octene | 90-170 | 15 | + 7.8 | -0.13 | | + 0.9 | -0.18 | + 3.0 | -0.08 | | | 0.14 |
| 11.09 | 1-Nonene | 90-170 | 15 | + 7.8 | -0.04** | | + 2.2 | -0.14** | + 3.5 | -0.03 | | | 0.16 |
| 11.10 | 1-Decene | 90-170 | 15 | + 7.7 | -0.02** | | + 1.6 | -0.15** | + 3.2 | -0.03 | | | 0.19 |
| *1-Alkynes* | | | | | | | | | | | | | |
| 12.05 | 1-Pentyne | 90-170 | 15 | + 30.5 | -0.12** | | + 8.5 | +0.39** | +13.5 | +0.21 | | | 0.38 |
| 12.06 | 1-Hexyne | 90-170 | 15 | + 31.2 | -0.20$^s$ | | + 9.7 | +0.18** | +14.1 | +0.11 | | | 0.40 |
| 12.07 | 1-Heptyne | 90-170 | 15 | + 32.1 | -0.03** | | +10.4 | +0.38* | +14.7 | +0.24 | | | 0.34 |
| 12.08 | 1-Octyne | 90-170 | 15 | + 31.8 | -0.11** | | + 9.3 | +0.24** | +14.2 | +0.16 | | | 0.43 |
| 12.09 | 1-Nonyne | 90-170 | 15 | + 31.9 | -0.20 | | + 9.1 | +0.20** | +14.2 | +0.12 | | | 0.32 |
| 12.10 | 1-Decyne | 90-170 | 15 | + 31.8 | -0.09** | | + 9.5 | +0.13** | +14.3 | +0.13 | | | 0.37 |
| *Alkynes* | | | | | | | | | | | | | |
| 13.01 | 2-Hexyne | 90-170 | 15 | + 23.0 | -0.16 | | + 5.7 | -0.63 | + 9.9 | -0.19 | | | 0.20 |
| 13.02 | 3-Hexyne | 90-170 | 15 | + 21.7 | -0.24 | | + 6.3 | -0.46* | + 9.7 | -0.16 | | | 0.36 |
| 13.03 | 4-Octyne | 90-170 | 15 | + 19.8 | -0.15* | | + 5.4 | -0.15** | + 8.7 | -0.03 | | | 0.36 |
| *Monocyclic hydrocarbons* | | | | | | | | | | | | | |
| 14.05 | Cyclopentane | 90-170 | 15 | + 3.0 | +0.06** | | - 0.3** | -0.36 | + 0.9 | -0.10 | | | 0.87 |
| 14.06 | Cyclohexane | 90-170 | 15 | + 2.7 | +0.36* | | - 0.6** | +0.45** | + 0.7 | +0.29 | | | 0.92 |
| 14.07 | Cycloheptane | 90-170 | 15 | + 3.0 | +0.58 | | + 0.0** | +0.35** | + 1.1 | +0.33 | | | 0.78 |
| 14.08 | Cyclooctane | 90-170 | 15 | + 4.0 | +0.61 | | - 0.5** | +1.17* | + 1.3 | +0.63 | | | 0.88 |
| 14.10 | Cyclodecane | 130-210 | 15 | + 6.7 | -0.06** | | + 3.6$^s$ | -0.51** | + 3.6 | -0.17 | | | 0.49 |
| *Bicyclic hydrocarbons* | | | | | | | | | | | | | |
| 15.01 | *cis*-Hydrindane | 130-210 | 15 | + 4.6 | +0.06** | | - 0.6** | +0.29** | + 1.4 | +0.13 | | | 0.92 |
| 15.02 | *trans*-Hydrindane | 130-210 | 15 | + 3.7 | +0.27** | | - 2.4** | +0.66** | + 0.5 | +0.33 | | | 0.91 |
| 15.03 | *cis*-Decalin | 130-210 | 15 | + 5.5 | +0.20** | | + 4.4** | -0.11** | + 3.4 | +0.06 | | | 0.91 |
| 15.04 | *trans*-Decalin | 130-210 | 15 | + 4.1 | -0.04** | | - 0.0** | -0.06** | + 1.4 | -0.02 | | | 0.58 |

| No. | Thermodynamic data : C78 / TMO | | | | | | | | |
|---|---|---|---|---|---|---|---|---|---|
| | TMO- C78 | | | Mixture | | id([$OCH_3$]=1) - C78 | | | σ |
| | $\Delta H$ (cal $mol^{-1}$) | $\Delta S$ | $\Delta C_P$ | $h$ (cal $mol^{-1}$) | $s$ (cal $mol^{-1}$ $K^{-1}$) | $\Delta H$ (cal l $mol^{-2}$) | $\Delta S$ | $\Delta C_P$ | (cal $mol^{-1}$) |
| | | (cal $mol^{-1}K^{-1}$) | | | | | (cal l $mol^{-2}K^{-1}$) | | |
| 10.11 | + 88 | +0.044** | - 1.0** | - 120* | -0.413 | - 24 | -0.159 | -0.4 | 2.2 |
| 10.12 | + 41 | -0.071 | + 2.5 | - 28** | -0.203 | - 9 | -0.126 | +0.8 | 1.0 |
| *1-Alkenes* | | | | | | | | | |
| 11.05 | - 59 | -0.223 | + 3.7s | - 308 | -0.880 | - 134 | -0.398 | +1.0 | 2.1 |
| 11.06 | - 93 | -0.294 | + 0.6** | - 370 | -1.012 | - 166 | -0.466 | -0.1 | 1.4 |
| 11.07 | - 82 | -0.277 | + 3.0 | - 277 | -0.785 | - 130 | -0.383 | +0.8 | 0.9 |
| 11.08 | - 114 | -0.373 | + 2.5s | - 186 | -0.585 | - 112 | -0.351 | +0.6 | 0.7 |
| 11.09 | - 106 | -0.366 | + 2.7 | - 186 | -0.583 | - 110 | -0.349 | +0.7 | 0.8 |
| 11.10 | - 112 | -0.388 | + 0.8** | - 179 | -0.592 | - 111 | -0.365 | +0.0 | 0.9 |
| *1-Alkynes* | | | | | | | | | |
| 12.05 | - 308 | -0.504 | + 3.1s | - 156s | -0.355s | - 146 | -0.262 | +0.9 | 2.1 |
| 12.06 | - 346 | -0.616 | + 4.0 | - 212 | -0.482 | - 179 | -0.345 | +1.2 | 1.8 |
| 12.07 | - 329 | -0.585 | + 3.4 | - 174 | -0.414 | - 161 | -0.315 | +1.0 | 1.7 |
| 12.08 | - 355 | -0.669 | + 3.7s | - 182 | -0.465 | - 175 | -0.367 | +1.0 | 2.1 |
| 12.09 | - 386 | -0.756 | + 2.5* | - 185 | -0.495 | - 189 | -0.411 | +0.6 | 1.9 |
| 12.10 | - 373 | -0.742 | + 3.9 | - 191 | -0.521 | - 187 | -0.418 | +1.1 | 2.0 |
| *Alkynes* | | | | | | | | | |
| 13.01 | - 261 | -0.522 | + 2.0 | - 338 | -0.873 | - 202 | -0.469 | +0.4 | 1.0 |
| 13.02 | - 264 | -0.539 | - 0.0** | - 309 | -0.790 | - 193 | -0.447 | -0.3 | 0.8 |
| 13.03 | - 245 | -0.544 | + 0.1** | - 221 | -0.618 | - 160 | -0.400 | -0.2 | 0.8 |
| *Monocyclic hydrocarbons* | | | | | | | | | |
| 14.05 | - 4** | -0.149s | + 5.9s | - 238s | -0.694 | - 93 | -0.314 | +1.8 | 3.4 |
| 14.06 | + 45** | -0.042** | + 4.7* | - 59** | -0.276** | - 17 | -0.138 | +1.5 | 3.8 |
| 14.07 | + 68* | +0.011** | + 2.2** | - 84** | -0.353** | - 18 | -0.149 | +0.7 | 3.9 |
| 14.08 | + 48* | -0.041** | + 4.4* | + 99** | +0.072** | + 37 | -0.024 | +1.5 | 3.8 |
| 14.10 | - 215 | -0.673 | + 3.9s | - 252 | -0.782 | - 173 | -0.531 | +1.0 | 2.0 |
| *Bicyclic hydrocarbons* | | | | | | | | | |
| 15.01 | - 190** | -0.620s | + 4.6** | - 78** | -0.379** | - 106 | -0.378 | +1.3 | 4.6 |
| 15.02 | - 28** | -0.232** | + 1.7** | - 3** | -0.207** | - 26 | -0.189 | +0.5 | 4.6 |
| 15.03 | - 222* | -0.699s | + 5.5* | - 191** | -0.616s | - 154 | -0.481 | +1.6 | 4.1 |
| 15.04 | - 252 | -0.787 | + 5.7 | - 146 | -0.553 | - 151 | -0.496 | +1.6 | 1.6 |

(*Continued on pages 400 and 401*)

Table 8 (*continued*)

| No. | Compound | Temp. range | n | Retention index : C78 / TMO | | | | | | | | | σ |
|---|---|---|---|---|---|---|---|---|---|---|---|---|---|
| | | | | TMO - C78 | | | Mixture | | id([OCH3]=1) - C78 | | | | |
| | | (°C) | | $\Delta I_{130}$ | $10 \times \Delta A_T$ ($K^{-1}$) | $100 \times \Delta A_{TT}$ ($K^{-2}$) | $A_L$ | $10 \times A_{LT}$ ($K^{-1}$) | $\Delta I'_{130}$ ($l\ mol^{-1}$) | $10 \times \Delta A'_T$ ($K^{-1} l\ mol^{-1}$) | $100 \times \Delta A'_{TT}$ ($K^{-2} l\ mol^{-1}$) | | |
| *Methylcyclohexanes (MCH)* | | | | | | | | | | | | | |
| 16.01 | Methylcyclohexane | 90-170 | 15 | + 2.3 | +0.14** | | - 1.8 | +0.34** | + 0.2 | +0.17 | | | 0.34 |
| 16.02 | *cis*-1,2-Di MCH | 90-170 | 15 | + 2.8 | +0.12** | | - 0.0** | +0.34** | + 0.8 | +0.17 | | | 0.55 |
| 16.03 | *trans*-1,2-Di MCH | 90-170 | 15 | + 2.2 | +0.18* | | - 0.5** | +0.20** | + 0.6 | +0.14 | | | 0.53 |
| 16.04 | *cis*-1,4-Di MCH | 90-170 | 15 | + 2.6 | +0.08** | | + 0.4** | +0.23** | + 1.0 | +0.12 | | | 0.27 |
| 16.05 | *trans*-1,4-Di MCH | 90-170 | 15 | + 2.4 | +0.24* | | + 0.1** | +0.15** | + 0.9 | +0.14 | | | 0.59 |
| *Cyclohexenes* | | | | | | | | | | | | | |
| 17.01 | Cyclohexene | 90-170 | 15 | + 9.6 | +0.14* | | + 1.6s | +0.40** | + 3.9 | +0.22 | | | 0.40 |
| 17.02 | 1,3-Cyclohexadiene | 90-170 | 15 | + 18.4 | +0.29s | | + 4.2 | +0.65* | + 7.8 | +0.39 | | | 0.60 |
| 17.03 | 1,4-Cyclohexadiene | 90-170 | 15 | + 18.8 | +0.28** | | + 4.6s | +0.19** | + 8.1 | +0.23 | | | 0.98 |
| *Alkylbenzenes* | | | | | | | | | | | | | |
| 18.00 | Benzene | 90-170 | 15 | + 28.9 | +0.46 | | + 8.2 | +0.79 | +12.9 | +0.54 | | | 0.39 |
| 18.01 | Toluene | 90-170 | 15 | + 27.9 | +0.41 | | + 7.2 | +0.80 | +12.2 | +0.52 | | | 0.38 |
| 18.02 | Ethylbenzene | 90-170 | 15 | + 27.5 | +0.30 | | + 7.6 | +0.80 | +12.2 | +0.48 | | | 0.48 |
| *Miscellaneous* | | | | | | | | | | | | | |
| 19.01 | Adamantane | 130-210 | 15 | + 5.7 | +0.59 | | + 0.4** | +0.47* | + 2.1 | +0.38 | | | 0.36 |
| 19.02 | Naphthalene | 130-210 | 15 | + 47.9 | +0.19** | | +18.3 | -0.51** | +22.9 | +0.08 | | | 0.75 |
| 19.03 | Azulene | 130-210 | 15 | + 56.4 | -0.77** | +0.23 | +18.3 | +1.42 | +25.8 | +0.45 | +0.08 | | 0.71 |
| *ALKANE DERIVATIVES* | | | | | | | | | | | | | |
| *1-Fluoroalkanes* | | | | | | | | | | | | | |
| 20.05 | 1-Fluoropentane | 90-170 | 15 | + 27.4 | -0.20* | | +10.1 | -0.46** | +12.9 | -0.12 | | | 0.52 |
| 20.06 | 1-Fluorohexane | 90-170 | 15 | + 27.7 | -0.16* | | +11.0 | -0.06** | +13.4 | +0.03 | | | 0.43 |
| 20.07 | 1-Fluoroheptane | 90-170 | 15 | + 27.8 | -0.21* | | +12.6 | +0.31** | +13.9 | +0.15 | | | 0.51 |
| 20.08 | 1-Fluorooctane | 90-170 | 15 | + 28.3 | -0.17 | | +12.0 | +0.23** | +13.9 | +0.14 | | | 0.30 |
| *1,1,1-Trifluoroalkanes* | | | | | | | | | | | | | |
| 21.08 | 1,1,1-Trifluorooctane | 90-170 | 15 | + 29.5 | -0.45 | | +12.1 | -0.19* | +14.4 | -0.10 | | | 0.15 |
| 21.10 | 1,1,1-Trifluorodecane | 90-170 | 15 | + 29.6 | -0.69 | | +11.9 | -0.48 | +14.3 | -0.29 | | | 0.20 |
| *1-Chloroalkanes* | | | | | | | | | | | | | |
| 22.04 | 1-Chlorobutane | 90-170 | 15 | + 30.1 | +0.04** | | +11.1 | -0.27** | +14.2 | +0.04 | | | 0.77 |

| No. | Thermodynamic data : C78 / TMO | | | | | | | | |
|---|---|---|---|---|---|---|---|---|---|
| | TMO- C78 | | | Mixture | | id([$OCH_3$]=1) - C78 | | | σ |
| | $\Delta H$ (cal $mol^{-1}$) | $\Delta S$ | $\Delta C_P$ | $h$ (cal $mol^{-1}$) | $s$ (cal $mol^{-1}$ $K^{-1}$) | $\Delta'H$ (cal l $mol^{-2}$) | $\Delta'S$ | $\Delta'C_P$ | (cal $mol^{-1}$) |
| | | (cal $mol^{-1}K^{-1}$) | | | | | (cal l $mol^{-2}K^{-1}$) | | |
| *Methylcyclohexanes (MCH)* | | | | | | | | | |
| 16.01 | - 4** | -0.168 | + 2.0* | - 69* | -0.326 | - 39 | -0.203 | +0.6 | 1.4 |
| 16.02 | - 26 | -0.227 | + 2.8 | - 78 | -0.343 | - 49 | -0.229 | +0.8 | 2.8 |
| 16.03 | - 3** | -0.177 | + 2.9* | - 101** | -0.401s | - 49 | -0.232 | +0.9 | 2.7 |
| 16.04 | - 30s | -0.235 | + 1.9* | - 103s | -0.395 | - 59 | -0.248 | +0.5 | 1.5 |
| 16.05 | + 10** | -0.143 | + 3.9s | - 119* | -0.435s | - 50 | -0.230 | +1.2 | 2.5 |
| *Cyclohexenes* | | | | | | | | | |
| 17.01 | - 74 | -0.245 | + 2.8s | - 94* | -0.335 | - 65 | -0.216 | +0.8 | 1.7 |
| 17.02 | - 138 | -0.291 | + 4.4s | - 60** | -0.216** | - 68 | -0.174 | +1.4 | 2.5 |
| 17.03 | - 135 | -0.289 | + 6.3s | - 152** | -0.443** | - 98 | -0.251 | +2.0 | 4.5 |
| *Alkylbenzenes* | | | | | | | | | |
| 18.00 | - 209 | -0.324 | + 2.3** | - 60** | -0.159** | - 84 | -0.145 | +0.7 | 2.2 |
| 18.01 | - 219 | -0.380 | + 1.7** | - 53** | -0.175** | - 88 | -0.177 | +0.5 | 2.2 |
| 18.02 | - 246 | -0.461 | + 1.4** | - 47** | -0.170** | - 96 | -0.206 | +0.3 | 2.7 |
| *Miscellaneous* | | | | | | | | | |
| 19.01 | + 34** | -0.071** | + 0.5** | - 70** | -0.359 | - 27 | -0.185 | +0.1 | 1.8 |
| 19.02 | - 604 | -1.134 | + 4.7* | - 391 | -0.949 | - 324 | -0.672 | +1.2 | 3.6 |
| 19.03 | - 793 | -1.516 | +11.3 | - 71** | -0.171** | - 275 | -0.526 | +3.5 | 3.2 |
| *ALKANE DERIVATIVES* | | | | | | | | | |
| *1-Fluoroalkanes* | | | | | | | | | |
| 20.05 | - 303 | -0.543 | + 4.3 | - 362 | -0.856 | - 217 | -0.452 | +1.2 | 2.1 |
| 20.06 | - 310 | -0.590 | + 4.4 | - 276 | -0.654 | - 191 | -0.403 | +1.3 | 1.5 |
| 20.07 | - 326 | -0.647 | + 4.5 | - 203 | -0.473 | - 173 | -0.362 | +1.3 | 2.1 |
| 20.08 | - 339 | -0.683 | + 3.1 | - 211 | -0.518 | - 181 | -0.394 | +0.8 | 1.5 |
| *1,1,1-Trifluroalkanes* | | | | | | | | | |
| 21.08 | - 388 | -0.769 | + 3.1 | - 399 | -0.709 | - 226 | -0.483 | +0.8 | 0.7 |
| 21.10 | - 461 | -0.974 | + 1.9 | - 344 | -0.860 | - 270 | -0.612 | +0.3 | 1.0 |
| *1-Chloroalkanes* | | | | | | | | | |
| 22.04 | - 292 | -0.518 | + 5.8s | - 322 | -0.765 | - 200 | -0.413 | +1.7 | 3.3 |

(Continued on pages 402 and 403)

Table 8 (*continued*)

| No. | Compound | Temp. range | n | Retention index : C78 / TMO | | | | | | | | | σ |
|---|---|---|---|---|---|---|---|---|---|---|---|---|---|
| | | | | TMO - C78 | | | Mixture | | id([OCH3]=1) - C78 | | | | |
| | | (°C) | | $\Delta I_{130}$ | 10 × $\Delta A_T$ ($K^{-1}$) | 100× $\Delta A_{TT}$ ($K^{-2}$) | $A_L$ | 10 × $A_{LT}$ ($K^{-1}$) | $\Delta I_{130}$ | 10 × $\Delta A_T$ ($K^{-1}l\ mol^{-1}$) | 100× $\Delta A_{TT}$ ($K^{-2}l\ mol^{-1}$) | | |
| 22.05 | 1-Chloropentane | 90-170 | 15 | + 29.8 | +0.36[s] | | +11.1 | +0.77** | +14.2 | +0.51 | | | 0.74 |
| 22.06 | 1-Chlorohexane | 90-170 | 15 | + 30.1 | +0.17** | | +11.2 | +0.79* | +14.3 | +0.45 | | | 0.71 |
| *1-Bromoalkanes* | | | | | | | | | | | | | |
| 23.03 | 1-Bromopropane | 90-170 | 15 | + 31.6 | +0.13* | | +11.8 | +0.35** | +15.0 | +0.29 | | | 0.34 |
| 23.04 | 1-Bromobutane | 90-170 | 15 | + 30.8 | +0.07** | | +11.0 | +0.38* | +14.5 | +0.28 | | | 0.31 |
| 23.05 | 1-Bromopentane | 90-170 | 15 | + 30.9 | +0.07** | | +10.7 | +0.62 | +14.4 | +0.36 | | | 0.26 |
| *1-Cyanoalkanes* | | | | | | | | | | | | | |
| 24.02 | Cyanoethane | 90-170 | 15 | + 85.2 | -0.67 | | +40.5 | -0.13** | +43.5 | +0.08 | | | 1.23 |
| 24.03 | 1-Cyanopropane | 90-170 | 15 | + 82.4 | -0.43 | | +40.5 | -0.19** | +42.5 | +0.14 | | | 0.66 |
| 24.04 | 1-Cyanobutane | 90-170 | 15 | + 81.8 | -0.25* | | +40.5 | +0.08** | +42.3 | +0.29 | | | 0.61 |
| 24.05 | 1-Cyanopentane | 90-170 | 15 | + 82.3 | -0.24* | | +41.5 | +0.36** | +42.8 | +0.40 | | | 0.65 |
| *1-Nitroalkanes* | | | | | | | | | | | | | |
| 25.02 | Nitroethane | 90-170 | 15 | + 92.4 | -0.79 | | +41.2 | -0.77 | +46.2 | -0.16 | | | 0.36 |
| 25.03 | 1-Nitropropane | 90-170 | 15 | + 86.8 | -0.64 | | +38.9 | -0.43** | +43.5 | -0.01 | | | 0.45 |
| 25.04 | 1-Nitrobutane | 90-170 | 15 | + 84.9 | -0.65 | | +37.7 | -0.15** | +42.4 | +0.07 | | | 0.39 |
| 25.05 | 1-Nitropentane | 90-170 | 15 | + 84.5 | -0.59 | | +38.6 | -0.21** | +42.6 | +0.08 | | | 0.43 |
| 1-Acetoxyalkanes | | | | | | | | | | | | | |
| 26.03 | 1-Acetoxypropane | 90-170 | 15 | + 45.9 | -0.17[s] | | +19.5 | -0.14** | +22.6 | +0.08 | | | 0.39 |
| 26.04 | 1-Acetoxybutane | 90-170 | 15 | + 46.0 | -0.11** | | +19.3 | +0.00** | +22.6 | +0.15 | | | 0.47 |
| 26.05 | 1-Acetoxypentane | 90-170 | 15 | + 46.3 | -0.17* | | +19.6 | -0.09** | +22.8 | +0.10 | | | 0.44 |
| *1-Alkanols* | | | | | | | | | | | | | |
| 27.04 | 1-Butanol | 90-170 | 15 | + 97.8 | -3.58 | +0.15 | +48.6 | -3.58 | +50.6 | -2.05 | +0.03 | | 0.51 |
| 27.05 | 1-Pentanol | 90-170 | 15 | + 99.6 | -3.49 | +0.19 | +49.4 | -3.25 | +51.5 | -1.89 | +0.05 | | 0.36 |
| 27.06 | 1-Hexanol | 90-170 | 15 | +101.3 | -3.68 | +0.15 | +50.6 | -3.37 | +52.5 | -1.99 | +0.04 | | 0.42 |
| 27.07 | 1-Heptanol | 90-170 | 15 | +102.3 | -3.47 | +0.13 | +51.3 | -3.47 | +53.1 | -1.96 | +0.03 | | 0.45 |
| *2-Alkanols* | | | | | | | | | | | | | |
| 28.04 | 2-Butanol | 90-170 | 15 | + 81.9 | -3.01 | +0.15 | +37.6 | -2.58 | +41.3 | -1.59 | +0.04 | | 0.37 |
| 28.05 | 2-Pentanol | 90-170 | 15 | + 83.0 | -2.80 | +0.14 | +38.9 | -2.26 | +42.1 | -1.39 | +0.04 | | 0.35 |
| 28.06 | 2-Hexanol | 90-170 | 15 | + 84.3 | -2.96 | +0.14 | +39.8 | -2.14 | +42.9 | -1.40 | +0.04 | | 0.32 |
| 28.07 | 2-Heptanol | 90-170 | 15 | + 85.3 | -2.99 | +0.14 | +41.2 | -2.47 | +43.7 | -1.52 | +0.04 | | 0.41 |

| No. | Thermodynamic data : C78 / TMO | | | | | | | | |
|---|---|---|---|---|---|---|---|---|---|
| | TMO - C78 | | | Mixture | | id([$OCH_3$]=1) - C78 | | | σ |
| | $\Delta H$ (cal $mol^{-1}$) | $\Delta S$ | $\Delta C_P$ | $h$ (cal $mol^{-1}$) | $s$ (cal $mol^{-1}$ $K^{-1}$) | $\Delta' H$ (cal l $mol^{-2}$) | $\Delta' S$ | $\Delta' C_P$ | (cal $mol^{-1}$) |
| | | (cal $mol^{-1}K^{-1}$) | | | | | (cal l $mol^{-2}K^{-1}$) | | |
| 22.05 | - 231 | -0.385 | + 5.1[s] | - 97[**] | -0.227[**] | - 103 | -0.186 | +1.6 | 2.9 |
| 22.06 | - 289 | -0.539 | + 4.8[s] | - 91[**] | -0.232[**] | - 122 | -0.244 | +1.5 | 3.1 |
| *1-Bromoalkanes* | | | | | | | | | |
| 23.03 | - 291 | -0.488 | + 3.9 | - 203 | -0.459 | - 157 | -0.294 | +1.2 | 1.3 |
| 23.04 | - 302 | -0.544 | + 3.5 | - 180 | -0.433 | - 156 | -0.311 | +1.0 | 1.1 |
| 23.05 | - 319 | -0.598 | + 3.1 | - 123 | -0.315 | - 143 | -0.293 | +0.9 | 1.3 |
| *1-Cyanoalkanes* | | | | | | | | | |
| 24.02 | - 980 | -1.432 | +10.7 | - 588 | -0.986 | - 473 | -0.667 | +3.2 | 4.8 |
| 24.03 | - 932 | -1.413 | + 6.9 | - 631 | -1.118 | - 477 | -0.721 | +1.9 | 2.8 |
| 24.04 | - 883 | -1.334 | + 5.6 | - 544 | -0.949 | - 435 | -0.646 | +1.5 | 2.9 |
| 24.05 | - 904 | -1.406 | + 6.3 | - 489 | -0.825 | - 424 | -0.632 | +1.8 | 3.0 |
| *1-Nitroalkanes* | | | | | | | | | |
| 25.02 | -1 114 | -1.705 | + 3.4[s] | - 760 | -1.389 | - 575 | -0.894 | +0.6 | 2.1 |
| 25.03 | -1 019 | -1.589 | + 3.4[*] | - 653 | -1.217 | - 516 | -0.818 | +0.6 | 2.7 |
| 25.04 | -1 011 | -1.622 | + 3.4[s] | - 555 | -1.020 | - 484 | -0.772 | +0.7 | 2.3 |
| 25.05 | -1 008 | -1.637 | + 2.3[**] | - 581 | -1.099 | - 493 | -0.809 | +0.3 | 2.5 |
| *1-Acetoxyalkanes* | | | | | | | | | |
| 26.03 | - 496 | -0.812 | + 3.6[s] | - 373 | -0.782 | - 274 | -0.486 | +0.9 | 2.3 |
| 26.04 | - 490 | -0.814 | + 2.5[**] | - 332 | -0.704 | - 259 | -0.464 | +0.6 | 2.8 |
| 26.05 | - 523 | -0.906 | + 1.6[**] | - 349 | -0.763 | - 278 | -0.519 | +0.2 | 2.5 |
| *1-Alkanols* | | | | | | | | | |
| 27.04 | -1 759 | -3.263 | +13.9 | -1 436 | -3.014 | -1 024 | -1.974 | +3.5 | 3.3 |
| 27.05 | -1 737 | -3.222 | +14.3 | -1 331 | -2.781 | - 982 | -1.884 | +3.7 | 2.4 |
| 27.06 | -1 806 | -3.400 | +13.8 | -1 360 | -2.864 | -1 017 | -1.976 | +3.5 | 2.8 |
| 27.07 | -1 775 | -3.327 | +12.4 | -1 364 | -2.886 | -1 008 | -1.960 | +3.0 | 2.7 |
| *2-Alkanols* | | | | | | | | | |
| 28.04 | -1 461 | -2.684 | +12.4 | -1 151 | -2.378 | - 834 | -1.582 | +3.2 | 2.1 |
| 28.05 | -1 427 | -2.647 | +11.9 | -1 047 | -2.185 | - 791 | -1.515 | +3.1 | 2.3 |
| 28.06 | -1 475 | -2.776 | +11.9 | - 987 | -2.053 | - 789 | -1.517 | +3.1 | 1.8 |
| 28.07 | -1 502 | -2.852 | +12.3 | -1 074 | -2.277 | - 828 | -1.622 | +3.2 | 2.5 |

(Continued on pages 404 and 405)

Table 8 (*continued*)

| No. | Compound | Temp. range (°C) | n | Retention index : C78 / TMO | | | | | | | | | σ |
|---|---|---|---|---|---|---|---|---|---|---|---|---|---|
| | | | | TMO- C78 | | | Mixture | | id([$OCH_3$]=1) - C78 | | | | |
| | | | | $\Delta I_{130}$ | $10\times \Delta A_T$ ($K^{-1}$) | $100\times \Delta A_{TT}$ ($K^{-2}$) | $A_L$ | $10\times A_{LT}$ ($K^{-1}$) | $\Delta I'_{130}$ ($l\ mol^{-1}$) | $10\times \Delta A'_T$ ($K^{-1} l\ mol^{-1}$) | $100\times \Delta A'_{TT}$ ($K^{-2} l\ mol^{-1}$) | | |
| *2-Methyl-2-alkanols* | | | | | | | | | | | | | |
| 29.04 | 2-Methyl-2-propanol | 90-170 | 15 | + 74.2 | -2.91 | +0.17 | +33.6 | -3.01 | +37.3 | -1.73 | +0.04 | | 0.51 |
| 29.05 | 2-Methyl-2-butanol | 90-170 | 15 | + 72.3 | -2.75 | +0.13 | +34.6 | -2.44 | +36.9 | -1.48 | +0.03 | | 0.47 |
| 29.06 | 2-Methyl-2-pentanol | 90-170 | 15 | + 72.1 | -2.68 | +0.15 | +34.7 | -2.07 | +36.9 | -1.33 | +0.04 | | 0.42 |
| 29.07 | 2-Methyl-2-hexanol | 90-170 | 15 | + 72.7 | -2.78 | +0.14 | +34.5 | -2.17 | +37.1 | -1.40 | +0.04 | | 0.42 |
| *1-Alkanethiols* | | | | | | | | | | | | | |
| 30.04 | 1-Butanethiol | 90-170 | 15 | + 30.1 | -0.83 | | +10.1 | -1.23 | +13.9 | -0.59 | | | 0.32 |
| 30.05 | 1-Pentanethiol | 90-170 | 15 | + 30.2 | -0.80 | | +10.1 | -1.18 | +13.9 | -0.57 | | | 0.32 |
| 30.06 | 1-Hexanethiol | 90-170 | 15 | + 30.5 | -0.70 | | +10.2 | -1.25 | +14.0 | -0.56 | | | 0.41 |
| *2-Alkanones* | | | | | | | | | | | | | |
| 31.04 | 2-Butanone | 90-170 | 15 | + 52.6 | -0.59 | | +22.0 | -1.32 | +25.8 | -0.45 | | | 0.26 |
| 31.05 | 2-Pentanone | 90-170 | 15 | + 52.1 | -0.38 | | +24.4 | -0.78 | +26.8 | -0.18 | | | 0.20 |
| 31.06 | 2-Hexanone | 90-170 | 15 | + 52.8 | -0.34 | | +25.2 | -0.36[s] | +26.9 | -0.02 | | | 0.22 |
| 31.07 | 2-Heptanone | 90-170 | 15 | + 53.3 | -0.36 | | +25.9 | -0.33* | +27.4 | -0.01 | | | 0.23 |
| *Aldehydes* | | | | | | | | | | | | | |
| 32.05 | Pentanal | 90-170 | 15 | + 49.2 | -0.88 | | +22.7 | -1.61 | +24.8 | -0.66 | | | 0.31 |
| 32.06 | Hexanal | 90-170 | 15 | + 50.3 | -0.78 | | +22.6 | -0.55** | +25.2 | -0.25 | | | 0.53 |
| 32.07 | Heptanal | 90-170 | 15 | + 50.8 | -0.51 | | +23.0 | -0.53 | +25.5 | -0.15 | | | 0.29 |
| *Ethers* | | | | | | | | | | | | | |
| 33.06 | Dipropylether | 90-170 | 15 | + 15.1 | -0.23 | | + 6.6 | -0.64 | + 7.5 | -0.24 | | | 0.24 |
| 33.08 | Dibutylether | 90-170 | 15 | + 14.8 | -0.15 | | + 6.6 | -0.36 | + 7.4 | -0.12 | | | 0.21 |
| *Halomethanes* | | | | | | | | | | | | | |
| 37.01 | Dichloromethane | 90-170 | 15 | + 59.3 | -0.78 | | +21.5 | +0.21** | +27.9 | +0.03 | | | 0.39 |
| 37.02 | Trichloromethane | 90-170 | 15 | + 65.2 | -1.52 | | +23.5 | -0.69* | +30.6 | -0.51 | | | 0.50 |
| 37.03 | Tetrachloromethane | 90-170 | 15 | + 19.7 | -0.34 | | + 2.6 | +0.21[s] | + 7.7 | +0.02 | | | 0.13 |
| 37.04 | $CF_2Br_2$ | 90-170 | 15 | + 24.8 | -0.59 | | + 3.8 | -1.04 | + 9.9 | -0.48 | | | 0.49 |
| *HALOBENZENES* | | | | | | | | | | | | | |
| 38.01 | Fluorobenzene | 90-170 | 15 | + 39.9 | -0.04** | | +12.2 | +0.10** | +18.0 | +0.17 | | | 0.33 |
| 38.02 | Hexafluorobenzene | 90-170 | 15 | + 36.9 | -0.66 | | +15.2 | -0.58[s] | +17.9 | -0.28 | | | 0.41 |
| 38.03 | Trifluoromethylbenzene | 90-170 | 15 | + 46.9 | -0.24 | | +16.4 | +0.16** | +21.9 | +0.15 | | | 0.33 |

| No. | Thermodynamic data : C78 / TMO | | | | | | | | |
|---|---|---|---|---|---|---|---|---|---|
| | TMO- C78 | | | Mixture | | id([$OCH_3$]=1) - C78 | | | σ |
| | $\Delta H$ (cal $mol^{-1}$) | $\Delta S$ | $\Delta C_P$ | $h$ (cal $mol^{-1}$) | $s$ (cal $mol^{-1}$ $K^{-1}$) | $\Delta' H$ (cal l $mol^{-2}$) | $\Delta' S$ | $\Delta' C_P$ | (cal $mol^{-1}$) |
| | | (cal $mol^{-1}K^{-1}$) | | | | | (cal l $mol^{-2}K^{-1}$) | | |
| *2-Methyl-2-alkanols* | | | | | | | | | |
| 29.04 | -1 383 | -2.562 | +12.6 | -1 175 | -2.526 | - 822 | -1.608 | +3.3 | 3.0 |
| 29.05 | -1 326 | -2.523 | +11.8 | -1 049 | -2.244 | - 765 | -1.512 | +3.1 | 2.8 |
| 29.06 | -1 294 | -2.468 | +11.6 | - 937 | -1.991 | - 718 | -1.412 | +3.1 | 2.4 |
| 29.07 | -1 330 | -2.573 | +11.9 | - 941 | -2.023 | - 733 | -1.463 | +3.2 | 2.4 |
| *1-Alkanethiols* | | | | | | | | | |
| 30.04 | - 480 | -0.991 | + 3.6 | - 506 | -1.248 | - 330 | -0.746 | +0.8 | 1.7 |
| 30.05 | - 489 | -1.028 | + 4.3 | - 489 | -1.224 | - 328 | -0.754 | +1.0 | 1.6 |
| 30.06 | - 478 | -1.011 | + 4.7 | - 496 | -1.255 | - 328 | -0.761 | +1.1 | 1.8 |
| *2-Alkanones* | | | | | | | | | |
| 31.04 | - 646 | -1.039 | + 2.0* | - 676 | -1.463 | - 420 | -0.775 | +0.2 | 1.7 |
| 31.05 | - 606 | -1.001 | + 2.3 | - 566 | -1.193 | - 371 | -0.676 | +0.4 | 1.2 |
| 31.06 | - 609 | -1.018 | + 1.4* | - 472 | -0.973 | - 341 | -0.609 | +0.1 | 1.2 |
| 31.07 | - 634 | -1.093 | + 1.7* | - 471 | -0.982 | - 350 | -0.641 | +0.2 | 1.2 |
| *Aldehydes* | | | | | | | | | |
| 32.05 | - 675 | -1.163 | + 3.9 | - 745 | -1.625 | - 455 | -0.877 | +0.8 | 1.7 |
| 32.06 | - 670 | -1.195 | + 7.2 | - 495 | -1.045 | - 371 | -0.697 | +2.0 | 1.5 |
| 32.07 | - 624 | -1.089 | + 3.8 | - 484 | -1.033 | - 353 | -0.660 | +0.9 | 1.4 |
| *Ethers* | | | | | | | | | |
| 33.06 | - 196 | -0.469 | + 3.4 | - 351 | -0.898 | - 188 | -0.469 | +0.9 | 0.9 |
| 33.08 | - 198 | -0.499 | + 1.3* | - 276 | -0.747 | - 166 | -0.436 | +0.2 | 0.9 |
| *Halomethanes* | | | | | | | | | |
| 37.01 | - 753 | -1.209 | + 2.0** | - 329 | -0.608 | - 334 | -0.530 | +0.3 | 2.4 |
| 37.02 | - 979 | -1.762 | + 7.1 | - 547 | -1.154 | - 485 | -0.905 | +1.9 | 2.0 |
| 37.03 | - 280 | -0.616 | + 1.6 | - 134 | -0.416 | - 142 | -0.355 | +0.3 | 0.7 |
| 37.04 | - 358 | -0.707 | + 4.2** | - 429 | -1.094 | - 263 | -0.601 | +1.1 | 2.7 |
| *HALOBENZENES* | | | | | | | | | |
| 38.01 | - 422 | -0.709 | + 3.8 | - 245 | -0.561 | - 212 | -0.394 | +1.1 | 1.2 |
| 38.02 | - 499 | -0.895 | + 4.2 | - 431 | -0.953 | - 299 | -0.584 | +1.1 | 2.1 |
| 38.03 | - 523 | -0.872 | + 4.7 | - 278 | -0.589 | - 252 | -0.443 | +1.3 | 1.4 |

(Continued on pages 406 and 407)

Table 8 (*continued*)

| No. | Compound | Temp. range (°C) | n | Retention index : C78 / TMO | | | | | | | | σ |
|---|---|---|---|---|---|---|---|---|---|---|---|---|
| | | | | TMO- C78 | | | Mixture | | id([OCH3]=1) - C78 | | | |
| | | | | $\Delta I_{130}$ | 10 × $\Delta A_T$ ($K^{-1}$) | 100× $\Delta A_{TT}$ ($K^{-2}$) | $A_L$ | 10 × $A_{LT}$ ($K^{-1}$) | $\Delta I_{130}$ ($l\ mol^{-1}$) | 10 × $\Delta A_T$ ($K^{-1}l\ mol^{-1}$) | 100× $\Delta A_{TT}$ ($K^{-2}l\ mol^{-1}$) | |
| 38.04 | Chlorobenzene | 90-170 | 15 | + 40.6 | +0.01** | | +11.7 | +0.23** | +18.1 | +0.23 | | 0.59 |
| 38.05 | Bromobenzene | 90-170 | 15 | + 42.9 | -0.03** | | +12.9 | +0.30** | +19.3 | +0.25 | | 0.43 |
| 38.06 | Iodobenzene | 130-210 | 15 | + 46.3 | +0.26s | | +13.0 | +0.54** | +20.5 | +0.45 | | 0.57 |
| *ALKYLPYRIDINES* | | | | | | | | | | | | |
| 39.01 | Pyridine | 90-170 | 15 | + 56.6 | -0.24 | | +28.5 | +0.15** | +29.4 | +0.21 | | 0.31 |
| 39.02 | 2-Picoline | 90-170 | 15 | + 48.3 | +0.09** | | +25.1 | +0.20** | +25.4 | +0.31 | | 0.30 |
| 39.03 | 3-Picoline | 90-170 | 15 | + 56.4 | +0.17* | | +33.9 | -0.23** | +31.2 | +0.24 | | 0.51 |
| 39.04 | 4-Picoline | 90-170 | 15 | + 57.0 | -0.03** | | +34.4 | -0.15** | +31.6 | +0.20 | | 0.29 |
| 39.05 | 2,3-Lutidine | 130-210 | 15 | + 48.9 | +0.42 | | +32.1 | -1.02 | +28.0 | +0.02 | | 0.32 |
| 39.06 | 2,4-Lutidine | 130-210 | 15 | + 48.1 | +0.49 | | +32.0 | -0.48 | +27.7 | +0.23 | | 0.27 |
| 39.07 | 2,5-Lutidine | 130-210 | 15 | + 46.2 | +0.53 | | +28.6 | +0.07** | +25.9 | +0.42 | | 0.52 |
| 39.08 | 2,6-Lutidine | 130-210 | 15 | + 42.3 | -0.19** | | +24.1 | -1.17** | +22.9 | -0.28 | | 1.21 |
| 39.09 | 3,4-Lutidine | 130-210 | 15 | + 60.5 | -0.23 | | +45.2 | -2.72 | +36.5 | -0.72 | | 0.24 |
| 39.10 | 3,5-Lutidine | 130-210 | 15 | + 56.5 | -0.19 | | +40.6 | -1.67 | +33.5 | -0.37 | | 0.27 |
| 39.11 | 2-Ethylpyridine | 130-210 | 15 | + 44.2 | +0.11s | | +25.8 | -1.27 | +24.2 | -0.20 | | 0.23 |
| 39.12 | 3-Ethylpyridine | 130-210 | 15 | + 51.4 | +0.01** | | +28.2 | -1.53 | +27.5 | -0.29 | | 0.22 |
| 39.13 | 4-Ethylpyridine | 130-210 | 15 | + 54.0 | +0.05* | | +32.6 | -1.44 | +29.9 | -0.23 | | 0.15 |
| 39.14 | 2-Propylpyridine | 130-210 | 15 | + 42.9 | +0.16** | | +21.9 | -1.56 | +22.4 | -0.30 | | 0.60 |
| 39.15 | 4-Propylpyridine | 130-210 | 15 | + 53.1 | +0.75 | | +23.8 | +1.20** | +26.6 | +0.89 | | 1.22 |
| 39.16 | 2,3,6-Collidine | 130-210 | 15 | + 40.8 | +0.19 | | +23.1 | -0.87 | +22.1 | -0.05 | | 0.24 |
| 39.17 | 2,4,6-Collidine | 130-210 | 15 | + 41.5 | -0.11 | | +25.4 | -0.93 | +23.1 | -0.17 | | 0.21 |
| 39.18 | 4-*tert*-Butylpyridine | 130-210 | 15 | + 53.4 | -0.02** | | +38.7 | -2.16 | +31.8 | -0.49 | | 0.35 |
| 39.19 | 3-Chloropyridine | 90-170 | 15 | + 57.6 | -0.03** | | +22.2 | -0.06** | +27.6 | +0.19 | | 0.51 |
| *ORGANOSILICON COMPOUNDS* | | | | | | | | | | | | |
| 40.01 | Tetramethylsilane | 90-170 | 15 | + 4.5 | -0.16** | | + 0.7** | +0.61** | + 1.8 | +0.17 | | 0.96 |
| 40.02 | Hexamethyldisilane | 90-170 | 15 | + 2.5 | -0.01** | | + 2.3s | -0.05** | + 1.7 | -0.01 | | 0.55 |
| 40.03 | Hexamethyldisiloxane | 90-170 | 15 | + 4.9 | -0.30 | | + 2.4 | -0.17** | + 2.5 | -0.14 | | 0.35 |
| *MISCELLANEOUS* | | | | | | | | | | | | |
| 41.01 | Carbon disulphide | 90-170 | 15 | + 11.7 | -0.03** | | - 0.4** | -0.47** | + 3.9 | -0.14 | | 0.51 |
| 41.02 | Tetramethyltin | 90-170 | 15 | + 6.7 | +0.43 | | + 2.8 | +0.73 | + 3.3 | +0.43 | | 0.22 |
| 41.03 | Tetrahydrofuran | 90-170 | 15 | + 31.2 | -0.08** | | +15.4 | -0.28** | +16.1 | -0.01 | | 0.36 |

| No. | Thermodynamic data : C78 / TMO | | | | | | | | |
|---|---|---|---|---|---|---|---|---|---|
| | TMO- C78 | | | Mixture | | id([OCH3]=1) - C78 | | | σ |
| | ΔH (cal mol-1) | ΔS (cal mol-1K-1) | ΔCP | h (cal mol-1) | s (cal mol-1 K-1) | Δ'H (cal l mol-2) | Δ'S (cal l mol-2K-1) | Δ'CP | (cal mol-1) |
| 38.04 | - 439 | -0.784 | + 5.8 | - 211 | -0.524 | - 209 | -0.414 | +1.7 | 1.8 |
| 38.05 | - 481 | -0.866 | + 3.8 | - 208 | -0.518 | - 222 | -0.439 | +1.0 | 1.9 |
| 38.06 | - 601 | -1.129 | + 5.5 | - 178[s] | -0.461 | - 252 | -0.507 | +1.6 | 2.2 |
| *ALKYLPYRIDINES* | | | | | | | | | |
| 39.01 | - 626 | -1.019 | + 4.5 | - 399 | -0.749 | - 316 | -0.524 | +1.2 | 1.4 |
| 39.02 | - 491 | -0.806 | + 4.1 | - 361 | -0.716 | - 266 | -0.457 | +1.1 | 1.3 |
| 39.03 | - 564 | -0.892 | + 4.8 | - 529 | -1.028 | - 340 | -0.572 | +1.3 | 2.3 |
| 39.04 | - 611 | -0.996 | + 3.7 | - 516 | -0.989 | - 351 | -0.593 | +0.9 | 1.5 |
| 39.05 | - 446 | -0.699 | + 2.2* | - 613 | -1.283 | - 336 | -0.611 | +0.4 | 1.5 |
| 39.06 | - 469 | -0.762 | + 3.2 | - 522 | -1.054 | - 312 | -0.553 | +0.7 | 1.0 |
| 39.07 | - 442 | -0.718 | + 3.1* | - 396 | -0.781 | - 262 | -0.451 | +0.8 | 2.5 |
| 39.08 | - 593 | -1.131 | + 5.0** | - 579 | -1.281 | - 380 | -0.773 | +1.2 | 5.3 |
| 39.09 | - 721 | -1.244 | + 4.1 | -1 006 | -2.108 | - 552 | -1.049 | +0.7 | 1.2 |
| 39.10 | - 720 | -1.284 | + 5.1 | - 806 | -1.656 | - 487 | -0.917 | +1.2 | 0.9 |
| 39.11 | - 493 | -0.866 | + 3.1 | - 601 | -1.321 | - 353 | -0.694 | +0.6 | 1.1 |
| 39.12 | - 572 | -0.979 | + 3.1 | - 672 | -1.477 | - 400 | -0.775 | +0.6 | 1.2 |
| 39.13 | - 610 | -1.041 | + 3.6 | - 699 | -1.489 | - 418 | -0.791 | +0.7 | 0.9 |
| 39.14 | - 364 | -0.582 | + 0.8** | - 598 | -1.379 | - 312 | -0.628 | -0.1 | 1.7 |
| 39.15 | - 446 | -0.661** | + 2.7** | - 124** | -0.187** | - 171 | -0.229 | +0.8 | 6.4 |
| 39.16 | - 397 | -0.691 | + 2.4[s] | - 484 | -1.087 | - 285 | -0.566 | +0.5 | 1.3 |
| 39.17 | - 502 | -0.937 | + 3.6 | - 525 | -1.154 | - 332 | -0.668 | +0.8 | 1.1 |
| 39.18 | - 630 | -1.116 | + 3.4[s] | - 864 | -1.847 | - 480 | -0.937 | +0.6 | 1.7 |
| 39.19 | - 543 | -0.830 | + 0.5** | - 367 | -0.782 | - 284 | -0.484 | -0.1 | 2.0 |
| *ORGANOSILICON COMPOUNDS* | | | | | | | | | |
| 40.01 | - 49** | -0.212[s] | + 2.3 | - 26** | -0.134** | - 32 | -0.135 | +0.7 | 6.2 |
| 40.02 | - 27** | -0.205 | - 1.4** | - 186[s] | -0.551 | - 84 | -0.285 | -0.7 | 2.6 |
| 40.03 | - 90 | -0.323 | + 0.6* | - 209 | -0.589 | - 110 | -0.332 | -0.0 | 1.9 |
| *MISCELLANEOUS* | | | | | | | | | |
| 41.01 | - 131 | -0.345 | + 2.9** | - 266 | -0.767 | - 141 | -0.395 | +0.7 | 2.9 |
| 41.02 | + 33 | -0.001** | + 1.4* | - 27** | -0.139* | - 5 | -0.064 | +0.4 | 1.2 |
| 41.03 | - 331 | -0.582 | + 0.4** | - 370 | -0.824 | - 226 | -0.447 | -0.1 | 1.4 |

(Continued on pages 408 and 409)

Table 8 (*continued*)

| No. | Compound | Temp. range (°C) | n | Retention index : C78 / TMO | | | | | | | | σ |
|---|---|---|---|---|---|---|---|---|---|---|---|---|
| | | | | TMO - C78 | | | Mixture | | id([OCH$_3$]=1) - C78 | | | |
| | | | | $\Delta I_{130}$ | $10 \times \Delta A_T$ ($K^{-1}$) | $100 \times \Delta A_{TT}$ ($K^{-2}$) | $A_L$ | $10 \times A_{LT}$ ($K^{-1}$) | $\Delta I'_{130}$ ($l\ mol^{-1}$) | $10 \times \Delta A'_T$ ($K^{-1} l\ mol^{-1}$) | $100 \times \Delta A'_{TT}$ ($K^{-2} l\ mol^{-1}$) | |
| 41.04 | 1,4-Dioxane | 90-170 | 15 | + 47.4 | -0.07** | | +19.4 | -0.18** | +23.1 | +0.11 | | 0.24 |
| 41.05 | Thiophene | 90-170 | 15 | + 38.5 | +0.47 | | +10.4 | +1.59 | +17.1 | +0.85 | | 0.39 |
| 41.06 | Cyclopentanone | 90-170 | 15 | + 62.8 | -0.13* | | +28.9 | -0.24** | +31.7 | +0.13 | | 0.32 |
| 41.07 | Cyclohexanone | 90-170 | 15 | + 61.6 | +0.45 | | +29.8 | +0.62s | +31.6 | +0.63 | | 0.36 |
| 41.08 | Cyclohexanol | 90-170 | 15 | + 89.6 | -2.99 | +0.16 | +43.9 | -2.81 | +46.2 | -1.62 | +0.04 | 0.43 |
| 41.11 | Nitrobenzene | 130-210 | 15 | + 87.2 | +0.05** | | +35.2 | -0.10** | +42.3 | +0.33 | | 0.88 |
| 41.12 | Benzyl alcohol | 130-210 | 15 | +152.3 | -4.70 | +0.20 | +78.2 | -3.61 | +79.7 | -2.21 | +0.05 | 0.69 |
| 41.13 | 2-Phenylethanol | 130-210 | 15 | +134.9 | -4.93 | +0.29 | +58.9 | -2.10 | +67.0 | -1.87 | +0.08 | 0.63 |
| 41.14 | Anisole | 130-210 | 15 | + 48.1 | -0.23 | | +17.6 | +0.24** | +22.7 | +0.19 | | 0.31 |
| 41.15 | Phenetole | 130-210 | 15 | + 45.1 | +0.07* | | +14.1 | +0.31 | +20.5 | +0.30 | | 0.17 |
| *ERROR OF THE COEFFICIENTS (STANDARD DEVIATION)* | | | | | | | | | | | | |
| | *f (n-alkanes* | *90-210* | | *def.* | | | | | | | | |
| | *f (n-alkanes)* | *150-210* | | *def.* | | | | | | | | |
| | *f (solutes)* | *90-170* | | *0.63* | *0.22* | *0.093* | *2.19* | *0.78* | *0.61* | *0.28* | *0.032* | |
| | *f (solutes)* | *130-210* | | *0.98* | *0.22* | *0.093* | *2.19* | *0.77* | *0.82* | *0.27* | *0.032* | |
| *CONVERSIONS* | | | | | | | | | | | | |
| *A* | *Data related to $K_D$* | | | *0* | *0* | *0* | *0* | *0* | *0* | *0* | *0* | |
| *B* | *Data related to 1 bar* | | | *0* | *0* | *0* | *0* | *0* | *0* | *0* | *0* | |

Table 8 (*continued*)

| No. | *Thermodynamic data : C78 / TMO* | | | | | | | | |
|---|---|---|---|---|---|---|---|---|---|
| | *TMO- C78* | | | *Mixture* | | *id([OCH$_3$]=1) - C78* | | | σ |
| | *ΔH* (cal mol$^{-1}$) | *ΔS* | *ΔC$_P$* | *h* | *s* | *Δ'H* | *Δ'S* | *Δ'C$_P$* | |
| | | (cal mol$^{-1}$K$^{-1}$) | | (cal mol$^{-1}$) | (cal mol$^{-1}$ K$^{-1}$) | (cal l mol$^{-2}$) | (cal l mol$^{-2}$K$^{-1}$) | | (cal mol$^{-1}$) |
| 41.04 | - 507 | -0.825 | + 3.0 | - 383 | -0.804 | - 280 | -0.496 | +0.7 | 1.4 |
| 41.05 | - 309 | -0.450 | + 2.1** | + 54** | +0.155** | - 72 | -0.064 | +0.7 | 2.1 |
| 41.06 | - 677 | -1.063 | + 1.3** | - 473 | -0.929 | - 276 | -0.249 | +0.6 | 1.7 |
| 41.07 | - 566 | -0.828 | + 2.9* | - 311 | -0.541 | - 266 | -0.382 | +0.7 | 2.0 |
| 41.08 | -1 560 | -2.942 | +12.9 | -1 184 | -2.516 | - 882 | -1.725 | +3.3 | 2.6 |
| 41.11 | -1 150 | -1.976 | + 8.8 | - 486 | -0.945 | - 511 | -0.877 | +2.5 | 2.9 |
| 41.12 | -2 514 | -4.559 | +16.5 | -1 418 | -2.716 | -1 240 | -2.226 | +4.2 | 3.8 |
| 41.13 | -2 367 | -4.423 | +17.8 | -1 035 | -2.018 | -1 079 | -1.990 | +4.8 | 2.8 |
| 41.14 | - 564 | -0.998 | + 2.3* | - 263 | -0.588 | - 264 | -0.494 | +0.5 | 1.7 |
| 41.15 | - 483 | -0.844 | + 2.3 | - 210 | -0.509 | - 222 | -0.425 | +0.5 | 0.9 |
| *ERROR OF THE COEFFICIENTS (STANDARD DEVIATION)* | | | | | | | | | |
| | *3.4* | *0.0082* | *0.40* | *8.6* | *0.0195* | *4.1* | *0.0095* | *0.14* | |
| | *3.4* | *0.0082* | *0.40* | *8.6* | *0.0195* | *4.1* | *0.0095* | *0.14* | |
| | *9.1* | *0.0223* | *0.76* | *31.3* | *0.0774* | *11.2* | *0.0277* | *0.26* | |
| | *33.8* | *0.0815* | *0.84* | *34.4* | *0.0774* | *16.5* | *0.0386* | *0.29* | |
| *CONVERSIONS* | | | | | | | | | |
| *A* | + 6 | -0.066 | + 0.1 | + 3 | +0.004 | + 3 | -0.021 | +0.0 | |
| *B* | 0 | 0 | 0 | 0 | 0 | 0 | 0 | 0 | |

Table 9
Retention indices and thermodynamic data for 152 solutes in C78/PCN mixtures where data for an ideal solvent with X = PCN, idPCN, are also given. For symbols and explanations see Table 8.

| No. | Compound | Temp. range | n | Retention index : C78 / PCN | | | | | | σ |
|---|---|---|---|---|---|---|---|---|---|---|
| | | | | PCN- C78 | | Mixture | | id([CN] =1) - C78 | | |
| | | | | $\Delta I_{130}$ | $10 \times \Delta A_T$ | $A_L$ | $10 \times A_{LT}$ | $\Delta' I_{130}$ | $10 \times \Delta' A_T$ | |
| | | (°C) | | | ($K^{-1}$) | | ($K^{-1}$) | ($l\ mol^{-1}$) | ($K^{-1} l\ mol^{-1}$) | |
| *HYDROCARBONS* | | | | | | | | | | |
| *n-Alkanes* | | | | | | | | | | |
| 00.05 | Pentane | 90-210 | 21 | | | | | | | |
| 00.06 | Hexane | 90-210 | 21 | | | | | | | |
| 00.07 | Heptane | 90-210 | 21 | | | | | | | |
| 00.08 | Octane | 90-210 | 21 | | | | | | | |
| 00.09 | Nonane | 90-210 | 21 | | | | | | | |
| 00.10 | Decane | 90-210 | 21 | | | | | | | |
| 00.11 | Undecane | 150-210 | 12 | | | | | | | |
| 00.12 | Dodecane | 150-210 | 12 | | | | | | | |
| 00.13 | Tridecane | 150-210 | 12 | | | | | | | |
| 00.14 | Tetradecane | 150-210 | 12 | | | | | | | |
| *Isoalkanes* | | | | | | | | | | |
| 10.01 | 2,2-Dimethylbutane | 90-170 | 15 | - 0.0** | -0.09** | + 0.6 | +0.04 | + 0.9 | -0.06 | 0.33 |
| 10.02 | 2,3-Dimethylbutane | 90-170 | 15 | - 0.0 | -0.14* | - 0.2** | -0.08** | - 0.3 | -0.32 | 0.37 |
| 10.03 | 2,2-Dimethylpentane | 90-170 | 15 | - 0.1** | -0.19 | - 0.3** | -0.33* | - 0.6 | -0.75 | 0.29 |
| 10.04 | 2,3-Dimethylpentane | 90-170 | 15 | + 0.1** | -0.11[s] | + 0.0** | +0.10** | + 0.1 | -0.01 | 0.23 |
| 10.05 | 2,4-Dimethylpentane | 90-170 | 15 | - 0.7 | -0.12 | + 0.4** | -0.23 | - 0.5 | -0.51 | 0.44 |
| 10.06 | 2,2-Dimethylhexane | 90-170 | 15 | - 0.3[s] | -0.23 | - 0.4** | -0.25* | - 1.1 | -0.70 | 0.22 |
| 10.07 | 2,3-Dimethylhexane | 90-170 | 15 | + 0.4 | +0.03** | - 0.0** | +0.26 | + 0.6 | +0.42 | 0.11 |
| 10.08 | 2,4-Dimethylhexane | 90-170 | 15 | - 0.3[s] | -0.01** | - 0.5** | +0.07** | - 1.1 | +0.08 | 0.26 |
| 10.09 | 3,4-Dimethylhexane | 90-170 | 15 | + 0.6 | +0.06* | - 1.5 | +0.25[s] | - 1.3 | +0.43 | 0.17 |
| 10.10 | 2,2,3-Trimethylbutane | 90-170 | 15 | + 0.4[s] | +0.34 | - 0.7** | +0.77 | - 0.3 | +1.59 | 0.27 |
| 10.11 | 2,2,4-Trimethylpentane | 90-170 | 15 | - 0.7 | +0.12[s] | - 0.6** | +0.39[s] | - 1.8 | +0.71 | 0.25 |
| 10.12 | 2,3,4-Trimethylpentane | 90-170 | 15 | + 0.6 | +0.26 | - 1.2 | +0.54 | - 0.8 | +1.14 | 0.18 |
| *1-Alkenes* | | | | | | | | | | |
| 11.05 | 1-Pentene | 90-170 | 15 | + 4.0 | -0.44 | - 0.6** | -0.93 | + 4.7 | -1.92 | 0.76 |
| 11.06 | 1-Hexene | 90-170 | 15 | + 4.0 | -0.55 | + 1.0* | +0.11** | + 7.1 | -0.56 | 0.28 |
| 11.07 | 1-Heptene | 90-170 | 15 | + 4.8 | -0.29 | + 1.5* | +0.19** | + 9.0 | -0.06 | 0.37 |
| 11.08 | 1-Octene | 90-170 | 15 | + 4.7 | -0.19* | + 0.4** | +0.41** | + 7.3 | +0.38 | 0.58 |
| 11.09 | 1-Nonene | 90-170 | 15 | + 5.0 | -0.06** | + 0.5** | +0.43** | + 7.9 | +0.60 | 0.67 |
| 11.10 | 1-Decene | 90-170 | 15 | + 4.6 | +0.20** | - 0.2** | +0.78** | + 6.4 | +1.46 | 0.86 |

| No. | Thermodynamic data : C78 / PCN | | | | | | | | |
|---|---|---|---|---|---|---|---|---|---|
| | PCN - C78 | | | Mixture | | id([CN] =1) - C78 | | | σ |
| | $\Delta H$ (cal mol$^{-1}$) | $\Delta S$ | $\Delta C_P$ (cal mol$^{-1}$K$^{-1}$) | $h$ (cal mol$^{-1}$) | $s$ (cal mol$^{-1}$ K$^{-1}$) | $\Delta' H$ (cal l mol$^{-2}$) | $\Delta' S$ | $\Delta' C_P$ (cal l mol$^{-2}$K$^{-1}$) | (cal mol$^{-1}$) |
| *HYDROCARBONS* | | | | | | | | | |
| *n-Alkanes* | | | | | | | | | |
| 00.05 | + 114 | +0.012 | -3.2 | -194 | -0.627 | - 189 | -1.058 | - 5.1 | 5.6 |
| 00.06 | + 101 | -0.029 | -3.0 | -193 | -0.627 | - 208 | -1.121 | - 4.9 | 4.8 |
| 00.07 | + 88 | -0.069 | -2.9 | -192 | -0.627 | - 227 | -1.182 | - 4.8 | 4.7 |
| 00.08 | + 74 | -0.110 | -2.7 | -190 | -0.627 | - 246 | -1.245 | - 4.5 | 4.2 |
| 00.09 | + 61 | -0.150 | -2.6 | -189 | -0.627 | - 265 | -1.306 | - 4.4 | 3.2 |
| 00.10 | + 48 | -0.191 | -2.4 | -188 | -0.627 | - 283 | -1.368 | - 4.2 | 3.6 |
| 00.11 | + 35 | -0.231 | -2.2 | -187 | -0.627 | - 302 | -1.429 | - 3.9 | 4.7 |
| 00.12 | + 21 | -0.272 | -2.1 | -185 | -0.627 | - 321 | -1.492 | - 3.8 | 4.3 |
| 00.13 | + 8 | -0.312 | -1.9 | -184 | -0.627 | - 339 | -1.553 | - 3.6 | 5.4 |
| 00.14 | - 5 | -0.353 | -1.8 | -183 | -0.627 | - 358 | -1.616 | - 3.5 | 6.3 |
| *Isoalkanes* | | | | | | | | | |
| 10.01 | + 87 | -0.057** | -3.2$^s$ | -191 | -0.612 | - 222 | -1.133 | - 5.2 | 2.1 |
| 10.02 | + 70 | -0.099 | -5.2 | -211 | -0.673 | - 278 | -1.287 | - 8.1 | 1.7 |
| 10.03 | + 58 | -0.138 | -2.9$^s$ | -261 | -0.798 | - 365 | -1.521 | - 5.0 | 1.7 |
| 10.04 | + 65 | -0.123 | -1.8$^s$ | -172 | -0.576 | - 229 | -1.183 | - 3.2 | 1.1 |
| 10.05 | + 76 | -0.093 | -6.3 | -248 | -0.758 | - 323 | -1.402 | - 9.7 | 0.8 |
| 10.06 | + 40 | -0.191 | -3.1 | -242 | -0.758 | - 368 | -1.545 | -5.3 | 1.2 |
| 10.07 | + 80 | -0.088 | -2.7 | -135 | -0.489 | - 157 | -1.015 | - 4.4 | 0.6 |
| 10.08 | + 84 | -0.082 | -4.4 | -174 | -0.592 | - 211 | -1.158 | - 6.9 | 1.2 |
| 10.09 | + 81 | -0.085 | -2.9 | -121 | -0.474 | - 140 | -0.997 | - 4.7 | 0.9 |
| 10.10 | + 160 | +0.118 | -2.7 | - 21** | -0.214$^s$ | + 117 | -0.333 | - 3.9 | 1.5 |
| 10.11 | + 120 | -0.001** | -2.3$^s$ | -102$^s$ | -0.413 | - 58 | -0.789 | - 3.7 | 1.4 |
| 10.12 | + 125 | +0.027 | -3.8 | - 67 | -0.335 | - 0 | -0.640 | - 5.7 | 0.9 |
| *1-Alkenes* | | | | | | | | | |
| 11.05 | - 24** | -0.270 | -4.5** | -393 | -1.125 | - 658 | -2.142 | - 7.7 | 4.1 |
| 11.06 | - 62 | -0.373 | -4.4 | -178 | -0.576 | - 406 | -1.506 | - 7.1 | 1.0 |
| 11.07 | - 23$^s$ | -0.273 | -4.7 | -165 | -0.541 | - 331 | -1.314 | - 7.4 | 1.2 |
| 11.08 | - 13** | -0.258 | -5.3 | -103* | -0.407 | - 235 | -1.116 | - 8.1 | 2.2 |
| 11.09 | - 2** | -0.237 | -4.7$^s$ | - 98** | -0.396* | - 213 | -1.073 | - 7.3 | 3.2 |
| 11.10 | + 42** | -0.144** | -4.1** | - 15** | -0.202** | - 38 | -0.677 | - 6.2 | 4.6 |

(*Continued on pages 412 and 413*)

Table 9 (*continued*)

| No. | Compound | Temp. range (°C) | n | Retention index : C78 / PCN | | | | | | σ |
|---|---|---|---|---|---|---|---|---|---|---|
| | | | | PCN- C78 | | Mixture | | id([CN] =1) - C78 | | |
| | | | | $\Delta I_{130}$ | $10 \times \Delta A_T$ ($K^{-1}$) | $A_L$ | $10 \times A_{LT}$ ($K^{-1}$) | $\Delta I'_{130}$ ($l\ mol^{-1}$) | $10 \times \Delta A'_T$ ($K^{-1} l\ mol^{-1}$) | |
| *1-Alkynes* | | | | | | | | | | |
| 12.05 | 1-Pentyne | 90-170 | 15 | +19.1 | -0.34 | + 6.0 | +1.43 | + 36.1 | +1.89 | 0.62 |
| 12.06 | 1-Hexyne | 90-170 | 15 | +19.9 | -0.39 | + 6.2 | +0.48** | + 37.4 | +0.47 | 0.57 |
| 12.07 | 1-Heptyne | 90-170 | 15 | +20.6 | -0.16** | + 8.6 | -0.13** | + 41.8 | -0.03 | 0.75 |
| 12.08 | 1-Octyne | 90-170 | 15 | +20.5 | -0.19s | + 5.6 | +0 21** | + 37.4 | +0.37 | 0.42 |
| 12.09 | 1-Nonyne | 90-170 | 15 | +20.6 | -0.08** | + 6.6 | -0.04** | + 38.9 | +0.18 | 0.52 |
| 12.10 | 1-Decyne | 90-170 | 15 | +20.8 | +0.03** | + 6.8 | +0.00** | + 39.5 | +0.40 | 0.59 |
| *Alkynes* | | | | | | | | | | |
| 13.01 | 2-Hexyne | 90-170 | 15 | +16.1 | -0.47s | + 1.6** | +0.55 | + 25.4 | +0.35 | 0.97 |
| 13.02 | 3-Hexyne | 90-170 | 15 | +14.0 | -0.07** | + 3.9 | -0.03** | + 25.6 | +0.09 | 0.56 |
| 13.03 | 4-Octyne | 90-170 | 15 | +12.9 | -0.02** | + 3.2 | -0.03** | + 23.1 | +0.14 | 0.50 |
| *Monocyclic hydrocarbons* | | | | | | | | | | |
| 14.05 | Cyclopentane | 90-170 | 15 | + 2.1 | -0.33 | - 1.5 | -0.17** | + 0.8 | -0.71 | 0.17 |
| 14.06 | Cyclohexane | 90-170 | 15 | + 1.7 | +0.05** | - 2.7 | +0.45 | - 1.4 | +0.70 | 0.22 |
| 14.07 | Cycloheptane | 90-170 | 15 | + 2.4 | +0.34 | - 3.1 | +0.37 | - 0.9 | +1.01 | 0.31 |
| 14.08 | Cyclooctane | 90-170 | 15 | + 3.0 | +0.57 | - 4.8 | +0.99 | - 2.4 | +2.21 | 0.27 |
| 14.10 | Cyclodecane | 130-210 | 15 | + 4.9 | +0.25 | - 4.4 | +0.36 | + 0.8 | +0.88 | 0.38 |
| *Bicyclic hydrocarbons* | | | | | | | | | | |
| 15.01 | *cis*-Hydrindane | 130-210 | 15 | + 3.3 | +0.30 | - 2.4 | -0.32s | + 1.3 | -0.02 | 0.20 |
| 15.02 | *trans*-Hydrindane | 130-210 | 15 | + 1.6 | +0.56 | - 0.8** | -0.11** | + 1.2 | +0.66 | 0.52 |
| 15.03 | *cis*-Decalin | 130-210 | 15 | + 4.4 | +0.47 | + 2.0** | -0.43** | + 9.2 | +0.14 | 0.42 |
| 15.04 | *trans*-Decalin | 130-210 | 15 | + 2.7 | +0.27 | - 3.4 | -0.22** | - 1.0 | +0.06 | 0.27 |
| *Methylcyclohexanes (MCH)* | | | | | | | | | | |
| 16.01 | Methylcyclohexane | 90-170 | 15 | + 1.1 | +0.09** | - 2.8 | -0.03** | - 2.4 | +0.06 | 0.31 |
| 16.02 | *cis*-1,2-Di MCH | 90-170 | 15 | + 2.3 | +0.16* | - 1.4* | +0.21** | + 1.3 | +0.54 | 0.40 |
| 16.03 | *trans*-1,2-Di MCH | 90-170 | 15 | + 1.6 | +0.17s | - 1.9 | +0.39* | - 0.4 | +0.79 | 0.36 |
| 16.04 | *cis*-1,4-Di MCH | 90-170 | 15 | + 2.0 | +0.16 | - 1.3 | -0.16** | + 1.0 | +0.01 | 0.19 |
| 16.05 | *trans*-1,4-Di MCH | 90-170 | 15 | + 1.4 | +0.17 | - 1.5 | +0.15* | - 0.1 | +0.46 | 0.16 |
| *Cyclohexenes* | | | | | | | | | | |
| 17.01 | Cyclohexene | 90-170 | 15 | + 6.9 | +0.11* | - 1.4s | +0.00** | + 7.9 | +0.23 | 0.33 |
| 17.02 | 1,3-Cyclohexadiene | 90-170 | 15 | +14.5 | +0.33 | + 1.4** | +1.23 | + 22.9 | +2.44 | 0.56 |
| 17.03 | 1,4-Cyclohexadiene | 90-170 | 15 | +14.7 | +0.51 | + 4.2 | +0.76 | + 27.2 | +2.07 | 0.25 |

| No. | Thermodynamic data : C78 / PCN | | | | | | | | |
|---|---|---|---|---|---|---|---|---|---|
| | PCN - C78 | | | Mixture | | id([CN] =1) - C78 | | | σ |
| | $\Delta H$ (cal mol$^{-1}$) | $\Delta S$ (cal mol$^{-1}$K$^{-1}$) | $\Delta C_P$ | $h$ (cal mol$^{-1}$) | $s$ (cal mol$^{-1}$ K$^{-1}$) | $\Delta' H$ (cal l mol$^{-2}$) | $\Delta' S$ (cal l mol$^{-2}$K$^{-1}$) | $\Delta' C_P$ | (cal mol$^{-1}$) |
| *1-Alkynes* | | | | | | | | | |
| 12.05 | - 156 | -0.383 | -6.3 | + 68** | +0.106** | - 139 | -0.430 | - 9.2 | 2.8 |
| 12.06 | - 185 | -0.464 | -3.9* | -160* | -0.445* | - 500 | -1.318 | - 6.3 | 3.3 |
| 12.07 | - 155 | -0.401 | -3.6** | -320s | -0.828 | - 684 | -1.770 | - 6.2 | 4.3 |
| 12.08 | - 172 | -0.459 | -2.5 | -203 | -0.583 | - 553 | -1.529 | - 4.5 | 2.4 |
| 12.09 | - 165 | -0.452 | -1.9** | -269 | -0.739 | - 637 | -1.741 | - 3.7 | 3.0 |
| 12.10 | - 159 | -0.442 | -2.7** | -261 | -0.721 | - 618 | -1.706 | - 4.9 | 3.3 |
| *Alkynes* | | | | | | | | | |
| 13.01 | - 163 | -0.493 | +4.6** | - 79** | -0.324** | - 377 | -1.245 | + 5.7 | 4.5 |
| 13.02 | - 62 | -0.244 | -5.7 | -234 | -0.678 | - 456 | -1.399 | - 8.9 | 1.8 |
| 13.03 | - 65 | -0.287 | -5.4 | -225 | -0.672 | - 458 | -1.472 | - 8.5 | 1.2 |
| *Monocyclic hydrocarbons* | | | | | | | | | |
| 14.05 | + 6** | -0.236 | -2.1 | -219 | -0.711 | - 377 | -1.528 | - 3.9 | 0.8 |
| 14.06 | + 76 | -0.074 | -3.3 | - 70* | -0.359 | - 72 | -0.815 | - 5.1 | 1.3 |
| 14.07 | + 107 | +0.004** | -5.1 | - 84 | -0.403 | - 52 | -0.773 | - 7.7 | 1.0 |
| 14.08 | + 129 | +0.055s | -4.7 | + 59* | -0.077** | + 176 | -0.252 | - 6.8 | 1.2 |
| 14.10 | + 41** | -0.162** | -3.1 | - 82 | -0.424 | - 146 | -1.047 | - 4.9 | 1.5 |
| *Bicyclic hydrocarbons* | | | | | | | | | |
| 15.01 | + 83 | -0.066** | -3.1 | -221 | -0.739 | - 279 | -1.349 | - 5.2 | 0.9 |
| 15.02 | + 209 | +0.223** | -4.7s | -199s | -0.666 | - 73 | -0.839 | - 7.1 | 2.5 |
| 15.03 | + 92** | -0.041** | -3.4* | -283 | -0.842 | - 346 | -1.435 | - 5.7 | 2.1 |
| 15.04 | + 92s | -0.059** | -3.6 | -192 | -0.684 | - 232 | -1.274 | - 5.8 | 1.2 |
| *Methylcyclohexanes (MCH)* | | | | | | | | | |
| 16.01 | + 81 | -0.072* | -4.4 | -172 | -0.615 | - 214 | -1.182 | - 6.9 | 1.6 |
| 16.02 | + 71 | -0.099 | -0.7 | -136 | -0.513 | - 173 | -1.064 | - 1.6 | 1.1 |
| 16.03 | + 85 | -0.072 | -0.6** | - 92 | -0.409 | - 92 | -0.885 | - 1.4 | 0.7 |
| 16.04 | + 77 | -0.079 | -3.5 | -211 | -0.696 | - 271 | -1.297 | - 5.7 | 1.2 |
| 16.05 | + 88 | -0.059 | -2.7 | -145 | -0.533 | - 162 | -1.041 | - 4.4 | 1.0 |
| *Cyclohexenes* | | | | | | | | | |
| 17.01 | + 33s | -0.115 | -4.3 | -179 | -0.613 | - 275 | -1.198 | - 6.8 | 1.7 |
| 17.02 | - 1** | -0.104* | -1.9** | + 50** | -0.011** | + 27 | -0.269 | - 2.8 | 2.6 |
| 17.03 | + 37 | -0.007** | -4.2 | - 79* | -0.294 | - 97 | -0.520 | - 6.2 | 1.4 |

(Continued on pages 414 and 415)

*Table 9 (continued)*

| No. | Compound | Temp. range | n | Retention index : C78 / PCN | | | | | | |
|---|---|---|---|---|---|---|---|---|---|---|
| | | | | PCN- C78 | | Mixture | | id([CN] =1) - C78 | | σ |
| | | (°C) | | $\Delta I_{130}$ | $10 \times \Delta A_T$ ($K^{-1}$) | $A_L$ | $10 \times A_{LT}$ ($K^{-1}$) | $\Delta' I_{130}$ ($l\ mol^{-1}$) | $10 \times \Delta' A_T$ ($K^{-1} l\ mol^{-1}$) | |
| *Alkylbenzenes* | | | | | | | | | | |
| 18.00 | Benzene | 90-170 | 15 | +24.6 | +0.38 | + 2.0 | +0.79 | + 38.2 | +2.02 | 0.35 |
| 18.01 | Toluene | 90-170 | 15 | +24.4 | +0.41 | + 3.1 | +0.24* | + 39.5 | +1.29 | 0.18 |
| 18.02 | Ethylbenzene | 90-170 | 15 | +23.8 | +0.51 | + 3.6 | +0.05** | + 39.3 | +1.16 | 0.33 |
| *Miscellaneous* | | | | | | | | | | |
| 19.01 | Adamantane | 130-210 | 15 | + 3.7 | +0.93 | - 1.2** | +0.38** | + 3.7 | +1.91 | 0.58 |
| 19.02 | Naphthalene | 130-210 | 15 | +42.9 | +0.60 | + 9.4 | -0.50** | + 74.9 | +0.82 | 0.78 |
| 19.03 | Azulene | 130-210 | 15 | +54.6 | +1.06 | +18.3 | +1.42** | +104.7 | +4.51 | 1.48 |
| *ALKANE DERIVATIVES* | | | | | | | | | | |
| *1-Fluoroalkanes* | | | | | | | | | | |
| 20.05 | 1-Fluoropentane | 90-170 | 15 | +25.3 | -0.07** | + 6.9 | -0.36** | + 46.1 | -0.19 | 0.44 |
| 20.06 | 1-Fluorohexane | 90-170 | 15 | +25.7 | -0.03** | + 7.2 | -0.31** | + 47.1 | -0.06 | 0.37 |
| 20.07 | 1-Fluoroheptane | 90-170 | 15 | +26.1 | +0.05** | + 7.7 | -0.21** | + 48.4 | +0.21 | 0.33 |
| 20.08 | 1-Fluorooctane | 90-170 | 15 | +26.6 | +0.03** | + 8.6 | -0.36s | + 50.4 | -0.01 | 0.24 |
| *1,1,1-Trifluoroalkanes* | | | | | | | | | | |
| 21.08 | 1,1,1-Trifluorooctane | 90-170 | 15 | +26.2 | +0.03** | +11.1 | -0.13** | + 53.4 | +0.35 | 0.26 |
| 21.10 | 1,1,1-Trifluorodecane | 90-170 | 15 | +26.6 | -0.25 | +11.4 | -0.55 | + 54.4 | -0.65 | 0.23 |
| *1-Chloroalkanes* | | | | | | | | | | |
| 22.04 | 1-Chlorobutane | 90-170 | 15 | +27.0 | +0.08** | + 6.2 | -0.60s | + 47.5 | -0.31 | 0.39 |
| 22.05 | 1-Chloropentane | 90-170 | 15 | +26.9 | +0.42 | + 6.2 | +0.63 | + 47.5 | +1.94 | 0.33 |
| 22.06 | 1-Chlorohexane | 90-170 | 15 | +27.1 | +0.35 | + 5.9 | +0.46 | + 47.4 | +1.59 | 0.51 |
| *1-Bromoalkanes* | | | | | | | | | | |
| 23.03 | 1-Bromopropane | 90-170 | 15 | +28.3 | +0.22* | + 6.4 | +0.15** | + 49.8 | +0.98 | 0.54 |
| 23.04 | 1-Bromobutane | 90-170 | 15 | +27.9 | +0.25s | + 5.4 | +0.36** | + 47.8 | +1.31 | 0.53 |
| 23.05 | 1-Bromopentane | 90-170 | 15 | +28.0 | +0.36 | + 5.0 | +0.46** | + 47.4 | +1.61 | 0.61 |
| *1-Cyanoalkanes* | | | | | | | | | | |
| 24.02 | Cyanoethane | 90-170 | 15 | +89.6 | -0.19** | +39.0 | -1.89s | +184.0 | -1.29 | 1.33 |
| 24.03 | 1-Cyanopropane | 90-170 | 15 | +88.5 | -0.35 | +32.6 | -1.12 | +173.4 | -0.52 | 0.34 |
| 24.04 | 1-Cyanobutane | 90-170 | 15 | +88.9 | -0.23 | +32.2 | -0.69s | +173.4 | +0.27 | 0.38 |
| 24.05 | 1-Cyanopentane | 90-170 | 15 | +89.7 | -0.05** | +33.1 | -0.54* | +175.9 | +0.76 | 0.48 |

| No. | Thermodynamic data : C78 / PCN | | | | | | | | |
|---|---|---|---|---|---|---|---|---|---|
| | PCN - C78 | | | Mixture | | id([CN] =1) - C78 | | | σ |
| | $\Delta H$ (cal mol$^{-1}$) | $\Delta S$ | $\Delta C_P$ | $h$ (cal mol$^{-1}$) | $s$ (cal mol$^{-1}$ K$^{-1}$) | $\Delta' H$ (cal l mol$^{-2}$) | $\Delta' S$ | $\Delta' C_P$ | (cal mol$^{-1}$) |
| | | (cal mol$^{-1}$K$^{-1}$) | | | | | (cal l mol$^{-2}$K$^{-1}$) | | |
| *Alkylbenzenes* | | | | | | | | | |
| 18.00 | - 92 | -0.195 | -2.6* | - 31** | -0.200** | - 191 | -0.604 | - 4.0 | 1.9 |
| 18.01 | - 99 | -0.227 | -3.5 | -171 | -0.536 | - 401 | -1.128 | - 5.6 | 0.9 |
| 18.02 | - 84 | -0.205 | -4.7 | -215 | -0.644 | - 447 | -1.257 | - 7.4 | 1.7 |
| *Miscellaneous* | | | | | | | | | |
| 19.01 | + 234 | +0.303** | -4.9s | -121** | -0.477s | + 77 | -0.454 | - 7.2 | 2.8 |
| 19.02 | - 179* | -0.249** | -5.4* | -365 | -0.955 | - 750 | -1.652 | - 8.7 | 3.7 |
| 19.03 | - 724 | -1.436 | +7.2 | -129** | -0.259** | -1 129 | -2.204 | + 8.8 | 3.2 |
| *ALKANE DERIVATIVES* | | | | | | | | | |
| *1-Fluoroalkanes* | | | | | | | | | |
| 20.05 | - 167 | -0.335 | -5.3 | -343 | -0.899 | - 721 | -1.744 | - 8.6 | 2.1 |
| 20.06 | - 178 | -0.386 | -4.3 | -331 | -0.874 | - 723 | -1.792 | - 7.2 | 1.7 |
| 20.07 | - 177 | -0.393 | -4.2 | -310 | -0.820 | - 694 | -1.729 | - 6.9 | 1.5 |
| 20.08 | - 202 | -0.461 | -3.4 | -350 | -0.914 | - 785 | -1.957 | - 6.0 | 1.2 |
| *1,1,1-Trifluroalkanes* | | | | | | | | | |
| 21.08 | - 174 | -0.383 | -3.3 | -326 | -0.817 | - 704 | -1.689 | - 5.7 | 1.4 |
| 21.10 | - 260 | -0.617 | -1.3** | -414 | -1.039 | - 953 | -2.342 | - 3.3 | 1.3 |
| *1-Chloroalkanes* | | | | | | | | | |
| 22.04 | - 166 | -0.346 | -1.5** | -378 | -1.003 | - 771 | -1.914 | -3.3 | 2.3 |
| 22.05 | - 107 | -0.211 | -2.8s | -112s | -0.352 | - 316 | -0.811 | -4.5 | 1.8 |
| 22.06 | - 140 | -0.303 | -3.2* | -143* | -0.437s | - 410 | -1.070 | -5.2 | 2.7 |
| *1-Bromoalkanes* | | | | | | | | | |
| 23.03 | - 150 | -0.287 | -2.7** | -216 | -0.600 | - 517 | -1.252 | - 4.6 | 2.9 |
| 23.04 | - 152 | -0.306 | -4.6 | -160s | -0.480 | - 448 | -1.127 | - 7.2 | 2.2 |
| 23.05 | - 149 | -0.309 | -4.6s | -136* | -0.431s | - 413 | -1.071 | - 7.2 | 2.9 |
| *1-Cyanoalkanes* | | | | | | | | | |
| 24.02 | - 839 | -1.102 | -6.7* | -988 | -2.045 | -2 349 | -3.867 | -11.9 | 4.9 |
| 24.03 | - 895 | -1.340 | -1.4* | -776 | -1.619 | -2 159 | -3.678 | - 4.3 | 1.2 |
| 24.04 | - 868 | -1.303 | -1.8 | -656 | -1.358 | -1 963 | -3.284 | - 4.6 | 1.9 |
| 24.05 | - 861 | -1.302 | -1.4** | -632 | -1.297 | -1 922 | -3.203 | - 4.0 | 2.8 |

(Continued on pages 416 and 417)

Table 9 (*continued*)

| No. | Compound | Temp. range (°C) | n | Retention index : C78 / PCN | | | | | | σ |
|---|---|---|---|---|---|---|---|---|---|---|
| | | | | PCN- C78 | | Mixture | | id([CN] =1) - C78 | | |
| | | | | $\Delta I_{130}$ | $10 \times \Delta A_T$ ($K^{-1}$) | $A_L$ | $10 \times A_{LT}$ ($K^{-1}$) | $\Delta' I_{130}$ ($l\ mol^{-1}$) | $10 \times \Delta' A_T$ ($K^{-1} l\ mol^{-1}$) | |
| *1-Nitroalkanes* | | | | | | | | | | |
| 25.02 | Nitroethane | 90-170 | 15 | +90.2 | -1.19 | +32.2 | -0.57** | +175.2 | -0.91 | 0.89 |
| 25.03 | 1-Nitropropane | 90-170 | 15 | +86.2 | -0.86 | +30.0 | -0.11** | +166.4 | +0.13 | 0.44 |
| 25.04 | 1-Nitrobutane | 90-170 | 15 | +85.2 | -0.69 | +29.9 | -0.36s | +164.8 | +0.00 | 0.25 |
| 25.05 | 1-Nitropentane | 90-170 | 15 | +84.4 | -0.55 | +30.6 | -0.30** | +164.7 | +0.29 | 0.29 |
| 1-Acetoxyalkanes | | | | | | | | | | |
| 26.03 | 1-Acetoxypropane | 90-170 | 15 | +41.2 | -0.21* | +12.4 | -0.57** | + 76.7 | -0.42 | 0.59 |
| 26.04 | 1-Acetoxybutane | 90-170 | 15 | +41.7 | -0.20** | +12.8 | -0.64** | + 77.9 | -0.49 | 0.69 |
| 26.05 | 1-Acetoxypentane | 90-170 | 15 | +42.1 | -0.28* | +12.4 | -0.58** | + 77.9 | -0.52 | 0.71 |
| *1-Alkanols* | | | | | | | | | | |
| 27.04 | 1-Butanol | 90-170 | 15 | +64.8 | -2.37 | +27.6 | -1.16** | +132.0 | -3.85 | 1.11 |
| 27.05 | 1-Pentanol | 90-170 | 15 | +66.5 | -2.18 | +28.4 | -0.99 | +135.6 | -3.29 | 1.13 |
| 27.06 | 1-Hexanol | 90-170 | 15 | +67.5 | -2.23 | +30.0 | -1.54* | +139.3 | -4.13 | 1.22 |
| 27.07 | 1-Heptanol | 90-170 | 15 | +67.6 | -1.84 | +32.6 | -2.02 | +143.2 | -4.22 | 1.06 |
| *2-Alkanols* | | | | | | | | | | |
| 28.04 | 2-Butanol | 90-170 | 15 | +54.3 | -1.49 | +19.5 | -0.85s | +105.5 | -2.39 | 0.55 |
| 28.05 | 2-Pentanol | 90-170 | 15 | +55.3 | -1.38 | +19.9 | -0.07** | +107.6 | -1.09 | 0.36 |
| 28.06 | 2-Hexanol | 90-170 | 15 | +56.3 | -1.41 | +21.2 | -0.37** | +110.9 | -1.54 | 0.38 |
| 28.07 | 2-Heptanol | 90-170 | 15 | +56.9 | -1.39 | +22.7 | -0.66s | +113.8 | -1.89 | 0.45 |
| *2-Methyl-2-alkanols* | | | | | | | | | | |
| 29.04 | 2-Methyl-2-propanol | 90-170 | 15 | +49.8 | -1.88 | +12.5 | -0.51** | + 89.0 | -2.61 | 0.52 |
| 29.05 | 2-Methyl-2-butanol | 90-170 | 15 | +49.2 | -1.68 | +15.2 | -0.65* | + 92.0 | -2.49 | 0.52 |
| 29.06 | 2-Methyl-2-pentanol | 90-170 | 15 | +49.3 | -1.42 | +16.4 | -0.76s | + 93.9 | -2.26 | 0.43 |
| 29.07 | 2-Methyl-2-hexanol | 90-170 | 15 | +49.6 | -1.32 | +16.9 | -1.22 | + 95.0 | -2.77 | 0.41 |
| *1-Alkanethiols* | | | | | | | | | | |
| 30.04 | 1-Butanethiol | 90-170 | 15 | +25.6 | -1.01 | + 5.5 | -0.56** | + 44.4 | -1.84 | 0.76 |
| 30.05 | 1-Pentanethiol | 90-170 | 15 | +26.3 | -0.82 | + 5.2 | -0.74 | + 44.9 | -1.82 | 0.86 |
| 30.06 | 1-Hexanethiol | 90-170 | 15 | +26.5 | -0.83 | + 4.5 | -0.24 | + 44.3 | -1.13 | 0.89 |
| *2-Alkanones* | | | | | | | | | | |
| 31.04 | 2-Butanone | 90-170 | 15 | +56.7 | -0.83 | +17.8 | -1.46 | +106.5 | -2.31 | 0.89 |
| 31.05 | 2-Pentanone | 90-170 | 15 | +56.1 | -0.55 | +17.9 | -0.92s | +105.9 | -1.14 | 0.56 |

| No. | Thermodynamic data : C78 / PCN | | | | | | | | |
|---|---|---|---|---|---|---|---|---|---|
| | PCN - C78 | | | Mixture | | id([CN] =1) - C78 | | | σ |
| | $\Delta H$ (cal mol$^{-1}$) | $\Delta S$ (cal mol$^{-1}$K$^{-1}$) | $\Delta C_P$ | $h$ (cal mol$^{-1}$) | $s$ (cal mol$^{-1}$ K$^{-1}$) | $\Delta'H$ (cal l mol$^{-2}$) | $\Delta'S$ (cal l mol$^{-2}$K$^{-1}$) | $\Delta'C_P$ | (cal mol$^{-1}$) |
| *1-Nitroalkanes* | | | | | | | | | |
| 25.02 | -1 089 | -1.771 | -4.5* | -659 | -1.301 | -2 257 | -3.809 | - 2.8 | 3.5 |
| 25.03 | - 974 | -1.588 | -2.6[s] | -532 | -1.063 | -1 944 | -3.287 | - 5.8 | 1.6 |
| 25.04 | - 941 | -1.547 | -0.9** | -561 | -1.151 | -1 947 | -3.766 | - 3.4 | 1.4 |
| 25.05 | - 926 | -1.528 | +0.2** | -564 | -1.159 | -1 932 | -3.367 | - 1.8 | 1.5 |
| *1-Acetoxyalkanes* | | | | | | | | | |
| 26.03 | - 366 | -0.666 | +2.2** | -437 | -1.066 | -1 090 | -2.337 | + 1.7 | 2.2 |
| 26.04 | - 378 | -0.705 | +2.1** | -451 | -1.104 | -1 129 | -2.452 | + 1.4 | 2.5 |
| 26.05 | - 417 | -0.813 | +3.1* | -431 | -1.065 | -1 159 | -2.557 | + 2.8 | 2.4 |
| *1-Alkanols* | | | | | | | | | |
| 27.04 | -1 070 | -2.102 | +5.6* | -743 | -1.616 | -2 427 | -4.917 | + 4.8 | 5.4 |
| 27.05 | -1 037 | -2.024 | +6.1[s] | -694 | -1.500 | -2 311 | -4.647 | + 5.7 | 4.2 |
| 27.06 | -1 073 | -2.123 | +7.7 | -820 | -1.802 | -2 540 | -5.211 | + 7.6 | 4.1 |
| 27.07 | -1 003 | -1.953 | +3.8** | -944 | -2.081 | -2 615 | -5.361 | + 2.0 | 4.7 |
| *2-Alkanols* | | | | | | | | | |
| 28.04 | - 769 | -1.434 | -1.1** | -593 | -1.340 | -1 824 | -3.668 | - 3.8 | 3.5 |
| 28.05 | - 761 | -1.456 | +0.8** | -411 | -0.905 | -1 563 | -3.106 | - 0.8 | 2.0 |
| 28.06 | - 780 | -1.508 | +0.1** | -479 | -1.064 | -1 686 | -3.404 | - 1.9 | 2.2 |
| 28.07 | - 801 | -1.571 | +1.1** | -556 | -1.245 | -1 825 | -3.747 | - 0.8 | 2.3 |
| *2-Methyl-2-alkanols* | | | | | | | | | |
| 29.04 | - 805 | -1.586 | +2.2** | -428 | -1.029 | -1 667 | -3.507 | + 0.9 | 2.9 |
| 29.05 | - 767 | -1.550 | +3.6 | -504 | -1.190 | -1 725 | -3.696 | + 2.8 | 1.9 |
| 29.06 | - 709 | -1.421 | +1.8* | -524 | -1.231 | -1 674 | -3.576 | + 0.3 | 1.5 |
| 29.07 | - 705 | -1.418 | +0.6** | -617 | -1.462 | -1 802 | -3.905 | - 1.6 | 1.9 |
| *1-Alkanethiols* | | | | | | | | | |
| 30.04 | - 383 | -0.924 | +3.6* | -360 | -0.971 | -1 059 | -2.701 | + 3.4 | 2.7 |
| 30.05 | - 365 | -0.886 | +5.0 | -392 | -1.058 | -1 080 | -2.774 | + 5.4 | 1.9 |
| 30.06 | - 380 | -0.930 | +5.4 | -275 | -0.781 | - 938 | -2.453 | + 6.1 | 2.6 |
| *2-Alkanones* | | | | | | | | | |
| 31.04 | - 655 | -1.109 | -4.2** | -693 | -1.612 | -1 803 | -3.591 | - 8.2 | 4.8 |
| 31.05 | - 598 | -1.032 | -3.5[s] | -563 | -1.307 | -1 551 | -3.085 | - 6.9 | 2.1 |

(Continued on pages 418 and 419)

Table 9 (*continued*)

| No. | Compound | Temp. range (°C) | n | Retention index : C78 / PCN | | | | | | |
|---|---|---|---|---|---|---|---|---|---|---|
| | | | | PCN- C78 | | Mixture | | id([CN] =1) - C78 | | σ |
| | | | | $\Delta I_{130}$ | $10 \times \Delta A_T$ ($K^{-1}$) | $A_L$ | $10 \times A_{LT}$ ($K^{-1}$) | $\Delta I_{130}$ ($l\ mol^{-1}$) | $10 \times \Delta A_T$ ($K^{-1} l\ mol^{-1}$) | |
| 31.06 | 2-Hexanone | 90-170 | 15 | +57.1 | -0.39 | +17.9 | -0.55* | +107.4 | -0.36 | 0.47 |
| 31.07 | 2-Heptanone | 90-170 | 15 | +57.6 | -0.28s | +18.5 | -0.36** | +108.9 | +0.08 | 0.60 |
| *Aldehydes* | | | | | | | | | | |
| 32.05 | Pentanal | 90-170 | 15 | +50.5 | -0.68 | +15.8 | -1.42 | + 94.8 | -2.14 | 0.42 |
| 32.06 | Hexanal | 90-170 | 15 | +51.9 | -0.48 | +14.9 | -0.74 | + 95.6 | -0.87 | 0.27 |
| 32.07 | Heptanal | 90-170 | 15 | +52.6 | -0.29 | +16.1 | -0.71 | + 98.3 | -0.53 | 0.19 |
| *Ethers* | | | | | | | | | | |
| 33.06 | Dipropylether | 90-170 | 15 | +12.9 | -0.29 | + 3.8 | +0.05** | + 23.9 | -0.13 | 0.12 |
| 33.08 | Dibutylether | 90-170 | 15 | +12.6 | -0.07* | + 3.7 | +0.11** | + 23.4 | +0.27 | 0.17 |
| *Halomethanes* | | | | | | | | | | |
| 37.01 | Dichloromethane | 90-170 | 15 | +42.8 | +0.26s | +12.4 | -0.21** | + 79.1 | +0.79 | 0.58 |
| 37.02 | Trichloromethane | 90-170 | 15 | +40.3 | -0.34 | +11.9 | -0.65* | + 74.7 | -0.74 | 0.48 |
| 37.03 | Tetrachloromethane | 90-170 | 15 | +10.3 | -0.07** | - 0.2** | -0.46* | + 14.4 | -0.63 | 0.41 |
| 37.04 | $CF_2Br_2$ | 90-170 | 15 | +14.8 | -0.68s | - 0.9** | +0.91** | + 19.9 | +0.51 | 1.35 |
| *HALOBENZENES* | | | | | | | | | | |
| 38.01 | Fluorobenzene | 90-170 | 15 | +30.9 | -0.03** | + 6.2 | +0.25** | + 53.2 | +0.80 | 0.28 |
| 38.02 | Hexafluorobenzene | 90-170 | 15 | +31.1 | -0.13** | +11.2 | -0.24** | + 60.6 | +0.02 | 0.43 |
| 38.03 | Trifluoromethylbenzene | 90-170 | 15 | +38.0 | +0.14* | +11.4 | +0.32** | + 70.8 | +1.31 | 0.37 |
| 38.04 | Chlorobenzene | 90-170 | 15 | +32.6 | +0.24* | + 5.2 | +0.65* | + 54.3 | +1.77 | 0.59 |
| 38.05 | Bromobenzene | 90-170 | 15 | +35.0 | +0.28* | + 4.2 | +0.88* | + 56.3 | +2.18 | 0.70 |
| 38.06 | Iodobenzene | 130-210 | 15 | +36.9 | +0.76 | + 4.4* | +0.52** | + 59.3 | +2.37 | 0.80 |
| *ALKYLPYRIDINES* | | | | | | | | | | |
| 39.01 | Pyridine | 90-170 | 15 | +53.7 | -0.30s | +15.5 | -0.29** | + 99.1 | +0.06 | 0.64 |
| 39.02 | 2-Picoline | 90-170 | 15 | +46.8 | -0.30* | +13.2 | -0.30** | + 85.9 | -0.07 | 0.88 |
| 39.03 | 3-Picoline | 90-170 | 15 | +57.1 | -0.18** | +18.4 | -0.17** | +108.1 | +0.49 | 0.95 |
| 39.04 | 4-Picoline | 90-170 | 15 | +58.8 | -0.39* | +19.2 | -0.75** | +111.6 | -0.61 | 1.04 |
| 39.05 | 2,3-Lutidine | 130-210 | 15 | +50.6 | +0.04** | +13.2 | +0.47** | + 91.5 | +1.57 | 0.68 |
| 39.06 | 2,4-Lutidine | 130-210 | 15 | +50.2 | +0.07** | +14.8 | +0.15** | + 93.2 | +1.17 | 0.79 |
| 39.07 | 2,5-Lutidine | 130-210 | 15 | +47.9 | +0.26 | +12.6 | +0.34* | + 86.7 | +1.65 | 0.24 |
| 39.08 | 2,6-Lutidine | 130-210 | 15 | +40.5 | -0.65 | +12.4 | -0.90s | + 75.6 | -1.53 | 0.62 |

| No. | Thermodynamic data : C78 / PCN | | | | | | | | |
|---|---|---|---|---|---|---|---|---|---|
| | PCN - C78 | | | Mixture | | id([CN] =1) - C78 | | | σ |
| | $\Delta H$ (cal mol$^{-1}$) | $\Delta S$ (cal mol$^{-1}$K$^{-1}$) | $\Delta C_P$ | $h$ (cal mol$^{-1}$) | $s$ (cal mol$^{-1}$ K$^{-1}$) | $\Delta'H$ (cal l mol$^{-2}$) | $\Delta'S$ (cal l mol$^{-2}$K$^{-1}$) | $\Delta'C_P$ | (cal mol$^{-1}$) |
| 31.06 | - 581 | -0.994 | -4.5 | -478 | -1.104 | -1 410 | -2.751 | - 8.1 | 0.6 |
| 31.07 | - 582 | -1.009 | -4.3 | -442 | -1.014 | -1 363 | -2.649 | - 7.7 | 1.9 |
| *Aldehydes* | | | | | | | | | |
| 32.05 | - 556 | -0.959 | -0.3** | -670 | -1.584 | -1 649 | -3.386 | - 2.5 | 2.4 |
| 32.06 | - 542 | -0.955 | -1.8** | -500 | -1.190 | -1 400 | -2.850 | - 4.3 | 1.7 |
| 32.07 | - 515 | -0.897 | -1.8* | -493 | -1.164 | -1 352 | -2.732 | - 4.2 | 1.2 |
| *Ethers* | | | | | | | | | |
| 33.06 | - 100 | -0.363 | -2.1 | -218 | -0.642 | - 490 | -1.522 | - 3.9 | 0.7 |
| 33.08 | - 77 | -0.327 | -3.3 | -202 | -0.611 | - 441 | -1.442 | - 5.5 | 0.5 |
| *Halomethanes* | | | | | | | | | |
| 37.01 | - 268 | -0.336 | -6.1 | -365 | -0.877 | - 838 | -1.574 | - 9.6 | 3.0 |
| 37.02 | - 389 | -0.720 | -2.8** | -460 | -1.129 | -1 159 | -2.513 | - 5.5 | 2.9 |
| 37.03 | - 35* | -0.239 | -2.6* | -290 | -0.869 | - 516 | -1.706 | - 4.7 | 2.4 |
| 37.04 | - 177 | -0.526 | +7.0** | + 40** | -0.060** | - 233 | -0.925 | + 9.3 | 7.1 |
| *HALOBENZENES* | | | | | | | | | |
| 38.01 | - 236 | -0.466 | -3.4 | -197 | -0.556 | - 606 | -1.432 | - 5.7 | 1.5 |
| 38.02 | - 235 | -0.424 | -4.1 | -352 | -0.862 | - 805 | -1.755 | - 6.9 | 1.9 |
| 38.03 | - 269 | -0.454 | -3.6 | -232 | -0.575 | - 674 | -1.372 | - 5.9 | 1.6 |
| 38.04 | - 230 | -0.455 | -4.4* | - 96** | -0.328** | - 460 | -1.106 | - 6.9 | 3.0 |
| 38.05 | - 257 | -0.502 | -4.4* | - 35** | -0.195** | - 413 | -0.982 | - 6.8 | 3.2 |
| 38.06 | - 257* | -0.505* | -0.9** | -141** | -0.456** | - 560 | -1.352 | - 2.1 | 4.2 |
| *ALKYLPYRIDINES* | | | | | | | | | |
| 39.01 | - 523 | -0.908 | +0.8** | -408 | -0.961 | -1 240 | -2.455 | - 0.4 | 2.8 |
| 39.02 | - 471 | -0.882 | +2.3** | -389 | -0.949 | -1 163 | -2.459 | + 1.7 | 4.2 |
| 39.03 | - 557 | -0.972 | +2.5** | -404 | -0.922 | -1 274 | -2.464 | + 1.9 | 4.7 |
| 39.04 | - 616 | -1.102 | +4.9* | -537 | -1.239 | -1 538 | -3.082 | + 5.0 | 2.9 |
| 39.05 | - 589 | -1.125 | +1.6** | -246 | -0.597 | -1 119 | -2.285 | + 0.8 | 2.2 |
| 39.06 | - 570 | -1.083 | +1.3** | -303 | -0.722 | -1 172 | -2.397 | + 0.3 | 3.7 |
| 39.07 | - 425 | -0.756 | -1.0** | -250 | -0.617 | - 904 | -1.815 | - 2.5 | 1.1 |
| 39.08 | - 602 | -1.278 | +1.5** | -458 | -1.134 | -1 462 | -3.319 | + 0.1 | 2.4 |

(*Continued on pages 420 and 421*)

Table 9 (*continued*)

| No. | Compound | Temp. range (°C) | n | Retention index : C78 / PCN | | | | | | σ |
|---|---|---|---|---|---|---|---|---|---|---|
| | | | | PCN- C78 | | Mixture | | id([CN] =1) - C78 | | |
| | | | | $\Delta I_{130}$ | $10 \times \Delta A_T$ ($K^{-1}$) | $A_L$ | $10 \times A_{LT}$ ($K^{-1}$) | $\Delta' I_{130}$ ($l\ mol^{-1}$) | $10 \times \Delta' A_T$ ($K^{-1} l\ mol^{-1}$) | |
| 39.09 | 3,4-Lutidine | 130-210 | 15 | +66.0 | -0.66 | +23.0 | -1.01 | +127.3 | -1.23 | 0.49 |
| 39.10 | 3,5-Lutidine | 130-210 | 15 | +61.1 | -0.58 | +21.2 | -1.05 | +117.7 | -1.26 | 0.51 |
| 39.11 | 2-Ethylpyridine | 130-210 | 15 | +42.9 | -0.31 | +10.9 | -0.61* | + 76.9 | -0.61 | 0.47 |
| 39.12 | 3-Ethylpyridine | 130-210 | 15 | +53.1 | -0.19s | +11.2 | -1.07 | + 91.9 | -0.96 | 0.42 |
| 39.13 | 4-Ethylpyridine | 130-210 | 15 | +57.6 | -0.25 | +14.8 | -0.16 | +103.7 | +0.36 | 0.65 |
| 39.14 | 2-Propylpyridine | 130-210 | 15 | +41.7 | -0.73 | + 8.5 | -0.34 | + 71.8 | -0.88 | 0.39 |
| 39.15 | 4-Propylpyridine | 130-210 | 15 | +56.1 | +0.53 | +12.8 | +1.31 | + 98.9 | +3.54 | 0.67 |
| 39.16 | 2,3,6-Collidine | 130-210 | 15 | +40.4 | -0.12* | + 9.6 | -0.47s | + 71.6 | -0.19 | 0.31 |
| 39.17 | 2,4,6-Collidine | 130-210 | 15 | +41.7 | -0.37 | +11.0 | -0.49 | + 75.4 | -0.54 | 0.27 |
| 39.18 | 4-*tert*-Butylpyridine | 130-210 | 15 | +57.2 | -0.48 | +17.5 | -0.99 | +106.9 | -1.13 | 0.37 |
| 39.19 | 3-Chloropyridine | 90-170 | 15 | +48.6 | +0.02** | +10.0 | -0.08** | + 83.9 | +0.68 | 0.46 |
| *ORGANOSILICON COMPOUNDS* | | | | | | | | | | |
| 40.01 | Tetramethylsilane | 90-170 | 15 | + 2.6 | +0.33s | + 6.7 | -0.17** | + 13.3 | +0.35 | 0.71 |
| 40.02 | Hexamethyldisilane | 90-170 | 15 | + 1.6 | +0.11* | + 2.6 | -0.40* | + 5.9 | -0.36 | 0.34 |
| 40.03 | Hexamethyldisiloxane | 90-170 | 15 | + 0.4** | -0.04** | + 2.8 | -0.64* | + 4.5 | -0.93 | 0.51 |
| *MISCELLANEOUS* | | | | | | | | | | |
| 41.01 | Carbon disulphide | 90-170 | 15 | + 8.0 | -0.81s | - 3.3** | +0.61** | + 6.7 | -0.23 | 1.63 |
| 41.02 | Tetramethyltin | 90-170 | 15 | + 5.8 | +0.38 | - 0.3** | +1.08 | + 8.0 | +2.16 | 0.31 |
| 41.03 | Tetrahydrofuran | 90-170 | 15 | +32.3 | -0.03** | + 8.4 | -0.28** | + 58.3 | +0.09** | 0.38 |
| 41.04 | 1,4-Dioxane | 90-170 | 15 | +40.7 | -0.12** | + 8.4 | -0.33** | + 70.3 | +0.00** | 0.39 |
| 41.05 | Thiophene | 90-170 | 15 | +27.8 | +0.82 | + 4.3 | +0.82 | + 46.2 | +2.77 | 0.56 |
| 41.06 | Cyclopentanone | 90-170 | 15 | +67.6 | -0.23 | +20.6 | -0.91 | +126.2 | -0.48 | 0.41 |
| 41.07 | Cyclohexanone | 90-170 | 15 | +68.4 | +0.19** | +21.3 | -0.59** | +128.5 | +0.60 | 0.76 |
| 41.08 | Cyclohexanol | 90-170 | 15 | +61.9 | -1.76 | +21.8 | -1.29* | +119.6 | -3.27 | 0.94 |
| 41.11 | Nitrobenzene | 130-210 | 15 | +81.7 | +0.35 | +22.9 | -0.35** | +149.9 | +1.37 | 0.46 |
| 41.12 | Benzyl alcohol | 130-210 | 15 | +99.4 | -1.41 | +36.2 | -0.57** | +194.1 | -1.06 | 0.95 |
| 41.13 | 2-Phenylethanol | 130-210 | 15 | +91.7 | -1.06 | +31.9 | -0.69s | +176.9 | -0.89 | 0.42 |
| 41.14 | Anisole | 130-210 | 15 | +42.9 | +0.01** | + 9.0 | -0.11** | + 74.3 | +0.54 | 0.29 |
| 41.15 | Phenetole | 130-210 | 15 | +40.1 | +0.14* | + 7.6 | +0.56* | + 68.4 | +1.63 | 0.43 |
| *ERRORS:* | *f (n-alkanes)* | *90-210* | | *def.* | | | | | | |
| | *f (n-alkanes)* | *150-210* | | *def.* | | | | | | |
| | *f (solutes)* | *90-170* | | *0.65* | *0.22* | *2.19* | *0.77* | *3.28* | *1.13* | |
| | *f (solutes)* | *130-210* | | *1.10* | *0.23* | *3.83* | *0.78* | *5.58* | *1.15* | |
| *CONVERSION TO $K_D$:* | | | | *0* | *0* | *0* | *0* | *0* | *0* | |

Table 9 (*continued*)

| No. | Thermodynamic data : C78 / PCN | | | | | | | | |
|---|---|---|---|---|---|---|---|---|---|
| | PCN - C78 | | | Mixture | | id([CN] =1) - C78 | | | σ |
| | ΔH (cal mol$^{-1}$) | ΔS (cal mol$^{-1}$K$^{-1}$) | ΔC$_P$ | h (cal mol$^{-1}$) | s (cal mol$^{-1}$ K$^{-1}$) | Δ'H (cal l mol$^{-2}$) | Δ'S (cal l mol$^{-2}$K$^{-1}$) | Δ'C$_P$ | (cal mol$^{-1}$) |
| 39.09 | - 882 | -1.668 | +3.1[s] | -571 | -1.288 | -1 942 | -3.900 | + 1.9 | 1.9 |
| 39.10 | - 778 | -1.469 | +1.8** | -579 | -1.325 | -1 820 | -3.706 | + 0.2 | 2.1 |
| 39.11 | - 527 | -1.065 | +0.4** | -400 | -1.010 | -1 273 | -2.841 | - 1.2 | 2.0 |
| 39.12 | - 593 | -1.109 | +0.3** | -485 | -1.220 | -1 466 | -3.149 | - 1.5 | 2.1 |
| 39.13 | - 732 | -1.392 | +2.5* | -376 | -0.901 | -1 488 | -3.045 | + 1.6 | 1.8 |
| 39.14 | - 462 | -0.939 | -2.3[s] | -332 | -0.873 | -1 099 | -2.502 | - 4.8 | 1.4 |
| 39.15 | - 512 | -0.880 | +0.6** | - 38** | -0.096** | - 710 | -1.213 | + 0.1 | 3.4 |
| 39.16 | - 431 | -0.876 | -0.1** | -349 | -0.906 | -1 078 | -2.458 | - 1.7 | 1.5 |
| 39.17 | - 532 | -1.105 | +1.1** | -372 | -0.943 | -1 245 | -2.815 | - 0.2 | 1.1 |
| 39.18 | - 679 | -1.290 | -0.4** | -524 | -1.242 | -1 625 | -3.390 | - 2.7 | 1.9 |
| 39.19 | - 517 | -0.969 | +0.1** | -305 | -0.785 | -1 114 | -2.361 | - 1.3 | 1.4 |
| *ORGANOSILICON COMPOUNDS* | | | | | | | | | |
| 40.01 | + 167 | +0.195[s] | -7.7 | -308 | -0.813 | - 253 | -1.006 | -11.5 | 3.7 |
| 40.02 | + 96 | -0.026** | -3.3[s] | -310 | -0.883 | - 372 | -1.459 | - 5.5 | 2.0 |
| 40.03 | + 92 | -0.045** | -2.9** | -363 | -1.009 | - 454 | -1.665 | - 5.1 | 2.8 |
| *MISCELLANEOUS* | | | | | | | | | |
| 41.01 | - 162[s] | -0.595 | +6.1** | - 25** | -0.255** | - 328 | -1.362 | + 7.8 | 8.5 |
| 41.02 | + 122 | +0.097 | -3.3 | + 45** | -0.042** | + 171 | -0.085 | - 4.6 | 1.8 |
| 41.03 | - 242 | -0.458 | -3.9 | -334 | -0.864 | - 800 | -1.834 | - 6.6 | 1.5 |
| 41.04 | - 363 | -0.654 | -4.7 | -336 | -0.867 | - 956 | -2.070 | - 7.9 | 1.6 |
| 41.05 | - 41* | -0.022** | -5.9 | - 71** | -0.270** | - 166 | -0.431 | - 8.5 | 2.9 |
| 41.06 | - 662 | -1.072 | -1.2** | -569 | -1.289 | -1 622 | -3.046 | - 3.6 | 2.4 |
| 41.07 | - 606 | -0.947 | +0.2** | -527 | -1.185 | -1 485 | -2.725 | - 1.4 | 3.9 |
| 41.08 | - 931 | -1.845 | +6.1 | -674 | -1.545 | -2 165 | -4.533 | + 5.8 | 2.3 |
| 41.11 | - 699 | -1.038 | -2.4** | -461 | -1.013 | -1 499 | -2.549 | - 5.0 | 2.4 |
| 41.12 | -1 552 | -2.904 | +9.3 | -619 | -1.238 | -2 848 | -5.310 | + 9.8 | 1.0 |
| 41.13 | -1 198 | -2.146 | +2.2** | -604 | -1.257 | -2 363 | -4.352 | + 0.4 | 1.6 |
| 41.14 | - 381 | -0.714 | -1.3** | -302 | -0.791 | - 936 | -2.052 | - 3.1 | 1.5 |
| 41.15 | - 334 | -0.643 | +0.9** | -140 | -0.411 | - 649 | -1.438 | + 0.4 | 1.9 |
| *E(contd)* | *4.5* | *0.0091* | *0.38* | *7.8* | *0.0176* | *17.4* | *0.0378* | *0.54* | |
| | *4.5* | *0.0091* | *0.38* | *7.8* | *0.0176* | *17.4* | *0.0378* | *0.54* | |
| | *9.1* | *0.0224* | *0.76* | *31.4* | *0.0776* | *46.1* | *0.1131* | *1.07* | |
| | *33.8* | *0.0812* | *0.84* | *34.5* | *0.0776* | *68.3* | *0.1580* | *1.19* | |
| *C(contd)* | - *0* | *-0.029* | *-0.0* | - *1* | *-0.003* | - *1* | *-0.045* | - *0.1* | |

Table 10
Retention indices and thermodynamic data for 152 solutes in C78/PSH mixtures where data for an ideal solvent with X = PSH, idPSH, are also given. For symbols and explanations see Table 8.

| No. | Compound | Temp. range (°C) | n | Retention index : C78 / PSH | | | | | | |
|---|---|---|---|---|---|---|---|---|---|---|
| | | | | PSH- C78 | | Mixture | | id([SH] =1) - C78 | | σ |
| | | | | $\Delta I_{130}$ | $10 \times \Delta A_T$ ($K^{-1}$) | $A_L$ | $10 \times A_{LT}$ ($K^{-1}$) | $\Delta' I_{130}$ ($l\ mol^{-1}$) | $10 \times \Delta' A_T$ ($K^{-1} l\ mol^{-1}$) | |
| *HYDROCARBONS* | | | | | | | | | | |
| *n-Alkanes* | | | | | | | | | | |
| 00.05 | Pentane | 90-210 | 21 | | | | | | | |
| 00.06 | Hexane | 90-210 | 21 | | | | | | | |
| 00.07 | Heptane | 90-210 | 21 | | | | | | | |
| 00.08 | Octane | 90-210 | 21 | | | | | | | |
| 00.09 | Nonane | 90-210 | 21 | | | | | | | |
| 00.10 | Decane | 90-210 | 21 | | | | | | | |
| 00.11 | Undecane | 150-210 | 12 | | | | | | | |
| 00.12 | Dodecane | 150-210 | 12 | | | | | | | |
| 00.13 | Tridecane | 150-210 | 12 | | | | | | | |
| 00.14 | Tetradecane | 150-210 | 12 | | | | | | | |
| *Isoalkanes* | | | | | | | | | | |
| 10.01 | 2,2-Dimethylbutane | 90-170 | 15 | - 1.5 | -0.28$^{s}$ | + 2.4 | +1.00 | + 1.4 | +1.09 | 0.29 |
| 10.02 | 2,3-Dimethylbutane | 90-170 | 15 | - 1.6 | -0.34$^{**}$ | + 3.2 | +0.84$^{*}$ | + 2.5 | +0.77 | 0.63 |
| 10.03 | 2,2-Dimethylpentane | 90-170 | 15 | - 1.2 | -0.37 | + 0.9 | +0.36 | - 0.5 | -0.02 | 0.09 |
| 10.04 | 2,3-Dimethylpentane | 90-170 | 15 | - 0.4 | -0.04$^{**}$ | + 0.8$^{s}$ | +0.08$^{**}$ | + 0.6 | +0.07 | 0.19 |
| 10.05 | 2,4-Dimethylpentane | 90-170 | 15 | - 1.2 | -0.66 | + 1.8$^{s}$ | +0.62$^{*}$ | + 0.9 | -0.05 | 0.41 |
| 10.06 | 2,2-Dimethylhexane | 90-170 | 15 | - 1.1 | -0.22 | + 0.2$^{**}$ | +0.12$^{**}$ | - 1.4 | -0.16 | 0.11 |
| 10.07 | 2,3-Dimethylhexane | 90-170 | 15 | - 0.3$^{*}$ | -0.19 | + 0.8$^{**}$ | +0.32$^{**}$ | + 0.8 | +0.20 | 0.30 |
| 10.08 | 2,4-Dimethylhexane | 90-170 | 15 | - 1.2 | -0.09 | + 0.2$^{**}$ | +0.36 | - 1.5 | +0.39 | 0.21 |
| 10.09 | 3,4-Dimethylhexane | 90-170 | 15 | + 0.0$^{**}$ | +0.17$^{s}$ | - 0.6$^{**}$ | -0.04$^{**}$ | - 0.9 | +0.19 | 0.19 |
| 10.10 | 2,2,3-Trimethylbutane | 90-170 | 15 | - 1.2 | +0.66 | + 0.1$^{**}$ | +0.18$^{**}$ | - 1.6 | +1.25 | 0.32 |
| 10.11 | 2,2,4-Trimethylpentane | 90-170 | 15 | - 1.5 | +0.20 | - 0.4$^{**}$ | +0.10$^{**}$ | - 2.8 | +0.43 | 0.20 |
| 10.12 | 2,3,4-Trimethylpentane | 90-170 | 15 | - 0.1$^{**}$ | +0.20$^{*}$ | + 0.1$^{**}$ | +0.44$^{*}$ | + 0.1 | +0.96 | 0.28 |
| *1-Alkenes* | | | | | | | | | | |
| 11.05 | 1-Pentene | 90-170 | 15 | + 1.1 | -1.56 | + 1.7$^{*}$ | -0.44$^{**}$ | + 3.9 | -2.97 | 0.45 |
| 11.06 | 1-Hexene | 90-170 | 15 | + 2.2 | -1.05 | + 1.4$^{*}$ | -0.82$^{s}$ | + 5.2 | -2.76 | 0.45 |
| 11.07 | 1-Heptene | 90-170 | 15 | + 2.6 | -0.78 | + 3.2 | -0.38 | + 8.6 | -1.66 | 0.15 |
| 11.08 | 1-Octene | 90-170 | 15 | + 2.2 | -0.53 | + 1.8 | -0.84 | + 5.9 | -2.01 | 0.16 |
| 11.09 | 1-Nonene | 90-170 | 15 | + 2.7 | -0.24 | + 0.7$^{**}$ | -0.64$^{s}$ | + 5.0 | -1.28 | 0.35 |
| 11.10 | 1-Decene | 90-170 | 15 | + 2.4 | -0.21$^{s}$ | + 0.4$^{**}$ | -0.46$^{s}$ | + 4.1 | -0.97 | 0.25 |

| No. | Thermodynamic data : C78 / PSH | | | | | | | | |
|---|---|---|---|---|---|---|---|---|---|
| | PSH - C78 | | | Mixture | | id([SH] =1) - C78 | | | σ |
| | ΔH | ΔS | $\Delta C_P$ | h | s | Δ'H | Δ'S | $\Delta' C_P$ | |
| | (cal mol$^{-1}$) | (cal mol$^{-1}$K$^{-1}$) | | (cal mol$^{-1}$) | (cal mol$^{-1}$ K$^{-1}$) | (cal l mol$^{-2}$) | (cal l mol$^{-2}$K$^{-1}$) | | (cal mol$^{-1}$) |
| *HYDROCARBONS* | | | | | | | | | |
| *n-Alkanes* | | | | | | | | | |
| 00.05 | + 80 | -0.021 | +0.6 | + 77 | +0.073 | + 165 | -0.070 | +0.8 | 6.1 |
| 00.06 | + 89 | -0.012 | +0.4 | + 92 | +0.073 | + 191 | -0.081 | +0.5 | 5.9 |
| 00.07 | + 99 | -0.003 | +0.1 | +107 | +0.073 | + 216 | -0.090 | +0.1 | 5.7 |
| 00.08 | +109 | +0.007 | -0.2 | +121 | +0.073 | + 241 | -0.097 | -0.3 | 4.8 |
| 00.09 | +119 | +0.016 | -0.5 | +136 | +0.073 | + 267 | -0.108 | -0.7 | 4.2 |
| 00.10 | +129 | +0.025 | -0.7 | +151 | +0.073 | + 293 | -0.119 | -1.0 | 4.6 |
| 00.11 | +138 | +0.034 | -1.0 | +165 | +0.073 | + 317 | -0.127 | -1.5 | 5.3 |
| 00.12 | +148 | +0.043 | -1.3 | +180 | +0.073 | + 343 | -0.138 | -1.9 | 4.8 |
| 00.13 | +158 | +0.052 | -1.6 | +195 | +0.073 | + 370 | -0.148 | -2.3 | 5.1 |
| 00.14 | +168 | +0.061 | -1.9 | +210 | +0.073 | + 395 | -0.159 | -2.7 | 6.2 |
| *Isoalkanes* | | | | | | | | | |
| 10.01 | + 66 | -0.084 | +1.0** | +211 | +0.421 | + 333 | +0.329 | +1.6 | 1.4 |
| 10.02 | + 66$^s$ | -0.097** | +4.2* | +168* | +0.315 | + 272 | +0.161 | +6.1 | 3.2 |
| 10.03 | + 63 | -0.097 | +0.7* | + 80 | +0.046** | + 133 | -0.246 | +0.9 | 0.6 |
| 10.04 | + 94 | -0.017** | +0.4** | + 97 | +0.069** | + 198 | -0.107 | +0.5 | 1.1 |
| 10.05 | + 34* | -0.171 | +1.2** | + 65** | +0.021** | + 73 | -0.381 | +1.5 | 2.3 |
| 10.06 | + 87 | -0.049 | +0.0** | + 82 | +0.009** | + 160 | -0.255 | -0.1 | 0.7 |
| 10.07 | + 87 | -0.047** | +0.3** | +130 | +0.118** | + 227 | -0.099 | +0.4 | 1.6 |
| 10.08 | +104 | -0.012** | +0.4** | +163 | +0.204$^s$ | + 298 | +0.071 | +0.6 | 1.2 |
| 10.09 | +122 | +0.042* | -0.1** | +147 | +0.137* | + 297 | +0.044 | -0.1 | 1.1 |
| 10.10 | +174 | +0.170 | +1.3** | +269 | +0.493 | + 554 | +0.757 | +2.3 | 1.5 |
| 10.11 | +133 | +0.060 | +0.3** | +164 | +0.212 | + 341 | +0.187 | +0.6 | 0.9 |
| 10.12 | +126 | +0.047 | +1.6 | +239 | +0.378 | + 436 | +0.399 | +2.5 | 0.6 |
| *1-Alkenes* | | | | | | | | | |
| 11.05 | -107 | -0.469 | +2.7** | -386 | -1.042 | - 749 | -2.266 | +2.6 | 2.5 |
| 11.06 | - 50$^s$ | -0.331 | +3.4* | -342 | -0.975 | - 613 | -1.993 | +3.7 | 2.4 |
| 11.07 | - 10* | -0.241 | +1.3 | -174 | -0.574 | - 323 | -1.310 | +1.1 | 0.7 |
| 11.08 | + 30 | -0.159 | +0.5** | -184 | -0.652 | - 293 | -1.336 | -0.0 | 0.9 |
| 11.09 | + 66 | -0.082 | +0.9 | - 54 | -0.383 | - 69 | -0.872 | +0.8 | 1.7 |
| 11.10 | + 82 | -0.061 | +0.8** | + 6 | -0.275 | + 29 | -0.715 | +0.8 | 0.9 |

(Continued on pages 424 and 425)

Table 10 (*continued*)

| No. | Compound | Temp. range | n | Retention index : C78 / PSH | | | | | | |
|---|---|---|---|---|---|---|---|---|---|---|
| | | | | PSH- C78 | | Mixture | | id([SH] =1) - C78 | | σ |
| | | | | $\Delta I_{130}$ | $10 \times \Delta A_T$ | $A_L$ | $10 \times A_{LT}$ | $\Delta I_{130}$ | $10 \times \Delta A_T$ | |
| | | (°C) | | | ($K^{-1}$) | | ($K^{-1}$) | ($l\ mol^{-1}$) | ($K^{-1} l\ mol^{-1}$) | |
| *1-Alkynes* | | | | | | | | | | |
| 12.05 | 1-Pentyne | 90-170 | 15 | + 6.6 | +0.09** | + 2.2$^s$ | -1.04 | +13.1 | -1.31 | 0.49 |
| 12.06 | 1-Hexyne | 90-170 | 15 | + 7.2 | -0.02** | + 1.5 | -0.92 | +12.9 | -1.29 | 0.22 |
| 12.07 | 1-Heptyne | 90-170 | 15 | + 7.5 | +0.19* | + 2.3 | -0.56$^s$ | +14.7 | -0.42 | 0.32 |
| 12.08 | 1-Octyne | 90-170 | 15 | + 7.4 | +0.31 | + 1.1* | -0.94 | +12.7 | -0.83 | 0.29 |
| 12.09 | 1-Nonyne | 90-170 | 15 | + 7.5 | +0.60 | + 0.1** | -0.84 | +11.4 | -0.26 | 0.35 |
| 12.10 | 1-Decyne | 90-170 | 15 | + 7.4 | +0.50 | + 1.9 | -0.18** | +14.0 | +0.61 | 0.31 |
| *Alkynes* | | | | | | | | | | |
| 13.01 | 2-Hexyne | 90-170 | 15 | + 6.2 | -0.01** | + 1.7 | -0.12** | +11.9 | -0.09 | 0.31 |
| 13.02 | 3-Hexyne | 90-170 | 15 | + 5.7 | -0.34$^s$ | + 1.4* | +0.46** | +10.7 | +0.28 | 0.39 |
| 13.03 | 4-Octyne | 90-170 | 15 | + 5.0 | -0.14** | + 0.2** | +0.34 | + 7.8 | +0.37 | 0.42 |
| *Monocyclic hydrocarbons* | | | | | | | | | | |
| 14.05 | Cyclopentane | 90-170 | 15 | + 2.7 | -0.45* | - 0.2** | -0.10** | + 3.7 | -0.79 | 0.58 |
| 14.06 | Cyclohexane | 90-170 | 15 | + 2.6 | -0.12** | + 0.6** | +0.40$^s$ | + 4.8 | +0.46 | 0.22 |
| 14.07 | Cycloheptane | 90-170 | 15 | + 3.9 | +0.49 | - 0.9** | -0.18** | + 4.5 | +0.51 | 0.31 |
| 14.08 | Cyclooctane | 90-170 | 15 | + 3.9 | +1.26 | - 0.7** | -0.56** | + 4.9 | +1.09 | 0.65 |
| 14.10 | Cyclodecane | 130-210 | 15 | + 4.4 | +0.84 | + 0.2** | -0.02** | + 7.0 | +1.29 | 0.63 |
| *Bicyclic hydrocarbons* | | | | | | | | | | |
| 15.01 | *cis*-Hydrindane | 130-210 | 15 | + 3.6 | +0.68 | - 1.2** | +0.19** | + 3.7 | +1.34 | 0.61 |
| 15.02 | *trans*-Hydrindane | 130-210 | 15 | + 1.2* | +0.94 | - 4.1* | +0.56** | - 4.2 | +2.22 | 0.60 |
| 15.03 | *cis*-Decalin | 130-210 | 15 | + 3.9 | +1.09 | - 0.8** | +0.50** | + 4.8 | +2.43 | 0.79 |
| 15.04 | *trans*-Decalin | 130-210 | 15 | + 2.8 | +0.68 | - 3.8* | +0.50** | - 1.4 | +1.76 | 0.69 |
| *Methylcyclohexanes (MCH)* | | | | | | | | | | |
| 16.01 | Methylcyclohexane | 90-170 | 15 | + 1.2 | -0.18** | - 0.2** | +0.54* | + 1.5 | +0.56 | 0.42 |
| 16.02 | *cis*-1,2-Di MCH | 90-170 | 15 | + 2.8 | -0.11** | + 0.6** | +0.46** | + 5.1 | +0.57 | 0.49 |
| 16.03 | *trans*-1,2-Di MCH | 90-170 | 15 | + 1.7 | -0.00** | + 1.0** | +0.20** | + 4.1 | +0.34 | 0.46 |
| 16.04 | *cis*-1,4-Di MCH | 90-170 | 15 | + 2.1 | -0.09** | + 0.6** | +0.04** | + 4.1 | -0.04 | 0.40 |
| 16.05 | *trans*-1,4-Di MCH | 90-170 | 15 | + 1.6 | -0.04** | + 1.5** | +0.46 | + 4.7 | +0.67 | 0.77 |
| *Cyclohexenes* | | | | | | | | | | |
| 17.01 | Cyclohexene | 90-170 | 15 | + 4.4 | -0.16** | + 0.3** | +0.74 | + 7.1 | +0.94 | 0.49 |
| 17.02 | 1,3-Cyclohexadiene | 90-170 | 15 | + 6.5 | -0.50* | + 1.8** | +0.84* | +12.5 | +0.62 | 0.62 |
| 17.03 | 1,4-Cyclohexadiene | 90-170 | 15 | + 7.6 | +0.26** | + 0.3** | -0.12** | +11.9 | +0.32 | 0.53 |

| No. | Thermodynamic data : C78 / PSH | | | | | | | | |
|---|---|---|---|---|---|---|---|---|---|
| | PSH - C78 | | | Mixture | | id([SH] =1) - C78 | | | σ |
| | ΔH (cal mol$^{-1}$) | ΔS (cal mol$^{-1}$K$^{-1}$) | ΔCP | h (cal mol$^{-1}$) | s (cal mol$^{-1}$ K$^{-1}$) | Δ'H (cal l mol$^{-2}$) | Δ'S (cal l mol$^{-2}$K$^{-1}$) | Δ'CP | (cal mol$^{-1}$) |
| *1-Alkynes* | | | | | | | | | |
| 12.05 | + 20* | -0.068s | -2.9 | -159 | -0.476 | - 234 | -0.864 | -4.6 | 1.4 |
| 12.06 | + 14** | -0.097 | -0.5** | -139 | -0.472 | - 223 | -0.921 | -1.2 | 1.3 |
| 12.07 | + 41 | -0.044** | -1.6** | - 2** | -0.159** | + 2 | -0.420 | -2.5 | 1.7 |
| 12.08 | + 66 | -0.003** | -0.3** | - 23** | -0.264s | - 4 | -0.541 | -0.7 | 1.6 |
| 12.09 | +103 | +0.071* | -0.2** | + 87** | -0.042** | + 193 | -0.149 | -0.3 | 2.0 |
| 12.10 | +103 | +0.057 | -1.6 | +195 | +0.211 | + 340 | +0.175 | -2.1 | 1.6 |
| *Alkynes* | | | | | | | | | |
| 13.01 | + 31* | -0.084s | +0.3** | + 56** | -0.009** | + 70 | -0.265 | +0.3 | 1.9 |
| 13.02 | - 3** | -0.163 | -2.1 | +110 | +0.128* | + 98 | -0.183 | -3.1 | 0.9 |
| 13.03 | + 44 | -0.088 | -2.2s | +165 | +0.179* | + 221 | -0.059 | -3.1 | 1.4 |
| *Monocyclic hydrocarbons* | | | | | | | | | |
| 14.05 | + 2** | -0.182 | -2.2** | - 42** | -0.256* | - 117 | -0.772 | -3.5 | 2.2 |
| 14.06 | + 50 | -0.089 | -0.5** | +141 | +0.167s | + 202 | -0.060 | -0.7 | 0.9 |
| 14.07 | +112 | +0.058** | -0.4** | +176 | +0.183** | + 326 | +0.138 | -0.5 | 1.9 |
| 14.08 | +197 | +0.258 | -1.5** | +266 | +0.360* | + 562 | +0.642 | -2.4 | 2.9 |
| 14.10 | +224s | +0.292** | -1.4** | +141** | -0.017** | + 408 | +0.117 | -1.9 | 3.0 |
| *Bicyclic hydrocarbons* | | | | | | | | | |
| 15.01 | +103** | +0.007** | +1.5** | +167* | +0.086** | + 284 | -0.114 | +2.1 | 2.7 |
| 15.02 | +198s | +0.216** | +0.8** | +260 | +0.291** | + 542 | +0.451 | +1.4 | 2.7 |
| 15.03 | +236* | +0.319** | -0.6** | +226* | +0.193** | + 545 | +0.453 | -0.6 | 3.9 |
| 15.04 | +176* | +0.162** | -0.4** | +253s | +0.238s | + 493 | +0.282 | -0.4 | 3.5 |
| *Methylcyclohexanes (MCH)* | | | | | | | | | |
| 16.01 | + 66 | -0.077* | -0.3** | +172s | +0.212** | + 259 | -0.005 | -0.4 | 2.4 |
| 16.02 | + 68 | -0.076s | +2.3* | +173 | +0.182** | + 258 | -0.057 | +3.3 | 1.7 |
| 16.03 | + 88 | -0.034** | +1.1** | +133s | +0.099** | + 231 | -0.114 | +1.5 | 2.0 |
| 16.04 | + 76 | -0.061* | +2.1* | + 94* | +0.001** | + 159 | -0.289 | +2.8 | 1.7 |
| 16.05 | + 84 | -0.044** | +2.8** | +173* | +0.213** | + 285 | +0.043 | +4.0 | 3.3 |
| *Cyclohexenes* | | | | | | | | | |
| 17.01 | + 30** | -0.119* | -0.0** | +209s | +0.327* | + 272 | +0.129 | +0.1 | 2.9 |
| 17.02 | - 26* | -0.239 | +2.1* | +145 | +0.196** | + 114 | -0.198 | +2.9 | 1.8 |
| 17.03 | + 48* | -0.043** | +2.0** | +127** | +0.118** | + 187 | -0.045 | +2.8 | 2.9 |

(Continued on pages 426 and 427)

Table 10 (*continued*)

| No. | Compound | Temp. range | n | Retention index : C78 / PSH | | | | | | |
|---|---|---|---|---|---|---|---|---|---|---|
| | | | | PSH- C78 | | Mixture | | id([SH] =1) - C78 | | σ |
| | | (°C) | | $\Delta I_{130}$ | $10 \times \Delta A_T$ ($K^{-1}$) | $A_L$ | $10 \times A_{LT}$ ($K^{-1}$) | $\Delta I'_{130}$ ($l\ mol^{-1}$) | $10 \times \Delta A'_T$ ($K^{-1} l\ mol^{-1}$) | |
| *Alkylbenzenes* | | | | | | | | | | |
| 18.00 | Benzene | 90-170 | 15 | + 9.7 | +0.76 | + 0.1** | -0.30** | +14.8 | +0.83 | 0.34 |
| 18.01 | Toluene | 90-170 | 15 | + 9.7 | +0.85 | + 0.9** | -0.22** | +16.0 | +1.09 | 0.38 |
| 18.02 | Ethylbenzene | 90-170 | 15 | + 9.9 | +0.82 | - 0.2** | +0.78s | +14.8 | +2.54 | 0.43 |
| *Miscellaneous* | | | | | | | | | | |
| 19.01 | Adamantane | 130-210 | 15 | + 5.8 | +1.18 | + 2.5** | -0.07** | +12.6 | +1.78 | 1.23 |
| 19.02 | Naphthalene | 130-210 | 15 | +18.6 | +0.70 | + 8.4s | -1.09** | +40.5 | -0.22 | 1.12 |
| 19.03 | Azulene | 130-210 | 15 | +21.4 | +1.36 | + 5.8 | +0.14 | +41.1 | +2.63 | 1.91 |
| *ALKANE DERIVATIVES* | | | | | | | | | | |
| *1-Fluoroalkanes* | | | | | | | | | | |
| 20.05 | 1-Fluoropentane | 90-170 | 15 | + 6.0 | -0.91 | + 0.2** | -0.56** | + 9.2 | -2.13 | 0.46 |
| 20.06 | 1-Fluorohexane | 90-170 | 15 | + 6.9 | -0.27s | + 1.6 | -0.36* | +12.7 | -0.83 | 0.28 |
| 20.07 | 1-Fluoroheptane | 90-170 | 15 | + 6.9 | -0.13 | + 1.9 | -0.10** | +13.2 | -0.23 | 0.11 |
| 20.08 | 1-Fluorooctane | 90-170 | 15 | + 7.1 | -0.19** | + 2.9 | +0.42* | +15.1 | +0.48 | 0.31 |
| *1,1,1-Trifluoroalkanes* | | | | | | | | | | |
| 21.08 | 1,1,1-Trifluorooctane | 90-170 | 15 | + 2.9 | -0.18** | + 3.6 | +0.66** | + 9.8 | +0.81 | 0.56 |
| 21.10 | 1,1,1-Trifluorodecane | 90-170 | 15 | + 2.9 | -0.53s | + 2.7 | +0.70* | + 8.4 | +0.33 | 0.53 |
| *1-Chloroalkanes* | | | | | | | | | | |
| 22.04 | 1-Chlorobutane | 90-170 | 15 | + 8.8 | -0.14** | + 0.2** | -0.40* | +13.5 | -0.69 | 0.31 |
| 22.05 | 1-Chloropentane | 90-170 | 15 | + 8.9 | +0.66 | + 0.4** | -0.22** | +14.0 | +0.79 | 0.39 |
| 22.06 | 1-Chlorohexane | 90-170 | 15 | + 9.0 | +0.50 | + 1.4** | +0.16** | +15.7 | +1.13 | 0.49 |
| *1-Bromoalkanes* | | | | | | | | | | |
| 23.03 | 1-Bromopropane | 90-170 | 15 | +11.2 | +0.40** | + 1.5** | -0.92** | +19.0 | -0.61 | 1.15 |
| 23.04 | 1-Bromobutane | 90-170 | 15 | +10.8 | +0.41** | + 2.5* | -0.12** | +20.0 | +0.62 | 0.79 |
| 23.05 | 1-Bromopentane | 90-170 | 15 | +10.8 | +0.32** | + 2.7** | +0.14** | +20.3 | +0.88 | 0.97 |
| *1-Cyanoalkanes* | | | | | | | | | | |
| 24.02 | Cyanoethane | 90-170 | 15 | +28.0 | +0.07** | +15.6 | -0.90** | +60.5 | -0.52 | 0.85 |
| 24.03 | 1-Cyanopropane | 90-170 | 15 | +23.9 | +0.77 | +13.3 | -0.94s | +55.9 | +0.25 | 0.49 |
| 24.04 | 1-Cyanobutane | 90-170 | 15 | +24.2 | +1.08 | +10.9 | -0.80** | +52.8 | +0.89 | 0.65 |
| 24.05 | 1-Cyanopentane | 90-170 | 15 | +24.6 | +1.13 | +10.6 | -0.72* | +52.9 | +1.09 | 0.45 |

| No. | Thermodynamic data : C78 / PSH | | | | | | | | |
|---|---|---|---|---|---|---|---|---|---|
| | PSH - C78 | | | Mixture | | id([SH] =1) - C78 | | | σ |
| | $\Delta H$ (cal mol$^{-1}$) | $\Delta S$ (cal mol$^{-1}$K$^{-1}$) | $\Delta C_P$ | $h$ (cal mol$^{-1}$) | $s$ (cal mol$^{-1}$ K$^{-1}$) | $\Delta'H$ (cal l mol$^{-2}$) | $\Delta'S$ (cal l mol$^{-2}$K$^{-1}$) | $\Delta'C_P$ | (cal mol$^{-1}$) |
| *Alkylbenzenes* | | | | | | | | | |
| 18.00 | + 73 | +0.059* | +0.4** | +179 | +0.261s | + 305 | +0.324 | +0.8 | 1.8 |
| 18.01 | + 87 | +0.083 | -3.1 | +225 | +0.346 | + 381 | +0.455 | -4.1 | 1.1 |
| 18.02 | + 91 | +0.078* | -2.6* | +445 | +0.841 | + 688 | +1.124 | -3.0 | 1.9 |
| *Miscellaneous* | | | | | | | | | |
| 19.01 | +109 | +0.039 | +2.5 | + 81** | -0.118** | + 176 | -0.345 | +3.4 | 4.4 |
| 19.02 | - 52** | -0.218** | +1.5** | -121** | -0.579* | - 309 | -1.288 | +1.4 | 4.7 |
| 19.03 | -122** | -0.363** | +5.2** | +116** | -0.063** | - 76 | -0.773 | +6.9 | 8.6 |
| *ALKANE DERIVATIVES* | | | | | | | | | |
| *1-Fluoroalkanes* | | | | | | | | | |
| 20.05 | - 79 | -0.334 | -1.3** | -245 | -0.741 | - 508 | -1.646 | -2.7 | 1.9 |
| 20.06 | - 1** | -0.160 | +1.6* | - 54** | -0.286 | - 131 | -0.764 | +1.9 | 1.2 |
| 20.07 | + 22 | -0.113 | -0.4** | + 46 | -0.072* | + 35 | -0.416 | -0.8 | 0.6 |
| 20.08 | + 23* | -0.124 | -1.6** | +147 | +0.151** | + 172 | -0.134 | -2.3 | 1.5 |
| *1,1,1-Trifluroalkanes* | | | | | | | | | |
| 21.08 | + 60 | -0.068** | +1.3** | +178 | +0.287* | + 274 | +0.154 | +1.9 | 2.4 |
| 21.10 | + 43* | -0.136s | -1.0** | +154* | +0.143** | + 195 | -0.199 | -1.5 | 2.9 |
| *1-Chloroalkanes* | | | | | | | | | |
| 22.04 | - 16** | -0.162 | -1.3** | - 30** | -0.239s | - 116 | -0.696 | -2.2 | 1.4 |
| 22.05 | + 77 | +0.055* | -2.6 | +191 | +0.269 | + 320 | +0.309 | -3.5 | 1.4 |
| 22.06 | + 66 | +0.015** | -3.7 | +237 | +0.359 | + 362 | +0.362 | -5.0 | 1.4 |
| *1-Bromoalkanes* | | | | | | | | | |
| 23.03 | + 9** | -0.054** | -6.9s | - 45** | -0.256** | - 94 | -0.548 | -9.1 | 4.2 |
| 23.04 | + 27* | -0.038** | -4.8 | +135s | +0.162 | + 178 | +0.048 | -6.8 | 1.9 |
| 23.05 | + 24** | -0.059 | -6.4 | +179s | +0.238** | + 227 | +0.103 | -8.9 | 2.6 |
| *1-Cyanoalkanes* | | | | | | | | | |
| 24.02 | -197 | -0.309 | -4.2* | -254 | -0.477 | - 576 | -0.928 | -6.7 | 3.3 |
| 24.03 | - 86 | -0.132 | +2.9 | -108s | -0.228s | - 252 | -0.454 | +3.8 | 1.5 |
| 24.04 | - 36s | -0.038** | +3.2 | + 27** | +0.019** | - 10 | -0.019 | +4.5 | 1.7 |
| 24.05 | - 29s | -0.031** | +1.7* | + 79* | +0.103** | + 63 | +0.083 | +2.5 | 1.4 |

(Continued on pages 428 and 429)

Table 10 (*continued*)

| No. | Compound | Temp. range (°C) | n | Retention index : C78 / PSH | | | | | | σ |
|---|---|---|---|---|---|---|---|---|---|---|
| | | | | PSH- C78 | | Mixture | | id([SH] =1) - C78 | | |
| | | | | $\Delta I_{130}$ | $10 \times \Delta A_T$ ($K^{-1}$) | $A_L$ | $10 \times A_{LT}$ ($K^{-1}$) | $\Delta I_{130}$ ($l\ mol^{-1}$) | $10 \times \Delta A_T$ ($K^{-1} l\ mol^{-1}$) | |
| *1-Nitroalkanes* | | | | | | | | | | |
| 25.02 | Nitroethane | 90-170 | 15 | +25.0 | +0.33 | + 8.1 | -1.50 | +49.6 | -1.31 | 0.30 |
| 25.03 | 1-Nitropropane | 90-170 | 15 | +23.2 | +0.37[s] | + 8.1 | -1.10 | +46.9 | -0.67 | 0.38 |
| 25.04 | 1-Nitrobutane | 90-170 | 15 | +23.0 | +0.48 | + 7.0 | -0.70* | +45.1 | +0.08 | 0.44 |
| 25.05 | 1-Nitropentane | 90-170 | 15 | +22.8 | +0.88 | + 7.6 | -1.00* | +45.7 | +0.23 | 0.79 |
| 1-Acetoxyalkanes | | | | | | | | | | |
| 26.03 | 1-Acetoxypropane | 90-170 | 15 | +11.7 | -0.37 | + 4.2 | -0.04** | +23.9 | -0.40 | 0.28 |
| 26.04 | 1-Acetoxybutane | 90-170 | 15 | +11.5 | -0.18 | + 3.0 | +0.10** | +21.8 | +0.08 | 0.17 |
| 26.05 | 1-Acetoxypentane | 90-170 | 15 | +11.2 | -0.15* | + 3.2 | +0.00** | +21.6 | -0.03 | 0.22 |
| *1-Alkanols* | | | | | | | | | | |
| 27.04 | 1-Butanol | 90-170 | 15 | +19.0 | -0.66 | +29.0 | -1.72 | +71.9 | -2.93 | 0.25 |
| 27.05 | 1-Pentanol | 90-170 | 15 | +18.3 | -0.05** | +23.9 | -1.48 | +63.3 | -1.73 | 0.37 |
| 27.06 | 1-Hexanol | 90-170 | 15 | +18.3 | -0.12** | +21.5 | -1.90 | +59.6 | -2.49 | 0.41 |
| 27.07 | 1-Heptanol | 90-170 | 15 | +18.4 | +0.39* | +22.2 | -2.54 | +60.8 | -2.68 | 0.58 |
| *2-Alkanols* | | | | | | | | | | |
| 28.04 | 2-Butanol | 90-170 | 15 | +15.5 | -0.14** | +17.9 | -1.16* | +50.1 | -1.50 | 0.77 |
| 28.05 | 2-Pentanol | 90-170 | 15 | +15.3 | +0.46** | +16.9 | -0.72** | +48.4 | +0.05 | 0.87 |
| 28.06 | 2-Hexanol | 90-170 | 15 | +15.5 | +0.24** | +15.0 | -0.40** | +45.8 | +0.17 | 0.76 |
| 28.07 | 2-Heptanol | 90-170 | 15 | +15.7 | +0.20** | +12.9 | +0.04** | +43.0 | +0.75 | 0.51 |
| *2-Methyl-2-alkanols* | | | | | | | | | | |
| 29.04 | 2-Methyl-2-propanol | 90-170 | 15 | +12.0 | -1.33 | +14.3 | +0.34** | +39.4 | -1.13 | 1.07 |
| 29.05 | 2-Methyl-2-butanol | 90-170 | 15 | +12.7 | -0.67 | + 9.7 | -0.52** | +33.5 | -1.49 | 0.56 |
| 29.06 | 2-Methyl-2-pentanol | 90-170 | 15 | +13.1 | -0.45** | + 9.2 | -0.46** | +33.4 | -1.07 | 0.77 |
| 29.07 | 2-Methyl-2-hexanol | 90-170 | 15 | +12.7 | -0.42 | + 8.4 | -0.36** | +31.6 | -0.89 | 0.36 |
| *1-Alkanethiols* | | | | | | | | | | |
| 30.04 | 1-Butanethiol | 90-170 | 15 | +10.4 | -1.47 | - 0.3** | -0.66** | +14.9 | -3.07 | 1.11 |
| 30.05 | 1-Pentanethiol | 90-170 | 15 | +11.4 | -1.12 | + 1.2* | -0.28** | +18.8 | -1.94 | 0.36 |
| 30.06 | 1-Hexanethiol | 90-170 | 15 | +11.7 | -0.42** | + 1.2** | -1.04* | +19.2 | -2.02 | 0.77 |
| *2-Alkanones* | | | | | | | | | | |
| 31.04 | 2-Butanone | 90-170 | 15 | +17.6 | -1.61 | + 8.2 | -1.42 | +38.5 | -4.21 | 0.63 |
| 31.05 | 2-Pentanone | 90-170 | 15 | +16.6 | -0.95 | + 6.0 | -0.78[s] | +33.8 | -2.29 | 0.46 |

| No. | Thermodynamic data : C78 / PSH | | | | | | | | |
|---|---|---|---|---|---|---|---|---|---|
| | PSH - C78 | | | Mixture | | id([SH] =1) - C78 | | | σ |
| | $\Delta H$ (cal mol$^{-1}$) | $\Delta S$ | $\Delta C_P$ | $h$ (cal mol$^{-1}$) | $s$ (cal mol$^{-1}$ K$^{-1}$) | $\Delta' H$ (cal l mol$^{-2}$) | $\Delta' S$ | $\Delta' C_P$ | (cal mol$^{-1}$) |
| | | (cal mol$^{-1}$K$^{-1}$) | | | | | (cal l mol$^{-2}$K$^{-1}$) | | |
| *1-Nitroalkanes* | | | | | | | | | |
| 25.02 | -129 | -0.202 | -0.3** | -269 | -0.697 | - 550 | -1.239 | -1.1 | 1.9 |
| 25.03 | -105 | -0.200 | -1.0** | -152s | -0.448 | - 368 | -0.927 | -1.9 | 2.2 |
| 25.04 | - 81 | -0.159 | -2.9 | - 15** | -0.161 | - 153 | -0.495 | -4.4 | 1.6 |
| 25.05 | - 34** | -0.062** | -4.4* | + 17** | -0.116** | - 51 | -0.319 | -6.4 | 3.4 |
| *1-Acetoxyalkanes* | | | | | | | | | |
| 26.03 | - 61 | -0.242 | +1.4** | - 28** | -0.182* | - 161 | -0.688 | +1.6 | 1.5 |
| 26.04 | - 28 | -0.179 | +0.7** | + 67 | -0.001** | + 8 | -0.374 | +0.8 | 0.8 |
| 26.05 | - 15* | -0.163 | -1.5* | + 64s | -0.044** | + 11 | -0.438 | -2.4 | 1.0 |
| *1-Alkanols* | | | | | | | | | |
| 27.04 | -181 | -0.436 | +2.1s | -731 | -1.576 | -1 250 | -2.747 | +1.4 | 1.2 |
| 27.05 | - 92 | -0.245 | +0.8** | -463 | -1.032 | - 771 | -1.770 | +0.1 | 2.1 |
| 27.06 | - 91 | -0.259 | +0.2** | -520 | -1.245 | - 866 | -2.132 | -0.9 | 2.4 |
| 27.07 | - 31** | -0.120* | -3.4* | -539 | -1.320 | - 817 | -2.063 | -5.9 | 3.0 |
| *2-Alkanols* | | | | | | | | | |
| 28.04 | - 88s | -0.226s | -0.7** | -398 | -0.873s | - 672 | -1.517 | -1.8 | 4.9 |
| 28.05 | - 11** | -0.074** | +1.4** | -147** | -0.315** | - 223 | -0.549 | +1.7 | 4.2 |
| 28.06 | - 26** | -0.126* | +0.8** | - 87** | -0.232** | - 174 | -0.541 | +0.8 | 3.7 |
| 28.07 | - 27** | -0.138s | -1.0** | + 31** | -0.006** | - 22 | -0.273 | -1.6 | 2.7 |
| *2-Methyl-2-alkanols* | | | | | | | | | |
| 29.04 | -193 | -0.524 | +0.0** | -294* | -0.638** | - 684 | -1.631 | -0.9 | 6.5 |
| 29.05 | -121 | -0.370 | +1.5** | -294 | -0.750 | - 604 | -1.628 | +1.2 | 3.1 |
| 29.06 | - 81 | -0.289 | +4.2s | -193s | -0.544 | - 413 | -1.242 | +5.3 | 2.7 |
| 29.07 | - 64 | -0.259 | -0.1** | -137s | -0.455 | - 323 | -1.107 | -0.7 | 2.0 |
| *1-Alkanethiols* | | | | | | | | | |
| 30.04 | -163 | -0.519 | -0.7** | -341s | -1.041s | - 771 | -2.351 | -2.3 | 5.5 |
| 30.05 | -126 | -0.437 | +0.9** | -190 | -0.689 | - 508 | -1.746 | +0.3 | 1.8 |
| 30.06 | - 49* | -0.253 | -2.5 | -191* | -0.726 | - 410 | -1.561 | -4.4 | 3.7 |
| *2-Alkanones* | | | | | | | | | |
| 31.04 | -272 | -0.657 | +1.5** | -686 | -1.715 | -1 359 | -3.366 | +0.2 | 3.9 |
| 31.05 | -176 | -0.461 | +1.4 | -338 | -0.921 | - 748 | -2.001 | +0.9 | 2.6 |

(Continued on pages 430 and 431)

Table 10 (*continued*)

| *No.* | *Compound* | *Temp. range* (°C) | *n* | *Retention index : C78 / PSH* | | | | | | |
|---|---|---|---|---|---|---|---|---|---|---|
| | | | | *PSH- C78* | | *Mixture* | | *id([SH] =1) - C78* | | σ |
| | | | | $\Delta I_{130}$ | $10 \times \Delta A_T$ ($K^{-1}$) | $A_L$ | $10 \times A_{LT}$ ($K^{-1}$) | $\Delta I'_{130}$ ($l\ mol^{-1}$) | $10 \times \Delta A'_T$ ($K^{-1} l\ mol^{-1}$) | |
| 31.06 | 2-Hexanone | 90-170 | 15 | +16.9 | -0.71 | + 5.8 | -0.62* | +33.9 | -1.69 | 0.49 |
| 31.07 | 2-Heptanone | 90-170 | 15 | +17.1 | -0.62 | + 5.8 | -0.44** | +34.3 | -1.28 | 0.47 |
| *Aldehydes* | | | | | | | | | | |
| 32.05 | Pentanal | 90-170 | 15 | +15.7 | +0.07** | + 7.0 | -1.28 | +33.9 | -1.51 | 0.43 |
| 32.06 | Hexanal | 90-170 | 15 | +16.2 | +0.34s | + 6.0 | -0.76s | +33.3 | -0.33 | 0.37 |
| 32.07 | Heptanal | 90-170 | 15 | +16.5 | +0.41 | + 6.1 | -0.79 | +33.8 | -0.32 | 0.31 |
| *Ethers* | | | | | | | | | | |
| 33.06 | Dipropylether | 90-170 | 15 | + 4.1 | -0.45* | + 1.1** | -0.82* | + 7.7 | -1.84 | 0.59 |
| 33.08 | Dibutylether | 90-170 | 15 | + 4.0 | -0.22s | + 1.2 | -0.94 | + 7.7 | -1.68 | 0.24 |
| *Halomethanes* | | | | | | | | | | |
| 37.01 | Dichloromethane | 90-170 | 15 | +13.1 | +0.78s | + 6.8 | +0.76** | +30.1 | +2.59 | 0.78 |
| 37.02 | Trichloromethane | 90-170 | 15 | +12.3 | +0.56 | + 4.2 | -0.16** | +24.8 | +0.83 | 0.53 |
| 37.03 | Tetrachloromethane | 90-170 | 15 | + 5.7 | +0.03** | + 0.1** | -0.24** | + 8.7 | -0.24 | 0.40 |
| 37.04 | $CF_2Br_2$ | 90-170 | 15 | + 4.3 | -0.10** | + 5.6 | +1.38 | +15.0 | +2.06 | 0.32 |
| *HALOBENZENES* | | | | | | | | | | |
| 38.01 | Fluorobenzene | 90-170 | 15 | + 9.9 | +0.29* | + 1.5* | +0.08** | +17.2 | +0.71 | 0.44 |
| 38.02 | Hexafluorobenzene | 90-170 | 15 | + 2.1 | -0.72 | + 6.3 | +2.40 | +12.8 | +2.64 | 0.52 |
| 38.03 | Trifluoromethylbenzene | 90-170 | 15 | + 7.4 | +0.10** | + 2.6* | +1.74 | +15.2 | +2.90 | 0.81 |
| 38.04 | Chlorobenzene | 90-170 | 15 | +12.3 | +0.72 | + 1.5** | +0.38** | +20.9 | +1.84 | 0.53 |
| 38.05 | Bromobenzene | 90-170 | 15 | +14.7 | +0.98 | + 2.6* | -0.12** | +26.1 | +1.53 | 0.72 |
| 38.06 | Iodobenzene | 130-210 | 15 | +16.8 | +1.19 | + 3.4* | +0.85s | +30.6 | +3.34 | 0.49 |
| *ALKYLPYRIDINES* | | | | | | | | | | |
| 39.01 | Pyridine | 90-170 | 15 | +19.1 | +0.59 | + 7.2 | -1.20 | +39.5 | -0.56 | 0.48 |
| 39.02 | 2-Picoline | 90-170 | 15 | +16.5 | +0.79 | + 4.0 | -0.84 | +30.8 | +0.20 | 0.34 |
| 39.03 | 3-Picoline | 90-170 | 15 | +20.1 | +0.91 | + 8.8 | -0.88 | +43.5 | +0.44 | 0.34 |
| 39.04 | 4-Picoline | 90-170 | 15 | +20.0 | +0.49 | + 7.5 | -0.94 | +41.3 | -0.30 | 0.28 |
| 39.05 | 2,3-Lutidine | 130-210 | 15 | +18.2 | +0.59 | + 2.9s | +1.06 | +31.9 | +2.77 | 0.34 |
| 39.06 | 2,4-Lutidine | 130-210 | 15 | +17.2 | +0.52 | + 4.5 | +0.40s | +32.7 | +1.68 | 0.24 |
| 39.07 | 2,5-Lutidine | 130-210 | 15 | +15.8 | +0.98 | + 2.9* | +1.51 | +28.4 | +4.00 | 0.75 |
| 39.08 | 2,6-Lutidine | 130-210 | 15 | +16.3 | -0.25 | + 5.0 | -0.14** | +31.9 | -0.29 | 0.24 |

| No. | Thermodynamic data : C78 / PSH | | | | | | | | |
|---|---|---|---|---|---|---|---|---|---|
| | PSH - C78 | | | Mixture | | id([SH] =1) - C78 | | | σ |
| | $\Delta H$ (cal mol$^{-1}$) | $\Delta S$ (cal mol$^{-1}$K$^{-1}$) | $\Delta C_P$ | $h$ (cal mol$^{-1}$) | $s$ (cal mol$^{-1}$ K$^{-1}$) | $\Delta' H$ (cal l mol$^{-2}$) | $\Delta' S$ (cal l mol$^{-2}$K$^{-1}$) | $\Delta' C_P$ | (cal mol$^{-1}$) |
| 31.06 | -141 | -0.338 | +0.6** | -233 | -0.704 | - 559 | -1.621 | -0.0 | 2.8 |
| 31.07 | -126 | -0.365 | -0.2** | -161[s] | -0.562 | - 445 | -1.410 | -1.1 | 2.7 |
| *Aldehydes* | | | | | | | | | |
| 32.05 | - 62 | -0.186 | -1.7** | -244 | -0.683 | - 455 | -1.285 | -3.1 | 2.4 |
| 32.06 | - 27* | -0.112 | -2.3* | - 46** | -0.247[s] | - 136 | -0.591 | -3.6 | 1.7 |
| 32.07 | - 28* | -0.108 | -1.9* | - 45** | -0.204[s] | - 109 | -0.430 | -2.7 | 2.1 |
| *Ethers* | | | | | | | | | |
| 33.06 | + 5** | -0.173 | -1.4** | -183* | -0.612 | - 314 | -1.266 | -2.7 | 3.2 |
| 33.08 | + 50 | -0.094 | -1.4[s] | -122 | -0.531 | - 181 | -1.083 | -2.6 | 0.9 |
| *Halomethanes* | | | | | | | | | |
| 37.01 | + 33** | +0.044** | +0.1** | +340[s] | +0.812[s] | + 518 | +1.187 | +0.8 | 4.7 |
| 37.02 | + 19** | -0.031** | +0.7** | +116** | +0.183** | + 160 | +0.138 | +1.1 | 3.2 |
| 37.03 | + 35* | -0.087* | +1.0** | + 38** | -0.089** | + 42 | -0.402 | +1.2 | 2.3 |
| 37.04 | + 21** | -0.104 | +0.8** | +295 | +0.695 | + 416 | +0.758 | +1.6 | 1.7 |
| *HALOBENZENES* | | | | | | | | | |
| 38.01 | + 22** | -0.064** | +1.4** | +151[s] | +0.215** | + 198 | +0.097 | +2.1 | 2.5 |
| 38.02 | - 11** | -0.225 | +1.5** | +407 | +0.958 | + 520 | +0.937 | +2.7 | 2.8 |
| 38.03 | + 31** | -0.072** | +1.0** | +470 | +1.019 | + 661 | +1.219 | +2.1 | 4.8 |
| 38.04 | + 53* | +0.014** | -0.7** | +320 | +0.557[s] | + 468 | +0.657 | -0.6 | 3.1 |
| 38.05 | + 62* | +0.050** | -1.7** | +265[s] | +0.401** | + 401 | +0.483 | -2.1 | 4.0 |
| 38.06 | +135* | +0.238** | -0.7** | +231 | +0.285* | + 452 | +0.576 | -0.7 | 2.4 |
| *ALKYLPYRIDINES* | | | | | | | | | |
| 39.01 | - 36* | -0.099* | -0.4** | -115** | -0.393* | - 235 | -0.750 | -1.0 | 2.8 |
| 39.02 | + 14** | -0.023** | +0.1** | + 44** | -0.068** | + 42 | -0.230 | +0.0 | 1.8 |
| 39.03 | - 5** | -0.032** | -0.5** | + 18** | -0.087** | - 8 | -0.235 | -0.8 | 1.9 |
| 39.04 | - 48 | -0.138 | -0.4** | - 68** | -0.317 | - 194 | -0.719 | -1.0 | 1.6 |
| 39.05 | + 27** | +0.010** | -0.3** | +275 | +0.443 | + 377 | +0.516 | -0.1 | 1.8 |
| 39.06 | - 21** | -0.115[s] | +0.9* | +148 | +0.152 | + 133 | -0.066 | +1.3 | 0.7 |
| 39.07 | - 29** | -0.146** | +3.3* | +348 | +0.629 | + 402 | +0.559 | +5.0 | 2.4 |
| 39.08 | -149 | -0.436 | +1.2** | + 52** | -0.063** | - 182 | -0.818 | +1.3 | 1.1 |

(Continued on pages 432 and 433)

Table 10 (*continued*)

| No. | Compound | Temp. range (°C) | n | Retention index : C78 / PSH | | | | | | σ |
|---|---|---|---|---|---|---|---|---|---|---|
| | | | | PSH- C78 | | Mixture | | id([SH] =1) - C78 | | |
| | | | | $\Delta I_{130}$ | $10\times\Delta A_T$ ($K^{-1}$) | $A_L$ | $10\times A_{LT}$ ($K^{-1}$) | $\Delta' I_{130}$ ($l\ mol^{-1}$) | $10\times\Delta' A_T$ ($K^{-1} l\ mol^{-1}$) | |
| 39.09 | 3,4-Lutidine | 130-210 | 15 | +23.8 | -0.04** | +10.0 | -0.48** | +50.8 | -0.32 | 0.49 |
| 39.10 | 3,5-Lutidine | 130-210 | 15 | +22.4 | -0.09** | + 9.5 | -0.66 | +47.9 | -0.69 | 0.32 |
| 39.11 | 2-Ethylpyridine | 130-210 | 15 | +15.2 | +0.17** | + 2.3** | +0.52** | +26.4 | +1.28 | 0.65 |
| 39.12 | 3-Ethylpyridine | 130-210 | 15 | +17.2 | -0.09** | + 2.3** | -1.22 | +29.2 | -1.71 | 0.45 |
| 39.13 | 4-Ethylpyridine | 130-210 | 15 | +18.9 | +0.28** | + 1.5** | +1.33* | +30.8 | +2.69 | 1.07 |
| 39.14 | 2-Propylpyridine | 130-210 | 15 | +14.4 | -0.05** | + 3.5** | -0.62** | +26.8 | -0.77 | 0.80 |
| 39.15 | 4-Propylpyridine | 130-210 | 15 | +18.2 | +0.92 | + 5.2 | +1.06 | +35.4 | +3.29 | 0.45 |
| 39.16 | 2,3,6-Collidine | 130-210 | 15 | +15.0 | +0.25 | + 3.4s | +0.17** | +27.7 | +0.88 | 0.41 |
| 39.17 | 2,4,6-Collidine | 130-210 | 15 | +14.1 | +0.20* | + 8.3 | -1.25 | +33.6 | -1.28 | 0.61 |
| 39.18 | 4-*tert*-Butylpyridine | 130-210 | 15 | +19.1 | -0.16** | + 4.6s | -0.35** | +35.6 | -0.45 | 0.62 |
| 39.19 | 3-Chloropyridine | 90-170 | 15 | +17.1 | +0.49 | + 5.4 | +0.04** | +33.9 | +1.10 | 0.54 |
| *ORGANOSILICON COMPOUNDS* | | | | | | | | | | |
| 40.01 | Tetramethylsilane | 90-170 | 15 | + 0.3* | +0.34 | + 2.9 | +0.26** | + 4.3 | +1.00 | 0.28 |
| 40.02 | Hexamethyldisilane | 90-170 | 15 | - 1.8 | -0.09** | - 0.6** | +0.28** | - 3.6 | +0.25 | 0.31 |
| 40.03 | Hexamethyldisiloxane | 90-170 | 15 | - 4.6 | -0.89 | - 0.8** | +1.58s | - 8.0 | +0.97 | 0.87 |
| *MISCELLANEOUS* | | | | | | | | | | |
| 41.01 | Carbon disulphide | 90-170 | 15 | + 8.1 | +0.59 | + 1.3s | -1.56 | +14.0 | -1.33 | 0.30 |
| 41.02 | Tetramethyltin | 90-170 | 15 | + 0.8 | +0.73 | - 1.5 | +0.38* | - 0.9 | +1.67 | 0.26 |
| 41.03 | Tetrahydrofuran | 90-170 | 15 | +12.4 | -0.55s | + 7.3 | +0.30** | +29.6 | -0.11 | 0.66 |
| 41.04 | 1,4-Dioxane | 90-170 | 15 | +14.2 | -0.16** | + 5.3 | +0.24** | +29.3 | +0.39 | 0.83 |
| 41.05 | Thiophene | 90-170 | 15 | +11.1 | +1.31 | + 1.9** | +0.66** | +19.8 | +3.14 | 0.90 |
| 41.06 | Cyclopentanone | 90-170 | 15 | +20.6 | -0.26** | + 7.5 | -0.02** | +42.2 | -0.04 | 0.74 |
| 41.07 | Cyclohexanone | 90-170 | 15 | +21.7 | +0.99 | + 7.2 | -0.40** | +43.5 | +1.28 | 0.73 |
| 41.08 | Cyclohexanol | 90-170 | 15 | +19.0 | -0.18** | +14.2 | -0.18** | +49.9 | -0.09 | 1.10 |
| 41.11 | Nitrobenzene | 130-210 | 15 | +24.8 | +0.70 | +16.0 | -0.51** | +61.4 | +0.84 | 0.74 |
| 41.12 | Benzyl alcohol | 130-210 | 15 | +30.0 | +0.40 | +13.7 | +2.24 | +65.9 | +4.56 | 0.54 |
| 41.13 | 2-Phenylethanol | 130-210 | 15 | +27.5 | +0.36 | + 9.6 | +2.14 | +56.0 | +4.26 | 0.54 |
| 41.14 | Anisole | 130-210 | 15 | +27.9 | +0.30 | +20.6 | +0.32 | +68.4 | +1.66 | 0.21 |
| 41.15 | Phenetole | 130-210 | 15 | +23.0 | +0.54 | +19.8 | +0.56 | +64.5 | +2.24 | 0.25 |
| *ERRORS:* | *f (n-alkanes)* | *90-210* | | *def.* | | | | | | |
| | *f (n-alkanes)* | *150-210* | | *def.* | | | | | | |
| | *f (solutes)* | *90-170* | | *0.63* | *0.22* | *2.19* | *0.77* | *3.21* | *1.13* | |
| | *f (solutes)* | *130-210* | | *1.09* | *0.22* | *3.79* | *0.77* | *5.56* | *1.13* | |
| *CONVERSION TO $K_D$:* | | | | *0* | *0* | *0* | *0* | *0* | *0* | |

Table 10 (*continued*)

| No. | Thermodynamic data : C78 / PSH | | | | | | | | |
|---|---|---|---|---|---|---|---|---|---|
| | PSH - C78 | | | Mixture | | id([SH] =1) - C78 | | | σ |
| | ΔH (cal mol$^{-1}$) | ΔS (cal mol$^{-1}$K$^{-1}$) | ΔC$_P$ | h (cal mol$^{-1}$) | s (cal mol$^{-1}$ K$^{-1}$) | Δ'H (cal l mol$^{-2}$) | Δ'S (cal l mol$^{-2}$K$^{-1}$) | Δ'C$_P$ | (cal mol$^{-1}$) |
| 39.09 | -202 | -0.492 | +1.6** | - 48** | -0.293* | - 383 | -1.184 | +1.6 | 2.4 |
| 39.10 | -192 | -0.481 | +1.4* | - 80$^s$ | -0.369 | - 416 | -1.281 | +1.3 | 1.1 |
| 39.11 | -157 | -0.467 | +3.3 | +174 | +0.202$^s$ | - 27 | -0.503 | +4.4 | 1.4 |
| 39.12 | - 75** | -0.256* | -0.4** | - 98* | -0.499 | - 303 | -1.214 | -1.2 | 2.0 |
| 39.13 | -188* | -0.506$^s$ | +3.6** | +310 | +0.514$^s$ | + 124 | -0.109 | +5.1 | 3.2 |
| 39.14 | + 33** | -0.034** | -2.1** | + 1** | -0.249** | - 17 | -0.564 | -3.3 | 3.2 |
| 39.15 | + 47** | +0.046** | +0.8** | +264 | +0.407 | + 387 | +0.508 | +1.4 | 1.7 |
| 39.16 | - 36** | -0.194** | +0.9** | +137$^s$ | +0.079** | + 80 | -0.319 | +1.1 | 1.9 |
| 39.17 | + 41** | -0.017** | -1.1** | -144* | -0.556 | - 202 | -0.953 | -2.1 | 2.9 |
| 39.18 | -185$^s$ | -0.523 | +1.5** | + 33** | -0.189** | - 273 | -1.153 | +1.5 | 2.7 |
| 39.19 | - 90** | -0.279* | +2.4** | + 67** | -0.027** | - 74 | -0.538 | +3.1 | 2.1 |
| *ORGANOSILICON COMPOUNDS* | | | | | | | | | |
| 40.01 | +109 | +0.066* | +0.7** | +137 | +0.343 | + 315 | +0.496 | +1.3 | 1.7 |
| 40.02 | +105 | -0.007** | -1.5** | +148 | +0.173* | + 278 | +0.034 | -2.1 | 1.4 |
| 40.03 | + 33 | -0.208 | -2.1 | +260 | +0.479 | + 335 | +0.185 | -2.8 | 5.3 |
| *MISCELLANEOUS* | | | | | | | | | |
| 41.01 | + 52 | -0.004** | +1.9** | -154 | -0.519 | - 191 | -0.856 | +2.2 | 1.9 |
| 41.02 | +157 | +0.169 | -1.1 | +340 | +0.667 | + 636 | +1.015 | -1.0 | 1.3 |
| 41.03 | - 97 | -0.317 | +1.1** | - 55** | -0.201** | - 240 | -0.795 | +1.1 | 3.6 |
| 41.04 | - 69* | -0.234$^s$ | +0.7** | + 41** | -0.011** | - 70 | -0.422 | +0.8 | 4.6 |
| 41.05 | +115 | +0.172* | +2.7** | +482 | +1.029 | + 801 | +1.591 | +4.7 | 4.3 |
| 41.06 | -135 | -0.330 | +0.6** | - 52** | -0.240** | - 284 | -0.855 | +0.4 | 3.8 |
| 41.07 | - 13** | -0.036** | +0.9** | +142** | +0.194** | + 156 | +0.156 | +1.4 | 3.4 |
| 41.08 | -104$^s$ | -0.299 | +3.1** | -125** | -0.378** | - 342 | -1.003 | +3.8 | 5.0 |
| 41.11 | - 81** | -0.191** | +1.0** | - 88** | -0.346** | - 260 | -0.812 | +1.0 | 3.4 |
| 41.12 | -245 | -0.518 | +3.2$^s$ | +369 | +0.798 | + 174 | +0.392 | +4.8 | 2.0 |
| 41.13 | - 50** | -0.088** | -1.8** | +395 | +0.780 | + 460 | +0.909 | -2.0 | 2.7 |
| 41.14 | -101 | -0.182$^s$ | -0.7** | - 73$^s$ | -0.123* | - 226 | -0.380 | -1.2 | 1.1 |
| 41.15 | - 65* | -0.161* | +0.8** | + 41** | +0.056** | - 41 | -0.167 | +1.0 | 1.2 |
| *E(contd)* | *5.2* | *0.0128* | *0.17* | *4.3* | *0.0102* | *9.5* | *0.0231* | *0.24* | |
| | *5.2* | *0.0128* | *0.17* | *4.3* | *0.0102* | *9.5* | *0.0231* | *0.24* | |
| | *9.1* | *0.0224* | *0.76* | *31.3* | *0.0776* | *45.9* | *0.1139* | *1.07* | |
| | *32.2* | *0.0812* | *0.83* | *34.3* | *0.0775* | *66.3* | *0.1582* | *1.17* | |
| *C(contd)* | *- 3* | *-0.044* | *-0.1* | *- 1* | *-0.003* | *- 6* | *-0.066* | *-0.1* | |

cal potential in the alkane C78, $\Delta\mu_j^A$, and the difference $\Delta\mu_j^P = \Delta\mu_j^P - \Delta\mu_j^A$ at a given composition by Eq. (9)

$$m_j^{A/P} = a + b\,\Delta\mu_j^A + c\Delta\mu_j^P \quad (9)$$

where the experimental value of the constant was calculated with data $h_j$ and $s_j$ listed in Tables 8–10, with Eq. (10)

$$m_j^{A/P} = h_j - Ts_j \quad (10)$$

The numerical values of the coefficients in Eq. (9) are as follows

| | $a$ | $b$ | $c$ | corr. coeff.:$r$ |
|---|---|---|---|---|
| TMO | 23.8 | −0.0055 | 0.509 | 0.972 |
| PCN | 27.2 | −0.0039 | 0.378 | 0.962 |
| PSH | 22.4 | −0.0292 | 0.521 | 0.872 |

Calculated values of the constant, $m_j^{A/P}$, as a function of those measured by experiment are plotted in Figs. 3, 4 and 5. Assuming that for a given A/P-mixture the values of the coefficients are independent of the solute, $j$, the $\Delta\mu$-value of an unknown solute can be estimated as described in Ref. [4].

The aim of the project stated in part I is the selection of a series of solvents where each solvent provides new information about interaction forces between the solute, $j$, and an interacting group, X. Let us characterize the additional interaction between $j$ and X by its $\Delta' I$-value (analogous to the $\Delta'\mu$-value), i.e. the retention index difference between the index measured in a one molar ideal solution of X in C78 and the index in pure C78. Obviously, if

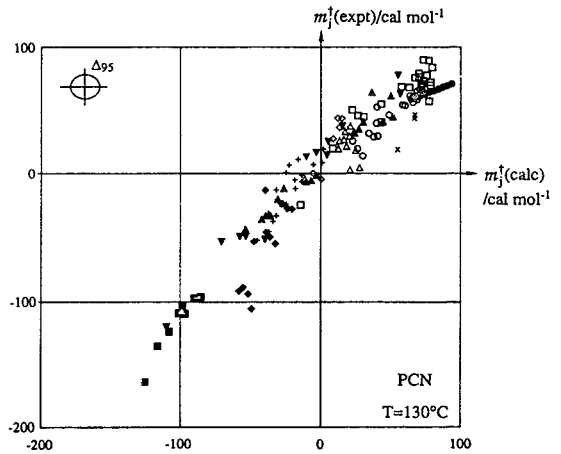


Fig. 4. Plot of the experimental constant, $m_j^{A/P}$ in Eq. (10), characterising the non-ideality of C78/PCN mixtures as a function of those calculated with Eq. (9) at 130°C.

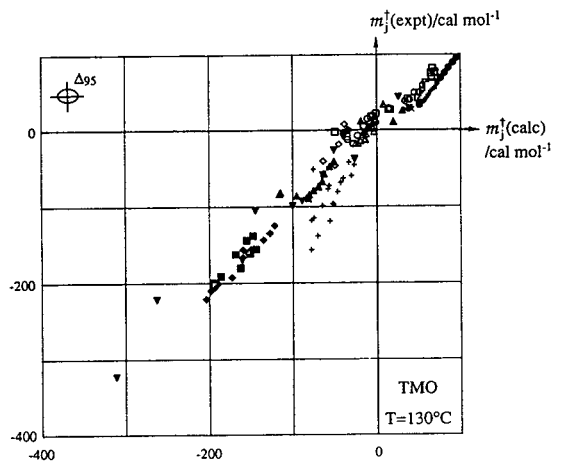


Fig. 3. Plot of the experimental constant, $m_j^{A/P}$ in Eq. (10), characterising the non-ideality of C78/TMO mixtures as a function of those calculated with Eq. (9) at 130°C.

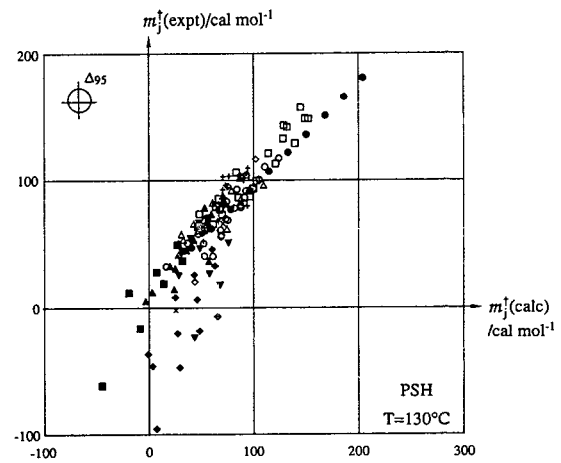


Fig. 5. Plot of the experimental constant, $m_j^{A/P}$ in Eq. (10), characterising the non-ideality of C78/PSH mixtures as a function of those calculated with Eq. (9) at 130°C.

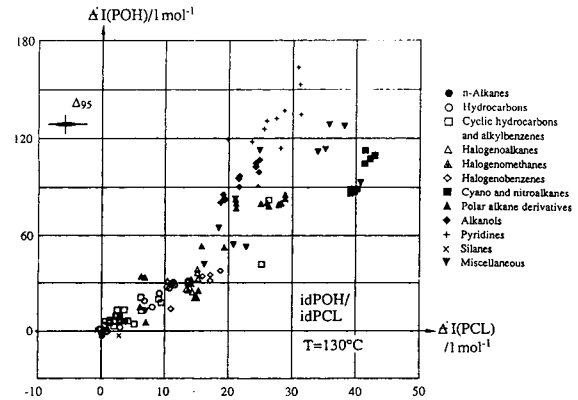


Fig. 6. Retention index difference of solutes in a hypothetical ideal one molar solution of the interacting groups POH in C78 as a function of the same difference in PCL and C78 ($\Delta'I$-values).

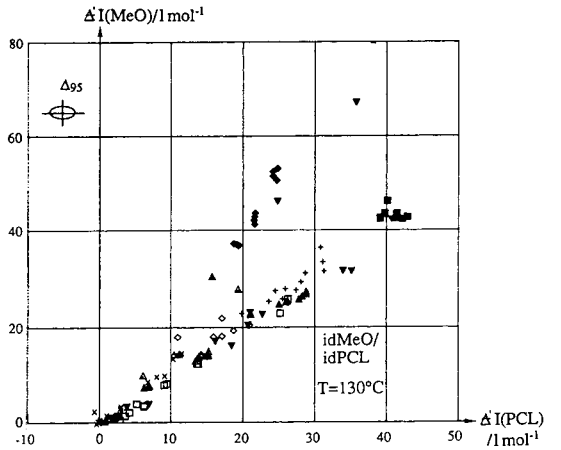


Fig. 8. Retention index difference of solutes in a hypothetical ideal one molar solution of the interacting groups MeO in C78 as a function of the same difference in PCL and C78 ($\Delta'I$-values).

$\Delta'I$-values on two ideal solvents correlate, one of the solvents can be excluded from the family. In the last five figures $\Delta'I$-values on primary hydroxyl (POH), trifluoromethylalkane ($CF_3$) from Refs. [1] and [4] as well as methoxyalkane (MeO), primary cyano (PCN) and primary thiol (PSH) data are plotted as a function of $\Delta'I$-values on a one molar ideal solution of primary chloroalkane (PCL) groups [5]. Latter was elected as standard as it approximates an ideal dipolar interacting group of average polarizability. In the following let us shortly comment on these figures:

– Primary hydroxyl can interact by its perma-

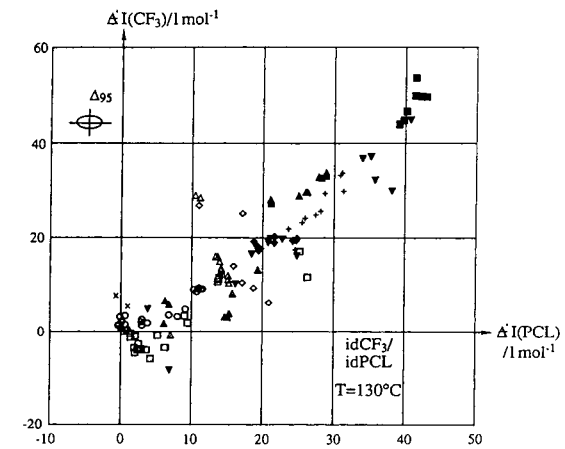


Fig. 7. Retention index difference of solutes in a hypothetical ideal one molar solution of the interacting groups $CF_3$ in C78 as a function of the same difference in PCL and C78 ($\Delta'I$-values).

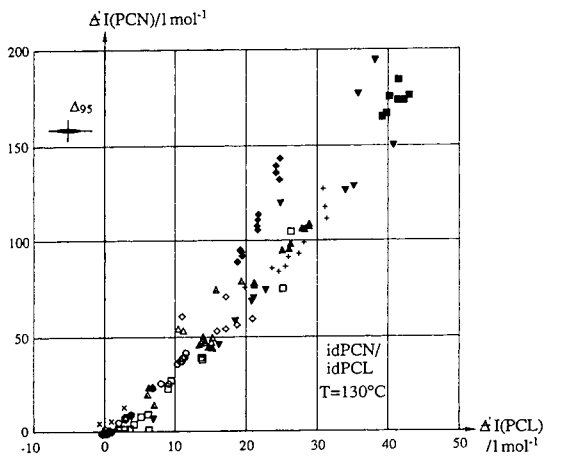


Fig. 9. Retention index difference of solutes in a hypothetical ideal one molar solution of the interacting groups PCN in C78 as a function of the same difference in PCL and C78 ($\Delta'I$-values).

nent polarity, and as a hydrogen bond donor and acceptor. Fig. 6 shows that alcohols, ethers, ketones etc. show a strong interaction.

– Trifluoromethylalkanes are similar to the primary chloroalkanes. Deviations in Fig. 7 were proposed to be due to the "hardness" of the trifluoromethyl group compared with the polariability of the chloro substituent [5].

– Methoxy groups can interact by permanent polarity and as hydrogen bond acceptors. Comparison of Fig. 8 with Fig. 6 shows that deviations are as awaited

– Cyano groups interact nearly exclusively by permanent polarity, they are weak hydrogen bond acceptors. In fact, in a "family of unlike solvents" this stationary phase might replace the PCL-solvent in which the chloro substituents are too reactive hence it cannot be used as stationary phase for certain solutes.

– The interaction forces of PSH groups are very interesting but for our purpose the behaviour of this phase is a deception. In fact, it was awaited that interaction forces between the slightly acidic thiol and basic compounds will be pronounced, i.e. that this phase measures the basicity of solutes. It is seen that pyridine derivatives are not retained more than other polar compounds. Interestingly this group is somewhat similar to the methoxy-alkane group. Fig. 10 shows that it seems to be a hydrogen bond acceptor and a very bad donor.

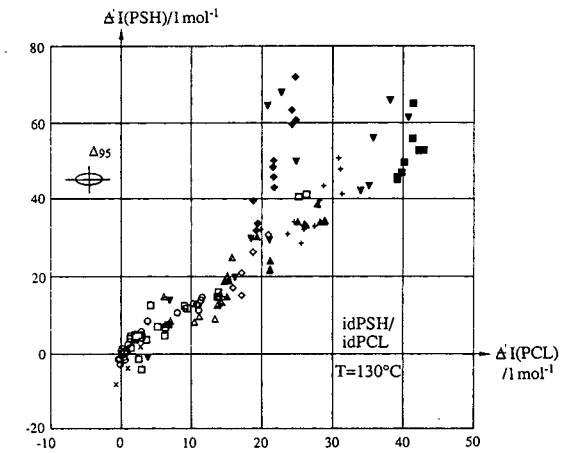


Fig. 10. Retention index difference of solutes in a hypothetical ideal one molar solution of the interacting groups PSH in C78 as a function of the same difference in PCL and C78 ($\Delta' I$-values).

## Acknowledgements

This paper reports on part of a project supported by the Fonds National Suisse de la Recherche Scientifique. The authors gratefully acknowledge Dr. A. Dallos and Dr. G. Défayes for providing density results.

## References

[1] K.S. Reddy, J.-Cl. Dutoit and E. sz. Kováts, J. Chromatogr., 609 (1992) 229.
[2] K.S. Reddy and E. sz. Kováts, Chromatographia, 34 (1992) 249.
[3] R. Cloux, G. Défayes, K. Fóti, J.-Cl.Dutoit and E. sz. Kováts, Synthesis (1993) 909.
[4] K.S. Reddy, R. Cloux and E. sz. Kováts, J. Chromatogr. A, 673 (1994) 181.
[5] G. Défayes, K.S. Reddy, A. Dallos and E. sz. Kováts, J. Chromatogr. A, 699 (1995) 131.
[6] P. Zeltner, G.A. Huber, R. Peters, F. Tátrai, L. Boksányi and E. sz. Kováts, Helv. Chim. Acta, 62 (1979) 2495.
[7] M. Tamura and J.K. Kochi, Synthesis (1971) 303.
[8] G. Körösi and E. sz. Kováts, J. Chem. Eng. Data, 26 (1981) 323.
[9] R.A. Fisher and F. Yates, Statistical Tables, Oliver and Boyd, Edinburgh, 6th ed., 1963.

ELSEVIER

Journal of Chromatography A, 704 (1995) 437–447

JOURNAL OF CHROMATOGRAPHY A

# Prediction of gas chromatographic retention times, column efficiency and resolution as a function of temperature and flow-rate
## Application for gas chromatographic separation of eight *p*-hydroxybenzoic esters

Y. Guillaume, M. Thomassin, C. Guinchard*

*Laboratoire de Chimie Analytique, UFR des Sciences Médicales et Pharmaceutiques, 25030 Besançon cedex, France*

First received 29 November 1994; revised manuscript received 21 February 1995; accepted 23 February 1995

**Abstract**

Using eight *p*-hydroxybenzoic esters, simple equations were developed to provide accurate gas chromatographic retention data and column efficiency represented by the height equivalent to a theoretical plate. With an experimental design, these equations have practical applications in the calculation of the resolution for a given pair of these compounds and for the determination of the isothermal conditions for their separation in minimum time. The method reduced the number of experiments to be carried out and provided good agreement between experimental results and predicted data.

## 1. Introduction

Qualitative and quantitative analysis in GC has been the subject of much debate. A paper listing some 900 Kovats indices for 400 monoterpenes on methylsilicone and Carbowax 20 M phases has been published [1].

Different methods have been reported for the determination of the universal retention index [2]. A procedure has been described that allowed the calculation of linear temperature-programmed retention indices from Kovats retention indices on a given stationary phase [3]. The use of the UNIFAC group contribution method to predict retention on low-molecular-mass stationary phases [4] and on polymer phases [5] was studied. Peng et al. discussed the prediction of retention indices for silylated derivatives of polar compounds [6]. Several studies examined the use of cubic splines to calculate temperature-programmed retention indices [7–9].

Fernandez-Sanchez et al. tested several methods to calculate programmed-temperature retention indices and preferred the cubic spline approach [10]. Prediction of retention data and/or structure–retention correlations were presented for the $C_9$–$C_{12}$ alkylbenzenes [11], polychlorobenzenes [12], chlorinated dibenzofuranes [13], bromo and bromo-chloro dioxins and furans [14], anabolic steroids [15], and for stimulants and narcotics [16].

Gerbino and Castello reported the GC identi-

* Corresponding author.

0021-9673/95/$09.50 
*SSDI* 0021-9673(95)00266-9

fication of complex mixtures of halomethanes and haloethanes by correlating retention with vapor pressure [17]. Practical guidelines for generating a simulated gas chromatogram and a new approach for the chromatographic indexing of organic compounds were presented by Mowery [18]. Jorgensen et al. described a model that could be used to accurately predict GC–flame ionization detector response factors from molecular structure [19].

Guillaume and Guinchard, using a molecular connectivity index, introduced a method for predicting retention indices for a series of *p*-hydroxybenzoic esters [20]. The use of chemometric methodology for the optimization of GC performance has been reported in several studies. Bautz et al. described the performance of a computer method to predict retention bandwidth, and resolution for programmed-temperature GC separations with an average error of better than 10% [21].

Dolan et al. investigated the changes on band spacing as a function of temperature through computer simulation [22]. A simplex method was used to optimize selectivity for the separation of 10 compounds by GC [23] and for the deconvolution of complex GC profiles [24].

This paper shows the interrelationships between the retention time of a *p*-hydroxybenzoic ester, its molecular connectivity index, the resolution between two solutes, column plate-height, carrier gas flow-rate and column temperature. To show this relationship, an experimental design has given suitable retention models. Thus the number of experiments used for the optimization of the separation of eight esters could be reduced with this chemometric methodology developed in our laboratory.

## 2. Experimental

### 2.1. Reagents

The chromatographed compounds were *p*-hydroxybenzoic esters. The straight chain esters, methyl to butyl (MetR, EtR, PrR, BuR) were purchased from Interchim (Montluçon, France). The branch chain esters isopropyl, isobutyl, *sec*-butyl and *tert*-butyl (IprR, IbuR, SbuR, TerR) were synthesized in our laboratory [20].

### 2.2. Apparatus

The analyses were performed using a DELSI DI200 gas chromatograph with a flame-ionization detector (Suresnes, France) and a Merck D2500 chromato-integrator (Nogent-sur-Marne, France).

A capillary column OV17 was used with a stationary phase of polymethylsiloxane (25 m × 300 μm I.D.) with a film thickness of 0.2 μm (Spiral, Dijon, France). The carrier gas was nitrogen with a flow-rate varying from 1.50 to 3 ml/min and the column temperature was varied from 145°C to 170°C with isothermal conditions.

### 2.3. Chemometric methodology

The chemometric approach is based on factorial designs. These are conveniently defined as a base, representing the number of levels of the factors, raised to an exponent, representing the number of factors under study. Thus in the general case of $k$ factors at two levels, $2^k$ factor combinations exist [25]. Two-level factorial designs allow for the fitting of a first order (linear) model to the data. If the effects of each factor do not vary linearly, a design which requires fewer experiments to detect curvature in the response is the composite central design developed by Box and Wilson [26]. The composite central design was developed specifically to enable a second-order response surface to be fitted to the data. An example of a two-factor factorial design is shown in Table 1, which illustrates the addition of levels to a $2^k$ factorial design. In general central composite designs are constructed of a total of $2^k + 2k + 1$ factor combinations [27] where $k$ is the number of factors under study. Thus the number of experiments required for two variables is 9.

Composite central designs provide sufficient data for the fitting of a quadratic model to a data set. Such models are amenable to regression analysis. For two factors this takes the form:

Table 1
Experiments required for a two variable experimental design

| Experiment N° | $x_1$ | $x_2$ |
|---|---|---|
| 1 | −1 | −1 |
| 2 | +1 | −1 |
| 3 | −1 | +1 |
| 4 | +1 | +1 |
| 5 | $-\sqrt{2}$ | 0 |
| 6 | $+\sqrt{2}$ | 0 |
| 7 | 0 | $-\sqrt{2}$ |
| 8 | 0 | $+\sqrt{2}$ |
| 9 | 0 | 0 |

$$y = a_0 + a_1x_1 + a_2x_2 + a_{11}x_1^2 + a_{22}x_2^2 + a_{12}x_1x_2 \quad (1)$$

where $y$ is the response or dependent variable and $x_1$, $x_2$ are the logarithm respectively of column temperature $T$ (°C) and carrier gas flow-rate $F$ (ml/min). The $a$ terms represent the parameters of the model.

## 3. Results and discussion

### 3.1. Height equivalent to a theoretical plate number study

A parameter that affects column efficiency is the average linear gas velocity ($u$):

$$u = \frac{L}{t_0} \quad (2)$$

where $L$ is the column length and $t_0$ the retention time of an unretained peak such as air or methane. The linear velocities encountered in capillary GC normally range from ≃10 to >100 cm/s.

The flow-rate at the column exit, $F_C^\circ$ relates to the average linear velocity by

$$F_C^\circ = [(u\pi r_C^2)/j] \quad (T_0/T) \quad (3)$$

where $r_C$ (column radius), $T_0$ (room temperature) and $T$ (column temperature) are included to adjust the column outlet flow for measurement at room temperature. The constant $j$ is a gas compressibility factor that compensates for the change in pressure across the column length.

Although often neglected, $j$ has a significant effect at column head pressures greater than ≃5 psi. Using the experimental design, $t_0$ was modelled by the two-order polynomial (Eq. 1) where $y$ is equal to $t_0$. From the full regression model (Table 2) a student T-test was used to provide the basis for a decision as to whether or not the model coefficients were significant. Results of the student $t$-test show that all the variables except $x_2$ and $x_2^2$ can be eliminated from the model; $t_0$ is then given by the equation:

$$t_0(\text{min}) = 0.890 - 0.223x_2 + 0.051x_2^2 \quad (4)$$

This generated model was assessed statistically using a Fischer Snedecor test and a coefficient of multiple determination $R^2$. The validity of the model was tested by a Fischer ratio and the value of $R^2$ was used as an indicator of the explanatory power and assumed a value from 0 to +1 indicating that these variables in the model perfectly explained the variation in the independent variable $t_0$.

The Fischer ratio was 6230 and 0.999 was $R^2$. These values show the excellent validity of the model. The predicted and measured $t_0$ values for seven experiments are given in Table 3. The retention of the second order term $x_2^2$ of the model showed that the flow-rate ($F$) influenced the degree of curvature of the curve. For a

Table 2
Estimates of regression parameters for the two regression models

| Independent variables | Parameter terms | $N/L$ [a] | $t_0$ [b] |
|---|---|---|---|
| Intercept | $a_0$ | +0.726 | +0.890 |
| $x_1$ | $a_1$ | −0.066 | −0.006 |
| $x_2$ | $a_2$ | −0.046 | −0.223 |
| $x_1^2$ | $a_{11}$ | −0.116 | +0.010 |
| $x_2^2$ | $a_{22}$ | −0.047 | +0.051 |
| $x_1x_2$ | $a_{12}$ | −0.051 | +0.002 |

[a] Reverse of the height to a theoretical plate ($mm^{-1}$).
[b] Column dead time (min).

Table 3
Predicted (p) and measured (m) values of the column dead time $t_0$ (min) and the reverse of the plate height $N/L$ ($mm^{-1}$) for different experimental conditions

| Experiment No. | Linear velocity (cm/s) | Temperature (°C) | $t_0^p$ | $t_0^m$ | $\Delta t_0(\%)$ | $N^p/L$ | $N^m/L$ | $\Delta(N/L)(\%)$ |
|---|---|---|---|---|---|---|---|---|
| 1 | 62.00 | 170.0 | 0.67 | 0.68 | 1.47 | 0.14 | 0.13 | 7.14 |
| 2 | 62.00 | 160.0 | 0.67 | 0.67 | 0.00 | 0.51 | 0.48 | 5.88 |
| 3 | 62.00 | 145.0 | 0.67 | 0.68 | 1.47 | 0.54 | 0.51 | 5.88 |
| 4 | 32.00 | 170.0 | 1.30 | 1.31 | 0.76 | 0.47 | 0.45 | 4.44 |
| 6 | 32.00 | 160.0 | 1.30 | 1.30 | 0.00 | 0.69 | 0.67 | 2.89 |
| 6 | 32.00 | 145.0 | 1.30 | 1.30 | 0.00 | 0.48 | 0.45 | 6.20 |
| 7 | 46.00 | 145.0 | 0.91 | 0.91 | 0.00 | 0.59 | 0.54 | 5.08 |

flow-rate ranging from 1.5 to 3 ml/min, the corresponding dead time $t_0$ was plotted on the $y$-axis (Fig. 1). The slight curvature in the plots is caused by the compressibility factor $j$. Eq. (4) can be written as the well known equation [28,29]

$$t_0(\text{min}) = \frac{\Phi_1}{F(\text{ml/min})} \quad (5)$$

where $\Phi_1$ is a constant calculated to be 2.02. Combining Eqs. (2) and (5) the following is obtained

$$u(\text{cm/s}) = \Phi_2 F(\text{ml/min}) \quad (6)$$

where $\Phi_2$ is equal to 20.70.

A similar method was used to study column dead time in reversed-phase chromatography [30].

In gas chromatography, the retention time of a solute molecule is given by the equation:

$$t = t_0(1 + k') \quad (7)$$

For this series of eight $p$-hydroxybenzoic esters, $k'$ was described by the following equation [20]:

$$\ln k' = {}^1\chi\left(\frac{\epsilon}{T} + \Phi\right) + \frac{\gamma}{T} + \delta \quad (8)$$

where $\epsilon$, $\Phi$, $\gamma$ and $\delta$ are constants, $T$ (K) is the column temperature and ${}^1\chi$ the ester molecular connectivity index [20].

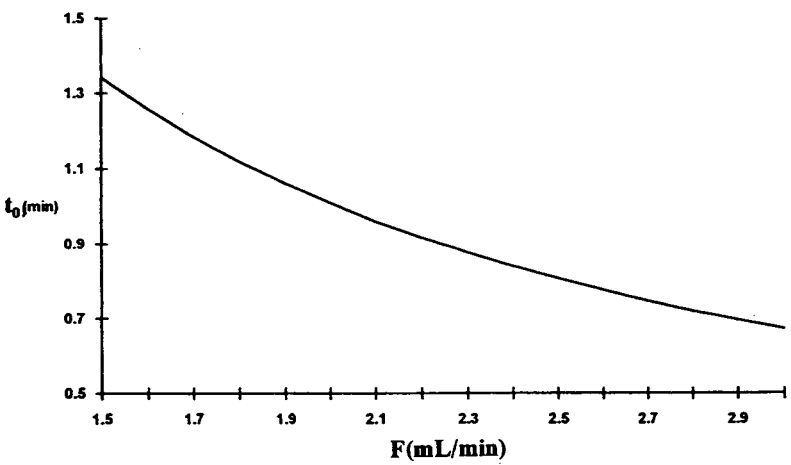


Fig. 1. Plot of column dead time vs. flow-rate.

Table 4
Predicted ($t^p$) and measured ($t^m$) retention time for the eight esters

| Compound[a] No. | [I] | | | | [II] | | | |
|---|---|---|---|---|---|---|---|---|
| | $t_I^p$(min) | $t_I^m$(min) | $\Delta t_I$(min) | $\Delta t_I$(%) | $t_{II}^p$(min) | $t_{II}^m$(min) | $\Delta t_{II}$(min) | $\Delta t_{II}$(%) |
| MeR = 1 | 10.11 | 9.74 | 0.37 | 3.70 | 2.22 | 2.21 | 0.01 | 0.45 |
| EtR = 2 | 14.07 | 13.54 | 0.53 | 3.74 | 2.81 | 2.79 | 0.02 | 0.71 |
| IprR = 3 | 17.65 | 16.94 | 0.71 | 4.00 | 3.33 | 3.33 | 0.00 | 0.00 |
| PrR = 4 | 18.77 | 18.00 | 0.77 | 4.10 | 3.49 | 3.48 | 0.01 | 0.29 |
| TerR = 5 | 21.23 | 20.19 | 1.04 | 4.89 | 3.84 | 3.82 | 0.02 | 0.52 |
| IbuR = 6 | 23.17 | 21.99 | 1.18 | 5.10 | 4.10 | 3.99 | 0.02 | 0.27 |
| SbuR = 7 | 24.25 | 23.06 | 1.19 | 4.90 | 4.25 | 4.22 | 0.03 | 0.71 |
| BuR = 8 | 25.00 | 23.72 | 1.28 | 5.12 | 4.39 | 4.32 | 0.07 | 0.16 |

[a] 1 = Methyl parahydroxybenzoic ester, 2 = ethyl parahydroxybenzoic ester, 3 = isopropyl parahydroxybenzoic ester, 4 = propyl parahydroxybenzoic ester, 5 = terbutyl parahydroxybenzoic ester, 6 = isobutyl parahydroxybenzoic ester, 7 = secbutyl parahydroxybenzoic ester, 8 = butyl parahydroxybenzoic ester.
Conditions: [I] Temperature = 145°C, flow-rate = 1.55 ml/min; [II] Temperature = 170°C, flow-rate = 3.00 ml/min.

Combining Eqs. (5), (7) and (8), a simple empirical equation was found relating the retention time $t$ to the column temperature $T$ (K) and gas flow-rate $F$ (ml/min).

$$t = \frac{\Phi_1}{F}\left(1 + \exp\left({}^1\chi\left(\frac{\epsilon}{T} + \Phi\right) + \frac{\gamma}{T} + \delta\right)\right) \quad (9)$$

Since the constant $\Phi_1$ and the connectivity index

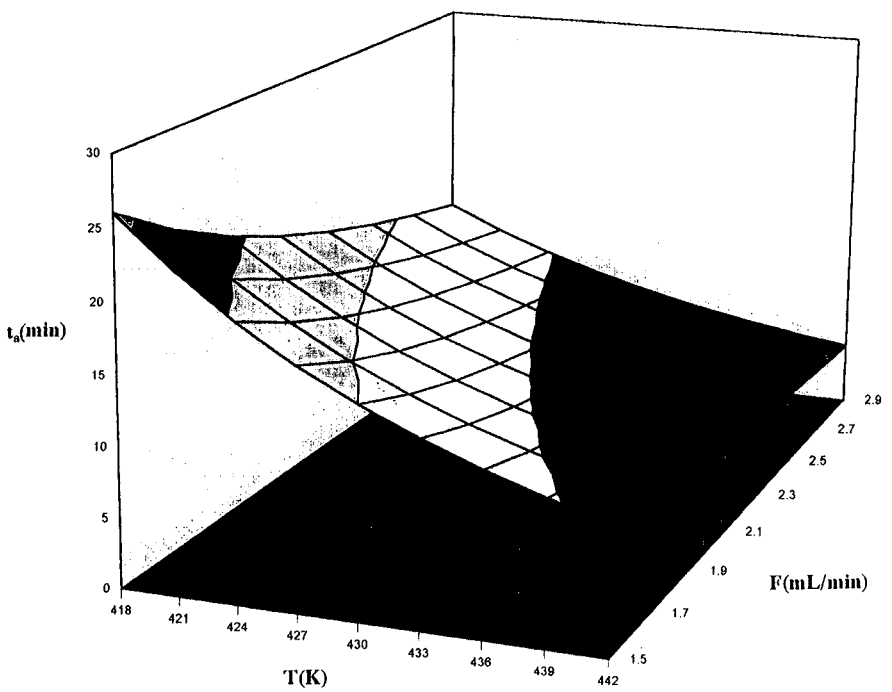


Fig. 2. Response surface for the analysis time $t_a$ vs. $F$ and $T$.

A

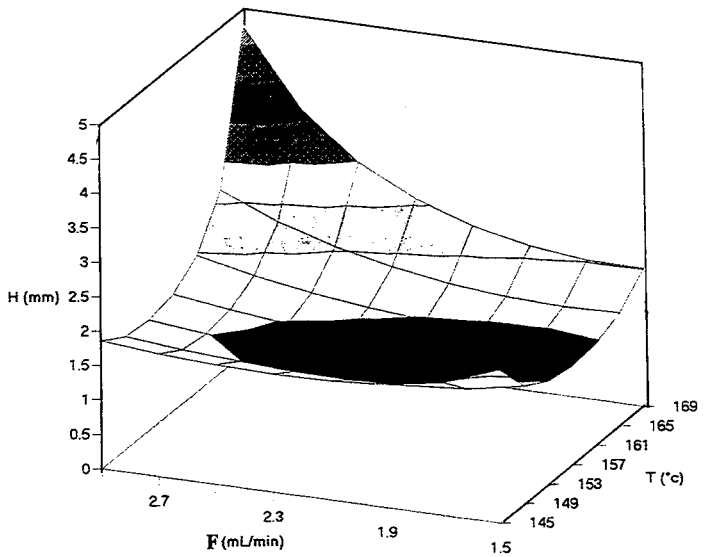


B

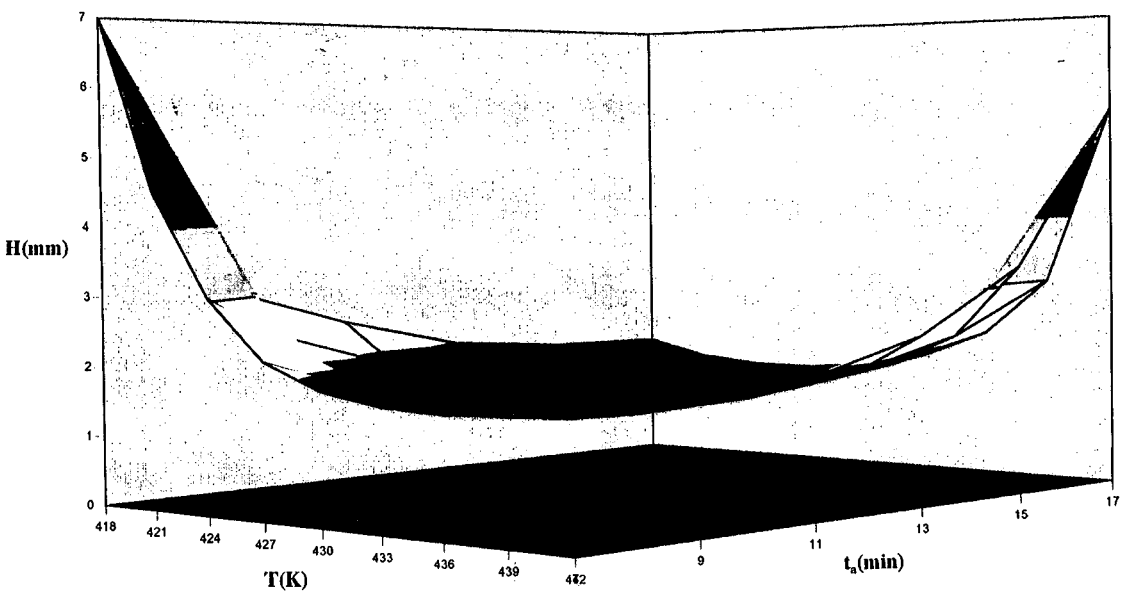


Fig. 3. Response surface of the height to a theoretical plate: (A) vs. column temperature/carrier gas flow-rate; (B) vs. analysis time/column temperature; (C) vs. analysis time/carrier gas flow-rate.

C

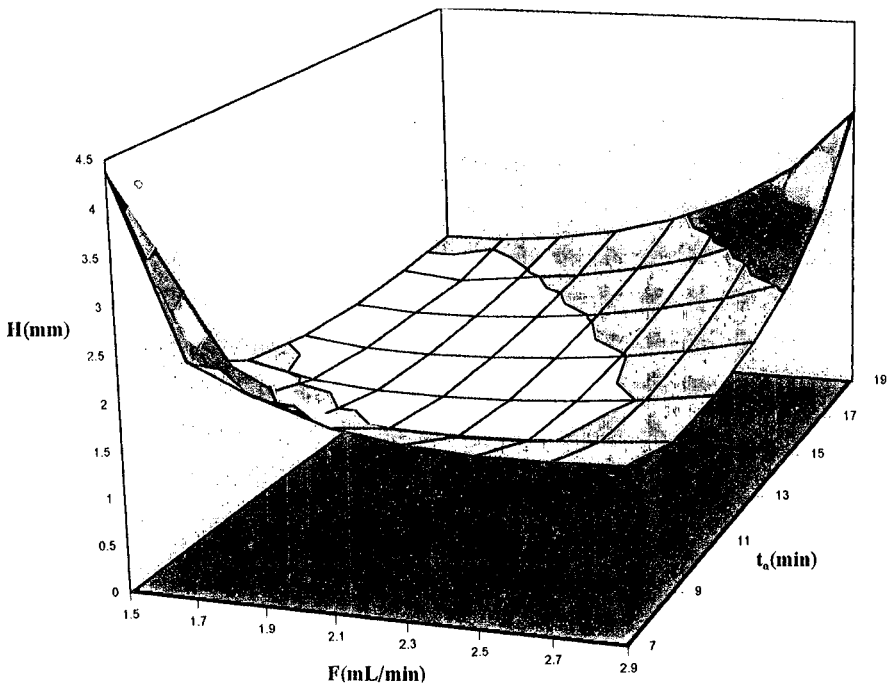


Fig. 3 (*Continued*).

$^1\chi$ of the eight compounds [20] were known, their retention times $t$ were calculated in accordance with the following experimental conditions: [I] $F = 1.55$ ml/min, $T = 145$°C; [II] $F = 3.00$ ml/min, $T = 170$°C.

The data for [I] varied as expected, i.e, a larger error at longer retention times. The good agreement observed between the predicted and experimental values shows the suitability of the model (Table 4). The response surface generated for the analysis time ($t_a$) model (Eq. 9) is given in Fig. 2 for the last compound on the chromatogram (butyl-*p*-hydroxy-benzoic ester).

In gas chromatography, the height equivalent to a theoretical plate ($H$) is used to study the sharpness of a peak. $H$ depends on the carrier gas flow-rate and column temperature. $H$ is given by the following equation:

$$H = \frac{L}{5.54}\left(\frac{W_{0.5}}{t}\right)^2 \qquad (10)$$

where $t$ is the retention time and $W_{0.5}$ the peak-width at half height. The corresponding column plate number ($N$) is:

$$N = \frac{L}{H} = 5.54\left(\frac{t}{W_{0.5}}\right)^2 \qquad (11)$$

The parameters estimates generated for the regression $N/L$ model are given in Table 2.

The values of the Fischer ratio and $R^2$ were 80.40 and 0.974, respectively. The results of the student $t$-test show that all the factors are significant. The predicted and measured $N/L$ values for seven experiments are given in Table 3. The response surface generated for the $H$-model is given in Fig. 3A. Using Eq. (9) relating separation analysis time $t_a$ to carrier gas flow-rate $F$ and column temperature $T$, two other response surfaces for the $H$-model are obtained (Figs. 3B,C). A similar chemometric methodology was used to study column efficiency in reversed-phase chromatography [30].

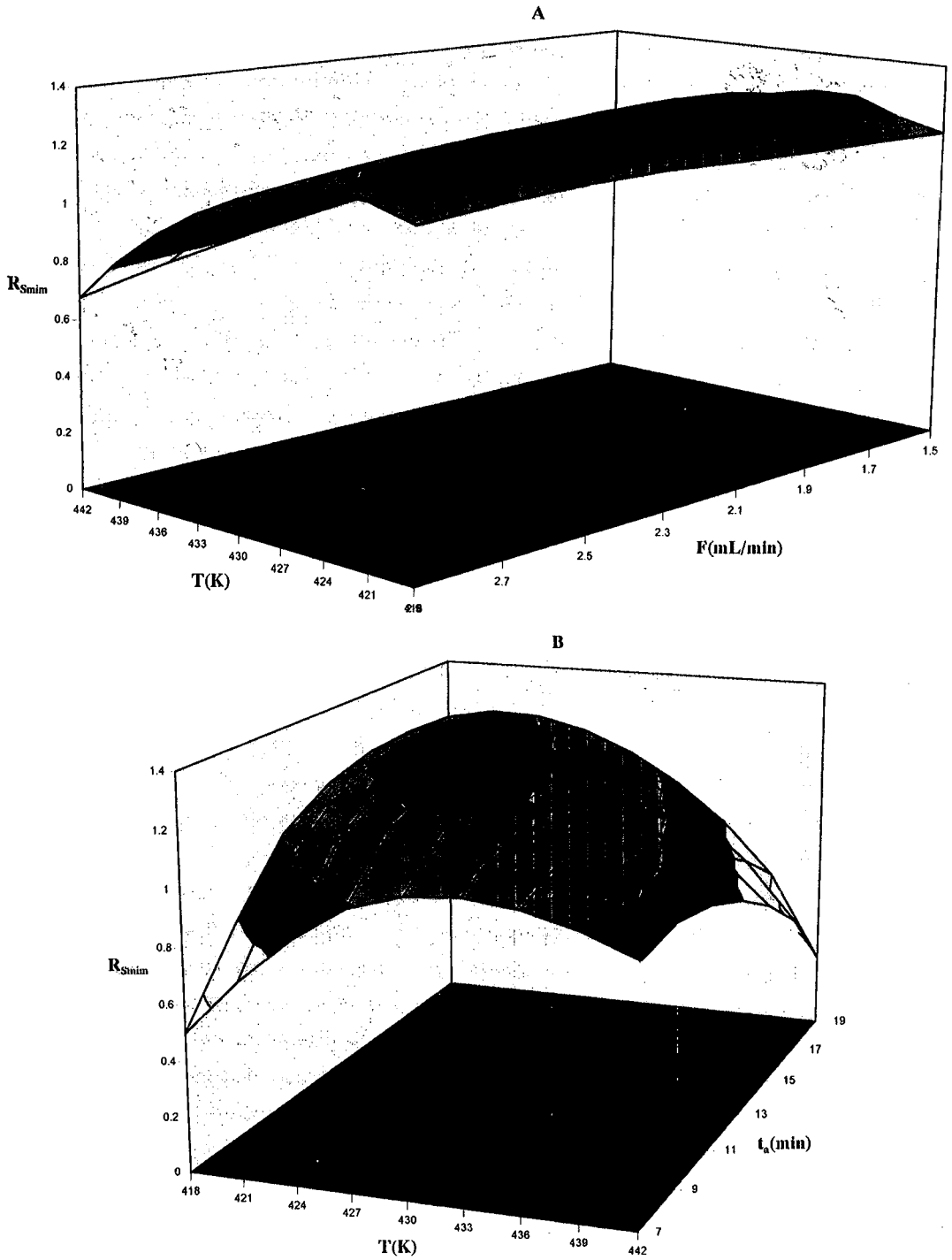


Fig. 4. Response surface of the minimal resolution $R_s$ min: (A) vs. column temperature/carrier gas flow-rate; (B) vs. analysis time/column temperature (C) vs. analysis time/carrier gas flow-rate.

C

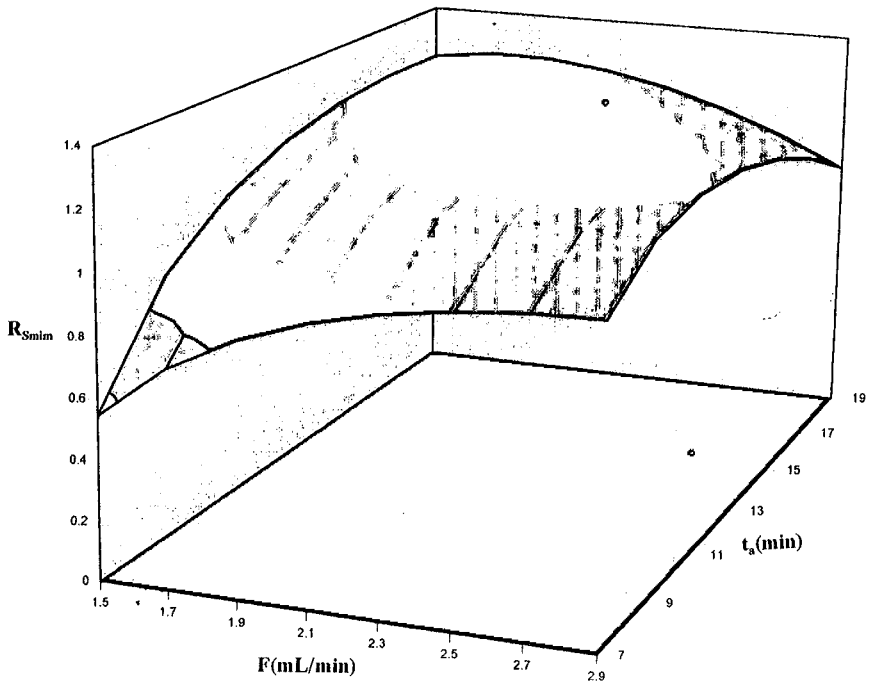


Fig. 4 (*Continued*).

Obviously, optimum column temperature and carrier gas flow-rate are minimum according respectively to the equation of De Wett and Pretorius [31] and Van Deemter et al. [32] which relate respectively $H$ to the column temperature and gas flow-rate. Further improvements and investigations made by others [33–41] do not take into account the simultaneous variation of $F$ and $T$. This chemometric methodology provided an equation relating $H$ to both gas velocity and temperature. The partial derivatives of the $H$-model against $x_1$ and $x_2$ were equal to zero and the optimal temperature and gas flow-rate were determined and found to be equal to 156°C and 1.90 ml/min. Figs. 3B and 3C present a global optimum, i.e, the maximal efficiency was obtained for a single combination of analysis time/gas flow-rate or analysis time/column temperature. In our case for optimal temperature and gas flow-rate, the optimum analysis time was calculated to be 12.00 min. The experimental optimum value of $t_a$ was 12.60 min. The theoretical value was good.

### 3.2. Eight compound separation study

Whatever the factor variation, all compounds were arranged on a chromatogram in the same order. The resolution ($R_S$) between two adjacent peaks can be affected by the three variables:

$$R_S = \frac{\sqrt{N}}{4}\left(\frac{k'}{1+k'}\right)\left(\frac{\alpha-1}{\alpha}\right) \quad (12)$$

where $\alpha$ is the separation factor given by the ratio of the capacity factor for the two solutes between which resolution is being calculated. Computer simulations have began to play an increasing role in the optimization of separations and in the understanding of retention data [21–24].

The interest of this method used here is that it takes into account the analyses time $t_a$ and the

simultaneous variation of column efficiency with the two factors $x_1$ and $x_2$. The experimental design reduced the number of experiments to be carried out. Therefore, knowing the variation of $N$, $k'$ and $\alpha$ with $x_1$ and $x_2$, $R_S$ can be calculated using Eq. (12) for the different values of the two factors. The highest resolution for the worst separated pair of peaks ($R_S$ min) (*sec*-butyl, butyl-*p*-hydroxy-benzoic esters) was used as criterion of separation.

Using Eqs. (9) and (12) there are three response surfaces generated for the $R_S$ min model (Fig. 4A,B,C). The maximum $R_S$ (1.260) was the highest for the worst separated pair of peaks. The optimum conditions were a gas flow-rate of 2.1 ml/min with a column temperature equal to 424 K with an analysis time of 13.20 min. The corresponding chromatogram is given in Fig. 5A.

Obviously, the objective must be to minimize the analysis time and not be too demanding with respect to resolution. If $R_s$ min was chosen to be equal to 1.10 for an analysis time of 8.00 min, Figs. 4B and 4C show that gas flow-rate and column temperature were respectively equal to 2.90 ml/min and 430 K. The corresponding chromatogram is given in Fig. 5B. It can be noted that column efficiency and optimum separation conditions were similar only in relation to the column temperature.

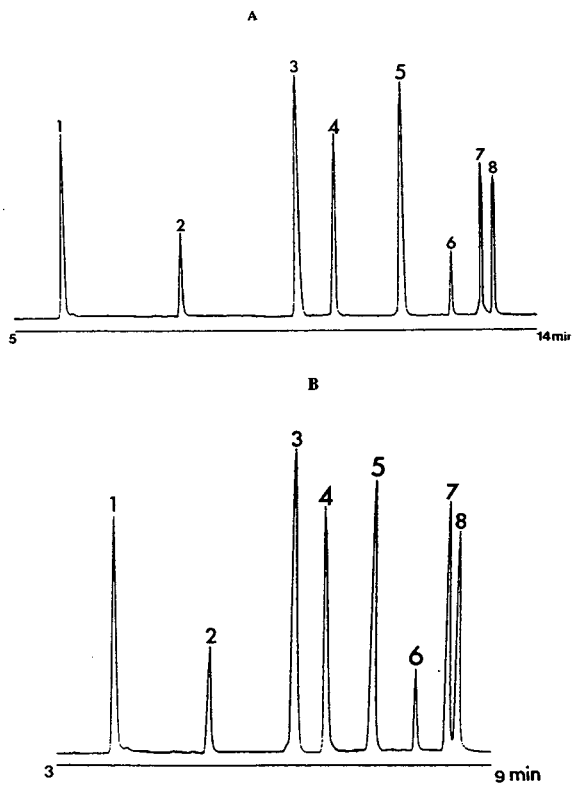


Fig. 5. *p*-Hydroxybenzoic ester chromatogram in the conditions: (A) $F = 2.1$ ml/min, $T = 424$K; (B) $F = 2.9$ ml/min, $T = 430$ K. Number above peaks refers to the eight compounds: see Table 4.

## 4. Conclusion

For a convenient way of ascertaining column temperature and gas flow-rate, this method which both reduces the number of experiments to be carried out and provides suitable retention models, is an attractive approach for optimization in GC.

This optimization procedure could be of interest to industrial process and control engineers as it both reduces analysis time and improves separation.

## References

[1] N.W. Davies, J. Chromatogr., 503 (1990) 1.
[2] M.S. Vigdergauz and N.F. Belyaev, Chromatographia, 30 (1990) 163.
[3] Y. Guan, J. Kiraly and J.A. Rijks, J. Chromatogr., 472 (1989) 129.
[4] G.J. Price and M.R. Dent, J. Chromatogr., 483 (1989) 1.
[5] G.J. Price and M.R. Dent, J. Chromatogr., 585 (1991) 83.
[6] C.T. Peng, Z.C. Yang and D. Maltby, J. Chromatogr., 586 (1991) 113.
[7] D. Messadi, F. Helaimia and S. Ali Mokhnache, C.R. Acad. Sci. Ser 2, 310 (1990) 1447.
[8] D.J.A. Garcia and J.M. Santiuste, Chromatographia, 32 (1991) 116.
[9] D. Messadi, F. Helaimia, S. Ali Mokhnache and M. Boumahraz, Chromatographia, 29 (1990) 429.
[10] E. Fernandez-Sanchez, J.A. Garcia-Dominguez, V. Menendez and J.M. Santiuste, J. Chromatogr., 498 (1990) 1.

[11] N. Dimov and E. Matisova, J. Chromatogr., 549 (1991) 325.
[12] M.N. Hasan and P.C. Jurs, Anal. Chem., 62 (1990) 2318.
[13] A. Robbat Jr. and C. Kalogeropoulos, Anal. Chem., 62 (1990) 2684.
[14] J.R. Donnely, W.D. Munslow, A.H. Grange, T.L. Petit, R.D. Simmons and G.W. Sovocool, J. Chromatogr., 540 (1991) 293.
[15] C.G. Georgakopoulos, O.G. Tsika and J.C. Kiburis, Anal. Chem., 63 (1991) 2025.
[16] C.G. Georgakopoulos, J.C. Kiburis and P.C. Jurs, Anal. Chem., 63 (1991) 2021.
[17] T.C. Gerbino and G. Castello, J. Chromatogr., 537 (1991) 305.
[18] R.A. Mowery Jr., J. Chromatogr. Sci., 29 (1991) 194.
[19] A.D. Jorgensen, K.C. Picel and V.C. Stamoudis, Anal. Chem., 62 (1990) 683.
[20] Y. Guillaume and C. Guinchard, Chromatographia, in press.
[21] D.E. Bautz, J.W. Dolan, W.D. Raddatz and L.R. Snyder, Anal. Chem., 62 (1990) 1560.
[22] J.W. Dolan, L.R. Snyder and D.E. Bautz, J. Chromatogr., 541 (1991) 21.
[23] Q. Wang, C. Zhu and B. Yan, J. Chromatogr., 513 (1990) 13.
[24] T. Aishima and S. Nakai, Anal. Chem. Acta, 248 (1991) 41.
[25] A.F. Fell, T.A.G. Noctor, J.E. Mama and B.J. Clark, J. Chromatogr., 434 (1988) 377.
[26] G.E.P. Box, K.B. Wilson and J. Roy. Stat. Soc. B., 13 (1951) 1.
[27] W.G. Cochran and G.M. Cox, Experimental Designs, Wiley, New York, 1957.
[28] L.A. Jonnes, J.J. Glennon and W.H. Reiss, J. Chromatogr., 595 (1992) 209.
[29] J.A. Perry, Introduction to analytical Gas Chromatography, Marcel Dekker, New York, NY, (1981).
[30] Y. Guillaume and C. Guinchard, J. Chromatogr. Sci., in press.
[31] W.J. De Wett and V. Pretorius, Anal. Chem., 30 (1958) 325.
[32] J.J. Van Deemter, F.J. Zwiderweg and A. Klinkenberg, Chem. Eng. Sci., 5 (1956) 271.
[33] M.J.E. Golay, in D.H. Desty (editor), Gas Chromatography, Butterworth, London, 1958, p. 36.
[34] H. Purnell, Gaz Chromatography, Wiley and Sons, New York, 1962.
[35] J.C. Giddings, Dynamics of Chromatography, Marcel Dekker, New York, 1965.
[36] A.B. Littlewood, Gas Chromatography, 2nd Edn., Academic Press, New York, 1970.
[37] J.N. Done, G.J. Kennedy and J.H. Knox, in S.G. Perry, (Editor), Gas Chromatography, Institute of petroleum, London, 1973.
[38] J.S. Fritz and D.M. Scott, J. Chromatogr., 271 (1983) 193.
[39] J. Ceulemans, J. Chromatogr. Sci., 22 (1984) 296.
[40] I.L. Moon, K.H. Row and W.K. Lee, Korean J. Chem. Eng., 2 (1985) 155.
[41] G. Gaspar, R. Annino, C. Vidal-Madjar and G. Guiochon, Anal. Chem., 50 (1978) 1512.

ELSEVIER

Journal of Chromatography A, 704 (1995) 449–454

JOURNAL OF CHROMATOGRAPHY A

# Comparison of gas chromatographic and spectrophotometric techniques for the determination of formaldehyde in water☆

Š. Velikonja*, I. Jarc, L. Zupančič-Kralj, J. Marsel

*Department of Chemistry, University of Ljubljana, Aškerčeva 5, Slovenia*

First received 13 October 1994; revised manuscript received 5 January 1995; accepted 11 January 1995

**Abstract**

Formaldehyde was determined in aqueous samples by four different analytical procedures (two spectrophotometric and two gas chromatographic). In the spectrophotometric procedures chromatogropic acid and 3-methyl-2-benzothiazolone hydrazone were used. For gas chromatography either an electron-captive or a flame ionization detector were used, and for sample preparation liquid–liquid extraction in the former and solid-phase extraction in the latter case were used. The concentration range covered was between 0.06 and 20 mg/l. Calibration plots and detection limits were optimized for all four procedures.

## 1. Introduction

Formaldehyde is a well known pollutant present in both industrial and non-industrial environments. It is a combustion product from many sources, including automobile engines and cigarette smoke [1]. As it is still widely used in the furniture industry [2], as a consequence it can be found in different building materials and furnishings. Formaldehyde is also known to be an irritant of the skin, eyes and nasopharyngial membranes [3] and has also been declared a suspected carcinogen [2] and mutagen [4].

Various methods can be used for formaldehyde determination [1,2]. In this work, two spectrophotometric and two gas chromatographic (GC) methods for the determination of formaldehyde in aqueous solutions were applied. The most frequently used method for the determination of formaldehyde is spectrophotometry with chromotropic acid (1,8-dihydroxy naphthalene-3,6-disulphonic acid) [3,5,6]. Another, less often used, method utilizes MBTH reagent (3-methyl-2-benzothiazolone hydrazone) [7,8]. An important problem associated with spectrophotometric determinations of formaldehyde is the interference of many substances, including acetaldehyde, acroleine, phenol and carbohydrates. For this reason, GC was applied as an alternative method for formaldehyde determination. Because of its high selectivity and efficiency of reaction at room temperature [9], derivatization with 2,4-dinitrophenylhydrazine was chosen. The 2,4-dinitrophenylhydrazine derivatisation products can be determined either by high-performance liquid chromatography (HPLC) [10–14] or by GC with electron-capture

* Corresponding author.

☆ Presented at the *International Symposium on Chromatographic and Electrophoretic Techniques, Bled, Slovenia, 10–13 October 1994.*

0021-9673/95/$09.50 
*SSDI* 0021-9673(95)00049-6

detector (ECD) or flame ionization detector (FID) [9,15–18]. However, all analytical methods for formaldehyde determination should permit its determination at concentrations below the maximum allowed concentration in different samples. The maximum allowed concentration of formaldehyde in waste water in Slovenia is 1 mg/l.

The two spectrophotometric methods were compared with the more reliable and rarely used GC–ECD and GC–FID methods. Few data on comparisons of methods for formaldehyde determination could be found in the literature [19].

## 2. Experimental

### 2.1. Apparatus

For spectrophotometric determinations a Milton Roy Spectronic 1201 spectrophotometer was used. A Hewlett-Packard Model 5890 A gas chromatograph with electron-capture and flame ionization detectors was used in combination with a Hewlett-Packard HP 3396 Series II integrator.

### 2.2. Reagents and materials

Formaldehyde solution (ca. 36%), iron(III) chloride hexahydrate and sulphamic acid were purchased from Kemika (Zagreb, Croatia). Chromotropic acid (CTA) (99%), 3-methyl-2-benzothiazolone hydrazone hydrochlorid (MBTH) reagent and gradient-grade toluene, *n*-hexane and acetonitrile were purchased from Merck (Darmstadt, Germany). Sulphuric acid (95–97%) was purchased from Merck-Alkaloid (Skopje, Macedonia). 2,4-Dinitrophenylhydrazine was purchased from BDH (Poole, UK), and, to avoid high blanks, was recrystallized twice from acetonitrile and stored in a closed glass vial. All solutions were prepared with purified water obtained from a Milli-Q water-purification system (Millipore) if not specified otherwise.

Supelclean 6-ml $C_{18}$ cartridges from Supelco (Bellafonte, PA, USA) were used for the solid-phase extraction associated with the GC–FID procedure.

### 2.3. Synthesis of standard

The standard derivative of 2,4-dinitrophenylhydrazine with formaldehyde was synthesized as described elsewhere [20] and recrystallized twice from acetonitrile. The product was stored in polypropylene vials in a dark and cool location prior to use.

### 2.4. Preparation of standard solutions and reagents

From formaldehyde solution (ca. 36%), a stock solution of formaldehyde at a concentration of ca. 10 g/l was prepared and standardized by the sulphite method [3]. The solution was stored in the dark and used for the preparation of other standards by dilution.

MBTH solution at a concentration of 0.037 g/l was prepared daily in water as reagent A. Reagent B consisted of iron(III) chloride (0.05 g/l) and sulphamic acid (0.09 g/l). A solution of 2,4-dinitrophenylhydrazone was prepared in acetonitrile. All solutions were stored in a dark and cool location.

2,4-Dinitrophenylhydrazine solution (for the GC–FID procedure) at a concentration of 1 mg/ml was prepared weekly by dissolving 10 mg of 2,4-dinitrophenylhydrazine in 1 ml of acetonitrile and diluting with HCl–$H_2O$ (1:3, v/v) to 10 ml and stored in a cool and dark location.

### 2.5. Analytical procedures

*Chromotropic acid procedure*

A 5-ml volume of the test solution was transferred into a 50-ml volumetric flask and 1 ml of 5% CTA solution was added. After addition of 43 ml of 50% $H_2SO_4$, the solution was mixed and closed with a glass stopper. The solution was heated on a water-bath at 100°C for 30 min, cooled and diluted to 50 ml with Milli-Q-purified water. The absorbance was measured against the blank at 572 nm.

*MBTH procedure*

A 1-ml volume of the test solution was placed into a 10-ml graduated tube and 0.5 ml of reagent A was added and mixed. After 1 min, 1 ml of reagent B was added, and after 10 min the mixture was diluted with water to 10 ml. The absorbance was measured against the blank at 632 nm.

*GC–ECD procedure*

This was based on a procedure described in the literature [15]; 1 ml of test solution was pipetted into a test-tube with a glass stopper and 1 ml of 2,4-dinitrophenylhydrazine solution was added and mixed. 2,4-Dinitrophenylhydrazone was extracted in 1 ml of toluene. Sodium sulphate was used to dry the toluene phase and the extract was analysed by capillary GC with a $^{63}Ni$ electron-capture detector and split–splitless injection. A 30 m × 0.32 mm I.D. fused-silica capillary column coated with DB-5 (J&W Scientific, Folson, CA, USA) with a 0.25-$\mu$m film thickness was used for chromatographic separation, and the nitrogen carrier gas flow-rate was 1.5 ml/min. The temperatures were as follows: injector, 200°C; detector, 290°C; and column oven, 200°C for 1 min, then increased to 250°C at 2°C/min. The purge activation time was 1 min. Peak heights for 2,4-dinitrophenylhydrazone were used for quantification.

*GC–FID procedure*

Preconcentration on $C_{18}$ cartridges was based on a procedure described elsewhere [11] with modification, i.e., after sample loading the cartridge was not washed with 17% acetonitrile solution, as 2,4-dinitriophenylhydrazones are eluted with this reagent.

From the stock solution, 0.2 ml of 2,4-dinitrophenylhydrazine solution was added to 100 ml of test solution, shaken and the reaction allowed to proceed for 1 h. The cartridge was activated with 20 ml of acetonitrile and 10 ml of water. The sample was pumped through at a flow-rate of ca. 5 ml/min. After passing all the sample, the cartridge was dried with air and 2,4-dinitrophenylhydrazones were eluted with 3 ml of acetonitrile. The solvent was evaporated with nitrogen, the residue was dissolved in 1 ml acetonitrile and the solution was analysed by capillary GC with a flame ionization detector and split–splitless injection. A 25 m × 0.20 mm I.D. fused-silica capillary column coated with HP-1 (Hewlett-Packard, Geneva, Switzerland) with a 0.22-$\mu$m film thickness was used for the separation, and the helium carrier gas flow-rate was 0.8 ml/min. The make-up gas was nitrogen. The temperatures were as follows: injector, 200°C; detector, 280°C; and column oven, 150°C for 1 min, then increased to 250°C at 3°C/min. The purge activation time was 1 min. Peak areas for 2,4-dinitrophenylhydrazone were used for quantification.

## 3. Results

### 3.1. Calibration

Calibration was performed with standard aqueous solutions of formaldehyde in tap water for all procedures and the linear regression analysis data are given in Table 1. With the CTA and GC–ECD procedures, each calibration point corresponds to a single analysis, while triplicate analyses were used with the MBTH and GC–FID procedures. Using the procedures described, formaldehyde can be determined in aqueous solutions over a wide concentration range. Each procedure covers a different concentration range, the CTA procedure from 1 to 20 mg/l and the MBTH procedure from 0.06 to 4 mg/l.

The major problem encountered with spectrophotometric methods for formaldehyde determination are interferences, hence these methods

Table 1
Regression parameters associated with calibration data

| Procedure | $a$ | $b$ | $r$ | $S_{y/x}$ |
|---|---|---|---|---|
| CTA | 0.0016 | 0.0487 | 0.9997 | 0.0069 |
| MBTH | 0.0004 | 0.1912 | 0.9998 | 0.0040 |
| GC–ECD | 0.5160 | 0.4334 | 0.9973 | 0.3977 |
| GC–FID | 0.3890 | 0.3775 | 0.9972 | 0.2762 |

are not reliable. GC methods do not suffer from interferences, but they are less precise (i.e., manual injection, etc). The GC–ECD procedure is capable of determining formaldehyde at concentrations between 0.8 and 10 mg/l, but saturation of the electron-capture detector at higher concentrations limits its linear range. The GC–FID method does not suffer from this problem and is capable of determining formaldehyde in the concentration range between 0.06 and 1 mg/l.

### 3.2. Recovery studies

To find the recovery of the extraction, 100 ml of a solution of 2,4-dinitrophenylhydrazone were prepared and treated as though it was a test sample. After preconcentration, 2 $\mu$l were injected into the gas chromatograph and the peak areas for 2,4-dinitrophenyl-hydrazone were compared with the areas obtained for pure standard solutions. Each experiment was repeated tree times. The recoveries were found to be between 87 and 101% for concentrations of formaldehyde between 3.0 and 0.1 mg/l.

### 3.3. Detection limit estimates

As formaldehyde is also of great concern in atmospheric chemistry research, e.g., tropospheric ozone formation, the detection limit for analytical methods is of interest. As is well known, Kaiser's approach to the estimation of the detection limit is most widely used [21], but it does not take into account $\beta$ errors, that is, the possibility of false-positive results, and errors associated with the calibration graph. Long and Winefordner [22] proposed a different approach for the estimation of detection limits, which includes errors in the calibration graph, but still fails to consider $\beta$ errors. A computer program, Detarchi [23], is based on the hypothesis testing method [24]. This makes it possible to choose the magnitude of $\alpha$ and $\beta$ errors (the probability of false-positive and false-negative results) and thus these errors can be adjusted depending on the problem. In our work we chose $\alpha$ to be equal to $\beta$ (0.05).

Table 2
Detection limit estimates

| Procedure | Detection limit (mg/l) | | |
|---|---|---|---|
| | Kaiser's method | Error propagation method[a] | Detarchi program[a] |
| CTA | 0.15 | 0.27 | **0.41** |
| MBTH | – | **0.06** | 0.04 |
| GC–ECD | 0.05 | **0.72** | 0.60 |
| GC–FID | – | 0.04 | **0.06** |

[a] Finally accepted detection limit estimates are printed in bold.

Blank determinations were repeated for all procedures and the detection limits estimated are given in Table 2. From the data in Table 2, the following conclusions about the estimation of the detection limit can be made. With the CTA and GC–ECD procedures, the detection limit estimates vary widely. The reason is that there are only a few calibration points near the detection limit and only one analysis was made for each calibration point. Detection limit estimates for the MBTH and GC–FID procedures are much closer, because there are more points in the lower concentration range and because every point corresponds to triplicate analysis. This makes the detection limit estimate lower, because there is lower uncertainty about the behaviour of the analyte near the detection limit region. Careful calibration design is essential for good detection limit estimates, as well as repetition of blanks. Careful attention must be paid to calibration points near the detection limit, and the calibration must be repeated several times to obtain sufficient information about the behaviour of the analyte over the whole calibration range and near the detection limit.

### 3.4. Water analysis

For the analysis of waste water with the CTA and GC–ECD methods, the sample was obtained from a retention pool in a factory that produces phenol–formaldehyde resins. A sample was taken in a glass bottle, which was closed immediately after sampling and was analysed on

the same day. For the CTA and GC–ECD procedures, the standard addition method was employed, because it was assumed that the sample contains phenol, which interferes with the analysis. The standard addition method was employed with three additions. The formaldehyde concentration in this waste water was found to be 0.9 mg/l with both methods, which is below the maximum allowed concentration for waste waters (1 mg/l).

River water was taken from a very polluted river in the region of Ljubljana (Slovenia) and analysed by the MBTH and GC–FID methods. A sample was taken in a glass bottle that had been prerinsed with river water. Each sample was taken at the surface in the countercurrent, closed with a glass stopper, transported to the laboratory and analysed on the same day. The standard addition method with six points was used for the MBTH procedure, but the estimated concentration of formaldehyde was found to be below the detection limit estimated for the MBTH procedure.

For the GC–FID procedure, three analyses were made and a typical chromatogram is shown in Fig. 1a. The peak height is negligible, because it lies on the tail of another peak. To confirm this small peak, the sample was spiked with 0.05 mg/l of formaldehyde and three additional determinations were made. The peak for 2,4-dinitrophenylhydrazone increased (Fig. 1b). The estimated concentration of formaldehyde in this water sample was below the limit of detection, which means that the concentrations of form-

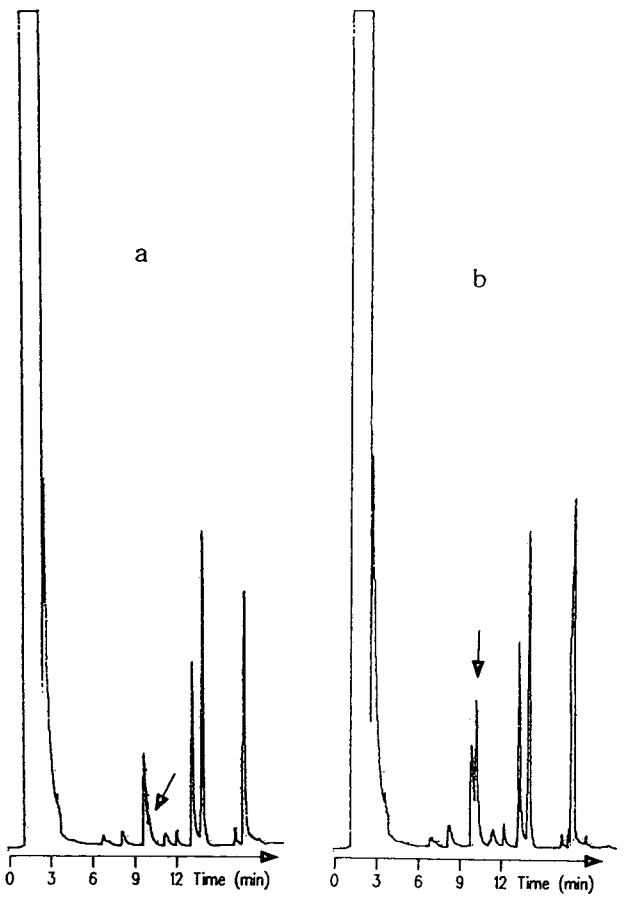


Fig. 1. Chromatograms of (a) river water and (b) river water spiked with 0.05 mg/l of formaldehyde.

aldehyde in that water were at approximately the same level as found elsewhere [4,11,14].

## 4. Conclusions

Both spectrophotometric procedures described suffer from interferences and therefore cannot be used for formaldehyde determination in water samples including interfering substances.

The GC–ECD procedure includes liquid–liquid extraction of 2,4-dinitrophenylhydrazone into toluene and its injection into the gas chromatograph. At higher concentrations the detector becomes saturated and this narrows the linear range. The GC–FID procedure uses a solid-phase extraction of 2,4-dinitrophenylhydrazone on $C_{18}$ cartridges and is able to cover a lower concentration range than the GC–ECD procedure.

The use of spectrophotometry allows formaldehyde determination in aqueous samples in the concentration range between 0.06 and 20 mg/l, and GC in the range between 0.06 and 10 mg/l.

If proper instrumentation is available, these methods can be used for the determination of formaldehyde in aqueous solutions over a broad concentration range. GC procedures are also a good alternative to the HPLC determination of formaldehyde, which is widely used [10–14].

Detection limit estimates for all four procedures show how important the calibration design is for detection limit estimation. If few calibration points are used for concentrations near the detection limit and with no replicates, the estimated detection limit can be very low, which can lead to false-positive results.

## Acknowledgements

The financial support of the Ministry of Science and Technology is gratefully acknowledged. One of us (Š.V.) thanks the Ministry of Education and Sport of Slovenia for financial support.

## References

[1] A.D. Pickard, and E.R. Clark, Talanta, 31 (1984) 763.
[2] M.P. Munoz, F.J.M. de Villena Ruenda and L.M.P. Diez, Analyst, 114 (1989) 1469.
[3] J.F. Walker, Formaldehyde, Robert Krieger, Huntington, NY, 3rd ed., 1975.
[4] F. van Hoof, A. Wittock, E. van Buggenhout and J. Janssens, Anal. Chim. Acta, 169 (1985) 419.
[5] A.P. Altshuller, D.A. Miller and S.F. Sleva, Anal. Chem., 33 (1961) 621.
[6] E. Sawicki, T.R. Hauser and S. McPherson, Anal. Chem., 34 (1962) 1460.
[7] T.G. Matthews and T.C. Howell, J. Air Pollut. Control Assoc., 31 (1981) 1181.
[8] E. Sawicki, T.R. Hauser, T.W. Stanley and W. Elbert, Anal. Chem., 33 (1961) 93.
[9] V.P. Uralets, J.A. Rijks and P.A. Leclercq, J. Chromatogr., 194 (1980) 135.
[10] P.J. Whittle and P.J. Rennie, Analyst, 113 (1988) 665.
[11] R.J. Kieber and K. Mopper, Environ. Sci. Technol., 24 (1990) 147.
[12] K. Fung and D. Grosjean, Anal. Chem., 53 (1981) 168.
[13] A. Benassu, A. Semenzato and F. Zaccaria, J. Chromatogr., 502 (1990) 193.
[14] K. Takami, K. Kuwata, A. Sugimae and M. Nakamoto, Anal. Chem., 57 (1985) 243.
[15] A.L. Pertsovskii and L.M. Kremko, Zh. Anal. Khim., 40 (1986) 1115.
[16] L.J. Papa and L.P. Turner, J. Chromatograph. Sci., 10 (1972) 744.
[17] T. Dumas, J. Chromatogr., 247 (1982) 289.
[18] K. Buckley and L. Fisher, J. Assoc. Off. Anal. Chem., 69 (1986) 655.
[19] M. Petreas, S. Twiss, D. Pon and M. Imada, Am. Ind. Hyg. Assoc., 47 (1986) 276.
[20] Vogel's Textbook of Practical Organic Chemistry, Longman, Harlow, 4th ed., 1978.
[21] P.C. Meier and R.E. Zünd, Statistical Methods in Analytical Chemistry, Wiley, New York, 1993.
[22] G.L. Long and J.D. Winefordner, Anal. Chem., 55 (1983) 712A.
[23] L. Sarabia and M.C. Oritz, Trends Anal. Chem., 13 (1994) 1.
[24] C.A. Clayton, J.W. Hines and P.D. Elkins, Anal. Chem., 59 (1987) 2508.

ELSEVIER

Journal of Chromatography A, 704 (1995) 455–463

JOURNAL OF CHROMATOGRAPHY A

# Accurate quantitation of short-, medium-, and long-chain fatty acid methyl esters by split-injection capillary gas–liquid chromatography

Franz Ulberth*, Franz Schrammel

*Department of Dairy Research and Bacteriology, Agricultural University, Gregor Mendel-Str. 33, A-1180 Vienna, Austria*

First received 8 December 1994; revised manuscript received 10 February 1995; accepted 17 February 1995

**Abstract**

Theoretical FID response factors were obtained with cold on-column injection for the major fatty acid methyl esters (FAMEs) occurring in bovine milk fat, except for methyl butyrate and methyl caproate. For these two substances the response factors were larger than expected by theory. Preliminary experiments showed that syringe handling is paramount for obtaining accurate results when a split injector was used for sampling. The solvent flush technique in combination with preheating of the needle and an additional dwell time after depressing the plunger proved to be best suited. Other operational parameters of the split injector were studied by two-level factorial designs. In the case of a FAME test mixture resembling the composition of bovine milk fat, temperature of the injector, septum penetration speed as well as the interaction of these two factors were found to govern the accuracy of the results. Using the same experimental set-up, all the factors tested (injector temperature, penetration speed, split liner design, and split vent flow) proved to be influential with a vegetable oil FAME test mixture. Nevertheless, the magnitude of these effects was so small that it seems justifiable to neglected them in routine testing of vegetable oil samples.

## 1. Introduction

It is widely accepted that gas–liquid chromatography (GLC) is the method of choice for the analysis of the fatty acid (FA) composition of fats and oils. In addition, the advent of inert and powerful fused-silica capillary columns fostered the attractiveness of this technique. Traditionally, lipid bound FAs are converted to methyl esters (FAMEs) by one of several possible basic procedures and the resulting esters separated by GLC. By theory, the area percentages of the recorded chromatogram should approximately represent the FA composition of the analysed fat. In some cases this assumption holds true, at least with modern instrumentation and simple FAME mixtures consisting of only 4 or 5 species with a similar number of carbon atoms. Accurate quantitation of mixtures of FAMEs whose boiling points differ to a greater extent represents a much more difficult task. Badings and De Jong [1] as well as Craske and Bannon [2] listed several factors which may adversely affect the accuracy of FAME analyses by GLC. Errors due to (i) inadequate sample preparation and (ii)

* Corresponding author.

0021-9673/95/$09.50 
*SSDI* 0021-9673(95)00224-3

faulty sample introduction seem to play the most prominent role.

The FA composition of milk fat (MF) from ruminant animals is not easily quantitated because it is made up of a unique mixture of components with low, medium and high boiling points. A base-catalysed transmethylation of the sample avoids losses of volatile and partly water-soluble short-chain FAMEs, hence ruling out a major source of error. As a consequence, failures in the GLC process per se or during calibration should account for inaccurate MF-FAME analyses. The necessity for special calibration runs results from the fact that the flame ionisation detector (FID) does not respond to the carbonyl carbon [3]. Therefore, the weight percentage of ionisable carbon varies with the chain length, thus giving rise to an unequal response for FAME with a different number of carbon atoms.

Sample introduction by split injection (SI) could aggravate this quantitation problem due to non-linear splitting. Several key factors involved in the process leading to sample discrimination have been identified so far [4]. Syringe handling techniques, temperature and design of the split injector seem to be most influential. In a series of articles the problems connected with the reliable GLC quantitation of FAMEs were addressed by Bannon, Craske and co-workers [2,5–9]. According to these studies, analytical parameters (ester preparation, FID linearity, injection technique, etc.) have to be optimised in such a way that only theoretical response factors (RFs), as proposed by Ackman and Sipos [3], have to be applied to convert FAME area percentages to mass percentages. By using packed-column technology they showed that this concept was also applicable to fats containing volatile, short-chain FAs like butyric acid in MF [5]. On the contrary, Badings and de Jong [1], working also with MF, reported empirical RFs, found by capillary-column GLC with cold on-column injection (OCI), which were close, but not identical with the theoretical factors.

A specially designed injector insert, high temperature of the injector (ca. 350°C), a high split ratio and rapid injection (preferably done by an automatic injector) were recommended for SI onto capillary columns to ensure high accuracy [2,7]. However, the appropriateness of these measures in case of FAME profiling of MF was not demonstrated. Although OCI injection is unequivocally regarded as the sampling technique best suited for quantitation, split injection is still very popular with lipid analysts. Therefore, we address, in this article, SI capillary GLC of FAMEs with large differences in chain length, with a focus on measures to minimise sample discrimination.

## 2. Experimental

### 2.1. Reagents

Reference methyl esters for gas chromatography (purity +99%) and solvents (AR grade) were obtained from Merck (Darmstadt, Germany). The AOCS Oil Reference Standard No. 1 was purchased from Sigma (Sigma-Aldrich, Vienna, Austria) and the CRM No. 162 (soya-maize oil blend) from the Community Bureau of Reference, Commission of the European Union, Brussels, Belgium. The Sep-Pak SiOH cartridge was from Waters Millipore (Millipore, Vienna, Austria).

### 2.2. Preparation of methyl esters

Methanolysis of the CRM No. 162 reference oil was done with KOH in methanol [10].

### 2.3. Gas–liquid chromatography

A Fisons/Carlo Erba MEGA 5300 gas chromatograph (Fisons Instruments, Vienna, Austria) equipped with both a cold on-column and a split/splitless injector was used. The FID signal was processed by a ChromJet integrator (Spectra-Physics, San Jose, CA, USA). FAMEs were separated with a 30 m × 0.32 mm I.D., 0.25 $\mu$m film thickness, J&W DB-Wax fused-silica capillary column (Fisons Instruments, Vienna, Austria). All experiments were run with the following oven temperature program: 40°C held for 4

min, 10°C/min to 140°C held there for 1 min, 5°C/min to 220°C held there for 10 min. Detector temperature was set at 250°C. Hydrogen was the carrier gas at 40 kPa head pressure (gas velocity: 45 cm/s determined at 40°C). Flow-rates of the FID fuel gases were: hydrogen 22 ml/min, nitrogen (make-up gas) 19 ml/min, air 290 ml/min. Secondary air cooling for OCI was turned on 2 min before an injection and shut off 5 s after injection. Sample introduction was done by means of a Hamilton (Bonaduz, Switzerland) 701N syringe (10-$\mu$l volume, 5-cm needle length, point style No. 2) for SI and a Hamilton 701SN syringe (5-$\mu$l volume, 7.5-cm needle length, point style No. 3) for OCI. Either an empty glass tube (79.5 × 4 mm I.D., Fisons Cat. No. 45300400) or a "laminar cup" splitter (79.5 × 5.5 mm I.D., Restek Cat. No. 20809, Bellefonte, PA, USA) were employed as splitter sleeves. Other splitter parameters are given in the text.

### 2.4. Needle handling techniques

The following needle handling techniques for SI were evaluated:

–(A) Filled needle injection: the needle of the syringe was cleaned with solvent and dried by applying vacuum. Sample was drawn up to the 1-$\mu$l mark, the syringe needle pushed through the septum and the plunger depressed immediately. Thereafter, the syringe was withdrawn rapidly.

–(B) Filled needle injection with post-injection dwell time: The injection was performed as described in (A) but the needle was left for an additional 2 s in the hot injector before being removed.

–(C) Hot needle injection: the syringe was cleaned as described in (A), sample was drawn up to the 1-$\mu$l mark and, thereafter, completely withdrawn into the barrel. The needle was pushed through the septum and, after a dwell time of 3 s, the plunger was depressed and the needle removed rapidly.

–(D) Solvent flush injection: first, the needle was filled with pure solvent. Second, the plunger was pulled back to the 1-$\mu$l mark to suck an air bubble into the syringe, followed by sample until the plunger reached the 2-$\mu$l mark. Finally, the sample was withdrawn from the needle into the barrel. Injection was performed as described under (C).

–(E) Solvent flush injection with post-injection dwell time: The injection was performed as described in (D) but the needle was left for an additional 2 s in the hot injector before being removed.

For OCI, the needle was filled with solvent followed by sample until the plunger reached the 1-$\mu$l mark. All the liquid was pulled back into the barrel before injection.

### 2.5. Error estimation

Analytical error was calculated in two ways. The first estimate was computed as proposed by Bannon et al. [5]: Total error (%) = $\Sigma$abs($C_i - c_i$), where $C_i$ was the known mass % of an individual FAME in the calibration mix, and $c_i$ the mass % found by converting GLC area %. Only theoretical RFs were used for conversion.

The second estimate was calculated as: Discrimination (%) = $\Sigma$abs($A_i - a_i$), where $A_i$ was the area % of an individual FAME in the calibration mixture found by OCI, and $a_i$ the area % found by SI.

### 2.6. Statistical analysis

Calculations were done using SAS/STAT Ver. 6.03 (SAS Institute, Cary, USA) procedures.

## 3. Results

### 3.1. On-column injection

Three calibration mixtures approximating the composition of bovine MF were prepared by gravimetry and analysed by GLC using OCI. Theoretical RFs and those obtained experimentally are listed in Table 1. C18:2 and C18:3 were omitted deliberately from the mixtures due to stability problems. This will not introduce a serious error in the analysis, since MF is not rich in polyunsaturated FAs. For all experimental

Table 1
Empirical response factors of fatty acid methyl esters as obtained by cold on-column GLC

| FAME | Relative response factors | | | | | |
|---|---|---|---|---|---|---|
| | Theor. | Mix 1[a] | Mix 2 | Mix 3 | Mean | S.D. |
| C4:0 | 1.540 | 1.730 | 1.734 | 1.754 | 1.739 | 0.013 |
| C6:0 | 1.308 | 1.430 | 1.427 | 1.398 | 1.418 | 0.018 |
| C8:0 | 1.193 | 1.224 | 1.226 | 1.212 | 1.214 | 0.019 |
| C10:0 | 1.123 | 1.132 | 1.141 | 1.145 | 1.139 | 0.007 |
| C12:0 | 1.077 | 1.079 | 1.099 | 1.074 | 1.084 | 0.013 |
| C14:0 | 1.044 | 1.066 | 1.047 | 1.046 | 1.053 | 0.011 |
| C16:0 | 1.019 | 1.031 | 1.023 | 1.032 | 1.029 | 0.005 |
| C18:0 | 1.000 | 1.000 | 1.000 | 1.000 | – | – |
| C18:1 | 0.993 | 1.002 | 0.993 | 1.000 | 0.998 | 0.005 |

[a] Mean values of quadruplicate injections.

mixtures the found RFs compared favourably with the theoretical values, except for C4:0 and C6:0. These factors were by 0.199 and 0.110 larger than the theoretical RFs.

### 3.2. Split injection: needle techniques

In a preliminary trial, we compared six needle-handling techniques for sample introduction by SI (Fig. 1). The % total error and the % discrimination figures were employed as criteria to judge the efficacy of the different techniques. Mean values of replicated OCI ($n = 5$) of the calibration mixture were taken as a basis for % discrimination calculations.

The widely used filled needle technique (A in Fig. 1) produced the largest error of all methods tested. Both methods for estimating analytical error yielded equivalent results. The same technique, but with an additional dwell time of the syringe needle in the injection port after releasing the sample, improved accuracy considerably (B1 in Fig. 1). An even better error estimate was observed when the needle was pushed as rapidly as possible through the septum (B2 in Fig. 1) compared to variant B1, where needle insertion was done in a smooth, normal way. Interestingly, the two methods to calculate analytical error did not agree. Hot needle injection (C in Fig. 1) led to error estimates which were comparable to B1 and B2 when % total error was used as criterion but was less accurate when % discrimination was employed. Solvent flush in combination with a hot syringe needle (D in Fig. 1) was best suited as judged by % total error, while a SI method recommended by Ackman [11] gave results which were closest to those obtained by OCI (E in Fig. 1). Therefore, we decided to use

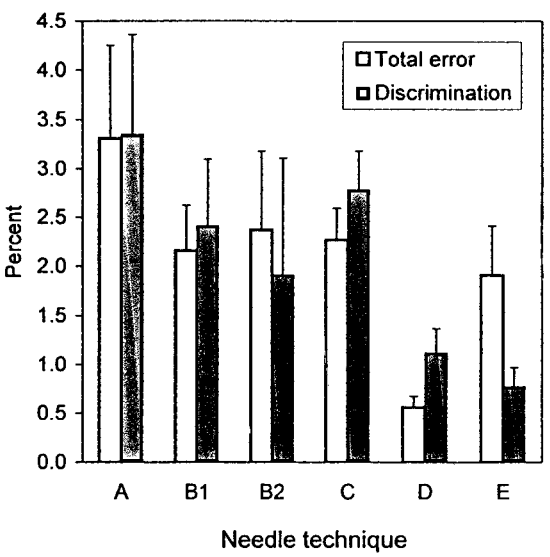


Fig. 1. Sample discrimination caused by different syringe needle handling techniques. (A) Filled needle. (B) Filled needle injection with post-injection dwell time; 1, normal septum penetration speed; 2, rapid septum penetration speed. (C) Hot needle injection. (D) Solvent flush injection. (E) Solvent flush injection with post-injection dwell time.

the latter technique in further experiments targeted at studying thoroughly those operating parameters which we expected to be of importance in SI of FAMEs.

### 3.3. Experimental design: milk fat

A two-level factorial design in the variables (a) temperature of the injector, (b) split-vent flow, (c) speed of needle penetration, and (d) injector sleeve design was set up to explore the experimental domain for an ester mixture simulating MF. The design matrix is given in Table 2. Injection technique E was termed injection with a "regular penetration speed ( = 4 s)". The same technique but with a penetration speed as rapidly as manually possible (ca. 1 s) and immediate release of the sample was termed "rapid injection". The design was blocked in factor (d). Each run was performed in duplicate and the average non-corrected area percentages of the 9 individual FAMEs for the 16 ($2^4$) factor combinations were taken for principal component analysis (PCA). This enabled us to visualise the outcome of the experiment without employing any response variable (Fig. 2). For ANOVA computation, the % discrimination parameter was chosen as response.

A plot of the first two principal components, which accounted for 91.8% of the total variation, revealed that the velocity of needle insertion was most influential and led to a clearly visible

Table 2
Factor and factor levels used in the $2^4$ experimental designs

| Factor | Factor level | |
|---|---|---|
| | Low (−) | High (+) |
| Injector temperature | 230°C | 330°C |
| Split vent flow | 50 ml/min | 250 ml/min |
| Liner design | Regular | Laminar cup |
| Penetration speed | 4 s[a] | 1 s[b] |

[a] Septum penetrated at regular speed and needle kept inside the hot injector for further 3 s before depressing the plunger.
[b] Septum penetrated as rapidly as possible and plunger depressed immediately thereafter.

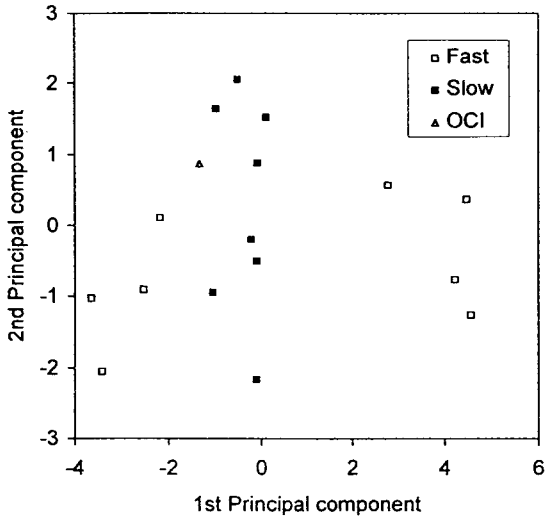


Fig. 2. Principal component plot of the milk fat experiment (fast, fast septum penetration; slow, slow septum penetration; OCI, on-column injection).

grouping of the results (Fig. 2). At normal penetration speed the points were homogeneously dispersed around the result obtained by OCI, whereas rapid penetration produced two distinct sub-groups. Mean values for the factor levels, using % deviation as response variable, are shown in Fig. 3. ANOVA of the data confirmed the influence of penetration speed ($p = 0.0001$). Temperature of the injector proved also to be statistically significant ($p = 0.0001$), in contrast to split-vent flow and liner design ($p = 0.2798$ and $p = 0.2589$). Of the two-factor interactions involving significant variables, only the temperature × liner design ($p = 0.0092$) and the temperature × penetration speed ($p = 0.0001$) interaction terms were significant. At an injector temperature of 230°C, rapid septum penetration produced the largest deviation value observed, whereas at 330°C the difference due to penetration speed was negligible (Fig. 3). Moreover, the effect was variable for different FAMEs, depending on chain length. Penetration of the injector at 330°C at regular speed, although giving satisfactory figures for % discrimination, overvalued short-chain FAMEs to a considerable extent.

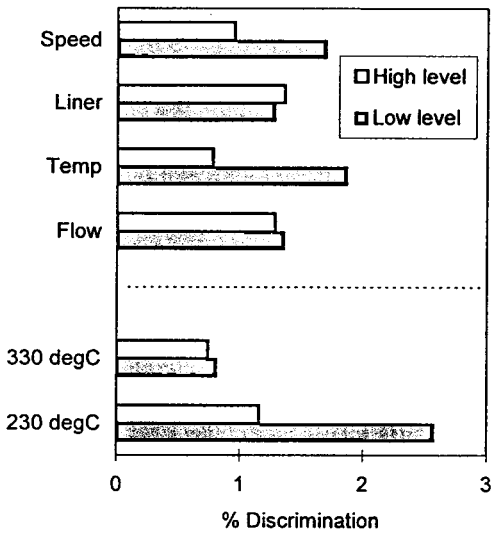


Fig. 3. Mean values at factor levels for the milk fat experiment.

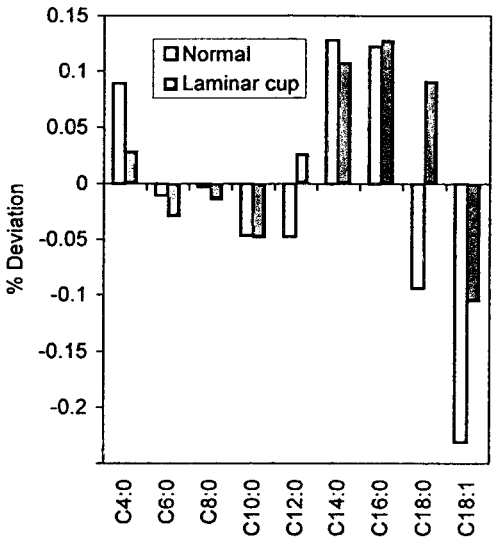


Fig. 4. Discrimination of individual FAMEs at an injector temperature of 280°C and normal septum penetration speed (peak areas obtained by cold on-column injection served as a basis for the evaluation of discrimination effects).

In a search for optimum conditions, the non-influential split vent flow was set to 50 ml/min, the septum was penetrated with a normal speed and the injector temperature set to 280°C (mid-point of the two factor levels). With these operating parameters both injector sleeves produced % deviation figures $<1$ (Fig. 4).

### 3.4. Experimental design: vegetable oil

The same factorial design was applied to a FAME standard resembling the composition of an average seed oil (ca. 10% C16:0, 10% C18:0, 30% C18:1 and 50% C18:2). To ensure that the C18:2 preparation was peroxide free, a solution of the ester in *n*-hexane was passed through a Sep-Pak silica cartridge, and the non-oxygenated C18:2 eluted with 5% diethyl ether in *n*-hexane.

As the chain lengths of the FAMEs in the vegetable oil standard did not differ to a greater extent, no particular influence of the factors tested was expected. PCA of the data strengthened this assumption since data points did not cluster in specific groups (Fig. 5). However, ANOVA revealed that all the factors tested were significant at $p < 0.05$. Nevertheless, the % discrimination response variable remained $<0.5\%$ for all factor combinations (Fig. 6). Therefore, the influence of the factors should be

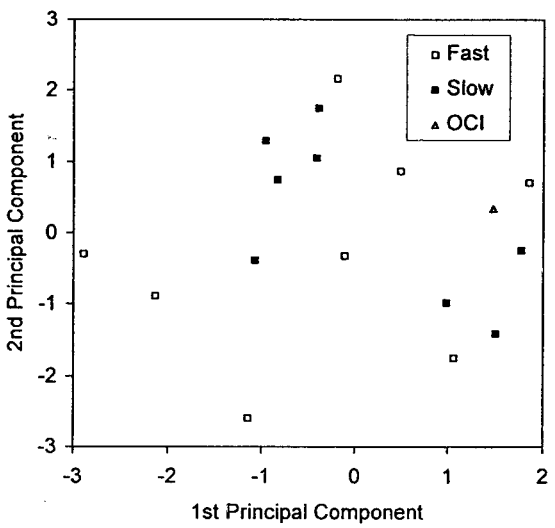


Fig. 5. Principal component plot of the vegetable oil experiment (fast, fast septum penetration; slow, slow septum penetration; OCI, on-column injection).

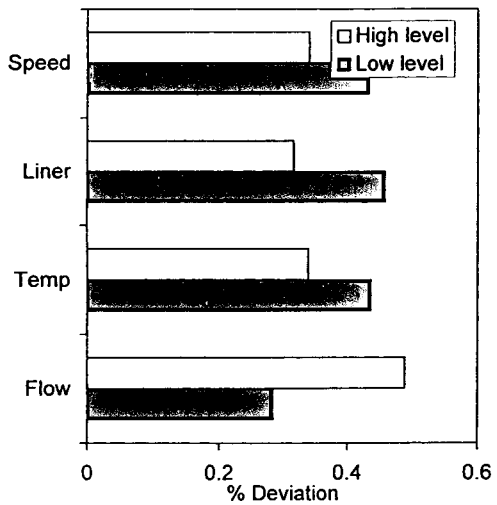


Fig. 6. Mean values at factor levels for the vegetable oil experiment.

only of minor importance in practical situations. This hypothesis was validated by analysis of commercially available standard mixtures (Oil Reference Standard AOCS No. 1 and BCR CRM 162) applying the same injection parameters as found in the MF optimisation trial. Only theoretical RFs were taken to convert % area to % weight. Excellent agreement between certified and experimentally determined values was observed (Table 3).

Table 3
Accuracy check by means of the AOCS reference mixture No. 1 and the BCR CRM 162

| FAME | Certified value | Uncertainty | Found value ($n = 4$) |
|---|---|---|---|
| *AOCS No. 1* | | | |
| C16:0 | 6.0 | | 6.02 ± 0.01 |
| C18:0 | 3.0 | | 2.92 ± 0.01 |
| C18:1 | 35.0 | | 34.92 ± 0.04 |
| C18:2 | 50.0 | | 50.25 ± 0.05 |
| C18:3 | 3.0 | | 2.98 ± 0.01 |
| C20:0 | 3.0 | | 2.92 ± 0.01 |
| *BCR CRM 162* | | | |
| C16:0 | 10.65 | 0.17 | 10.69 ± 0.02 |
| C18:0 | 2.87 | 0.07 | 2.92 ± 0.03 |
| C18:1 | 24.14 | 0.28 | 24.21 ± 0.03 |
| C18:2 | 56.66 | 0.54 | 56.59 ± 0.05 |
| C18:3 | 4.48 | 0.21 | 4.74 ± 0.06 |

## 4. Discussion

### 4.1. Response factors of fatty acid methyl esters

Although serious shortcomings of classical SI have been reported, it is still the preferred sample introduction technique in most lipid laboratories [11]. In particular, whether SI allows the accurate quantitation of multi component mixtures is under discussion [12,13]. The most common remedy for this problem is to determine empirical correction factors by analysing a calibration mixture with known composition. Methyl esters of short-chain FAs are notoriously volatile. As a result, the accurate preparation of a calibration mixture resembling bovine MF is a delicate task. Using large amounts of FAME to lessen weighing errors is prohibitive due to the high price of pure standard substances. In addition, a one-pot preparation of the calibration mixture where nine individual standards are weighed in a suitable flask and made up to the mark with solvent, is time consuming. Thus, the risk that some of the volatile components evaporate gradually during handling is strongly increased. As a compromise we prepared 5–10 fold concentrated stock solutions of individual short and medium chain FAMEs (C4:0–C12:0) and added aliquots to the less-volatile long chain FAMEs, whose weight can be obtained with sufficient accuracy.

Remaining errors due to evaporation of volatile esters during mixture preparation were ruled out on two grounds. Firstly, three independently prepared FAME mixtures gave RFs whose relative S.D.s were well below 2% (Table 1). Furthermore, it is unlikely that mixtures flawed by evaporative losses, which is an uncontrolled process, will give such estimates of analytical precision. Secondly, a faulty mass taken for only one of the individual FAME during weighing will bias the percentages for all mixture components. This, in turn, will be reflected in deviations of all RFs from their theoretical values.

The validity of theoretical RFs, as originally proposed by Ackman and Sipos [3] and further advocated by an Australian research group [2,5–8], was confirmed, except for C4:0 and C6:0. Both behaved aberrantly in that their carbon deficiency was $>1$. This anomaly has even been recognised by Ackman and Sipos, who postulated in another publication [14] a carbon deficiency of 1.4 for C4:0 and C6:0, and 1.2 for C8:0. A re-calculation of RF (relative to C18:0) taking into account this deficiency, resulted in values of 1.7107, 1.4016 and 1.2232 for C4:0, C6:0 and C8:0, respectively. Experimentally found values (Table 1) were in close agreement with these factors. Shehata et al. [15] and Kemppinen and Kalo [16] also reported RFs value for C4:0 which were larger than the theoretical factors, viz. 1.62 and 1.64, although their factor for C6:0 agreed well (1.31) or was smaller (1.26). In a very carefully conducted study, employing OCI, RF values of 1.43, 1.18 and 1.09 were found for C4:0–C8:0 [1]. These RF values were intended to express the final result on a FA instead of a FAME basis. Conversion with appropriate factors leads to FAME-based figures of 1.579, 1.262, and 1.140, respectively [17].

Factors other than the relative proportion of "effective" carbon atoms in the molecule may thus relate to its FID response. A study aimed at predicting FID response by a quantitative structure–property relationship (QSPR) approach revealed that, besides the relative weight of "effective" carbon atoms, other features referred from quantum-chemical modelling of the molecules were involved [18].

Other possible sources of error, which could have been responsible for the deviation of our results from those found in the literature, such as irreversible adsorption, detector overload, or non-linearity of the detector, were ruled out, because adsorption is very unlikely to occur with fused-silica capillary columns and highly diluted samples were injected (ca. 100 ng total sample mass).

### 4.2. Discrimination caused by split injection

Processes taking place during sample introduction into a hot, vaporising injector are complex and may cause a serious alteration of the composition of that part of the sample actually reaching the column [13]. Numerous parameters are known to influence sample splitting [4]. Bannon et al. [7] identified three critical factors which governed accuracy of FAME analysis by SI to a large extent. Avoidance of the so-called needle discrimination by high injection speed, rapid vaporisation of the sample, ensured by high injector temperature, small sample volume and low sample concentration, and intensive mixing of the sample with carrier gas, facilitated by specially designed injector sleeves, were the key measures they recommended to achieve linear splitting. Our results confirmed the crucial importance of factors related to needle discrimination (syringe handling and injector temperature) but no indication about the significance of the other parameters mentioned were seen in the MF experiments. Needle handling exerted the most prominent influence on accuracy (Fig. 1). In agreement with the findings of Grob [13], filled needle techniques were least suited.

Interestingly, the solvent flush/hot needle technique (method D) produced results where total error, calculated according to the Bannon and Craske method, was as small as $0.56 \pm 0.11$ (3 different calibration mixtures). With this injection technique individual RFs did not differ by more than 0.038 from their theoretical values (largest difference found with C4:0: 1.578 vs. 1.540), but non-corrected area % did not agree with results obtained by OCI, a technique which is generally accepted to be non-discriminative [12,13,19]. Therefore, we believe that this particular type of sample introduction created such peculiar conditions that the resulting RFs were, misleadingly, close to the theoretical values put forward by Bannon et al. [5,7].

The factorial design with simulated MF showed clearly that neither split vent flow nor injector insert design was influential, while others [20–22] stressed the importance of high split ratios and/or special inlets to obtain linear sample splitting. In agreement with earlier reports [2,7,13], a high injector temperature was paramount for achieving high accuracy. On the other hand, the high temperature demanded rapid penetration of the septum to avoid needle

discrimination. Use of special autosamplers capable of performing injections in $<0.2$ s as recommended by Bannon et al. [7] is, therefore, mandatory for productivity since manual high speed injections, though possible, are prone to errors, and are likely to result in bent needles. A somewhat lower injector temperature (280°C) in combination with regular penetration speed, which promotes pre-heating of the needle, was an effective means to obviate this difficulty without loss of accuracy.

## Acknowledgement

This work was supported financially by the University Foundation of the City of Vienna.

## References

[1] H.T. Badings and C.E. De Jong, J. Chromatogr., 279 (1983) 493.
[2] J.D. Craske and C.D. Bannon, J. Am. Oil Chem. Soc., 64 (1987) 1413.
[3] R.J. Ackman and J.C. Sipos, J. Am. Oil Chem. Soc., 41 (1964) 377.
[4] E. Bayer and G.H. Liu, J. Chromatogr., 256 (1983) 201.
[5] C.D. Bannon, J.D. Craske, A.E. Hilliker, J. Am. Oil Chem. Soc., 62 (1985) 1501.
[6] C.D. Bannon, J.D. Craske, A.E. Hilliker, J. Am. Oil Chem. Soc., 63 (1986) 105.
[7] C.D. Bannon, J.D. Craske, D.L. Felder, I.J. Garland and L.M. Norman, J. Chromatogr., 407 (1987) 231.
[8] J.D. Craske and C.D. Bannon, J. Am. Oil Chem. Soc., 65 (1988) 1190.
[9] J.D. Craske, J. Am. Oil Chem. Soc., 70 (1993) 325.
[10] S.W. Christopherson and R.L. Glass, J. Dairy Sci., 52 (1969) 1289.
[11] R.J. Ackman, in E.G. Perkins (Editor), Analysis of Fats, Oils and Lipoproteins, American Oil Chemists' Society, Champaign, IL, USA, 1991, p. 270.
[12] G. Schomburg, H. Behlau, R. Dielmann, F. Weeke and H. Husmann, J. Chromatogr., 142 (1977) 87.
[13] K. Grob, Classical Split and Splitless Injection in Capillary GC, 2nd edn., Huethig Verlag, Heidelberg, Germany, 1988.
[14] R.G. Ackman and J.C. Sipos, J. Chromatogr., 16 (1964) 298.
[15] A.Y. Shehata, J.M. de Man and J.C. Alexander, Can. Inst. Food Technol. J., 3 (1979) 85.
[16] A. Kemppinen and P. Kalo, J. Am. Oil Chem. Soc., 70 (1993) 1203.
[17] H.T. Badings and C.E. De Jong, J. Am. Oil Chem. Soc., 65 (1988) 659.
[18] A.R. Katritzky, E.S. Ignatchenko, R.A. Barcock, V.S. Lobanov and M. Karelson, Anal. Chem., 66 (1994) 1799.
[19] G. Schomburg, H. Husmann and R. Rittmann, J. Chromatogr., 204 (1981) 85.
[20] J.E. Purcell, Chromatographia, 15 (1982) 546.
[21] K. Grob and C. Wagner, J. High Resolut. Chromatogr., 16 (1993) 429.
[22] W. Jennings, Gas Chromatography with Glass Capillary Columns, 2nd edn., Academic Press, New York–London, 1980, p. 71.

ELSEVIER

Journal of Chromatography A, 704 (1995) 465–471

JOURNAL OF CHROMATOGRAPHY A

# Breakthrough volume of monoterpenes on Tenax TA: influence of temperature and concentration for α-pinene

Valérie Simon, Marie-Louise Riba, Ana Waldhart, Liberto Torres*

*Ecole Nationale Supérieure de Chimie de Toulouse, Laboratoire Chimie–Energie et Environnement, 118 route de Narbonne, 31077 Toulouse Cédex, France*

First received 1 November 1994; revised manuscript received 13 February 1995; accepted 15 February 1995

**Abstract**

The breakthrough volumes (BTV) of several monoterpenes (α- and β-pinene, myrcene, sabinene, $\Delta^3$-carene and limonene) on Tenax TA were determined at very low mixing ratios (0.2–30 ppb, v/v). α-Pinene, which exhibits the lowest BTV of all the terpenes studied (16.3 l $g^{-1}$ at 24°C for a mixing ratio of 3 ppb, v/v) was taken as a standard during the atmospheric sampling. A study of the influence of temperature and mixing ratio on its BTV was carried out. The influence of temperature is shown to follow a Van't Hoff-type law of the form log (BTV) = $a + b/T$, whereas the influence of the concentration follows Freundlich's adsorption isotherm, expressed as log (BTV) = log $a + b$ log $C$.

## 1. Introduction

Perturbations of the equilibrium between the biosphere and atmosphere constitute a major environmental problem. Such perturbations are induced by variations in the concentration of trace components of the troposphere, namely carbon and nitrogen oxides, hydrocarbons, ozone, sulfur compounds and aerosols.

Among the hydrocarbons susceptible to modifying this equilibrium on a local or region scale, isoprenoid compounds are of particular importance owing to their predominance in vegetal emissions and their high chemical reactivity in the gaseous phase [1,2].

A better understanding of the role of these compounds can be assessed by the development of physico-chemical models able to predict their evolution. However, the validation of such models requires experimental data on the precursors, the intermediates and the products of chemical pollution. Here, a difficulty is the lack of qualitative and quantitative data on the sources of biogenic hydrocarbons.

There is also a technical difficulty in the determination of these compounds close to their source, owing to their very low mixing ratio in the atmosphere (between a few tens of ppt and a few ppb, v/v).

Among different analytical techniques, gas chromatography is the only one that can provide qualitative and quantitative data on most volatile organic compounds that are present in the neighbourhood of sources. In general, the analytical procedure requires the preconcentration of trace components. This is achieved by passing the gaseous samples through a trap in which the

* Corresponding author.

0021-9673/95/$09.50 
*SSDI* 0021-9673(95)00213-8

organic compounds are retained on a solid adsorbent [3].

The solid adsorbent must satisfy a number of requirements, such as (i) total chemical inertness relative to the adsorbed compounds, (ii) a capacity for total desorption and (iii) an adsorption capacity as large as possible for a maximum number of compounds.

The adsorption capacity of an adsorbent towards a given compound is characterized by the breakthrough volume (BTV), which represents the gas volume above which a given compound is no longer totally trapped [4]. This means that the preconcentration of such a compound on an adsorbent can only be quantitative at sampling volumes that do not exceed the BTV of the compound.

Our studies on the quantification of a biogenic monoterpenic source are based on analytical techniques requiring preconcentration of terpenes on Tenax TA. For this purpose, we need to determine the BTV of these compounds on this adsorbent.

Although the adsorption capacity of Tenax GC has been evaluated earlier, there are only very few data available on Tenax TA. A study of the BTV of the principal monoterpenes on Tenax TA is presented here.

It has been demonstrated that the BTV depends on numerous factors, such as the temperature [5–7], the concentration of the compound being studied [8,9], the chemical composition of the gaseous mixture [10,11], the relative humidity [12,13], the flow-rate and linear velocity of the carrier gas [14,15], the dimensions of the trap [16], a number parameters relating to the adsorbent, such as mass [16], granulometry, pore diameter and specific surface area [17,18], repeated re-use and thermal pretreatment [13,19].

However, it appears that the adsorption temperature and the concentration of the adsorbed compound are the main critical parameters affecting the BTV value. We therefore investigated the influence of these two parameters on the adsorption of $\alpha$-pinene on Tenax TA. The range of volume mixing ratios considered is representative of that encountered in the atmosphere, where the mixing ratio in $\alpha$-pinene ranges between a fraction of ppb and a few ppb (v/v).

$\alpha$-Pinene was selected as a standard as the value of its BTV on Tenax TA is lower than those of other terpenes.

## 2. Experimental

### 2.1. Apparatus

The apparatus used for this study has been described in detail previously [20,21] and is shown in Fig. 1. It includes principally (i) a generator of standard atmospheric samples which functions by permeation or by diffusion, (ii) a preconcentration–thermodesorption module connected with a Hewlett–Packard Model 5890 gas chromatograph equipped with a 30-m Megabore DB5 column (film thickness 1.5 $\mu$m), flame ionization detector and an OMRON C28K programmable controller. The whole device is fully automated and operates in a continuous manner.

The preconcentration–thermodesorption module contains a Pyrex glass tube packed with 150 mg of 60–80 mesh Tenax TA (Chrompack) and mounted directly on the chromatograph injector. The adsorbent bed is located in a zone of the trap where the temperature is regulated at ±1°C.

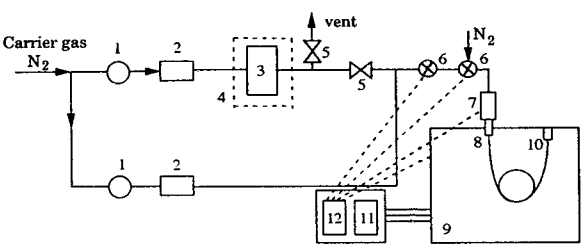


Fig. 1. Experimental device used for the determination of BTV values. 1 = Manometer; 2 = mass flow controller; 3 = terpenes generator (permeation or diffusion); 4 = thermostated bath; 5 = flow controller valve; 6 = three-way electrovalve; 7 = thermoregulated trap module; 8 = injector; 9 = gas chromatograph; 10 = detector; 11 = integrator; 12 = programmable controller.

During trapping experiments, the flow-rate of nitrogen was adjusted to 150 ml $min^{-1}$, corresponding to a linear velocity of 13.95 m $min^{-1}$.

### 2.2. Reagents

The monoterpenes used ($\alpha$- and $\beta$-pinene, myrcene, sabinene, $\Delta^3$-carene and limonene) were obtained as guaranteed products from Extrasynthese (Genay, France).

### 2.3. Procedure

Standard atmospheric samples were obtained either by permeation ($\alpha$-pinene) or by a diffusion process ($\beta$-pinene, myrcene, sabinene and mixture of $\alpha$- and $\beta$-pinene). A dilution step was necessary to obtain very low volume mixing ratios in monoterpenes (between a few hundred ppt and a few tens of ppb, v/v).

The BTV was determined by passing a gaseous mixture through the trap. By varying the concentration of the gaseous mixture and the trapping time, it is possible to pass different volumes of gas and different amounts of samples through the trap. It should be noted that the experimental temperatures and the monoterpene volume mixing ratios selected for this study were of the same magnitude as those recorded in the natural atmosphere.

The trapped sample was subsequently desorbed and analysed. The peak area obtained is a function of the mass of compound adsorbed, which was evaluated by comparison with a calibration graph determined for monoterpenes [22].

The masses of adsorbed compounds were plotted against sample volumes. An example is provided in Fig. 2, showing a case in which the mixing ratio in $\alpha$-pinene is 1.1 ppb (v/v). Each point represented on the plot is the average of 5–7 experimental measurements. Table 1 gives experimental data with their estimated standard deviations.

The BTV is defined as the sampled volume corresponding to the end of the linear domain. The extreme value of the linear domain is evaluated by calculation of the intersection between linear and non-linear domains. The linear calibration equation $y = ax$ is calculated by the least-squares method. Data in the non-linear domain are fitted by a power law, $y = cx^d$. The parameters $c$ and $d$ are obtained by the least-squares method. Such a mathematical method to determine the BTV was preferred to the statistical method developed by Liteanu et al. [23], which requires a large number of experimental points close to the actual value of the BTV.

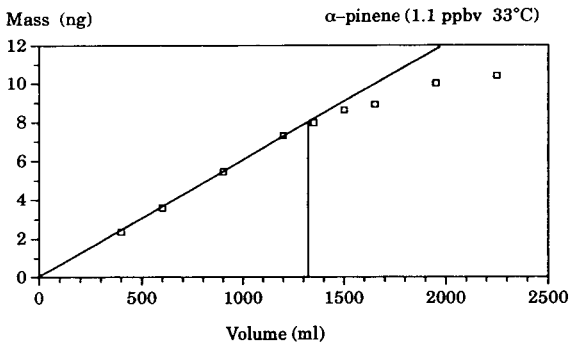


Fig. 2. Plot of mass of $\alpha$-pinene (1.1 ppb, v/v) adsorbed on Tenax TA versus sampling volume.

Among various direct and indirect methods available for the determination of the BTV [4], the one we employed is well adapted to our automatic device, which can generate very low

Table 1
Statistical characteristics of the measurements corresponding to Fig. 2

| Volume sampled (ml) | Average mass sampled (ng) | No. of measurements | R.S.D. (%) |
|---|---|---|---|
| 400 | 2.35 | 6 | 1.5 |
| 600 | 3.59 | 6 | 1.2 |
| 900 | 5.45 | 5 | 1.9 |
| 1200 | 7.30 | 5 | 2.4 |
| 1350 | 7.97 | 6 | 6.3 |
| 1500 | 8.61 | 5 | 1.8 |
| 1650 | 8.90 | 7 | 1.9 |
| 1950 | 10.00 | 5 | 1.4 |
| 2250 | 10.40 | 5 | 7.6 |

concentrations and allows automatic programming of the sampling time.

## 3. Results and discussion

### 3.1. BTV determination for a series of monoterpenes

The BTV values measured on Tenax TA for six monoterpenes characteristic of biogenic emissions are displayed in Table 2. The mixing ratio of these monoterpenes was adjusted to 3 ppb (v/v) and the adsorption temperature on Tenax TA was 24 ± 1°C.

It appears that the experimental BTV values are of the same magnitude, and increase in the order α-pinene < myrcene <sabinene < β-pinene <$\Delta^3$-carene ≈limonene. As α-pinene exhibits the lowest BTV of the series, it may be selected as a standard and the capacity of Tenax TA for α-pinene may be reasonably used as a threshold value for all monoterpenes or mixtures of these compounds, provided that their BTV is not modified when they are mixed. Taking α-pinene as a reference compound, we set out to examine the principal parameters that may influence the value of its BTV on Tenax TA.

### 3.2. Influence of temperature

Adsorption is an exothermic phenomenon, the BTV being related to the temperature by a Van't Hoff-type relationship:

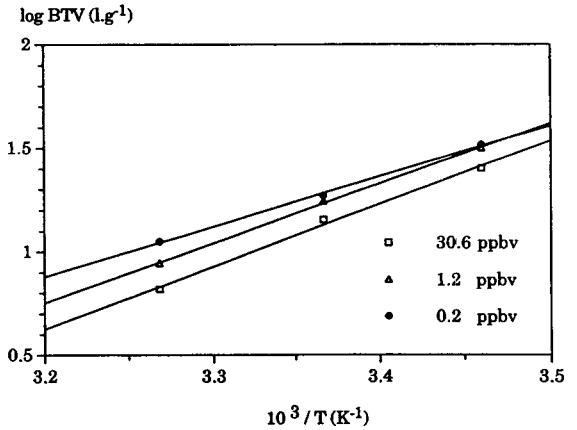


Fig. 3. Variation of α-pinene BTV versus sampling temperature.

$$\frac{d[\log(BTV)]}{d\left(\frac{1}{T}\right)} = -\frac{\Delta H_{ad}}{2.3R} \quad (1)$$

where $\Delta H_{ad}$ is the adsorption enthalpy, $R$ is the gas constant and $T$ is the absolute temperature. Considering $\Delta H_{ad}$ as a constant, Eq. 1 can be expressed as

$$\log(BTV) = -\frac{\Delta H_{ad}}{2.3RT} + K \quad (2)$$

or, more generally,

$$\log(BTV) = a + \frac{b}{T} \quad (3)$$

Fig. 3 shows that the experimental values follow this law for the three mixing ratios volumes considered here, namely 0.2, 1.2 and 30.6

Table 2
BTV on Tenax TA for different monoterpenes in mixtures where the mixing ratio is 3 ppb (v/v) at 24°C

| Monoterpene | BTV at 24 ± 1°C (l g$^{-1}$) | Boiling temperature (°C) | Vapour pressure (mmHg, 24°C) |
|---|---|---|---|
| α-pinene | 16.3 | 156 | 4.6 |
| β-pinene | 21.4 | 164 | 3.1 |
| Myrcene | 17.9 | 167 | 1.9 |
| Sabinene | 20.9 | 164 | 3.1 |
| $\Delta^3$-carene | >21.4 | 167 | 2.5 |
| Limonene | >21.4 | 178 | 2.0 |

Table 3
Values of the parameters for the experimental law log (BTV) = $a + b/T$

| Mixing ratios (ppb, v/v) | $a$ | $b$ | Correlation coefficient | $-\Delta H_{ad}$ (kJ mol$^{-1}$) |
|---|---|---|---|---|
| 30.6 | −9.07 | 3031 | 0.99 | 58.1 |
| 1.2 | −8.47 | 2883 | 1 | 55.2 |
| 0.2 | −6.88 | 2426 | 0.99 | 46.4 |

ppb (v/v). The characteristic parameters $a$ and $b$ and the correlation coefficients are displayed in Table 3. The influence of temperature seems more pronounced for the two highest mixing ratios considered here (>1 ppb, v/v).

The adsorption enthalpies of α-pinene on Tenax TA were also determined (Table 3). The average enthalpy, $\Delta H_{ad}$, equal to −53.2 kJ mol$^{-1}$, is of the same magnitude as that reported by Gallant et al. [24] for the adsorption of various hydrocarbons on Tenax GC.

According to Kiselev's classification (see [25]) and considering the value obtained here for the adsorption enthalpy, one may reasonably conclude that α-pinene–Tenax TA interactions involve both non-specific interactions of the Van der Waals type and London dispersion forces [26] and also specific interactions of the π–π type.

The knowledge of $a$ and $b$ is of great interest as they allow one by extrapolation, to determine theoretical BTV values of α-pinene on Tenax TA for any sampling temperature.

### 3.3. Influence of concentration

Fig. 4 represents the variation of the BTV of α-pinene on Tenax TA as a function of the various mixing ratios considered. The resulting relationship, of linear log–log type, is consistent with the expression of an adsorption isotherm satisfying Freundlich's equation:

$$\log(\mathrm{BTV}) = \log a + b \log C \quad (4)$$

where $C$ is the mixing ratio volume.

For each isotherm we determined the parameters $a$ and $b$ as well as the correlation coefficients (Table 4). The slope of the linear isotherm at 33°C is greater than those obtained at 24 and 16°C.

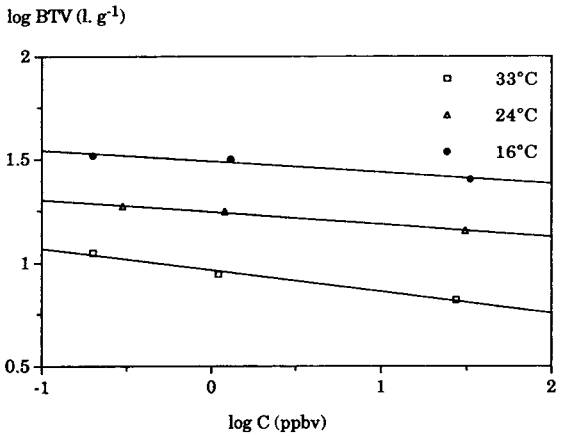


Fig. 4. Variation of α-pinene BTV versus α-pinene mixing ratio.

Thus, prior to any sampling experiment, the BTV value can be evaluated from Eqs. 3 and 4, depending on the sampling temperature selected by the operator and the concentration range to be measured, which should be estimated by excess.

For example, let us calculate the BTV of α-pinene for sampling temperatures of 16 and 33°C, considering an atmosphere containing α-pinene at a volume mixing ratio of 100 ppb (v/v). Eq. 4 leads to the corresponding BTV values (Table 5). Considering that the trap contains 400 mg of Tenax TA, volumes lower than 9.6 and 2.2 l would be the maximum sampling values not to exceed the BTV value at 16 and 33°C, respective-

Table 4
Values of the parameters for the experimental law log (BTV) = log $a$ + $b$ log $C$

| Temperature (°C) | Log $a$ | $b \times 10^2$ | Correlation coefficient |
|---|---|---|---|
| 16 | 1.49 | −5.35 | 0.97 |
| 24 | 1.24 | −5.89 | 1 |
| 33 | 0.96 | −10.51 | 0.99 |

Table 5
BTV of α-pinene on Tenax TA at different temperatures and mixing ratios

| Parameter | Mixing ratio of α-pinene | | | |
|---|---|---|---|---|
| | 100 ppbv | | 10 pptv | |
| | 16°C | 33°C | 16°C | 33°C |
| BTV ($l\,g^{-1}$) | 24.1 | 5.6 | 39.4 | 14.7 |
| BTV (l)[a] | 9.6 | 2.2 | 15.8 | 5.9 |

[a] Calculated for 400 mg of Tenax TA.

ly. Atmospheric α-pinene mixing ratios are generally lower than 100 ppb (v/v).

Let us also consider the example of an atmosphere characterized by an α-pinene mixing ratio as low as 10 ppt (v/v). In that case, the calculated BTV values (Table 5) indicate that it would be possible to adsorb on 400 mg of Tenax TA a maximum of 15.8 l of α-pinene at 16°C and 5.9 l at 33°C. In the latter example, the masses of α-pinene sampled (0.9 and 0.3 ng, respectively) would only be detectable for a sampling temperature of 16°C on our apparatus, and the mass sampled at 16°C would be three times greater than at 33°C, yet not exceeding the BTV value. This clearly means that low values of the sampling temperature favour the detection of the lowest quantifiable concentration.

It is clear that the BTV is a volume threshold value above which the sampling operation is no longer quantitative. Even in the case where this critical volume is collected, the sampling may be subject to uncontrolled variations during the manipulations. As shown above, if one does not control the sampling temperature or the concentration of the compound being studied, the BTVs corresponding to different samplings will be subject to large deviations. One should keep in mind that the temperatures and the concentrations may be subject to large variations at the experimental site, especially between night and day.

Hence it is generally recommended to remain far below this value during sampling experiments. A safe sampling volume (SSV) has been defined for this purpose, corresponding to a certain percentage of the actual BTV value. Different percentages have been used by different workers. The SSV suggested by Harper [27] corresponds to two thirds of the BTV, whereas the value indicated by the HSE [28] is 70%. In our determinations, we took an SSV value equal to two thirds of the BTV.

## References

[1] R. Atkinson, Atmos. Environ., 24A (1990) 1.
[2] F. Fehswenfeld, J. Calvert, R. Fall, P. Goldan, A.B. Guenther, C.N. Hewitt, B. Lamb, S. Liu, M. Trainer, H. Westberg and P. Zimmerman, Global Biogeochem. Cycles, 6 (1992) 389.
[3] P. Ciccioli, in H.J.TH. Bloemen and J. Burn (Editors), Chemistry and Analysis of Volatile Organic Compounds in the Environment, Blackie, Glasgow, 1993, p. 92.
[4] J. Namiesnik, Talanta, 35 (1988) 567.
[5] X.L. Cao, J. Chromatogr., 586 (1991) 161.
[6] K. Ventura, M. Dostal and J. Churacek, J. Chromatogr., 642 (1993) 379.
[7] I. Maier and M. Fieber, J. High Resolut. Chromatogr. Chromatogr. Commun., 11 (1988) 566.
[8] R.H. Brown and C.J. Purnell, J. Chromatogr., 178 (1979) 79.
[9] M.L. Riba, E. Randrialimanana, J. Mathieu and L. Torres, Int. J. Environ. Anal. Chem., 19 (1985) 133.
[10] R.J.B. Peters and H.A. Bakkeren, Analyst, 119 (1994) 71.
[11] P. Comes, N. Gonzalez-Flesca and T. Menard, Anal. Chem., 65 (1993) 1048.
[12] S.E. Maljaars and M.W.F. Nielen, Int. J. Environ. Anal. Chem., 34 (1988) 333.
[13] K.A. Persson and S. Berg, Chromatographia, 27 (1989) 55.
[14] W.T. Sturges and J.W. Elkins, J. Chromatogr., 642 (1993) 123.
[15] S. Seshadri and J.W. Bozzelli, Chemosphere, 12 (1983) 809.
[16] H. Hori, I. Tanaka and T. Akiyama, J. Air Pollut. Control Assoc., 38 (1988) 269.
[17] S.F. Patil and S.T. Lonkar, J. Chromatogr., 600 (1992) 344.
[18] A. Przyjazny, J. Chromatogr., 346 (1985) 61.
[19] S. Coppi, A. Betti, G. Blo and C. Bighi, J. Chromatogr., 267 (1983) 91.
[20] M.L. Riba, N. Tsiropoulos, B. Clement, A. Golfier and L. Torres, J. Chromatogr., 456 (1988) 165.
[21] B. Clement, M.L. Riba, V. Simon and L. Torres, Int. J. Environ. Anal. Chem., 50 (1993) 19.
[22] M.L. Riba, N. Tsiropoulos and L. Torres, J. Chromatogr., 437 (1988) 139.

[23] C. Liteanu, I.C. Popescu and E. Hopirtean, Anal. Chem., 48 (1976) 2010.
[24] R.F. Gallant, J.W. King, P.L. Levins and J.F. Piecewicz, EPA-600/7-78-054, 1978.
[25] S.J. Gregg and K.S.W. Sing, Adsorption, Surface Area and Porosity, Academic Press, London, 2nd ed., 1982.
[26] B.A. Demian, K. Lam, A. Schindler and E.D. Pellizzari, in L.H. Keith (Editors), Identification and Analysis of Organic Pollutants in Air, Butterworth, Guildford, 1984, p. 95.
[27] M. Harper, R. Soc. Chem. (Clean Air Work), (1992) 182.
[28] Health and Safety Executive, Methods for the Determination of Hazardous Substances. Laboratory Method Using Pumped Solid Sorbent Tubes, Thermal Desorption and Gas Chromatography, MDHS 72, HSE, London, 1992.

ELSEVIER

Journal of Chromatography A, 704 (1995) 473–482

JOURNAL OF CHROMATOGRAPHY A

# Chromatographic determination of trace amounts of amines using a surface ionization detector

U.Kh. Rasulev*, E.G. Nazarov, G.B. Khudaeva

*Arifov Institute of Electronics, 700143 Tashkent, Uzbekistan*

First received 17 May 1994; revised manuscript received 21 October 1994; accepted 14 November 1994

**Abstract**

The results of comparative investigations showed the possibility of the chromatographic detection of trace amounts of amines (primary, secondary, tertiary and quaternary) in mixtures using a modified surface ionization detector. The potential (theoretical) characteristics of the surface ionization detector (ionization efficiency, sensitivity, detection limits, linear ranges, etc.) were calculated on the basis of an experimental study of the concentration dependences of the detector signal on the amount of substance under analysis ($10^{-4}$–$10^{-9}$ g). The unique sensitivity of the detector with respect to tertiary amines, $10^{-14}$ g/s, is shown, in addition to the possibility of the selective registration and identification of quaternary ammonium salts.

## 1. Introduction

The wide application of nitrogen-containing bases in various areas of the chemical and chemical–pharmaceutical industries and the necessity to determine trace amounts of physiologically active and carcinogenic substances in complex mixtures have stimulated the development of highly sensitive selective and rapid methods for the determination of amine containing substances [1,2]. Among the methods considered, recording of amines, hydrazines and their derivatives based on the surface ionization (SI) phenomenon is of particular interest [3–5]. Surface ionization consists in the formation of ions during thermal desorption of particles from a solid surface. Positive ions are formed as a result of the isoenergetic tunnel transition of an electron from a desorbing particle into the solid. The detection of the SI of organic compounds and subsequent systematic mass spectrometric study have revealed the general regularities of the SI of organic compounds of different classes [4–5]. It has been found that as a rule it is not the initially adsorbed molecules that become ionized but the products of their heterogeneous reactions, followed by the formation of particles with relatively small ionization potentials; more often these are the products of dissociation, and rarely of associations with the formation of quasi-molecular particles: (M + H), (M − H), (M − R), where M is a molecule, H is a hydrogen atom and R is a radical. Nitrogen-containing organic compounds such as amines, hydrazines and their derivatives appeared to be the most effectively ionizable. The efficiency of the ionization of these substances depends on the nature of the functional group. It increases, for example,

* Corresponding author.

0021-9673/95/$09.50 
*SSDI* 0021-9673(94)01126-5

in the series of primary, secondary and tertiary alkylamines, for the tertiary type reaching values of 0.1–0.05 A/Pa · $cm^2$. Thus, one ion is formed by every 2–5 adsorbed molecules. Organic compounds of other classes are significantly more weakly ionized and molecules of simple gases appeared to be virtually non-ionizable. This led to the development of a simple selective detector for amines, hydrazines and their derivatives on the basis of SI [6,7].

The first instruments for surface ionization detection (SID) demonstrated unique sensitivity and selectivity of amine registration and good prospects for employment as selective detectors in gas chromatography [7,8]. Later, SID was used in a number of studies [9–11] as an illustration of the possibility of determining trace amounts of series of alkylamines, polyaromatic hydrocarbons, terpenes, steroids and some nitrogen-containing medicinal preparations in complex mixtures [8–10]. However, at present the wide application SID is restricted by the lack of systematic data from investigations of its analytical characteristics. For this reason, this paper presents the results of comparative investigations that show the possibility of detecting chromatographically trace amounts of alkylamines (primary, secondary, tertiary and quaternary) in complex mixtures using SID. The data permit a complete set of unified characteristics of SID to be obtained that will allow specialists to establish the practical problems where this detector could be employed with the highest efficiency.

## 2. Experimental

The results presented here were obtained under the same experimental conditions using a chromatograph (TSVET-500) equipped with an experimental model of a surface ionization detector with an indirect incandescence emitter. The detector was designed specially for chromatographs of this kind [12]; later an analogous detector was connected to other types of chromatographs and the same characteristics were obtained in these experiments. Fig. 1 shows the design and the scheme of the electric circuitry for

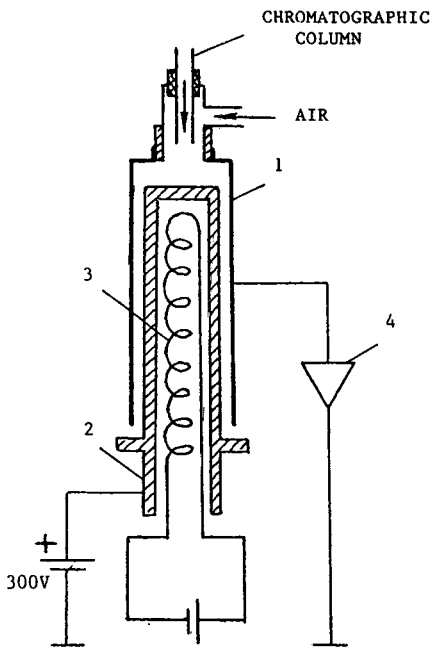


Fig. 1. Design of surface ionization detector with indirect incandescence emitter and the connecting circuitry. 1 = Collector; 2 = Thermoemitter; 3 = Nichrome heater; 4 = charge amplifier.

the detector and indirect incandescence emitter. The detector consists of a two-electrode device containing the thermoemitter (2) in the form of a hollow cylinder and enclosed by cylindrical ion collector (1). The thermoemitter is heated to the operating temperature of 650–700 K by a Nichrome heater (3) located in the inner cavity of the thermoemitter. To provide effective collection of ions desorbing from the thermoemitter, a potential difference (300 V) is applied between the thermoemitter and the collector. Provided that stability of the emission and catalytic characteristics of the thermoemitter obtain, the ion current recorded by the electrometer (4) is proportional to the number of molecules of analyte amines adsorbing on the thermoemitter and, hence, proportional to the concentration of ionizing molecules in the mixture.

The detector with an indirect incandescence emitter has the following advantages over detectors with direct incandescence wire thermoemitters used previously [7,9]: owing to the high heat

conductivity of the massive thermoemitter, rectangular distribution of temperature all over its operating length (38 mm) is provided; the noise immunity increases owing to complete isolation of the incandescence circuit and the circuit of ion current measurements; and the thermoemitter operating period rises considerably and the degree of influence of outside factors (temperature variations, flow velocity of the mixture under analysis through the detector, vibrations, etc.) on the detector characteristics decreases.

The material from which the thermoemitter is constructed influences the main characteristics of the detector. The operating surface of the thermoemitter should have a maximum work function and maintain constant emission and catalytic properties with prolonged heating in gas–air mixtures (air or inert gas) containing organic compound vapours. Oxidized refractory metals are known to meet these requirements, primarily molybdenum [13] and some other metals (e.g., Ir, Re, Pt) [10], when oxygen or air is passed continuously through the detector. In addition, very rigid requirements are placed on the purity of the material, as there should be no impurities of elements with small ionization potentials, e.g., alkali metals. On heating the thermoemitter their atoms diffuse from the bulk to the surface and evaporate from it as ions that generate considerable background currents. To purify them from admixtures, the thermoemitters produced must be subjected to prolonged vacuum annealing at >2000 K. We have found a continuous decrease with time (during a year of operation) in the ionization efficiency of thermoemitters made from polycrystalline molybdenum. A brown coating was formed on the operating external surface of such emitters, and appeared not only on thermoemitters operated with organic vapours but also on control thermoemitters intended for registering background currents only. This indicates that surface degradation is the result of diffusion from the bulk of hardly evaporating elements. It is likely that these are compounds of chromium evaporating into the inner cavity of the thermoemitter from the Nichrome heater. To prevent such degradation, it has been recommended to use single-crystal molybdenum as the initial material [14]. The diffusion rate of foreign atoms through the single-crystal lattice is an order of magnitude less than that over grain boundaries of polycrystalline molybdenum, so even at the same purity of the initial materials the degree of long-term degradation of the single-crystal surface by diffusion flow from the bulk is essentially less than that of polycrystals.

In our experiments the chromatograms were recorded simultaneously using two types of detection, namely surface ionization detection (SID) and conventional flame ionization detection (FID), the detector being connected in parallel to the outlet of the chromatograph column. The carrier gas flow on the outlet of the column was divided in the ratio SID : FID = 1 : 3. This arrangement allowed not only the ratio of detector signals, $I_{SID}/I_{FID}$, to be obtained with high accuracy, which was necessary for functional group analysis of amines (as was shown previously [15]), but also permitted the sample dose ($m$) entering the evaporator to be controlled independently by the signal of each detector. Moreover, the constancy of the $I_{SID}/I_{FID}$ ratio with changes in the amount of sample entering the evaporator indicated that the characteristics of each detector remained constant during comparative analyses. After careful training of the thermoemitter and special steps for purification of the carrier gas and air, the background current did not exceed $10^{-10}$ A with a noise level of $10^{-13}$ A.

### 2.1. Procedure

Comparative analyses of the efficiency of amine ionization were performed using solutions in which standards of alkylamines of various classes were used: primary = hexylamine (HEA), allylamine (ALA) and *n*-butylamine (BA); secondary = diethylamine (DEA), diisobutylamine (DiBA), diisopentylamine (DiPA) and dipentylamine (DPA); tertiary = triethylamine (TEA), tributylamine (TBA), tripropylamine (TPA) and dipropylpropargylamne (DPPA). The following simplest structures were used as representatives of quaternary amines: tetraethylam-

monium chloride, tetraethylammonium bromide and acetylcholine (ACH), the last being more complex in structure.

For all substances under analysis, the SID characteristics were determined by the procedure of calibrated insertion of a sample into the detector [16]. As a rule, the dependences of the charge in coulombs, $Q = \int i(t)\,dt$, obtained in SID on the dose of the substance under analysis inserted into the chromatograph evaporator were monitored. Toward this end, six calibration solutions were prepared by successive dilution with concentrations $C = 10$, 1, $10^{-1}$, $10^{-2}$, $10^{-3}$ and $10^{-4}$% (v/v). Samples with volume $V = 5$ ml were injected into the evaporator of the chromatograph with a microsyringe and they contained $m = V\rho C/100$ g of the substance under analysis (where $\rho$ is the specific gravity of the component under analysis), which corresponded to the amine doses from $10^{-4}$ up to $10^{-9}$ g. In check experiments with a solution of tributylamine in acetone, a wider dose range was used (from $10^{-12}$ up to $10^{-4}$ g). However, in this instance the requirements on the conditions for preparing and carrying out the analysis (purity of carrier gas, preparation of samples and injection into the evaporator) became more rigid. At the same time, the relative error in the doses increased significantly. Therefore, subsequently the dose range in all experiments was limited to $10^{-9}$–$10^{-4}$ g.

A separate syringe was used for each kind of amine and when using different concentrations the syringe was washed thoroughly in the solvent. Each time the experiment began with the use of the solution with the minimum amine concentration.

Acetone, hexadecane and sometimes distilled water and ethanol were used as solvents for the amines. Before the preparation of the solutions a chromatogram of the solvent was first taken.

Glass columns (200 cm × 3 mm I.D.) were used for chromatographic separation. Depending on the substance–solvent pair, various sorbents were used: non-polar 4% Apiezon (Ap) + 1% KOH on Chromatone G and polar 0.5% $Na_3PO_4$ + 5% PEG-1000 on Chromosorb G AW [17].

All experiments were carried out within the same temperature regime: thermostated columns, 100°C; evaporation cell, 140°C; and thermoemitter, 660 K. Helium was used as the carrier gas with a flow-rate of 30 ml/min. The flow-rate of air necessary to stabilize the characteristics of the operating surface of the thermoemitter was 100 ml/min.

Quaternary salts (QAS) were dissolved in ethanol or distilled water, in view of the practical problems of their determination in biological liquids.

SID characteristics were calculated using plots of the dependences $Q = f(m)$ in the following way:

(i) ionization efficiency (according to Lovelock):

$$E = \frac{MQ}{meN_a}$$

where $M$ is the relative molecular mass and $N_a$ is Avogadro's number;

(ii) sensitivity ($K$):

$$K = \frac{Q}{m}\ (\mathrm{C/g})$$

(iii) detection limit:

$$m_{min} = -\frac{Q_{min}}{K} = \frac{2\int i_n\,dt}{K}\ (\mathrm{g/s})$$

where $i_n$ is the level of noise;

(iv) linear dynamic range (LDR):

$$\mathrm{LDR} = m_{max}/m_{min}$$

where $m_{max}$ is the amount of substance under analysis at which deviation from linearity of the $Q = f(m)$ dependence begins;

(v) selectivity ($S$):

$$S = \frac{K_1}{K_2}$$

where $K_1$ is the sensitivity of SID relative to the amines under analysis and $K_2$ is the sensitivity of SID relative to the substance with respect to which the selectivity is estimated;

(vi) the coefficient of relative sensitivity, $I_{SID}$/

$I_{FID}$, i.e., the ratio of the SID and FID signals with parallel registration; and

(vii) reproducibility of the results, which characterizes the similarity of the results of repeated measurements performed under the same conditions.

## 3. Results and discussion

### 3.1. Determination of primary, secondary and tertiary amines

Fig. 2 (lines 1–11) shows the results of the chromatographic determination of the dependences of the amount of the charge registered in SID on the dose of various kinds of amines inserted into the evaporator. It can be seen that all dependences have the same slope. Deviation from linearity for all substances begins when the charge $Q \sim 10^{-5}$ C is collected from the thermoemitter, which corresponds to a current density $j = 5.1 \cdot 10^{-6}$ A/cm$^2$. Depending on the functional group of the amines, their plots are arranged at various levels corresponding to various sensitivities $K$ (C/g). The first part with $K > 1$ includes the plots corresponding to all tertiary amines, the second part (dashed region) with $10^{-2} < K < 1$ contains all plots of secondary amines and the third part with $K < 10^{-2}$ contains all plots of primary amines. The main SID characteristics calculated relative to various kinds of amines are given in Table 1. It is seen that the ionization efficiency $E$ of SID for ter-

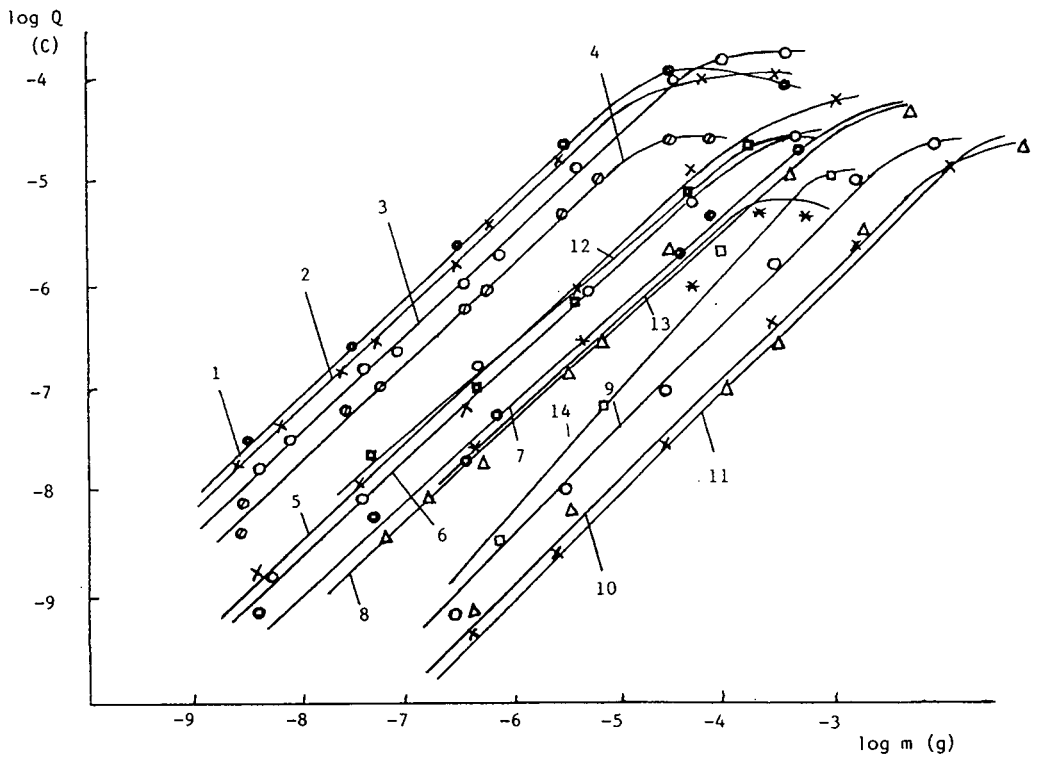


Fig. 2. Plots of the dependences of SID output signals on the amount of substance introduced. Tertiary amines: 1 = dipropylpropargylamine (DPPA); 2 = tripropylamine (TPA); 3 = tributylamine (TBA); 4 = triethylamine (TEA). Secondary amines: 5 = dipentylamine (DPA); 6 = diisopentylamine (DiPA); 7 = diisobutylamine (DiBA); 8 = diethylamine (DEA). Primary amines: 9 = hexylamine (HEA); 10 = alkylamine (ALA); 11 = *n*-butylamine (BA). Quaternary amines: 12 = tetraethylammonium chloride; 13 = tetraethylammonium bromide; 14 = acethylcholine.

Table 1
Characteristics of the surface ionization detector

| Amine | Ionization efficiency, $E$ | Sensitivity, $K$(C/g) | Detection limit (g/s) | Linear dynamic range (LDR) | Selectivity (relative to ketone hydrocarbons), $S_k$ | $I_{SID}/I_{FID}$ | Reproducibility (%) |
|---|---|---|---|---|---|---|---|
| *Tertiary* | | | | | | | |
| DPPA | $1.3 \cdot 10^{-1}$ | 7.2 | $2.7 \cdot 10^{-14}$ | | | 10000 | |
| TPA | $1.8 \cdot 10^{-1}$ | 6.0 | $3.3 \cdot 10^{-14}$ | $10^8$ | $10^6$–$10^8$ | 8000 | 3–4 |
| TBA | $1.6 \cdot 10^{-2}$ | 3.0 | $6.6 \cdot 10^{-14}$ | | | 6000 | |
| TEA | $2.0 \cdot 10^{-2}$ | 2.1 | $9.0 \cdot 10^{-14}$ | | | 4000 | |
| *Secondary* | | | | | | | |
| DPA | $2.5 \cdot 10^{-2}$ | $2.9 \cdot 10^{-1}$ | $3.4 \cdot 10^{-13}$ | | | 100 | |
| DiPA | $1.8 \cdot 10^{-2}$ | $1.4 \cdot 10^{-2}$ | $7.0 \cdot 10^{-13}$ | $10^6$ | $10^6$–$10^5$ | 488 | <5 |
| DiBA | $2.8 \cdot 10^{-3}$ | $3.3 \cdot 10^{-2}$ | $3.0 \cdot 10^{-12}$ | | | 80 | |
| DEA | $1.4 \cdot 10^{-3}$ | $3.0 \cdot 10^{-2}$ | $3.3 \cdot 10^{-12}$ | | | 90 | |
| *Primary* | | | | | | | |
| HEA | $8.0 \cdot 10^{-5}$ | $2.8 \cdot 10^{-3}$ | $3.4 \cdot 10^{-11}$ | | | 30 | |
| ALA | $2.5 \cdot 10^{-5}$ | $1.4 \cdot 10^{-3}$ | $1.0 \cdot 10^{-10}$ | $10^5$ | $10^4$ | 5 | <5 |
| BA | $3.5 \cdot 10^{-5}$ | $3.5 \cdot 10^{-4}$ | $2.8 \cdot 10^{-10}$ | | | 70 | |
| *Quaternary* | | | | | | | |
| Tetraethylammonium chloride | $2.5 \cdot 10^{-3}$ | $1.5 \cdot 10^{-1}$ | $1.0 \cdot 10^{-13}$ | $10^6$ | | 3000 | 5–6 |
| Tetraethylammonium bromide | $4.5 \cdot 10^{-3}$ | $1.9 \cdot 10^{-1}$ | $1.0 \cdot 10^{-13}$ | $10^6$ | $10^6$–$10^5$ | 4000 | 5–6 |
| ACH | $2.5 \cdot 10^{-4}$ | $1.0 \cdot 10^{-2}$ | $2.0 \cdot 10^{-11}$ | $10^5$ | | 2000 | 5–6 |

tiary amines is $10^{-1}$–$10^{-2}$. This value is defined by Lovelock as the ratio of ion flows, $\nu_k^+$, of all recorded kinds of ions to the total flow, $\nu$, of ionizing molecules directed to the detector inlet. By introducing $\nu_{mol}$ (the fraction of molecules from the flow $\nu$ that is incident on the thermoemitter surface) into this ratio one can obtain [7]

$$E = \frac{\sum_k \nu_k^+}{\nu} = \frac{\sum_k \nu_k^+}{\nu_{mol}} \cdot \frac{\nu_{mol}}{\nu} = \beta_{mol} \cdot \xi$$

where $\beta_{mol} = \nu_k^+ / \nu_{mol}$ is an integral coefficient of the surface ionization detector defined by the thermoemission and catalytic properties of thermoemitter material; $\xi$ is a factor characterizing the perfection of the detector design as it defines the coefficient of utilization of a substance.

Using mass spectrometric data, $\beta_{mol}$ was calculated for tertiary amines to be 0.2–0.1 [3,4,17]. Hence, the coefficient of utilization of a substance for a given design of the detector is close to the maximum value. The limit of detection of tertiary amines is $m_{min} = 10^{-14}$ g/s, which exceeds considerably those with the best models of flame ionization [18] and thermoionic detectors [19]. One can obtain analogous sensitivity using an electron–capture detector, but then the preliminary conversion of amines into halogen-containing compounds is necessary, which makes the analysis complex [20]. It should be noted that limits of detection and the linear dynamic ranges (LDR) given in Table 1 are of a relative character as they were calculated on the assumption that the linearity of all plots that applies in the small-dose region is maintained up to the double noise of $2I_n = 2 \cdot 10^{-13}$ A, but this requires experimental confirmation. As we pointed out, such attempts have been made and at best reproducible results and linearity were obtained only for doses of $10^{-11}$ g. The high sensitivity of SID is confirmed by the ratio of the SID and FID signals: for tertiary amines it equals $10^3$ with an error of 5%, for secondary amines $10^2$ with an error of 10% and for primary amines less than $10^2$ but with an error of 25%. As is known, the different sensitivities relative to amine subclasses may be used for functional group analysis [15]. The unique selectivity of SID towards nitrogen-containing bases is known from direct mass spectrometric investigations surface ionization [5]. The chromatogram in Fig. 3 illustrates this effect, from which it is seen that the values of the recorded peaks for acetone and for TBA are almost the same, although the amount of TBA introduced ($3.1 \cdot 10^{-9}$ g) is $6.2 \cdot 10^6$ times less than that of acetone ($1.58 \cdot 19^{-3}$ g). When using samples containing amines and saturated hydrocarbons as solvent only one amine peak was registered for such concentrations.

The reproducibility of the analytical results obtained by SID is determined by the SID operating conditions and by the thermoemitter state. This could be revealed during operation with simultaneous SID and FID. When a solvent and the ionizing component are very different from each other, then the reproducibilities of the results for both detectors correlate independently of the kind of solvent and are within the range 5–6%. However, if the retention time of an amine is close to that of the solvent, then with non-selective FID the main peak of the solvent overlaps the peak of the dissolved component under analysis. In this event owing to its high selectivity, only one amine peak is registered by SID, but the reproductibilty of the results becomes worse owing to oversaturation of the thermoemitter by the solvent vapours. Hexadecane proved to be the most convenient solvent. When using columns packed with Apiezon sorbent (4% Ap + 1% KOH), the retention time of amines is of the order of minutes whereas that of the solvent is up to 8 h, so the continuous

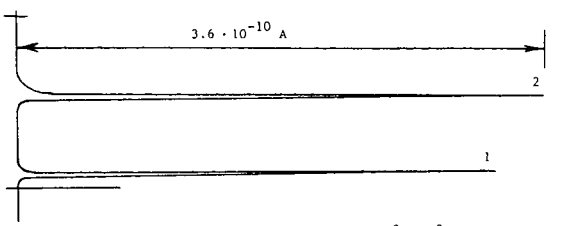


Fig. 3. Chromatogram of a mixture ($2 \cdot 10^{-3}$ cm$^3$) containing $2 \cdot 10^{-4}$% (v/v) of tributylamine in acetone: 1 = acetone (retention time $t_r$ = 15 s); 2 = tributylamine ($t_r$ = 180 s). The ion current was registered on the same scale of the charge amplifier.

analysis of amines may be carried out using both detectors during the whole operating time, as has been recommended [21].

### 3.2. Determination of quaternary amines

The results of the chromatographic determination of the dependence of the amount of charge registered in SID on the dose of quaternary ammonium salts (QAS) inserted into the chromatographic evaporator, namely tetraethylammonium chloride $(C_2H_5)_4N^+Cl^-$, tetraethylammonium bromide, $(C_2H_5)_4N^+Br^-$, and a typical representative of a mediator of natural origin, acetylcholine chloride, $CH_3COOCH_2$-$CH_2N^+(CH_3)_3Cl^-$, are presented in Fig. 2 (plots 12–14). Such dependences were obtained irrespective of the kind of solvent employed, distilled water or ethanol. The results of calculations of the SID characteristics relative to QAS are given in Table 1.

Fig. 4 shows typical chromatograms for comparison that were registered using SID and FID simultaneously under various conditions of analysis with the same dose $m = 2 \cdot 10^{-5}$ g of triethylamine and tetraethylammonium chloride. One can see that the high selectivity of SID allows amines to be reliably registered irrespective of the conditions of the chromatographic separation of the solvent and amine under analysis, whereas for the analysis with non-selective FID it is necessary to achieve the effective chromatographic separation of the amines and solvent. The sensitivity $K$ of SID when registering QAS is in the range 0.01–1 C/g, which corresponds to the sensitivity of secondary amines, and the ratio of signals $I_{SID}/I_{FID} = 4000$ corresponds to tertiary amines. Moreover, the times of sample retention in the column when inserting both tetraethylammonium chloride and bromide into the chromatographic evaporator are the same and coincide with the retention time of triethylamine.

Having analysed these data, the following conclusion could be drawn: QAS decompose in the chromatographic evaporator into tertiary amines, e.g., in accordance with Hoffman degradation:

$$(C_2H_5)_4N^+Cl^- \xrightarrow{t^0} (C_2H_5)_3N + (C_2H_5)Cl$$

(where $t^0$ denotes thermal heating) and the products of this reaction then are subjected to chromatographic separation, which is in accordance with the generalized conclusions concerning the chromatography of quaternary amines presented in detail by Anderson [18].

To locate where QAS are transformed into tertiary amines, experiments were carried out with various temperatures of the evaporator and a constant temperature of the column.

Fig. 5 shows the alteration of the peak shape registered during the injection of $10^{-5}$ g of acetylcholine at a constant column temperature $T_c = 150$°C for different temperatures of the evaporator ($T_{ev}$). One can see that the peak at $T_{ev} = 180$°C has a diffuse shape that could be explained by the low rate of transformation of acetylcholine into tertiary amine. With the increase in $T_{ev}$ the rate of the transformation reaction in the evaporator increases. This process affects the peak width, making it more symmetric. At $T_{ev} > 260$°C, the peak width becomes independent of $T_{ev}$, but it is anyway slightly wider than that of the peak registered for the injection of the corresponding tertiary amine (Fig. 4a–d).

In analogous experiments with triethylamine, the peak shape appeared to be independent of $T_{ev}$ as low as 120°C. This evidence indicates that decomposition of QAS into tertiary amines takes place mainly in the evaporation cell. Nevertheless, even at high $T_{ev}$, a certain fraction of QAS enters the chromatographic column where they may also be transformed into tertiary amines. This results in specific differences in the shape of the chromatographic peak of QAS from that of the corresponding tertiary amine. The latter may be used for the determination of QAS in complex mixtures by the analysis of data including the retention times and the shapes of the peaks recorded.

## 4. Conclusions

Systematic studies have been made of the main characteristics of a modification of the

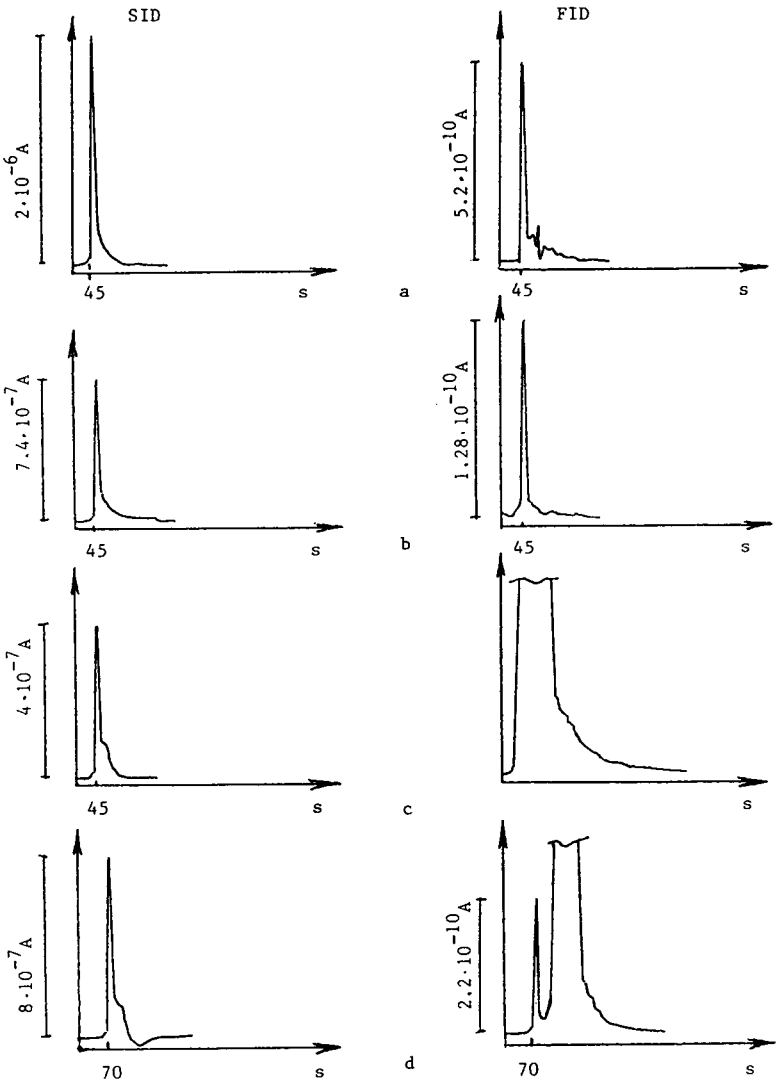


Fig. 4. Comparison of chromatograms obtained for injection of (a, b) aqueous and (c, d) alcoholic solutions of (a) triethylamine and (b–d) solutions of tetraethylammonium chloride using the columns with various sorbents: (a–c) Apiezon with potassium hydroxide and (d) PEG-1000.

surface ionization detector with an indirect incandescence emitter. The values of the characteristics obtained confirm the excellent sensitivity and selectivity of nitrogen-containing bases registered by the surface ionization method. By using SID the functional group analysis of trace amounts of amines in various mixtures can be carried out. The highest sensitivity was obtained relative to tertiary amines and the detection limit is ca. $10^{-14}$ g/s.

The present detector may be used for the selective registration and identification of quaternary amines. The detection limit of QAS in solutions is ca. $10^{-13}$ g/s.

The high sensitivity and selectivity of SID relative to nitrogen-containing bases suggest the

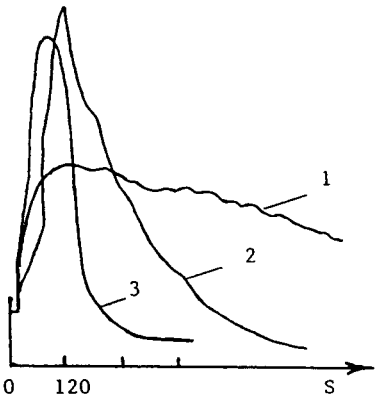


Fig. 5. Alteration of peak shape registered on injection of the acetycholine obtained with constant temperature of the chromatographic column (150°C) and different temperatures of the evaporator: $T_{ev}$ = (1) 180, (2) 220 and (3) 260°C.

development of improved methods for the detection and identification of various amines and their derivatives.

## References

[1] B.D. Taosh and J.N. Duscall, *Am. Lab.*, 14 (1982) 59–62.
[2] *Pollution of Atmospheric Air and Soil, Proceedings of IVth All-Union Meeting, Obninsk, 1989.*
[3] E.Ya. Zandberg, U.Kh. Rasulev, and B.N. Shustrov, *Dokl. Akad. Nauk SSSR*, 172 (1967) 885–888.
[4] E.Ya. Zandbegr and U.Kh. Rasulev, *Usp. Khim.*, 6 (1982) 1425.
[5] U.Kh. Rasulev and E.Ya. Zandberg, *Prog. Surf. Sci.*, 28 (1988) 181–412.
[6] U.Kh. Rasulev, E.Ya. Zandberg, A.M. Drobiz and K.U. Beldi, in *Proceedings of All-Union Conference, Tula, 1975*, p. 142.
[7] E.Ya. Zandberg, A.G. Kamenev, V.I. Paleev and U.Kh. Rasulev, *Zh. Anal. Khim.*, 35 (1980) 1188–1194.
[8] L.Ya., Gavrilina, V.I. Djeivot and O.A. Emelyanova, *Zh. Usp. Khim.*, 53 (1984) 2078–2100.
[9] T. Fujii and A. Arimoto, *Anal. Chem.*, 57 (1985) 2625–2628.
[10] T. Fujii and A. Arimoto, *J. Chromatogr.*, 355 (1986) 375–385.
[11] T. Fujii, H. Jimba, M. Ogura, H. Arimoto and K. Osaki, *Analyst* 113 (1988) 789–792.
[12] *Surface Ionization Detector, DPI. Technical Description and Operating Instructions*, OKBA, Dzerdzinsk, 1988.
[13] E.Ya. Zandbegr, U.Kh. Rasulev and Sh.Sh. Khalikov, *Zh. Tekh. Fiz.*, 46 (1976) 832.
[14] U.Kh. Rasulev, E.G. Nazarov, E.E. Petushkov, M.I. Nazarova and A.A. Stamov, *Visokochistie Veshestva*, No. 5–6 (1992) 203.
[15] R.V. Golovnya, I.L. Zhuravleva, M.B. Terenina, U.Kh. Rasulev and E.Ya. Zandberg, *Zh. Anal. Khim.*, 36 (1981) 533–539.
[16] V.V. Brazhnikov, *Differential Detector for Gas Chromatography*, Nauka, Moskow, 1974.
[17] R.V. Golovnya and I.L. Zhuravleva, *Zh. Anal. Khim.*, 29 (1974) 1406–1410.
[18] A.A. Anderson, *Gas Chromatography of Amine Compounds*, Zinatie, Riga, 1982.
[19] A. Karmen, *Adv. Chromatogr.*, 2 (1986) 293–336.
[20] E.D. Pellizzari, *J. Chromatogr.*, 98 (1974) 323–361.
[21] U.Kh. Rasulev, A.A. Balaukhin, V.G. Vtorov, E.G. Nazarov and G.B. Khudaeva, *Information Report No. 470*, FAN RU, Tashkent, 1989.

ELSEVIER

Journal of Chromatography A, 704 (1995) 483–494

JOURNAL OF CHROMATOGRAPHY A

# Hygrine, bona fide alkaloid or artifact: its chemical reduction, novel di-heptafluorobutyrylation and sensitive detection in South American coca leaves using capillary gas chromatography–electron capture detection

James M. Moore*, John F. Casale, Patrick A. Hays, Robert F.X. Klein, Donald A. Cooper

*Special Testing and Research Laboratory, United States Drug Enforcement Administration, 7704 Old Springhouse Road, McLean, VA 22102-3494, USA*

First received 31 August 1994; revised manuscript received 16 February 1995; accepted 16 February 1995

**Abstract**

Methodology is described for the isolation of hygrine, along with the related compound cuscohygrine, from South American coca leaf and its major tropane alkaloids. The isolated hygrine was reduced with lithium aluminum hydride to yield diastereomeric alcohols, which were subsequently derivatized with heptafluorobutyric anhydride in the presence of 4-dimethylaminopyridine. The resultant diastereomeric di-heptafluorobutyryl derivatives could be detected on-column at femtogram levels when using a polar fused-silica capillary column interfaced with a $^{63}Ni$ electron-capture detector. The artifactual formation of hygrine, resulting from the degradation of cuscohygrine, is discussed. Quantitative data are provided for hygrine and cuscohygrine levels in South American coca.

## 1. Introduction

Most known alkaloids in the leaf of the South American coca plant, *Erythroxylum coca*, possess a tropane moiety [1]. Two exceptions are the N-methylpyrrolidine alkaloids hygrine, 1, and cuscohygrine, 2, seen in Fig. 1. Recently, and for the first time, quantitative data were reported for 1 and 2 in coca leaf, along with the tropane alkaloids cocaine, *cis*- and *trans*-cinnamoylcocaine, the truxillines, tropacocaine and ecgonine methyl ester [2]. In that study, detailed analytical methodology, reaction pathways and derivative structures were not given for 1 and are, therefore, reported here. Furthermore, it was suspected that the presence of 1 in some coca leaf might be in part or in whole artifactual, resulting from the degradation of 2.

In the study described herein, methodology is provided for the isolation of 1 and 2 from coca leaf tissue and the bulk tropane alkaloid matrix. Once isolated, 1 was subjected to chemical reduction using lithium aluminum hydride ($LiAlH_4$), followed by derivatization with heptafluorobutyric anhydride (HFBA)/4-dimethylaminopyridine (4-DMAP) and analysis of the resultant di-heptafluorobutyryl (di-HFB) derivatives using capillary gas chromatography–elec-

* Corresponding author.

0021-9673/95/$09.50 
*SSDI* 0021-9673(95)00219-7

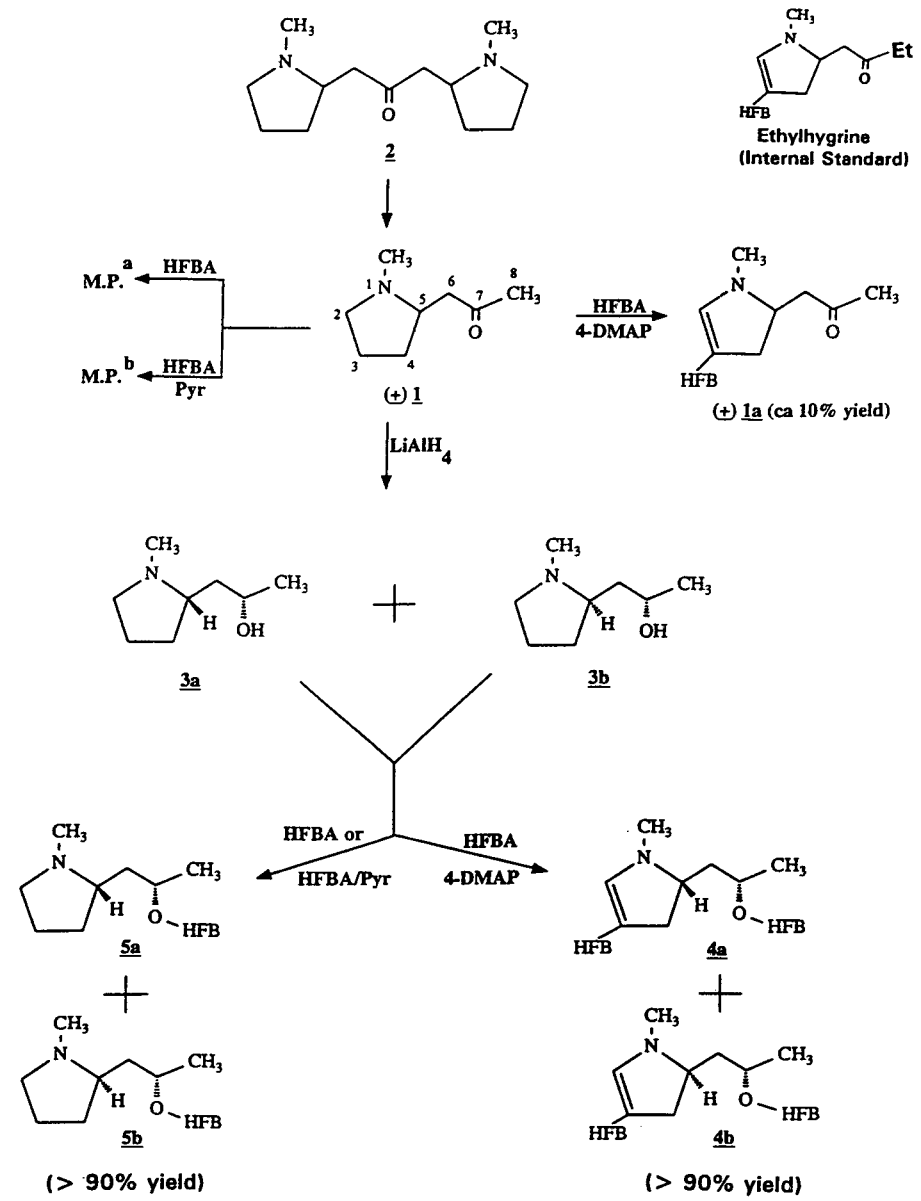


Fig. 1. Formation of hygrine (1) from cuscohygrine (2); lithium aluminum hydride reduction of 1 to yield diastereomeric hygrinols (3a and 3b), followed by heptafluorobutyrylation, with or without catalyst, to yield either heptafluorobutyryl (HFB) derivatives 5a and 5b or di-heptafluorobutyryl (di-HFB) derivatives 4a and 4b. [a] M.P. = Multiple perfluorinated cGC–ECD peaks, none of which appeared analytically useful; [b] M.P. = multiple perfluorinated cGC–ECD peaks, none of which appeared analytically useful; peaks differed from those generated using HFBA without pyridine catalyst.

electron capture detection (cGC–ECD). The relationship between 1 and 2, with respect to the formation of the former from the latter, is discussed.

## 2. Experimental

### 2.1. Solvents, chemicals and materials

All solvents were distilled-in-glass products of Burdick and Jackson Labs (Muskegon, MI, USA). HFBA was supplied in 1-ml sealed glass ampules and obtained from Pierce (Rockford, IL, USA). A 1.0 *M* solution of $LiAlH_4$ in diethyl ether and 4-DMAP were supplied by Aldrich (Milwaukee, WI, USA). Celite was provided by J.T. Baker (Jackson, TN, USA) and was used without further treatment. A pH 4.0 acid phthalate buffer was prepared according to the United States Pharmacopeia XIX. All other chemicals were of reagent-grade quality.

### 2.2. Standards

The syntheses of 1 (Fig. 1) and an internal standard analogue, ethylhygrine (Fig. 1), were accomplished using the methods of Thomsen et al. [3] and Ghirlando et al. [4]. The $LiAlH_4$ reduction of 1 and ethylhygrine yielded diastereomeric hygrinols 3a and 3b, and ethylhygrinols, respectively. The procedure of de Boer and Speckamp [5] was used for the preparation of 2.

### 2.3. Gas chromatography

Two gas chromatographs (GCs) and three capillary columns were used in this study. The first, a Hewlett-Packard 5880A GC–$^{63}$Ni ECD interfaced with a Level IV data processor, was used in the initial phase of this study for the determination of 1 in coca leaves. This GC was operated in the splitless mode and was fitted with a 15 m × 0.25 mm I.D. fused-silica capillary column coated with DB-5+ (0.25 μm) (J&W Scientific, Rancho Cordova, CA, USA). The oven temperature was programmed as follows: (level 1) initial temperature, 90°C; initial hold, 5.5 min; temperature program rate, 5°C/min; final temperature, 160°C; final hold, 5 min; (level 2) temperature program rate, 4°C/min; final temperature, 275°C; final hold, 10 min. Injector and detector temperatures were both held at 300°C. Hydrogen was used as a carrier gas at 30–40 cm/s and argon–methane (95:5) as detector make-up gas at 30–40 ml/min.

The second chromatograph was a Hewlett-Packard 5890 Series II GC with dual $^{63}$Ni ECD detectors interfaced with two 30 m × 0.25 mm I.D. fused-silica capillary columns, one coated with DB-1701 (0.25 μm) and the other with DB-1 (0.25 μm). The GC oven temperature was programmed as follows for both columns: initial temperature, 90°C; initial hold, 1.0 min; program rate, 6.0°C/min; final temperature, 275°C; final hold, 5 min. Injector and detector temperatures were maintained at 230 and 300°C, respectively. Hydrogen was used as the carrier gas at a velocity of 35–40 cm/s measured at an oven temperature of 90°C. Argon–methane (95:5) was the make-up gas at a flow of 30–40 ml/min.

### 2.4. Mass spectrometry

A Hewlett-Packard Model 5972 quadrupole mass-selective detector (MSD) interfaced with a Hewlett-Packard 5890 Series II GC was used for the characterization of 1 and 1a, 4a and 4b, and 5a and 5b (Fig. 1). The MSD was operated in the electron ionization mode with an ionization potential of 70 eV, an EMV of 1541 and at 1.2 scans/s. The GC was fitted with a 30 m × 0.25 mm I.D. fused-silica capillary column coated with DB-1 (0.25 μm) and used helium as the carrier gas. The oven was temperature-programmed as follows: initial temperature, 80°C; initial hold, 5 min; program rate, 4°C/min; final temperature, 285°C.

### 2.5. Nuclear magnetic resonance spectrometry

A Varian Unity 500 NMR spectrometer operating at 500 MHz for proton and equipped with a 5 mm I.D. indirect detection probe was used for the structural determination of 4a and

4b. Sample analysis was accomplished at 25°C. The sample was run in deuterated chloroform (Aldrich, Milwaukee, WI, USA), with tetramethylsilane (TMS) added as an internal standard.

### 2.6. Coca leaf

The leaf material used in this study was cultivated in the South American countries of Bolivia, Peru, Ecuador and Colombia. After harvesting, the leaves were air-dried and then shipped to our laboratory, where they were stored under ambient conditions prior to analysis. At the time of analysis most leaf had an approximate age of 1–2 years from the time of harvesting.

### 2.7. Isolation of 1 from coca leaf

Dried leaf tissue was powdered in a Wiley mill to pass a 2-mm sieve. About 1–5 g of the powdered coca leaf was accurately weighed, thoroughly mixed with 1–5 ml of saturated aqueous sodium bicarbonate, and placed in a 50-ml centrifuge tube containing an appropriate quantity of ethylhygrine internal standard. For a 1-g sample weight, about 25–30 ml of water-saturated toluene, containing a known quantity of ethylhygrine internal standard, was added and the tube was heated at 60–65°C for 1 h with occasional mixing. The tube was then centrifuged and the toluene layer transferred to a flask. The coca leaf powder residue was re-extracted twice more in the same manner; the combined toluene extracts were transferred to a chromatographic column (260 mm × 22 mm), packed with a mixture of 4 ml of 0.18 *M* sulfuric acid and 8 g of Celite 545. After passing the toluene extracts through the column, an additional 20 ml of water-saturated toluene, followed by 30 ml of water-saturated chloroform, were added; all eluates were discarded. The tropane alkaloids, 1, 2 and the ethylhygrine internal standard were then all eluted from the column with 25 ml of water-saturated chloroform containing 250 μl diethylamine (DEA), followed by 30 ml of water-saturated chloroform.

### 2.8. Isolation of 1 and 2 from other major coca alkaloids

A 5.0-ml aliquot from the chloroform–DEA eluate above was extracted with 7 ml of a pH 4.0 phthalate buffer and the chloroform phase (containing cocaine and the cinnamoylcocaines) discarded. The buffer (containing 1 and 2) was then back-extracted with 15 ml of chloroform, the latter being discarded. A 1-ml aliquot of 4 *M* sodium hydroxide was added to the buffer, which was then extracted with 3 × 3-ml aliquots of chloroform, filtering the extracts through anhydrous sodium sulfate into a 10-ml volumetric flask. After dilution to volume with chloroform, a 3.0-ml aliquot was transferred to a tube containing 0.3 ml of 0.05 *M* HCl gas in methanol. After vortex-mixing, the solution was evaporated to dryness.

### 2.9. $LiAlH_4$ reduction of 1

To the residue above was added 1 ml of methylene chloride and the resulting solution heated at 50°C for several minutes with occasional vortex-mixing. Upon cooling, 5 ml of anhydrous ethyl ether was added to the tube, followed by 0.2 ml of 1 *M* $LiAlH_4$ in ethyl ether. After vortex-mixing, the solution was reduced in volume to about 0.5 ml by heating at 50–55°C. About 6 ml of acetone was slowly added to the tube and the contents cooled to 0°C and held there for 10 min. After centrifugation, the acetone supernatant was transferred to another tube containing 5 ml of the methanol–HCl solution and evaporated to dryness.

### 2.10. HFBA derivatization of diastereomeric 3a and 3b and ethylhygrinols

To the residue above was added 1 ml of acetonitrile, 50 μl of HFBA and 100 mg of 4-DMAP, and the tube was heated at 75°C for 1 h. After cooling, 5.0 ml of isooctane was added to the tube, followed by 5 ml of saturated

aqueous sodium bicarbonate, and the contents mixed vigorously without delay. After centrifugation, the isooctane was back-extracted with 5 ml of 0.18 *M* sulfuric acid (to remove 4-DMAP) and the isooctane layer was then dried over anhydrous sodium sulfate.

### 2.11. cGC–ECD analysis

About 2 μl of the isooctane extract from above was injected onto the 15 m DB-5+ capillary column using conditions described under Experimental. Also injected was a mixed standard containing the di-HFB derivatives of standard diastereomeric hygrinols and ethylhygrinol internal standards of known concentration. For calculation purposes the peak areas for each diastereomeric pair were summed.

## 3. Results and discussion

### 3.1. Isolation of 1 from coca leaf and other coca alkaloids

Toluene was found to be an effective solvent for the high-yield extraction of 1, 2 and other alkaloids from powdered coca leaf tissue [2]. The bulk alkaloid matrix, including 1 and 2, was quantitatively isolated from non-alkaloidal leaf components by acid/Celite column chromatography. After removal from the column, 1 and 2 were isolated from cocaine and the bulk of other tropane alkaloids by partitioning between chloroform and the pH 4.0 phthalate buffer. The higher $pK_b$ of 1 and 2 allowed for their quantitative extraction into the buffer (along with small quantities of isomeric truxillines), while most of the cocaine and other alkaloids were retained in the chloroform phase. Because of its higher volatility, subsequent reduction-in-volume steps involving 1 (as well as 2) were always preceded by its conversion to the hydrochloride ion pairs. It should also be noted that the method recoveries of 1 and the ethylhygrine internal standard were similar and both $>80\%$.

### 3.2. Reduction and/or chemical derivatization of 1 and diastereomeric 3a and 3b

Given the suspected low levels of 1 in coca leaf, it was believed that the more sensitive $^{63}Ni$ ECD detector would be required for their analyses, as opposed to the less sensitive flame-ionization detector (FID). This required the high-yield introduction of an electrophilic group onto 1. We have previously described the unusual quantitative attachment of HFB or HFBO groups at carbon sites in other, similar nitrogen heterocycles, including nicotine, itself an N-methylpyrrolidine alkaloid [6–8].

The reactions outlined in Fig. 1 used racemic (synthetic) 1 as the precursor compound. Early in this study, standard 1 was subjected directly to HFBA derivatization in the presence of 4-DMAP, with the intention of incorporating an HFB group into 1; this would allow for its sensitive detection by cGC–ECD. Although this reaction produced the desired product 1a, as seen in Fig. 1, the yield was unacceptably low ($<10\%$). This was surprising, given the intense coloration of the reaction solution, which suggested a higher yield. Furthermore, little or no unreacted 1 was detected. Modest attempts to improve the yield of 1a were unsuccessful. It is also seen in Fig. 1 that the reaction of 1 with HFBA in the presence or absence of pyridine yielded multiple HFB-substituted products, none of which appeared analytically useful. It should be noted that no 1a was produced from these latter reactions; nor was there a significant presence of unreacted 1. Furthermore, the mass spectra of these diverse derivatization products contained no base peak ion at $m/z$ 84, suggesting that modification of the N-methylpyrrolidine ring had occurred.

Given the low yield of 1a, additional attempts were made at providing an improved ECD-responsive derivative from racemic 1. This included the $LiAlH_4$ reduction of 1 to yield diastereomeric alcohols, 3a and 3b (Fig. 1). Subsequent derivatization of these compounds with HFBA in the presence or absence of pyridine yielded two major products in high yield, believed to be the diastereomeric 5a and 5b (Fig.

1). No 4a or 4b were detected as products of this reaction. When 3a and 3b were treated with HFBA in the presence of 4-DMAP, the diastereomeric pair 4a and 4b were afforded in good yield. In fact, the yield of 4a + 4b was markedly greater than that for 1a, obtained by the reaction of 1 with HFBA/4-PMAP (Fig. 1).

It was concluded, as outlined in Fig. 1, that the LiAlH4 reduction of 1 to give 3a and 3b, followed by HFBA/4-PMAP derivatization to yield 4a and 4b, provided the methodology of highest sensitivity for the detection of 1. Not only was the derivatization yield for 4a and 4b high, but the introduction of two HFB groups into a small molecule such as 3a,b provided highly electrophilic derivatives which were ideally suited for sensitive cGC–ECD detection.

### 3.3. Mass spectral analysis of 1a, 4a and 4b, and 5a and 5b

Given that the structure of 1 was known, characterization of 1a (Fig. 1) could be rationally derived from its EI mass spectrum, seen in Fig. 2a. The molecular ion at $m/z$ 335 supported the introduction of a single HFB group and the concomitant formation of a double bond in 1. This was in agreement with our previous observations regarding the heptafluorobutyrylation of tertiary nitrogen heterocyclic compounds

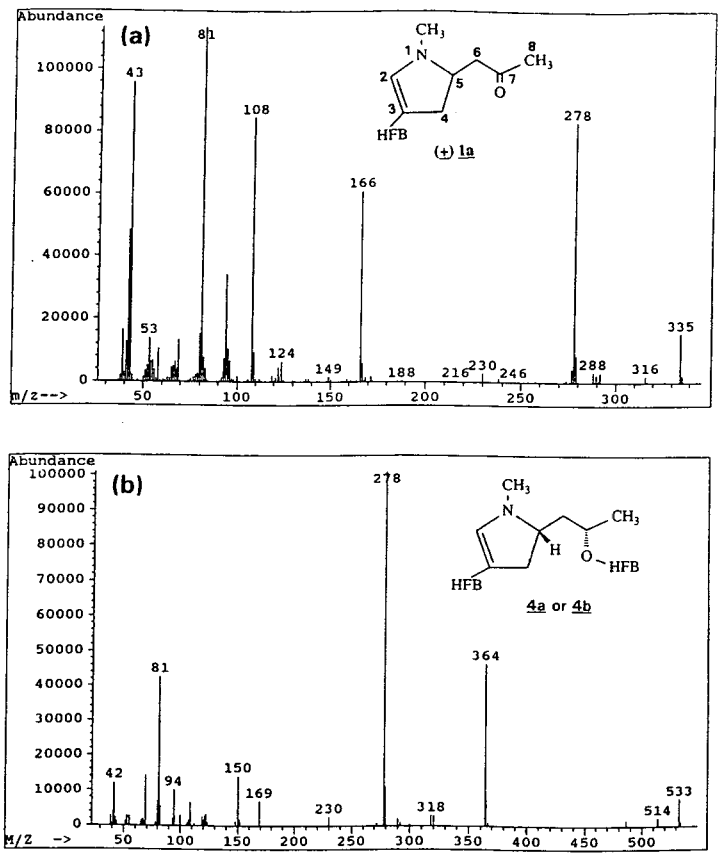


Fig. 2. Electron-ionization mass spectra of (a) derivatization product 1a, obtained by the reaction of hygrine (1a) with heptafluorobutyric anhydride (HFBA) in the presence of 4-dimethylpyridine (4-DMAP) (see Fig. 1) and (b) diastereomeric derivatization product 4a or 4b, obtained by the reaction of hygrinol diastereomers (3a and 3b) with HFBA in the presence of 4-DMAP (see Fig. 1).

[6,7]. The fragment ion at $m/z$ 278 was accounted for by loss of the 2-propanone side chain, also confirming the presence of the HFB/C = C grouping in the N-methylpyrrolidine ring, probably arranged in a vinylogous amide configuration. Supporting this modification of the N-methylpyrrolidine ring was the absence of a fragment ion at $m/z$ 84, which in the mass spectrum of untreated 1 is due to the N-methylpyrrolidinium ion. A prominent ion at $m/z$ 166 is almost certainly due to the loss of the $CF_3CF_2CF_2$ radical. The extraction characteristics of 1a suggested a reduced basicity for this derivative, supporting a vinylogous amide, with (a) the double bond at C2 = C3 and HFB at C3, or (b) double bond at C4 = C5 and HFB at C4, or (c) double bond at C5 = C6 with HFB at C6. The presence of the intense $m/z$ 278 ion (see above and Fig. 2a) discounted proposal (c), as loss of the side chain would not be likely. The intense ion at $m/z$ 108, believed to be due to the loss of $CF_3CF_2CF_2$ and acetone (involving carbon nos. 6, 7 and 8 and the proton at C4) from the molecular ion, discounted proposal (b). The loss of acetone inferred the presence of a proton at C5, which accommodated the structure in proposal (a). The base peak ion at $m/z$ 81 was believed to be due to losses of the HFB moiety and the $-CH_2-CO-CH_3$ side chain from the 1a molecular ion.

The mass spectra of 5a and 5b (see structures in Fig. 1) were virtually identical, with each exhibiting what was believed to be a low-intensity molecule ion at $m/z$ 339, indicating the presence of a sole HFB moiety. A base peak ion at $m/z$ 84 represented loss of the side chain and concomitantly placed the HFB substituent on that leaving group, almost certainly at the secondary alcohol site. The appearance of a low-intensity ion at $m/z$ 126 was probably due to loss of the heptafluorobutyryloxy group from the molecular ion. The presence of a fragment ion at $m/z$ 169 was believed to be due to $[CF_3CF_2CF_2]^+$.

As expected, the EI mass spectra of diastereomeric 4a and 4b, seen in Fig. 2b, were also virtually identical. The molecular ion at $m/z$ 533 necessitated the presence of two HFB groups, with one site of HFB substitution again being at the secondary alcohol. The fragment ion at $m/z$ 364 was due probably to loss of $CF_3CF_2CF_2$ from the molecular ion. The base peak ion at $m/z$ 278 was accounted for by the loss of the $CH_2$-CH(OHFB)-$CH_3$ side chain. Amide extraction characteristics were also evident for 4a and 4b and suggested, (a) a double bond at C2 = C3 with HFB attachment at C3, or (b) a double bond at C4 = C5 with an HFB substituent at C4 or (c) a double bond at C5 = C6 with the HFB group at C6. Since 4a and 4b are diastereomers (the result of perfluoroacylation of the diastereomeric precursors 3a and 3b and as evidenced by 2 GC peaks), a proton at C5 was required. This necessitated placement of the double bond at C2 = C3 with HFB attachment at C3.

### *3.4. Nuclear magnetic resonance spectral analysis of 4a and 4b*

NMR spectroscopy verified that two compounds were present in nearly equal amounts and that they were diastereomers. Proton and carbon assignments are found in Table 1, with proton–proton scalar coupling constants in Table 2.

An indirect detection 2D heteronuclear multiple-quantum coherence (HMQC) experiment was used to determine carbon–proton bonding ($^1J_{CH}$). An indirect detection 2D heteronuclear multiple-bond coherence (HMBC) experiment was used to establish skeletal connections between carbons and protons with $^2J_{CH}$ and $^3J_{CH}$ couplings. A 2D correlation spectroscopy (COSY) experiment was used for proton–proton coupling correlations with $^2J_{HH}$ and $^3J_{HH}$ couplings. These 2D experiments and the normal, direct detection proton and carbon spectra allowed for the assignment of all chemical shifts to the two compounds.

The 2D COSY experiment detected a linear five carbon chain $CH_2$-CH-$CH_2$-CH-$CH_3$ for both compounds. This chain corresponds with carbons C4 through C8 respectively. All other protons are isolated from this chain.

The methine at C7 and proton and carbon chemical shifts verify that HFB substitution

Table 1
NMR assignments for 4a and 4b

| Position | Compound 4a | | Compound 4b | |
|---|---|---|---|---|
| | Proton[a] | Carbon[a] | Proton[a] | Carbon[a] |
| NCH3 | 3.11 s | 34.9 or 35.1 | 3.11 s | 34.9 or 35.1 |
| 2 | 7.36 s | 156.0 | 7.32 s | 156.2 |
| 3 | – | approx. 108[b] | – | approx. 108[b] |
| 4 | 2.70 dd, 3.13 dd | 33.4 | 2.76 dd, 3.20 dd | 33.6 |
| 5 | 3.75 m | 60.8 | 3.86 m | 61.1 |
| 6 | 1.72 ddd, 2.27 ddd | 38.4 | 2.04 ddd, 2.11 p | 37.9 |
| 7 | 5.25 ddq | 73.2 | 5.32 as | 73.5 |
| 8 | 1.45 d | 20.2 | 1.42 d | 19.6 |

s = singlet, d = doublet, t = triplet, q = quartet, p = pentet, as = apparent sextet.
[a] Chemical shifts are in ppm relative to TMS.
[b] Approximate value. C3 was indirectly detected using HMBC.
Chemical shifts of the carbons in the HFB groups were not determined due to peak splitting from the fluorine atoms.

occurred at the alcohol. The methine at C5 and proton and carbon chemical shifts confirm the nitrogen substitution. The methylene at C4 indicates that the alkene double bond is from C2 to C3. A singlet in the proton spectrum at 3.11 ppm has two corresponding carbon chemical shifts (34.9 and 35.1 ppm) indicating N-methyl groups for 4a and 4b. The remaining olefinic proton is found as a singlet at 7.36 (4a) and 7.32 ppm (4b) with its carbon at 156.0 (4a) and 156.2 ppm (4b). Because this proton is a singlet and is not coupled to any other protons (i.e., the C4 methylene), its position is at C2, verifying HFB substitution at C3.

Table 2
Coupling constants for 4a and 4b ($^{2,3}J_{HH}$ in Hz)

| Positions | Compound 4a | Compound 4b |
|---|---|---|
| 4ab | 15.4 | 15.4 |
| 4a,5 | 6.8 | 7.1 |
| 4b,5 | 5.1 | 11.2 |
| 5,6a | 10.9 | 3.8 |
| 5,6b | 2.9 | 7.5 |
| 6ab | 14.0 | 14.6 |
| 6a,7 | 2.6 | 5.2 |
| 6b,7 | 10.2 | 7.5 |
| 7,8 | 6.2 | 6.3 |

The 5-membered ring is verified by using the 2D HMBC experiment. Through-bond connections are present between the N-methyl protons and C1 and C7. This experiment also confirms a link between the C4 protons and C1 and C2.

Tentative assignments of compounds 4a versus 4b was accomplished using a molecular modelling program. After minimizing energy for these molecules, dihedral angles were determined for H4a/H5, H4b/H5, H5/H6a, H5/H6b, H6a/H7, and H6b/H7, and their coupling constants estimated [9]. These estimates were then compared with experimental values taken from the proton spectrum.

### *3.5. Yield of 4a and 4b versus derivatization time*

At a temperature of 75°C, the diastereomeric mixture of 3a and 3b was subjected to derivatization with HFBA/4-PDAP at reaction times of 10, 20, 45 and 60 min. After summation of the diastereomeric pair peak areas for each of the four reactions, it was determined that the yields

of 4a and 4b did not vary significantly with time. However, it was noted that at the reduced reaction times, the levels of undesirable by-products increased.

### 3.6. Chromatography and on-column MDQ of 4a and 4b

The chromatography of 4a and 4b, along with the di-HFB derivatives of the corresponding ethylhygrinol diastereomeric internal standard, were investigated using three capillary columns of differing polarity. These included two 30 m × 0.25 mm I.D. fused-silica capillary columns, one coated with DB-1 (0.25 μm) and the other with DB-1701 (0.25 μm). The third column was a 15 m × 0.25 mm I.D. fused-silica capillary column coated with DB-5+ (0.25 μm). Retention time data for 4a and 4b and the di-HFB derivatives of the ethylhygrinol diastereomers for the three columns are presented in Table 3. The most suitable columns were found to be DB-5+ and DB-1701. Fig. 3 illustrates the cGC–ECD chromatography on the DB-5+ column for the determination of 1 in Colombian coca leaves.

The on-column minimum detectability quantity (OC-MDQ) of 4a and 4b was determined on the 30-m DB-1701 column. About 1 mg of 3a+3b was derivatized with HFBA/4-DMAP and then serially diluted with isooctane until no cGC–ECD response for the derivatives 4a and 4b was observed. The OC-MDQ value for each diastereomer was approximately 400–600 fg.

Table 3
Retention time data for 4a, 4b and the di-HFB derivatives of diastereomeric ethylhygrinol internal standard (see Fig. 1)

| Compound | Retention time (min)[a] | | |
|---|---|---|---|
| | DB-1 | DB-1701 | DB-5+ |
| 4a[b] | 15.07 | 19.58 | 18.62 |
| 4b[b] | 15.20 | 19.83 | 18.85 |
| Ethygr-ISa[c] (di-HFB) | 16.23 | 20.35 | 20.00 |
| Ethygr-ISb[c] (di-HFB) | 16.33 | 20.58 | 20.20 |
| Aldrin IS[d] | 20.07 | 21.26 | – |

[a] See Experimental for column dimensions and oven temperature parameters.
[b] The di-HFB derivatives of diastereomeric hygrinol (see Fig. 1).
[c] The di-HFB derivatives of diastereomeric ethylhygrinol internal standard.
[d] Aldrin used as instrumental internal standard (IS).

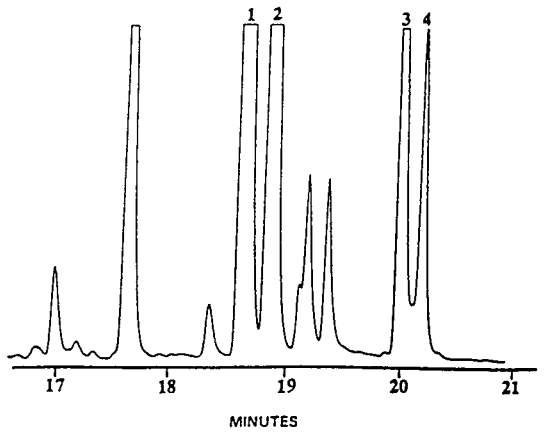


Fig. 3. The cGC–ECD chromatogram of hygrine (1) determined in Colombian coca leaves. Peaks: 1,2 (18.6 min, 18.8 min) = 4a and 4b in Fig. 1; 3,4 (20.0 min and 20.2 min) = di-HFB derivatives of diastereomeric ethylhygrinol (obtained via $LiAlH_4$ reduction and HFBA derivatization of ethylhygrine internal standard).

### 3.7. Content of 1 in coca leaves–bona fide alkaloid or artifact

The content of 1 in coca leaf from Bolivia, Peru, Ecuador and Colombia was determined soon after the samples were reduced to powder form. After storage of the coca powder under ambient conditions for 2–3 weeks, the analyses were repeated for the Bolivian and Peruvian samples. This data is presented in Table 4. As seen, the low levels of 1 in the Bolivian and Peruvian coca justified the use of the more sensitive cGC–ECD methodology. It is also seen that the same coca leaf powder yielded higher results for 1 after storage under ambient conditions for several weeks. This clearly indicates that 1 can be formed as an artifact in situ. For this reason, the data in Table 4 should be considered the "maximum" level for "true" 1 in the leaf sample. It was surmised that the artifact-

Table 4
Hygrine (1) content of South American coca leaf samples from Bolivia, Peru, Ecuador and Colombia[a]

| Country | Hygrine content[b] (%) | |
|---|---|---|
| | 1 Day[c] | 2–3 Weeks[c] |
| Bolivia | 2.3 | 5.2 |
| Peru | 1.4 | 4.8 |
| Ecuador | 4.2 | – |
| Colombia | 24 | – |

[a] Coca leaf samples were harvested and maintained as dry whole leaf under ambient conditions 1–2 years prior to cGC–ECD analyses.
[b] Hygrine (1) content expressed as % (w/w) relative to cocaine content.
[c] Period of time between powdering of the coca leaf and the determination of 1.

ual formation of 1 was enhanced by powdering of the sample and subsequent storage at room temperature (as opposed to sub-ambient temperatures). The preliminary results of a parallel study [10] suggested that keeping the powder at or near 0°C before analysis may retard the increase in 1. However, further work is needed to confirm this observation. It is not known whether 1 is produced in the whole leaf between the time of harvesting and analyses, a period that can be rather lengthy. It is recommended that for maximum accuracy, the determination of 1 and 2 should be carried out soon after harvesting of the leaf. If this is not possible, then the leaf material should be air-dried and stored at or near 0°C over a dehydrating agent prior to reduction to a powder and immediate analysis.

It was concluded that the content of 1 in the Colombian leaf (Table 4) was mostly bona fide. However, although it is not believed that artifactual 1 contributed significantly to this result, it is likely that at least trace levels are present. The level of 1 in the Colombian coca was in general agreement with a relatively high content of 1 in a "fresh" leaf sample harvested in northern Peru [10]. It was estimated that for this latter sample, the time between harvesting and analysis was less than one month; in addition, the sample was analyzed for 1 immediately after powdering, thus establishing 1 as a bona fide alkaloid.

Given the artifactual increase of 1 seen in Table 4, it was reasoned that there should be a concomitant decrease in the levels of 2. To substantiate this hypothesis, a Peruvian coca leaf sample was powdered and then analyzed for 2 over a 2-month period. During this time, the powdered sample was stored under ambient conditions. The results, seen in Table 5, revealed a marked decrease in the level of 2 over the defined time period. As was the case with 1, it is not known if the level of 2 begins decreasing immediately upon harvesting and continues with storage of the whole leaf at ambient temperature.

In addition to the artifactual formation of 1 described above, we have observed that during routine column and thin-layer chromatographic analyses of coca leaf extracts, small amounts of 1 can be created, (again) presumably from the degradation of 2. It is believed that the levels of artifactual 1 formed in this manner are quite small and probably represent $<2\%$ w/w (relative to cocaine). Work is currently on-going in the development of methodology for the isolation of 1 from 2 using column chromatographic techniques. It has also been observed that during cGC–FID analyses of coca leaf for 2, a relationship existed between the formation of 1 from 2 and injection port temperature. This can be seen

Table 5
Degradation of cuscohygrine (2) in powdered Peruvian coca leaf as a function of storage and time[a]

| Date of analysis | Cuscohygrine content[b] (%) |
|---|---|
| 3/7/90 | 95 |
| 3/28/90 | 67 |
| 5/8/90 | 36 |

[a] Coca leaf sample was harvested and maintained as dry whole leaf under ambient conditions 1–2 years prior to cGC–ECD analyses; sample was powdered prior to the first analysis and subsequently stored at room temperature.
[b] Cuscohygrine content express as % (w/w) relative to the cocaine content.

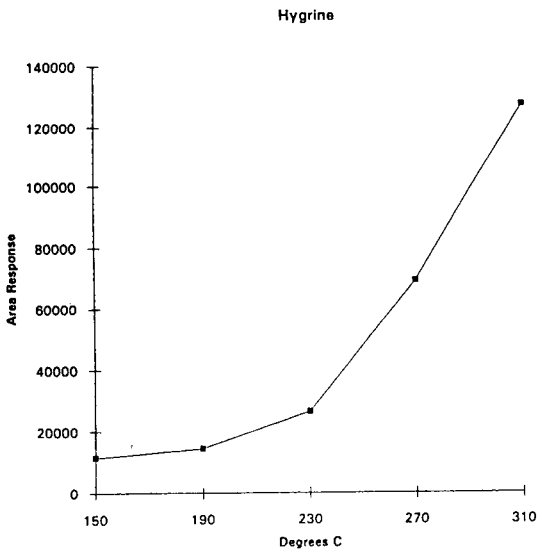


Fig. 4. Artifactual formation of 1 after cGC–FID injection of chloroform solution of standard 2 at increasing injection port temperatures; injections carried out in fused-silica injection port liner at a split ratio of 20:1.

in Fig. 4 for standard 2, from which marked increases of 1 were observed at injection port temperatures in excess of 230°C. It should be emphasized, however, that for the cGC–ECD methodology described herein, the injection port conversion of 2 to 1 is a non-factor, since 1 is first reduced and then heptafluorobutyrylated prior to chromatographic determination.

In summary, it is clear that 1 is a bona fide alkaloid in some coca leaf. It is also apparent that this compound can be produced artifactually, due to improper storage of the coca powder (and perhaps of the whole leaf as well). It also appears that trace levels of 1 can be formed during routine acid–base extractions. Artifactual 1 almost certainly results from the degradation of 2. As mentioned previously, it is not known whether significant amounts of 1 are produced from 2 during prolonged storage of the whole, dry coca leaf under ambient conditions. It is recommended, therefore, that for the determination of both 1 and 2, the analyses be carried out soon after harvesting of the leaf. If this is not feasible, then storage of the air-dried whole leaf over a dehydration agent at or near 0°C is recommended. Although it appears that by storing powdered coca leaf at 0°C the degradation of 2 to 1 was retarded, it is recommended that determination of these alkaloids in stored leaf be done immediately after the sample is powdered.

## 4. Conclusions

Sensitive methodology has been described for the detection and quantitation of hygrine in cocaine-bearing plants of South America. After isolation of hygrine and cuscohygrine from the leaf and other alkaloids, it is reduced with lithium aluminum hydride and the resultant diastereomeric hygrinols derivatized with heptafluorobutyric anhydride in the presence of 4-dimethylaminopyridine. The resulting di-heptafluorobutyryl derivatives could be detected on-column at femtogram levels when using a cGC–ECD equipped with a fused-silica capillary column. Hygrine levels of 1% w/w or less (relative to cocaine) in coca leaf could be determined when using a structurally-related internal standard. Although hygrine has been confirmed as a bona fide alkaloid of coca leaf, the storage of leaf in the powdered form at room temperature can result in the artifactual formation of this compound, due probably to the degradation of cuscohygrine. It is not known if artifactual hygrine is produced when whole coca leaf is stored for prolonged time periods at room temperature. Hygrine can also be produced as an artifact during work-up of the coca leaf sample and in the injection port of the gas chromatograph, due to the thermal degradation of cuscohygrine.

## References

[1] C.E. Turner, B.S. Urbanek, G.M. Waller, in Cocaine–An Annotated Bibliography, Vols. I and II, Research Institute of Pharmaceutical Sciences, University of Mississippi, Oxford, MS, 1988.

[2] J.M. Moore, J.F. Casale, R.F.X. Klein, D.A. Cooper and J. Lydon, J. Chromatogr. A, 659 (1994) 163–175.

[3] I. Thomsen, K. Clausen, S. Scheibye and S.O. Lawesson, Org. Synth., 62 (1984) 158–163.
[4] R. Ghirlando, A.S. Howard, R.B. Katz and J.P. Michael, Tetrahedron, 40 (1984) 2879–2884.
[5] J.J. de Boer and W.N. Speckamp, Proc. 11th IUPAC Int. Symp. Chem. Nat. Prod., 1978, Vol. 3, pp. 129–132.
[6] J.M. Moore, A.C. Allen and D.A. Cooper, Anal. Chem., 56 (1984) 642–646.
[7] J.M. Moore, A.C. Allen, D.A. Cooper and S. Carr, Anal. Chem., 58 (1986) 1656–1660.
[8] J.M. Moore, D.A. Cooper, T.C. Kram and R.F.X. Klein, J. Chromatogr., 645 (1993) 273–281.
[9] R.M. Silverstein, G.C. Bassler, T.C. Morrill, in Spectrometric Identification of Organic Compounds, 4th edn., John Wiley and Sons, New York, NY, 1981.
[10] J.M. Moore and J.F. Casale, unpublished results.

ELSEVIER

Journal of Chromatography A, 704 (1995) 495–502

JOURNAL OF CHROMATOGRAPHY A

# Improved chromatographic analysis of volatile sulfur compounds by the static headspace technique on water–alcohol solutions and brandies with chemiluminescence detection

Mustapha Nedjma*, Alain Maujean

*Faculté des Sciences, Laboratoire d'Oenologie, "Moulin de la Housse", B.P. 347, 51062 Reims Cedex, France*

Received 20 December 1994; accepted 16 February 1995

**Abstract**

Volatile sulfur compounds are renowned for their nauseous character in alcoholic beverages at an extremely low concentration. In this work, a quantitative analytical method was developed for their detection with the static headspace technique using a Sievers chemiluminescence detector (SCD 355). It gives a linear response over the concentration range 10–100 $\mu$g/l with a repeatability or reproducibility error of less than 5%. It was found that the headspace concentration of sulfur compounds in water–alcohol solutions or brandies rises with increasing ratio between the gas and liquid phase volumes and is proportional to the temperature. However, it diminishes with increasing ethanol content and is barely sensitive to the liquid-phase salt concentration.

## 1. Introduction

Nauseous volatile sulfur products such as hydrogen sulfide ($H_2S$), carbonyl sulfide (COS), sulfur dioxide ($SO_2$), thiols (RSH), sulfides (RSR), polysulfides ($RS_nR$, $n = 2, 3, \ldots$) or thioesters (RCOSR') are found in grape juices [1], wines [2,3], beers [4–6] and spirits [7,8]. Most of these compounds are the cause of olfactory problems and in some cases organoleptic defects, because of their nauseous nature and their very low perception levels [9–11]. However, some of them (with medium and high boiling points) may have a positive influence [12,13].

Sulfur products have diverse origins: (1) natural, from plant cell breakdown products; (2) plant protection via breakdown of vine plant treatment products in wines [14,15]; (3) fermentation [16–19]; (4) thermal, via Maillard and Strecker reactions during distillation; and (5) photochemistry, in the case of white wines [20,21].

The determination of these compounds in wines and spirits is difficult because of their volatility and their very low olfactory perception levels, which require the use of highly sensitive detectors. Among the different analytical techniques, gas chromatographic separation coupled with sulfur-specific detection, namely flame photometric detection (FPD), is the most widely used [22,23]. The detection principle is based on

* Corresponding author.

0021-9673/95/$09.50 
*SSDI* 0021-9673(95)00218-9

the burning of sulfur products to place the sulfur atom in an excited state ($S_2$), which emits light that can be detected at 393 nm with a photomultiplier (PMT) [24].

More recently, a new type detector has been developed. This chemiluminescence detector (SCD type) works through the burning of sulfur products to yield sulfur monoxide (SO). A highly pure ceramic is subsequently used to collect 90% of the related combustion products, which are then channelled under vacuum towards the chemiluminescence detector [25,26]. In the reaction cell, SO reacts with ozone to yield a sulfur oxide molecule in the excited state. This latter compound emits light while returning to its ground state, and this light signal can be detected with a PMT (Fig. 1).

This type of detection is more sensitive than FPD, because sulfur monoxide is the main combustion product [24]. Moreover, in contrast to FPD, it overcomes quenching phenomena due to the presence of carbon dioxide, water or hydrocarbons [24,27–29], and yields a linear response with increasing sulfur product concentration.

Two types of SCD exist: the SCD 350 and the SCD 355. The SCD 350 is coupled to a flame ionization detection (FID) instrument. The sulfur monoxide and other combustion products are formed in the FID flame [30]. It has the advantage of double detection (FID and SCD), while displaying a reduced sensitivity because of the positioning of the salvage probe and its relative lack of stability with time. The flameless SCD 355 is more sensitive. In fact, the probe is directly linked after the column to a combustion chamber and a regulator to control gas flows (hydrogen and air), the temperature and the pressure [31,32].

In this work, we further evaluated the capacity of the SCD 355 and improved the analytical conditions using the static headspace technique. In that respect, several parameters were studied: the temperature, the ratio between the sample gas- and liquid-phase volumes, the liquid salt concentration (sodium chloride, ammonium sulfate and sodium sulfate) and the ethanol content.

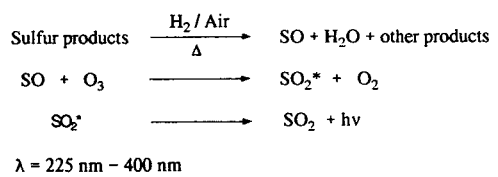


Fig. 1. Principle of chemiluminescence detection

## 2. Experimental

### 2.1. Quantitative analysis of sulfur products

All chromatograms were obtained using a Shimadzu GC 17 A gas chromatograph coupled to an SCD 355 chemiluminescence detector (Sievers). The detector signals were sent to a Kontron 450 MT2 data processing unit. Chromatographic separations were effected on a 30 m × 0.32 mm I.D. polydimethylpolysiloxane (4 μm film thickness) capillary column (SPB-1-Sulfur from Supelco).

The GC temperature programme was set as follows: 1 min at 35°C followed by a 10°C/min gradient to 55°C and then a 25°C/min gradient to 250°C. The injection temperature was 115°C.

In order to speed up the analytical separation and to enhance the sensitivity, pressure variations were used: 1 min at 82 kPa followed by a 30 kPa/min increase to 320 kPa. This shortened each analysis by 8 min and improved the peak detection and integration by yielding a better signal-to-noise ratio.

All gases used were highly pure (analytical-reagent grade). The hydrogen and air inputs into the burner were set at 100 and 40 ml/min, respectively. The oxygen pressure in the ozone generator was maintained at 48 kPa (7 p.s.i.g.).

Glass vials of 250 ml were used to generate the headspace. They were all tightly capped with silicone-rubber septa (sleeve stoppers).

Samples were obtained with a Hamilton 5-ml gas-tight Teflon Luer-Lock (1005 LTN). A 2-ml volume of the headspace volume was taken into the syringe before being adjusted to 1 ml 2 min later, and injected in the GC system with a splitting ratio of 1:5.

Ethyl methyl sulfide (EMS) was used as an internal standard. Calibration graphs were ob-

tained by plotting peak surface-area ratios, $A$ (S-Pdts)/$A$ (EMS), versus concentration ratios, [S-Pdts]/[EMS]. EMS was elected as an internal standard for several reasons: it does not exist in the solutions to be tested, it does not react with the other compounds studied and it displays physico-chemical properties similar to those of the sulfur products under scrutiny.

### 2.2. Reagents and chemicals

Ethanol was of Normapur analytical-reagent grade, L-(+)-tartaric acid (TH2) and sodium sulfate were purchased from Prolabo, highly pure potassium hydrogentartrate (THK) from Merck, gaseous methanethiol (MeSH), diethyl sulfide (DES), ethanethiol (EtSH), thiophene, dimethyl disulfide (DMDS) and diethyl disulfide (DEDS) from Aldrich and dimethyl sulfide (DMS), ethyl methyl sulfide (EMS), carbon disulfide ($CS_2$), ammonium sulfate and sodium chloride from Fluka (all at least 97% pure). Sodium sulfide (Merck) was dissolved in aqueous solution buffered at pH 3.2 (TH2–THK) in order to generate hydrogen sulfide. Distilled, deionized water (resistivity 18.2 MΩ/cm) was used throughout. All brandies used were a generous gift from the Bureau National Interprofessionnel de Cognac (BNIC).

### 2.3. Solution preparation

Stock standard solutions of sulfur compounds (10–20 g/l) were prepared in ethanol to reduce losses by volatilization, and subsequently stored at 0°C until used. They were then diluted with cold ethanol or cold brandies in a cold room at 4°C to yield intermediate standard solutions at $4 \cdot 10^{-2}$ g/l that were kept at 0°C in closed test-tubes until used to prepare the final working standard solutions (concentrations and compositions are described in the figure legends). All standard solutions were stored in vials with headspace volumes as small as possible.

Water–alcohol (20:80) solutions were prepared by first dissolving 3 g/l of tartaric acid and 3 g/l of potassium hydrogentartrate (pH adjusted to 3.2) in water and by mixing in the desired volume of ethanol (medium 1). Medium 2 was obtained by diluting 70% brandy solutions to 20% ethanol and by adjusting the solution pH from 4.5 to 3.2. A given volume ($V_L$ in Eq. 1) of these solutions was placed in 250-ml vials that were kept overnight at 4°C before addition of standard sulfur product (at 4°C).

$$V_L = V_1 + V_s \quad (1)$$

where $V_L$ = total volume of the liquid phase, $V_1$ = volume of the water–alcohol solution or other medium and $V_s$ = total volume of the introduced sulfur products.

All vials were hermetically capped with silicone-rubber septa (sleeve stoppers) and stored away from light in a thermostat-regulated water-bath before injection. The conditions used for the study of the various factors affecting the partition coefficient at a 50 μg/l concentration were a sample equilibrium temperature of 25°C with a partitioning equilibrium time of 72 h before injection.

## 3. Results and discussion

The performance of the detection of various substances with the headspace technique is generally higher in the dynamic than in the static mode [33]. However, the results obtained by the latter method are more realistically closer to the taster viewpoint, and the method is easier to set up. We therefore tried to improve the detection of volatile sulfur products obtained by the static headspace method. An SPB1-Sulfur column was used for the determination of volatile sulfur compounds at low concentration in the headspace [34].

### 3.1. Role of the water–alcohol medium for the partitioning of volatile compounds into the gas phase

Brandies are complex solutions and several substances in addition to water and ethanol can hinder the transfer of volatile sulfur products to the gas phase. We therefore followed the partitioning of nine sulfur compounds (among the most commonly found in brandies) from two

liquid phases: a pure synthetic water–alcohol solution and a commercial brandy solution (Figs. 2 and 3). Both of these solutions had similar pH (3.2) and ethanol content (20%).

It appears that, from brandy solutions only, the thiols ($H_2S$, EtSH, MeSH) cannot be detected in the gas phase even at concentrations up to 100 $\mu$g/l, whereas they can easily (at 10 $\mu$g/l in the liquid phase) be detected if the liquid phase is a synthetic water–alcohol solution. Certain substances such as carbonylated compounds and heavy metals must exist in brandies that can interact with the thiols to lock them in the liquid phase.

### *3.2. Reliability of the detection and preparation method*

The results in Table 1 show the reliability of the experimental protocol used for the study of sulfur compounds in medium 1. In fact, the performances are similar for any sulfur compounds, except for thiols, which cannot be detected in medium 2. The repeatability and reproducibility of the method were determined at concentrations of 10, 20, 50 and 100 $\mu$g/l. This concentration range was used because it covers the olfactory perception limit of most compounds in alcoholic beverages (0.02–100 $\mu$g/l). After establishing the reliability of the method at 10 $\mu$g/l, it was then necessary to determine the linearity of the detection response at concentrations up to 100 $\mu$g/l.

Calibration graphs were calculated for $H_2S$, $CH_3SH$, $C_2H_5SH$, DMS, $CS_2$, DES, thiophene, DMDS and DEDS in both media 1 and 2. All nine standards yielded a linear response in the concentration range 10–100 $\mu$g/l with an average correlation coefficient of 0.998. Typical calibration graphs for a thiol (EtSH), a sulfide (DES) and a disulfide (DEDS) are shown in Figs. 4–6.

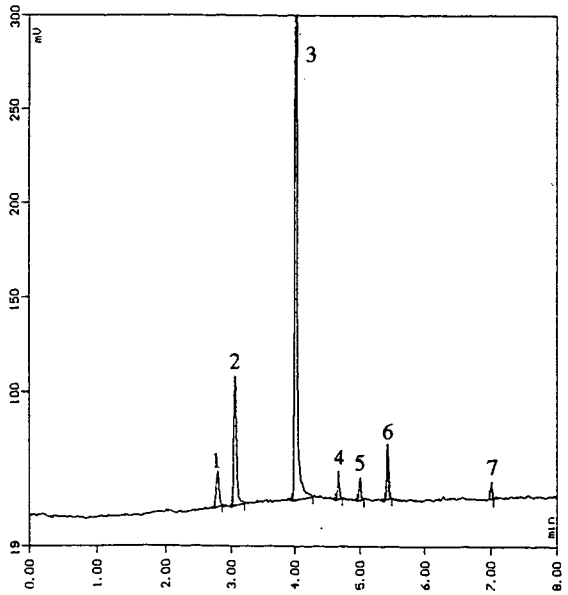


Fig. 3. Chromatograms of volatile sulfur compounds from medium 2. The initial concentration of each compound in the liquid phase was 10 $\mu$g/l, except for the EMS (internal standard), which was at 100 $\mu$g/l. Peaks: 1 = DMS; 2 = $CS_2$; 3 = EMS; 4 = DES; 5 = thiophene; 6 = DMDS; 7 = DEDS.

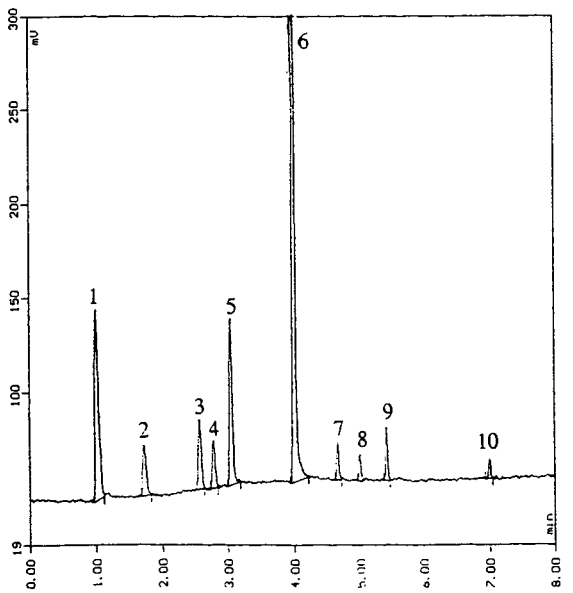


Fig. 2. Chromatograms of volatile sulfur compounds from medium 1. The initial concentration of each compound in the liquid phase was 10 $\mu$g/l, except for EMS (internal standard), which was at 100 $\mu$g/l. Peaks: 1 = $H_2S$; 2 = MeSH; 3 = EtSH; 4 = DMS; 5 = $CS_2$; 6 = EMS; 7 = DES; 8 = thiophene; 9 = DMDS; 10 = DEDS.

Table 1
Determination of repeatability and reproducibility

| Sulfur compound | Retention time (min) | *A* S-Pdts/*A* EMS[a] | | Repeatability[b,c] | | Reproducibility[b,d] | |
|---|---|---|---|---|---|---|---|
| | | Medium 1 | Medium 2 | R.S.D.$_1$ (%) | R.S.D.$_2$ (%) | R.S.D.$_1$ (%) | R.S.D.$_2$ (%) |
| $H_2S$ | 1.00 | 0.362 | ND[e] | 1.20 | – | 1.27 | – |
| MeSH | 1.72 | 0.094 | ND | 1.71 | – | 4.31 | – |
| EtSH | 2.57 | 0.119 | ND | 1.94 | – | 1.54 | – |
| DMS | 2.78 | 0.081 | 0.077 | 1.34 | 1.32 | 1.48 | 1.64 |
| $CS_2$ | 3.06 | 0.320 | 0.300 | 2.71 | 1.70 | 4.51 | 2.32 |
| DES | 4.66 | 0.043 | 0.039 | 1.56 | 2.08 | 3.26 | 2.60 |
| Thiophene | 5.00 | 0.033 | 0.032 | 4.52 | 2.50 | 3.06 | 2.12 |
| DMDS | 5.43 | 0.06 | 0.069 | 3.67 | 2.32 | 4.02 | 2.32 |
| DEDS | 7.00 | 0.021 | 0.020 | 2.94 | 2.75 | 3.53 | 3.25 |

[a] Mean of three values.
[b] R.S.D. = relative standard deviation obtained with medium 1 and R.S.D.$_2$ = that obtained with medium 2.
[c] The repeatability was obtained from three independent injections of the same sample.
[d] The reproducibility was obtained using three independently prepared samples.
[e] ND = not detected.

### 3.3. *Influence of various physico-chemical factors on the partitioning of volatile sulfur products between a gas and a liquid phase*

The liquid-to-gas volume ratio, $V_l/V_g$, has an influence on the detection of sulfur products. The results obtained are shown in Fig. 7 for a thiol, a sulfide and a disulfide, all with an ethyl group. The highest sensitivity is obtained for a $V_l/V_g$ ratio of 4. This value was adopted for the study of the other parameters.

Similar results were obtained with methyl-containing substances, hydrogen sulfide, carbon disulfide and thiophene. A closer look at the data, however, reveals that the value of the $V_l/V_g$ ratio has a greater influence on sulfur products having a lower partition coefficient. A similar observation was made by Penton [35].

As described in the literature [36], the partition coefficient varies with temperature according to the Van't Hoff law [$\log K_i = f(1/T)$]. We

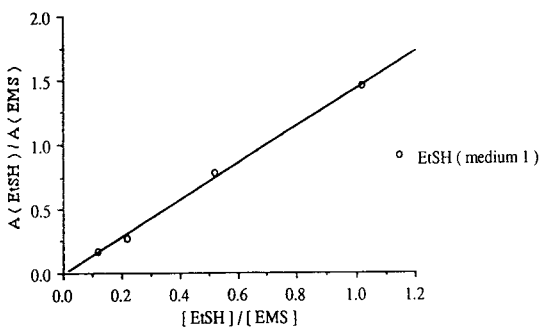


Fig. 4. Calibration graph for ethanethiol from medium 1. Each point represents the average value of three independent measurements. $y_1 = -3.3986 \cdot 10^{-2} + 1.4519x$; $r^2 = 0.997$.

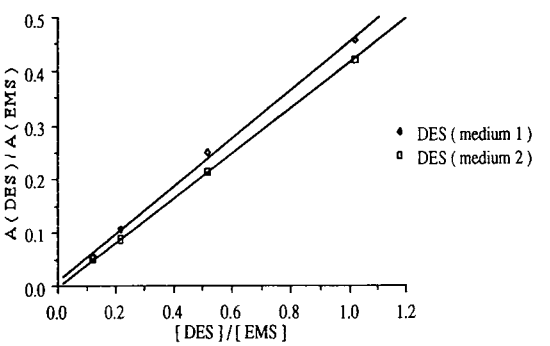


Fig. 5. Calibration graph for diethyl sulfide from media 1 and 2. Each point represents the average value of three independent measurements. $y_1 = 5.918 \cdot 10^{-3} + 1.4519x$; $r^2 = 0.998$. $y_2 = -5.0116 \cdot 10^{-3} + 0.41416x$; $r^2 = 1.000$.

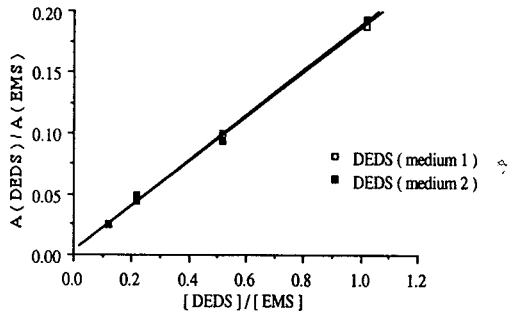


Fig. 6. Calibration graph for diethyl disulfide from media 1 and 2. Each point represents the average value of three independent measurements. $y_1 = 2.7016 \cdot 10^{-3} + 0.18174x$; $r^2 = 1.000$. $y_2 = 2.528 \cdot 10^{-3} + 0.18395x$; $r^2 = 0.997$.

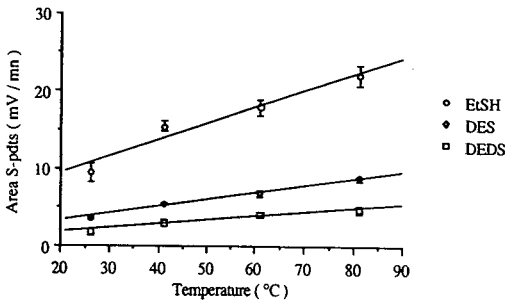


Fig. 8. Dependence on the gas concentration of volatile sulfur compounds from medium 1 on equilibrium temperature. Each point represents the average value of three independent measurements. $y_{EtSH} = 4.5242 + 0.21369x$; $r^2 = 0.951$. $y_{DES} = 0.73470 + 9.2038 \cdot 10^{-2}x$; $r^2 = 0.991$. $y_{DEDS} = -5.4556 \cdot 10^{-2} + 5.3666 \cdot 10^{-2}x$; $r^2 = 0.971$.

therefore followed the temperature-dependent variations in partition coefficient in order to find the optimum analytical conditions in terms of detection. After leaving samples for 72 h at 25°C away from light, they were brought to 40, 60 and 80°C and analysed 2 h later.

The results obtained with ethanethiol, diethyl sulfide and diethyl disulfide on medium 1 and diethyl sulfide and diethyl disulfide on medium 2 are displayed in Figs. 8 and 9, respectively. They show linear increases in detectability with increasing temperature. However, a standard temperature of 25°C was selected for samples analysis because it better reflects the olfactory sensations of the taster. Different sulfur products exhibit different temperature dependences. For example, ethanethiol, which is more hydrophilic and alcoholophilic at 80°C, displays larger temperature-dependent variations than sulfides and disulfides.

Among the many physico-chemical factors that influence the detection of sulfur products, the ionic strength of the liquid phase was studied in order to alleviate the matrix effect encountered in brandies. For this purpose, medium 2 was modified with increasing sodium chloride, sodium sulfate or ammonium sulfate concentration. Surprisingly, Fig. 10 shows that increasing sodium chloride concentrations do not modify the response of thiols and hydrogen sulfide, whereas

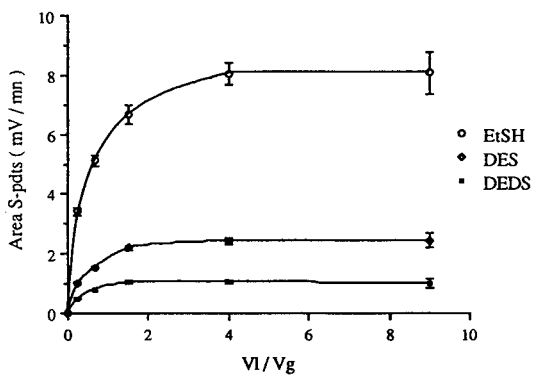


Fig. 7. Influence of the volume ratio $V_l/V_g$ on partitioning of sulfur compounds in the liquid and gas phases. Each point represents the average value of three independent measurements.

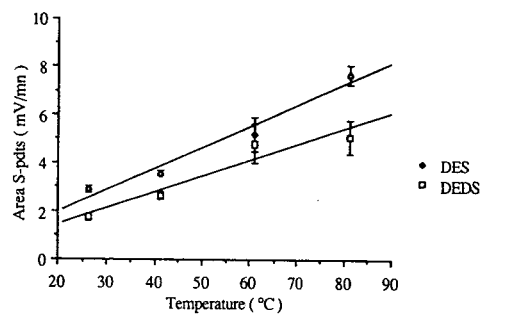


Fig. 9. Dependence on the gas concentration of volatile sulfur compounds from medium 2 on equilibrium temperature. Each point represents the average value of three independent measurements. $y_{DES} = 6.24054 \cdot 10^{-2} + 8.8197 \cdot 10^{-2}x$; $r^2 = 0.967$. $y_{DEDS} = -4.1406 \cdot 10^{-2} + 6.5751 \cdot 10^{-2}x$; $r = 0.921$.

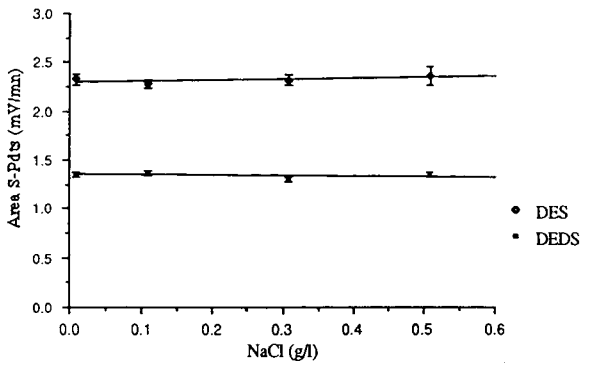


Fig. 10. Effect of increasing amounts of dissolved salts on the liquid–gas partitioning of volatile sulfur compounds from medium 2. Each point represents the average value of three independent measurements.

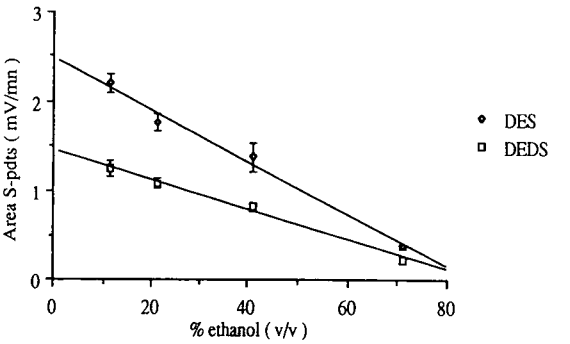


Fig. 12. Effect of increasing amounts of ethanol (v/v) in brandy solution. Each point represents the average value of three independent measurements. $y_{DES} = 2.3809 - 2.9315 \cdot 10^{-2}x$; $r^2 = 0.989$. $y_{DEDS} = 1.3634 - 1.6851 \cdot 10^{-2}x$; $r^2 = 0.990$.

they affect those of the less hydrophilic sulfides and disulfides. Similar results were obtained with other salts such as sodium sulfate and ammonium sulfate.

Przyjazny et al. [36] reported that for sulfur products the partition coefficients increase and hence their gas concentrations decrease with increasing solubility in water at 25°C. Such a result prompted us to evaluate the detectability of the standards used in the headspace according to the ethanol content of the liquid phase in water–alcohol solutions and brandies.

The results in Figs. 11 and 12 clearly show that a constant increase in ethanol content leads to a gradual and linear decrease in the amount of product detected. In order to minimize this "ethanol effect" in brandies, the ethanol content was decreased to 20% by adding distilled, deionized water. This choice was made as a compromise between a lower ethanol effect and a not too large dilution of the samples.

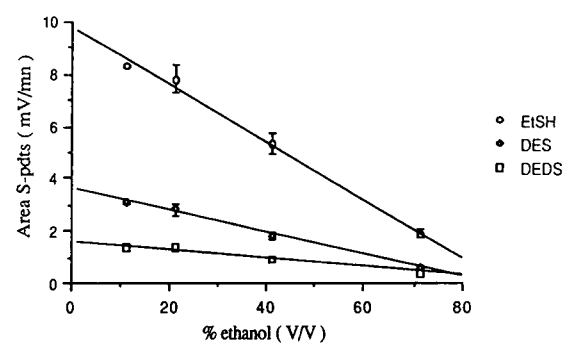


Fig. 11. Effect of increasing amounts of ethanol in water–alcohol solution. Each point represents the average value of three independent measurements. $y_{EtSH} = 9.4250 - 0.11026x$; $r^2 = 0.992$. $y_{DES} = 3.3289 - 4.2778 \cdot 10^{-2}x$; $r^2 = 0.995$. $y_{DEDS} = 1.3283 - 1.67380 \cdot 10^{-2}x$; $r^2 = 0.980$.

## 4. Conclusion

The results presented in this paper illustrate the high performance of the Sievers SCD 355 detector. Its direct connection to the output of the column, without an intermediate FID instrument such as is used with the SCD 350, makes it more stable with time and results in higher reliability in terms of repeatability and reproducibility. Moreover, it exhibits a linear response over a wide concentration range, in contrast to the FPD instrument. We have also demonstrated that the static headspace technique is simple and reliable.

Several new pieces of information have originated from this work: (i) the linearity and repeatability of the SCD 355 detector and the reproducibility of the sample preparation; (ii) the importance of the $V_l/V_g$ ratio, which yields optimum detection at a value of 4; (iii) the role of the ethanol content; (iv) the addition of salt has no effect on the release of thiols from the

liquid phase; and (v) even though increasing temperatures enhance the response much more than a change in the above parameters, we decided to work at 25°C in order to prevent undesirable reactions between sulfur products or with the electrophilic substances present in complex solutions (wines, brandies, etc.) and to reflect better the olfactory impression obtained during tasting. This choice of temperature will not be a limitation if the chromatographic unit is equipped with a pressure gradient system, which greatly shortens the retention times while lowering the detection limit.

## Acknowledgements

This work was supported by the Ministère de l'Agriculture, R. Cantagrel and J.P. Vidal of BNIC (Bureau National Interprofessionnel de Cognac). L. Legendre is thanked for his helping in the translation of the manuscript.

## References

[1] R. Eschenbruch, S.J. De Mora, S.J. Knowles, W.K. Leonard, T. Forrester and D.J. Spedding, Vitis, 25 (1986) 53–57.
[2] D.J. Spedding, R. Eschenbruch and P.J. McGregor, Food Technol. Aust. 35 (1983) 22–23.
[3] A. Rapp, M. Güntert and J. Almy, Am. J. Enol. Vitic, 36 (1985) 219–221.
[4] O. Leppänen, J. Denslow and P. Ronkainen, J. Inst. Brew, 85 (1979) 350–353.
[5] M.S. Burmeister, C.J. Drummond, E.A. Pfisterer and D.W. Hysert, J. Am. Soc. Brew. Chem., 50 (1992) 54–58.
[6] M.D. Walker, J. Inst. Brew, 98 (1992) 283–287.
[7] K. McNamara, Élaboration and Connaissance des Spiritueux, Lavoisier Tec&Doc, 1993, pp. 1–12.
[8] M. Masuda and K.I.C. Nishimura, J. Food. Sci., 47 (1981) 101–105.
[9] M.C. Meilgaard, MBAA Tech. Q., 12 (1975) 151–168.
[10] C.S. du Plessis and G.J. Loubser, Agrochem. Phys., 6 (1974) 49–52.
[11] R.F. Simpson, Vitis, 18 (1979) 148–154.
[12] K. Mizushima, K. Takashima, T. Takashima and A. Totsuka, J. Brew. Soc. Jpn., 85 (1990) 120–126.
[13] P. Darriand, D. Dubourdieu, Thesis, Université de Bordeaux II, Bordeaux, 1993.
[14] A. Maujean, M. Nedjma, J.P. Vidal, R. Cantagrel and L. Lurton, Élaboration et Connaissance des Spiritueux, Lavoisier Tec&Doc, 1993, pp. 110–122.
[15] D. Rauhut, in Comptes Rendus, 4-ème Symposium International d'Oenologie, Bordeaux, 15–17 Juin 1989, Dunod, Paris, 1989, pp. 482–487.
[16] S.J. de Mora, R. Eschenbruch, S.J. Knowles and D.J. Spedding, Food Microbiol., 3 (1986) 27–32.
[17] P.R. Monk, Wine Ind. J., (1986) 10–17.
[18] C.S. Thomas, R.B. Boulton, M.W. Silacci and W.D. Gubler, Am. J. Enol. Vitic., 44 (1993) 211–214.
[19] G.W.A. Fowles, J. Wine Res., 5 (1994) 103–112.
[20] A. Maujean and N. Seguin, Sci. Aliment., 3 (1983) 589–601.
[21] A. Maujean and N. Seguin, Sci. Aliment., 3 (1983) 603–613.
[22] S.S. Brody and J.E. Chaney, J. Gas Chromatogr., (1966) 42–45.
[23] S.O. Farwell and C.J. Baringa, J. Chromatogr. Sci., 24 (1986) 483–494.
[24] R.L. Benner and D.H. Stedman, Anal. Chem., 61 (1989) 121–122.
[25] R.S. Hutte, R.E. Sievers and J.W. Birks, J. Chromatogr. Sci., 24 (1986) 499–505.
[26] J.R. Burdge and S.O. Farwell, J. High Resolut. Chromatogr., 17 (1994) 22–24.
[27] S.S. Lee and K.J. Siebert, J. Am. Soc. Brew. Chem., 44 (1986) 57–66.
[28] F. Magnani and F. Bruner, Anal. Chem., 55 (1983) 2193–2194.
[29] K.K. Gaines, W.H. Chatham and S.O. Farwell, J. High Resolut. Chromatogr., 13 (1990) 489–493.
[30] R.L. Shearer, D.L. O'Neal, R. Rios and M.D. Baker, J. Chromatogr. Sci., 28 (1990) 24–28.
[31] R.L. Shearer and E.B. Poole, J. Chromatogr. Sci., 31 (1993) 82–87.
[32] R.L. Shearer, Int. Chromatogr. Lab., 19 (1994) 4–8.
[33] W.M. Coleman and B.M. Lawrence, J. Chromatogr. Sci., 30 (1992) 396–98.
[34] R.S. Hutte, N.G. Johansen and M.F. Legier, J. High Resolut. Chromatogr., 13 (1990) 421–426.
[35] Z. Penton, J. High Resolut. Chromatogr., 15 (1992) 834–836.
[36] A. Przyjazny, W. Janicki, W. Chrzanowski and R. Staszewski, J. Chromatogr., 280 (1983) 249–260.

ELSEVIER

Journal of Chromatography A, 704 (1995) 503–512

JOURNAL OF CHROMATOGRAPHY A

# Capillary zone electrophoresis of aldose enantiomers: separation after derivatization with *S*-(−)-1-phenylethylamine ☆

Christian R. Noe*, Jerome Freissmuth

*Institute of Pharmaceutical Chemistry, Christian Doppler Laboratory for Chemistry of Chiral Compounds, Johann Wolfgang Goethe University, Marie-Curie-Str. 9, D-60439 Frankfurt, Germany*

First received 12 October 1994; revised manuscript received 28 December 1994; accepted 20 February 1995

**Abstract**

A method for the analysis of monosaccharide enantiomers of the aldose-type is described. Aminoalditols resulting from derivatization with *S*-(−)-1-phenylethylamine were subjected to capillary electrophoresis in a borate buffer. Standard on-column UV detection at 200 nm was applied. Studies of the dependence of separation selectivity and electrophoretic mobility on temperature, electrolyte composition and pH were carried out. Single-run resolution of all 16 derivatized aldohexoses and 3 out of 4 aldotetroses was achieved at pH 10.3 in a 50 m*M* borate buffer using acetonitrile as organic modifier.

## 1. Introduction

Although the biological pathways of sugar formation are well established, there is an alternative approach to sugar total synthesis, which recently has been investigated and discussed as a potential way for prebiotic sugar formation [2–5]. This alternative pathway encompasses the aldolization of glycol aldehyde, the first step of which opens a way to all four aldotetroses and the second step to all 16 aldohexoses. Studies on asymmetric induction in this reaction require–beyond analysis of the diastereomer distribution–consideration of the sugar enantiomer distribution. Development of an efficient analytical procedure, which allows fast and reliable identification of all 20 products together with detection of by-products, is a major prerequisite for successful work on this topic. Before developing the capillary electrophoretic method described in this paper analyses were performed using an HPLC method, which included several derivatization steps and was by far more time-consuming [4,5].

It is known that a certain number of naturally occurring L-sugars exist, e.g. L-(−)-galactose in agar or L-(−)-glucose in the leaves of jute. However, the data available suggest that systematic studies on sugar enantiomer distribution in nature are still far from being comprehensive. Therefore we believe that an efficient analytical technique for the separation of sugar enantiomers is of considerable importance in biological and chemical research.

Separation of neutral carbohydrates by electrophoresis is generally not feasible. In addition, sugars exhibit very low UV absorbance, because

* Corresponding author.

☆ Parts of the results were presented as a poster at the 2nd European Congress of Pharmaceutical Sciences, Berlin, Germany, Sep. 28–Oct. 1, 1994 [1].

0021-9673/95/$09.50 
*SSDI* 0021-9673(95)00237-5

in solution, due to their tendency to form pyranose or furanose rings, only an extremely small percentage exists in the open-chain form with its easily detectable carbonyl group. Thus sugars are not ideal analytes for capillary zone electrophoresis. Even so, in recent years an increasing number of separation methods using this technique has been reported. One basis for this development has been the well-known fact that sugar molecules form negatively charged complexes with tetrahydroxyborate and that the stability and electrophoretic mobility of these complexes strongly depend on the configuration of the sugar hydroxy groups [6–8]. Using this approach Hofstetter-Kuhn et al. [9] showed that even underivatized sugars can be separated by capillary zone electrophoresis at elevated temperatures.

The low UV absorbance of underivatized sugars has been effectively overcome by the use of various derivatization reagents [10], the most common method being the reductive amination of the carbonyl group with an aromatic amine, such as 2-aminopyridine, *p*-aminobenzoic acid, ethyl-*p*-aminobenzoic acid or *p*-aminobenzonitrile [11,12]. When a chiral amine such as *S*-(−)-1-phenylethylamine is used for derivatization, sugar enantiomers are transformed into diastereomers and separation in an achiral environment may be achieved. This approach was first introduced for liquid chromatography and gas chromatography by Oshima et al. [13,14]. It has been successfully applied in the HPLC separation of various aldoses and–depending on the amine–ketoses of mono- and oligosaccharides. In gas chromatography further derivatization of the remaining hydroxy groups is unavoidable to render the analytes volatile and thus compatible with the technique.

Recently, Vorndran et al. [15] described a separation technique for sugars by capillary zone electrophoresis using a different approach based on indirect UV detection. The separation of several sugars and sugar acids was achieved by use of an UV-active buffer–in this case sorbic acid–as background electrolyte.

All these capillary electrophoretic methods do not take into account resolution of sugar enantiomers. Only recently a separation of sugar enantiomers using capillary electrophoresis has been reported [16]. Several monosaccharides were derivatized by reductive amination with 2-aminopyridine, 5-aminonaphthalene-2-sulfonic acid or 4-amino-5-hydroxynaphthalene-2,7-disulfonic acid. Enantiomer discrimination was achieved by addition of various chiral additives to the electrolyte solution. Laser-induced fluorescence was used as detection method.

Here, we present a method which for the first time allows separation of all sixteen D- and L-aldohexoses in a single run using capillary zone electrophoresis (CZE). Discrimination of sugar enantiomers was achieved by reductive amination with enantiomerically pure (*S*)-(−)-1-phenylethylamine [13]. A standard on-column UV detector was used for detection at 200 nm. To optimize and validate the method extensive studies were carried out on the dependence of the electrophoretic mobility on various factors, such as temperature, electrolyte concentration, pH and others.

## 2. Experimental

### 2.1. Chemicals

Chemicals used for the preparation of the various buffers were of analytical grade. Sodium tetraborate and NaOH were obtained from E. Merck (Darmstadt, Germany). The reagents used for the reductive amination of the various aldohexoses and aldotetroses, *R*-(+)-1-phenylethylamine, *S*-(−)-1-phenylethylamine, *rac*-1-phenylethylamine and sodium cyanoborhydride, were also obtained from E. Merck.

Sugars were used in the best available quality without any further purification. Among the aldohexoses D-(+)-talose, L-(−)-talose, L-(−)-glucose, L-(−)-galactose, L-(−)-allose, D-(+)-mannose, L-(−)-mannose, D-(+)-altrose, D-(−)-gulose and L-(+)-gulose were obtained from Janssen Chimica (Neuss, Germany). L-(−)-Idose and D-(+)-idose were obtained from Sigma (Deisenhofen, Germany). D-(+)-Glucose and D-(+)-galactose were obtained from E.

Merck. D-(+)-Allose was obtained from Aldrich-Chemie (Steinheim, Germany). The aldotetrose D-(−)-erythrose was obtained from Aldrich-Chemie, and L-(+)-threose was obtained from Sigma.

### 2.2. Equipment

All separations were carried out using a Beckman P/ACE System 2210. The resulting electropherograms were analysed by Gold Software Version 7.12 SSC 2.00. For the photometric detection of the derivatized carbohydrates on-column UV detection was performed at 200 nm.

### 2.3. Electrophoretic conditions

All experiments were carried out with open-tube fused-silica capillaries (Beckman, 338472) of 50 μm I.D. (400 μm O.D.). Capillary lengths were 127, 107 or 77 cm and the UV–Vis detector was situated 7 cm from the cathodic end of the capillary. Temperature control during separation was achieved by liquid cooling (capillary cartridge coolant, Beckman, No. 359976). All samples were introduced into the capillary by pressure (3.45 kPa). Prior to separation the capillary was rinsed for 5 min with 0.1 *M* NaOH and for 10 min with the buffer solution.

### 2.4. Buffers

The buffers were prepared using HPLC-grade water (E. Merck). The pH was adjusted with 10 *M* NaOH or 10 *M* HCl (dissolved in HPLC-grade water). Organic modifiers, such as tetrahydrofuran (THF), methanol or acetonitrile were of HPLC quality (Carl Roth, Karlsruhe, Germany).

### 2.5. Reductive amination of aldohexoses and aldotetroses

A 1 *M* solution of each sugar was prepared in water (HPLC-grade quality) and stored at −20°C. The amines were dissolved in water (1 *M* solutions in HPLC-grade water). The pH of these solutions was adjusted to 6.5 with 10 *M* HCl. A solution of 9 mg of the reducing agent sodiumcyanoborohydride in 30 μl of water was prepared. The derivatization of the various sugars was carried out as follows: 12 μl of amine solution was added to 10 μl of the corresponding sugar solution. This reaction mixture was kept at 90°C for 10 min. The resulting solution of Schiff-base was treated with 4.5 μl sodiumcyanoborohydride solution at 90°C for 1 h to form a stable amine. After addition of 100 μl water the reaction mixture was stored at −20°C. Prior to sample introduction these solutions were further diluted.

## 3. Results and discussions

### 3.1. Derivatization

Derivatization of the analytes with the enantiomerically pure amine could be achieved under the conditions described above. Instead of a reaction temperature of 40°C and a reaction time of 3 h, as described by Oshima et al. [13], a reaction temperature of 90°C was applied in reductive amination with *S*-(−)-1-phenylethylamine. These conditions resulted in complete and efficient derivatization of the aldoses within 1 h. (In a preparative scale experiment D-(+)-glucose was derivatized with *R*-(+)-1-phenylethylamine as described in Section 2.5. and gave the corresponding aminoalditol in quantitative yield.) The time course of derivatization was studied using three selected sugars, namely D-(+)-glucose, L-(−)-glucose and L-(−)-galactose. As indicated in Fig. 1 reaction was completed after 20 min and no further change in peak areas was observed. Epimerization of the sugars during derivatization could be excluded since after derivatization of pure monosaccharides as described above only the peak corresponding to the pure diastereomer was detected in the electropherograms.

Unfortunately L-(−)-altrose and L-(+)-erythrose were not commercially available. Therefore the available enantiomers D-(+)-altrose, D-(−)-erythrose were derivatized with *rac*-1-phenylethylamine, resulting in two diastereomer-

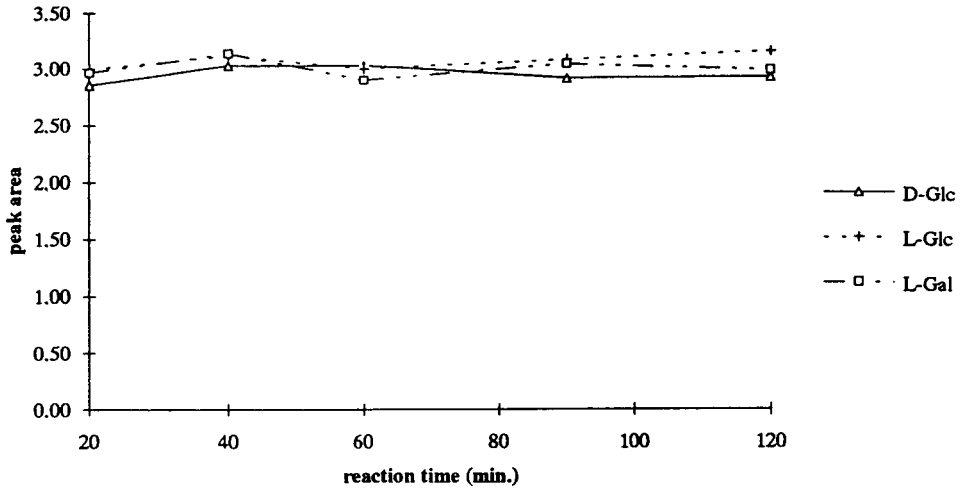


Fig. 1. Dependency of the peak area on the reaction time for the derivatization. Concentrations of the monosaccharides, *S*-(−)-1-phenylethylamine and sodium cyanoborhydride appear in Section 2.5. Reaction temperature, 90°C; capillary: fused-silica, L (total length) = 77 cm, l (lenght to detector) = 70 cm; carrier, 50 m*M* borate buffer; voltage, 30 kV; temperature, 20°C; UV detection, 200 nm; injection, 2.0 s by pressure (3.45 kPa).

ic products for each sugar. One of these products was the expected derivative of the sugar with *S*-(−)-1-phenylethylamine (1a and 2a in Fig. 2). The other diastereomer was the derivative of the sugar with *R*-(+)-1-phenylethylamine. Due to the achiral separation mechanism the diastereomers of D-sugars with *R*-(+)-1-phenylethylamine migrate with the same velocity as their enantiomers, which are the derivatives of the corresponding L-sugars with *S*-(−)-1-phenylethylamine (1b and 2b in Fig. 2). In Fig. 2 the derivatives of the non-available sugars L-(−)-

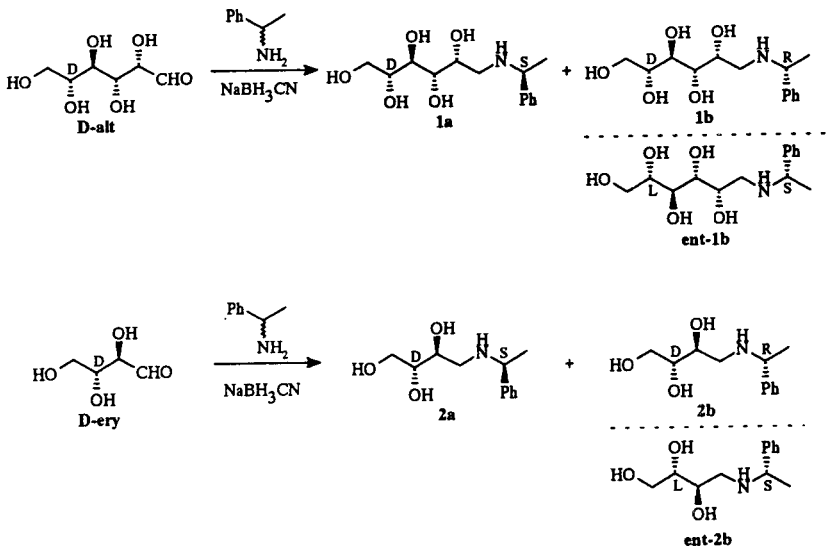


Fig. 2. Structures and derivatization reactions.

altrose and L-(+)-erythrose with *S*-(−)-1-phenylethylamine are specified as ent-1b and ent-2b.

In order to ensure that the derivatization reagent did not react preferably with one of the sugar enantiomers, a mixture of D-(+)- and L-(−)-galactose in a ratio of 1.8:1 was derivatized with *S*-(−)-1-phenylethylamine. Sodium cyanoborohydride was added to the reaction mixture after 2.5, 6, 8, 10 and 15 min, and after 1 h these solutions were diluted with water. The samples were analysed by capillary electrophoresis using the conditions described in Fig. 6. In the resulting electropherograms the ratios between D-(+)- and L-(−)-galactose ranged from 1.78:1 to 1.82:1, which clearly indicates that there is no preferable reaction of *S*-(−)-1-phenylethylamine with one of the sugar enantiomers.

### 3.2. Influence of pH and buffer concentration

First a mixture of 14 aldohexoses [no L-(−)-glucose and L-(−)-altrose] was derivatized with *S*-(−)-1-phenylethylamine as described above. To study the relationship between the pH-value and separation selectivity $\alpha$ ($\alpha = [t_m(D) - t_0]/[t_m(L) - t_0]$) of these sugar derivatives, the pH was increased from 8.3 to 10.8 with the borate concentration of the carrier electrolyte kept constant at 50 m*M*. For selected sugars the separation selectivities $\alpha$ as a function of pH are shown in Fig. 3. For some sugar derivatives increase in pH caused an increase in separation selectivity $\alpha$, while for others a decrease in selectivity was observed. At the same time the electrophoretic mobility of the analytes was increased due to several factors such as enhanced complex formation with the tetrahydroxyborate anion at higher pH values. Configurational differences at carbon atoms C-2 to C-5 determine the stability of the borate complexes of the various carbohydrates. Selectivities, including differences in the dependence of the mobility on pH, strongly depend upon these complex stabilities. With the complex mixture of the 14 aldohexose-derivatives optimum selectivities were achieved at pH 10.3 (Fig. 4). Further increase in pH caused long separation times as well as a decrease in separation selectivity. With the exception of L-(−)-mannose/D-(+)-glucose and, as indicated in Table 1, D-(+)-mannose/L-(−)-glucose all sugar derivatives could be resolved.

The effect of borate concentration of the carrier electrolyte on the separation selectivity $\alpha$

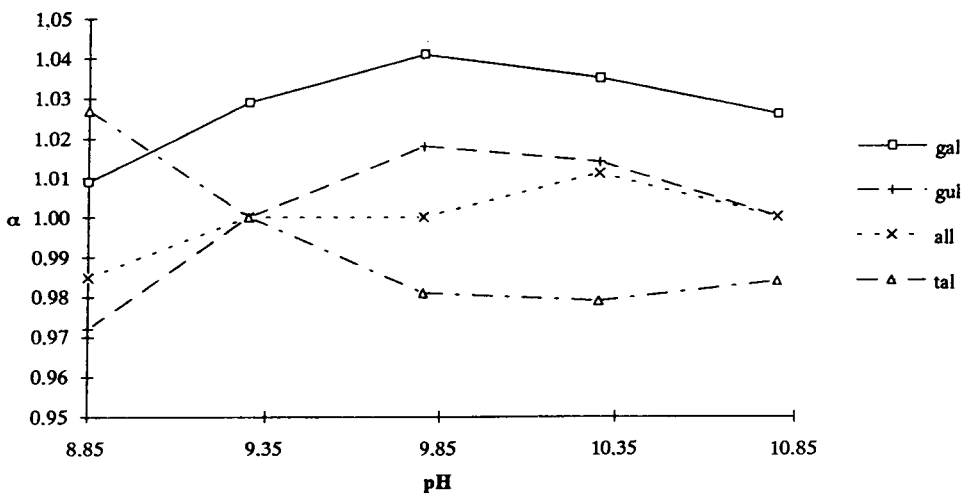


Fig. 3. Dependency of separation selectivity $\alpha$ on pH for selected aminoalditols. Capillary, fused-silica, L = 107 cm, l = 100 cm; carrier, 50-m*M* borate buffer; voltage, 30 kV; temperature, 25°C; UV detection, 200 nm.

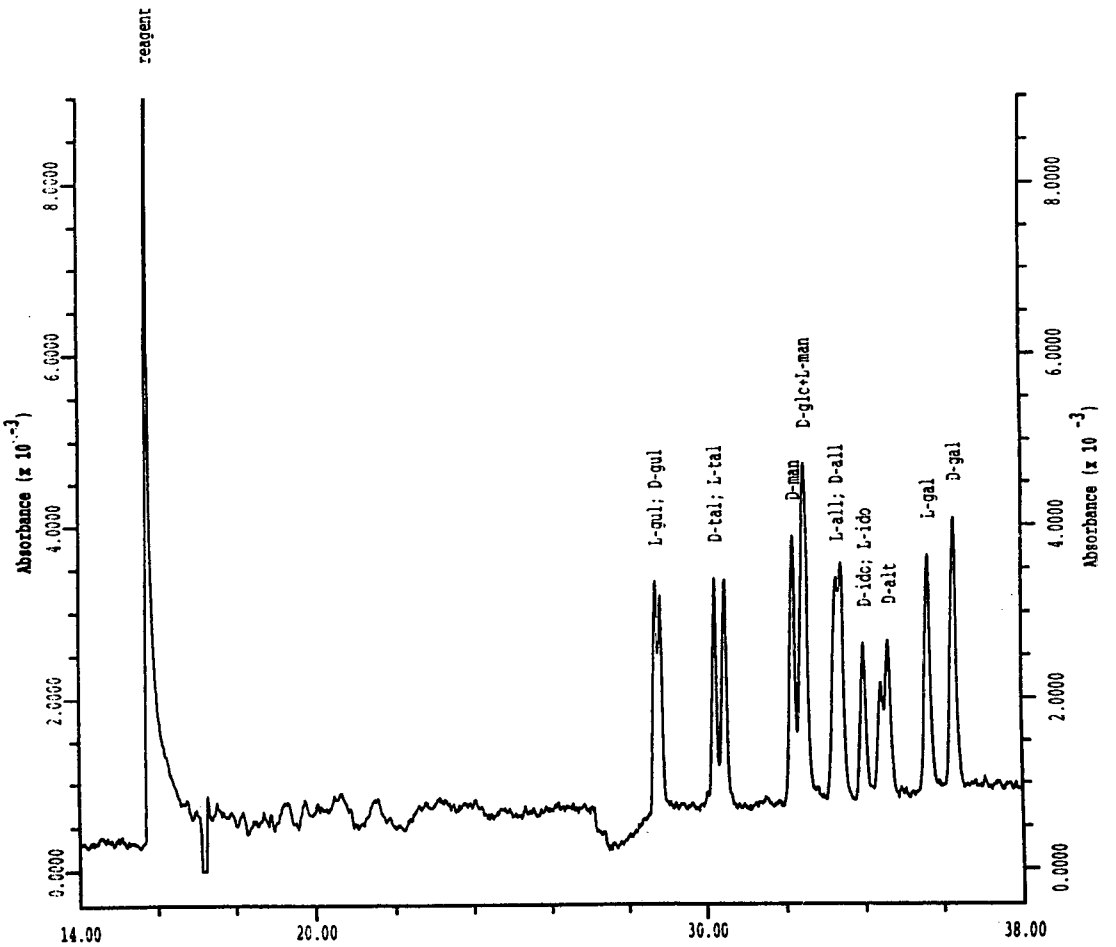


Fig. 4. Separation of a mixture of 14 aldohexoses [no L-(−)-altrose and L-(−)-glucose] derivatized with *S*-(−)-1-phenylethylamine. Capillary, fused-silica, L = 107 cm, l = 100 cm; carrier, 50 m*M* borate, pH 10.3; voltage, 30 kV; temperature, 25°C; UV detection, 200 nm; injection, 3.0 s by pressure (3.45 kPa).

was studied at a constant pH-value of 10.3 and increasing buffer concentrations from 25 m*M* to 100 m*M* (Fig. 5). An increase of borate concentration led to a reduction of the electroosmotic flow and, as a consequence, to very long separation times. Although an increase in separation selectivity could be achieved at higher borate concentration the two diastereomers of D-(+)-glucose and L-(−)-allose could not be separated. At pH 8.8 an increase of buffer concentration up to 200 m*M* improved resolution and decreased time of analysis. However, the results obtained at pH 10.3 using a 50-m*M* borate buffer could not be reached.

### 3.3. Temperature control

Hoffstetter-Kuhn et al. [9] in their electrophoretic separation of underivatized carbohydrate–borate complexes obtained narrow peaks and thus acceptable selectivities at a temperature of 60°C. According to their study formation of borate complexes with underivatized sugars is a complex reaction, because there are six different

Table 1
Migration time of sugar derivatives depending on the concentration of the organic modifier acetonitrile

| Sugar derivative | Migration time (min) | | | | |
|---|---|---|---|---|---|
| | 0% AN | 9% AN | 13% AN | 17% AN | 23% AN |
| L-Gul | 28.7 | 35.2 | 38.5 | 41.3 | 49.0 |
| D-Gul | 28.8 | 35.4 | 38.7 | 41.6 | 49.3 |
| D-Tal | 30.1 | 37.9 | 41.8 | 45.2 | 54.5 |
| L-Tal | 30.5 | 38.3 | 42.3 | 45.8 | 55.2 |
| L-Glc | 32.1 | 41.0 | 45.4 | 49.4 | 60.2 |
| D-Glc | 32.5 | 41.3 | 45.7 | 49.7 | 60.7 |
| D-Man | 32.1 | 41.3 | 45.7 | 50.1 | 61.5 |
| L-Man | 32.5 | 41.7 | 46.3 | 50.5 | 61.9 |
| D-Ido | 34.0 | 43.0 | 47.8 | 52.2 | 63.5 |
| L-Ido | 34.4 | 43.2 | 48.3 | 52.8 | 64.2 |
| L-All | 33.2 | 43.2 | 47.8 | 52.3 | 64.8 |
| D-All | 33.4 | 43.6 | 48.3 | 52.8 | 65.6 |
| D-Alt | 34.6 | 44.9 | 50.3 | 55.3 | 68.9 |
| L-Alt | 35.0 | 45.4 | 50.8 | 56.0 | 69.7 |
| L-Gal | 35.6 | 46.3 | 51.9 | 57.4 | 71.9 |
| D-Gal | 36.3 | 47.2 | 52.9 | 58.5 | 73.5 |

AN = acetonitrile. Capillary: fused-silica, L (total length) = 107 cm, l (length to detector) = 100 cm; carrier, 50 m*M* borate, pH 10.3; voltage, 30 kV; temperature, 25°C; UV detection, 200 nm; injection: 3.0 s by pressure (3.45 kPa).

structures for a sugar molecule dissolved in water: the $\alpha$- and $\beta$-pyranose rings, the $\alpha$- and $\beta$-furanose rings, the open-chain form and the hydrated open-chain form. Since at higher temperature the equilibrium for complexation with the tetrahydroxyborate anion is reached faster,

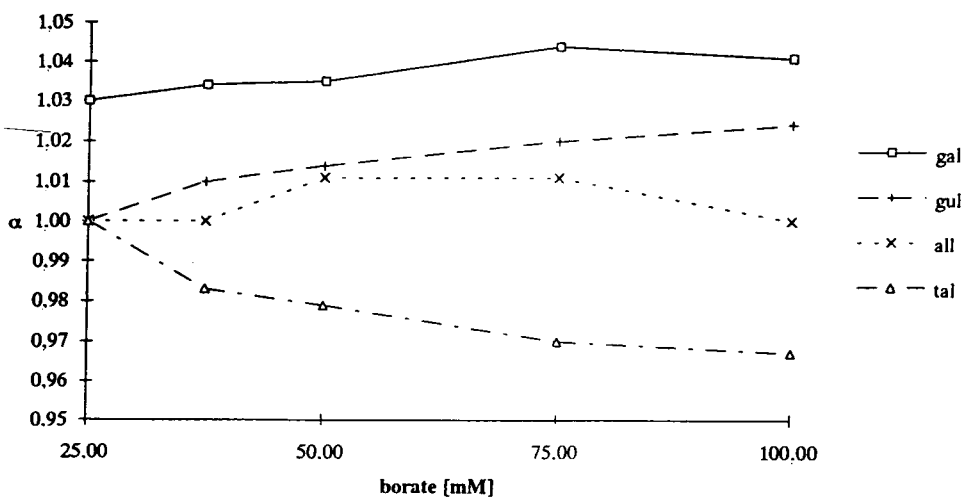


Fig. 5. Dependency of separation selectivity $\alpha$ on borate concentration for selected aminoalditols. Capillary, fused-silica, L = 107 cm, l = 100 cm; carrier, borate, pH 10.3; voltage, 30 kV; temperature, 25°C; UV detection, 200 nm.

narrower peaks are obtained. In addition, an increase in temperature results in higher proportions of the open-chain carbonyl form and due to the decreased viscosity a larger volume is introduced into the capillary. All these effects explain the improvement both in selectivity and in efficiency of the separation.

*

In contrast to the underivatized carbohydrates, our attempts to run the electrophoretic separation at higher temperatures resulted in a dramatic loss of resolution and in broad peaks. P. Jandik and G. Bonn had observed the same effect with carbohydrates derivatized with *p*-aminobenzoic acid [17]. Reductive amination reduces the number of possible solution isomers to the open-chain form and thus the equilibrium for complexation with the tetrahydroxyborate anion is less affected by an increase in temperature. It may be assumed that the observed loss of

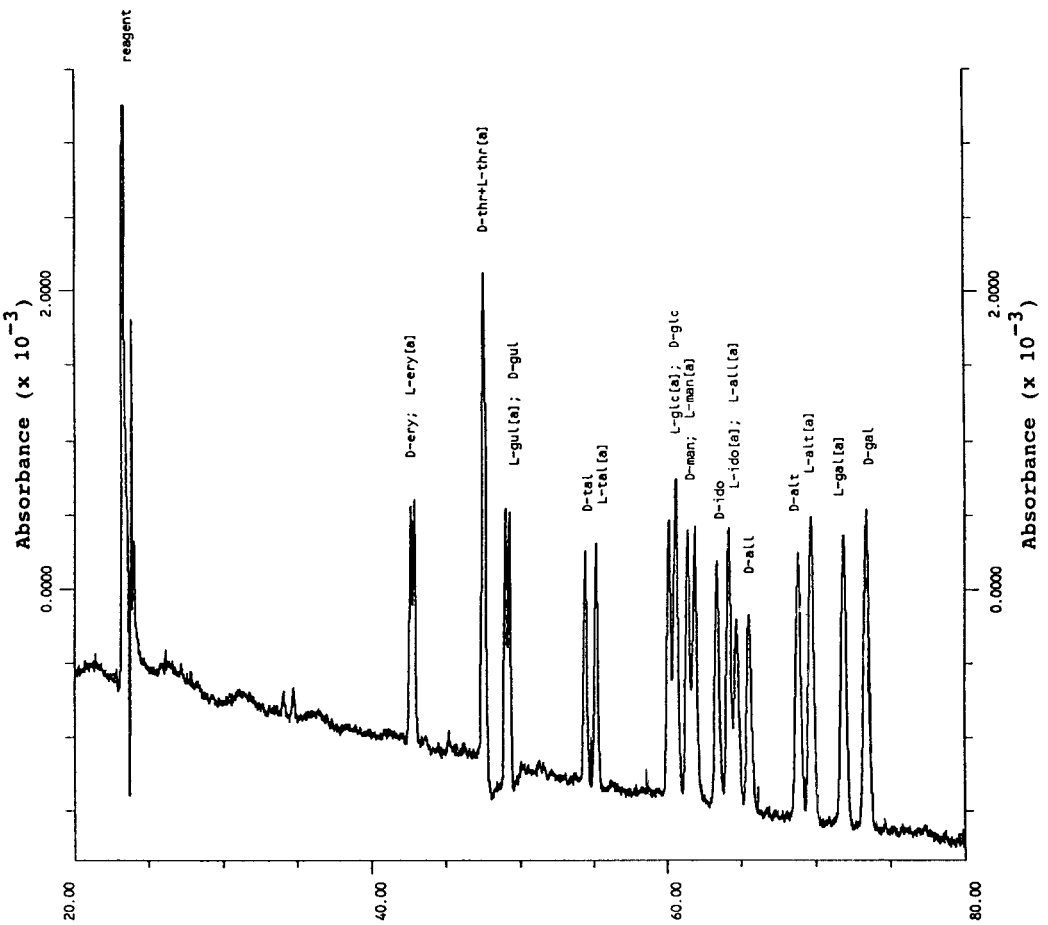


Fig. 6. Separation of a mixture of 8 D-aldohexoses and 2 aldotetroses derivatized with *rac*-1-phenylethylamine. Capillary: fused-silica, L = 107 cm, l = 100 cm; carrier, 50 m*M* borate, pH 10.3 and 23% acetonitrile; voltage, 30 kV; temperature, 25°C; UV detection, 200 nm; injection, 3.0 s by pressure (3.45 kPa). In the electropherogram the signals of derivatives of D-sugars with *R*-(+)-1-phenylethylamine are assigned as L-sugars marked with [a]. They are enantiomers of the derivatives of L-sugars and *S*-(−)-1-phenylethylamine and have the same electrophoretic mobility in the separation system.

resolution for derivatized carbohydrates is caused by larger longitudinal diffusion of the analytes.

### 3.4. Further modifications

To obtain resolution of all 16 aldohexoses further modifications of the buffer were attempted. It is well known that various organic modifiers are capable to reduce the electroosmotic flow to a certain extent. With the common organic additives THF, methanol and acetonitrile the strongest decrease of the electroosmotic flow is effected by acetonitrile, followed by THF and methanol. Methanol was added up to 30% to the buffer solution and THF up to 5%, but both of these solvents did not lead to an increase in resolution. Acetonitrile was added to the electrolyte up to 30%. Best results were obtained by addition of 23% of acetonitrile to the carrier electrolyte. Although electroosmotic flow velocity was strongly reduced resulting in a considerable increase of migration times, this effect was compensated by an improvement in resolution. Table 1 shows migration times of all aldohexose-derivatives with increasing percentage of acetonitrile. The selectivity $\alpha$ for derivatized sugar enantiomers is hardly affected by the addition of the organic modifier. The increasing amount of organic modifier led to a separation of the diastereomeric sugar derivatives of L-(−)-glucose/D-(+)-mannose and D-(+)-glucose/L-(−)-mannose, which in a 50 m*M* borate buffer, pH 10.3 had the same electrophoretic mobilities. An amount of 9% acetonitrile in the electrolyte resulted in a separation of the derivatives L-(−)-glucose and L-(−)-mannose, whereas the derivatives of D-(+)-glucose and D-(+)-mannose under these conditions had the same mobility. With addition of more acetonitrile all four diastereomers could be separated. A similar effect was observed for the sugar derivatives of D-(+)-/L-(−)-idose and D-(+)-/L-(−)-allose. Here an increasing amount of acetonitrile in the electrolyte led to an inversion of the electrophoretic mobility of the sugar derivatives of D-(+)-/L-(−)-allose and D-(+)-/L-(−)-idose. Fig. 6 shows the electropherogram of a standard mixture of 8 D-aldohexoses and 2 aldotetroses derivatized with *rac*-1-phenylethylamine. With the exception of the diastereomers corresponding to D-(−)- and L-(+)-threose all sugar derivatives could be resolved. The reproducibility of migration times in the electrolyte system used for this separation was 0.9% ($n = 6$). Without the organic modifier the reproducibility of migration times is 0.3%.

## 4. Conclusions

The capillary zone electrophoretic method presented in this paper allows easy and efficient analysis of sugar enantiomers after derivatization with *S*-(−)-1-phenylethylamine. In contrast to GC or HPLC methods [13,14] there is no need for further purification or derivatization of the aminoalditols. All 16 aldohexoses could be resolved in a single run. From a mixture of aldohexoses and aldotetroses 19 out of 20 products were separated in one run.

## References

[1] C.R. Noe and J. Freissmuth, Eur. J. Pharm. Sci., 2 (1994) 151.
[2] C.R. Noe, M. Knollmüller and P. Ettmayer, Liebigs Ann. Chem., (1989) 637.
[3] A. Eschenmoser, D. Müller, S. Pitsch, A. Kittaka, E. Wagner and C.E. Wintner, Helv. Chim. Acta, 73 (1990) 1410.
[4] C.R. Noe, M. Knollmüller and P. Ettmayer, Liebigs Ann. Chem., (1991) 417.
[5] C.R. Noe, M. Knollmüller and J. Freissmuth, Liebigs Ann. Chem., (1994) 611.
[6] J. Böseken, Adv. Carbohydr. Chem., 4 (1949) 189.
[7] C.F. Bell, R.D. Beauchamp and E.L. Short, Carbohydr. Res., 185 (1989) 39.
[8] M. van Duin, J.A. Peters, A.P.G. Kieboom and H. van Bekuum, Tetrahedron, 41 (1985) 3411.
[9] S. Hofstetter-Kuhn, A. Paulus, E. Gassmann and H.M. Widmer, Anal. Chem., 63 (1991) 1541.
[10] P.J. Oefner and C. Chiesa, Glycobiology, 4 (1994), 397.
[11] P.J. Oefner, A.E. Vorndran, E. Grill, C. Huber and G.K. Bonn, Chromatographia, 34 (1992) 308.

[12] A.E. Vorndran, E. Grill, C. Huber, P.J. Oefner and G.K. Bonn, Chromatographia, 34 (1992) 109.
[13] R. Oshima, Y. Yamauchi and J. Kumanotani, Carbohydr. Res., 107 (1982) 169.
[14] R. Oshima and J. Kumanotani, J. Chromatogr., 259 (1983) 159.
[15] A.E. Vorndran, P.J. Oefner, H. Scherz and G.K. Bonn, Chromatographia, 33 (1992) 163.
[16] M. Stefansson and M. Novotny, J. Am. Chem. Soc., 115 (1993) 11573.
[17] E. Grill, C. Huber, P. Oefner, A. Vorndran and G. Bonn, Electrophoresis, 14 (1993) 1004.

ELSEVIER

Journal of Chromatography A, 704 (1995) 513–517

JOURNAL OF CHROMATOGRAPHY A

Short communication

# Determination of benzoylurea insecticides in apples by high-performance liquid chromatography

T. Tomšej[a,*], J. Hajšlová[b]

[a]*District Hygienic Centre, Bezručova 10, 360 21 Karlovy Vary, Czech Republic*

[b]*Institute of Chemical Technology, Department of Food Chemistry and Analysis, Technická 5, 166 28 Prague 6, Czech Republic*

First received 25 August 1994; revised manuscript received 7 February 1995; accepted 21 February 1995

**Abstract**

A method for the simultaneous determination of the benzoylurea insecticides diflubenzuron, flufenoxuron, flucycloxuron chlorfluazuron and triflumuron in apples using reversed-phase HPLC is described. The separation of analytes was performed on a Separon SGX $C_8$ column (150 × 3 mm I.D., 5 μm) with methanol–water (55:45, v/v) as the mobile phase. Benzoylurea residues were extracted with acetone and then partitioned into dichloromethane. The final clean-up step was conducted by gel permeation chromatography on Bio- Beads SX-3 using cyclohexane–chloroform (3:2, v/v) as the mobile phase.

## 1. Introduction

Benzoylureas (BU) are promising insecticides, used for the control of insects attacking a wide range of crops, especially fruits and vegetables. These compounds act as powerful growth regulators which inhibit the synthesis of cuticle chitin in target pests, causing death or abortive development [1–3]. BUs are considered to be a fourth generation of insecticides with many attractive properties such as high selectivity, low acute toxicity for mammals and high biological activity, resulting in low application rates [4,5].

There are nine BUs registered [6] in the Czech Republic as active ingredients of pesticide formulations (apples being the main protected crop). Structures and solubility data for the most common BUs are shown in Table 1.

Reversed-phase HPLC with UV detection is predominantly employed for the determination of BUs [7–12] because they are thermally unstable and, consequently, their GC properties are poor [7,13]. The latter technique has occasionally been applied after derivatization of the parent analytes or their hydrolytic products [7,14,15].

Most of the above analytical studies were concerned with the determination of a single BU only. In this paper, a rapid isocratic reversed-phase HPLC method applicable to the simultaneous determination of five extensively used BUs is described. Whereas time-consuming multiple partitioning of extracts followed by adsorption chromatography on Florisil was commonly utilized in previous methods, in this work

* Corresponding author.

0021-9673/95/$09.50 
*SSDI* 0021-9673(95)00258-8

Table 1
Structures and solubility data for the most common BUs

| Common name | Structure | Molecular mass | Solubility in water (mg/l) |
|---|---|---|---|
| Diflubenzuron | 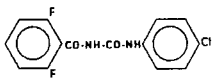 | 310 | 0.1 |
| Triflumuron | 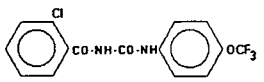 | 358 | <0.001 |
| Flufenoxuron | 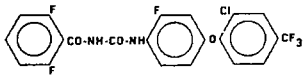 | 488 | 0.001 |
| Chlorfluazuron | 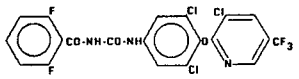 | 540 | <0.01 |
| Flucycloxuron | 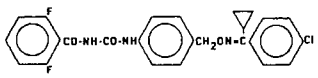 | 483 | <0.001 |

a significant simplification of the clean-up step was achieved by using gel permeation chromatography (GPC).

## 2. Experimental

### 2.1. Materials

All chemicals were of analytical-reagent grade. Methanol, cyclohexane, acetonitrile and chloroform (Lachema, Brno, Czech Republic) were glass distilled prior to the use. Anhydrous sodium sulphate was purified by heating at 600°C for 3 h. Standards of BUs (diflubenzuron, flucycloxuron, flufenoxuron, triflumuron and chlorfluazuron) of purity not less than 99% were provided by Solvay-Duphar, Shell International Petroleum, Bayer and Ciba-Geigy. Stock standard solutions prepared by dissolution in methanol were stable for 2 weeks when held at 4°C.

### 2.2. Equipment

A Hewlett-Packard Model 1090 M liquid chromatograph equipped with an HP Model 1040 M diode-array detector was used. The columns were CGC glass cartridges (150 × 3 mm I.D.) filled with (i) Separon SGX $C_{18}$, (ii) Separon SGX Phenyl and (iii) Separon SGX $C_8$, all 5 $\mu$m (Tessek, Prague, Czech Republic). Separation of BUs was tested on these columns at 40°C using methanol–water and acetonitrile–water mixtures as mobile phases at a flow-rate of 0.5 ml/min. The detection wavelength was set at 260 nm.

Gel permeation chromatography was performed on a 500 × 8 mm I.D. column filled with Bio Beads SX-3, 200–400 mesh (Bio-Rad, Richmond, CA, USA). Mobile phases consisting of cyclohexane–chloroform (1:1, 3:2 and 4:1, v/v) were tested. The flow-rate was 0.6 ml/min and a 2-ml sample loop was used.

### 2.3. Sample preparation

*GPC: determination of the elution profile*

Volumes of 2 ml of standard solutions of BUs or crude apple extract (see below), dissolved in the mobile phase, were loaded on to the column. Fifteen 2-ml fractions of the eluate were collected in order to obtain an elution curve. The amount of apple wax and other co-extracts in each fraction was determined gravimetricaly

after evaporation of solvent. BUs were determined by HPLC after dissolving residue in the mobile phase.

*Isolation of BUs from apples*

A 50-g amount of a representative sample was homogenized in 100 ml of acetone. The homogenate was filtered through glass-wool into a separating funnel. After addition of 10 g of NaCl and 10 ml of distilled water, partitioning with 50 ml of dichloromethane was carried out. The organic layer was separated and dried over anhydrous sodium sulphate. After evaporation to dryness, the residue was dissolved prior to GPC clean-up in the respective mobile phase [cyclohexane–chloroform (3:2, v/v)].

*Isolation of BUs from surface layer of apples*

Approximately 200 g of apples (intact fruit) were washed by immersing them in two 150-ml portions of dichloromethane in an appropriately shaped beaker. The combined extracts were dried over anhydrous sodium sulphate and then evaporated to dryness. After dissolving of residue in cyclohexane–chloroform, an aliquot corresponding to 50 g of apple was cleaned up by GPC.

## 3. Results and discussion

Despite the effort spent on optimization of the HPLC conditions, it was not possible to achieve a satisfactory resolution of all analytes on an HPLC column packed with reversed-phase $C_{18}$: flucycloxuron and flufenoxuron exhibited very similar $k'$ values in tested mobile phases [16]. For this reason, the separation of BUs on several other stationary phases was examined. The best results were achieved on the Separon SGX $C_8$ column. All analytes were resolved under isocratic conditions with methanol–water (55:45, v/v) as the mobile phase. The time of analysis did not exceed 10 min. Detection at 260 nm provided the most sensitive and relatively selective detection of the analytes. Minimum detectable amounts are summarized in Table 2. The values recorded for diflubenzuron and flufenoxuron are comparable to those published by other workers [8,12]; there are no previous data available for the remaining BUs.

"Classical" clean-up based on adsorption chromatography was replaced by GPC in this work. Mobile phases consisting of cyclohexane–chloroform in three different proportions (4:1, 3:2 and 1:1, v/v), i.e., mixtures with different "polarity", were tested in preliminary experiments. An increased content of chloroform in the mobile phase resulted in narrower elution bands of co-extracts (see Fig. 1). No significant differences in the elution patterns of compounds extracted from homogenized (disintegrated) apples and those washed from the surface of the intact fruit were observed. The best resolution of BUs from co-extracts was obtained using the GPC system employing cyclohexane–chloroform (2:3, v/v) as the mobile phase. The main portion (approximately 95%) of co-extracts was eluted in a volume of 6–14 ml and, as can be seen from Fig. 2, elution of BUs occurred afterwards, in the

Table 2
Detection limits of BUs with relative standard deviations

| Compound | Minimum detectable amount (ng) | Method detection limit (mg/kg) | R.S.D. (%)[a] | |
|---|---|---|---|---|
| | | | 0.1 mg/kg level | 1 mg/kg level |
| Diflubenzuron | 5 | 0.01 | 9 | 5 |
| Flufenoxuron | 8 | 0.02 | 9 | 7 |
| Flucycloxuron | 10 | 0.02 | 13 | 10 |
| Chlorfluazuron | 15 | 0.03 | 11 | 9 |
| Triflumuron | 5 | 0.01 | 14 | 9 |

[a] $n = 4$.

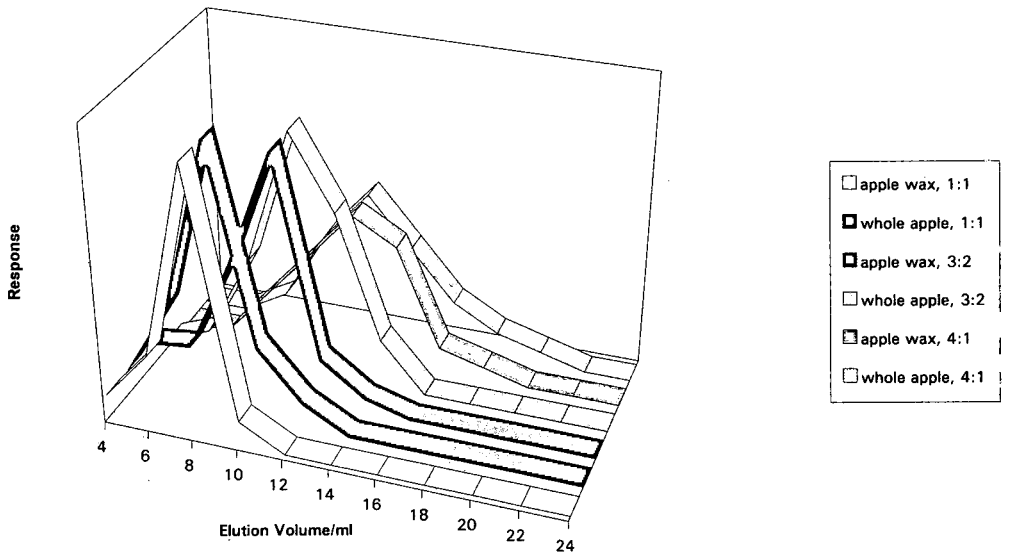


Fig. 1. Elution profiles of co-extracts from (whole) apples and apple wax in three mobile phases with different cyclohexane–chloroform ratios.

range 14–22 ml. A size-exclusion mechanism evidently predominated in the GPC system employed. In accordance with theory, BUs were eluted in order of their molecular mass (Table 1), i.e., in the descending order chlorfluazuron, flufenoxuron, flucycloxuron, trifumuron and diflubenzuron.

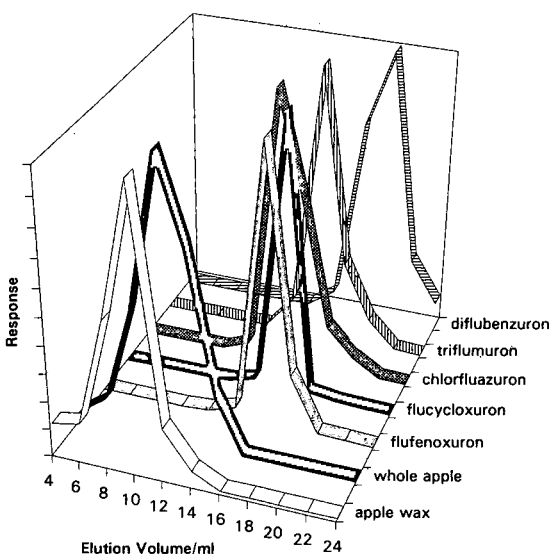


Fig. 2. Elution profiles of BUs and co-extracts from (whole) apples and apple wax. Mobile phase: cyclohexane–chloroform (3:2, v/v).

The efficiency of the applied clean-up procedure for isolated surface wax (which can be assumed to represent the main portion of co-extracts) is well illustrated in Fig. 3, showing chromatograms of apple extracts (blank and spiked) together with a standard mixture. Several additional co-extracts adsorbing at 260 nm appeared in chromatograms corresponding to extracts obtained from homogenized apples (Fig. 3c), but no interference with the peaks of the analytes occurred. The recoveries of diflubenzuron, flufenoxuron, flucycloxuron, chlorfluazuron and triflumuron measured at the 0.1 mg/kg level were 92, 72, 75, 71 and 79%, respectively.

## 4. Conclusions

A reversed-phase ($C_8$-bonded silica) HPLC method employing GPC clean-up (Bio Beads SX-3) can be recommended for the sensitive and

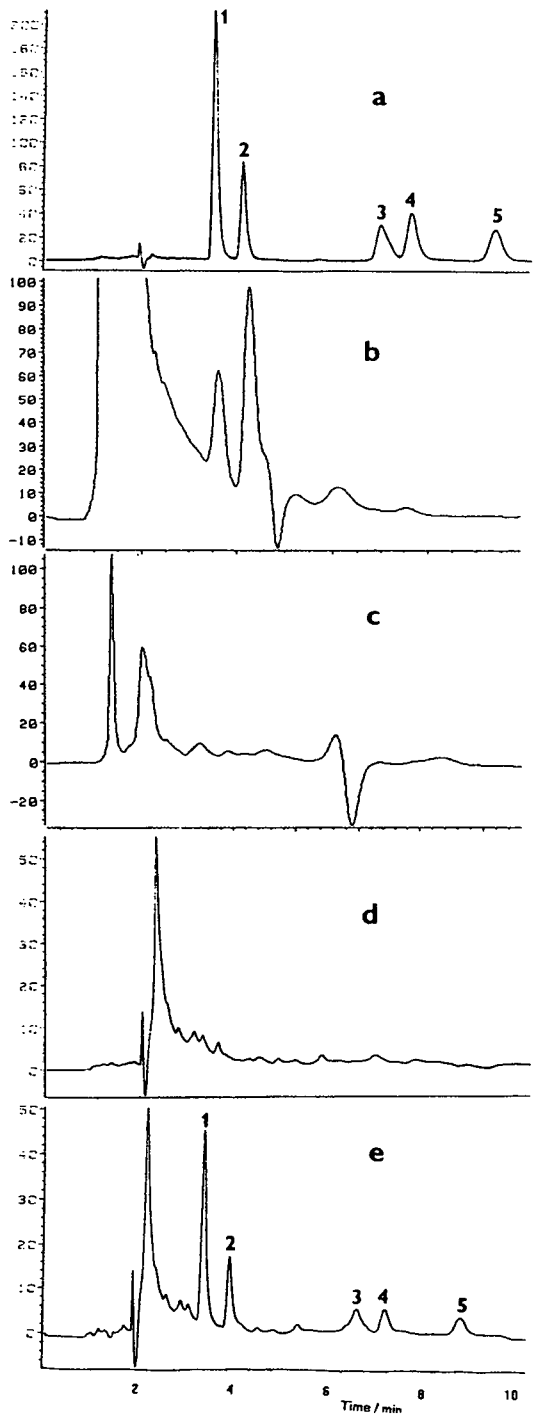


Fig. 3. Chromatograms of (a) standard mixture of BUs (1 diflubenzuron; 2 triflumuron; 3 flufycloxuron; 4 flufenoxuron; 5 chlorfluazuron), (b) crude apple extract, (c) apple extract after clean-up, (d) apple wax after clean-up and (e) apple wax spiked at 0.05 mg/kg with flucycloxuron, flufenoxuron and chlorfluazuron and 0.1 mg/kg with diflubenzuron and triflumuron.

reproducible determination of BU residues in apples. Because of their hydrophobic nature, BU residues are expected to be located predominantly in the surface layers of treated fruit, dissolved in the wax layer, As a result, homogenization of samples and more complicated isolation of residues from homogenates can be avoided by a simpler and more rapid examination (especially for screening purposes) of wax contamination.

## Acknowledgement

This work was carried out within the sponsorship of COST project 66.30 "Pesticides–Soil–Environment".

## References

[1] N.P. Hajjar and J.E. Casida, Science, 200 (1978) 1499.
[2] A.R. Horowitz, M. Klein, S. Yablonski and I. Ishaaya, Crop Protect., 11 (1992) 465.
[3] R. Mussarelli, Chitin in Nature and Technology, Plenum Press, New York, 1986.
[4] R.L. Metcalf, P. Lu and S. Bowlus, J. Agric. Food Chem., 23 (1975) 359.
[5] C.R. Worthing, The Pesticide Manual, British Crop Protection Council, 9th ed., 1990.
[6] List of Approved Agents for Plant Preservation, Czech Ministry of Agriculture, 1994.
[7] C. Corley, R.W. Miller and K.R. Hill, J. Assoc. Off. Anal. Chem., 57 (1974) 1269.
[8] E.R. Bogus, P.A. Gallagher, E.A. Cameron and R.O. Mumma, J. Agric. Food Chem., 33 (1985) 1018.
[9] D.J. Austin and K.J. Hall, J. Pestic. Sci., 12 (1981) 495.
[10] D.J. Austin and K.J. Carter, J. Pestic. Sci., 17 (1986) 73.
[11] W.A. Hopkins and D.R. Lauren, J. Chromatogr., 516 (1990) 442.
[12] K.M.S. Sundram and R. Nott, J. Liq. Chromatogr., 12 (1989) 2333.
[13] S. Smith, G.H. Willis and L.L. McDowell, J. Agric. Food Chem., 31 (1983) 610.
[14] N.H. Nigg, R.D. Canizzaro and J.H. Stamper, Bull. Environ. Contam. Toxicol., 36 (1986) 833.
[15] H.J. Stan and P. Klaffenbach, Fresenius' J. Anal. Chem., 339 (1991) 40.
[16] T. Tomšej, J. Hajšlová, P. Outrata and J. Landesková, Agrochémia, 33 (1993) 255.

ELSEVIER

Journal of Chromatography A, 704 (1995) 518–523

JOURNAL OF CHROMATOGRAPHY A

Short communication

# Determination of eight constituents of Hsiao-cheng-chi-tang by high-performance liquid chromatography

Shuenn-Jyi Sheu*, Chyong-Fang Lu

*Department of Chemistry, National Taiwan Normal University, 88, Sec. 4, Tingchow Road, Taipei, Taiwan*

First received 29 November 1994; revised manuscript received 13 February 1995; accepted 16 February 1995

**Abstract**

A high-performance liquid chromatographic method for the simultaneous determination of eight constituents (gallic acid, sennoside B, sennoside A, naringin, hesperidin, honokiol, magnolol and emodin) of the Chinese herbal formula Hsiao-cheng-chi-tang was established. Various samples of the formula were separated using a Cosmosil $5C_{18}$ column with a linear gradient elution system consisting of acetate buffer as mobile phase. Contents of these marker substances in an unpretreated Hsiao-cheng-chi-tang extract could be easily determined within 60 min. The effects of pH, buffer concentration and column selectivity for this method are described.

## 1. Introduction

Chinese herbal preparations have been used for several hundred years and are still widely used, especially in China, Japan and Taiwan. Therefore, suitable assay methods are urgently needed for quality control purposes. Recently, high-performance liquid chromatography (HPLC) [1–5] and capillary electrophoresis (CE) [6–10] have been employed to establish the optimum conditions for examining two or three constituents of the preparations. However, as our knowledge of the effective components of Chinese herbal preparations is still limited and their chemical compositions are very complicated, the exact determination of the quality of a Chinese herbal preparation is very difficult. Efforts to develop simpler and more rapid methods that can assay all the bioactive constituents known are therefore necessary.

Hsiao-cheng-chi-tang (Minor Rhubarb Combination) is a herbal prescription often used for treating patients with bloating, constipation, moist fever and a sinking pulse, and is composed of Rhei Rhizoma, Aurantii Fructus Immaturus and Magnoliae Cortex [11]. It is well known that Aurantii Fructus Immaturus and Magnoliae Cortex can dispel distention and contain a number of bioactive components such as naringin (**4**) and hesperidin (**5**) in the former and magnolol (**7**) and honokiol (**6**) in the latter. Rhei Rhizoma is an antipyretic and has gallic acid (**1**), sennoside A (**3**), sennoside B (**2**) and emodin (**8**) as its major bioactive components [12]. Using these eight compounds (as shown in Fig. 1) as marker substances, an HPLC method was developed. The difference in column selectivity and the suitability of this method are also discussed.

* Corresponding author.

0021-9673/95/$09.50 
*SSDI* 0021-9673(95)00216-2

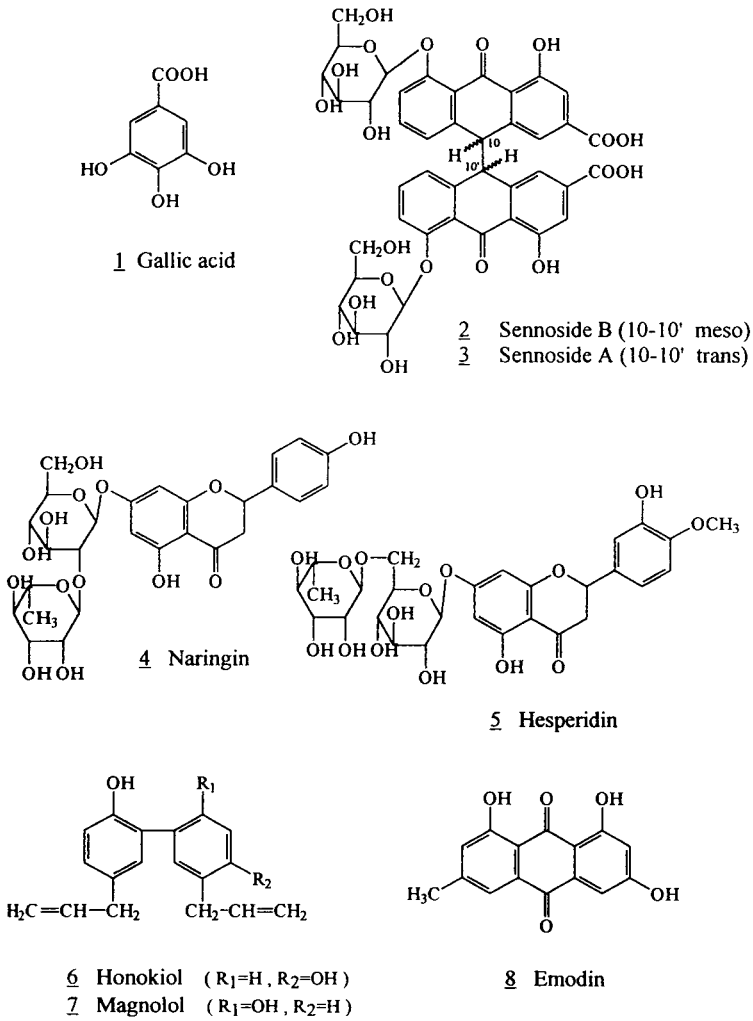


Fig. 1. Structures of the eight marker substances.

## 2. Experimental

### 2.1. Reagents and materials

Sennoside A and B were purchased from Yoneyama (Osaka, Japan), emodin and hesperidin from Sigma (St. Louis, MO, USA), naringin from Aldrich (St. Louis, MO, USA), *p-tert.*-octylphenol from Nacalai Tesque (Kyoto, Japan), acetic acid and gallic acid from Merck (Darmstadt, Germany) and sodium acetate from Kanto (Tokyo, Japan). Acetonitrile and methanol were of LC grade (Mallinckrodt, St. Louis, MO, USA). Magnolol and honokiol were isolated from Magnoliae Cortex [13]. Hsiao-cheng-chi-tang was provided by a Chinese pharmaceutical company in Taipei (Taiwan). Peak identification and purity checking of all the marker substances and test samples were done with a photodiode-array detector.

### 2.2. Preparation of Chinese herbal preparation extract

A 0.5170-g sample of Hsiao-cheng-chi-tang was extracted with 70% methanol (7 ml) by

stirring at room temperature for 30 min, then centrifuged at 1500 *g* for 5 min. Extraction was repeated three times. The extracts were combined and filtered through a No. 1 filter-paper. After adding 2.5 ml of internal standard solution (0.1172 g of *p-tert.*-octylphenol in 100 ml of methanol), the herbal preparation extract was diluted to 25 ml with 70% methanol. A 5-$\mu$l volume of this solution was injected directly into the HPLC system.

### 2.3. Apparatus and conditions

The HPLC system consisted of two Waters Model 510 pumps, a Waters Model 680 automated gradient controller and a Waters Model 991 photodiode-array detector (280 nm). The separations were obtained with a reversed-phase column (Cosmosil $5C_{18}$, 5 $\mu$m, 25 cm × 4.6 mm I.D.) (Nacalai Tesque) and by linear gradient elution, using eluents A and B [A = buffer–$CH_3CN$ (9:1), the buffer being an aqueous solution consisting of 0.02 *M* sodium acetate and 0.4197 *M* acetic acid (24 ml of acetic acid was made to a 1000 ml aqueous solution); B = $CH_3OH$–$CH_3CN$–1% acetic acid (9:9:2)] according to the following A–B profile: 0 min, 90:10; 14–22 min, 75:25; 30 min, 70:30; 35 min, 20:80; 45–55 min, 0:100; 60 min, 90:10. The flow-rate was kept constant at 0.8 ml/min. A precolumn of $\mu$Bondapak $C_{18}$ (Millipore, Milford, MA, USA) was used to protect the column.

## 3. Results and discussion

### 3.1. Analytical conditions

Two methods for the determination of naringin and hesperidin in Aurantii Fructus Immaturus or herbal preparations containing it have been developed by Ishihara et al. [14] and Wu and Sheu [15]. The former used acetonitrile–water containing 0.05 *M* phosphate as the mobile phase whereas the latter used a mixture of acetonitrile and 0.5% acetic acid. However, with these solvent systems, analysis for the eight marker substances did not afford a satisfactory result. The HPLC separation of Hsiao-cheng-chi-tang extract was conducted by addition of $CH_3COONa$ and $CH_3COOH$ to the mobile phase.

After a series of experiments, it was found that a pH 3.56 solution (mixture of 0.02 *M* sodium acetate and 0.4197 *M* acetic acid) could separate all the constituents well. At lower pH (3.40), the peaks of sennoside A and naringin could not be separated. At higher pH (3.86, adjusted by either increasing the acetate concentration or decreasing the acetic acid concentration), the separation was satisfactory for the eight authentic marker substances but it was unsuitable for the analysis of the extract owing to the overlapping of the sennoside A and B peaks with those of some unknown components of the drug.

Acetic acid (1%) was added to the mixture of the methanol and acetonitrile in reservoir B of the gradient system in order to obtain an ideal chromatogram with a much smoother baseline.

The mobile phase and stationary phase have mutual influences on each other. We therefore fixed the concentration of buffer at 0.02 *M* $CH_3COONa$ and 0.4197 *M* $CH_3COOH$ as discussed above and compared the selectivities of nine commercial $C_{18}$ columns (all 25 cm in length, except column IX, which was 30 cm, as shown in Table 1). After a series of experiments, the capacity factors ($k'$) of the constituents were as shown in Fig. 2.

The data in Fig. 2 show that all the columns except I, V and VIII failed to separate the eight compounds completely. Among columns I, V and VIII, which can give a fairly good separation of all the constituents, column I was found to be the best as it gave a higher resolution in the separation of the crude extract. There was seriously overlapping between the trace sennoside B and some unknown components of the extract when columns V and VIII were used.

From the above results, the best resolution was obtained with a buffer containing 0.02 *M* $CH_3COONa$ and 0.4197 *M* $CH_3COOH$ and with the reversed-phase Cosmosil $5C_{18}$ column. Fig. 3 presents a chromatogram showing the separation

Table 1
Columns used

| No. | Column | Producer and location | Column length (cm) | Column I.D. (mm) |
|---|---|---|---|---|
| I | Cosmosil $5C_{18}$ | Nacalai Tesque (Kyoto, Japan) | 25 | 4.6 |
| II | Cosmosil $5C_{18}$-MS | Nacalai Tesque | 25 | 4.6 |
| III | Cosmosil $5C_{18}$-AR | Nacalai Tesque | 25 | 4.6 |
| IV | Intersil ODS-2 | GL Science (Tokyo, Japan) | 25 | 4.6 |
| V | LiChrosorb RP-18 | Merck (Darmstadt, Germany) | 25 | 4.0 |
| VI | LiChrospher 60RP-Select B | Merck | 25 | 4.0 |
| VII | Purosphere RP-18 | Merck | 25 | 4.0 |
| VIII | Nucleosil 100 $5C_{18}$ | Macherey–Nagel (Düren, Germany) | 25 | 4.0 |
| IX | Novapak $C_{18}$ | Millipore (Milford, MA, USA) | 30 | 3.9 |

Particle size = 5 $\mu$m for all columns.

of the eight marker substances in a sample of Hsiao-chen-chi-tang extract. The tailing factors (half the peak width at 5% of the peak height divided by the distance between the peak front and the peak maximum measured at 5% of the peak height) of all the peaks to be determined are very close to unity.

### 3.2. Calibration graphs for marker substances

Calibration graphs (peak-area ratio, $y$, vs. concentration, $x$, in $\mu$g ml$^{-1}$) were constructed

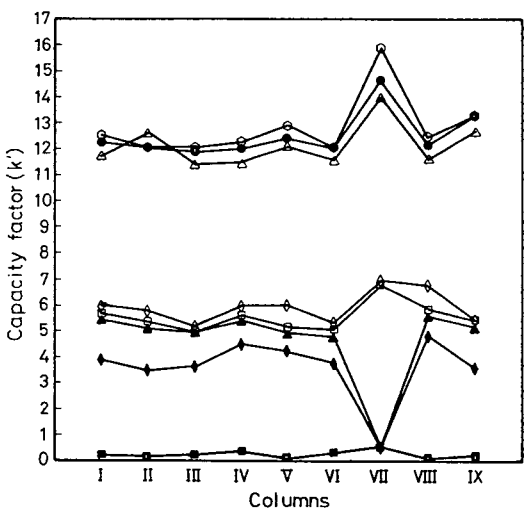


Fig. 2. Effect of column selectivity on capacity factor ($k'$). (■) **1** = gallic acid; (◆) **2** = sennoside B; (▲) **3** = sennoside A; (□) **4** = naringin; (◇) **5** = hesperidin; (△) **6** = honokiol; (●) **7** = magnolol; (○) **8** = emodin.

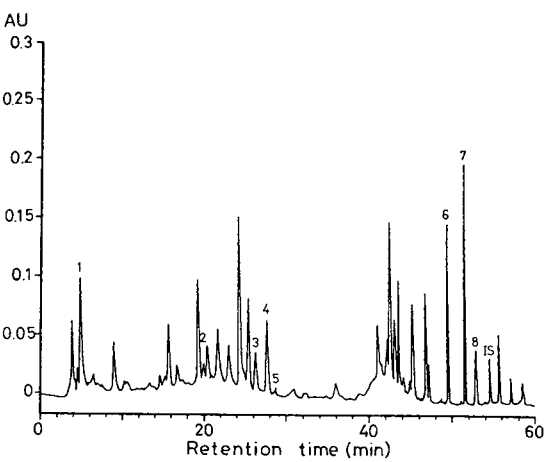


Fig. 3. Chromatogram of Hsiao-cheng-chi-tang. IS = internal standard (*p-tert.*-octylphenol); other peaks as in Fig. 1.

in the range 0.0282–0.2112 mg $ml^{-1}$ for gallic acid, 0.0026–0.0528 mg $ml^{-1}$ for sennoside B, 0.0046–0.0159 mg $ml^{-1}$ for sennoside A, 0.0089–0.1680 mg $ml^{-1}$ for naringin, 0.0010–0.0204 mg $ml^{-1}$ for hesperidin, 0.0089–0.4480 mg $ml^{-1}$ for honokiol, 0.0385–0.7236 mg $ml^{-1}$ for magnolol and 0.0022–0.0426 mg $ml^{-1}$ for emodin. The retention times of the marker substances and the regression equations of these graphs and their correlation coefficients were as follows: gallic acid, 5.0 min, $y = 0.0512x + 1.0448$ ($r = 0.9997$); sennoside B, 19.8 min, $y = 0.0141x + 3.4872$ ($r = 0.9997$); sennoside A, 25.8 min, $y = 0.0159x + 2.6812$ ($r = 0.9997$); naringin, 27.8 min, $y = 0.0260x + 9.3242$ ($r = 0.9997$); hesperidin, 28.2 min, $y = 0.0365x + 0.1172$ ($r = 0.9997$); honokiol, 49.5 min, $y = 0.0335x + 2.3599$ ($r = 0.9999$); magnolol, 51.5 min, $y = 0.0213x + 18.3838$ ($r = 0.9996$); emodin, 53.0 min, $y = 0.0735x + 0.8804$ ($r = 0.9997$); and *p-tert.*-octylphenol (internal standard), 54.2 min.

### 3.3. Determination of the constituents of Hsiao-cheng-chi-tang sample

When the test solution of Hsiao-cheng-chi-tang extract was analysed by HPLC under the selected conditions, the graph shown in Fig. 3 was obtained. The calculated contents of the individual constituents of two commercial Hsiao-cheng-chi-tang samples are given in Table 2. The data in Table 2 show that the quality of the formula in different commercial products varied.

Table 2
Contents of marker substances in two commercial concentrated herbal preparations of Hsiao-cheng-chi-tang (mg/g)

| Constituent | Sample 1 | Sample 2 |
|---|---|---|
| Gallic acid | 1.72 | 1.79 |
| Sennoside B | 0.60 | 0.64 |
| Sennoside A | 2.49 | 3.27 |
| Naringin | 2.73 | 3.05 |
| Hesperidin | 0.13 | 0.99 |
| Honokiol | 1.84 | 0.62 |
| Magnolol | 5.02 | 3.72 |
| Emodin | 0.37 | 0.69 |

The relative standard deviations of the proposed method, on the basis of peak-area ratios for six replicate injections, were 1.26% (intra-day) and 2.09% (inter-day) for gallic acid, 2.26 and 2.51% for sennoside B, 1.86 and 1.40% for sennoside A, 1.11 and 1.61% for naringin, 1.54 and 1.56% for hesperidin, 1.37 and 1.94% for honokiol, 1.24 and 1.67% for magnolol and 1.05 and 1.32% for emodin, respectively. Suitable amounts (2.33–69.29 mg) of the eight marker substances were added to a sample of Hsiao-cheng-chi-tang of known content and the mixture was extracted and analysed using the proposed procedure. The recoveries were 99.04% for gallic acid, 94.70% for sennoside B, 92.55% for sennoside A, 99.56% for naringin, 97.94% for hesperidin, 94.43% for honokiol, 97.89% for magnolol and 99.54% for emodin.

## Acknowledgement

Financial support from the National Science Council, Republic of China, is gratefully acknowledged.

## References

[1] M. Harada, Y. Ogihara, Y. Kano, A. Akahori, Y. Ichio, O. Miura and H. Suzuki, Iyakuhin Kenkyu, 19 (1988) 852.
[2] M. Harada, Y. Ogihara, Y. Kano, A. Akahori, Y. Ichio, O. Miura, K. Yamamoto and H. Suzuki, Iyakuhin Kenkyu, 20 (1989) 1300.
[3] K.C. Wen, C.Y. Huang and F.S. Liu, J. Chromatogr., 593 (1992) 191.
[4] K.C. Wen, C.Y. Huang and F.L. Lu, J. Chromatogr., 631 (1993) 241.
[5] L.C. Chang and S.J. Sheu, J. Food Drug Anal., 1 (1993) 33.
[6] Y.M. Liu and S.J. Sheu, J. Chromatogr., 637 (1993) 219.
[7] Y.M. Liu and S.J. Sheu, J. Chromatogr., 639 (1993) 323.
[8] H.R. Chen and S.J. Sheu, J. Chromatogr. A, 653 (1993) 184.
[9] Y.M. Liu and S.J. Sheu, J. High Resolut. Chromatogr., 17 (1994) 559.
[10] S.J. Sheu and H.R. Chen, Anal. Chim. Acta., in press.

[11] H.Y. Hsu and C.S. Hsu, Commonly Used Chinese Herb Formulas with Illustrations, Oriental Healing Arts Institute, Los Angeles, 1980, pp. 141–142.
[12] H.Y. Hsu, Y.P. Chen, S.J. Sheu, C.S. Hsu, C.C. Chen and H.C. Chang, Chinese Material Medica—A Concise Guide, Modern Drug Press, Taipei, 1985, pp. 61–62, 300–301 and 312–313.
[13] M. Fujita, H. Itokawa and Y. Sashida, Chem. Pharm. Bull., 20 (1972) 212.
[14] S. Ishihara, S. Yoshid, S. Tosa, H. Nakazawa and T. Tomimatsu, Shoyakugaku Zasshi, 45 (1991) 52.
[15] F.J. Wu and S.J. Sheu, Chin. Pharm. J., 44 (1992) 257.

ELSEVIER

Journal of Chromatography A, 704 (1995) 524–529

JOURNAL OF CHROMATOGRAPHY A

Short communication

# Separation and quantification of tetraethylene glycol monoheptanoate and diheptanoate by high-performance liquid chromatography

V. Baudrand, Z. Mouloungui*, A. Gaset

*Laboratoire de Chimie Agro-industrielle, École Nationale Supérieure de Chimie de Toulouse INPT, 118 Route de Narbonne, 31077 Toulouse, France*

First received 2 August 1994; revised manuscript received 14 February 95; accepted 21 February 1995

**Abstract**

Tetraethylene glycol mono- and diheptanoate were prepared by direct esterification of heptanoic acid with tetraethylene glycol. The constituents of the reaction were separated by thin layer chromatography with flame ionization detection, but only tetraethyleneglycol diheptanoate could be determined by this method. The main constituents of the reaction mixture were quantified by HPLC using two different mobile phases on a non-bonded silica column. Acetonitrile acidified with 0.3% acetic acid was used to separate and quantify the monoester and tetraethylene glycol, while hexane–isopropanol (80:20, v/v) acidified with 0.3% acetic acid was used to separate and quantify heptanoic acid and the diester. The starting compounds and the products of the reaction could be thus separated and quantified accurately using these two eluents without derivatization of the hydroxylated compounds.

## 1. Introduction

Tetraethylene glycol monoheptanoate (TEGMH) is a non-ionic surfactant belonging to the family of short hydrophobic alkyl chain wetting agents [1] and is employed in numerous industrial and domestic cleansing formulations [2]. The polyoxyalkylene moiety with a free terminal hydroxyl group is an important structural feature which enhances the properties of these wetting agents.

Tetraethylene glycol diheptanoate (TEGDH) is a diester with plastifying properties used as an adhesion control agent in conjunction with polyvinylbutyral (PVB) [3]. It is also employed as an additive in solid photopolymerisable compositions used in the manufacture of optical components in imaging equipment [4].

Analytical data on the separation of commercial polyethoxy fatty acids by HPLC on a silica column have been reported [5], although the main objective of the study was to identify the fatty acids and determine the number of ethylene oxide units in these surfactants.

TEGMH and TEGDH were synthesized from heptanoic acid (HA) and tetraethyleneglycol (TEG) at moderate temperature in the absence of catalyst and solvent [6] (Eq. 1).

* Corresponding author.

0021-9673/95/$09.50 
*SSDI* 0021-9673(95)00245-6

$$3\,\underset{\text{HA}}{CH_3(CH_2)_5COOH} + 2\,\underset{\text{TEG}}{H(OC_2H_4)_4OH}$$
$$\rightleftharpoons \underset{\text{TEGMH}}{CH_3(CH_2)_5CO(OC_2H_4)_4OH}$$
$$+ \underset{\text{TEGDH}}{CH_3(CH_2)_5CO(OC_2H_4)_4OCO(CH_2)_5CH_3}$$
$$+ 3\,H_2O$$

The reaction mixture was analyzed using a combination of TLC–FID and HPLC with silica as stationary phase, which enabled the determination of the content of non-ionic surfactants and starting compounds (HA and TEG) in the reaction mixture.

## 2. Experimental

### 2.1. Reagents and analytical set-up

TEG (99%) was supplied by Aldrich (St. Quentin Fallavier, France). HA (99%) was supplied by Fluka (St. Quentin Fallavier, France), and 2,7-difluorescein was purchased from Merck (Nogent-sur-Marne, France). The silica chromagel (60 Å, 60–200 $\mu$) used for the flash-chromatography was obtained from SDS (Peypin, France).

The TLC silica plates (60 $F_{254}$) were supplied by Merck (Nogent-sur-Marne, France). The detector was a Bioblock Scientific UV lamp (Illkich, France).

An Iatroscan MK-5 was used for TLC–FID, and the samples were applied on S-III chromarods (Iatron Laboratories, Tokyo, Japan) (Flotech, Paris, France). Five 1-$\mu$l aliquots (0.25 g reaction mixture in 10 ml ethyl ether) of each sample were applied using a semi-automatic pipette (SES 3202). The chromarods were then placed in a chamber previously saturated with the elution solvent [ethyl ether–pentane–acetic acid (80:20:1, v/v)], removed after 30 min migration and then oven dried (Rod Dryer TK-8; Iatron Laboratories) at 110°C for 5 min. After temperature stabilisation in a desiccator under vacuum, the chromarods were transformed to the flame ionization detector and burned using the following parameters: hydrogen flow 160 ml/min, air flow 2 ml/min, burn rate 35 s/rod. The results were analyzed using BOREAL software.

The HPLC system was equipped with a Spectra System AS 3000 automatic injector and a Spectra-Physics Analytical P 1500 pump (Spectra-Physics, Paris, France). Samples of 20 $\mu$l (0.1 g reaction mixture in 1.4 ml acetonitrile or hexane) were injected. The analytical column was a Nucleosil S 100 5 $\mu$m type NC04 (250 × 4.0 mm I.D.) (Bischoff Chromatography) (ICS, Toulouse, France) fitted with a 10 $\mu$m Lichrosorb SI 100 precolumn (Bischoff Chromatography). A Car H (30 cm × 7.8 mm I.D.) fitted with a Sarasep precolumn (5 cm × 4.6 mm) (Touzard-Matignon, Grabels, France) eluted with acetonitrile–water (60:40, v/v) acidified with 0.005 *M* sulfuric acid (flow-rate, 0.4 ml/min; oven temperature, 40°C), and a 5 $\mu$m Nucleosil $C_{18}$ column (25 × 4.6 mm I.D.) (Touzard-Matignon) fitted with a precolumn eluted with methanol acidified with 0.3% acetic acid (flow-rate, 0.8 ml/min; oven temperature, 40°C) were also tested. A refractometer (Refractomonitor IV Milton Roy) (LDC, Paris, France) was employed as detector, and the chromatograms were recorded on a Spectra-Physics chromjet integrator.

### 2.2. Synthesis and purification of TEGMH and TEGDH

TEGMH and TEGDH were synthesized by reacting different amounts of TEG and HA in the absence of solvent in a 100-ml three-necked flask fitted with a cooling system, mechanical stirrer and temperature probe. The reaction mixture was heated to 145°C on a thermostated oil bath for 480 min. The reaction mixture was washed with 0.1 *M* KOH to extract HA and saturated NaCl to extract TEG. The TEGMH and TEGDH were then separated on a silica column by flash-chromatography using two eluents: ether and ethanol. Analytical grade solvents (SDS; Peypin, France) were employed for the HPLC and TLC–FID.

## 3. Results and discussion

### 3.1. Separation by TLC and TLC–FID–Quantification of TEGDH by TLC–FID

In preliminary experiments, the progress of the esterification reaction was followed by TLC. The plates were eluted with ethyl ether–pentane–formic acid (80:20:5, v/v) and the products TEGMH ($R_F$: 0.10) and TEGDH ($R_F$: 0.42) along with the starting compounds HA ($R_F$: 0.50) and TEG ($R_F$: 0.02) were detected under UV illumination (254 nm) after spraying the plates with 2,7-difluorescein. This produced light yellow spots for the mono- and diester, dark yellow spots for heptanoic acid and orange spots for TEG.

TLC–FID, combining the advantages of TLC and flame ionization detection [7], was carried out using thin silica rods coated with silica (5 $\mu$m), and eluted with a mixture of ethyl ether–pentane–acetic acid (80:20:1, v/v). The presence of TEGMH (retention time: 17.90 min) and TEGDH (retention time: 12.11 min) was detected along with HA (retention time: 5.80 min) and TEG (retention time: 23.68 min).

In TLC–FID both TEGMH and TEG were strongly retained on the silica. These highly polar mono- and dihydroxylated compounds interact with silica and are thus strongly bound to the support. TEG with two hydroxyl groups migrated only a little, and tended to contaminate the rods close to the point of sample application. Heptanoic acid is not readily quantified by TLC–FID as it has a low molecular mass and is highly volatile. It tends to evaporate during the drying stage at 110°C and leads to errors in the calculation of mass conservation.

This system was found to be sufficiently linear and reproducible only for accurate quantification of TEGDH. Each point on the calibration curve for the diester corresponds to five separate determinations. The surface areas corresponding to each concentration were calculated to an error of ±3%. The calibration curve for the diester was described by the equation $y = 900.62 + 3379.4\,x$ with a correlation coefficient $r = 0.989$, which was thus suitable for quantification of the non-ionic surfactant [8].

### 3.2. Optimization of analytical conditions for HPLC

In view of the limitations of TLC–FID, we turned to HPLC for quantification of TEGMH, TEGDH, TEG and HA. Using a refractometer as detector we obtained linear and reproducible responses for both standards and samples.

*Reversed-phase (Nucleosil $C_{18}$) and high-capacity acid resin (Car H) columns*

Various types of columns with different eluents were tested:

(a) A reversed-phase column (5 $\mu$m) filled with Nucleosil $C_{18}$ was eluted with methanol acidified with 0.3% acetic acid. TEG (retention time: 4 min) was eluted first followed by HA and TEGMH (retention time: 5 min) and TEGDH (retention time: 6 min). (b) A Car H column filled with a high-capacity cation-exchange resin in the $H^+$-form has been described for analysis of organic acids and polyols using acetonitrile–water (60:40, v/v) acidified with sulfuric acid (0.005 $M$) as eluent [9]. Using this system, TEGDH was eluted first (retention time: 8.37 min) followed by HA and TEGMH (retention time: 9.85 min) and TEG (retention time: 20.13 min).

In both cases, TEGMH and HA were eluted together, while the order of elution of TEG and TEGDH was reversed on the two different supports.

Varughèse et al. [10] have investigated the HPLC behavior on reversed-phase supports of a series of non-ionic surfactants bearing different functional and alkyl groups. They found that the chromatographic behavior depended on interactions between the alkyl group of the surfactant and the stationary phase. We assume that the retention of TEGMH and HA on the Car H acid support was influenced by the hydrophobic part of the molecule consisting of the hydrocarbon chain of heptanoic acid.

A drawback of the Car H column was that it

required a perfect match between the eluent and dilution solvent (equal proportions of water and acetonitrile). If these two solvents are not the same, a negative peak was observed just after the TEGMH and HA peak, which tended to interfere with the quantification of these compounds.

*Silica column (Nucleosil S100)*

The qualitative results obtained with TLC–FID and literature data [5] on HPLC separations using silica columns prompted us to employ a non-coated silica column (Nucleosil S100). Two solvent systems were employed for separation of both starting compounds and products of the esterification reaction:

(a) Hexane–isopropanol (80:20, v/v) acidified with 0.3% acetic acid for separation of HA and TEGDH (Fig. 1). These two compounds were quantified after calibration of the column with external standards. There was a linear relationship between the concentrations injected and the peak heights of HA and the peak areas of TEGDH. The following equations governed the relationships between the peaks and concentrations injected: for HA, $y = 0.26832 + 9.1946 \cdot 10^{-2}x$, $r = 0.994$; for TEGDH, $y = 68.685 + 3004.3\ X$, $r = 0.999$. If the dilution solvent differed from the eluent, a negative peak was observed at time $t_0$ before emergence of HA (Fig. 1). The other compounds (TEG and TEGMH) were too strongly retained for reliable detection and their peak could not be discriminated from baseline noise. To avoid accumulation of polar compounds under these analytical conditions, the column was rinsed with isopropanol after each analysis.

(b) Acetonitrile acidified with 0.3% acetic acid for separation and quantification of TEG and TEGMH (Fig. 2). In this case, HA and TEGDH were eluted first and were not separated. TEG and TEGMH were quantified after calibration using ethylene glycol (EG) as internal standard. Linear relationships were observed between the concentrations injected and the areas of the peaks of TEG, TEGMH and EG. The concentrations of TEG and TEGMH were derived from the following equations: For TEG, $y =$

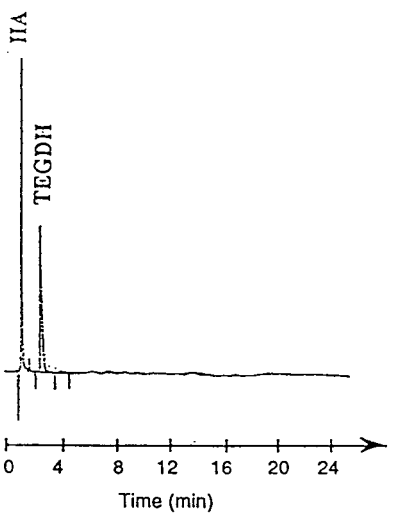


Fig. 1. Chromatogram of HA and TEGDH on a Nucleosil S100 column. Operating conditions: oven temperature, 40°C; duration of analysis, 6 min; retention time (min), HA: 0.8, TEGDH: 3.53.

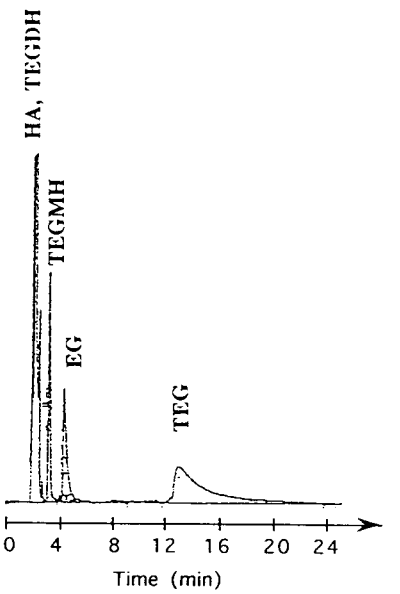


Fig. 2. Chromatogram of TEGMH and TEG on a Nucleosil S 100 column. Operating conditions: eluent, acetonitrile acidified with 0.3% acetic acid; flow-rate, 1.4 ml/min; oven temperature, 40°C; duration of analysis, 25 min; retention time (min), TEGMH: 3.53, TEG: 12.93, EG: 4.27.

$-5623 + 3409.10x$, $r = 0.991$; for TEGMH, $y = -13285 + 2383.70x$, $r = 0.991$; for EG, $y = -2826 + 644.96x$, $r = 0.992$.

### 3.3. Adaptation of HPLC system to separation of components of esterification medium

*Injection system*

The esterification reaction between heptanoic acid and tetraethylene glycol depends on the initial ratio of the reactants. A large excess of TEG minimizes formation of TEGDH, whereas an excess of HA maximizes formation of this ester. We thus investigated ratios of HA/TEG ranging from 0.1 to 10. The following conditions were employed: (a) HPLC system with automatic sample loader to gain time and minimize errors on routine analyses, (b) an injection loop which enabled an increase in injection volumes (20–250 μl) and could be adapted to different proportions of reactants and products.

*Refractometric detection*

The refractometer detected 0.5, 2, 0.15 and 1 μmole respectively of HA, TEG, TEGDH and TEGMH. As in the previous experiments, the refractometric detector could not be employed with a dilution gradient and was highly sensitive to changes in temperature and pressure.

*Analysis of media from esterification of HA and TEG*

Fig. 3 shows the progress of the esterification reaction for an HA/TEG ratio of 7.52.

The operating conditions with excess HA gave a conversion rate of 100% for TEG and 70% for HA. TEGMH and TEGDH were obtained as a mixture, and the relative proportions of the two depended on the duration of the reaction. TEGMH was obtained in 60% yield after 50 min reaction, while TEGDH was obtained in 95% yield after 480 min.

*Analysis of other esterification mixtures*

Hexane–isopropanol (80:20, v/v) acidified with 0.3% acetic acid was also employed to separate and quantify compounds from reaction mixtures containing: (a) tetraethyleneglycol monoundecanoate (retention time: 7.17 min), tetraethyleneglycol diundecanoate (retention time: 2.39 min) and undecylenic acid (retention time: 1.86 min); (b) tetraethyleneglycol monooleate (retention time: 6.09 min) tetraethyleneglycol dioleate (retention time: 2.05 min), and oleic acid (retention time: 1.77 min).

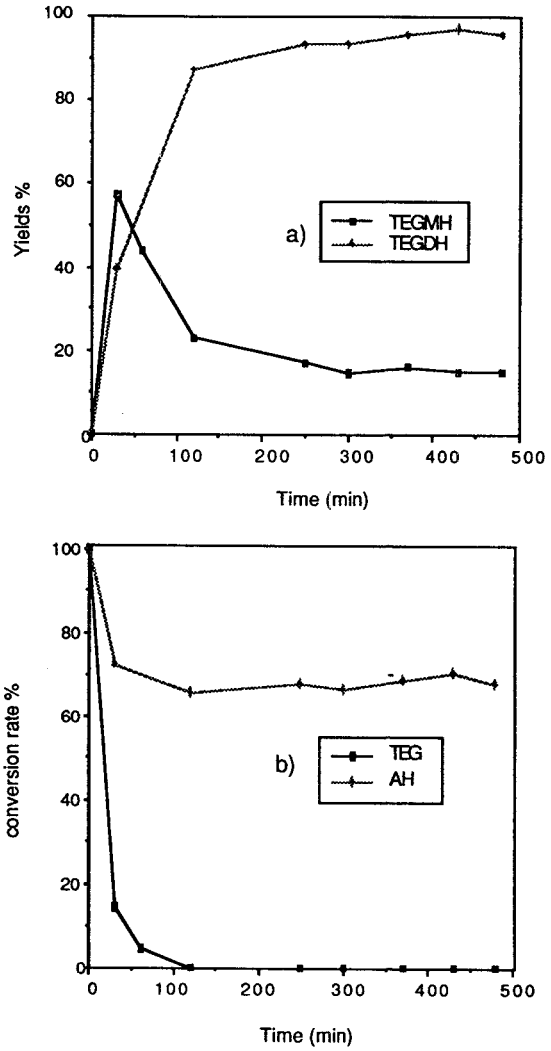


Fig. 3. Reaction progress with HA in excess (HA/TEG: 7.52). (a) Yields of TEGDH and TEGMH, (b) HA and TEG conversion rate. Operating conditions: temperature: 167°C; AH: 6 moles, TEG: 0.79 moles.

## 4. Conclusion

The various components of the reaction mixture from esterification of a fatty acid (HA) with tetraethylene glycol (TEG) were separated by TLC, TLC–FID or HPLC on acidified silica supports. A mobile phase of hydrocarbons (pentane, hexane) mixed with polar solvents such as isopropanol, formic and acetic acid [11], or acetonitrile acidified with acetic acid were found to be suitable for separation of the neutral components, and for separation and quantification of the acid components. Two mobile phases were developed to optimize separation of HA from TEGDH, and TEG from TEGMH by HPLC. The esterification reaction carried out in the absence of solvent could thus be followed both qualitatively and quantitatively by HPLC. The method was adapted for quantification of non-ionic surfactants.

## References

[1] J.K. Weil, R.E. Koos, W.M. Linfield and N. Parris, J. Am. Oil Chem. Soc., 139 (1979) 873.
[2] R.A. Reck, in R.W. Johnson and E. Fritz (Editors), Fatty acids in industry, Marcel Dekker, New York, 1989, Ch. 8, p. 177.
[3] T.R. Phillips, Polyvinyl butyral plasticized with tetraethyleneglycol di-*n*-heptanoate, EP 80105092.3 (1980).
[4] W.K. Smothers, Storage stable photopolymerisable composition and element for refractive index imaging, US 4,994,347 (1991).
[5] N. Garti, V.R. Kaufman and A. Aserin, in J. Cross (Editor), Non-ionic surfactant chemical analysis, Marcel Dekker, New York, 1988, Ch. 7, p. 225.
[6] V. Baudrand, Unpublished results.
[7] K.D. Mukherjee, in J. Sherma and B. Fried (Editors), Handbook of Thin-Layer Chromatography, Marcel Dekker, New York, 1991, Ch. 13, p. 339.
[8] H. Pakdel and C. Roy, Biomass, 13 (1987) 155.
[9] Catalogue Touzart-Matignon France (1994), p. 19.
[10] P. Varughèse, M.E. Gangoda and R.K. Gilpin, J. Chromatogr., 499 (1990) 469.
[11] W.W. Christie, Lipid Technol., 5 (1993) 121.

ELSEVIER

Journal of Chromatography A, 704 (1995) 530–534

JOURNAL OF CHROMATOGRAPHY A

Short communication

# Determination of chlorine, sulphur and phosphorus in organic materials by ion chromatography using electrodialysis sample pretreatment☆

M. Novič[a,*], A. Dovžan[a], B. Pihlar[b], V. Hudnik[a]

[a]*National Institute of Chemistry, P.O. Box 30, 61115 Ljubljana, Slovenia*

[b]*Department of Chemistry and Chemical Technology, University of Ljubljana, Ljubljana, Slovenia*

First received 16 November 1994; revised manuscript received 19 January 1995; accepted 25 January 1995

**Abstract**

Wet decomposition of an organic material results in a residue of strong acid or alkali which should be neutralized before ion chromatographic (IC) analysis. Oxidative sample decomposition by sodium peroxide fusion in a Parr bomb and subsequent chloride, phosphate and sulphate determination by IC are described. Residual NaOH, formed during the decomposition procedure, was neutralized in an electrodialysis sample pretreatment step. Samples were neutralized in a commercially available electrodialysis cell. Using the described procedure, real samples were analysed and the results compared with those obtained by other analytical procedures. Detection limits of 0.005% for chlorine and 0.008% for sulphur and phosphorus were achieved when 0.1–0.3 g of sample was analysed.

## 1. Introduction

To employ ion chromatography (IC) for the determination of elements such as chlorine, sulphur and phosphorus in organic materials, these materials should be previously decomposed by an appropriate procedure in order to convert the mentioned elements into chloride, sulphate and orthophosphate, respectively. Classical wet chemical decomposition procedures often result in a very acidic or alkaline decomposition mixture, very rich in ions, which makes IC analysis impossible. Decomposition in a Schöniger oxygen flask with an absorbing solution composed of dilute $H_2O_2$ or NaOH [1–4] or combustion of organic material in a flow of oxygen and consequent trapping of the component of interest in dilute $H_2O_2$ [5] allows the IC determination of the mentioned elements. Several workers [1–4] have reported a high efficiency of these decomposition procedures. Recent results report by Umali et al. [6] confirm the quantitative conversion of chlorine and sulphur into chloride and sulphate using the Schöniger oxygen flask decomposition procedure. When phosphorus is also to be determined, an additional hydrolysis

* Corresponding author.

☆ Presented at the *International Symposium on Chromatographic and Electrophoretic Techniques, Bled, Slovenia, 10–13 October 1994.*

0021-9673/95/$09.50 
*SSDI* 0021-9673(95)00105-0

step, following the decomposition procedure, was necessary to ensure the complete conversion of different forms of phosphorus into orthophosphate [6].

The number of decomposition procedures compatible with IC analysis became much broader after the introduction of Donnan dialysis as a sample pretreatment step. Cox and coworkers [7,8] reported the determination of some anions in carbonate- and NaOH-based samples after carbonate fusion or oxygen combustion. Instead of Donnan dialysis, a dual ion-exchange method was used [7,8] to prevent sample contamination by the anion of the acid used as the source of $H_3O^+$ ions. Further improvement in the selectivity of the Donnan dialysis sample pretreatment was achieved with the introduction of electrodialysis Donnan pretreatment [9–14]. In the work cited, different electrodialysis devices were constructed and tested. The electrodialysis cell described by Siriraks and Stillian [11] allows the in-cell generation of hydronium ions by electrolysis of pure demineralized water (of 18 MΩ/cm resistance). In that way contamination of the sample by acid co-ions is completely prevented.

Sodium peroxide fusion decomposition results in complete mineralization of organic materials [15], quantitatively converting halogens into halides, sulphur into sulphate and phosphorus into orthophosphate. This method is often used as the sample preparation procedure in the classical, usually titrimetric, determination of chlorine and sulphur contents in organic material. Owing to the formation of an equivalent amount of NaOH from $Na_2O_2$, this method was avoided as a decomposition procedure for IC analysis. With the introduction of Donnan or electrodialysis sample neutralization before IC analysis, the drawback of $Na_2O_2$ fusion decomposition (strongly alkaline solution after the decomposition), can be easily overcome. The described analytical procedure has not previously been published and is the main objective of this paper. The proposed method was optimized and the accuracy and precision of the results obtained were validated by the analysis of some certified reference materials.

## 2. Experimental

### 2.1. Reagents

All reagents were of analytical-reagent grade. A sodium hydrogencarbonate–carbonate-based eluent was prepared according to Dionex [16]. Stock standard solutions of inorganic anions ($Cl^-$, $HPO_4^{2-}$, $SO_4^{2-}$) were prepared by dissolving appropriate amounts of their sodium salts in water purified with a Milli-Q system (Millipore). The accuracy of the procedure was tested by the analysis of some certified standard reference materials (SRMs) provided by NIST (Washington, DC, USA) (SRM 1084 Wear-Metals in Lubricating Oil, SRM 1085 Wear-Metals in Lubricating Oil, SRM 1548 Total Diet and SRM 1577b Bovine Liver).

### 2.2. Instrumentation

All chromatographic measurements were done with a Dionex 4000i chromatographic system. The electrodialysis system that was used for the off-line neutralization of alkaline samples is presented schematically in Fig. 1.

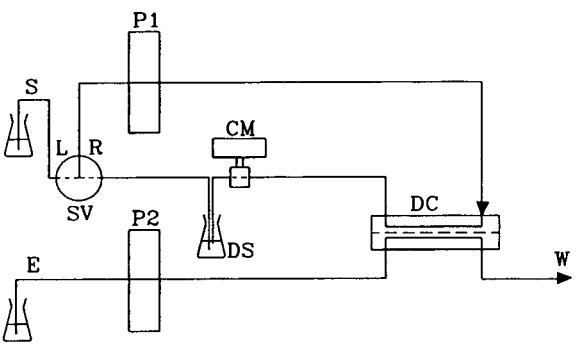


Fig. 1. Scheme of the Donnan dialysis system for the neutralization of alkaline samples after oxidative sample decomposition by sodium peroxide fusion in a Parr bomb. S = Sample; E = donor of $H_3O^+$ ions ($H_2SO_4$ or electrolysed 18 MΩ/cm water); P1 = peristaltic pump; P2 = pneumatic donor delivery system; SV = selection valve; DC = dialysis cell; CM = conductivity meter; DS = dialysed sample; W = waste.

### 2.3. Chromatographic conditions

The following conditions were used: sample loop volume, 50 μl; guard column, HPIC-AG4A SC (4 mm) (Dionex); separation column, HPIC-AS4A SC (4 mm) (Dionex); eluent, 180 m*M* $Na_2CO_3$–1.7 m*M* $NaHCO_3$; eluent flow-rate, 2.0 ml/min; suppressor, ASRS-1, Dionex (4 mm), current setting 1; regenerant, electrolysed 18 MΩ/cm water; and regenerant flow-rate, 3.0 ml/min.

### 2.4. Dialysis conditions

The conditions were as follows: dialysis cell, ASRS-1, Dionex (4 mm), current setting 2 or 3; sample flow-rate, ca. 1 ml/min; donor of $H_3O^+$; electrolysed 18 MΩ/cm water; and donor flow-rate, 3.0 ml/min.

### 2.5. Analytical procedure

A 150–300-mg amount of a sample was decomposed by 7.0 g of $Na_2O_2$ according to the standard procedure for organic material decomposition by sodium peroxide fusion in a Parr bomb [15]. After the decomposition, the reaction mixture was dissolved in 250 ml of 18 MΩ/cm water (obtained with a Milli-Q system). The concentration of the residual NaOH was between 0.7 and 0.8 mol/l. An aliquot (20 ml) was filtered through a 0.45-μm pore size membrane filter. The whole dialysis system was rinsed with the filtered sample. On selecting valve position L (load) (Fig. 1), about 5 ml of the sample were collected in a volumetric flask, whereas on selecting valve position R (recycle), sample from the volumetric flask was dialysed until the neutralization was finished (constant conductivity, usually achieved in about 30 min). The concentrations of individual anions in the dialysed sample were determined by subsequent IC analysis using the standard addition method.

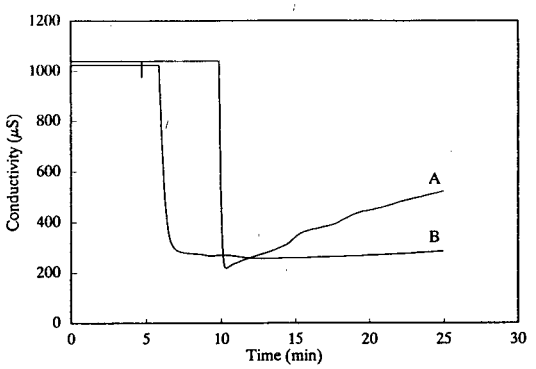


Fig. 2. Effect of (A) Donnan dialysis and (B) electrodialysis neutralization on the integral sample conductivity. The sample contained 2 mg/l $F^-$, 3 mg/l $Cl^-$, 8 mg/l $NO_2^-$, 10 mg/l $Br^-$, 10 mg/l $NO_3^-$, 15 mg/l $HPO_4^{2-}$ and 15 mg/l $SO_4^{2-}$ in 1.0 mol/l NaOH. Dialysis cell, ASRS-1; donor of hydronium ions (A) 12 m*M* $H_2SO_4$ and (B) electrolysed 18 MΩ/cm water.

## 3. Results and discussion

### 3.1. Selection of the source of $H_3O^+$ ions

To ascertain the influence of the source of hydronium ions on the sample contamination for the tested electrodialysis cell, an experiment was carried out in which the overall conductivity of the sample was monitored during its dialysis neutralization. Because a commercially available electrodialysis cell was used, only the sources of hydronium ions suggested by the manufacturer were tested. Two series of experiments were performed; in first 12 m*M* $H_2SO_4$ and in the second electrolysed 18 MΩ/cm water were used as the source of $H_3O^+$ ions. The results of these experiments are demonstrated in Fig. 2. The minimum values of the overall conductivity on both curves (A and B) represent neutralization of NaOH present in the sample. In the experiment, in which $H_2SO_4$ was used as the donor of $H_3O^+$ ions (curve A), the conductivity increased slowly after the minimum had been reached. This effect can be attributed to the non-ideal permselectivity of the cation-exchange membrane incorporated in the dialysis cell, which allows $SO_4^{2-}$ ions to permeate into the sample. Permeation of the $SO_4^{2-}$ ions was proved by IC analysis of the dialysed sample. The concentration of sulphate increased almost linearly with the time of dialysis, whereas the concentrations of other anions of interest (chloride and phos-

phate) remained constant during the neutralization. The recoveries of other ions (fluoride, nitrite and bromide) were also tested and the results obtained were very close to published values [12].

In the experiment in which electrolysed 18 MΩ/cm water was used as the donor of $H_3O^+$ ions, the conductivity of the dialysed sample remained fairly constant after the minimum value has been reached (curve B). This experiment confirms the superiority of in-dialysis cell generation of $H_3O^+$ ions by electrolysis of 18 MΩ/cm water for the electrodialysis sample neutralization, because no sample contamination was observed and therefore a constant dialysis time was not needed.

### 3.2. Validation of $Na_2O_2$ fusion decomposition in combination with IC analysis

To evaluate the analytical procedure for Cl, S and P determination in organic materials, the proposed method was verified by an independent analytical method and/or by the analysis of standard reference materials with certified Cl, S and P contents.

The accuracy of the IC determination of chlorine after sodium peroxide fusion decomposition and electrodialysis neutralization was verified titrimetrically with 0.1 *M* $AgNO_3$ with potentiometric indication of the equivalence point. The results of the comparison of chlorine content determinations in different used lubricating oils by titrimetric and electrodialysis–IC determination after sodium peroxide fusion decomposition are summarized in Table 1. It is evident that IC determination of chlorine after electrodialysis neutralization gives results comparable to those obtained titrimetrically, with the exception of sample 802, for which the result obtained titrimetrically is 32% higher than that obtained by IC. In that sample, the concentration of chloride was only slightly higher than the detection limit for the applied titrimetric method, which resulted in an inaccurate chloride determination.

The accuracy and precision of the determination of chlorine, sulphur and phosphorus in an organic material were tested by determining these elements in a used lubricating oil and in SRM 1557b Bovine Liver. When used lubricating oil was analysed, the precision of the proposed method for the determination of chlorine and sulphur content was tested. The used lubricating oil contained 0.40% of chlorine and 0.16% of sulphur. The calculated R.S.D. for chlorine and sulphur was found to be 7.1% and 9.0% ($n = 6$), respectively. Using SRM 1557b Bovine Liver, the accuracy and precision of the proposed procedure were tested. The certified values for chlorine, phosphorus and sulphur in the SRM were 0.278% (R.S.D. 2.2%), 1.10% (R.S.D. 2.7%) and 0.785% (R.S.D. 0.8%), respectively. The same three elements were determined using the proposed analytical procedure and in five parallel determinations the results obtained were 0.23% (R.S.D. 9.4%), 1.19% (R.S.D. 3.5%) and 0.78% (R.S.D. 5.5%), respectively (Table 2). It is evident that the accuracy of the simultaneous determination of chlorine, sulphur and phosphorus using the proposed procedure is within required limits.

The accuracy and precision of chlorine, sulphur and phosphorus determinations using the proposed procedure were additionally verified by analysing different SRMs. The results, summarized in Table 2, show good agreement in the accuracy of the simultaneous determination of chlorine, sulphur and phosphorous with the certified values even in organic materials with significant differences in matrix composition.

Table 1
Comparison of the chlorine content (%) in used lubricating oils obtained titrimetrically and by IC analysis after $Na_2O_2$ decomposition

| Sample No. | Potentiometric titration with $Ag^+$ | HPIC determination after dialysis neutralization |
|---|---|---|
| 798 | 7.63 | 7.46 |
| 799 | 1.16 | 1.19 |
| 801 | 8.85 | 8.93 |
| 802 | 0.53 | 0.40 |
| 803 | 6.61 | 6.64 |

Table 2
Results of the determination of chlorine, sulphur and phosphorus in different standard reference materials

| Sample | Determined concentration (%) (±R.S.D., %) | | | Certified concentration (%) (R.S.D., %) | | |
|---|---|---|---|---|---|---|
| | Cl | P | S | Cl | P | S |
| SRM 1084 Wear-Metals in Lubricating Oil | – | – | 0.19 (±5.0) | – | – | 0.220[a] |
| SRM 1085 Wear-Metals in Lubricating Oil | – | – | 0.42 (±5.1) | – | – | 0.480[a] |
| SRM 1548 Total Diet | 0.88 (±3.1) | – | 0.24 (±5.0) | 0.872 (±4.6) | – | 0.258 (±10.1) |
| SRM 1577b Bovine Liver | 0.23 (±9.4) | 1.19 (±3.5) | 0.78 (±5.5) | 0.278 (±2.2) | 1.102 (±2.7) | 0.785 (±0.8) |

[a] R.S.D. not stated.

## 4. Conclusions

The efficiency and compatibility of sodium peroxide fusion decomposition of organic samples as a sample preparation step for the IC determination of the anions of interest have been demonstrated and validated. The decomposition process results in a strongly alkaline solution, and this can be successfully neutralized by electrodialysis. To prevent sample contamination by hydronium co-anion in classical Donnan dialysis neutralization, a commercially available electrodialysis cell was used. This cell permits the in-cell generation of $H_3O^+$ ions in the anode compartment and $OH^-$ ions in the cathode compartment. By electrolysis of 18 MΩ/cm water, further contamination of the sample was avoided. In the validation of the proposed procedure, both the precision and the accuracy of the results were found to be within acceptable limits. In proposed procedure, detection limits of 0.005% for chlorine and 0.008% for sulphur and phosphorus were achieved when 0.1–0.3 g of sample was analysed.

## References

[1] J.F. Colaruotolo and R.S. Eddy, Anal. Chem., 49 (1977) 885.
[2] J.R. Kreling, F. Block, G.T. Louthan and J. Dezwaan, Microchem. J., 34 (1986) 158.
[3] A.M. Quinn, K.W.M. Siu, G.J. Gardner and S.S. Berman, J. Chromatogr., 370 (1986) 203.
[4] H. Assenmacher and J. Frigge, Fresenius' Z. Anal. Chem., 332 (1988) 41.
[5] M. Andrew, I.M.V. Burholt, N.J. Kernoghan, T.P. Lynch, R. Mackison, D. Mealor, J.A. Price and P. Schofield, J. Chromatogr., 640 (1993) 111.
[6] J.C. Umali, G. Morgan and P.R. Haddad, presented at the International Ion Chromatography Symposium IICS '94, 19–22 September 1994, Turin, Italy.
[7] J.A. Cox and N. Tanaka, Anal. Chem., 57 (1985) 383.
[8] J.A. Cox, E. Dabek-Zlotorzynska, R. Saari and N. Tanaka, Analyst, 113 (1988) 1401.
[9] A. Henshall, S. Rabin, J. Statler and J. Stillian, Am. Lab., November (1992) 20R.
[10] S. Rabin, J. Stillian, V. Barreto, K. Friedman and M. Toofan, J. Chromatogr., 640 (1993) 97.
[11] A. Siriraks and J. Stillian, J. Chromatogr., 640 (1993) 151.
[12] P.R. Haddad, S. Laksana and R.G. Simons, J. Chromatogr., 640 (1993) 135.
[13] P.R. Haddad and S. Laksana, J. Chromatogr., 671 (1994) 131.
[14] A.J.J. Debts, K.-P. Hupe, W.Th. Kok and U.A.Th. Brinkman, J. Chromatogr., 600 (1992) 163.
[15] N.H. Furman (Editor), Standard Methods of Chemical Analysis, Van Nostrand, New York, 6th ed., 1962, p. 964.
[16] Dionex Ion Chromatography Cookbook, Issue 1, Dionex, Sunnyvale, CA, 1987.

ELSEVIER

Journal of Chromatography A, 704 (1995) 535–539

JOURNAL OF CHROMATOGRAPHY A

Short communication

# Monitoring the esterification of sorbitol and fatty acids by gas chromatography

Jasminka Giacometti[a,*], Čedomila Milin[a], Nikola Wolf[b]

[a]*Medical Faculty, Department of Chemistry and Biochemistry, University of Rijeka, Braće Branchetta 20/1, HR 51000 Rijeka, Croatia*

[b]*Faculty of Chemical Engineering and Technology, Department of Polymer Engineering and Organic Chemical Tehnology, University of Zagreb, HR 41000 Zagreb, Croatia*

First received 3 November 1994; revised manuscript received 8 February 1995; accepted 21 February 1995

**Abstract**

Lauric acid esters of sorbitol, 1,4-sorbitan and 1,4:3,6-isosorbide were synthesized in laboratory. Esterification was carried out at 160°C with a catalyst for sorbitol cyclization and esterification, viz., *p*-toluenesulfonic acid. Lipid classes and polyols were separated and analysed by GC as trimethylsilyl ethers and esters. The purpose of the study was to determine the suitability of GC analysis of these products as a means of following the progress of reactions. The results confirmed the possibility of monitoring lauric acid and sorbitol esterification via the GC determination of lauric acid concentration.

## 1. Introduction

Non-ionic surfactants with ester groups (NSEG) such as sorbitan fatty acid esters (SFAE) are widely used as emulsifiers and stabilizers in the food and cosmetics industries. They are usually complex mixtures, because they have varying distributions of the alkyl chain length of the fatty acids.

Chemically, SFAE are complex mixtures of fatty acid esters of several polyols derived from sorbitol. These compounds are prepared by heating sorbitol and fatty acids at 160°C in the presence of a catalyst such as *p*-toluenesulfonic acid (*p*-TSA).

Two of the known polyols other than sorbitol itself are its anhydride, 1,4-sorbitan (1,4-anhydro-D-sorbitol), and the dianhydride, 1,4-3,6-isosorbide (1,4:3,6-dianhydro-D-sorbitol). The polyols are esterified, with and without cyclization at 160°C, with fatty acids, resulting in a complex mixture of mono-, di- and tri-fatty acids esters (Fig. 1).

SFAE have been determined by means of thin-layer chromatography (TLC) [1–4], gas chromatography (GC) [1,5–7] and high-performance liquid chromatography (HPLC) [8]. However, TLC has poor separation and quantitative capabilities and SFAE of high molecular mass cannot be measured by GC because they are non-volatile. Many studies have been reported on the application of HPLC to SFAE, as HPLC is very suitable for the determination of non-volatile compounds [8].

This paper describes a simple solution to the monitoring of synthetic and production activities.

* Corresponding author.

0021-9673/95/$09.50 
*SSDI* 0021-9673(95)00257-X

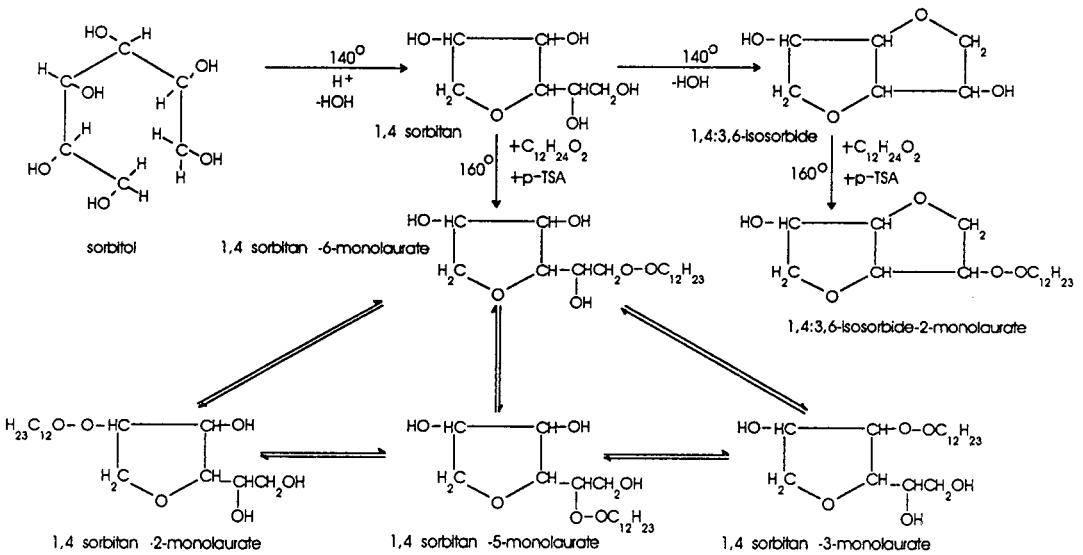


Fig. 1. Esterification of sorbitol with lauric acid with *p*-TSA as catalyst at 160°C.

Silyl derivatives are probably the most widely used derivatives for GC applications. Usually they are formed by the replacement of the active hydrogens of acids, alcohols, thiols, amines, amides and enolizable ketones and aldehydes with trimethylsilyl groups. The reaction of hydroxyl groups and carboxylic acids present in surface-active agents with hexamethyldisilazane and trimethylchlorosilane was used in this work [9]. The products are volatile trimethylsilyl ether and ester derivatives that are suitable for GC. The reaction is simple and quantitative without any undesirable side-reactions.

This paper describes the optimization of the GC separation. The extent of conversion of acid into sorbitan esters was calculated as mass-% (acid value) and vol.-% (GC analysis).

## 2. Experimental

### 2.1. Materials

The following were used: lauric acid ($C_{12}H_{24}O_2$), purum 98% (GC), (Fluka, Buchs, Switzerland), D-sorbitol ($C_6H_{14}O_6$), 99.5% (Hefti, Zurich, Switzerland), *p*-toluenesulfonic acid hydrate ($CH_3C_6H_4SO_3H \cdot xH_2O$) (Carlo Erba, Milan, Italy), Tri-Sil reagent (Pierce, Rockford, IL, USA), N,N-dimethylformamide, analytical-reagent grade (Merck, Darmstadt, Germany), Pyridine, analytical-reagent grade (Merck), 0.1 *M* KOH–ethanol (Kemika, Zagreb, Croatia), sorbitan monolaurate (Hefti) and 1,4:3,6-dianhydro-D-sorbitol (Aldrich, Milwaukee, WI, USA).

### 2.2. Apparatus

Analyses were performed using a Perkin-Elmer Model 8410 gas chromatograph with a flame ionization detector and fitted with a glass column [2 m × 5 mm I.D., packed with 3% SE-30 on Chromosorb G (60–80 mesh)] [7]. The column temperature was programmed from 150 to 220°C at 5°C/min. The injector and detector temperatures were 240°C. The carrier gas (nitrogen) flow-rate was 30 ml/min. The sample injection volume was 0.4 μl.

### 2.3. Preparations of esters

Individual fatty acid esters were prepared in the laboratory by two procedures. Sorbitol and

lauric acid (1:1, w/w), in the presence 0.1% w/w *p*-toluenesulfonic acid as catalyst were esterified at 160°C (method A, without cyclization) [10]. The reaction course was followed by taking samples after 15, 30, 45, 60, 90, 120 and 150 min determination of acid value and chromatographic analyses.

Sorbitol was cyclized with *p*-toluenesulfonic acid at 140°C (1 h) and esterified with lauric acid (1:1, w/w) at 160°C (method B, with cyclization) [11]. The reaction course was followed as in method A.

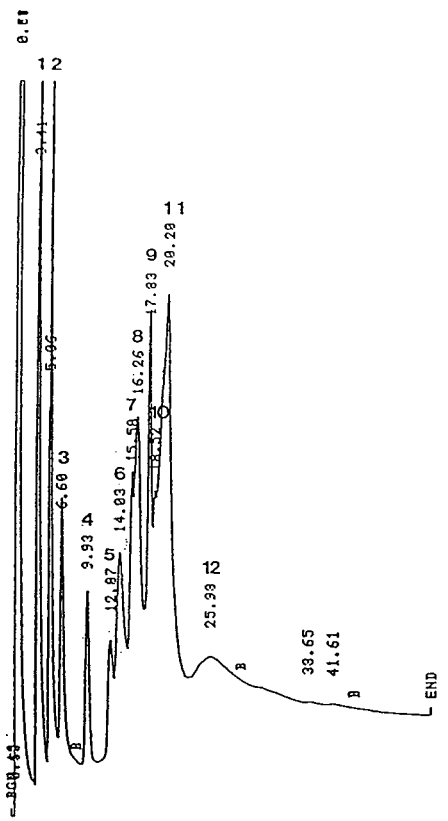


Fig. 2. Chromatogram of TMS derivative of cyclized sorbitol (method B) on a glass column (2 m × 5 mm I.D.) packed with 3% SE-30 on Chromosorb G (60–80 mesh). Column temperature, increased from 150 to 220°C at 5°C/min; carrier gas (nitrogen) flow-rate, 30 ml/min. Retention times (min) are shown on the peaks. Peaks: 1 = 1,4:3,6-isosorbide (1,4:3,6-dianhydro-D-sorbitol); 2 = 1,4-sorbitan (anhydro-D-sorbitol); 3–11 = unspecified isomers of cyclized sorbitol; 12 = unreacted sorbitol.

### 2.4. Preparation of derivatives

The samples withdrawn from reactor were silylated with Tri-Sil reagent. The reagent contains hexamethyldisilazane (HMDS) as the active ingredient, trimethylchlorosilane (TMCS) as catalyst and pyridine as solvent, all premixed in the appropriate proportions (2:1:9). The TMS derivatives were prepared by treating 50–60-mg samples [1] in N,N-dimethylformamide (DMF). Tri-Sil reagent (0.1 ml) and 0.3 ml of ester dissolved in DMF were added and shaken and allowed to stand for 15 min [1,5,7]. The supernatant (0.4 μl) was injected into the gas chromatograph. The amount injected was required for packed column application.

The assignment of peak 1 (Fig. 2) and peak 3 (Fig. 3) in the chromatograms was made according to chromatograms of standard compounds.

### 2.5. Conversion of fatty acids

The extent of conversion of acid into sorbitan esters was determined as follows: samples of the reaction mixture were taken periodically during the reaction, and the concentration of the residual fatty acid was determined GC and by titration with 0.1 *M* KOH–ethanol. The extent of conversion was calculated [4].

## 3. Results and discussion

The purpose of this study was to show possible ways of following the course of esterification reactions using GC. In this way it was possible to show which of the isomers present undergoes the esterification reaction with lauric acid. The conversion of lauric acid was determined, and the presence of cyclized sorbitol isomers was defined using GC.

Fig. 1 shows the hypothetical sequence of the esterification reaction up to monolaurate on the basis of the results obtained using GC. Fig. 2 shows gas chromatogram of the cyclized sorbitol with the corresponding isomers and their retention times (method B). The retention times of individual specific isomers, isosorbide and 1,4-

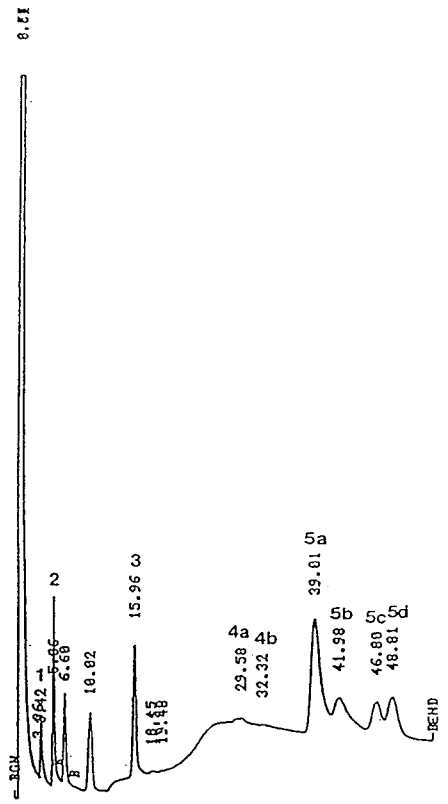


Fig. 3. Chromatogram of TMS derivative of reaction mixture of sorbitan monolaurate (method B) on a glass column (2 m × 5 mm I.D.) packed with 3% SE-30 on Chromosorb G (60–80 mesh). Conditions as in Fig. 2. Retention times (min) are shown on the peaks. Peaks: 1 = 1,4:3,6-isosorbide; 2 = 1,4-sorbitan; 3 = lauric acid, 4a and b = 1,4:3,6-isosorbide monolaurate; 5a–d = sorbitan monolaurate.

sorbitan, were separately determined [1,6] and compared with the mixture of isomers of cyclized sorbitol. The retention time of 1,4:3,6-isosorbide (peak 1) was 3.41 min and that of 1,4-sorbitan (peak 2) was 5.06 min. These compounds are present at higher concentrations in the mixture of cyclized sorbitol relation in comparison with other isomers.

The gas chromatogram of sorbitan monolaurate (prepared by method B) with characteristic peaks of sorbitol anhydrides (peaks 1 and 2), lauric acid (peak 3) and sorbitan monolaurate (peaks 4a and b and 5a–d) is shown in Fig. 3 [1,6]. Peaks 4a and b represent possible isomers

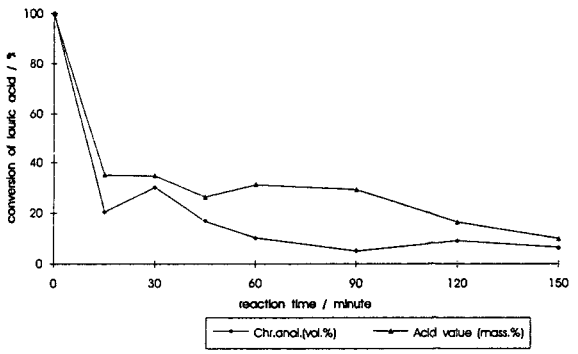


Fig. 4. Change in concentration of lauric acid reacted in the course of reaction with sorbitol at 160°C without previous cyclization of sorbitol with *p*-TSA as catalyst. ◆ = GC analysis (vol-%); ▲ = acid value (mass-%).

of sorbitan monolaurate obtained by the esterification reaction of 1,4:3,6-isosorbide with lauric acid. Peaks 5a–d could represent isomers of sorbitan monolaurate obtained by the esterification reaction of 1,4-sorbitan with lauric acid [1]. The retention time of lauric acid standard was separately determined (peak 3) [1,6]. The retention times of mono-, di, tri- and tetralaurates obtained by the esterification reaction of sorbitol anhydrides with lauric acid were theoretically explainable.

Figs. 4 and 5 show the conversion of lauric acid with [11] (method B) and without [9] (method A) previous sorbitol cyclization, as obtained using GC (vol.-%) and by determi-

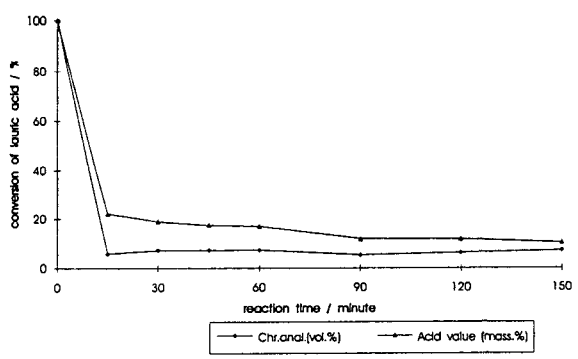


Fig. 5. Change in concentration of lauric acid reacted in the course of reaction with sorbitol at 160°C with previous cyclization of sorbitol with *p*-TSA as catalyst. ◆ = GC analysis (vol. %); ▲ = acid value (mass-%).

nation of the acid number (mass-%), demonstrating the quality of the sorbitol esterification reaction with lauric acid. It can be seen that the conversion was better when the sorbitol was previously cyclized (method B).

This work represents the solution to a real problem that should be of interest to surfactant and carbohydrate chemists. Workers in the food, cosmetic, detergents and general surfactants industries should also benefit from this work.

## 4. Conclusions

Trimethylsilyl derivatives of sorbitan fatty acid esters can be determined by GC. The conversion of lauric acid can be followed by GC analysis. The results of these analyses confirm the possibility of monitoring lauric acid and sorbitol esterification via the GC determination of lauric acid concentration.

## References

[1] M.R. Sahasrabudhe and R.K. Chadha, J. Am. Oil Chem. Soc., 46 (1969) 8.
[2] J. Cerdas, A. Carlier, F. Puisieux and A. Le Hir, Ann. Pharm. Fr. 25 (1967) 553.
[3] R. Von Neissner, SÖFW-J., 74 (1972) 198.
[4] H. Seino, T. Uchibori, T. Nishitani and S. Inamasu, J. Am. Oil Chem. Soc., 61 (1984) 1761.
[5] R. Suffis, T.J. Sullivan and W.S. Henderson, J. Soc. Cosmet. Chem., 16 (1965) 783.
[6] S. Ropuszyński and E. Sczesna, Tenside Surf. Deterg., 27 (1990) 350.
[7] R. Novina, Kem. Ind., 33, No. 1 (1984) 13.
[8] Y. Kondoh, A. Yamada and S. Takano, J. Chromatogr., 541 (1991) 431.
[9] A.E. Pierce, Silylation of Organic Compounds, Pierce, Rockford, IL, 1968.
[10] K.R. Brown (Atlas Powder), US Pat., 2 322 820 (1943).
[11] G.J. Stockburger, US Pat., 4 297 290 (1981).

ELSEVIER

Journal of Chromatography A, 704 (1995) 540–543

JOURNAL OF CHROMATOGRAPHY A

Short communication

# Thin-layer chromatographic detection of dichlorvos and dimethoate using orcinol

B.D. Mali*, M.V. Garad, V.B. Patil, S.V. Padalikar

*Regional Forensic Science Laboratory, State of Maharashtra, Cantonment, Aurangabad-431 002, India*

First received 21 July 1994; revised manuscript received 18 January 1995; accepted 19 January 1995

**Abstract**

A sensitive and selective thin-layer chromatographic method for the detection of dichlorvos and dimethoate using orcinol is described. The alkali hydrolysis product of dichlorvos or dimethoate with orcinol produces a yellow fluorescent compound. The reagent does not react with other organophosphorus, organochlorine and carbamate insecticides. The constituents of viscera (amino acids, peptides, proteins, etc.) and plant materials do not interfere with the test. The fluorescence detection limits for dichlorvos and dimethoate are ca. 1 $\mu$g per spot (1.40 $\mu g/cm^2$) and ca. 15 $\mu$g per spot (21 $\mu g/cm^2$), respectively.

## 1. Introduction

Dichlorvos and dimethoate are organophosphorous insecticides widely used in agriculture for crop protection. Owing to their ready availability they are often misused for homicidal or suicidal purpose. During 1992, the Forensic Laboratories of Maharashtra detected 97 and 459 human poisoning cases with dichlorvos and dimethoate, respectively. The detection of these insecticides in routine forensic work is achieved using thin-layer chromatography (TLC). For instrumental methods, the biological material (vomitus, blood, viscera etc.) needs to be cleaned up before assay in order to remove biological impurities such as amino acids, peptides and proteins. Although these instrumental methods are sensitive, they are expensive and there are limitations to their use in routine forensic work owing to the large number of samples to be analysed. Hence TLC is the procedure of choice owing to its availability, simplicity and rapidity.

A number of chromogenic reagents, such as mercury (II) nitrate–potassium hexacyanaferrate(II) [1], potassium iodate–starch [2], alkaline resorcinol [3], iodine [4,5] and zinc chloride–diphenyalamine [6], have been reported for the detection of these insecticides, but none is selective for dichlorvos and dimethoate. In a search for selective and sensitive reagent, orcinol was found to be suitable for detection of dichlorvos and dimethoate.

## 2. Experimental

All reagents were of analytical-reagent grade and distilled water was used throughout.

Solutions of technical-grade dichlorvos (Ciba-

* Corresponding author.

0021-9673/95/$09.50 
*SSDI* 0021-9673(95)00091-7

Geigy, Bombay, India, 1 mg/ml, and dimethoate (Rallis, India), 4 mg/ml, were prepared in ethanol. Aqueous solutions of anthranilic acid (1 mg/ml), 2% (w/v) sodium hydroxide and 0.5% (w/v) orcinol (BDH, Poole, UK) were prepared.

### 2.1. Thin-layer chromatography

TLC plates were prepared as described previously [7]. Known concentrations of dichlorvos or dimethoate together with anthranilic acid were spotted on the plate, which was then developed in a presaturated TLC chamber using two solvent systems, *n*-hexane–acetone–methanol (8:3:0.5) and benzene–ethyl acetate–methanol (9:1:1). After the solvent had migrated ca. 10 cm, the plate was removed and allowed to dry at room temperature. It was sprayed uniformly with 2% sodium hydroxide solution followed by 0.5% orcinol solution, then placed in an oven at 100°C for about 10 min. The plate was removed and allowed to cool to room temperature. A yellow-brown spot for dichlorvos and a yellow spot for dimethoate were observed. The plate was viewed under long-wavelength (365 nm) UV light. Both insecticides appeared as yellow fluorescent spots, whereas the anthranilic acid spot demonstrated a blue fluorescence. The $R_F$ values of dichlorvos and dimethoate with respect to anthranilic acid are given in Table 1.

### 2.2. Recovery of dichlorovos and dimethoate from biological materials

For the semi-quantitative determination of dichlorovos, 1 mg of insecticide was added to ca. 50 g of minced visceral tissue (stomach, intestine, liver, etc.) and kept for a day. The insecticide was then extracted with diethyl ether, the solvent was evaporated at room temperature and the residue was dissolved in 1 ml of ethanol. A 10-$\mu$l volume of this solution was spotted on an activated plate along with 10 $\mu$l each of standard solutions containing 8.5, 9.0, 9.5 and 10.0 $\mu$g of dichlorovos. The plate was then developed as described above. The intensity of the yellow fluorescent spot produced by the visceral extract was comparable to that of the spot corresponding to 9.0 $\mu$g of dichlorvos (average of three experiments). Hence the recovery was ca. 90%. Likewise, the recovery of dimethoate was also found to be ca. 90%.

## 3. Results and discussion

Dichlorvos and dimethoate are the derivatives of phosphoric and dithiophosphoric acid, respectively, and both are readily hydrolysed in an alkaline medium. Dichlorvos on alkali hydrolysis [8] produce dimethylphosphoric acid (**I**) and dichloroacetaldehyde (**II**). Orcinol (**III**) reacts with dichloroacetaldehyde (**II**) as shown in Fig. 1. Similar reactions of chloral with resorcinol [9] and chloroform with orcinol [10] have been reported.

Dichlorovos and dimethoate gives visible spots at amounts of 4 $\mu$g and 90 $\mu$g, respectively. Under UV radiation, the detection limit of the reagent is lowered to 1 $\mu$g per spot (1.40 $\mu$g/cm$^2$) for dichlorvos and 15 $\mu$g per spot (21 $\mu$g/cm$^2$) for dimethoate. The colour of the spots

Table 1
$R_F$ values with respect to anthranilic acid

| Insecticide | $R_F \pm$ S.D.[a] | | Colour of spot under 365-nm UV radiation |
|---|---|---|---|
| | I[b] | II[b] | |
| Dichlorvos | 2.92 ± 0.04 | 2.16 ± 0.03 | Yellow |
| Dimethoate | 0.68 ± 0.02 | 0.63 ± 0.03 | Yellow |
| Anthranilic acid | 1.00 | 1.00 | Blue |

[a] Standard deviations based on ten measurements.
[b] Solvent systems: I = *n*-hexane–acetone– methanol (8:3:0.5) (anthranilic acid $R_F = 0.18$); II = benzene–ethyl acetate–methanol (9:1:1) (anthranilic acid $R_F = 0.33$).

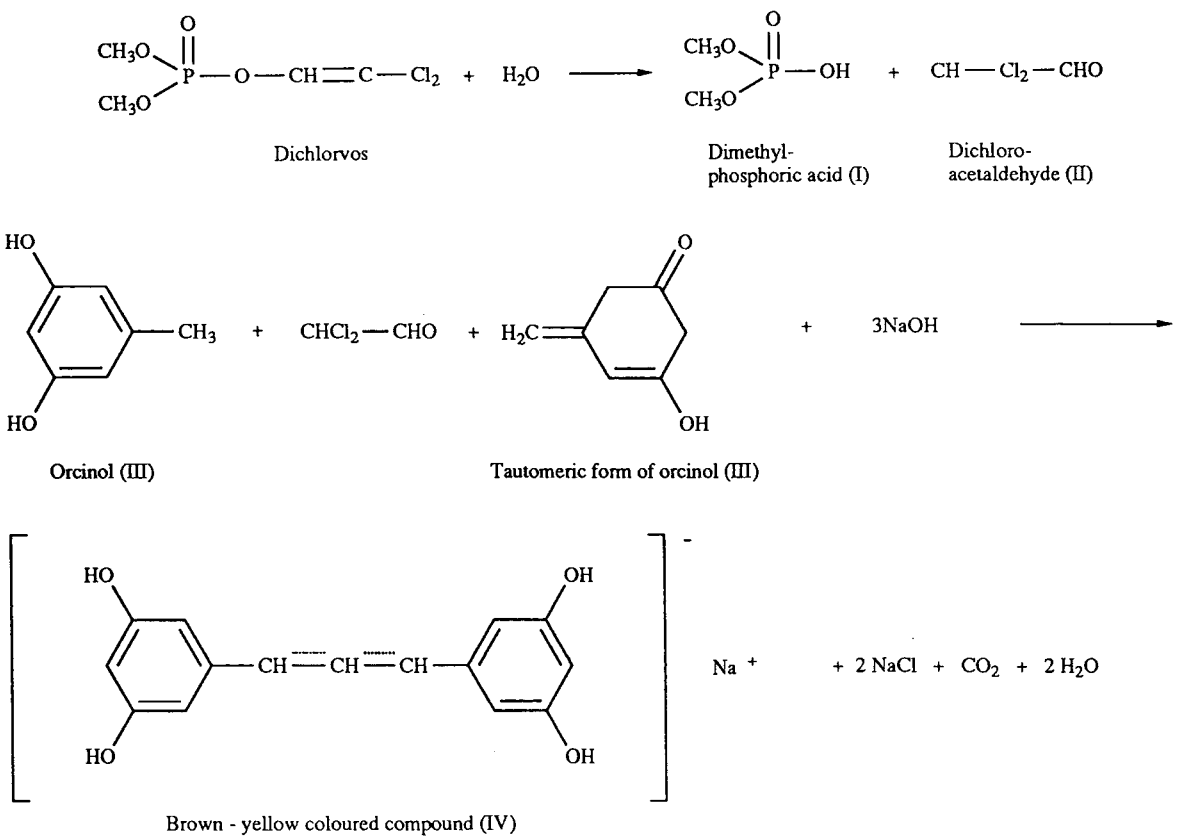


Fig. 1. Formation of coloured compounds.

remains stable for about 2 days. The solvent systems used gives compact spots. It was seen that dichlorvos and dimethoate are not fluorescent. Anthranilic acid does not react with orcinol, hence it was used for obtaining relative $R_F$ values.

Orcinol was found to give yellow fluorescence with chloral hydrate and trichloroacetic acid with detection limits of 25 and 48 $\mu$g, respectively. It does not give a colour reaction with other organophosphorus insecticides (malathion, fenthion, phorate, parathion, quinolphos, ekatin and fenitrothion), organochlorine insecticides (endosulphan, DDT and benzene hexachloride) and carbamate insecticides (baygon, carbaryl and carbofuran) as such or after their alkali hydrolysis. The constituents of viscera (amino acids, peptides, proteins, etc.) generally co-extracted with these insecticides and plant materials do not interfere with the test. Hence the proposed reagent, owing to its sensitivity and selectivity, can be useful for detection and semi-quantitative determination of dichlorvos and dimethoate insecticides in biological and vegetable materials.

## Acknowledgement

The authors are grateful to Mr. S.O. Baisane, Director, Forensic Science Laboratories, State of Maharashtra, Bombay, for his keen interest and valuable guidance in this work.

## References

[1] H.N. Katkar and V.P. Barve, Curr. Sci., 45 (1976) 662.
[2] V.B. Patil, S.V. Padalikar and G.B. Kawale, Analyst, 112 (1987) 1765.

[3] B. Xie and Z. Zhou, Lihua Jianyan Huaxue Fence, 25 (1989) 126.
[4] R. Kumar and C.B. Sharma, J. Liq. Chromatogr., 10 (1987) 3681.
[5] B. Xie, Lihua Jianyan Huaxue Fence, 28 (1992) 178.
[6] M.T. Sevalkar, V.B. Patil and H.N. Katkar, J. Assoc. Off. Anal. Chem., 74 (1991) 545.
[7] B.D. Mali and P.P. Parulekar, J. Chromatogr., 457 (1988) 383.
[8] U.S. Sree Ramulu, Chemistry of Insecticides and Fungicides, IBH, New Delhi, 2nd ed., 1985, p. 125.
[9] M. Pesez and P. Poirier, Méthodes et Réactions de l'Analyse Organique, Vol. III, Masson, Paris, 1954, p. 173.
[10] F. Feigl, Spot Tests in Organic Analysis, Elsevier, Amsterdam, 7th ed., 1983, p. 424.

ELSEVIER

Journal of Chromatography A, 704 (1994) 544–545

JOURNAL OF CHROMATOGRAPHY A

# Book Review

*Carbohydrate Analysis–High-Performance Liquid Chromatography and Capillary Electrophoresis*, edited by Z. El Rassi, (Journal of Chromatography Library, Vol. 58), Elsevier, Amsterdam, 1995, XX + 672 pp., including index; Price Dfl 425.00; ISBN 0-444-89981-2, hardbound

Retailing at around £160 for 692 pages this is an expensive tome, but with this nicely layed out hardbound book you are getting more than a treatise on chromatography. The well balanced contents include an excellent introduction to glycoconjugate structure and analysis for both novice and expert alike. The diversity of oligosaccharides structure covered is only matched by the comprehensive methodology necessary to unravel it. The expert authors guide you through the complexity with both theoretical and practical implications written around solid description of techniques. And it is very up-to-date. The opening chapter (A.J. Mart and M.L. Pierce) is a highly readable account of oligosaccharide structure and properties including very helpful details on the preparation of carbohydrates for analysis (the title of the chapter) and a useful table of suppliers. Chapter 2 by Z. El Rassi compares reversed-phase (RP) and hydrophobic interaction chromatography (HIC) with reviews of column types, organic modifiers and labelling strategies and including ion-pair RP and porous graphitised carbon (PGC) chromatography. Chapter 3 (S.C. Churms) draws the contrast between HIC and HILIC, a useful distinction introduced by Alpert, the latter being the agreed abbreviation for hydrophilic interaction chromatography which is an all encompassing term for normal phase. The column packings and amine modifiers used in HPLC are also discussed in their other context of capillary electrophoresis (i.e. silica for derivatised or less polar oligosaccharides, diol columns, soluble amine modifiers, amino bonded silica phases, etc). A comprehensive matrix is presented of retention times in 4–7 different HPLC systems of 22 monosaccharides, 18 disaccharides, 10 alditols, 60 glycoprotein-derived oligosaccharides and 14 glycolipids, an exhausting but not an exhaustive list of all the published literature. The coverage is accurate (except for a single misspelt GalNAc-ol on p140!). Chapter 4 (C.G. Huber and G.K. Bonn) is on "HPLC of Carbohydrates with Cation- and Anion-Exchange silica and Resin-Based Stationary Phases" which, besides discussing well the column packings marketed for CE or AE, again shows the diversity of silica (with $Ag^{2+}$, $Pb^{2+}$ etc) and amino bonded silica (as a weak-base anion exchanger). Similar aspects are discussed for electrophoretic methods (Ch. 8; Z El Rassi and W. Nashabeh). Chapter 5 (R.R. Townsend) is an obligatory chapter on the now no longer new pellicular-phase anion exchangers (PAE) which have particular application in high pH anion-exchange chromatography (HPAEC) of oligosaccharides and monosaccharides (which are weak acids at $pH > 11$). The indispensable nature of this technique is exemplified by many diverse examples from viral, bacterial and mam-

*SSDI* 0021-9673(95)00287-1

malian glycoconjugate studies. This chapter is complemented by an equally authoritative discussion (Ch. 10 D.C. Johnson and W.R. Lacourse) of pulsed electrochemical detection at high pH for both carbohydrates and, interestingly, amino acids.

Several of the chapters give novel slants on HPLC analysis: Ch. 6 (S. Honda) covers the estimation of binding constants using lectin immobilised columns and by electrophoresis; Ch. 7 (S.C. Churms) outlines the development of modern size exclusion chromatography; Ch. 13 (M. Dreux and M. Lafosse) introduces evaporative light scattering (ELS) detection and Ch. 16 (L.J. Nagels and P.C. Maes) details post-column enzyme reactors. Other detection methods covered are refractive index (Ch. 11; A.E. Bruno and B. Krattiger), mass spectrometry (Ch. 12; C.A. Settineri and A.L. Burlingame), chiroptics (Ch. 14; N. Purdie), pre- and post-column derivatisation (Ch. 15; S. Hase) and, catalogued together in Ch. 17 (Z. El Rassi and J.T. Smith), UV, fluorescence, conductrometry, NMR, radioactivity and constant-potential amperometry. Disappointingly there was no crossreferencing between this last section, Ch. 5 or Ch. 10 where, for some maybe confusingly, PAD and PED are used interchangeably. Ch. 5 does have an abbreviations section but it would have been helpful if this had extended to the whole book. The nomenclature in the MS and derivatisation chapters (12 and 15) in particular could become challenging for those not familiar with the field (as LSIMS, LC/ESI/CID/MS, MALDI-TOFMS, PFBAB, ABEE, ABOE, ABH, ACP, AMC, ANTS, DAAB, CBQCA, are included, for example). Otherwise these are excellent chapters which go beyond chromatography and provide route maps for those wanting to know the best way to analyse their glycoconjugates. One slight niggle is the misspelling of Hakomori throughout Ch. 12 and his initial (S) in the references. As far as the other detection methods are concerned it was not always clear as to their particular advantages/disadvantages. ELS looked very good for stoichiometric detection (p. 533) but what is its sensitivity? Not until the end of Ch. 13 was this technique compared to RI, but neither method was compared with the most widely used, UV. Fluorescence detection, in particular of electrophoresis eluates, is the most sensitive (at the attomole level), but I was interested to see on p. 628 that Linhardt et al. had previously achieved pmole detection of proteoglycan oligosaccharides by suppressed conductivity detection. For sensitivity coupled with specificity the details in Ch. 16 given on different hydrolases, oxidases, dehydrogenases etc. used in series are invaluable.

At the other end of the extreme from high sensitive detection, is the ability of HPLC to work at a preparative scale. K.B. Hicks in Ch. 9 goes over the analytical techniques introduced in the earlier chapters, giving useful hints as to their practicality for large scale and high yields.

*London, UK* E.F. Hounsell

# Author Index


Abram, V., see Kukman, I.L. 704(1995)113
Aggarwal, S.K., see Batta, A.K. 704(1995)228
Albert, K., see Bayer, E. 704(1995)37
Andersson, P.E., see Wan, H. 704(1995)179
Batta, A.K., Aggarwal, S.K., Tint, G.S., Batta, M. and Salen, G.
Capillary gas–liquid chromatography of 6-hydroxylated bile acids 704(1995)228
Batta, M., see Batta, A.K. 704(1995)228
Baudrand, V., Mouloungui, Z. and Gaset, A.
Separation and quantification of tetraethylene glycol monoheptanoate and diheptanoate by high-performance liquid chromatography 704(1995)524
Baumeister, E., see Bayer, E. 704(1995)37
Bayer, E., Baumeister, E., Tallarek, U., Albert, K. and Guiochon, G.
NMR imaging of the chromatographic process. Deposition and removal of gadolinium ions on a reversed-phase liquid chromatographic column 704(1995)37
Beigi, F., Yang, Q. and Lundahl, P.
Immobilized-liposome chromatographic analysis of drug partitioning into lipid bilayers 704(1995)315
Benčina, M., see Friedrich, J. 704(1995)363
Blaschke, G., see Chankvetadze, B. 704(1995)234
Blomberg, L.G., see Wan, H. 704(1995)179
Boonkerd, S., Detaevernier, M.R., Michotte, Y. and Vindevogel, J.
Suppression of chiral recognition of 3-hydroxy-1,4-benzodiazepines during micellar electrokinetic capillary chromatography with bile salts 704(1995)238
Bossányi, F., see Piotte, M. 704(1995)377
Bousquet, O. and Le Goffic, F.
Counter-current chromatographic separation of polyunsaturated fatty acids 704(1995)211
Boyd-Boland, A.A. and Pawliszyn, J.B.
Solid-phase microextraction of nitrogen-containing herbicides 704(1995)163
Brinkman, U.A.T., see Van de Nesse, R.J. 704(1995)1
Bruno, T.J.
Permeation tube approach to long-term use of automatic sampler retention index standards 704(1995)157
Bult, A., see Cui, H. 704(1995)27
Caccamese, S., Principato, G., Viaud, M.-C. and Guillaumet, G.
Direct high-performance liquid chromatographic separation of the enantiomers of methoxy and hydroxy derivatives of 3,4-dihydro-3-(dipropylamino)-2*H*-1-benzopyrans with dopaminergic activity 704(1995)83
Caccialanza, G., see Massolini, G. 704(1995)55
Casale, J.F., see Moore, J.M. 704(1995)483
Chankvetadze, B., Endresz, G. and Blaschke, G.
Enantiomeric resolution of anionic *R*/*S*-1,1′-binaphthyl-2,2′-diyl hydrogen phosphate by capillary electrophoresis using anionic cyclodextrin derivatives as chiral selectors 704(1995)234
Chen, H.-R., see Sheu, S.-J. 704(1995)141
Cimerman, A., see Friedrich, J. 704(1995)363
Cloux, R., see Reddy, K.S. 704(1995)387
Cooper, D.A., see Moore, J.M. 704(1995)483
Cui, H., Leon, J., Reusaet, E. and Bult, A.
Selective determination of peptides containing specific amino acid residues by high-performance liquid chromatography and capillary electrophoresis 704(1995)27
De Lorenzi, E., see Massolini, G. 704(1995)55
Detaevernier, M.R., see Boonkerd, S. 704(1995)238
Dorsey, J.G., see Siles, B.A. 704(1995)289
Dovžan, A., see Novič, M. 704(1995)530
Effmert, U., see Schoor, A. 704(1995)89
Endresz, G., see Chankvetadze, B. 704(1995)234
Engström, A., see Wan, H. 704(1995)179
Erdmann, N., see Schoor, A. 704(1995)89
Fahey, J., see Redden, P.R. 704(1995)99
Favrou, A., see Roussel, C. 704(1995)67
Ferretti, R., Gallinella, B., La Torre, F. and Villani, C.
Direct high-performance liquid chromatography resolution on chiral columns of tiaprofenic acid and related compounds in bulk powder and pharmaceutical formulations 704(1995)217
Fischer, J.B. and Michael, J.L.
Thermospray ionization liquid chromatography–mass spectrometry and chemical ionization gas chromatography–mass spectrometry of hexazinone metabolites in soil and vegetation extracts 704(1995)131
Foucault, A., see Ma, Y. 704(1995)75
Freissmuth, J., see Noe, C.R. 704(1995)503
Friedrich, J., Žužek, M., Benčina, M., Cimerman, A., Štrancar, A. and Radež, I.
High-performance liquid chromatographic analysis of mevinolin as mevinolinic acid in fermentation broths 704(1995)363
Gachanja, A.N., Lewis, S.W. and Worsfold, P.J.
Determination of aldehydes in used engine oils by liquid chromatography with chemiluminescence detection 704(1995)329
Gallinella, B., see Ferretti, R. 704(1995)217
Gandini, C., see Massolini, G. 704(1995)55
Garad, M.V., see Mali, B.D. 704(1995)540
Gaset, A., see Baudrand, V. 704(1995)524
Giacometti, J., Milin, Č. and Wolf, N.
Monitoring the esterification of sorbitol and fatty acids by gas chromatography 704(1995)535
Gill, D.S., see Roush, D.J. 704(1995)339
Giumanini, A.G., Verardo, G., Strazzolini, P. and Hepburn, H.R.
Rapid detection of high-molecular-mass dienes in beeswax 704(1995)224
Gooijer, C., see Van de Nesse, R.J. 704(1995)1

Guillaume, Y., Thomassin, M. and Guinchard, C.
Prediction of gas chromatographic retention times, column efficiency and resolution as a function of temperature and flow-rate. Application for gas chromatographic separation of eight *p*-hydroxybenzoic esters 704(1995)437
Guillaumet, G., see Caccamese, S. 704(1995)83
Guinchard, C., see Guillaume, Y. 704(1995)437
Guiochon, G., see Bayer, E. 704(1995)37
Guiochon, G. and Sarker, M.
Consolidation of the packing material in chromatographic columns under dynamic axial compression. I. Fundamental study 704(1995)247
Haginaka, J., Seyama, C. and Murashima, T.
Retentive and enantioselective properties of ovomucoid-bonded silica columns. Influence of protein purity and isolation method 704(1995)279
Hajšlová, J., see Tomšej, T. 704(1995)513
Halsall, H.B., see Siles, B.A. 704(1995)289
Hays, P.A., see Moore, J.M. 704(1995)483
Hepburn, H.R., see Giumanini, A.G. 704(1995)224
Horrobin, D.F., see Redden, P.R. 704(1995)99
Hounsell, E.F.
Carbohydrate Analysis–High-Performance Chromatography and Capillary Electrophoresis (by Z. El Rassi) (Book Review) 704(1995)544
Hsu, K.-Y., see Lee, W.-C. 704(1995)307
Hu, Z.-D., see Zhang, H.-W. 704(1995)242
Hudnik, V., see Novič, M. 704(1995)530
Ito, Y., see Ma, Y. 704(1995)75
Jarc, I., see Velikonja, Š. 704(1995)449
Jarm, V., see Šegudović, N. 704(1995)149
Jia, L., see Zhang, H.-W. 704(1995)242
Jolicoeur, C., see Piotte, M. 704(1995)377
Kaneko, S., see Nobuhara, K. 704(1995)45
Kaštelan-Macan, M., see Petrović, M. 704(1995)173
Kato, M., see Nobuhara, K. 704(1995)45
Kemmery, B., see Thompson, C.O. 704(1995)203
Khudaeva, G.B., see Rasulev, U.K. 704(1995)473
Klein, R.F.X., see Moore, J.M. 704(1995)483
Klyushnichenko, V.E., Yakimov, S.A., Tuzova, T.P., Syagailo, Ya.V., Kuzovkina, I.N., Wulfson, A.N. and Miroshnikov, A.I.
Determination of indole alkaloids from *R. serpentina* and *R. vomitoria* by high-performance liquid chromatography and high-performance thin-layer chromatography 704(1995)357
Kovač-Filipović, M., see Šegudović, N. 704(1995)149
Kováts, E.s., see Reddy, K.S. 704(1995)387
Kukman, I.L., Zelenik-Blatnik, M. and Abram, V.
Isolation of low-molecular-mass hydrophobic bitter peptides in soybean protein hydrolysates by reversed-phase high-performance liquid chromatography 704(1995)113
Kuzovkina, I.N., see Klyushnichenko, V.E. 704(1995)357
La Torre, F., see Ferretti, R. 704(1995)217
Le Goffic, F., see Bousquet, O. 704(1995)211
Lee, W.-C., Lin, C.-H., Ruaan, R.-C. and Hsu, K.-Y.
High-performance affinity chromatography of proteins on non-porous polystyrene beads 704(1995)307
Leister, W.H., Weaner, L.E. and Walker, D.G.
Analysis and purification of modified methoxy(polyethylene glycol) compounds of similar molecular mass by high-performance liquid chromatography 704(1995)369
Leon, J., see Cui, H. 704(1995)27
Lewis, S.W., see Gachanja, A.N. 704(1995)329
Lin, C.-H., see Lee, W.-C. 704(1995)307
Lin, X., see Redden, P.R. 704(1995)99
Lu, C.-F., see Sheu, S.-J. 704(1995)518
Lundahl, P., see Beigi, F. 704(1995)315
Ma, Y., Ito, Y. and Foucault, A.
Resolution of gram quantities of racemates by high-speed counter-current chromatography 704(1995)75
Mali, B.D., Garad, M.V., Patil, V.B. and Padalikar, S.V.
Thin-layer chromatographic detection of dichlorvos and dimethoate using orcinol 704(1995)540
Marsel, J., see Prosen, H. 704(1995)121
Marsel, J., see Velikonja, Š. 704(1995)449
Massolini, G., De Lorenzi, E., Ponci, M.C., Gandini, C., Caccialanza, G. and Monaco, H.L.
Egg yolk riboflavin binding protein as a new chiral stationary phase in high-performance liquid chromatography 704(1995)55
Maujean, A., see Nedjma, M. 704(1995)495
Michael, J.L., see Fischer, J.B. 704(1995)131
Michotte, Y., see Boonkerd, S. 704(1995)238
Mikkat, S., see Schoor, A. 704(1995)89
Milin, Č., see Giacometti, J. 704(1995)535
Miroshnikov, A.I., see Klyushnichenko, V.E. 704(1995)357
Monaco, H.L., see Massolini, G. 704(1995)55
Moore, J.M., Casale, J.F., Hays, P.A., Klein, R.F.X. and Cooper, D.A.
Hygrine, bona fide alkaloid or artifact: its chemical reduction, novel di-heptafluorobutyrylation and sensitive detection in South American coca leaves using capillary gas chromatography–electron capture detection 704(1995)483
Mouloungui, Z., see Baudrand, V. 704(1995)524
Murashima, T., see Haginaka, J. 704(1995)279
Nakamura, M., see Nobuhara, K. 704(1995)45
Nazarov, E.G., see Rasulev, U.K. 704(1995)473
Nedjma, M. and Maujean, A.
Improved chromatographic analysis of volatile sulfur compounds by the static headspace technique on water–alcohol solutions and brandies with chemiluminescence detection 704(1995)495
Nobuhara, K., Kato, M., Nakamura, M., Takami, M. and Kaneko, S.
Preparation and evaluation of magnesia-coated silica as column packing material for high-performance liquid chromatography 704(1995)45
Noe, C.R. and Freissmuth, J.
Capillary zone electrophoresis of aldose enantiomers: separation after derivatization with *S*-(−)-1-phenylethylamine 704(1995)503
Novič, M., Dovžan, A., Pihlar, B. and Hudnik, V.
Determination of chlorine, sulphur and phosphorus in organic materials by ion chromatography using electrodialysis sample pretreatment 704(1995)530

Ondra, P., Válka, I., Vičar, J., Sütlüpinar, N. and Šimánek, V.
Chromatographic determination of constituents of the genus *Colchicum* (Liliaceae) 704(1995)351
Padalikar, S.V., see Mali, B.D. 704(1995)540
Patil, V.B., see Mali, B.D. 704(1995)540
Pawliszyn, J.B., see Boyd-Boland, A.A. 704(1995)163
Perreault, F., see Piotte, M. 704(1995)377
Petrović, M. and Kaštelan-Macan, M.
Validation of quantitative chromatographic analysis on laboratory-prepared thin layers 704(1995)173
Pihlar, B., see Novič, M. 704(1995)530
Piotte, M., Bossányi, F., Perreault, F. and Jolicoeur, C.
Characterization of poly(naphthalenesulfonate) salts by ion-pair chromatography and ultrafiltration 704(1995)377
Pirkle, W.H. and Terfloth, G.J.
Naproxen-derived segmented and sidechain-modified polysiloxanes as chiral stationary phases 704(1995)269
Ponci, M.C., see Massolini, G. 704(1995)55
Principato, G., see Caccamese, S. 704(1995)83
Prosen, H., Zupančič-Kralj, L. and Marsel, J.
Optimization of an analytical procedure for the determination of triazine herbicides in environmental samples 704(1995)121
Radež, I., see Friedrich, J. 704(1995)363
Rasulev, U.K., Nazarov, E.G. and Khudaeva, G.B.
Chromatographic determination of trace amounts of amines using a surface ionization detector 704(1995)473
Redden, P.R., Lin, X., Fahey, J. and Horrobin, D.F.
Stereospecific analysis of the major triacylglycerol species containing γ-linolenic acid in Evening Primrose oil and borage oil 704(1995)99
Reddy, K.S., Cloux, R. and Kováts, E.s.
Pair-wise interactions by gas chromatography.
VI. Interaction free enthalpies of solutes with primary methoxyalkane, cyanoalkane and alkanethiol groups 704(1995)387
Reusaet, E., see Cui, H. 704(1995)27
Riba, M.-L., see Simon, V. 704(1995)465
Roush, D.J., Gill, D.S. and Willson, R.C.
Preferred high-performance liquid chromatographic anion-exchange chromatographic contact region for recombinant rat cytochrome $b_5$ 704(1995)339
Roussel, C. and Favrou, A.
Cationic β-cyclodextrin: a new versatile chiral additive for separation of drug enantiomers by high-performance liquid chromatography 704(1995)67
Ruaan, R.-C., see Lee, W.-C. 704(1995)307
Salen, G., see Batta, A.K. 704(1995)228
Sarker, M., see Guiochon, G. 704(1995)247
Schoor, A., Erdmann, N., Effmert, U. and Mikkat, S.
Determination of the cyanobacterial osmolyte glucosylglycerol by high-performance liquid chromatography 704(1995)89
Schrammel, F., see Ulberth, F. 704(1995)455
Šegudović, N., Sertić, S., Kovač-Filipović, M. and Jarm, V.
Salt effect on size-exclusion chromatography of partially sulfonated alternating copolymers of maleic acid and styrene in a polar solvent 704(1995)149
Sertić, S., see Šegudović, N. 704(1995)149
Seyama, C., see Haginaka, J. 704(1995)279
Sheu, S.-J. and Chen, H.-R.
Simultaneous determination of twelve constituents of I-tzu-tang, a Chinese herbal preparation, by high-performance liquid chromatography and capillary electrophoresis 704(1995)141
Sheu, S.-J. and Lu, C.-F.
Determination of eight constituents of Hsiao-cheng-chi-tang by high-performance liquid chromatography 704(1995)518
Siles, B.A., Halsall, H.B. and Dorsey, J.G.
Retention and selectivity of flavanones on homopolypeptide-bonded stationary phases in both normal- and reversed-phase liquid chromatography 704(1995)289
Šimánek, V., see Ondra, P. 704(1995)351
Simon, V., Riba, M.-L., Waldhart, A. and Torres, L.
Breakthrough volume of monoterpenes on Tenax TA: influence of temperature and concentration for α-pinene 704(1995)465
Štrancar, A., see Friedrich, J. 704(1995)363
Strazzolini, P., see Giumanini, A.G. 704(1995)224
Sütlüpinar, N., see Ondra, P. 704(1995)351
Syagailo, Ya.V., see Klyushnichenko, V.E. 704(1995)357
Takami, M., see Nobuhara, K. 704(1995)45
Tallarek, U., see Bayer, E. 704(1995)37
Terfloth, G.J., see Pirkle, W.H. 704(1995)269
Thomassin, M., see Guillaume, Y. 704(1995)437
Thompson, C.O. and Trenerry, V.C.
Determination of synthetic colours in confectionery and cordials by micellar electrokinetic capillary chromatography 704(1995)195
Thompson, C.O., Trenerry, V.C. and Kemmery, B.
Determination of cyclamate in low joule foods by capillary zone electrophoresis with indirect ultraviolet detection 704(1995)203
Tint, G.S., see Batta, A.K. 704(1995)228
Tomšej, T. and Hajšlová, J.
Determination of benzoylurea insecticides in apples by high-performance liquid chromatography 704(1995)513
Torres, L., see Simon, V. 704(1995)465
Trenerry, V.C., see Thompson, C.O. 704(1995)195
Trenerry, V.C., see Thompson, C.O. 704(1995)203
Tuzova, T.P., see Klyushnichenko, V.E. 704(1995)357
Ulberth, F. and Schrammel, F.
Accurate quantitation of short-, medium-, and long-chain fatty acid methyl esters by split-injection capillary gas–liquid chromatography 704(1995)455
Válka, I., see Ondra, P. 704(1995)351
Van de Nesse, R.J., Velthorst, N.H., Brinkman, U.A.T. and Gooijer, C.
Laser-induced fluorescence detection of native-fluorescent analytes in column liquid chromatography, a critical evaluation 704(1995)1
Velikonja, Š., Jarc, I., Zupančič-Kralj, L. and Marsel, J.
Comparison of gas chromatographic and spectrophotometric techniques for the determination of formaldehyde in water 704(1995)449
Velthorst, N.H., see Van de Nesse, R.J. 704(1995)1
Verardo, G., see Giumanini, A.G. 704(1995)224

Viaud, M.-C., see Caccamese, S. 704(1995)83
Vičar, J., see Ondra, P. 704(1995)351
Villani, C., see Ferretti, R. 704(1995)217
Vindevogel, J., see Boonkerd, S. 704(1995)238
Waldhart, A., see Simon, V. 704(1995)465
Walker, D.G., see Leister, W.H. 704(1995)369
Wan, H., Andersson, P.E., Engström, A. and Blomberg, L.G.
Direct and indirect chiral separation of amino acids by capillary electrophoresis 704(1995)179
Weaner, L.E., see Leister, W.H. 704(1995)369
Willson, R.C., see Roush, D.J. 704(1995)339
Wolf, N., see Giacometti, J. 704(1995)535
Worsfold, P.J., see Gachanja, A.N. 704(1995)329
Wulfson, A.N., see Klyushnichenko, V.E. 704(1995)357
Yakimov, S.A., see Klyushnichenko, V.E. 704(1995)357
Yamauchi, S.
Nitrobenzenes in reversed-phase liquid chromatography. New candidates for internal standards 704(1995)323
Yang, Q., see Beigi, F. 704(1995)315
Zelenik-Blatnik, M., see Kukman, I.L. 704(1995)113
Zhang, H.-W., Jia, L. and Hu, Z.-D.
Determination of palladium(II) as a chloro complex by capillary zone electrophoresis 704(1995)242
Zupančič-Kralj, L., see Prosen, H. 704(1995)121
Zupančič-Kralj, L., see Velikonja, Š. 704(1995)449
Žužek, M., see Friedrich, J. 704(1995)363

# Retention and Selectivity in Liquid Chromatography

## Prediction, Standardisation and Phase Comparisons

Edited by **R.M. Smith**

**Journal of Chromatography Library Volume 57**

This book brings together a number of studies which examine the ways in which the retention and selectivity of separations in high-performance liquid chromatography are dependent on the chemical structure of the analytes and the properties of the stationary and mobile phases. Although previous authors have described the optimisation of separations by alteration of the mobile phase, little emphasis has previously been reported of the influence of the structure and properties of the analyte.

The initial chapters describe methods based on retention index group increments and log P increments for the prediction of the retention of analytes and the ways in which these factors are influenced by mobile phases and intramolecular interactions. The values of a wide range of group increments in different eluents are tabulated.

Different scales of retention indices in liquid chromatography are described for the comparison of separations, the identification of analytes and the comparison of stationary phases. Applications of these methods in the pharmaceutical, toxicology, forensic, metabolism, environmental, food and other fields are reviewed. The effects of different mobile phases on the selectivity of the retention indices are reported. A compilation of sources of reported retention index values are given.

Methods for the comparison of stationary phases based on the interactions of different analytes are covered, including lipophilic and polar indices, shape selectivity comparisons, their application to novel stationary phases, and chemometric methods for column comparisons.

**Contents:**


1. Retention prediction based on molecular structure (R.M. Smith).
2. Retention prediction of pharmaceutical compounds (K. Valkó).
3. Retention index scales used in high-performance liquid chromatography (R.M. Smith).
4. Application of retention indices for identification in high-performance liquid chromatography (R.M. Smith).
5. Application of nitroalkanes and secondary retention index standards for the identification of drugs (M. Bogusz).
6. Identification using retention indices in gradient HPLC (P. Kuronen).
7. Characterization of retention and selectivity in reversed-phase LC using interaction indices (P. Jandera).
8. Lipophilic and polar indices (P. Jandera).
9. Solvent selectivity (S.D. West).
10. Retention and selectivity for polycyclic aromatic hydro carbons in reversed-phase liquid chromatography (L.C. Sander, S.A. Wise).
11. Comparison of novel stationary phases (J.J. Pesek, E.J. Williamsen).
12. Multivariate characterization of RP-HPLC stationary phases (A. Bolck, A.K. Smilde).

Subject index.



**©1995 480 pages Hardbound**
**Price: Dfl. 425.00 (US$ 250.00)**
**ISBN 0-444-81539-2**




ELSEVIER
An imprint of Elsevier Science


## ORDER INFORMATION


**ELSEVIER SCIENCE B.V.**
Order Fulfilment Department
P.O. Box 211
1000 AE Amsterdam
The Netherlands
Fax: +31 (20) 485 3598

For USA and Canada:
**ELSEVIER SCIENCE B.V.**
P.O. Box 945, New York
NY 10159-0945
Fax: +1 (212) 633 3680

*US$ prices are valid only for the USA & Canada and are subject to exchange rate fluctuations; in all other countries the Dutch guilder price (Dfl.) is definitive. Customers in the European Union should add the appropriate VAT rate applicable in their country to the price(s). Books are sent postfree if prepaid.*

## PUBLICATION SCHEDULE FOR THE 1995 SUBSCRIPTION

*Journal of Chromatography A* and *Journal of Chromatography B: Biomedical Applications*

| MONTH | 1994 | J | F | M | A | M[a] | J | |
|---|---|---|---|---|---|---|---|---|
| Journal of Chromatography A | Vols. 683–688 | 689/1<br>689/2<br>690/1<br>690/2 | 691/1 + 2<br>692/1 + 2<br>693/1<br>693/2 | 694/1<br>694/2<br>695/1<br>695/2 | 696/1<br>696/2<br>697/1 + 2<br>698/1 + 2 | 699/1 + 2<br>700/1 + 2<br>702/1 + 2<br>703/1 + 2 | 704/1<br>704/2<br>705/1<br>705/2 | The publication schedule for further issues will be published later. |
| Bibliography Section | | | | 713/1 | | | 713/2 | |
| Journal of Chromatography B: Biomedical Applications | | 663/1<br>663/2 | 664/1<br>664/2 | 665/1<br>665/2 | 666/1<br>666/2 | 667/1<br>667/2 | 668/1<br>668/2 | |

[a] Vol. 701 (Cumulative Indexes Vols. 652–700) expected in October.

## INFORMATION FOR AUTHORS

(Detailed *Instructions to Authors* were published in *J. Chromatogr. A*, Vol. 657, pp. 463–469. A free reprint can be obtained by application to the publisher, Elsevier Science B.V., P.O. Box 330, 1000 AH Amsterdam, Netherlands.)

**Types of Contributions.** The following types of papers are published: Regular research papers (full-length papers), Review articles, Short Communications and Discussions. Short Communications are usually descriptions of short investigations, or they can report minor technical improvements of previously published procedures; they reflect the same quality of research as full-length papers, but should preferably not exceed five printed pages. Discussions (one or two pages) should explain, amplify, correct or otherwise comment substantively upon an article recently published in the journal. For Review articles, see inside front cover under Submission of Papers.

**Submission.** Every paper must be accompanied by a letter from the senior author, stating that he/she is submitting the paper for publication in the *Journal of Chromatography A* or *B*.

**Manuscripts.** Manuscripts should be typed in **double spacing** on consecutively numbered pages of uniform size. The manuscript should be preceded by a sheet of manuscript paper carrying the title of the paper and the name and full postal address of the person to whom the proofs are to be sent. As a rule, papers should be divided into sections, headed by a caption (*e.g.*, Abstract, Introduction, Experimental, Results, Discussion, etc.). All illustrations, photographs, tables, etc., should be on separate sheets.

**Abstract.** All articles should have an abstract of 50–100 words which clearly and briefly indicates what is new, different and significant. No references should be given.

**Introduction.** Every paper must have a concise introduction mentioning what has been done before on the topic described, and stating clearly what is new in the paper now submitted.

**Experimental conditions** should preferably be given on a *separate* sheet, headed "Conditions". These conditions will, if appropriate, be printed in a block, directly following the heading "Experimental".

**Illustrations.** The figures should be submitted in a form suitable for reproduction, drawn in Indian ink on drawing or tracing paper. Each illustration should have a caption, all the *captions* being typed (with double spacing) together on a *separate sheet*. If structures are given in the text, the original drawings should be provided. Coloured illustrations are reproduced at the author's expense, the cost being determined by the number of pages and by the number of colours needed. The written permission of the author and publisher must be obtained for the use of any figure already published. Its source must be indicated in the legend.

**References.** References should be numbered in the order in which they are cited in the text, and listed in numerical sequence on a separate sheet at the end of the article. Please check a recent issue for the layout of the reference list. Abbreviations for the titles of journals should follow the system used by *Chemical Abstracts*. Articles not yet published should be given as "in press" (journal should be specified), "submitted for publication" (journal should be specified), "in preparation" or "personal communication".

Vols. 1–651 of the *Journal of Chromatography*; *Journal of Chromatography, Biomedical Applications* and *Journal of Chromatography, Symposium Volumes* should be cited as *J. Chromatogr.* From Vol. 652 on, *Journal of Chromatography A* (incl. Symposium Volumes) should be cited as *J. Chromatogr. A* and *Journal of Chromatography B: Biomedical Applications* as *J. Chromatogr. B.*

**Dispatch. Before sending the manuscript to the Editor please check that the envelope contains four copies of the paper complete with references, captions and figures. One of the sets of figures must be the originals suitable for direct reproduction. Please also ensure that permission to publish has been obtained from your institute.**

**Proofs.** One set of proofs will be sent to the author to be carefully checked for printer's errors. Corrections must be restricted to instances in which the proof is at variance with the manuscript.

**Reprints.** Fifty reprints will be supplied free of charge. Additional reprints can be ordered by the authors. An order form containing price quotations will be sent to the authors together with the proofs of their article.